Cochrane Library

Cochrane Database of Systematic Reviews

Irinotecan chemotherapy combined with fluoropyrimidines versus irinotecan alone for overall survival and progression-free survival in patients with advanced and/or metastatic colorectal cancer (Review)

Wulaningsih W, Wardhana A, Watkins J, Yoshuantari N, Repana D, Van Hemelrijck M

Wulaningsih W, Wardhana A, Watkins J, Yoshuantari N, Repana D, Van Hemelrijck M.
Irinotecan chemotherapy combined with fluoropyrimidines versus irinotecan alone for overall survival and progression-free survival in patients with advanced and/or metastatic colorectal cancer.
Cochrane Database of Systematic Reviews 2016, Issue 2. Art. No.: CD008593.
DOI: 10.1002/14651858.CD008593.pub3.

www.cochranelibrary.com

TABLE OF CONTENTS

[Intervention Review]

Irinotecan chemotherapy combined with fluoropyrimidines versus irinotecan alone for overall survival and progression-free survival in patients with advanced and/or metastatic colorectal cancer

Wahyu Wulaningsih[1,2,3], Ardyan Wardhana[3,4], Johnathan Watkins[3,5], Naomi Yoshuantari[3,6], Dimitra Repana[7], Mieke Van Hemelrijck[1]

[1]Cancer Epidemiology Group, Division of Studies, Faculty of Life Sciences and Medicine, King's College London, London, UK. [2]Division of Haematology and Oncology, Department of Internal Medicine, Gadjah Mada University, Yogyakarta, Indonesia. [3]PILAR Research and Education, Cambridge, UK. [4]Department of Anesthesiology, Faculty of Medicine, Gadjah Mada University, Yogyakarta, Indonesia. [5]Institute for Mathematics and Molecular Biomedicine, King's College London, London, UK. [6]Department of Cellular and Anatomic Pathology, Faculty of Medicine, Gadjah Mada University, Yogyakarta, Indonesia. [7]Department of Medical Oncology, Guy's and St Thomas' NHS Foundation Trust, London, UK

Contact address: Wahyu Wulaningsih, Cancer Epidemiology Group, Division of Studies, Faculty of Life Sciences and Medicine, King's College London, Research Oncology, 3rd floor Bermondsey Wing, Guy's Hospital, London, England, SE1 9RT, UK. wahyu.wulaningsih@kcl.ac.uk.

Editorial group: Cochrane Colorectal Cancer Group.
Publication status and date: New, published in Issue 2, 2016.

Citation: Wulaningsih W, Wardhana A, Watkins J, Yoshuantari N, Repana D, Van Hemelrijck M. Irinotecan chemotherapy combined with fluoropyrimidines versus irinotecan alone for overall survival and progression-free survival in patients with advanced and/or metastatic colorectal cancer. *Cochrane Database of Systematic Reviews* 2016, Issue 2. Art. No.: CD008593. DOI: 10.1002/14651858.CD008593.pub3.

ABSTRACT

Background

Chemotherapy is the treatment of choice in patients with advanced or metastatic colorectal cancer (CRC) where surgical resection of metastases is not an option. Both irinotecan (IRI) and fluoropyrimidines are often included in first- or second- line chemotherapy treatment regimens in such patients. However, it is not clear whether combining these agents is superior to irinotecan alone.

Objectives

To compare the efficacy and safety of two chemotherapeutic regimens, irinotecan monotherapy or irinotecan in combination with fluoropyrimidines, for patients with advanced CRC when administered in the first or second-line settings.

Search methods

We searched the following electronic databases to identify randomized controlled trials: Cochrane Colorectal Cancer Group Specialised Register (January 13, 2016), Cochrane Central Register of Controlled Trials (CENTRAL)(The Cochrane Library Issue 12, 2016), Ovid MEDLINE (1950 to January 13, 2016), Ovid EMBASE (1974 to January 13, 2016), registers of controlled trials in progress, references cited in relevant publications and conference proceedings in related fields (BioMed Central and Medscape's Conference). The key authors or investigators of all eligible studies, and professionals in the field were contacted when necessary. The search from January 2016 identified one eligible study, an ongoing trial currently presented as an abstract, to be considered in an update of this review.

Selection criteria

Randomized controlled trials (RCTs) investigating the efficacy and safety of IRI chemotherapy combined with fluoropyrimidine compared with IRI alone for the treatment of patients with advanced CRC, regardless of treatment line settings.

Data collection and analysis

Study eligibility and methodological quality were assessed independently by the two authors, and any disagreement was solved by a third author. The data collected from the studies were reviewed qualitatively and quantitatively using the Cochrane Collaboration statistical software RevMan 5.3.

Main results

Five studies were included in this review with a total of 1,726 patients. The top-up search resulted in an additional ongoing trial, the results of which have not been incorporated in this review. Among five included studies, no reduction in all-cause mortality was observed in the combination arm, with a summary hazard ratio (HR) of 0.91 (95% CI: 0.81-1.02). Longer progression-free survival was observed in those treated with the combination chemotherapy (HR: 0.68, 95% CI: 0.53-0.87), however, this result may have been driven by findings from the single first-line treatment setting study.
The quality of evidence for overall survival was low and for progression-free survival was moderate, mainly due to study limitation from the lack of information on randomisation methods and allocation concealment.
There were higher risks of toxicity outcomes grade 3 or 4 diarrhoea and grade 1 or 2 alopecia, and a lower risk of grade 3 or 4 neutropenia in controls compared to the invervention group. Evidence for toxicity has been assessed to be low to moderate quality.

Authors' conclusions

There was no overall survival benefit of the irinotecan and fluoropyrimidine treatment over irinotecan alone, thus both regimens remain reasonable options in treating patients with advanced or metastatic CRC. Given the low and moderate quality of the evidence, future studies with sufficient numbers of patients in each treatment arms are needed to clarify the benefit observed in progression-free survival with combination irinotecan and fluoropyrimidines.

PLAIN LANGUAGE SUMMARY

Irinotecan chemotherapy combined with fluoropyrimidines versus irinotecan alone for overall survival and progression-free survival in patients with advanced and/or metastatic colorectal cancer

Background:

Patients with inoperable colorectal cancer (CRC) are likely to receive chemotherapy drugs as their primary treatment. Irinotecan (IRI) and fluoropyrimidines are two such drugs widely used in this setting, either alone or as part of multi-drug chemotherapy treatments.

Objectives:

Currently, there is lack of evidence comparing the combination of IRI and fluoropyrimidine with IRI alone. Therefore it was the aim of this review to compare the two treatments for patients with inoperable advanced or metastatic CRC.

Investigation and study characteristics:

We searched the literature on January 13, 2016. We identified five randomised controlled trials with a total of 1,726 patients comparing the combination of IRI and fluoropyrimidine with IRI alone. The search in January 2016 resulted in an additional ongoing trial, the results of which have not been incorporated in this review.
This review compared IRI and fluoropyrimidine with IRI alone in terms of overall survival, progression-free survival, toxicity, response rates and quality of life.

Main results:

There is no evidence to suggest any superiority of the combination of IRI and fluoropyrimidine over IRI alone, but our results on overall survival are limited by the number of studies available to date. Longer progression-free survival was seen from adding fluoropyrimidines to IRI. Based on current evidence, both the combination regimens and IRI alone seem equally effective for treating advanced or metastatic patients. Patients in the intervention arm were less likely to develop grade 3 or 4 diarrhea and grade 1 or 2 alopecia, and more likely to have grade 3 or 4 neutropenia, compared to patients receiving IRI alone.

Quality of the evidence:

There was moderate quality evidence from these studies suggesting longer progression-free survival from adding fluoropyrimidines to IRI. However, findings need to be confirmed by larger, high-quality randomised clinical trials.

SUMMARY OF FINDINGS

Summary of findings for the main comparison. IRI with fluoropyrimidines versus single agent IRI for advanced and/or metastatic colorectal cancer

IRI with fluoropyrimidines versus single agent IRI for advanced and/or metastatic colorectal cancer

Patient or population: patients with advanced and/or metastatic colorectal cancer
Settings: first- and second- line treatments
Intervention: IRI with fluoropyrimidines

Control: Single agent IRI.

Outcomes	Illustrative comparative risks* (95% CI)		Relative effect (95% CI)	No of Participants (studies)	Quality of the evidence (GRADE)
	Assumed risk	Corresponding risk			
	Control	IRI with fluoropyrimidines			
Overall survival (Death) Follow-up: 12 months	**47 per 100**	**44 per 100** (40 to 48)	**HR 0.91** (0.81 to 1.02)	1728 (5 studies)	⊕⊕⊖⊖ **low** [1]
Progression-free survival (Disease progression) Follow-up: 12 months	**92 per 100**	**81 per 100** (74 to 88)	**HR 0.68** (0.53 to 0.83)	600 (3 studies)	⊕⊕⊕⊖ **moderate[2]**
Grade 3/4 diarrhea	**Study Population**		**RR 0.66** (0.51 to 0.85)	1179 (5 studies)	⊕⊕⊕⊖ **moderate[3]**
Follow-up:	**213 per 1000**	**140 per 1000** (109 to 181)			
	Moderate				
	185 per 1000	**122 per 1000** (94 to 157)			
Grade 3/4 nausea	**Study Population**		**RR 0.33** (0.07 to 1.58)	209 (3 studies)	⊕⊕⊖⊖ **low[4]**
Follow-up:	**49 per 1000**	**16 per 1000** (3 to 77)			
	Moderate				
	33 per 1000	**11 per 1000**			

(2 to 52)

*The basis for the **assumed risk** (e.g. the median control group risk across studies) is provided in footnotes. The **corresponding risk** (and its 95% confidence interval) is based on the assumed risk in the comparison group and the **relative effect** of the intervention (and its 95% CI).
CI: Confidence interval; **HR:** Hazard ratio.

GRADE Working Group grades of evidence
High quality: Further research is very unlikely to change our confidence in the estimate of effect.
Moderate quality: Further research is likely to have an important impact on our confidence in the estimate of effect and may change the estimate.
Low quality: Further research is very likely to have an important impact on our confidence in the estimate of effect and is likely to change the estimate.
Very low quality: We are very uncertain about the estimate.

1 Downgraded one level for study limitations (Allocation concealment was only clear for one of the five studies, open-label intervention) and one level for imprecision (Lack of sufficient number of samples may have reduced the statistical power of the analysis)
2 Downgraded one level for study limitations (Allocation concealment was only clear for one of the five studies, open-label intervention)
3 Downgraded one level for study limitations (Allocation concealment was only clear for one of the five studies, open-label intervention)
4 Downgraded one level for study limitations (Allocation concealment was only clear for one of the five studies, open-label intervention) and one level for imprecision (Lack of sufficient number of samples may have reduced the statistical power of the analysis)

BACKGROUND

Description of the condition

Colorectal cancer (CRC) is currently the third most commonly diagnosed cancer for men and the second most common for women, as well as a leading cause of death worldwide (Ferlay 2010). In the United States, it was estimated that 136,830 people (71,830 men and 65,000 women) were diagnosed with CRC and 50,310 died from the disease in 2014 (Siegel 2014). Despite the higher incidence and mortality rates of CRC in more developed countries , these rates have been decreasing over the last two decades, particularly in the United States (Jemal 2011; Siegel 2013). Conversely, both CRC incidence and mortality have increased in less developed countries, largely owing to limited resources and inadequate healthcare infrastructure (Center 2009).

Early stage CRC is potentially curable by surgery (Kuhry 2008). However, 20-25% of CRC patients are first diagnosed with metastatic disease, where curative surgical resection is unlikely to be carried out (Siegel 2014; Van Cutsem 2014), and many patients relapse with metastatic disease after potentially curative resections. For these patients systemic chemotherapy is often the treatment of choice, with the objectives of relieving symptoms, increasing survival and improving quality of life (Simmonds 2000; Ragnhammar 2001).

Description of the intervention

Antimetabolite fluoropyrimidines have been the backbone of CRC chemotherapy for the past 40 years. For decades, treatment efficacy from fluorouracil (FU) monotherapy has been limited. The subsequent combination of 5-fluorouracil (5-FU) with leucovorin (LV), a reduced folate that increases thymidylate synthetase inhibition, was used to modulate effects of 5-FU and improve its efficacy (ACCMAP 1992). This combination has resulted in better response rates than 5-FU alone for advanced CRC (Thirion 2004) and remains the main component of most chemotherapy regimens in CRC, either as an intravenous (IV) bolus injection, infusion, or both (Chau 2005; Maiello 2005).

Irinotecan is a semisynthetic derivative of the natural alkaloid camptothecin which inhibits topoisomerase I, thus impeding DNA uncoiling and leading to double-stranded DNA breaks (Hsiang 1985). This drug was shown to have antitumour activity against CRC when administered intravenously alone in a first-line setting, or as a second-line regimen for patients with advanced CRC that is refractory to FU (Conti 1996; Pitot 1997; Rothenberg 1999; Rougier 1997; Rougier 1998)

In more recent years, a number of oral fluoropyrimidines such as capecitabine have become available. In addition to its more convenient use as an oral agent, capecitabine has been shown in clinical trials to have superior safety profiles compared to IV 5-FU/LV with similar (non-inferior) overall survival (OS), progression-free survival (PFS) and time to progression (TTP) for patients with metastatic CRC (Petrelli 2012; Van Cutsem 2004). These encouraging results suggest that oral fluoropyrimidine agents may serve as a suitable alternative to IV agents for CRC chemotherapy treatment. However, when both treatment arms were combined with irinotecan (IRI), IV 5-FU/LV regimens demonstrated longer PFS and less toxicity in metastatic CRC compared to capecitabine (Montagnani 2010), and the combination of capecitabine and IRI is used less commonly now.

How the intervention might work

As a first-line chemotherapeutic regimen for CRC, IV IRI alone was demonstrated to have comparable antitumour activity to 5-FU/LV (Cao 2000, Saltz 2000). Besides a different mechanism of action from 5-FU, the lack of cross-resistance of IRI to previous 5-FU/LV treatment, as shown by its similar activity against untreated and 5-FU-pretreated CRC, is the rationale for combining it with fluoropyrimidines as first-line therapy for this disease (Rougier 1997). The synergistic effects between IRI and fluoropyrimidines have been suggested to be comparable with that of IRI and oxaliplatin despite difference different toxicity profiles (Colucci 2005; Tournigand 2004). As the second-line treatment for advanced CRC, two phase III studies have shown modest benefits in survival with IRI of 2.3 months and 2.7 months compared to IV 5-FU and best supportive care, respectively (Rougier 1998; Cunningham 1998). Until now, the superiority of IRI combined with fluoropyrimidines over fluoropyrimidines alone has been assumed and the combination regimen is now widely used for advanced CRC patients in clinical practice (Douillard 2000; Maiello 2000; Folprecht 2008; Giessen 2011; Muro 2010).

Why it is important to do this review

Several randomized controlled trials (RCTs) comparing IRI in combination with fluoropyrimidines against IRI alone suggested that the combination regimen leads to better outcomes in OS and TTP for advanced CRC (Saltz 2000; Seymour 2007), while the results of another trial and a meta-analysis indicated that IRI monotherapy had equivalent efficacy and toxicity (Clarke 2011; Graeven 2007). However, the meta-analysis comparing IRI and IV 5-FU/LV combination regimen (FOLFIRI) for second-line treatment of CRC was not specific for trials concurrently including both treatment arms (Clarke 2011). Thus the benefit of IRI and fluoropyrimidines over IRI monotherapy remains unclear. Taking their efficacy and toxicity into account, we therefore undertook this study to systematically compare the combination regimen with IRI alone to determine which regimen is more suitable for advanced CRC patients, either as a first-line or a second-line therapy.

OBJECTIVES

The aim of this systematic review was to compare the efficacy and safety of two chemotherapeutic regimens, IRI monotherapy or IRI in combination with fluoropyrimidines, for patients with advanced CRC when administered in the first or second-line setting.

METHODS

Criteria for considering studies for this review

Types of studies

Randomised controlled trials (RCTs) investigating the efficacy and safety of chemotherapeutic regimens that compared IRI combined with fluoropyrimidine against IRI alone for the treatment of patients with advanced CRC, regardless of treatment line settings, were eligible for the inclusion. If trials enrolled more than two groups, we only extracted data that related to the two regimens. Relevant cluster RCTs were eligible for this review.

Types of participants

Studies involving patients diagnosed histologically or cytologically with locally advanced and/or metastatic CRC were included.

Types of interventions

The experimental group received the combination regimen, namely IRI with fluoropyrimidines administered intravenously or orally; the control group received single agent IRI. Other agents were acceptable as long as they were common to both treatment arms, except LV, which is specific to IV 5-FU.

Types of outcome measures

Primary outcomes

The primary outcome measures were:

- Overall survival (OS),
- Time to progression (TTP) or progression-free survival (PFS)

All outcomes were analysed on an intention to treat (ITT) basis. Studies which reported survival outcomes either directly or by curves were included, if the relevant data could be obtained by using Parmar methods (Parmar 1998; Tierney 2007).

Secondary outcomes

The secondary outcome measures were:

- toxicity, classified according to the National Cancer Institute Common Toxicity Criteria (NCI-CTC version 2.0),
- response rates, classified according to the RECIST criteria (see below),
- quality of life, measured by the European Organisation for Research and Treatment of Cancer quality of life questionnaire (EORTC QLQ-C30)

Response rates were classified according to Response Evaluation Criteria In Solid Tumors (RECIST version 1.0) (Therasse 2000), where measurable target and non-target lesions were determined at baseline and evaluated during follow up. A complete response (CR) was defined as disappearance of full lesion, while partial response (PR) referred to a decrease of at least 30% of lesion and progressive disease (PD) an increase of at least 20% of the lesion. Those with insufficient changes to be categorized as either PR or PD were classified as stable disease (SD). CR and PR were used as outcomes in this review.

Search methods for identification of studies

We performed an updated search in January 2016, resulting in identification of an ongoing trial added to 'Studies awaiting classification'.

Electronic searches

Published or unpublished trials eligible for inclusion were identified by performing searches in the following databases:

- Cochrane Colorectal Cancer Group Specialized Register (December 2014);
- Cochrane Central Register of Controlled Trials (CENTRAL)(The Cochrane Library Issue 12, 2014) (Appendix 1);
- Ovid MEDLINE from 1950 to 8 December 2014 (Appendix 2)
- Ovid EMBASE from 1974 to 8 December 2014 (Appendix 3)
- Science Citation Index from 1900 to 8 December 2014 (Appendix 4)

In each database, both medical subject headings and free-text searching were performed in order to improve the sensitivity of the searches. All above databases were searched from the beginning of electronic records to the time at which the search was conducted and eligible studies in both English and non-English languages were identified without any publication date or publication status limitations.

Searching other resources

Published meta-analyses and relevant reviews, registers of controlled trials in progress (World Health Organization's International Clinical Trials Registry and ClinicalTrials.gov), references cited in relevant publications and conference proceedings in related fields were also searched (BioMed Central and Medscape's Conference). The key authors or investigators of all eligible studies, and professionals in the field were contacted if necessary in order to obtain other relevant information on the topic. In addition, bibliographies of identified trials and relevant references were hand-searched.

Data collection and analysis

Selection of studies

The title, abstract and keywords of every record from retrieved studies obtained by applying the above search strategies were checked independently against the inclusion criteria by two reviewers (AW and NY). All eligible studies were included irrespective of whether measured outcome data were reported on. Disagreements were resolved by a third reviewer (WW). Potentially eligible trials were retrieved in full for further assessment. Where more than one publication of a single trial existed, only the publication with the most complete data was included unless the relevant outcomes were only published in earlier versions.

Data extraction and management

Data was extracted from published papers independently by two reviewers (WW and NY). Any disagreement was resolved by a third reviewer (MVH). Data for overall survival and progression-free survival was extracted from the publications or estimated from survival curves where necessary. The following data of each study was requested: response rates (complete and partial), toxicity, the outcomes of quality life measurements, if any, the schedule and dosing of IRI or fluoropyrimidines, and baseline characteristics including age, sex, performance status, site of metastatic disease, whether or not patients had received previous adjuvant chemotherapy, site of primary tumor (rectum versus colon). If a study did not include one of the comparators of interest, only available results on the other interventions were included. The investigators of included studies were asked to supply updated data where possible.

Assessment of risk of bias in included studies

The methodological quality of the included studies was evaluated independently by two reviewers (WW and AW) with disagreements resolved by a third reviewer (MVH) according to the Cochrane Handbook. For each study, the following domains were assessed (Higgins 2011):

1. Selection bias: the generation of allocation schedule (truly random, quasi random, systematic) & concealment of treatment allocation.
2. Performance bias: blinding of study participants and personnel.
3. Detection bias: blinding of outcome assessors.
4. Attrition bias: completeness of follow-up, withdrawal and drop-out rates and whether analyses were performed by ITT.
5. Selective outcome reporting: evidence that outcome data have been reported based on the nature of the results.
6. Other biases, such as deviation from the study protocol in a way that does not reflect clinical practice.

The methods and procedures within each domain were judged as low, high or unclear risk of bias based on criteria specified in the Cochrane Risk of Bias tool (see Appendix 5)(Higgins 2011). Any disagreements were resolved by discussion between the reviewers. Investigators were contacted where this information could not be extracted from the publication.

Measures of treatment effect

The absolute effects of treatment at different time points were obtained from publication data or read from simple (non-stratified) Kaplan Meier curves of included trials. Median survivals and TTP (or PFS) were also estimated from Kaplan-Meier curves.

The information on survival and progress from each study was summarised as a log hazard ratio (HR). When HRs were not reported, observed (O) and the log-rank expected (E) number of events and variance (V) were calculated from the numbers of events and the numbers at risk at each time interval in published Kaplan-Meier survival curves (Parmar 1998; Tierney 2007). These numbers were used to estimate the HRs for all time intervals. When estimates from Cox regression were reported, the HRs were included in the analysis instead of those manually derived from the log-rank method (O-E/V). The general inverse variance method was used to obtain summary log HRs from combined studies.

All time to event analyses were performed by ITT.

Unit of analysis issues

For individual trials, the unit of analysis used was individual patients. For any eligible cluster RCTs, meta-analysis was conducted based on results from analysis that took into account clustering design. For studies in which control of clustering was not performed or reported, and individual patient data was not available, the intervention effects of cluster RCT were corrected by reducing the size of each trial to its 'effective sample size', which is the number of original sample size divided by the 'design effect'. The design effect were calculated as 1 + (M-1)* ICC, where M is the average cluster size and ICC is the intracluster correlation coefficient (Higgins 2011b).

Dealing with missing data

All principal investigators of the selected trials were contacted and asked to provide data that were missing or information which could not be extracted from the publication. Among five authors contacted, two immediately complied, another two no longer had any data at hand, one did not respond. Fortunately, most of the authors whose additional information was unavailable have provided detailed survival data on their published papers.

Assessment of heterogeneity

The studies were evaluated clinically and methodologically to assess if it was reasonable to consider combining data. Statistical heterogeneity was measured by the visual inspection of the forest plots and statistically through an assessment of homogeneity based on the Chi^2 test for which a p-value of less than 0.10 was considered an indication of substantial heterogeneity. The I^2 measurement was calculated as an indicator of the amount of statistical variation not attributable to sampling error. A value of more than 50% was considered to represent substantial heterogeneity. Where necessary, further investigations were undertaken to determine the source of the observed heterogeneity and in particular, whether there were any outlying studies driving this heterogeneity. Analyses were then conducted both with and without the outlying studies as part of a sensitivity analysis.

Assessment of reporting biases

Funnel plots were visually inspected to assess publication bias. The presence of publication bias was indicated by an asymmetrical distribution of data points derived from HR estimates and standard errors of log HRs from individual studies in relation to the pooled estimate effect.

Data synthesis

The statistical package Review Manager 5.3 (RevMan 5.3) provided by the Cochrane Collaboration was used for analysing data. For primary outcomes, pooled results on overall survival or progression-free survival were expressed as HRs with 95% confidence intervals (CI) by calculating the overall HRs and its variance across the trials. A random effects model was used to address potential statistical heterogeneity among included studies. All time-to-event analyses were performed by ITT.

For secondary outcomes, data on toxicity, response rates and quality of life, where available, were analysed as dichotomous data and the outcomes were reported as relative risks (RRs) with 95% CI. A Mantel-Haenszel test was employed to obtain pooled estimates across studies under a random effects model.

Subgroup analysis and investigation of heterogeneity

Where different routes of administration were used, studies were grouped according to whether fluoropyrimidines were administered orally or intravenously. A second subgroup analysis was performed according to the different settings (first- or second-line) under which individual trials were categorised. We also explored possible interactions between different methods of administration of 5-FU in combination with IRI (infusion versus bolus) in order to investigate possible sources of heterogeneity. The Chi^2 test for interaction was used to test for consistency of effects across these subsets of trials.

Sensitivity analysis

Sensitivity analyses were performed in order to assess the robustness of our results to heterogeneity, different assumptions or methodological approaches:

1. Removing studies at a high risk of bias in all domains assessed using the Cochrane Risk of Bias Tool

2. Exclusion of studies that used other agents (in both study arms) that may affect treatment effects of study regimen.

Summary of findings

We evaluated the quality of evidence of the two primary outcomes (Overall survival and Progression-free survival), and one secondary outcome (Toxicity) using the Grading of Recommendations Assessment, Development and Evaluation (GRADE) approach and presented it in 'Summary of Findings' tables.

The GRADE system classifies the quality of evidence in one of four grades:

1. High: Further research is very unlikely to change our confidence in the estimate of effect;
2. Moderate: Further research is likely to have an impact on our confidence in the estimate of effect and may change the estimate;
3. Low: Further research is very likely to have an important impact on our confidence on the estimate og effect and is likely to change the estimate; or
4. Very low: Any estimate of effect is very uncertain.

The quality of evidence were to be downgraded by one (serious concern) or two levels (very serious concern) for the following reasons: risk of bias, inconsistency (unexplained heterogeneity, inconsistency of results), indirectness (indirect population, intervention, control, outcomes) and imprecision (wide confidence intervald, single trial). The quality could also be upgraded by one level due to large summary effect.

RESULTS

Description of studies

Results of the search

We identified a total of 3,117 records through the electronic searches. After removing duplicates, a total of 2,006 records were left to be checked for eligibility, of which 1,997 studies were clearly irrelevant and thus excluded. The updated search in January 2016 resulted in one ongoing trial, which has been added to 'Studies awaiting classification' (Bendell 2014). We retrieved full text of the remaining 8 records for further assessment (Bécouarn 2001; Clarke 2011; Graeven 2007; Saltz 2000; Seymour 2007; Fiorentini 2012; Mitchell 2011; Popov 2006). We excluded 3 studies for reasons listed in the Characteristics of excluded studies. In total, 5 RCTs fulfilled the inclusion criteria (Bécouarn 2001, Clarke 2011, Graeven 2007,Saltz 2000, Seymour 2007). All included studies were individual trials and no relevant cluster RCTs were identified. The study flow diagram is shown in Figure 1.

Figure 1. Study flow diagram

Included studies

Five studies were included in this review, and details on IRI and fluoropyrimidine regimens are presented in Table 1. A total of 1,726 patients were randomised: 686 in the IRI-fluoropyrimidine combination group and 1,040 in the control group. Four of the studies administered IRI and the combination of IRI with fluoropyrimidine as a second-line treatment (Bécouarn 2001; Clarke 2011; Graeven 2007; Seymour 2007) and one study as a first-line treatment (Saltz 2000); all used 5-FU IV as the fluoropyrimidine of choice in the combination arm. No additional chemotherapeutic agents apart from LV in the 5-FU arm were used except in Bécouarn 2001, where oxaliplatin was administered in both treatment arms in addition to IRI and 5FU/LV. Seymour 2007 compared three strategies of sequential chemotherapy, where a second-line treatment with IRI was administered in the control group and the IRI and 5-FU combination was used as a second-line treatment in one of the intervention groups, both groups had previously been treated with 5-FU as the first-line drug of choice. Randomisation occurred prior to first-line treatments and therefore, the numbers of patients actually assigned to the combination IRI + 5-FU and IRI groups (185 and 356 patients, respectively) were lower than those at randomisation (365 and 710 patients, respectively). All randomised patients were included when combining results from time-to-event analyses. One study (Saltz 2000) administered three treatment arms: IRI alone, 5-FU/LV alone, and a combination of IRI and 5-FU-LV, but a comparison was only made between the latter two. ITT analyses were conducted in all studies.

Excluded studies

Among the remaining three studies from the search, two trials did not have randomized allocations of IRI regimens and thus were excluded (Mitchell 2011; Popov 2006). One study was excluded because it used intra-arterial administration of IRI-loaded drug-eluting beads (DEBIRI) instead of an IV or oral route (Fiorentini 2012).

Risk of bias in included studies

Risk of bias was assessed from the available information reported by the authors and summarised in the Characteristics of included studies section. This assessment is also presented as the risk of bias graph (Figure 2) and risk of bias summary (Figure 3). Randomisation technique was one of the main components of the assessment. All studies randomised their patients when allocating treatments. Except for Seymour 2007, randomisation took place prior to treatment with experimental and control regimens. Further details on risk of bias in included studies are as following.

Figure 2. Risk of bias graph: review authors' judgements about each risk of bias item presented as percentages across all included studies.

Figure 3. Risk of bias summary: review authors' judgements about each risk of bias item for each included study.

Allocation

The methods used for randomisation and allocation concealment were less explicit. Only two RCTs described the technique used for randomization, minimisation (Clarke 2011; Seymour 2007). Allocation concealment was only clear for one study (Clarke 2011), which conducted central randomisation by telephone, resulting in 20% of the studies to have shown low risk of selection bias based on allocation concealment and 40% based on randomisation methods (Figure 2).

Blinding

One trial was open label and therefore judged to have had high risk of bias (Saltz 2000). Blinding of personnel or study participants was not reported in any of other included studies. No mention of blinding of outcome assessors was made in any publication. Hence, 20% of all studies had high risk of bias from the lack of blinding (Figure 2).

Incomplete outcome data

A total of 15 patients withdrew from the studies Bécouarn 2001; Clarke 2011; Graeven 2007; Saltz 2000: 8 in the experimental group, 7 in the control group, and 2 had no mention of their allocated group. In Seymour 2007, 154 patients who failed first-line treatment with 5-FU did not receive the allocated combination of IRI + fluoropyrimidines and 302 did not receive allocated IRI as second-line treatment. Except for two patients withdrawing from the study in Graeven 2007 and one patient that refused the use of their data after withdrawing from the study in Clarke 2011, all patients were included in the analysis. No reason was reported for patient withdrawal in the Graeven 2007 study, hence we regarded this study to have unclear risk of attrition bias, Overall, this showed 80% of included trials to have low risk of attrition bias (Figure 2).

Selective reporting

Limited information on pre-specified outcomes was found when assessing reporting bias in individual studies, however, most studies reported both significant and insignificant findings in their publications. Figure 4 shows the funnel plot for results on OS. From visual inspection, all data points representing the estimates and precision of individual studies fell within the triangle comprising 95% confidence interval of the pooled effect estimate, with larger and more precise studies occupying the top of the inverted funnel and smaller and less precise studies more diversely scattered at the bottom. Most smaller and less precise studies (Bécouarn 2001; Graeven 2007) reported positive results. Although an assymetrical funnel plot was shown, interpretation is hampered given the small number of studies. Therefore, more studies are needed to determine a true reporting bias.

Figure 4. Funnel plot for comparisons of overall survival

Other potential sources of bias

No other potential sources of bias were identified from the studies and thus we assessed all studies (100%) to have low risk of other bias.

Effects of interventions

See: **Summary of findings for the main comparison** IRI with fluoropyrimidines versus single agent IRI for advanced and/or metastatic colorectal cancer

1. Primary outcomes

The primary outcomes of this review were Overall Survival (OS) and Progression-free Survival (PFS)

1.1 Overall survival

As seen in Table 1, median OS ranged between 9.5-15.4 months in the intervention arms across all studies, and between 10.7-13.9 months in the control arms. When comparing efficacy, subgroup analyses was performed according to the line of treatment, although only one study was found for the first-line treatment setting (Saltz 2000). For OS, analysis of both subgroups combined failed to show any statistically significant difference in overall mortality risk between the combination IRI + 5-FU regime and IRI monotherapy arms (Figure 5) (HR 0.91, with 95% CI of 0.81 to 1.02). No heterogeneity within and between subgroups was observed. Results were downgraded from high to low due to study limitations (Allocation concealment was only clear for one of the five studies, open-label intervention) and imprecision (Lack of sufficient number of samples may have reduced the statistical power of the analysis) (Summary of findings for the main comparison).

Figure 5. Overall survival.

1.2 Progression-free survival

Three studies provided data on PFS (Clarke 2011; Graeven 2007; Saltz 2000). An increase in progression-free survival was seen in the combination IRI + 5-FU arm overall, with a hazard ratio of 0.68 (95% CI: 0. 53-0.87). Overall, no substantial heterogeneity was found (I^2 = 13%), and the difference between subgroups failed to reach significance (p=0.13). Nevertheless, results may have been largely driven by the study with first-line setting (Saltz 2000), and the summary HR for second-line treatments showed no difference in risk of disease progression between the experimental and control group (Figure 6). This finding was downgraded from high to moderate due to study limitations (Allocation concealment was only clear for one of the five studies, open-label intervention) (Summary of findings for the main comparison).

Figure 6. Progression-free survival

2. Secondary outcomes

2.1 Response to treatment

Response rates to treatment in the two arms were compared, which included CR and PR as the outcome of interest. No difference was observed with all studies combined. Individually or second-line treatments by themselves (Figure 7), first-line treatment with the combination IRI + 5-FU chemotherapy were shown to result in higher response rates (RR for CR and PR: 2.18 (95% CI: 1.50-3.02)) compared to the controls. However, there was substantial heterogeneity overall (I^2 > 50%). We therefore performed a sensitivity analysis in which we excluded a study with an additional chemotherapeutic agent in both arms (Bécouarn 2001), which may have introduced bias. Re-running the random effects model with this study excluded eliminated the overall heterogeneity and yielded a summary RR of 1.77 (95% CI: 1.32-2.39; results not shown in figures), indicating better responses to treatment in the intervention arm compared to controls.

Figure 7. Response to treatment (CR + PR)

2.2 Toxicity

Toxicity profiles were reported in both first- and second-line treatments and combined, where information on individual toxicities was available. For grade 3/4 diarrhoea, a reduced overall risk was observed in the combination IRI + 5-FU arm (RR: 0.66 (95% CI: 0.48-0.91) compared to the controls (Figure 8). A similar risk reduction was seen for grade 1/2 alopecia (RR: 0.45 (95% CI: 0.28-0.74), while an increased risk of grade 3/4 neutropenia was observed in the experimental group (RR: 1.98 (95% CI: 1.48-2.67) compared to the IRI arm. No marked difference was seen for other toxicities including grade 3 or 4 mucositis, nausea, and vomiting, and neuropathy (Figure 9; Figure 10; Figure 11; Figure 12; Figure 13; Figure 14; Figure 15). For grade 1 or 2 alopecia and neuropathy, only estimates from 2 studies were available. However, a decision to pool the results was made based on similar treatment arms. No marked heterogeneity was found unless for analysis of grade 3 or 4 neutropenia (I^2: 48%). A sensitivity analysis for grade 3 or 4 neutropenia excluding a study by Bécouarn 2001, which included oxaliplatin in both treatment arms, revealed less heterogeneity without altering the findings (RR: 1.79 (95% CI: 1.49-2.28); I^2: 28%, results not shown in figures). Summary of findings table 2showed downgrading of evidence for toxicity outcomes grade 3/4 diarrhea to moderate due to study limitation, and grade 3/4 nausea to low due to study limitations and imprecision.

Figure 8. Grade 3/4 diarrhea

Figure 9. Grade 3/4 mucositis

Figure 10. Grade 3/4 nausea

Figure 11. Grade 3/4 vomiting

Figure 12. Grade 3/4 neutropenia

Figure 13. Febrile neutropenia

Figure 14. Grade 1/2 alopecia

Figure 15. Neuropathy

2.3 Quality of life

Quality of life was assessed in three studies (Clarke 2011; Saltz 2000; Seymour 2007). However, no detailed results were reported to enable a meta-analysis. Findings varied for comparisons of overall quality of life between the experimental and control arms. Saltz 2000 reported higher global health status for the combination IRI and 5-FU regimen, although these results were not statistically significant. On the contrary, Clarke 2011 showed a statistically significant lower overall quality of life with the combination chemotherapy. No benefit or disadvantage was observed between the two groups in Seymour 2007.

DISCUSSION

Summary of main results

Five studies fulfilled the inclusion criteria and were included in this review. High risk of bias due to the lack of blinding was seen with the Saltz 2000 study. Low risk of selection bias based on allocation concealment was shown in one study (Clarke 2011), whereas low risk based on randomisation techniques was seen in two studies (Clarke 2011; Seymour 2007). There was a lack of sufficient information to fully assess other sources of bias. Overall, no OS benefit was seen by combining IRI with fluoropyrimidine for treating advanced or metastatic CRC compared to using IRI alone. Longer PFS and higher response rates were seen in the combination IRI + 5-FU arms. However, these results may have been driven by the single first-line treatment study, and for treatment response rates there was substantial heterogeneity. Toxicity profiles were different, with higher risks of grade 3 or 4 diarrhoea and grade 1 or 2 alopecia and a lower risk of grade 3 or 4 neutropenia in the control group compared to the combination arm. No conclusive results were available for quality of life.

Overall completeness and applicability of evidence

Overall, our findings indicate no clinical advantage of the combination of IRI and fluoropyrimidine treatment over IRI alone for patients with advanced or metastatic CRC, but our results were limited by the number of studies available for each treatment line. The significant heterogeneity between first- and second- line groups indicate that results may only be interpreted with respect to treatment settings.

Quality of the evidence

The quality of evidence in this review was classified as low and moderate (Summary of findings for the main comparison). This was mostly due to high risk of bias assessed through the meta-analysis and imprecision of results due to a lack of statistical power. When substantial heterogeneity was found such as in the assessment of response rates, lthough it was likely that the line of treatment is the major determinant of this heterogeneity, the plausible mechanism underlying the different effects on survival with respect to treatment setting is unclear. It is possible that treatment setting is a proxy of other prognostic factors in advanced or metastatic CRC, and therefore the observed heterogeneity reflects the difference in population characteristics rather than the interventions. Additionally, the small numbers of participants and a lack of studies with first-line settings as mentioned above may indicate the necessity of confirming our findings through larger clinical studies sufficiently addressing each line of treatment.

Potential biases in the review process

The inclusion of randomised studies comprising first- and second-line treatments strengthened this current review. However, even though similar drugs and routes of administration were used in all the included studies, there was variation in dosage and timings that may have affected the overall findings. Nevertheless, several studies suggested similar efficacy in treating advanced and metastatic CRC across IRI-based regimens with different intervals of IRI administration (Aranda 2009; Bouzid 2003), although further investigations are needed to delineate the impact of administration routes and other agents in combination with IRI. Additionally, only 5-FU-based regimens represented the fluoropyrimidine arm in this review. As differences in clinical outcomes have been reported with different fluoropyrimidine agents in IRI-based regimens (Fuchs 2007), this may limit the generalisability of our findings.

In the study conducted by Seymour and colleagues (Seymour 2007), a sequential strategy was employed in which allocation to both first- and second-line chemotherapy was performed at the start of the study. Patient eligibility was assessed prior to first-line of treatment and this may have explained the high proportions of patients who did not receive the allocated second-line treatments after failure in the first-line setting. Insufficient patients may also have limited the results of this review, since a number of analyses had hazard ratios with wide CI. However, this is not likely the case for OS since a consistency between subgroups with first- and second-line treatments was observed. For PFS and response rates, the benefit in the combination group was affected by inclusion of the first-line treatment setting study (Saltz 2000). Since marked heterogeneity between subgroups was found, this signified the importance of conducting subgroup analyses based on first- or second-line treatments. Such individualised interpretation may also be more useful when translating these findings to clinical context. Through the sensitivity analyses, we observed that including studies with an additional agent in both arms (oxaliplatin in this case) (Bécouarn 2001) increased heterogeneity in the final analyses. The different associations observed in presence of common additional agents, i.e. oxaliplatin, suggest that great care should be made when designing studies and choosing statistical methods to compare IRI with and without fluoropyrimidine where additional chemotherapeutic or biological agents are used. Finally, the fact that one ongoing study from the additional search have not yet been incorporated may be a source of potential bias.

Agreements and disagreements with other studies or reviews

A similar review was published in 2011, focusing on the use of IRI and 5-FU compared to IRI alone as a second-line treatment for advanced or metastatic CRC (Clarke 2011), which included three studies that were also selected here (Clarke 2011; Graeven 2007; Seymour 2007). In this previous review, there was no significant benefit or disadvantage in OS or PFS by adding 5-FU to IRI, which was similar to what we found for the second-line treatment setting. In the current review, comparisons of toxicities were performed only for studies providing toxicity profiles of both experimental and control arms in both first- and second-line treatments instead of combining results from single-arm trials. Interestingly, for grade 3 or 4 diarrhea and grade 1 or 2 alopecia, the findings presented here were similar to that obtained from the single-arm studies in Clarke 2011, with higher risks observed in the single IRI arm. We also observed an increased risk of grade 3 or 4 neutropenia in the experimental arm. This may occur because neutropenia is a well-known adverse effect of both IRI and 5-FU. o Nevertheless, no difference in febrile neutropenia was observed between treatment arms.

AUTHORS' CONCLUSIONS

Implications for practice

Given available data from clinical trials and large heterogeneity in reported findings, there is no evidence to suggest any superiority in OS of the combination of IRI and fluoropyrimidine over IRI alone. Patients in the combination arm were shown to have longer PFS, but the moderate quality of the evidence indicates the necessity to confirm findings from this review in clinical studies with adequate sample size to address potential subgroup effects. Risks of grade 3 or 4 diarrhea and grade 1 or 2 alopecia were higher in the intervention arm compared to in controls, whereas the risk of grade 3 or 4 neutropenia was higher in the control group. These different toxicity profiles indicate the need for further consideration when selecting a suitable treatment based on individual characteristics of the patients at baseline.

Implications for research

Despite the emergence of targeted therapies, IRI and fluoropyrimidine remain an important components of the regimens used in treating advanced and metastatic CRC. Therefore, more clinical trials with sufficient numbers of patients in each line of treatment are needed to confirm any benefit seen with regimens containing the combination of IRI and fluoropyrimidine for CRC treatment compared to those containing IRI alone. It would be of interest for trialists to assess both regimens in combination with more recent biological agents, and include other administration routes, in order to achieve optimal clinical benefits. The ongoing study in 'Studies awaiting classification' may alter the conclusions of the review once results are available and incorporated.This also calls for designs of RCT protocols that allow for an unbiased comparison between groups of patients receiving IRI with and without the addition of fluoropyrimidine.

ACKNOWLEDGEMENTS

The authors wish to thank the Managing Editor, Trial Search Coordinator and the editorial team from the Cochrane Colorectal Cancer Group for the support and advice provided throughout the preparation of this review.

REFERENCES

References to studies included in this review

Bécouarn 2001 *{published data only}*

Bécouarn Y, Gamelin E, Coudert B, Ne´grier S, Pierga JY, Raoul JL, et al. Randomized multicenter phase II study comparing a combination of fluorouracil and folinic acid and alternating irinotecan and oxaliplatin with oxaliplatin and irinotecan in fluorouracil-pretreated metastatic colorectal cancer patients. *Journal of Clinical Oncology* 2001;**19**(22):4195-201.

Clarke 2011 *{published data only}*

Clarke SJ, Yip S, Brown C, van Hazel GA, Ransom DT, Goldstein D, et al. Single-agent irinotecan or FOLFIRI as second-line chemotherapy for advanced colorectal cancer; results of a randomised phase II study (DaVINCI) and meta-analysis [corrected]. *European Journal of Cancer* 2011;**47**(12):1826-36.

Graeven 2007 *{published data only}*

Graeven U, Arnold D, Reinacher-Schick A, Heuer T, Nusch A, Porschen R, et al. A randomised phase II study of irinotecan in combination with 5-FU/FA compared with irinotecan alone as second-line treatment of patients with metastatic colorectal carcinoma. *Onkologie* 2007;**30**(4):169-74.

Saltz 2000 *{published data only}*

Saltz LB, Cox JV, Blanke C, Rosen LS, Fehrenbacher L, Moore MJ, et al. Irinotecan plus fluorouracil and leucovorin for metastatic colorectal cancer. Irinotecan Study Group. *New England Journal of Medicine* 2000;**343**(13):905-14.

Seymour 2007 *{published data only}*

Seymour MT, Maughan TS, Ledermann JA, Topham C, James R, Gwyther SJ, et al. Different strategies of sequential and combination chemotherapy for patients with poor prognosis advanced colorectal cancer (MRC FOCUS): a randomised controlled trial. *Lancet* 2007;**30**(9582):143-52.

References to studies excluded from this review

Fiorentini 2012 *{published data only}*

Fiorentini G, Aliberti C, Tilli M, Mulazzani L, Graziano F, Giordani P, et al. Intra-arterial infusion of irinotecan-loaded drug-eluting beads (DEBIRI) versus intravenous therapy (FOLFIRI) for hepatic metastases from colorectal cancer: final results of a phase III study. *Anticancer Research* 2013;**33**(11):5211.

Mitchell 2011 *{published data only}*

Mitchell EP, Piperdi B, Lacouture ME, Shearer H, Iannotti N, Pillai MV, et al. The efficacy and safety of panitumumab administered concomitantly with FOLFIRI or Irinotecan in second-linetherapy for metastatic colorectal cancer: the secondary analysis from STEPP (Skin Toxicity Evaluation ProtocolWith Panitumumab) by KRAS status. *Clinical Colorectal Cancer* 2011;**10**(4):333-9.

Popov 2006 *{published data only}*

Popov I, Jelic S, Krivokapic Z, Micev M, Babic D, Zdrale Z. What is the best sequence of chemotherapy in advanced colorectal cancer? Final results of a five-arm study. *Chemotherapy* 2006;**52**:20–2.

References to studies awaiting assessment

Bendell 2014 *{published data only}*

Bendell JC, Tan BR, Reeves JA, Xiong HQ, Laeufle R, Byrtek M, et al. STEAM: A randomized, open-label, phase 2 trial of sequential and concurrent FOLFOXIRI-bevacizumab (BEV) versus FOLFOX-BEV for the first-line (1L) treatment (tx) of patients (pts) with metastatic colorectal cancer (mCRC).. *Journal of Clinical Oncology* 2014;**32:5s**:suppl; abstr TPS3652.

Additional references

ACCMAP 1992

Advanced Colorectal Cancer Meta-Analysis Project. Modulation of fluorouracil by leucovorin in patients with advanced colorectal cancer: evidence in terms of response rate. *Journal of Clinical Oncology* 1992;**10**(6):896-903.

Aranda 2009

Aranda E, Valladares M, Martinez-Villacampa M, Benavides M, Gomez A, Massutti B, et al. Randomized study of weekly irinotecan plus high-dose 5-fluorouracil (FUIRI) versus biweekly irinotecan plus 5-fluorouracil/leucovorin (FOLFIRI) as first-line chemotherapy for patients with metastatic colorectal cancer: a Spanish Cooperative Group for the Treatment of Digestive Tumors Study. *Annals of Oncology* 2009;**20**(2):251-7.

Bouzid 2003

Bouzid K, Khalfallah S, Tujakowski J, Piko B, Purkalne G, Plate S, et al. A randomized phase II trial of irinotecan in combination with infusional or two different bolus 5-fluorouracil and folinic acid regimens as first-line therapy for advanced colorectal cancer. *Annals of Oncology* 2003;**14**(7):1106-14.

Cao 2000

Cao S, Rustum YM. Synergistic antitumor activity of irinotecan in combination with 5-fluorouracil in rats bearing advanced colorectal cancer: role of drug sequence and dose. *Cancer Research* 2000;**60**(14):3717-21.

Center 2009

Center MM, Jemal A, Smith RA, Ward E. Worldwide variations in colorectal cancer. *CA: a cancer journal for clinicians* 2009;**59**(6):366-78.

Chau 2005

Chau I, Norman AR, Cunningham D, Iveson T, Hill M, Hickish T, et al. Longitudinal quality of life and quality adjusted survival in a randomised controlled trial comparing six months of bolus fluorouracil/leucovorin vs twelve weeks of protracted venous infusion fluorouracil as adjuvant chemotherapy for colorectal cancer. *European Journal of Cancer* 2005;**41**(11):1551-9.

Colucci 2005

Colucci G, Gebbia V, Paoletti G, Giuliani F, Caruso M, Gebbia N, Gruppo Oncologico Dell'Italia Meridionale. Phase III randomized trial of FOLFIRI versus FOLFOX4 in the treatment of advanced colorectal cancer: a multicenter study of the Gruppo Oncologico Dell'Italia. *Journal of Clinical Oncology* 2005;**23**:4866-75.

Conti 1996

Conti JA, Kemeny NE, Saltz LB, Huang Y, Tong WP, Chou TC, et al. Irinotecan is an active agent in untreated patients with metastatic colorectal cancer. *Journal of Clinical Oncology* 1996;**14**(3):709-15.

Cunningham 1998

Cunningham D, Pyrhonen S, James RD, Punt CJ, Hickish TF, Heikkila R, et al. Randomised trial of irinotecan plus supportive care versus supportive care alone after fluorouracil failure for patients with metastatic colorectal cancer. *Lancet* 1998;**352**(9138):1413-8. [PUBMED: 9807987]

Douillard 2000

Douillard JY, Cunningham D, Roth AD, Navarro M, James RD, Karasek P, et al. Irinotecan combined with fluorouracil compared with fluorouracil alone as first-line treatment for metastatic colorectal cancer: a multicentre randomised trial. *Lancet* 2000;**355**(9209):1041-7.

Ferlay 2010

Ferlay J, Shin HR, Bray F, Forman D, Mathers C, Parkin DM. Estimates of worldwide burden of cancer in 2008: GLOBOCAN 2008. *International Journal of Cancer* 2010;**127**(12):2893-917.

Folprecht 2008

Folprecht G, Seymour MT, Saltz L, Douillard JY, Hecker H, Stephens RJ, et al. Irinotecan/fluorouracil combination in first-line therapy of older and younger patients with metastatic colorectal cancer: combined analysis of 2,691 patients in randomized controlled trials. *Journal of Clinical Oncology* 2008;**26**(9):1443-51.

Fuchs 2007

Fuchs CS, Marshall J, Mitchell E, Wierzbicki R, Ganju V, Jeffery M, et al. Randomized, controlled trial of irinotecan plus infusional, bolus, or oral fluoropyrimidines in first-line treatment of metastatic colorectal cancer: results from the BICC-C Study. *Journal of Clinical Oncology* 2007;**25**(30):4779-86.

Giessen 2011

Giessen C, von Weikersthal LF, Hinke A, Stintzing S, Kullmann F, Vehling-Kaiser U, et al. A randomized, phase III trial of capecitabine plus bevacizumab (Cape-Bev) versus capecitabine plus irinotecan plus bevacizumab (CAPIRI-Bev) in first-line treatment of metastatic colorectal cancer: the AIO KRK 0110 trial/ML22011 trial. *BMC cancer* 2011;**11**:367.

Higgins 2011

Higgins JPT, Altman DG, Gøtzsche PC, Jüni P, Moher D, Oxman AD, Cochrane Bias Methods Group. The Cochrane Collaboration's tool for assessing risk of bias in randomised trials. *British Medical Journal* 2011;**343**:d5928.

Higgins 2011b

Higgins JPT, Green S. Cochrane Handbook for Systematic Reviews of Interventions Version 5.1.0. The Cochrane Collaboration, March 2011.

Hsiang 1985

Hsiang YH, Hertzberg R, Hecht S, Liu LF. Camptothecin induces protein-linked DNA breaks via mammalian DNA topoisomerase I. *Journal of Biological Chemistry* 1985;**260**(27):14873-8.

Jemal 2011

Jemal A, Bray F, Center MM, Ferlay J, Ward E, Forman D. Global cancer statistics. *CA: a cancer journal for clinicians* 2011;**61**(2):69-90.

Kuhry 2008

Kuhry E, Schwenk W, Gaupset R, Romild U, Bonjer J. Long-term outcome of laparoscopic surgery for colorectal cancer: a cochrane systematic review of randomised controlled trials. *Cancer Treatment Reviews* 2008;**34**(6):498-504.

Maiello 2000

Maiello E, Gebbia V, Giuliani F, Paoletti G, Gebbia N, Cigolari S, et al. 5-Fluorouracil and folinic acid with or without CPT-11 in advanced colorectal cancer patients: a multicenter randomised phase II study of the Southern Italy Oncology Group. *Annals of Oncology* 2000;**11**(8):1045-51.

Maiello 2005

Maiello E, Gebbia V, Giuliani F, Paoletti G, Gebbia N, Borsellino N, et al. FOLFIRI regimen in advanced colorectal cancer: the experience of the Gruppo Oncologico dell'Italia Meridionale (GOIM). *Annals of Oncology: Official Journal of the European Society for Medical Oncology / ESMO* 2005;**16 Suppl 4**:iv56-60.

Montagnani 2010

Montagnani F, Chiriatti A, Licitra S, Aliberti C, Fiorentini G. Differences in efficacy and safety between capecitabine and infusional 5-fluorouracil when combined with irinotecan for the treatment of metastatic colorectal cancer. *Clinical Colorectal Cancer* 2010;**9**(4):243-7.

Muro 2010

Muro K, Boku N, Shimada Y, Tsuji A, Sameshima S, Baba H, et al. Irinotecan plus S-1 (IRIS) versus fluorouracil and folinic acid plus irinotecan (FOLFIRI) as second-line chemotherapy for metastatic colorectal cancer: a randomised phase 2/3 non-inferiority study (FIRIS study). *The Lancet Oncology* 2010;**11**(9):853-60.

Parmar 1998

Parmar MK, Torri V, Stewart L. Extracting summary statistics to perform meta-analyses of the published literature for survival endpoints. *Statistics in Medicine* 1998;**17**(24):2815-34. [PUBMED: 9921604]

Petrelli 2012

Petrelli F, Cabiddu M, Barni S. 5-Fluorouracil or capecitabine in the treatment of advanced colorectal cancer: a pooled-analysis of randomized trials. *Medical Oncology* 2012;**29**(2):1020-9.

Pitot 1997

Pitot HC, Wender DB, O'Connell MJ, Schroeder G, Goldberg RM, Rubin J, et al. Phase II trial of irinotecan in patients with metastatic colorectal carcinoma. *Journal of Clinical Oncology* 1997;**15**(8):2910-9.

Ragnhammar 2001

Ragnhammar P, Hafström L, Nygren P, Glimelius B. A systematic overview of chemotherapy effects in colorectal cancer. *Acta Oncologica* 2001;**40**(2-3):282-308.

Rothenberg 1999

Rothenberg ML, Cox JV, DeVore RF, Hainsworth JD, Pazdur R, Rivkin SE, et al. A multicenter, phase II trial of weekly irinotecan (CPT-11) in patients with previously treated colorectal carcinoma. *Cancer* 1999;**85**(4):786-95.

Rougier 1997

Rougier P, Bugat R, Douillard JY, Culine S, Suc E, Brunet P, et al. Phase II study of irinotecan in the treatment of advanced colorectal cancer in chemotherapy-naive patients and patients pretreated with fluorouracil-based chemotherapy. *Journal of Clinical Oncology* 1997;**15**(1):251-60.

Rougier 1998

Rougier P, Van Cutsem E, Bajetta E, Niederle N, Possinger K, Labianca R, et al. Randomised trial of irinotecan versus fluorouracil by continuous infusion after fluorouracil failure in patients with metastatic colorectal cancer. *Lancet* 1998;**352**(9138):1407-12.

Siegel 2013

Siegel R, Naishadham D, Jemal A. Cancer statistics, 2013. *CA: A Cancer Journal for Clinicians* 2013;**63**(1):11-30.

Siegel 2014

Siegel R, DeSantis S, Jemal A. Colorectal Cancer Statistics, 2014. *CA: A Cancer Journal for Clinicians* 2014;**64**:104-17.

Simmonds 2000

Simmonds PC. Palliative chemotherapy for advanced colorectal cancer: systematic review and meta-analysis. Colorectal Cancer Collaborative Group. *British Medical Journal* 2000;**321**(7260):531-5.

Therasse 2000

Therasse P, Arbuck SG, Eisenhauer EA, Wanders J, Kaplan RS, Rubinstein L, et al. New guidelines to evaluate the response to treatment in solid tumors. European Organization for Research and Treatment of Cancer, National Cancer Institute of the United States, National Cancer Institute of Canada. *Journal of the National Cancer Institute* 2000;**92**(3):205-16.

Thirion 2004

Thirion P, Michiels S, Pignon JP, Buyse M, Braud AC, Carlson RW, et al. Modulation of fluorouracil by leucovorin in patients with advanced colorectal cancer: an updated meta-analysis. *Journal of Clinical Oncology* 2004;**22**(18):3766-75.

Tierney 2007

Tierney JF, Stewart LA, Ghersi D, Burdett S, Sydes MR. Practical methods for incorporating summary time-to-event data into meta-analysis. *Trials* 2007;**8**:16. [PUBMED: 17555582]

Tournigand 2004

Tournigand C, André T, Achille E, Lledo G, Flesh M, Mery-Mignard D, et al. FOLFIRI followed by FOLFOX6 or the reverse sequence in advanced colorectal cancer: a randomized GERCOR study. *Journal of Clinical Oncology* 2004;**22**:229-37.

Van Cutsem 2004

Van Cutsem E, Hoff PM, Harper P, Bukowski RM, Cunningham D, Dufour P, et al. Oral capecitabine vs intravenous 5-fluorouracil and leucovorin: integrated efficacy data and novel analyses from two large, randomised, phase III trials. *British Journal of Cancer* 2004;**90**(6):1190-7.

Van Cutsem 2014

Van Cutsem E, Cervantes A, Nordlinger B, Arnold D, on behalf of the ESMO Guidelines Working Group. Metastatic colorectal cancer: ESMO Clinical Practice Guidelines for diagnosis, treatment and follow-up. *Annals of Oncology* 2014;**25 (Supplement 3)**:iii1–iii9.

CHARACTERISTICS OF STUDIES

Characteristics of included studies *[ordered by study ID]*

Bécouarn 2001

Methods	Randomized controlled trial Phase II, multicenter
Participants	CRC with progressive disease after no more than one regimen of optimal 5-FU FA-based chemotherapy for metastatic disease and/or no more than one line of 5-FU–containing treatment after prior adjuvant chemotherapy if discontinued less than 6 months
Interventions	IRI + 5-FU/LV + oxaliplatin vs IRI + oxaliplatin
Outcomes	Overall survival

Bécouarn 2001 *(Continued)*

	Progression-free survival
	Toxicity
Notes	Oxaliplatin IV was administered in both treatment arms
	IR + oxaliplatin had longer survivals and better toxicity profile

Risk of bias

Bias	Authors' judgement	Support for judgement
Random sequence generation (selection bias)	Unclear risk	No mention of how randomization sequence was generated
Allocation concealment (selection bias)	Unclear risk	No mention of any allocation concealment
Blinding of participants and personnel (performance bias) All outcomes	Unclear risk	No mention of blinding of participants and personnel
Blinding of outcome assessment (detection bias) All outcomes	Unclear risk	No mention of blinding of outcome assessment
Incomplete outcome data (attrition bias) All outcomes	Low risk	Two patients in the control arm did not received any treatment due to a move to a nonparticipating study site in one case and worsening of general status in the other. However they were included in the analysis.
Selective reporting (reporting bias)	Unclear risk	No reported pre-specified outcomes
Other bias	Low risk	None

Clarke 2011

Methods	Randomized controlled trial
	Phase II, multicenter
Participants	Incurable locally advanced or metastatic CRC, progressive disease after one prior chemotherapy regimen for advanced disease and/or after prior adjuvant therapy, provided that relapse had occurred within 6 months of that treatment
Interventions	IRI + 5-FU/LV vs IRI
Outcomes	Overall survival
	Progression-free survival
	Toxicity
Notes	Trial was terminated due to slow recruitment.

Clarke 2011 *(Continued)*

	Similar efficacy between the two arms but IRI + 5-FU/LV had slightly less toxicities

Risk of bias

Bias	Authors' judgement	Support for judgement
Random sequence generation (selection bias)	Low risk	Minimisation
Allocation concealment (selection bias)	Low risk	Central randomization/allocation by telephone
Blinding of participants and personnel (performance bias) All outcomes	Unclear risk	No mention of blinding of participants and personnel
Blinding of outcome assessment (detection bias) All outcomes	Unclear risk	No mention of blinding of outcome assessment
Incomplete outcome data (attrition bias) All outcomes	Low risk	Four patients withdrew early (2 in the intervention and 2 in the control arm). Three withdrew before baseline tumour assessment and did not receive any treatment. The fourth one opted 3 days after consent to receive off-study irinotecan and cetuximab. These patients were included in the analysis, except one who explicitly refused.
Selective reporting (reporting bias)	Unclear risk	No reported pre-specified outcomes
Other bias	Low risk	None

Graeven 2007

Methods	Randomized controlled trial Phase II, multicenter
Participants	Metastatic CRC after failure of a first-line chemotherapy, pretreatment was to consist of either 5-FU/LV, capecitabine or 5-FU/LV in combination with oxaliplatin, whereas irinotecan-containing regimens were not allowed
Interventions	IRI + 5-FU/LV vs IRI
Outcomes	Overall survival Progression-free survival Toxicity
Notes	No marked difference was observed between the two groups.

Risk of bias

Bias	Authors' judgement	Support for judgement

Graeven 2007 *(Continued)*

Random sequence generation (selection bias)	Unclear risk	No mention of how randomization sequence was generated
Allocation concealment (selection bias)	Unclear risk	No mention of any allocation concealment
Blinding of participants and personnel (performance bias) All outcomes	Unclear risk	No mention of blinding of participants and personnel
Blinding of outcome assessment (detection bias) All outcomes	Unclear risk	No mention of blinding of outcome assessment
Incomplete outcome data (attrition bias) All outcomes	Unclear risk	Two patients were withdrawn prior to the first administration, but reasons for this were not reported and there was no mention of which treatment arm they were randomized to. Both patients were not included in the analysis.
Selective reporting (reporting bias)	Unclear risk	No reported pre-specified outcomes
Other bias	Low risk	None

Saltz 2000

Methods	Randomized controlled trial Phase III, multicenter
Participants	Metastatic CRC, no prior therapy for metastatic disease; patients who had received adjuvant 5-FU-based therapy were eligible if they had remained free of disease for at least one year after the completion of adjuvant therapy
Interventions	IRI + 5-FU/LV vs IRI
Outcomes	Overall survival Progression-free survival Toxicity
Notes	The study had another treatment arm with 5-FU/LV alone. IRI + 5-FU/LV was superior to FU/LV alone but not directly compared with IRI

Risk of bias

Bias	**Authors' judgement**	**Support for judgement**
Random sequence generation (selection bias)	Unclear risk	No mention of how randomization sequence was generated
Allocation concealment (selection bias)	Unclear risk	No mention of any allocation concealment

Saltz 2000 *(Continued)*

Blinding of participants and personnel (performance bias) All outcomes	High risk	Open-label, thus no blinding of participants and personnel was performed
Blinding of outcome assessment (detection bias) All outcomes	Unclear risk	No mention of blinding of outcome assessment
Incomplete outcome data (attrition bias) All outcomes	Low risk	Six patients in the intervention group and three patients in the control arm either did not receive any treatment or received the wrong treatment. However, they were included in the analysis.
Selective reporting (reporting bias)	Unclear risk	No reported pre-specified outcomes
Other bias	Low risk	None

Seymour 2007

Methods	Randomized controlled trial
Participants	Inoperable metastatic or locoregional CRC
Interventions	IRI + 5-FU/LV vs IRI
Outcomes	Overall survival Progression-free survival Toxicity
Notes	The intervention arms were part of sequential treatments with three strategies. Two among these administered 5-FU as the first-line treatment, followed by a second-line treatment with IRI in the control group and either IRI + 5-FU or oxaliplatin in the intervention group. The third strategy used the combination of IRI or oxaliplatin with 5-FU as the first-line treatment.

Risk of bias

Bias	**Authors' judgement**	**Support for judgement**
Random sequence generation (selection bias)	Low risk	Minimisation
Allocation concealment (selection bias)	Unclear risk	No mention of any allocation concealment
Blinding of participants and personnel (performance bias) All outcomes	Unclear risk	No mention of blinding of participants and personnel
Blinding of outcome assessment (detection bias) All outcomes	Unclear risk	No mention of blinding of outcome assessment

Seymour 2007 *(Continued)*

Incomplete outcome data (attrition bias) All outcomes	Low risk	Among 339 patients in the intervention group who failed first-line treatment, 110 died or progressed to terminal care prior to administration and 44 received alternative second-line regimen. Among 666 patients in the control group who failed first-line treatment, 251 died or progressed to terminal care prior to administration and 51 received alternative second-line regimen. However, these patients were included in the analysis.
Selective reporting (reporting bias)	Unclear risk	No reported pre-specified outcomes
Other bias	Low risk	None

Characteristics of excluded studies *[ordered by study ID]*

Study	Reason for exclusion
Fiorentini 2012	IRI was not administered via an IV or oral route
Mitchell 2011	Assignments to IRI or IRI + 5-FU were not randomized
Popov 2006	Assignments to IRI or IRI + 5-FU were not randomized

Characteristics of studies awaiting assessment *[ordered by study ID]*

Bendell 2014

Methods	Open label RCT / three arm study
Participants	280 adult patients (both gender), aged 18-75, with a histologically confirmed colorectal cancer with at least on measurable metastatic lesion.
Interventions	Exp A – FOLFOXFIRI + Bevacizumab; Exp B – sequential FOLFOXFIRI + Bevacizumab; Exp C – FOLFOX + Bevacizumab
Outcomes	Primary – Overall response rate (ORR1); and progression-free survival (PFS1) during first line therapy. Secondary – Overall response rate during second line therapy (ORR2); progression-free survival during second line therapy (PFS2); Time to PFS2; Overall survival (OS); Liver resection rate; Rates of conversion from unresectable to resectable disease; Adverse events.
Notes	The study is ongoing but not recruiting. Estimated primary completion December 2016.

DATA AND ANALYSES

Comparison 1. Overall Survival

Outcome or subgroup title	No. of studies	No. of participants	Statistical method	Effect size
1 Overall survival	5	1728	Hazard Ratio (Random, 95% CI)	0.91 [0.81, 1.02]
1.1 First-line treatments	1	457	Hazard Ratio (Random, 95% CI)	0.88 [0.69, 1.12]
1.2 Second-line treatments	4	1271	Hazard Ratio (Random, 95% CI)	0.92 [0.75, 1.14]
2 Overall survival	5	1728	Hazard Ratio (95% CI)	0.88 [0.75, 1.05]

Analysis 1.1. Comparison 1 Overall Survival, Outcome 1 Overall survival.

Study or subgroup	IRI + 5-FU N	IRI N	log[Hazard Ratio] (SE)	Hazard Ratio IV, Random, 95% CI	Weight	Hazard Ratio IV, Random, 95% CI
1.1.1 First-line treatments						
Saltz 2000	231	226	-0.1 (0.124)		22.49%	0.88[0.69,1.12]
Subtotal (95% CI)					**22.49%**	**0.88[0.69,1.12]**
Heterogeneity: Not applicable						
Test for overall effect: Z=1.03(P=0.3)						
1.1.2 Second-line treatments						
Bécouarn 2001	32	30	0.5 (0.508)		1.34%	1.65[0.61,4.46]
Clarke 2011	44	44	-0.3 (0.229)		6.63%	0.72[0.46,1.13]
Graeven 2007	28	27	0.3 (0.335)		3.1%	1.31[0.68,2.52]
Seymour 2007	356	710	-0.1 (0.072)		66.44%	0.91[0.79,1.05]
Subtotal (95% CI)					**77.51%**	**0.92[0.75,1.14]**
Heterogeneity: Tau^2=0.01; Chi^2=3.6, df=3(P=0.31); I^2=16.77%						
Test for overall effect: Z=0.75(P=0.45)						
Total (95% CI)					**100%**	**0.91[0.81,1.02]**
Heterogeneity: Tau^2=0; Chi^2=3.68, df=4(P=0.45); I^2=0%						
Test for overall effect: Z=1.67(P=0.1)						
Test for subgroup differences: Chi^2=0.09, df=1 (P=0.76), I^2=0%						

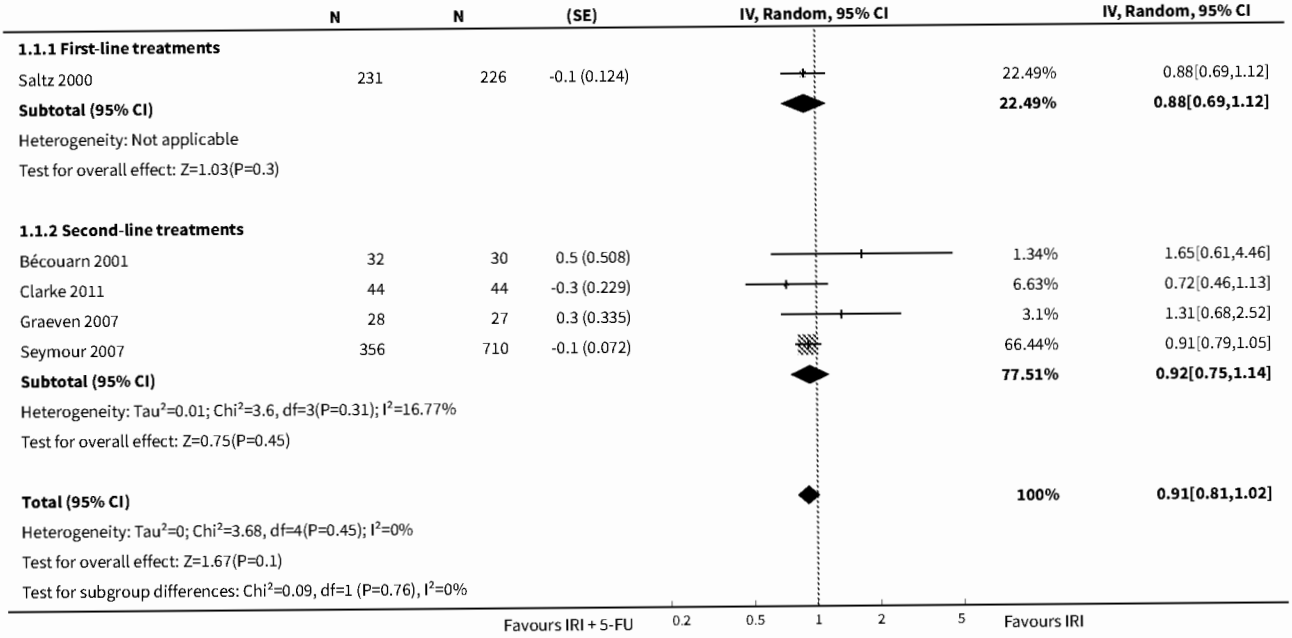

Analysis 1.2. Comparison 1 Overall Survival, Outcome 2 Overall survival.

Study or subgroup	IRI + 5-FU n/N	IRI n/N	Hazard Ratio 95% CI	Weight	Hazard Ratio 95% CI
Clarke 2011	18/44	26/44		5.7%	0.67[0.33,1.36]
Saltz 2000	102/231	116/226		29.34%	0.84[0.61,1.14]
Seymour 2007	149/356	313/710		58.06%	0.89[0.71,1.11]
Graeven 2007	21/28	20/27		3.97%	1.13[0.48,2.64]
Bécouarn 2001	19/32	14/30		2.93%	1.65[0.61,4.45]

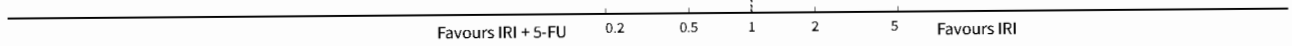

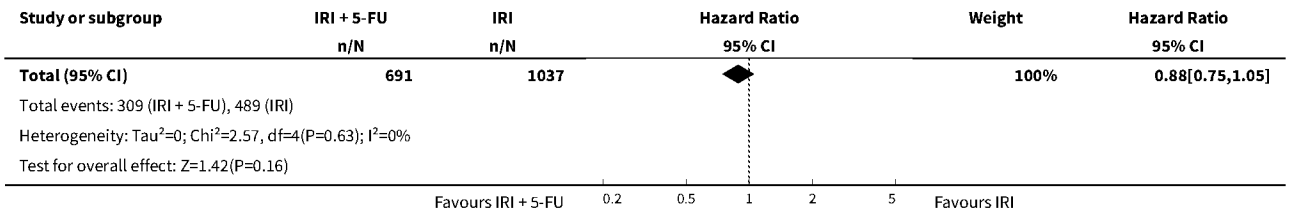

Comparison 2. Progression-Free Survival

Outcome or subgroup title	No. of studies	No. of participants	Statistical method	Effect size
1 Progression-free survival	3	600	Hazard Ratio (Random, 95% CI)	0.68 [0.53, 0.87]
1.1 First-line treatments	1	457	Hazard Ratio (Random, 95% CI)	0.59 [0.45, 0.77]
1.2 Second-line treatments	2	143	Hazard Ratio (Random, 95% CI)	0.83 [0.58, 1.19]

Analysis 2.1. Comparison 2 Progression-Free Survival, Outcome 1 Progression-free survival.

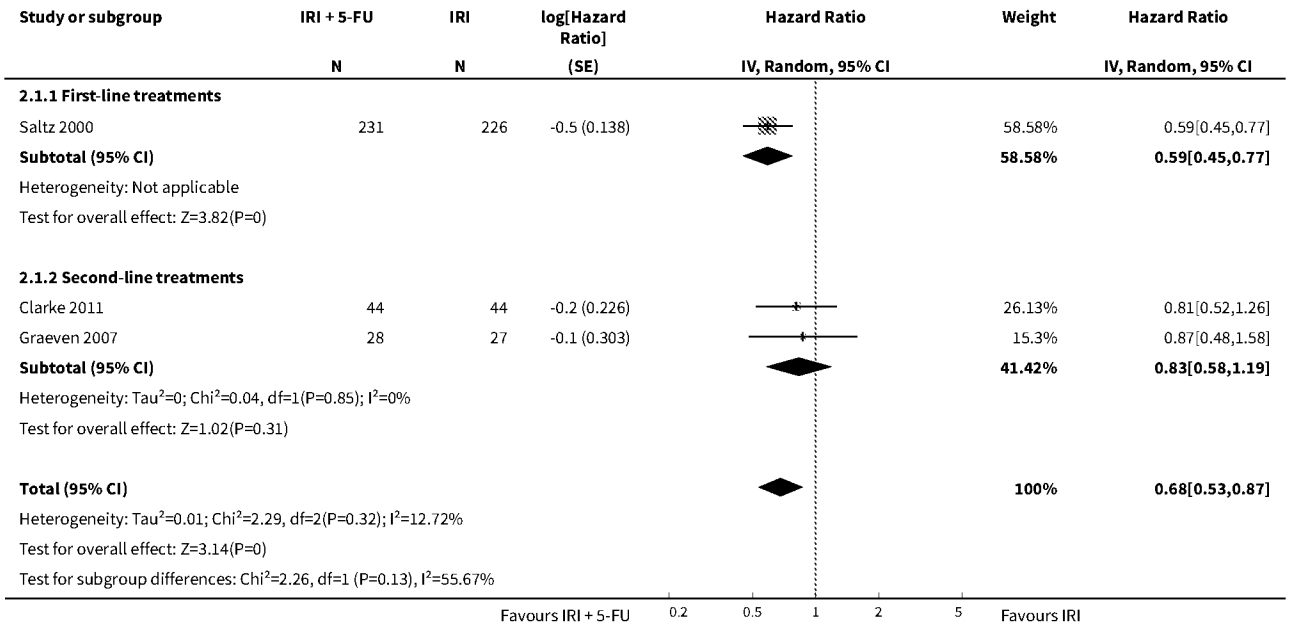

Comparison 3. Response to Treatment

Outcome or subgroup title	No. of studies	No. of participants	Statistical method	Effect size
1 Objective response (CR + PR)	5	1199	Risk Ratio (M-H, Random, 95% CI)	1.34 [0.80, 2.24]
1.1 First-line treatments	1	448	Risk Ratio (M-H, Random, 95% CI)	2.18 [1.58, 3.02]
1.2 Second-line treatments	4	751	Risk Ratio (M-H, Random, 95% CI)	0.99 [0.50, 1.96]

Analysis 3.1. Comparison 3 Response to Treatment, Outcome 1 Objective response (CR + PR).

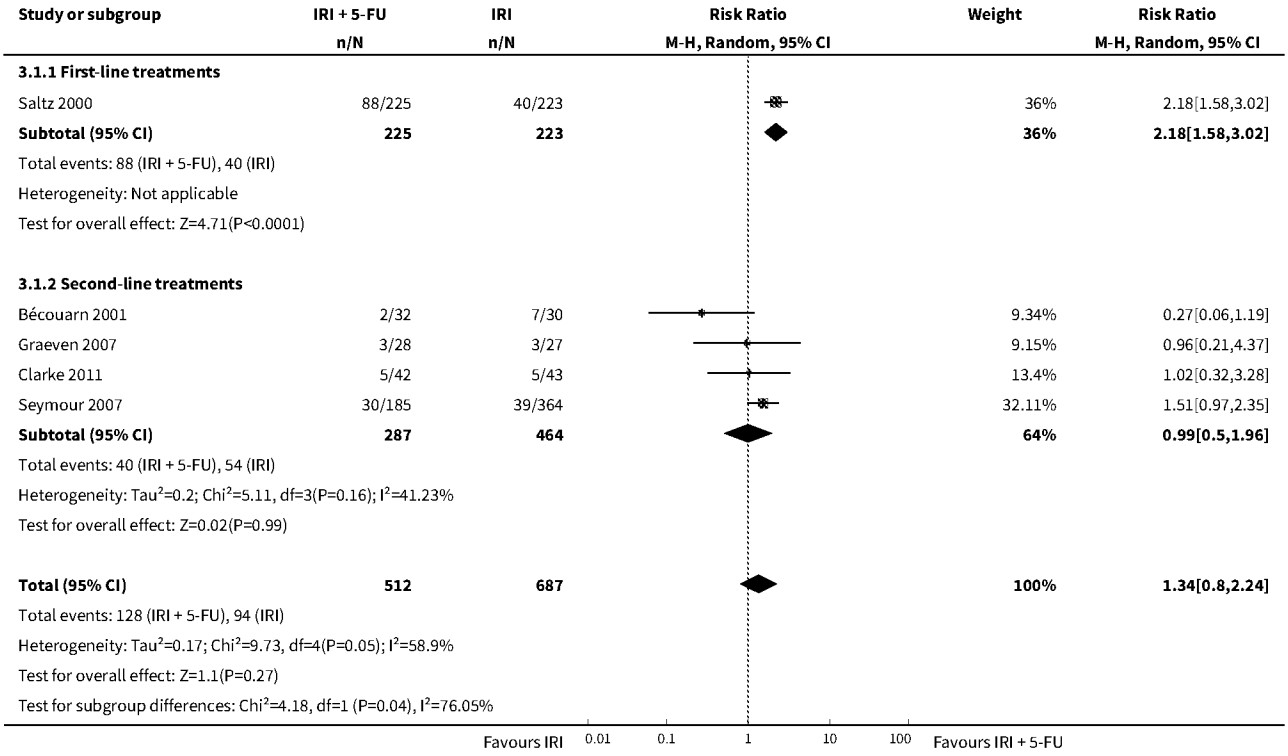

Comparison 4. Toxicity

Outcome or subgroup title	No. of studies	No. of participants	Statistical method	Effect size
1 Grade 3/4 diarrhea	5	1179	Risk Ratio (M-H, Random, 95% CI)	0.66 [0.48, 0.91]
2 Grade 3/4 mucositis	4	1117	Risk Ratio (M-H, Random, 95% CI)	1.19 [0.45, 3.11]
3 Grade 3/4 nausea	3	209	Risk Ratio (M-H, Random, 95% CI)	0.33 [0.07, 1.58]

Outcome or subgroup title	No. of studies	No. of participants	Statistical method	Effect size
4 Grade 3/4 vomiting	4	650	Risk Ratio (M-H, Random, 95% CI)	0.76 [0.47, 1.24]
5 Grade 3/4 neutropenia	5	1179	Risk Ratio (M-H, Random, 95% CI)	1.79 [1.29, 2.48]
6 Febrile neutropenia	3	595	Risk Ratio (M-H, Random, 95% CI)	1.21 [0.53, 2.78]
7 Grade 1/2 alopecia	2	140	Risk Ratio (M-H, Random, 95% CI)	0.45 [0.28, 0.74]
8 Neuropathy	2	591	Risk Ratio (M-H, Random, 95% CI)	1.22 [0.27, 5.42]
9 Grade 3/4 anemia	2	117	Risk Ratio (M-H, Random, 95% CI)	0.66 [0.08, 5.19]

Analysis 4.1. Comparison 4 Toxicity, Outcome 1 Grade 3/4 diarrhea.

Study or subgroup	IRI + 5-FU n/N	IRI n/N	Risk Ratio M-H, Random, 95% CI	Weight	Risk Ratio M-H, Random, 95% CI
Bécouarn 2001	6/32	3/30		5.71%	1.88[0.51,6.83]
Clarke 2011	4/42	8/43		7.46%	0.51[0.17,1.57]
Graeven 2007	3/28	5/27		5.41%	0.58[0.15,2.19]
Saltz 2000	51/225	69/223		55.8%	0.73[0.54,1]
Seymour 2007	14/180	58/349		25.62%	0.47[0.27,0.82]
Total (95% CI)	**507**	**672**		**100%**	**0.66[0.48,0.91]**
Total events: 78 (IRI + 5-FU), 143 (IRI)					
Heterogeneity: Tau^2=0.02; Chi^2=4.66, df=4(P=0.32); I^2=14.07%					
Test for overall effect: Z=2.55(P=0.01)					

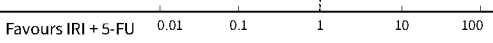

Analysis 4.2. Comparison 4 Toxicity, Outcome 2 Grade 3/4 mucositis.

Study or subgroup	IRI + 5-FU n/N	IRI n/N	Risk Ratio M-H, Random, 95% CI	Weight	Risk Ratio M-H, Random, 95% CI
Clarke 2011	1/42	0/43		9.19%	3.07[0.13,73.3]
Graeven 2007	0/28	0/27			Not estimable
Saltz 2000	5/225	5/223		61.6%	0.99[0.29,3.38]
Seymour 2007	2/180	3/349		29.2%	1.29[0.22,7.67]
Total (95% CI)	**475**	**642**		**100%**	**1.19[0.45,3.11]**
Total events: 8 (IRI + 5-FU), 8 (IRI)					
Heterogeneity: Tau^2=0; Chi^2=0.44, df=2(P=0.8); I^2=0%					
Test for overall effect: Z=0.35(P=0.73)					

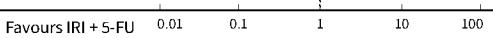

Analysis 4.3. Comparison 4 Toxicity, Outcome 3 Grade 3/4 nausea.

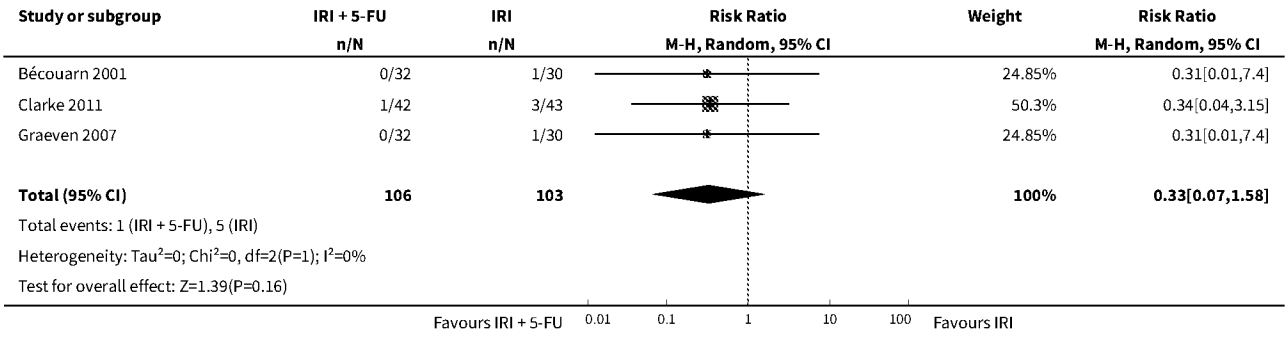

Analysis 4.4. Comparison 4 Toxicity, Outcome 4 Grade 3/4 vomiting.

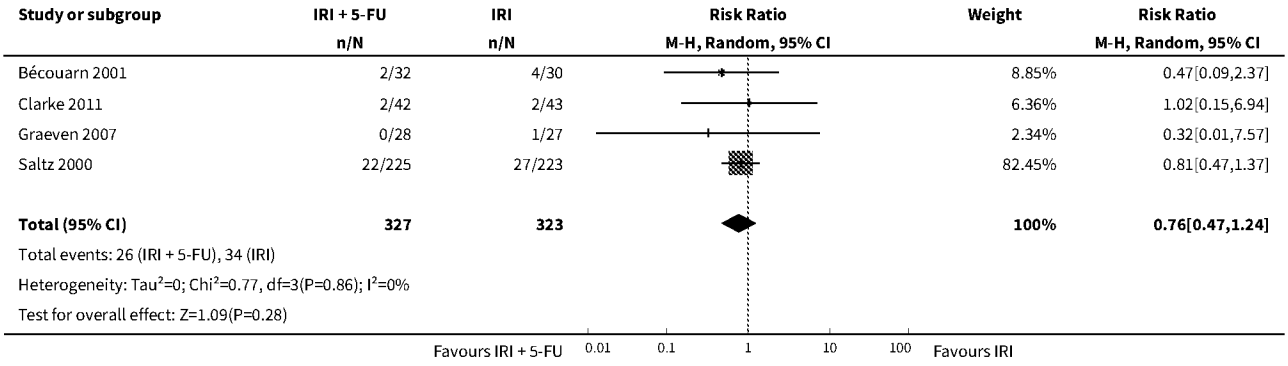

Analysis 4.5. Comparison 4 Toxicity, Outcome 5 Grade 3/4 neutropenia.

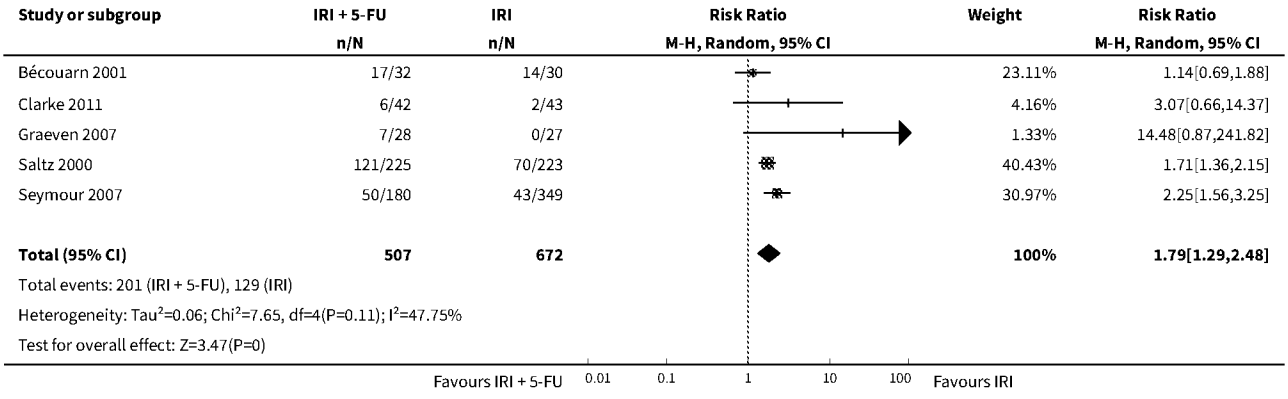

Analysis 4.6. Comparison 4 Toxicity, Outcome 6 Febrile neutropenia.

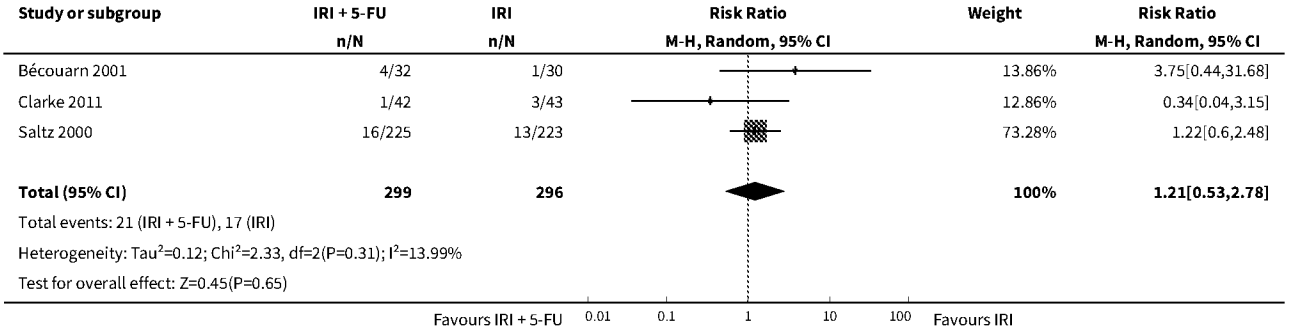

Analysis 4.7. Comparison 4 Toxicity, Outcome 7 Grade 1/2 alopecia.

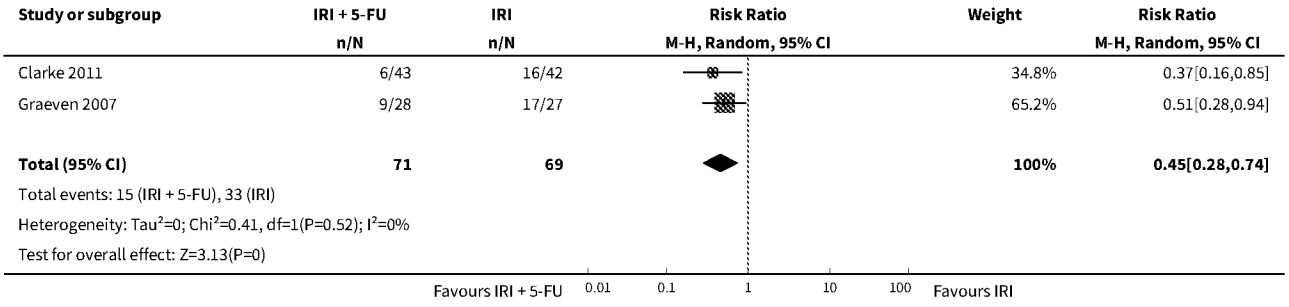

Analysis 4.8. Comparison 4 Toxicity, Outcome 8 Neuropathy.

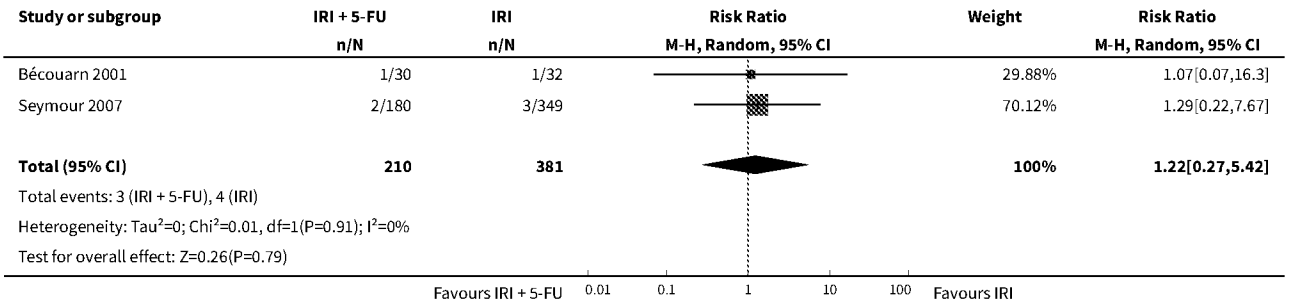

Analysis 4.9. Comparison 4 Toxicity, Outcome 9 Grade 3/4 anemia.

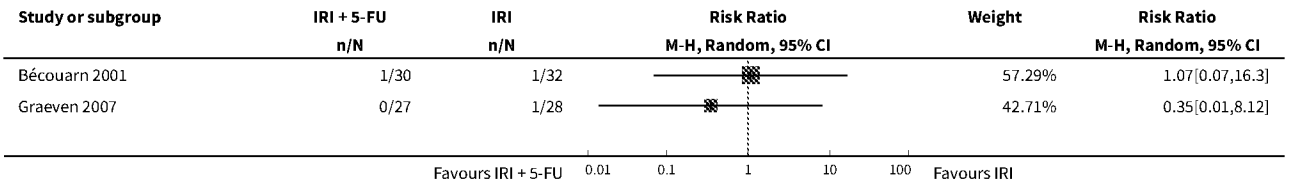

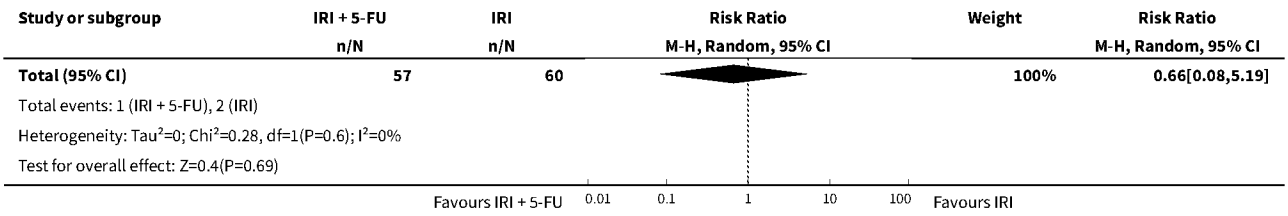

ADDITIONAL TABLES

Table 1. Characteristics of studies

Study	Group	Chemotherapy agent(s)	Additional agent(s)	Cycle interval	Median overall survival (months)
Bécouarn 2001	Intervention	IRI 180 mg/m2 IV 90 min on Day 1 5-FU 400 mg/m2 IV bolus and 600 mg/m2 IV 22 hrs on Day 1,2,15,16	Oxaliplatin on Day 1	4 weeks	9.8 (6.4-13)
	Control	IRI 200 mg/m2 IV 30 min on Day 1	Oxaliplatin on Day 15	3 weeks	12.3 (9.8-14.8)
Clarke 2011	Intervention	IRI 180 mg/m2 IV 90 min on Day 1 5-FU 400 mg/m2 IV bolus and 2400 mg/m2 IV 46 hrs on Day 1		2 weeks	15.4 (8.1-18)
	Control	IRI 300-350 mg/m2 IV 90 min on Day 1		3 weeks	11.2 (8.3-13.3)
Graeven 2007	Intervention	IRI 80 mg/m2 IV 60 min on Day 1,8,15,22,29,36 5-FU 2000 mg/m2 IV 24 hrs on Day 1,8,15,22,29,36		7 weeks	9.5 (6.5-13)
	Control	IRI 125 mg/m2 IV 30-60 min on Day 1,8,15,22		6 weeks	10.7 (8-12.9)
Saltz 2000	Intervention	IRI 125 mg/m2 IV 90 min on Day 1,8,15,22 5-FU 500 mg/m2 IV bolus on Day 1,8,15,22 and 5-FU 425 mg/m2 IV bolus on Day 1-5		6 weeks	14.8
	Control	IRI 125 mg/m2 IV 90 min on Day 1,8,15,22		6 weeks	12
Seymour 2007	Intervention	IRI 180 mg/m2 IV 30 min on Day 1 5-FU 400 mg/m2 IV bolus and 2400 mg/m2 IV 46 hrs on Day 1		2 weeks	15
	Control	IRI 350 mg/m2 IV 30-90 min on Day 1		3 weeks	13.9

APPENDICES

Appendix 1. CENTRAL search strategy

#1 MeSH descriptor: [Colorectal Neoplasms] explode all trees
#2 ((colorect* or colon or colonic or rect* or anal* or anus* or intestin* or bowel*) near/3 (carcinom* or neoplas* or adenocarcinom* or cancer* or tumor* or tumour* or sarcom* or metastas*)):ti,ab,kw
#3 (#1 or #2)
#4 MeSH descriptor: [Camptothecin] explode all trees
#5 (irinotecan* or camptothecin* or biotecan or Camptosar or camptothecin-11 or CPT-11 or SN-38):ti,ab,kw
#6 (#4 or #5)
#7 (#3 and #6)

Appendix 2. MEDLINE search strategy

1. *Colorectal Neoplasms/
2. ((colorect* or colon or colonic or rect* or anal* or anus* or intestin* or bowel*) and (carcinom* or neoplas* or adenocarcinom* or cancer* or tumor* or tumour* or sarcom* or metastas*)).m_titl.
3. 1 or 2
4. exp Camptothecin/
5. (irinotecan* or camptothecin* or biotecan or Camptosar or camptothecin-11 or CPT-11 or SN-38).m_titl.
6. 4 or 5
7. 3 and 6
8. randomized controlled trial.pt.
9. controlled clinical trial.pt.
10. randomized.ab.
11. placebo.ab.
12. clinical trial as topic.sh.
13. randomly.ab.
14. trial.ti.
15. 8 or 9 or 10 or 11 or 12 or 13 or 14
16. Exp animals/ not humans.sh.
17. 15 not 16
18. 7 and 17

Appendix 3. EMBASE search strategy

1. *colorectal cancer/
2. ((colorect* or colon or colonic or rect* or anal* or anus* or intestin* or bowel*) and (carcinom* or neoplas* or adenocarcinom* or cancer* or tumor* or tumour* or sarcom* or metastas*)).m_titl.
3. 1 or 2
4. *irinotecan/
5. (irinotecan* or camptothecin* or biotecan or Camptosar or camptothecin-11 or CPT-11 or SN-38).m_titl.
6. 4 or 5
7. 3 and 6
8. CROSSOVER PROCEDURE.sh.
9. DOUBLE-BLIND PROCEDURE.sh.
10. SINGLE-BLIND PROCEDURE.sh.
11. (crossover* or cross over*).ti,ab.
12. placebo*.ti,ab.
13. (doubl* adj blind*).ti,ab.
14. allocat*.ti,ab.
15. trial.ti.
16. RANDOMIZED CONTROLLED TRIAL.sh.
17. random*.ti,ab.
18. 8 or 9 or 10 or 11 or 12 or 13 or 14 or 15 or 16 or 17
19. (exp animal/ or exp invertebrate/ or animal.hw. or nonhuman/) not (exp human/ or human cell/ or (human or humans or man or men or wom?n).ti.)
20. 18 not 19
21. 7 and 20

Appendix 4. Science Citation Index search strategy

#1 Title: ((colorect* or colon or colonic or rect* or anal* or anus* or intestin* or bowel*) near/3 (carcinom* or neoplas* or adenocarcinom* or cancer* or tumor* or tumour* or sarcom* or metastas*))
#2 Title: (irinotecan* or camptothecin* or biotecan or Camptosar or camptothecin-11 or CPT-11 or SN-38)
#3 TOPIC: (controlled trial or controlled clinical trial or placebo or clinical trial or random* or trial or cct or rct)
#4 (#3 AND #2 AND #1)

Appendix 5. Criteria for judging risk of bias in the 'Risk of bias' assessment tool

RANDOM SEQUENCE GENERATION	
Selection bias (biased allocation to interventions) due to inadequate generation of a randomised sequence.	
Criteria for a judgement of 'Low risk' of bias.	The investigators describe a random component in the sequence generation process such as: · Referring to a random number table; · Using a computer random number generator; · Coin tossing; · Shuffling cards or envelopes; · Throwing dice; · Drawing of lots; · Minimization*. *Minimization may be implemented without a random element, and this is considered to be equivalent to being random.
Criteria for the judgement of 'High risk' of bias.	The investigators describe a non-random component in the sequence generation process. Usually, the description would involve some systematic, non-random approach, for example: · Sequence generated by odd or even date of birth; · Sequence generated by some rule based on date (or day) of admission; · Sequence generated by some rule based on hospital or clinic record number. · Other non-random approaches happen much less frequently than the systematic approaches mentioned above and tend to be obvious. They usually involve judgement or some method of non-random categorization of participants, for example: · Allocation by judgement of the clinician; · Allocation by preference of the participant; · Allocation based on the results of a laboratory test or a series of tests; · Allocation by availability of the intervention.
Criteria for the judgement of 'Unclear risk' of bias.	Insufficient information about the sequence generation process to permit judgement of 'Low risk' or 'High risk'.
ALLOCATION CONCEALMENT	
Selection bias (biased allocation to interventions) due to inadequate concealment of allocations prior to assignment.	
Criteria for a judgement of 'Low risk' of bias.	Participants and investigators enrolling participants could not foresee assignment because one of the following, or an equivalent method, was used to conceal allocation:

(Continued)

	· Central allocation (including telephone, web-based and pharmacy-controlled randomization); · Sequentially numbered drug containers of identical appearance; · Sequentially numbered, opaque, sealed envelopes.
Criteria for the judgement of 'High risk' of bias.	Participants or investigators enrolling participants could possibly foresee assignments and thus introduce selection bias, such as allocation based on: · Using an open random allocation schedule (e.g. a list of random numbers); · Assignment envelopes were used without appropriate safeguards (e.g. if envelopes were unsealed or nonopaque or not sequentially numbered); · Alternation or rotation; · Date of birth; · Case record number; · Any other explicitly unconcealed procedure.
Criteria for the judgement of 'Unclear risk' of bias.	Insufficient information to permit judgement of 'Low risk' or 'High risk'. This is usually the case if the method of concealment is not described or not described in sufficient detail to allow a definite judgement – for example if the use of assignment envelopes is described, but it remains unclear whether envelopes were sequentially numbered, opaque and sealed.
BLINDING OF PARTICIPANTS AND PERSONNEL Performance bias due to knowledge of the allocated interventions by participants and personnel during the study.	
Criteria for a judgement of 'Low risk' of bias.	Any one of the following: · No blinding or incomplete blinding, but the review authors judge that the outcome is not likely to be influenced by lack of blinding; · Blinding of participants and key study personnel ensured, and unlikely that the blinding could have been broken.
Criteria for the judgement of 'High risk' of bias.	Any one of the following: · No blinding or incomplete blinding, and the outcome is likely to be influenced by lack of blinding; · Blinding of key study participants and personnel attempted, but likely that the blinding could have been broken, and the outcome is likely to be influenced by lack of blinding.
Criteria for the judgement of 'Unclear risk' of bias.	Any one of the following: · Insufficient information to permit judgement of 'Low risk' or 'High risk'; · The study did not address this outcome.
BLINDING OF OUTCOME ASSESSMENT Detection bias due to knowledge of the allocated interventions by outcome assessors.	
Criteria for a judgement of 'Low risk' of bias.	Any one of the following: · No blinding of outcome assessment, but the review authors judge that the outcome measurement is not likely to be influenced by lack of blinding; · Blinding of outcome assessment ensured, and unlikely that the blinding could have been broken.

(Continued)

Criteria for the judgement of 'High risk' of bias.	Any one of the following: · No blinding of outcome assessment, and the outcome measurement is likely to be influenced by lack of blinding; · Blinding of outcome assessment, but likely that the blinding could have been broken, and the outcome measurement is likely to be influenced by lack of blinding.
Criteria for the judgement of 'Unclear risk' of bias.	Any one of the following: · Insufficient information to permit judgement of 'Low risk' or 'High risk'; · The study did not address this outcome.

INCOMPLETE OUTCOME DATA

Attrition bias due to amount, nature or handling of incomplete outcome data.

Criteria for a judgement of 'Low risk' of bias.	Any one of the following: · No missing outcome data; · Reasons for missing outcome data unlikely to be related to true outcome (for survival data, censoring unlikely to be introducing bias); · Missing outcome data balanced in numbers across intervention groups, with similar reasons for missing data across groups; · For dichotomous outcome data, the proportion of missing outcomes compared with observed event risk not enough to have a clinically relevant impact on the intervention effect estimate; · For continuous outcome data, plausible effect size (difference in means or standardized difference in means) among missing outcomes not enough to have a clinically relevant impact on observed effect size; · Missing data have been imputed using appropriate methods.
Criteria for the judgement of 'High risk' of bias.	Any one of the following: · Reason for missing outcome data likely to be related to true outcome, with either imbalance in numbers or reasons for missing data across intervention groups; · For dichotomous outcome data, the proportion of missing outcomes compared with observed event risk enough to induce clinically relevant bias in intervention effect estimate; · For continuous outcome data, plausible effect size (difference in means or standardized difference in means) among missing outcomes enough to induce clinically relevant bias in observed effect size; · 'As-treated' analysis done with substantial departure of the intervention received from that assigned at randomization; · Potentially inappropriate application of simple imputation.
Criteria for the judgement of 'Unclear risk' of bias.	Any one of the following: · Insufficient reporting of attrition/exclusions to permit judgement of 'Low risk' or 'High risk' (e.g. number randomized not stated, no reasons for missing data provided); · The study did not address this outcome.

SELECTIVE REPORTING

(Continued)

Reporting bias due to selective outcome reporting.	
Criteria for a judgement of 'Low risk' of bias.	Any of the following: · The study protocol is available and all of the study's pre-specified (primary and secondary) outcomes that are of interest in the review have been reported in the pre-specified way; · The study protocol is not available but it is clear that the published reports include all expected outcomes, including those that were pre-specified (convincing text of this nature may be uncommon).
Criteria for the judgement of 'High risk' of bias.	Any one of the following: · Not all of the study's pre-specified primary outcomes have been reported; · One or more primary outcomes is reported using measurements, analysis methods or subsets of the data (e.g. subscales) that were not pre-specified; · One or more reported primary outcomes were not pre-specified (unless clear justification for their reporting is provided, such as an unexpected adverse effect); · One or more outcomes of interest in the review are reported incompletely so that they cannot be entered in a meta-analysis; · The study report fails to include results for a key outcome that would be expected to have been reported for such a study.
Criteria for the judgement of 'Unclear risk' of bias.	Insufficient information to permit judgement of 'Low risk' or 'High risk'. It is likely that the majority of studies will fall into this category.
OTHER BIAS	
Bias due to problems not covered elsewhere in the table.	
Criteria for a judgement of 'Low risk' of bias.	The study appears to be free of other sources of bias.
Criteria for the judgement of 'High risk' of bias.	There is at least one important risk of bias. For example, the study: · Had a potential source of bias related to the specific study design used; or · Has been claimed to have been fraudulent; or · Had some other problem.
Criteria for the judgement of 'Unclear risk' of bias.	There may be a risk of bias, but there is either: · Insufficient information to assess whether an important risk of bias exists; or · Insufficient rationale or evidence that an identified problem will introduce bias.

HISTORY

Protocol first published: Issue 7, 2010
Review first published: Issue 2, 2016

Date	Event	Description
14 December 2014	New search has been performed	New search performed. 945 additional studies found in initial search, but no new trials identified in full-text search and checked for inclusion
24 June 2013	New search has been performed	Updated protocol with new author team

CONTRIBUTIONS OF AUTHORS

TASKS	WHO WILL UNDERTAKE TASKS?
Draft the protocol	**Wahyu Wulaningsih and Mieke Van Hemelrijck**
Develop a search strategy	**Wahyu Wulaningsih and Mieke Van Hemelrijck**
Search for trials	**Ardyan Wardhana and Naomi Yoshuantari**
Select which trials to include	**Wahyu Wulaningsih and Ardyan Wardhana**
Extract data from trials	**Wahyu Wulaningsih and Naomi Yoshuantari**
Enter data into RevMan	**Wahyu Wulaningsih and Ardyan Wardhana**
Carry out the analysis	**Wahyu Wulaningsih, Ardyan Wardhana, Johnathan Watkins**
Interpret the analysis	**All authors**
Draft the final review	**All authors**

DECLARATIONS OF INTEREST

None declared.

SOURCES OF SUPPORT

Internal sources

- No sources of support supplied, Other.

External sources

- No sources of support supplied, Other.

DIFFERENCES BETWEEN PROTOCOL AND REVIEW

In the protocol, we specified that only English publications would be included in the review. However, during initial search and selection of studies, we included trials in all languages and when limiting to studies in English in the latter stage, this made no difference in studies selected. Therefore, in the current review we no longer limited the studies to publications in English.

The method used to pool estimates from binary outcomes was not specified in the protocol. The use of a Mantel-Haenszel test has now been included in the review.

In the protocol, we specified that random effects model will be used when heterogeneity is indicated. However, in the review, random effects model selection was performed for all analyses, and investigations of sources of any results inconsistency by sensitivity analyses were performed when heterogeneity was indicated.

INDEX TERMS

Medical Subject Headings (MeSH)

Alopecia [chemically induced]; Antimetabolites, Antineoplastic [adverse effects] [therapeutic use]; Antineoplastic Agents, Phytogenic [adverse effects] [therapeutic use]; Antineoplastic Combined Chemotherapy Protocols [adverse effects] [*therapeutic use]; Camptothecin [administration & dosage] [adverse effects] [analogs & derivatives]; Colorectal Neoplasms [*drug therapy] [mortality] [pathology]; Diarrhea [chemically induced]; Disease-Free Survival; Fluorouracil [administration & dosage] [adverse effects]; Irinotecan; Nausea [chemically induced]; Neutropenia; Quality of Life; Randomized Controlled Trials as Topic

MeSH check words

Humans

XELODA®
(capecitabine)
TABLETS

DESCRIPTION: XELODA (capecitabine) is a fluoropyrimidine carbamate with antineoplastic activity. It is an orally administered systemic prodrug of 5'-deoxy-5-fluorouridine (5'-DFUR) which is converted to 5-fluorouracil.

The chemical name for capecitabine is 5'-deoxy-5-fluoro-N-[(pentyloxy)carbonyl]-cytidine and has a molecular weight of 359.35. Capecitabine has the following structural formula:

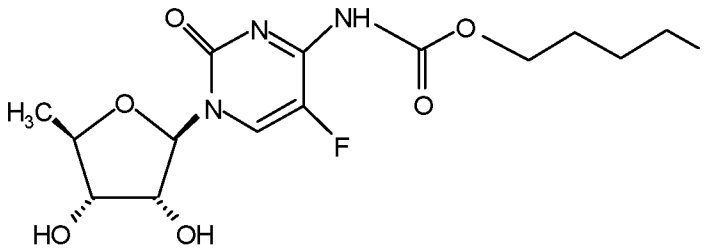

Capecitabine is a white to off-white crystalline powder with an aqueous solubility of 26 mg/mL at 20ºC.

XELODA is supplied as biconvex, oblong film-coated tablets for oral administration. Each light peach-colored tablet contains 150 mg capecitabine and each peach-colored tablet contains 500 mg capecitabine. The inactive ingredients in XELODA include: anhydrous lactose, croscarmellose sodium, hydroxypropyl methylcellulose, microcrystalline cellulose, magnesium stearate and purified water. The peach or light peach film coating contains hydroxypropyl methylcellulose, talc, titanium dioxide, and synthetic yellow and red iron oxides.

CLINICAL PHARMACOLOGY: Capecitabine is relatively non-cytotoxic in vitro. This drug is enzymatically converted to 5-fluorouracil (5-FU) in vivo.

Bioactivation: Capecitabine is readily absorbed from the gastrointestinal tract. In the liver, a 60 kDa carboxyesterase hydrolyzes much of the compound to 5'-deoxy-5-fluorocytidine (5'-DFCR). Cytidine deaminase, an enzyme found in most tissues, including tumors, subsequently converts 5'-DFCR to 5'-deoxy-5-fluorouridine (5'-DFUR). The enzyme, thymidine phosphorylase (dThdPase), then hydrolyzes 5'-DFUR to the active drug 5-FU. Many tissues throughout the body express thymidine phosphorylase. Some human carcinomas express this enzyme in higher concentrations than surrounding normal tissues.

XELODA® (capecitabine)

Metabolic Pathway of capecitabine to 5-FU

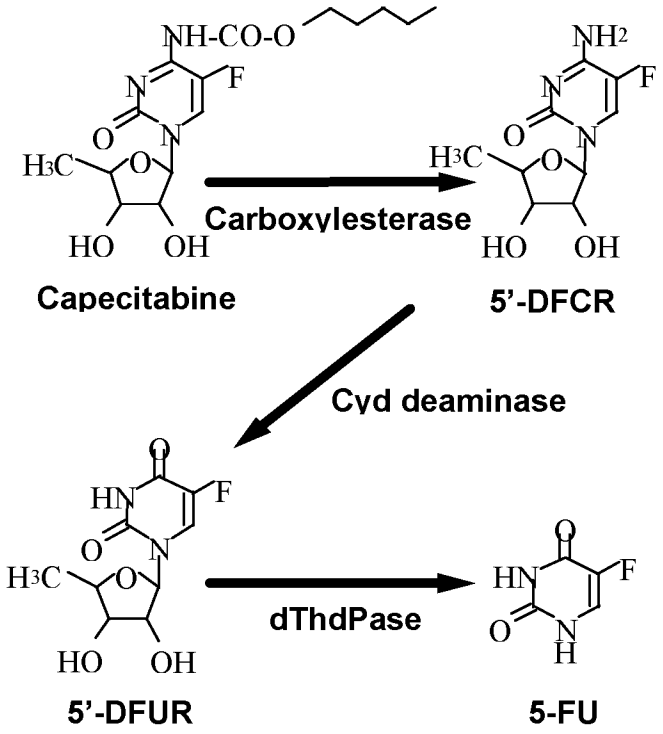

Mechanism of Action: Both normal and tumor cells metabolize 5-FU to 5-fluoro-2-deoxyuridine monophosphate (FdUMP) and 5-fluorouridine triphosphate (FUTP). These metabolites cause cell injury by two different mechanisms. First, FdUMP and the folate cofactor, N^{5-10}-methylenetetrahydrofolate, bind to thymidylate synthase (TS) to form a covalently bound ternary complex. This binding inhibits the formation of thymidylate from uracil. Thymidylate is the necessary precursor of thymidine triphosphate, which is essential for the synthesis of DNA, so that a deficiency of this compound can inhibit cell division. Second, nuclear transcriptional enzymes can mistakenly incorporate FUTP in place of uridine triphosphate (UTP) during the synthesis of RNA. This metabolic error can interfere with RNA processing and protein synthesis.

Pharmacokinetics in Colorectal Tumors and Adjacent Healthy Tissue: Following oral administration of capecitabine 7 days before surgery in patients with colorectal cancer, the median ratio of 5-FU concentration in colorectal tumors to adjacent tissues was 2.9 (range from 0.9 to 8.0). These ratios have not been evaluated in breast cancer patients or compared to 5-FU infusion.

Human Pharmacokinetics: The pharmacokinetics of XELODA and its metabolites have been evaluated in about 200 cancer patients over a dosage range of 500 to 3500 mg/m^2/day. Over this range, the pharmacokinetics of capecitabine and its metabolite, 5'-DFCR were dose proportional and did not change over time. The increases in the AUCs of 5'-DFUR and 5-FU, however, were greater than proportional to the increase in dose and the AUC of 5-FU was 34% higher on day 14

than on day 1. The elimination half-life of both parent capecitabine and 5-FU was about ¾ of an hour. The inter-patient variability in the C_{max} and AUC of 5-FU was greater than 85%.

Absorption, Distribution, Metabolism and Excretion: Capecitabine reached peak blood levels in about 1.5 hours (T_{max}) with peak 5-FU levels occurring slightly later, at 2 hours. Food reduced both the rate and extent of absorption of capecitabine with mean C_{max} and $AUC_{0-\infty}$ decreased by 60% and 35%, respectively. The C_{max} and $AUC_{0-\infty}$ of 5-FU were also reduced by food by 43% and 21%, respectively. Food delayed T_{max} of both parent and 5-FU by 1.5 hours (see PRECAUTIONS and DOSAGE AND ADMINISTRATION).

Plasma protein binding of capecitabine and its metabolites is less than 60% and is not concentration-dependent. Capecitabine was primarily bound to human albumin (approximately 35%).

Capecitabine is extensively metabolized enzymatically to 5-FU. The enzyme dihydropyrimidine dehydrogenase hydrogenates 5-FU, the product of capecitabine metabolism, to the much less toxic 5-fluoro-5,6-dihydro-fluorouracil (FUH_2). Dihydropyrimidinase cleaves the pyrimidine ring to yield 5-fluoro-ureido-propionic acid (FUPA). Finally, β-ureido-propionase cleaves FUPA to α-fluoro-β-alanine (FBAL) which is cleared in the urine.

Capecitabine and its metabolites are predominantly excreted in urine; 95.5% of administered capecitabine dose is recovered in urine. Fecal excretion is minimal (2.6%). The major metabolite excreted in urine is FBAL which represents 57% of the administered dose. About 3% of the administered dose is excreted in urine as unchanged drug.

Special Populations:

Age, Gender and Ethnicity: No formal studies were conducted to examine the effect of age or gender or ethnicity on the pharmacokinetics of capecitabine and its metabolites.

Hepatic Insufficiency: XELODA has been evaluated in 13 patients with mild to moderate hepatic dysfunction due to liver metastases defined by a composite score including bilirubin, AST/ALT and alkaline phosphatase following a single 1255 mg/m^2 dose of capecitabine. Both $AUC_{0-\infty}$ and C_{max} of capecitabine increased by 60% in patients with hepatic dysfunction compared to patients with normal hepatic function (n=14). The $AUC_{0-\infty}$ and C_{max} of 5-FU was not affected. In patients with mild to moderate hepatic dysfunction due to liver metastases, caution should be exercised when XELODA is administered. The effect of severe hepatic dysfunction on XELODA is not known (see PRECAUTIONS and DOSAGE AND ADMINISTRATION).

Drug-Drug Interactions:

Drugs Metabolized by Cytochrome P450 Enzymes: In vitro enzymatic studies with human liver microsomes indicated that capecitabine and 5'-DFUR had no inhibitory effects on substrates of cytochrome P450 for the major isoenzymes such as 1A2, 2A6, 3A4, 2C9, 2C19, 2D6, and 2E1, suggesting a low likelihood of interactions with drugs metabolized by cytochrome P450

enzymes.

Antacid: When Maalox®* (20 mL), an aluminum hydroxide- and magnesium hydroxide-containing antacid, was administered immediately after capecitabine (1250 mg/m^2, n=12 cancer patients), AUC and C_{max} increased by 16% and 35%, respectively, for capecitabine and by 18% and 22%, respectively, for 5'-DFCR. No effect was observed on the other three major metabolites (5'-DFUR, 5-FU, FBAL) of capecitabine.

XELODA has a low potential for pharmacokinetic interactions related to plasma protein binding.

CLINICAL STUDIES: In a phase 1 study with XELODA in patients with solid tumors, the maximum tolerated dose as a single agent was 3000 mg/m^2 when administered daily for 2 weeks, followed by a 1-week rest period. The dose-limiting toxicities were diarrhea and leukopenia.

Breast Carcinoma: The antitumor activity of XELODA was evaluated in an open-label single-arm trial conducted in 24 centers in the US and Canada. A total of 162 patients with stage IV breast cancer were enrolled. The primary endpoint was tumor response rate in patients with measurable disease, with response defined as a ≥50% decrease in sum of the products of the perpendicular diameters of bidimensionally measurable disease for at least 1 month. XELODA was administered at a daily dose of 2510 mg/m^2 for 2 weeks followed by a 1-week rest period and given as 3-week cycles. The baseline demographics and clinical characteristics for all patients (n=162) and those with measurable disease (n=135) are shown in the table below. Resistance was defined as progressive disease while on treatment, with or without an initial response, or relapse within 6 months of completing treatment with an anthracycline-containing adjuvant chemotherapy regimen.

XELODA® (capecitabine)

Table 1. Baseline Demographics and Clinical Characteristics

	Patients with Measurable Disease (n=135)	All Patients (n=162)
Age (median, years)	55	56
Karnofsky PS	90	90
No. Disease Sites		
1-2	43 (32%)	60 (37%)
3-4	63 (46%)	69 (43%)
>5	29 (22%)	34 (21%)
Dominant Site of Disease		
Visceral[1]	101 (75%)	110 (68%)
Soft Tissue	30 (22%)	35 (22%)
Bone	4 (3%)	17 (10%)
Prior Chemotherapy		
Paclitaxel	135 (100%)	162 (100%)
Anthracycline[2]	122 (90%)	147 (91%)
5-FU	110 (81%)	133 (82%)
Resistance to Paclitaxel	103 (76%)	124 (77%)
Resistance to an Anthracycline[2]	55 (41%)	67 (41%)
Resistance to both Paclitaxel and an Anthracycline[2]	43 (32%)	51(31%)

[1]Lung, pleura, liver, peritoneum
[2]Includes 2 patients treated with an anthracenedione

Antitumor responses for patients with disease resistant to both paclitaxel and an anthracycline are shown in the table below.

XELODA® (capecitabine)

Table 2. Response Rates in Doubly-Resistant Patients

	Resistance to Both Paclitaxel and an Anthracycline (n=43)
CR	0
PR[1]	11
CR + PR[1]	11
Response Rate[1] (95% C.I.)	25.6% (13.5, 41.2)
Duration of Response,[1] Median in days[2] (Range)	154 (63 to 233)

[1]Includes 2 patients treated with an anthracenedione
[2]From date of first response

For the subgroup of 43 patients who were doubly resistant, the median time to progression was 102 days and the median survival was 255 days. The objective response rate in this population was supported by a response rate of 18.5% (1 CR, 24 PRs) in the overall population of 135 patients with measurable disease, who were less resistant to chemotherapy (see Table 1). The median time to progression was 90 days and the median survival was 306 days.

INDICATIONS AND USAGE: XELODA is indicated for the treatment of patients with metastatic breast cancer resistant to both paclitaxel and an anthracycline-containing chemotherapy regimen or resistant to paclitaxel and for whom further anthracycline therapy is not indicated, eg, patients who have received cumulative doses of 400 mg/m^2 of doxorubicin or doxorubicin equivalents. Resistance is defined as progressive disease while on treatment, with or without an initial response, or relapse within 6 months of completing treatment with an anthracycline-containing adjuvant regimen.

This indication is based on demonstration of a response rate. No results are available from controlled trials that demonstrate a clinical benefit resulting from treatment, such as improvement in disease-related symptoms, disease progression, or survival.

CONTRAINDICATIONS: XELODA is contraindicated in patients who have a known hypersensitivity to 5-fluorouracil.

XELODA is also contraindicated in patients with severe renal impairment (creatinine clearance below 30 mL/min [Cockroft and Gault]).

WARNINGS: *Renal Insufficiency:* In patients with moderate renal impairment (creatinine clearance 30-50 mL/min [Cockroft and Gault]) at baseline, a dose reduction to 75% of the XELODA starting dose is recommended. In patients with mild renal impairment (creatinine clearance 51-80 mL/min) no adjustment in starting dose is recommended. (see DOSAGE AND ADMINISTRATION). Careful monitoring and prompt treatment interruption is recommended if

the patient develops a grade 2, 3, or 4 adverse event with subsequent dose adjustments as outlined in the table in DOSAGE AND ADMINISTRATION.

Coagulopathy: Altered coagulation parameters and/or bleeding have been reported in patients taking XELODA concomitantly with coumarin-derivative anticoagulants such as warfarin and phenprocoumon. These events occurred within several days and up to several months after initiating XELODA therapy and, in a few cases, within one month after stopping XELODA. These events occurred in patients with and without liver metastases. Patients taking coumarin-derivative anticoagulants concomitantly with XELODA should be monitored regularly for alterations in their coagulation parameters (PT or INR) (see PRECAUTIONS: *Drug-Drug Interactions*).

Diarrhea: XELODA can induce diarrhea, sometimes severe. Patients with severe diarrhea should be carefully monitored and given fluid and electrolyte replacement if they become dehydrated. The median time to first occurrence of grade 2-4 diarrhea was 31 days (range from 1 to 322 days). National Cancer Institute of Canada (NCIC) grade 2 diarrhea is defined as an increase of 4 to 6 stools/day or nocturnal stools, grade 3 diarrhea as an increase of 7 to 9 stools/day or incontinence and malabsorption, and grade 4 diarrhea as an increase of ≥10 stools/day or grossly bloody diarrhea or the need for parenteral support. If grade 2, 3 or 4 diarrhea occurs, administration of XELODA should be immediately interrupted until the diarrhea resolves or decreases in intensity to grade 1. Following grade 3 or 4 diarrhea, subsequent doses of XELODA should be decreased (see DOSAGE AND ADMINISTRATION). Standard antidiarrheal treatments (eg, loperamide) are recommended.

Necrotizing enterocolitis (typhlitis) has been reported.

Geriatric Patients (gastrointestinal toxicity): Patients ≥80 years old may experience a greater incidence of gastrointestinal grade 3 or 4 adverse events (see PRECAUTIONS: *Geriatric Use*). Among the 14 patients 80 years of age and greater treated with capecitabine, three (21.4%), three (21.4%) and one (7.1%) patients experienced reversible grade 3 or 4 diarrhea, nausea and vomiting, respectively.

Among the 313 patients age 60 to 79 years old, the incidence of gastrointestinal toxicity was similar to that in the overall population.

Pregnancy: XELODA may cause fetal harm when given to a pregnant woman. Capecitabine at doses of 198 mg/kg/day during organogenesis caused teratogenic malformations and embryo death in mice. In separate pharmacokinetic studies, this dose in mice produced 5'-DFUR AUC values about 0.2 times the corresponding values in patients administered the recommended daily dose. Teratogenic malformations in mice included cleft palate, anophthalmia, microphthalmia, oligodactyly, polydactyly, syndactyly, kinky tail and dilation of cerebral ventricles. At doses of 90 mg/kg/day, capecitabine given to pregnant monkeys during organogenesis caused fetal death. This dose produced 5'-DFUR AUC values about 0.6 times the corresponding values in patients administered the recommended daily dose. There are no adequate and well-controlled studies in pregnant women using XELODA. If the drug is used during pregnancy, or if the patient becomes

pregnant while receiving this drug, the patient should be apprised of the potential hazard to the fetus. Women of childbearing potential should be advised to avoid becoming pregnant while receiving treatment with XELODA.

PRECAUTIONS: ***General:*** Patients receiving therapy with XELODA should be monitored by a physician experienced in the use of cancer chemotherapeutic agents. Most adverse events are reversible and do not need to result in discontinuation, although doses may need to be withheld or reduced (see DOSAGE AND ADMINISTRATION).

Hand-and-Foot Syndrome: Hand-and-foot syndrome (palmar-plantar erythrodysesthesia or chemotherapy induced acral erythema) is characterized by the following: numbness, dysesthesia/paresthesia, tingling, painless or painful swelling, erythema, desquamation, blistering and severe pain. Grade 2 hand-and-foot syndrome is defined as painful erythema and swelling of the hands and/or feet and/or discomfort affecting the patient's activities of daily living. Grade 3 hand-and-foot syndrome is defined as moist desquamation, ulceration, blistering and severe pain of the hands and/or feet and/or severe discomfort that causes the patient to be unable to work or perform activities of daily living. If grade 2 or 3 hand-and-foot syndrome occurs, administration of XELODA should be interrupted until the event resolves or decreases in intensity to grade 1. Following grade 3 hand-and-foot syndrome, subsequent doses of XELODA should be decreased (see DOSAGE AND ADMINISTRATION).

Cardiac: There has been cardiotoxicity associated with fluorinated pyrimidine therapy, including myocardial infarction, angina, dysrhythmias, cardiogenic shock, sudden death and electrocardiograph changes. These adverse events may be more common in patients with a prior history of coronary artery disease.

Hepatic Insufficiency: Patients with mild to moderate hepatic dysfunction due to liver metastases should be carefully monitored when XELODA is administered. The effect of severe hepatic dysfunction on the disposition of XELODA is not known (see CLINICAL PHARMACOLOGY and DOSAGE AND ADMINISTRATION).

Hyperbilirubinemia: Grade 3 or 4 hyperbilirubinemia occurred in 17% (n=97) of 570 patients with either metastatic breast or colorectal cancer who received a dose of 2510 mg/m^2 daily for 2 weeks followed by a 1-week rest period. Of 339 patients who had hepatic metastases at baseline and 231 patients without hepatic metastases at baseline, grade 3 or 4 hyperbilirubinemia occurred in 21.2% and 10.4%, respectively. Seventy-four (76%) of the 97 patients with grade 3 or 4 hyperbilirubinemia also had concurrent elevations in alkaline phosphatase and/or hepatic transaminases; 6% of these were grade 3 or 4. Only 4 patients (4%) had elevated hepatic transaminases without a concurrent elevation in alkaline phosphatase. If drug related grade 2-4 elevations in bilirubin occur, administration of XELODA should be immediately interrupted until the hyperbilirubinemia resolves or decreases in intensity to grade 1. NCIC grade 2 hyperbilirubinemia is defined as 1.5 x normal, grade 3 hyperbilirubinemia as 1.5-3 x normal and grade 4 hyperbilirubinemia as >3 x normal. (See recommended dose modifications under DOSAGE AND ADMINISTRATION.)

XELODA® (capecitabine)

Hematologic: In 570 patients with either metastatic breast or colorectal cancer who received a dose of 2510 mg/m^2 administered daily for 2 weeks followed by a 1-week rest period, 4%, 2%, and 3% of patients had grade 3 or 4 neutropenia, thrombocytopenia and decreases in hemoglobin, respectively.

Carcinogenesis, Mutagenesis and Impairment of Fertility: Long-term studies in animals to evaluate the carcinogenic potential of capecitabine have not been conducted. Capecitabine was not mutagenic in vitro to bacteria (Ames test) or mammalian cells (Chinese hamster V79/HPRT gene mutation assay). Capecitabine was clastogenic in vitro to human peripheral blood lymphocytes but not clastogenic in vivo to mouse bone marrow (micronucleus test). Fluorouracil causes mutations in bacteria and yeast. Fluorouracil also causes chromosomal abnormalities in the mouse micronucleus test in vivo.

Impairment of Fertility: In studies of fertility and general reproductive performance in mice, oral capecitabine doses of 760 mg/kg/day disturbed estrus and consequently caused a decrease in fertility. In mice that became pregnant, no fetuses survived this dose. The disturbance in estrus was reversible. In males, this dose caused degenerative changes in the testes, including decreases in the number of spermatocytes and spermatids. In separate pharmacokinetic studies, this dose in mice produced 5'-DFUR AUC values about 0.7 times the corresponding values in patients administered the recommended daily dose.

Information for Patients (see Patient Package Insert): Patients and patients' caregivers should be informed of the expected adverse effects of XELODA, particularly nausea, vomiting, diarrhea, and hand-and-foot syndrome, and should be made aware that patient-specific dose adaptations during therapy are expected and necessary (see DOSAGE AND ADMINISTRATION). Patients should be encouraged to recognize the common grade 2 toxicities associated with XELODA treatment.

Diarrhea: Patients experiencing grade 2 diarrhea (an increase of 4 to 6 stools/day or nocturnal stools) or greater should be instructed to stop taking XELODA immediately. Standard antidiarrheal treatments (eg, loperamide) are recommended.

Nausea: Patients experiencing grade 2 nausea (food intake significantly decreased but able to eat intermittently) or greater should be instructed to stop taking XELODA immediately. Initiation of symptomatic treatment is recommended.

Vomiting: Patients experiencing grade 2 vomiting (2 to 5 episodes in a 24-hour period) or greater should be instructed to stop taking XELODA immediately. Initiation of symptomatic treatment is recommended.

Hand-and-Foot Syndrome: Patients experiencing grade 2 hand-and-foot syndrome (painful erythema and swelling of the hands and/or feet and/or discomfort affecting the patients' activities of daily living) or greater should be instructed to stop taking XELODA immediately.

XELODA® (capecitabine)

Stomatitis: Patients experiencing grade 2 stomatitis (painful erythema, edema or ulcers of the mouth or tongue, but able to eat) or greater should be instructed to stop taking XELODA immediately. Initiation of symptomatic treatment is recommended (see DOSAGE AND ADMINISTRATION).

Fever and Neutropenia: Patients who develop a fever of 100.5°F or greater or other evidence of potential infection should be instructed to call their physician.

Drug-Food Interaction: In all clinical trials, patients were instructed to administer XELODA within 30 minutes after a meal. Since current safety and efficacy data are based upon administration with food, it is recommended that XELODA be administered with food (see DOSAGE AND ADMINISTRATION).

Drug-Drug Interactions:

Antacid: The effect of an aluminum hydroxide- and magnesium hydroxide-containing antacid (Maalox)* on the pharmacokinetics of capecitabine was investigated in 12 cancer patients. There was a small increase in plasma concentrations of capecitabine and one metabolite (5'-DFCR); there was no effect on the 3 major metabolites (5'-DFUR, 5-FU and FBAL).

Coumarin Anticoagulants: Altered coagulation parameters and/or bleeding have been reported in patients taking capecitabine concomitantly with coumarin-derivative anticoagulants such as warfarin and phenprocoumon. Patients taking coumarin-derivative anticoagulants concomitantly with capecitabine should be monitored regularly for alterations in their coagulation parameters (PT or INR) (see WARNINGS: *Coagulopathy*).

Phenytoin: Postmarketing reports indicate that some patients receiving capecitabine and phenytoin had toxicity associated with elevated phenytoin levels. The level of phenytoin should be carefully monitored in patients taking XELODA and phenytoin dose may need to be reduced (see DOSAGE AND ADMINISTRATION: *Dose Modification Guidelines*).

Leucovorin: The concentration of 5-fluorouracil is increased and its toxicity may be enhanced by leucovorin. Deaths from severe enterocolitis, diarrhea, and dehydration have been reported in elderly patients receiving weekly leucovorin and fluorouracil.

Pregnancy: *Teratogenic Effects:* Category D (see WARNINGS). Women of childbearing potential should be advised to avoid becoming pregnant while receiving treatment with XELODA.

Nursing Women: It is not known whether the drug is excreted in human milk. Because many drugs are excreted in human milk and because of the potential for serious adverse reactions in nursing infants, it is recommended that nursing be discontinued when receiving XELODA therapy.

XELODA® (capecitabine)

Pediatric Use: The safety and effectiveness of XELODA in persons <18 years of age have not been established.

Geriatric Use: No separate studies have been conducted to examine the effect of age on the pharmacokinetics of capecitabine and its metabolites. Patients ≥80 years old may experience a greater incidence of gastrointestinal grade 3 or 4 adverse events (see WARNINGS). Among the 14 patients 80 years of age and greater treated with capecitabine, 21.4%, 21.4% and 7.1% experienced grade 3 or 4 diarrhea, nausea and vomiting, respectively. Among the 313 patients 60 to 79 years old, the incidence was similar to the overall population.

The elderly may be pharmacodynamically more sensitive to the toxic effects of 5-FU. Physicians should pay particular attention to monitoring the adverse effects of XELODA in the elderly.

ADVERSE REACTIONS:

The following table shows the adverse events occurring in ≥5% of patients reported as at least remotely related to the administration of XELODA. Rates are rounded to the nearest whole number. The data are shown both for the study in stage IV breast cancer and for a group of 570 patients with breast and colorectal cancer who received a dose of 2510 mg/m^2 administered daily for 2 weeks followed by a 1-week rest period. The 570 patients were enrolled in 6 clinical trials (162 from the breast cancer trial described under CLINICAL STUDIES, 83 other patients with breast cancer and 325 patients with colorectal cancer). The mean duration of treatment was 121 days. A total of 71 patients (13%) discontinued treatment because of adverse events/intercurrent illness.

Table 3. Percent Incidence of Adverse Events Considered Remotely, Possibly or Probably Related to Treatment in ≥5% of Patients

Adverse Event	Phase 2 Trial in Stage IV Breast Cancer (n=162)			Overall Safety Database (n=570)		
Body System/Adverse Event	**Total**	**Grade 3**	**Grade 4**	**Total**	**Grade 3**	**Grade 4**
GI						
Diarrhea	57	12	3	50	11	2
Nausea	53	4	–	44	4	–
Vomiting	37	4	–	26	3	–
Stomatitis	24	7	–	23	4	–
Abdominal pain	20	4	–	17	4	–
Constipation	15	1	–	9	1	–
Dyspepsia	8	–	–	6	–	–
Skin and Subcutaneous						
Hand-and-Foot Syndrome	57	11	–	45	13	–
Dermatitis	37	1	–	31	1	–
Nail disorder	7	–	–	4	–	–

XELODA® (capecitabine)

Adverse Event	Phase 2 Trial in Stage IV Breast Cancer (n=162)			Overall Safety Database (n=570)		
Body System/Adverse Event	**Total**	**Grade 3**	**Grade 4**	**Total**	**Grade 3**	**Grade 4**
General						
Fatigue	41	8	–	34	5	–
Pyrexia	12	1	–	10	–	–
Pain in limb	6	1	–	4	–	–
Neurological						
Paraesthesia	21	1	–	12	–	–
Headache	9	1	–	7	1	–
Dizziness	8	–	–	5	–	–
Insomnia	8	–	–	3	–	–
Metabolism						
Anorexia	23	3	–	20	2	–
Dehydration	7	4	1	5	2	1
Eye						
Eye irritation	15	–	–	10	–	–
Musculoskeletal						
Myalgia	9	–	–	4	–	–
Cardiac						
Edema	9	1	–	6	–	–
Blood						
Neutropenia	26	2	2	22	3	2
Thrombocytopenia	24	3	1	21	1	1
Anemia	72	3	1	74	2	1
Lymphopenia	94	44	15	94	36	10
Hepatobiliary						
Hyperbilirubinemia	22	9	2	34	14	3

– Not observed or applicable.

Shown below by body system are the adverse events in <5% of patients reported as related to the administration of XELODA and that were clinically at least remotely relevant. In parentheses is the incidence of grade 3 or 4 occurrences of each adverse event.

Gastrointestinal: intestinal obstruction (1.1), rectal bleeding (0.4), GI hemorrhage (0.2), esophagitis (0.4), gastritis, colitis, duodenitis, haematemesis, necrotizing enterocolitis

Skin: increased sweating (0.2), photosensitivity (0.2), radiation recall syndrome (0.2)

General: chest pain (0.2)

Neurological: ataxia (0.4), encephalopathy (0.2), depressed level of consciousness (0.2), loss of consciousness (0.2)

XELODA® (capecitabine)

Metabolism: cachexia (0.4), hypertriglyceridemia (0.2)

Respiratory: dyspnea (0.5), epistaxis (0.2), bronchospasm (0.2), respiratory distress (0.2)

Infections: oral candidiasis (0.2), upper respiratory tract infection (0.2), urinary tract infection (0.2), bronchitis (0.2), pneumonia (0.2), sepsis (0.4), bronchopneumonia (0.2), gastroenteritis (0.2), gastrointestinal candidiasis (0.2), laryngitis (0.2), esophageal candidiasis (0.2)

Musculoskeletal: bone pain (0.2), joint stiffness (0.2)

Cardiac: angina pectoris (0.2), cardiomyopathy

Vascular: hypotension (0.2), hypertension (0.2), venous phlebitis and thrombophlebitis (0.2), deep venous thrombosis (0.7), lymphoedema (0.2), pulmonary embolism (0.4), cerebrovascular accident (0.2)

Blood: coagulation disorder (0.2), idiopathic thrombocytopenic purpura (0.2), pancytopenia (0.2)

Psychiatric: confusion (0.2)

Renal and Urinary: nocturia (0.2)

Hepatobiliary: hepatic fibrosis (0.2), cholestatic hepatitis (0.2), hepatitis (0.2)

Immune System: drug hypersensitivity (0.2)

OVERDOSAGE: *Acute:* Based on experience in animals and in humans treated up to doses of 3514 mg/m^2/day, the anticipated manifestations of acute overdose would be nausea, vomiting, diarrhea, gastrointestinal irritation and bleeding, and bone marrow depression. Medical management of overdose should include customary supportive medical interventions aimed at correcting the presenting clinical manifestations. Although no clinical experience has been reported, dialysis may be of benefit in reducing circulating concentrations of 5'-DFUR, a low-molecular weight metabolite of the parent compound.

Single doses of XELODA were not lethal to mice, rats, and monkeys at doses up to 2000 mg/kg (2.4, 4.8, and 9.6 times the recommended human daily dose on a mg/m^2 basis).

DOSAGE AND ADMINISTRATION: The recommended dose of XELODA is 2500 mg/m^2 administered orally daily with food for 2 weeks followed by a 1-week rest period given as 3 week cycles. The XELODA daily dose is given orally in two divided doses (approximately 12 hours apart) at the end of a meal. XELODA tablets should be swallowed with water. The following table displays the total daily dose by body surface area and the number of tablets to be taken at each dose.

XELODA® (capecitabine)

Table 4. XELODA Dose Calculation According to Body Surface Area

Dose level 2500 mg/m^2/day		Number of tablets to be taken at each dose (morning and evening)	
Surface Area (m^2)	**Total Daily* Dose (mg)**	**150 mg**	**500 mg**
≤ 1.24	3000	0	3
1.25 - 1.36	3300	1	3
1.37 - 1.51	3600	2	3
1.52 - 1.64	4000	0	4
1.65 - 1.76	4300	1	4
1.77 - 1.91	4600	2	4
1.92 - 2.04	5000	0	5
2.05 - 2.17	5300	1	5
≥ 2.18	5600	2	5

*Total Daily Dose divided by 2 to allow equal morning and evening doses.

Dose Modification Guidelines: Patients should be carefully monitored for toxicity. Toxicity due to XELODA administration may be managed by symptomatic treatment, dose interruptions and adjustment of XELODA dose. Once the dose has been reduced it should not be increased at a later time.

The phenytoin dose may need to be reduced when phenytoin is concomitantly administered with XELODA (see PRECAUTIONS: *Drug-Drug Interactions*).

Table 5. Recommended Dose Modifications

Toxicity NCIC Grades*	During a Course of Therapy	Dose Adjustment for Next Cycle (% of starting dose)
• *Grade 1*	Maintain dose level	Maintain dose level
• *Grade 2*		
-1st appearance	Interrupt until resolved to grade 0-1	100%
-2nd appearance	Interrupt until resolved to grade 0-1	75%
-3rd appearance	Interrupt until resolved to grade 0-1	50%
-4th appearance	Discontinue treatment permanently	
• *Grade 3*		
-1st appearance	Interrupt until resolved to grade 0-1	75%
-2nd appearance	Interrupt until resolved to grade 0-1	50%
-3rd appearance	Discontinue treatment permanently	

XELODA® (capecitabine)

Toxicity NCIC Grades*	During a Course of Therapy	Dose Adjustment for Next Cycle (% of starting dose)
• *Grade 4*		
-1st appearance	Discontinue permanently *or* If physician deems it to be in the patient's best interest to continue, interrupt until resolved to grade 0-1	50%

*National Cancer Institute of Canada Common Toxicity Criteria were used except for the Hand-and-Foot Syndrome (see PRECAUTIONS).

Dosage modifications are not recommended for grade 1 events. Therapy with XELODA should be interrupted upon the occurrence of a grade 2 or 3 adverse experience. Once the adverse event has resolved or decreased in intensity to grade 1, then XELODA therapy may be restarted at full dose or as adjusted according to the above table. If a grade 4 experience occurs, therapy should be discontinued or interrupted until resolved or decreased to grade 1, and therapy should be restarted at 50% of the original dose. Doses of capecitabine omitted for toxicity are not replaced or restored; instead the patient should resume the planned treatment cycles.

Adjustment of Starting Dose in Special Populations:

Hepatic Impairment: In patients with mild to moderate hepatic dysfunction due to liver metastases, no starting dose adjustment is necessary; however, patients should be carefully monitored. Patients with severe hepatic dysfunction have not been studied.

Renal Impairment: In patients with moderate renal impairment (creatinine clearance 30-50 mL/min [Cockroft and Gault, as shown below]) at baseline, a dose reduction to 75% of the XELODA starting dose (from 2500 mg/m^2/day to 1900 mg/m^2/day) is recommended. In patients with mild renal impairment (creatinine clearance 51-80 mL/min) no adjustment in starting dose is recommended. Careful monitoring and prompt treatment interruption is recommended if the patient develops a grade 2, 3, or 4 adverse event with subsequent dose adjustments as outlined in the table above. XELODA is contraindicated in patients with severe renal impairment (creatinine clearance below 30 mL/min [Cockroft and Gault]).

Cockroft and Gault Equation:

$$\text{Creatinine clearance for males} = \frac{(140 - \text{age [yrs]})\ (\text{body wt [kg]})}{(72)\ (\text{serum creatinine [mg/dL]})}$$

Creatinine clearance for females = 0.85 x male value

XELODA® (capecitabine)

Geriatrics: The elderly may be pharmacodynamically more sensitive to the toxic effects of 5-FU and therefore, physicians should exercise caution in monitoring the effects of XELODA in the elderly. Insufficient data are available to provide a dosage recommendation.

HOW SUPPLIED: XELODA is supplied as biconvex, oblong film-coated tablets, available in bottles as follows:

150 mg

color: light peach
engraving: XELODA on one side, 150 on the other
150 mg tablets packaged in bottles of 120 (NDC 0004-1100-51)

500 mg

color: peach
engraving: XELODA on one side, 500 on the other
500 mg tablets packaged in bottles of 240 (NDC 0004-1101-16)

Storage Conditions: **Store at 25°C (77°F); excursions permitted to 15° to 30°C (59° to 86°F), keep tightly closed.** [See USP Controlled Room Temperature]

*Maalox is a registered trademark of Novartis.

R_X only

Pharmaceuticals

Roche Laboratories Inc.
340 Kingsland Street
Nutley, New Jersey 07110-1199

27897445-1100

Revised: November 2000
Printed in USA

XELODA® (capecitabine)

PATIENT PACKAGE INSERT (text only):

Patient Information About XELODA® (capecitabine) Tablets

This information will help you learn more about XELODA® (capecitabine) Tablets. It cannot, however, cover all possible precautions or side effects associated with XELODA nor does it list all the benefits and risks of XELODA. Your doctor should always be your first choice for detailed information about your medical condition and your treatment. Be sure to ask your doctor about any questions you may have.

What is XELODA?

- XELODA [zeh-LOE-duh] is an oral medication for the treatment of advanced breast cancer resistant to treatment with paclitaxel [pak-lih-TAK-sil] and an anthracycline [ann-thruh-SYE-kleen]-containing chemotherapy regimen. Paclitaxel is also known as Taxol®*. Anthracyclines include Adriamycin®† or doxorubicin.

- XELODA tablets come in two strengths: 150 mg (light peach) and 500 mg (peach).

How does XELODA work?

XELODA is converted in the body to the substance 5-fluorouracil. In some patients, this substance kills cancer cells and decreases the size of the tumor.

Who should not take XELODA?

- Patients allergic to 5-fluorouracil.

- Studies in animals suggest that XELODA may cause serious harm to an unborn child. No studies have been done with pregnant women. If you are pregnant, be sure to discuss with your doctor whether XELODA is right for you. Also, tell your doctor if you are nursing.

- Patients with severe renal impairment. Please inform your doctor if you know of any renal impairment that you may have. Your doctor may either prescribe a different drug or reduce the XELODA dose.

How should I take XELODA?

Your doctor will prescribe a dose and treatment regimen that is right for *you*. Your doctor may want you to take a combination of *150 mg* and *500 mg* tablets for each dose. If a combination of tablets is prescribed, it is very important that you correctly identify the tablets. Taking the wrong tablets could result in an overdose (too much medication) or underdose (too little medication). The 150 mg tablets are light peach in color and have 150 engraved on one side. The 500 mg tablets are peach in color and have 500 engraved on one side.

XELODA® (capecitabine)

- Take the tablets in the combination prescribed by your doctor for your **morning and evening** doses.
- Take the tablets within **30 minutes after the end of a meal** (breakfast and dinner).
- XELODA tablets should be **swallowed with water.**
- It is important that you take all your medication as prescribed by your doctor.
- If you are taking the vitamin folic acid, please inform your doctor.
- If you are taking phenytoin (also known as Dilantin®‡), please inform your doctor. Your doctor may need to more frequently test the levels of phenytoin in your blood and/or change the dose of phenytoin that you are taking.
- If you are taking warfarin (also known as Coumadin®§), please inform your doctor. Your doctor may need to more frequently check how quickly your blood is clotting.

How long will I have to take XELODA?

It is recommended that XELODA be taken for 14 days followed by a 7-day rest period (no drug) given as a 21-day cycle. Your doctor will determine how many cycles of treatment you will need.

What if I miss a dose?

If you miss a dose of XELODA, do not take the missed dose at all and do not double the next one. Instead, continue your regular dosing schedule and check with your doctor.

What are the most common side effects of XELODA?

The most common side effects of XELODA are:

- diarrhea, nausea, vomiting, stomatitis (sores in mouth and throat), abdominal pain, constipation, loss of appetite or decreased appetite, and dehydration (excessive water loss from the body).
- hand-and-foot syndrome (palms of the hands or soles of the feet tingle, become numb, painful, swollen or red), rash, dry or itchy skin.
- tiredness, weakness, dizziness, headache, and fever.

When should I call my doctor?

It is important that you **CONTACT YOUR DOCTOR IMMEDIATELY** if you experience the following side effects. This will help reduce the likelihood that the side effect will continue or

become serious. Your doctor may instruct you to decrease the dose and/or temporarily discontinue treatment with XELODA.

STOP taking XELODA immediately and contact your doctor if any of these symptoms occur:

- ***Diarrhea:*** if you have more than 4 bowel movements each day or any diarrhea at night.
- ***Vomiting:*** if you vomit more than once in a 24-hour time period.
- ***Nausea:*** if you lose your appetite, and the amount of food you eat each day is much less than usual.
- ***Stomatitis:*** if you have pain, redness, swelling, or sores in your mouth.
- ***Hand-and-foot syndrome:*** if you have pain, swelling or redness of hands and/or feet.
- ***Fever or Infection:*** if you have a temperature of 100.5°F or greater, or other evidence of infection.

If caught early, most of these side effects usually improve within 2 to 3 days after you stop taking XELODA. If they don't improve within 2 to 3 days, call your doctor again. After side effects have improved, your doctor will tell you whether to start taking XELODA again or what dose to use.

How should I store and use XELODA?

- Never share XELODA with anyone.
- XELODA should be stored at normal room temperature (about 65° to 85°F).
- Keep this and all other medications out of the reach of children.
- In case of accidental ingestion or if you suspect that more than the prescribed dose of this medication has been taken, contact your doctor or local poison control center or emergency room IMMEDIATELY.
- Medicines are sometimes prescribed for uses other than those listed in this leaflet. If you have any questions or concerns, or want more information about XELODA, contact your doctor or pharmacist.

* Taxol is a registered trademark of Bristol-Myers Squibb Company.
† Adriamycin is a registered trademark of Pharmacia & Upjohn Company.
‡ Dilantin is a registered trademark of Parke-Davis.
§ Coumadin is a registered trademark of DuPont Pharma.

Convection-enhanced delivery of a topoisomerase I inhibitor (nanoliposomal topotecan) and a topoisomerase II inhibitor (pegylated liposomal doxorubicin) in intracranial brain tumor xenografts[1]

Yoji Yamashita, Michal T. Krauze, Tomohiro Kawaguchi, Charles O. Noble,[2] Daryl C. Drummond,[2] John W. Park,[2] and Krystof S. Bankiewicz[3]

Department of Neurological Surgery, Brain Tumor Research Center (Y.Y., M.T.K., T.K., K.S.B.), and Division of Hematology-Oncology (C.O.N., J.W.P.), University of California, San Francisco, San Francisco, CA 94103; and Hermes Biosciences, Inc., South San Francisco, CA 94080 (D.C.D., J.W.P.); USA

Despite multimodal treatment options, the response and survival rates for patients with malignant gliomas remain dismal. Clinical trials with convection-enhanced delivery (CED) have recently opened a new window in neuro-oncology to the direct delivery of chemotherapeutics to the CNS, circumventing the blood-brain barrier and reducing systemic side effects. Our previous CED studies with liposomal chemotherapeutics have shown promising antitumor activity in rodent brain tumor models. In this study, we evaluated a combination of nanoliposomal topotecan (nLs-TPT) and pegylated liposomal doxorubicin (PLD) to enhance efficacy in our brain tumor models, and to establish a CED treatment capable of improving survival from malignant brain tumors. Both liposomal drugs decreased key enzymes involved in tumor cell replication in vitro. Synergistic effects of nLs-TPT and PLD on U87MG cell death were found. The combination displayed excellent efficacy in a CED-based survival study 10 days after tumor cell implantation. Animals in the control group and those in single-agent groups had a median survival of less than 30 days, whereas the combination group experienced a median survival of more than 90 days. We conclude that CED of two liposomal chemotherapeutics (nLs-TPT and PLD)

Received January 27, 2006; accepted May 30, 2006.

[1]Grant support for this study was received from the National Cancer Institute Specialized Program of Research Excellence grant (K.S.B. and J.W.P.) and from Accelerate Brain Cancer Cure (K.S.B.), NIH/NCI grant U54 CA90788 (J.W.P.), NIH/NCI contract N01-CO-27031-16 (Hermes Biosciences, Inc.), and CBCRP grant 7KB-0066 (D.C.D.)

[2]Charles Noble and Daryl Drummond hold stock options in Hermes Biosciences, Inc., a company developing the liposomal drug described in this article. John Park has a financial interest in and a management/advisory relationship with Hermes Biosciences and a consulting relationship with Johnson & Johnson. John Park and/or Hermes has a planned patent related to this work.

[3]Address correspondence to Krystof S. Bankiewicz, Department of Neurological Surgery, University of California, San Francisco, 1855 Folsom Street, Mission Center Building Room 226, San Francisco, CA 94103, USA (Krystof.Bankiewicz@ucsf.edu)

[4]Abbreviations used are as follows: BBB, blood-brain barrier; CED, convection-enhanced delivery; DiI-DS, $DiIC_{18}(3)$-DS; DSPE, disteroyl phosphatidylethanolamine; EC, effective concentration; HBS, HEPES-buffered saline; HBSS, Hanks' balanced salt solution without Ca^{2+} and Mg^{2+}; H&E, hematoxylin and eosin; HEPES, *N*-(2-hydroxyethyl)piperazine-*N*'-(2-ethanesulfonic acid); MS, median survival; MTD, maximum tolerated dose; nLs, nanoliposomal; PEG, polyethylene glycol; PLD, pegylated liposomal doxorubicin; TEA_8SOS, triethylammonium sucrose octasulfate; topo, topoisomerase; TPT, topotecan.

may be an effective treatment option for malignant gliomas. *Neuro-Oncology 9, 20–28, 2007 (Posted to Neuro-Oncology [serial online], Doc. D06-00015, October 3, 2006. URL www.dukeupress.edu/neuro-oncology; DOI: 10.1215/15228517-2006-016)*

Keywords: brain tumor, CED, convection-enhanced delivery, glioma, liposome, topotecan

Despite intensive multimodal treatment such as surgical resection, malignant glioma (e.g., glioblastoma multiforme) remains the most difficult neoplasm to treat. Poor penetration of most anticancer drugs across the blood-brain barrier (BBB)[4] into the CNS after systemic administration is the one of the major obstacles to improvement in survival for this group of patients. Even with drugs that penetrate the BBB, it is difficult to reach sufficient drug concentrations in brain tumor tissue without causing considerable systemic toxicity (Groothuis, 2000).

Convection-enhanced delivery (CED) is a promising local delivery technique. This technique uses bulk flow to deliver small or large molecules directly to targeted sites in clinically significant volumes of tissue, and it provides wider distribution as compared with simple diffusion techniques (Bobo et al., 1994). CED of therapeutic agents circumvents the BBB, delivering a high concentration of therapeutic agent in the immediate vicinity of the tumor, minimizing systemic exposure, and thus results in a significant shift in the toxicity profile for the drug.

However, because CED distributes therapeutic agents not only to the tumor mass, but also beyond the tumor margin into normal surrounding brain tissue, a strategy for minimizing toxicity to normal brain tissue is needed. Liposomal drugs are promising candidates for local delivery in this regard, because they are inert until the drug is released from the confines of the nanocarrier. Liposomes, microscopic phospholipid nanoparticles with a bilayered membrane structure, are vehicles for administering therapeutic agents, such as drugs and genes, to areas of the body afflicted with cancer. Liposomes have been shown to provide stable encapsulation for various anticancer drugs and have many advantages over the corresponding free drugs for the systemic treatment of cancer (Allen and Martin, 2004; Drummond et al., 1999). One potential advantage of liposome-encapsulated cytotoxic drugs over corresponding unencapsulated agents is prolongation of systemic drug half-life (Allen et al., 1995; Drummond et al., 1999; Gabizon et al., 2003). We have recently developed a novel intraliposomal stabilization strategy for preparing highly stable nanoliposomal drugs (Drummond et al., 2005). In conjunction with CED, it was expected that antineoplastic drugs would be released slowly in the brain, prolonging exposure of brain tumor cells to the drugs, and that this delivery pattern would provide greater efficacy and less toxicity than treatment with free drugs. In fact, CED of liposomal antineoplastic agents demonstrated an excellent selective toxicity against tumor tissue (Noble et al., 2006; Saito et al., 2006a, b). We have also demonstrated that CED of liposomal CPT-11 resulted in no apparent leakage of drug from the CNS to the systemic circulation and produced no signs of systemic side effects (Noble et al., 2006).

Topoisomerase inhibitors have played an important role in cancer chemotherapy. There has therefore been considerable interest in combining topoisomerase I (topo I) inhibitors with topoisomerase II (topo II) inhibitors, because agents that target topo I and topo II exert their principal effects on the two major classes of enzymes involved in regulating DNA topology, which overlap functionally. The feasibility of administering a combination of topo I and topo II inhibitors to patients with advanced solid malignancies has been evaluated in numerous clinical studies (Ando et al., 1997; Hammond et al., 1998; Herben et al., 1997; Penson et al., 2004). In the treatment of patients with brain tumors, both topo I and topo II inhibitors have been found to be promising agents (Gross et al., 2005; Hau et al., 2004; Pipas et al., 2005). We have started to evaluate the combination of nanoliposomal topotecan (nLs-TPT) to inhibit topo I and pegylated (polyethylene glycol–coated) liposomal doxorubicin (PLD) to inhibit topo II, in conjunction with CED in intracranial glioblastoma xenografts. Our previous studies with each liposomal agent alone in the treatment of various intracranial glioblastoma xenografts encouraged us to explore this combination further (Saito et al., 2006a, b; Yamashita et al., 2006). In this study, we used PLD and nLs-TPT to treat U87MG intracranial xenografts. The liposomal drug combination displayed synergy in our in vitro studies and excellent efficacy in large tumors (U87MG, day 10) in our survival studies.

Materials and Methods

Liposome Preparation

Pegylated liposomal doxorubicin (Doxil; Alza Pharmaceuticals, Mountain View, Calif.) was obtained commercially. The commercial PLD solution contained 2 mg/ml of doxorubicin. The PLD was diluted with HEPES (*N*-[2-hydroxyethyl]piperazine-*N*′-[2-ethanesulfonic acid]; pH 6.5)-buffered saline (HBS).

Topotecan and nLs-TPT were provided by Hermes Bioscience, Inc. (South San Francisco, Calif.). Topotecan-loaded liposomes were prepared with a modified remote-loading ion gradient and intraliposomal drug stabilization method, as described previously (Saito et al., 2006a). Briefly, after the lipids were dried in a solution of chloroform and methanol (9:1, vol/vol), they were next dried by rotary evaporation and then under vacuum for a minimum of 2 h. The lipids were subsequently resuspended in one volume of ethanol at 60°C. An aqueous solution of triethylammonium sucrose octasulfate (TEA_8SO5; 0.65 M TEA) was prepared by cation-exchange chromatography as described previously (Drummond et al., 2005) and was also heated to 60°C. Nine volumes of the TEA_8SO5 solution were then injected rapidly into the ethanolic lipid solution to form liposomes. The liposomes were sized by extrusion through polycarbonate filters of average size 0.1 μm, which resulted in an aver-

age size of 100–120 nm. Unencapsulated TEA_8SOS was removed by Sepharose CL-4B size-exclusion chromatography and eluted with water. HEPES and NaCl were added to adjust the final concentrations to 5 mM and 145 mM, respectively. Topotecan was added at a ratio of 350 g of TPT/mol of phospholipid, and loading was initiated by adjusting the pH to 6.5 and incubating the mixture for 30 min at 60°C, followed by quenching on ice for 15 min. Unencapsulated TPT was removed by Sephadex G-75 gel filtration chromatography, eluting with HBS (5 mM HEPES and 145 mM NaCl, pH 6.5), and the drug concentration and the phospholipid concentration of the purified solution were determined spectrophotometrically at 375 nm after dissolution in acidic methanol and by a standard phosphate assay (Bartlett et al., 1959), respectively. The loading efficiency was always greater than 95% for the preparations used in these studies.

$DiIC_{18}(3)$-DS (DiI-DS) liposomes (control liposomes) were prepared with the fluorescent membrane dye 1,1'-dioctadecyl-3,3,3',3'-tetramethylindocarbocyanine perchlorate ($DiIC_{18}$; Sigma, St. Louis, Mo.) as described previously by Saito et al. (2006a). Briefly, dioleoylphosphatidylcholine (DOPC), cholesterol (molar ratio, 3:2), polyethylene glycol–disteroyl phosphatidylethanolamine (PEG-DSPE; 0.5 mol% of phospholipid), and DiI-DS (0.5 mol%) were codiluted in chloroform and dried in a vacuum by rotary evaporation to form a lipid film. The lipid film was hydrated by shaking it in HBS, followed by six successive cycles of freezing at –80°C and thawing at 37°C. The resulting multilamellar liposomes were extruded through 0.1-μm polycarbonate membrane filters, yielding liposomes of an average diameter of 95.8 nm as determined by dynamic light scattering. The liposome concentration was measured by a standard phosphate assay, and the final liposome concentration was adjusted to 20 mM of phospholipid by diluting the suspension with HBS.

Distribution of Liposomes in Rodent CNS

The role of pegylation in regulating the distribution of liposomes in the brain upon administration by CED appears to be relatively complex. MacKay et al. (2005) have recently observed that liposomes stabilized with the neutral PEG2000-distearoylglycerol lipid displayed a volume of distribution that was 40% greater than observed for similarly constructed nonpegylated liposomes. However, we have recently observed that CED of liposomes prepared with the negatively charged PEG2000-DSPE lipid, similar to the highly pegylated liposomal doxorubicin employed in this study, had a volume of distribution that was nearly identical to nonpegylated liposomes (Saito et al., 2006b). Thus, we expect that the PLD and nLs-TPT coinfused in these studies will have similar distributions in the brain, despite the difference in pegylation of the carrier.

Tumor Cell Line

An established human glioblastoma multiforme cell line, U87MG, was obtained from the Brain Tumor Research Center Tissue Bank at the University of California, San Francisco. Cells were maintained as monolayers in a complete medium that consisted of Eagle's minimal essential medium supplemented with 10% fetal calf serum and nonessential amino acids. Cells were cultured at 37°C in a humidified atmosphere of 95% air and 5% CO_2.

Western Blotting for Topoisomerase I, Topoisomerase II, Cleaved Caspase-3, and α-Tubulin

One day prior to treatment, 4×10^5 cells per well were seeded into six-well multiwells (Corning Inc., Corning, N.Y.). After 24 h of incubation, cells were exposed to DiI-DS liposomes, PLD (5 μg doxorubicin/ml), nLs-TPT (1 μg TPT/ml), or both (PLD at 2.5 μg doxorubicin/ml + topotecan liposomes at 0.5 μg TPT/ml) in complete medium. After a 24-h incubation, cells were collected, and protein was extracted in cell lysis buffer (Cell Signaling Technology, Beverly, Mass.). Equal amounts of protein (10 μg) were separated on a 12% bis-tris gel (Invitrogen, Carlsbad, Calif.) and electroblotted onto an Immobilon-P membrane (Millipore, Bedford, Mass.). The membrane was blocked in 5% skim milk and incubated with primary antibodies against topoisomerase I (1:2000; TopoGEN, Port Orange, Fla.), topoisomerase IIα (1:1000; Chemicon, Calif.), cleaved caspase-3 (1:1000; Cell Signaling Technology), or α-tubulin (1:2000; Santa Cruz Biotechnology, Calif.) overnight at 4°C. Bound antibody was detected with horseradish peroxidase–conjugated secondary antibodies by using ECL Western blotting detection reagents (Amersham, Piscataway, N.J.).

Cell Cycle Analysis

One day prior to treatment, 2×10^5 cells/well were seeded into each well of a six-well plate (Corning Inc.). After a 24-h incubation, cells were exposed to DiI-DS liposomes (control liposomes), PLD (2.5 μg doxorubicin/ml), nLs-TPT (0.5 μg TPT/ml), or both (PLD, 2.5 μg doxorubicin/ml, + topotecan liposomes, 0.5 μg TPT/ml) in complete medium. After 24 h, cells were fixed in 70% ethanol, washed, digested with RNaseA (Sigma), stained with propidium iodide (Sigma), and subjected to flow cytometry in a FACScan machine (Becton-Dickinson, San Jose, Calif.) with 10,000 events per determination. ModFit LT software (Verity Software House, Inc., Topsham, Maine) was used to assess the cell cycle distribution.

MTT Cell Viability Assay

Cells were seeded at 1000 cells per well in 96-well plates (Corning Inc.), allowed to attach for 24 h, and then exposed to DiI-DS liposomes (control liposomes), PLD, nLs-TPT, or both, in complete medium. MTT (3-[4,5-dimethylthiazol-2-yl]-5-[3-carboxymethoxyphenyl]-2-[4-sulfophenyl]-2*H*-tetrazolium) reagent was added 48 h after initiation of treatment, and plates were read at an absorbance of 490 nm 3 h later with a Spectra-

Max microplate reader (Molecular Device Corporation, Sunnyvale, Calif.). All treatments were performed in triplicate. The background absorbance was determined by incubating media with substrate alone and subtracting the values from wells containing cells only.

Animals and Intracranial Xenograft Technique

Male Sprague-Dawley rats (250 g) were obtained from Charles-River Laboratories (Wilmington, Mass.). Congenitally athymic, male, homozygotic, nude rats (*rnu/rnu*; 150–200 g) were purchased from the National Cancer Institute (Bethesda, Md.) and housed under aseptic conditions that included filtered air, as well as sterilized food, water, bedding, and cages. All protocols were approved by the Institutional Animal Care and Use Committee at the University of California, San Francisco. For the intracranial xenograft tumor model, U87MG cells were harvested by trypsinization, washed once with Hanks' balanced salt solution without Ca^{2+} and Mg^{2+} (HBSS), and resuspended in HBSS for implantation. A cell suspension containing 5×10^5 cells/10 μl of HBSS was implanted into the striatal region of the athymic rat brains. Under deep isoflurane anesthesia, rats were placed in a small-animal stereotactic frame (David Kopf Instruments, Tujunga, Calif.). A sagittal incision was made through the skin to expose the cranium, and a burr hole was made in the skull at 0.5 mm anterior and 3 mm lateral from the bregma with a small dental drill. At a depth of 4.5 mm from the brain surface, 5 μl of cell suspension was injected; 2 min later, another 5 μl was injected at a depth of 4 mm; and 2 min later, the needle was removed and the wound sutured.

Convection-Enhanced Delivery

Throughout this study, free doxorubicin or PLD was delivered in a volume of 20 μl with the CED method described previously (Bankiewicz et al., 2000; Saito et al., 2004). Briefly, the infusion system consisted of a fused-silica needle cannula that was connected to a loading line (containing liposomes) and an oil-infusion line. A 1-ml syringe (filled with oil) was mounted onto a microinfusion pump (BeeHive; Bioanalytical Systems, West Lafayette, Ind.) that regulated the flow of fluid through the system. By referring to tumor injection site coordinates, the step-design cannula was mounted onto stereotactic holders and guided to the targeted region of the brain through burr holes made in the skull (see the previous section for details). The following ascending infusion rates were applied to achieve the 20-μl infusion: 0.2 μl/min (15 min) + 0.5 μl/min (10 min) + 0.8 μl/min (15 min). The step-design cannula used for all CED procedures in this study was reflux free and backflow free at infusion rates up to 50 μl/min (Krauze et al., 2005a).

Evaluation of Toxicity

Three normal Sprague-Dawley rats were evaluated for potential local toxicity after CED-mediated coinfusion of PLD and nLs-TPT. CED was performed as described in the previous section. Rats were monitored daily for general health (alertness, grooming, feeding, excreta, skin, fur, mucous membrane condition, ambulation, breathing, and posture). Animal weights were reported weekly. Both liposomal drugs were used at half the maximum tolerated dose (MTD) that was determined in previous studies (Saito et al., 2006b; Yamashita et al., 2006). Sixty days after CED of 20 μl of PLD (0.1 mg/ml) and 20 μl of nLs-TPT (0.25 mg/ml) into the striatum, rats were euthanized and their brains fixed in 4% formaldehyde. Fixed brain tissue was subjected to paraffin sectioning (5 μm) and stained with hematoxylin and eosin (H&E).

Combination Therapy Against the U87MG Intracranial Xenograft Model

Thirty-two rats, implanted with U87MG tumor cells, were randomly divided into four CED treatment groups of eight rats each: (1) a control group treated with DiI-DS fluorescent liposomes, (2) a group treated with PLD (0.1 mg/ml doxorubicin), (3) a group treated with nLs-TPT (0.25 mg/ml), and (4) a group receiving a combination treatment of PLD (0.1 mg/ml) together with nLs-TPT (0.25 mg/ml) ($n = 8$). Ten days after tumor cell implantation, a CED of 20 μl of the specified drug was performed for each group. Rats were monitored daily for survival and general health (alertness, grooming, feeding, excreta, skin, fur, mucous membrane conditions, ambulation, breathing, and posture). Animal weights were reported weekly. The study was terminated 90 days after tumor implantation, surviving animals were euthanized, and their brains were stained with H&E. An additional three rats were implanted with U87MG tumor cells and euthanized 10 days after implantation to estimate the tumor size on the treatment day used in this study.

Statistical Analysis

Results for the survival studies were expressed as a Kaplan-Meier curve. Survival of the treatment groups was compared with a log-rank test and median survival.

Results

Expression of Topoisomerase I and Topoisomerase IIα in U87MG Cells

Both topo I and topo II were highly expressed in U87MG cells (Fig. 1A). After treatment with nLs-TPT, depletion of topo I expression was observed (Fig. 1C). A similar decrease in topo II was seen (Fig. 1C), confirming that no compensatory increase in topo II occurred. Treatment with PLD resulted in a reduction in topo II expression, but there was no significant effect on the expression of topo I (Fig. 1B). After simultaneous exposure to PLD and nLs-TPT, a significant reduction in both topoisomerase isoforms was observed (Fig. 1D).

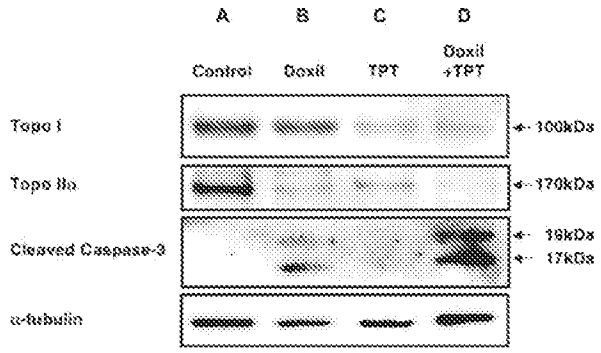

Fig. 1. Western blotting for topo I, topo IIα, and cleaved caspase-3. U87MG cells were incubated for 24 h with PLD (5 μg/ml), nLs-TPT (1 μg/ml), or a combination of PLD (2.5 μg/ml) and nLs-TPT (0.5 μg/ml). Western blotting was used for detection of topo I, topo IIα, cleaved caspase-3, and α-tubulin. A. The untreated control cells (U87MG) show high levels of topo I and topo IIα expression. B. Cells incubated with PLD (Doxil) show downregulation of topo IIα, upregulation of cleaved caspase-3, and similar levels of topo I when compared with control cells. C. Cells incubated with nLs-TPT show downregulation of topo I and topo IIα and no signal for cleaved caspase-3. D. The combination of PLD and nLs-TPT shows downregulation of topo I and topo IIα and increased levels of cleaved caspase-3.

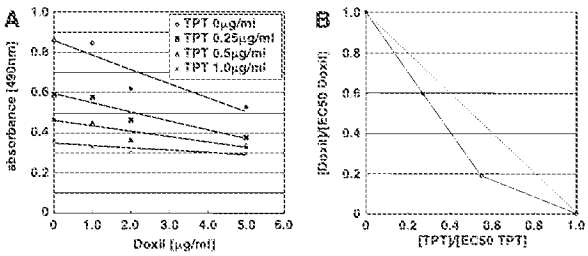

Fig. 2. Synergistic induction of cell death by PLD and nLs-TPT in U87MG glioma cells. A. U87MG cells were treated for 48 h with increasing nLs-TPT concentrations (0–1 μg/ml) and 24 h with increasing PLD concentrations (0–5 μg/ml). B. Synergy between the two agents is expressed in an isobologram.

The molecular events occurring during synergistic induction of cell death by PLD and nLs-TPT were characterized in U87MG cells at approximate EC_{50} concentrations (concentrations that were effective in inducing death in 50% of the U87MG cells). Western blots for cleaved caspase-3 detected the activation of caspase-3 in U87MG cells treated with PLD (5 μg/ml) (Fig. 1B), or at considerably higher levels upon coexposure to PLD (2.5 μg/ml) and nLs-TPT (1 μg/ml) (Fig. 1D). After treatment with the combination of PLD and nLs-TPT, caspase-3 activation increased considerably, even though both liposomal drugs were used at approximate EC_{25} concentration, half of the dose employed in the single-drug treatment groups.

Synergistic Cytotoxic Effects of PLD and Topotecan Liposome In Vitro

Synergy, as determined by isobologram analysis (Berenbaum, 1981), was observed between the two agents (Fig. 2). EC_{50} values (median effect doses) calculated from this experiment were 6.08 μg/ml for PLD and 0.91 μg/ml for topotecan liposome and were plotted on a graph to show synergy (values under the dashed line Fig. 2B).

Cell Cycle Distributions In Vitro

Although activation of caspase-3 was not observed within 24 h after treatment with nLs-TPT in U87MG cells, prolonged exposure of these cells to nLs-TPT resulted in marked S-phase accumulation (62% with topotecan liposomes vs. 19% with control liposomes; Fig. 3C and Fig. 3A, respectively). In contrast, cells treated with PLD, a G2/M-active antineoplastic drug, underwent G2 arrest, with the percentage of cells in G2/M increasing from 21% prior to PLD treatment to 34% 24 h later (Fig. 3B). At 24 h after combination treatment with PLD and nLs-TPT, both S-phase accumulation and G2 arrest were observed in U87MG cells (Fig. 3D).

Toxicity of Combination Treatment in Normal Rat Brain

The rats receiving the combination treatment (CED infusion with 0.1 mg/ml of doxorubicin as PLD and 0.25 mg/ml of nLs-TPT) survived without any neurological symptoms, and the tissue damage was negligible (Fig. 4). The MTD for each therapeutic was determined in previous studies, that is, 0.2 mg/ml for doxorubicin as PLD and 0.5 mg/ml for nLs-TPT. No increase in tissue damage was observed in comparison with similar data

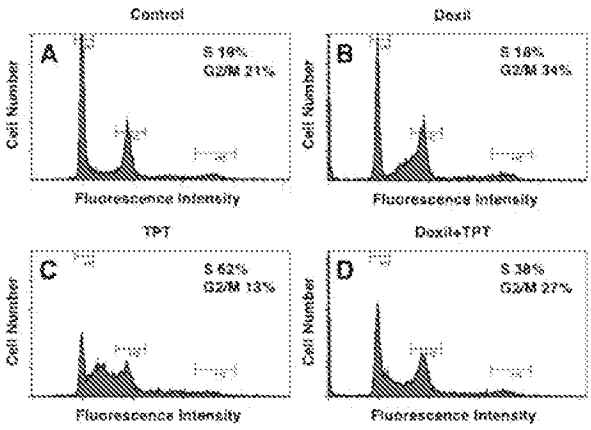

Fig. 3. Cell cycle profiles of U87MG cells examined by flow cytometry. U87MG cells were harvested for analysis and exposed to A. DiI-DS fluorescent liposomes (control), B. PLD (2.5 μg/ml), C. topotecan liposomes (TPT) (0.5 μg/ml), or D. a combination of PLD (2.5 μg/ml) and TPT (0.5 μg/ml) for 24 h.

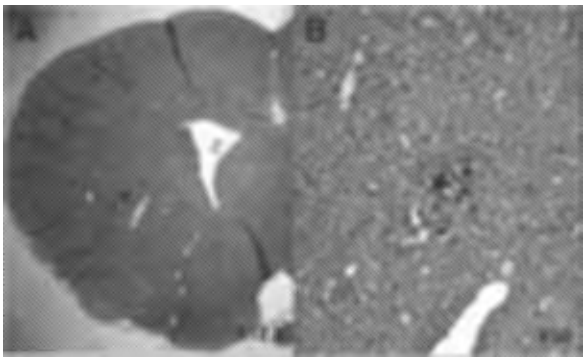

Fig. 4. Toxicity evaluation. Sixty days after CED infusion of 0.1 mg/ml of doxorubicin as PLD and 0.25 mg/ml of topotecan as liposomal drug into the striatum of intact Sprague-Dawley rats (n = 3), rats were euthanized, and 5-μm paraffin sections of their brains were obtained. A. Representative H&E sections from a single rat are shown. B. Only a small region of inflammation was detected just adjacent to the needle tract.

from previous studies (Saito et al., 2006a; Yamashita et al., 2006).

Combined Effect of PLD and nLs-TPT in U87MG Brain Tumor Xenografts In Vivo

Rats in the control group, which received liposomes tagged with the fluorescent dye DiI-DS, were all euthanized 19 to 22 days after tumor cell implantation because of neurological symptoms indicative of tumor progression. The median survival (MS) for this group was 20 days (Fig. 5A-1). One of eight rats that received 0.1 mg/ml PLD by CED survived until termination of the study. However, neurological symptoms caused by large tumor formations were observed in the seven other rats, requiring euthanasia at 16 to 31 days after tumor cell implantation. No significant improvement in survival was noted in this treatment group ($P = 0.0789$), with an MS of 21.5 days (Fig. 5A-2). Two of eight rats that received treatment at 0.25 mg/ml nLs-TPT by CED survived until termination of the study. Because of neurological symptoms indicating tumor progression, the six other rats in this group had to be euthanized 20 to 46 days after tumor cell implantation. In contrast with treatment with PLD, a significant survival benefit for nLs-TPT was found ($P = 0.002$), with an MS for this group of 27.5 days (Fig. 5A-3). However, rats in the group that received the combination treatment of PLD and nLs-TPT demonstrated a significant improvement in survival ($P = 0.0004$), surviving significantly longer than the rats in the single-agent therapy groups, with six of eight rats surviving until termination of the study (MS > 90 days) (Fig. 5A-4). To estimate tumor size at time of treatment, three additional rats from the control group were euthanized on day 10 after tumor implantation (Fig. 5B).

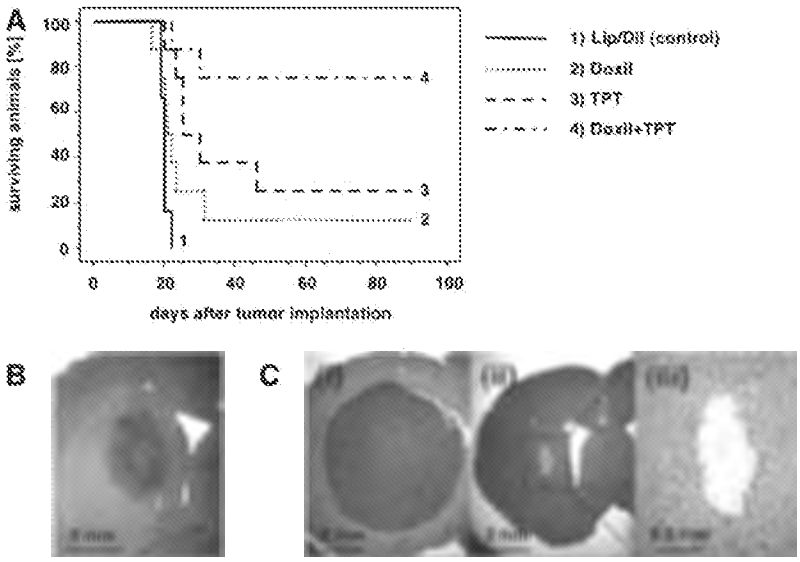

Fig. 5. Survival study. A. Chemotherapy with a combination of PLD and topotecan liposomes prolongs the survival of U87MG brain tumor xenografts. Survival of treated animals was observed for 90 days and is expressed as a Kaplan-Meier curve. Eight rats for each group were used in the experimental design of the survival study. B. U87MG xenograft size on day 10 after tumor cell implantation after treatment with DiI liposomes (control) (n = 3, H&E staining). In histological findings at necropsy, H&E staining of the brains of rats that failed to survive the observation period revealed large tumor formation C. (i), whereas in the brains of rats that received combination therapy and survived the observation period, fibrous scar tissues were detected C. (ii), (iii).

Discussion

Clinical trials to evaluate the combination of topo I and topo II inhibitors via intravenous administration in patients with solid neoplasms have demonstrated substantial toxicity (Ando et al., 1997; Hammond et al., 1998; Herben et al., 1997). Because the defined MTD was frequently lower than the typical dose level for the respective individual agent, the efficacy with systemic treatment was often limited by hematologic toxicities (Penson et al., 2004). For patients with brain tumors, systemic delivery of therapeutics is usually associated with systemic side effects while achieving marginal therapeutic concentrations in the CNS; thus the efficacy of systemic treatment is also limited. In an effort to improve drug delivery to the brain and to reduce systemic side effects caused by antineoplastic agents, recent studies have demonstrated the advantages of CED (Saito et al., 2004). Chemotherapeutic agents delivered locally by CED have produced favorable therapeutic outcomes (Bruce et al., 2000; Degen et al., 2003; Kaiser et al., 2000). However, highly cytotoxic agents with extensive distribution in the CNS have resulted in brain damage (Kaiser et al., 2000). Hence, good candidates for CED administration into brain tumors would ideally be the agents that show the highest possible therapeutic index against tumor cells over healthy neuronal cells. Liposomal drug delivery offers the potential for avoiding the high peak concentrations of bioavailable drug that are so often associated with pronounced toxicity (Noble et al., 2006).

In preclinical studies, topo I and topo II inhibitors have already been combined in many schedules and models. Topo I mRNA and protein levels in the tumor decreased, whereas topo II mRNA and protein levels rose after treatment with topo I inhibitor. The reverse effect, a fall in topo II and concurrent rise in topo I levels with topo II–active drug treatment, was also observed. The conclusion was that topo I and II agents can be combined to produce greater than additive tumor cytotoxicity without increase in host toxicity (Eder et al., 1998). In addition, initial treatment with topotecan was associated with increasing responsiveness of the xenografts to subsequent doses of doxorubicin (Kim et al., 1992). On the basis of these observations, we designed this study to determine whether a synergistic effect in vitro and in the U87MG intracranial rodent xenograft model in vivo could be observed.

It is generally accepted that the sensitivity of proliferating tumor cells to DNA-damaging agents is higher than that of quiescent tumor cells. Topo I inhibition increases the number of covalent topo I–DNA complexes within cells, and the interaction of these complexes with replication forks results in the formation of double-strand DNA breaks (Kaufmann et al., 1996; Rowinsky and Kaufmann, 1997). These DNA lesions are thought to be responsible for topotecan-induced cell death. This mechanism accounts for the maximum cytotoxicity of topotecan observed during the S phase of the cell cycle (Sinha, 1995; Taron et al., 2000). It has already been reported that prolonged exposure to low doses of topo I inhibitors, such as topotecan, results in an increase in G2-phase and/or S-phase cells (Cliby et al., 2002; Kim et al., 1992). S-phase cells increased in our U87MG cells after treatment with a novel, highly stable nanoliposomal topotecan. Furthermore, it was found that after topotecan administration, the subsequent administration of DNA-damaging antineoplastic drugs, at the interval of maximal topotecan-induced S-phase cell cycle arrest, could increase DNA damage, inhibiting DNA repair and G2/M transit, thus synergistically increasing cytotoxicity (Taron et al., 2000). It was expected that doxorubicin would be released slowly from the liposomes, to prolong the exposure of brain tumor cells that showed S-phase accumulation induced by topotecan liposomes, and that this delivery pattern would thereby provide a synergistic increase in efficacy (Allen and Martin, 2004). Additionally, we have shown previously that locally administered topotecan liposomes work as a drug source for effective antiangiogenic chemotherapy in malignant glioma xenografted models (Saito et al., 2006a). It was also reported that the breakdown of tumor vasculature induced by doxorubicin-containing liposomes might arise both from the vascular accumulation of liposomes and from cytotoxic effects on tumor vascular endothelial cells (Zhou et al., 2002).

In our previous study (Saito et al., 2006a), CED of nLs-TPT eradicated tumors and significantly enhanced survival of tumor-bearing rats, in comparison to similar animals that received only systemic administration of topotecan, a result that encouraged further exploration. On the other hand, the limited efficacy observed in a late treatment of a U87MG xenograft model clearly showed the necessity not only of highly selective toxicity, but also of improved cytotoxic activity toward tumor cells in vivo in more developed tumors (Saito et al., 2006a). In this study, by means of CED of a combination of PLD and nLs-TPT, we significantly prolonged the survival of tumor-bearing rats without increasing toxicity in the normal brain, even though the start of treatment was delayed as compared with the earlier study.

Our main aim in this study was to develop an effective treatment for the eradication of large intracranial U87MG tumor xenografts (day 10). As malignant human brain tumors are usually detected at an advanced stage, our study also focused on advanced tumor xenografts with an established vasculature. Rats receiving treatment on day 10 after U87MG implantation were approximately halfway through their average life expectancy after tumor inoculation. The combination of PLD and nLs-TPT showed impressive effects in vitro, and CED of this chemotherapeutic combination significantly improved therapeutic outcome in a large human U87MG glioma intracranial xenograft model.

We propose that this CED approach be used in future clinical studies. It seems likely that this new combination therapy may offer a new and potentially effective chemotherapeutic regimen in glioma therapy. As demonstrated in our previous reports (Krauze et al., 2005b; Mamot et al., 2004; Saito et al., 2004), liposomal gadolinium constructs can be imaged directly in the CNS during CED by MRI, and liposomes containing a marker for

imaging can be combined with liposome-encapsulated drugs, enabling real-time guidance of CED (Saito et al., 2005). Although current clinical CED protocols must be improved to translate our recent findings into the clinic, we believe that patients with inoperable glioblastoma are amenable to MRI-guided CED of liposomal drugs aided by the implantation of several catheters within and around tumor tissue. The introduction of our step-design catheter enables especially more precise distribution in the targeted area of the CNS (Krauze et al., 2005b). In our ongoing studies, we have shown that current CED difficulties in clinical trials, such as spillover or reflux in the vicinity of sulci and ventricles, are almost negligible when a step-design catheter is used (unpublished data). Moreover, to prevent relapse, patients undergoing tumor debulking might benefit from postoperative CED for tumor margins. Efficient future brain tumor therapies require three important steps: (1) visualized and controlled direct delivery of therapeutics to CNS, (2) therapeutic combination with high toxicity against malignant cells but low toxicity against healthy brain, and (3) pharmacokinetic profile of therapeutics that enables a long half-life and the introduction of metronomic chemotherapy that targets dormant cancer cells. Considerable progress regarding step 1 has been shown in our previous work. The search for optimal therapeutic combinations is under evaluation and forms part of the current work. Step 3 has been achieved by liposome encapsulation of therapeutics, which has improved the pharmacokinetic profile tremendously in CNS, and it is expected that further research in this expanding field will impact brain tumor treatment modalities. In summary, our approach may represent significant progress toward defining promising chemotherapeutic liposome combinations for future clinical application of CED for the treatment of gliomas.

Acknowledgment

Special thanks are extended to John Forsayeth for proofreading and editing this work.

References

Allen, T.M., and Martin, F.J. (2004) Advantages of liposomal delivery systems for anthracyclines. *Semin. Oncol.* **31**, 5–15.

Allen, T.M., Newman, M.S., Woodle, M.C., Mayhew, E., and Uster, P.S. (1995) Pharmacokinetics and anti-tumor activity of vincristine encapsulated in sterically stabilized liposomes. *Int. J. Cancer* **62**, 199–204.

Ando, M., Eguchi, K., Shinkai, T., Tamura, T., Ohe, Y., Yamamoto, N., Kurata, T., Kasai, T., Ohmatsu, H., Kubota, K., Sekine, I., Hojo, N., Matsumoto, T., Kodama, T., Kakinuma, R., Nishiwaki, Y., and Saijo, N. (1997) Phase I study of sequentially administered topoisomerase I inhibitor (irinotecan) and topoisomerase II inhibitor (etoposide) for metastatic non-small-cell lung cancer. *Br. J. Cancer* **76**, 1494–1499.

Bankiewicz, K.S., Eberling, J.L., Kohutnicka, M., Jagust, W., Pivirotto, P., Bringas, J., Cunningham, J., Budinger, T.F., and Harvey-White, J. (2000) Convection-enhanced delivery of AAV vector in parkinsonian monkeys; in vivo detection of gene expression and restoration of dopaminergic function using pro-drug approach. *Exp. Neurol.* **164**, 2–14.

Bartlett, G.R. (1959) Colorimetric assay methods for free and phosphorylated glyceric acids. *J. Biol. Chem.* **234**, 469–471.

Berenbaum, M.C. (1981) Criteria for analyzing interactions between biologically active agents. *Adv. Cancer Res.* **35**, 269–335.

Bobo, R.H., Laske, D.W., Akbasak, A., Morrison, P.F., Dedrick, R.L., and Oldfield, E.H. (1994) Convection-enhanced delivery of macromolecules in the brain. *Proc. Natl. Acad. Sci. USA* **91**, 2076–2080.

Bruce, J.N., Falavigna, A., Johnson, J.P., Hall, J.S., Birch, B.D., Yoon, J.T., Wu, E.X., Fine, R.L., and Parsa, A.T. (2000) Intracerebral clysis in a rat glioma model. *Neurosurgery* **46**, 683–691.

Cliby, W.A., Lewis, K.A., Lilly, K.K., and Kaufmann, S.H. (2002) S phase and G2 arrests induced by topoisomerase I poisons are dependent on ATR kinase function. *J. Biol. Chem.* **277**, 1599–1606.

Degen, J.W., Walbridge, S., Vortmeyer, A.O., Oldfield, E.H., and Lonser, R.R. (2003) Safety and efficacy of convection-enhanced delivery of gemcitabine or carboplatin in a malignant glioma model in rats. *J. Neurosurg.* **99**, 893–898.

Drummond, D.C., Meyer, O., Hong, K., Kirpotin, D.B., and Papahadjopoulos, D. (1999) Optimizing liposomes for delivery of chemotherapeutic agents to solid tumors. *Pharmacol. Rev.* **51**, 691–743.

Drummond, D.C., Marx, C., Guo, Z., Scott, G., Noble, C., Wang, D., Pallavicini, M., Kirpotin, D.B., and Benz, C.C. (2005) Enhanced pharmacodynamic and antitumor properties of a histone deacetylase inhibitor encapsulated in liposomes or ErbB2-targeted immunoliposomes. *Clin Cancer Res.* **11**, 3392–3401.

Eder, J.P., Chan, V., Wong, J., Wong, Y.W., Ara, G., Northey, D., Rizvi, N., and Teicher, B.A. (1998) Sequence effect of irinotecan (CPT-11) and topoisomerase II inhibitors in vivo. *Cancer Chemother. Pharmacol.* **42**, 327–335.

Gabizon, A., Shmeeda, H., and Barenholz, Y. (2003) Pharmacokinetics of pegylated liposomal doxorubicin: Review of animal and human studies. *Clin. Pharmacokinet.* **42**, 419–436.

Groothuis, D.R. (2000) The blood-brain and blood-tumor barriers: A review of strategies for increasing drug delivery. *Neuro-Oncology* **2**, 45–59.

Gross, M.W., Altscher, P., Brandtner, M., Haeusser-Mischlich, H., Chiricuta, I.C., Siegmann, A.D., and Engenhart-Cabillic, R. (2005) Open-label simultaneous radio-chemotherapy of glioblastoma multiforme with topotecan in adults. *Clin. Neurol. Neurosurg.* **107**, 207–213.

Hammond, L.A., Eckardt, J.R., Ganapathi, R., Burris, H.A., Rodriguez, G.A., Eckhardt, S.G., Rothenberg, M.L., Weiss, G.R., Kuhn, J.G., Hodges, S., Von Hoff, D.D., and Rowinsky, E.K. (1998) A phase I and translational study of sequential administration of the topoisomerase I and II inhibitors topotecan and etoposide. *Clin. Cancer Res.* **4**, 1459–1467.

Hau, P., Fabel, K., Baumgart, U., Rümmele, P., Grauer, O., Bock, A., Dietmaier, C., Dietmaier, W., Dietrich, J., Dudel, C., Hübner, F., Jauch, T., Drechsel, E., Kleiter, I., Wismeth, C., Zellner, A., Brawanski, A., Steinbrecher, A., Marienhagen, J., and Bogdahn, U. (2004) Pegylated liposomal doxorubicin-efficacy in patients with recurrent high-grade glioma. *Cancer* **100**, 1199–1207.

Herben, V.M., ten Bokkel Huinink, W.W., Dubbelman, A.C., Mandjes, I.A., Groot, Y., van Gortel-van Zomeren, D.M., and Beijnen, J.H. (1997) Phase I and pharmacological study of sequential intravenous topotecan and oral etoposide. *Br. J. Cancer* **76**, 1500–1508.

Kaiser, M.G., Parsa, A.T., Fine, R.L., Hall, J.S., Chakrabarti, I., and Bruce, J.N. (2000) Tissue distribution and antitumor activity of topotecan delivered by intracerebral clysis in a rat glioma model. *Neurosurgery* **47**, 1391–1398.

Kaufmann, S.H., Peereboom, D., Buckwalter, C.A., Svingen, P.A., Grochow, L.B., Donehower, R.C., and Rowinsky, E.K. (1996) Cytotoxic effects of topotecan combined with various anticancer agents in human cancer cell lines. *J. Natl. Cancer Inst.* **88**, 734–741.

Kim, R., Hirabayashi, N., Nishiyama, M., Jinushi, K., Toge, T., and Okada, K. (1992) Experimental studies on biochemical modulation targeting topoisomerase I and II in human tumor xenografts in nude mice. *Int. J. Cancer* **50**, 760–766.

Krauze, M.T., Saito, R., Noble, C., Tamas, M., Bringas, J., Park, J.W., Berger, M.S., and Bankiewicz, K. (2005a) Reflux-free cannula for convection-enhanced high-speed delivery for therapeutic agents. *J. Neurosurg.* **103**, 923–929.

Krauze, M.T., Mcknight, T.R., Yamashita, Y., Bringas, J., Noble, C.O., Saito, R., Geletneky, K., Forsayeth, J., Berger, M.S., Jackson, P., Park, J.W., and Bankiewicz, K.S. (2005b) Real-time visualization and characterization of liposomal delivery into the monkey brain by magnetic resonance imaging. *Brain Res. Brain Res. Protoc.* **16**, 20–26.

MacKay, J.A., Deen, D.F., and Szoka, F.C., Jr. (2005) Distribution in brain of liposomes after convection enhanced delivery; modulation by particle charge, particle diameter, and presence of steric coating. *Brain Res.* **1035**, 139–153.

Mamot, C., Nguyen, J.B., Pourdehnad, M., Hadaczek, P., Saito, R., Bringas, J.R., Drummond, D.C., Hong, K., Kirpotin, D.B., McKnight, T., Berger, M.S., Park, J.W., and Bankiewicz, K.S. (2004) Extensive distribution of liposomes in rodent brains and brain tumors following convection-enhanced delivery. *J. Neurooncol.* **68**, 1–9.

Noble, C.O., Krauze, M.T., Drummond, D.C., Yamashita, Y., Saito, R., Berger, M.S., Kirpotin, D.B., Bankiewicz, K.S., and Park, J.W. (2006) Novel nanoliposomal CPT-11 infused by convection-enhanced delivery in intracranial tumors: Pharmacology and efficacy. *Cancer Res.* **66**, 2801–2806.

Penson, R.T., Seiden, M.V., Goodman, A., Fuller, A.F., Jr., Berkowitz, R.S., Matulonis, U.A., Krasner, C., Lee, H., Atkinson, T., and Campos, S.M., for the Gynecologic Oncology Research Program at Dana Farber/Partners CancerCare (2004) Phase I trial of escalating doses of topotecan in combination with a fixed dose of pegylated liposomal doxorubicin in women with mullerian malignancies. *Gynecol. Oncol.* **93**, 702–707.

Pipas, J.M., Meyer, L.P., Rhodes, C.H., Cromwell, L.D., McDonnell, C.E., Kingman, L.S., Rigas, J.R., and Fadul, C.E. (2005) A phase II trial of paclitaxel and topotecan with filgrastim in patients with recurrent or refractory glioblastoma multiforme or anaplastic astrocytoma. *J. Neurooncol.* **71**, 301–305.

Rowinsky, E.K., and Kaufmann, S.H. (1997) Topotecan in combination chemotherapy. *Semin. Oncol.* **24** (suppl.), S20-11–S20-S26.

Saito, R., Bringas, J.R., McKnight, T.R., Wendland, M.F., Mamot, C., Drummond, D.C., Kirpotin, D.B., Park, J.W., Berger, M.S., and Bankiewicz, K.S. (2004) Distribution of liposomes into brain and rat brain tumor models by convection-enhanced delivery monitored with magnetic resonance imaging. *Cancer Res.* **64**, 2572–2579.

Saito, R., Krauze, M.T., Bringas, J.R., Noble, C., McKnight, T.R., Jackson, P., Wendland, M.F., Mamot, C., Drummond, D.C., Kirpotin, D.B., Hong, K., Berger, M.S., Park, J.W., and Bankiewicz, K.S. (2005) Gadolinium-loaded liposomes allow for real-time magnetic resonance imaging of convection-enhanced delivery in the primate brain. *Exp. Neurol.* **196**, 381–389.

Saito, R., Krauze, M.T., Noble, C.O., Drummond, D.C., Kirpotin, D.B., Berger, M.S., Park, J.W., and Bankiewicz, K.S. (2006a) Convection-enhanced delivery of Ls-TPT enables an effective, continuous, low-dose chemotherapy against malignant glioma xenograft model. *Neuro-Oncology* **8**, 205–214.

Saito, R., Krauze, M.T., Noble, C.O., Tamas, M., Drummond, D.C., Kirpotin, D.B., Berger, M.S., Park, J.W., and Bankiewicz, K.S. (2006b) Tissue affinity of the infusate affects distribution volume during convection-enhanced delivery into rodent brains: Implications for local drug delivery. *J. Neurosci. Methods* **154**, 225–232.

Sinha, B.K. (1995) Topoisomerase inhibitors. A review of their therapeutic potential in cancer. *Drugs* **49**, 11–19.

Taron, M., Plasencia, C., Abad, A., Martin, C., and Guillot, M. (2000) Cytotoxic effects of topotecan combined with various active G2/M-phase anticancer drugs in human tumor-derived cell lines. *Invest. New Drugs* **18**, 139–147.

Yamashita Y., Saito R., Krauze, M.T., Kawaguchi, T., Noble, C., Drummond, D.C., Kirpotin, D.B., Park, J.W., Berger, M.S., and Bankiewicz, K.S. (2006) Convection-enhanced delivery of liposomal doxorubicin in intracranial brain tumor xenografts. *Targeted Oncol.* **1**, 79–85.

Zhou, R., Mazurchuk, R., and Straubinger, R.M. (2002) Antivasculature effects of doxorubicin-containing liposomes in an intracranial rat brain tumor model. *Cancer Res.* **62**, 2561–2566.

Targ Oncol (2006) 1: 79–85
DOI 10.1007/s11523-006-0011-8

ORIGINAL RESEARCH

Yoji Yamashita · Ryuta Saito · Michal T. Krauze · Tomohiro Kawaguchi · Charles Noble · Daryl C. Drummond · Dmitri B. Kirpotin · John W. Park · Mitchel S. Berger · Krystof S. Bankiewicz

Convection-enhanced delivery of liposomal doxorubicin in intracranial brain tumor xenografts

Received: 28 October 2005 / Revised: 19 January 2006 / Accepted: 24 January 2006 / Published online: 21 March 2006

Abstract We previously reported that convection-enhanced delivery (CED) of liposomes into brain tissue and intracranial brain tumor xenografts produced robust tissue distribution that can be detected by magnetic resonance imaging. Considering image-guided CED of therapeutic liposomes as a promising strategy for the treatment of brain tumors, we evaluated the efficacy of pegylated liposomal doxorubicin delivered by CED in an animal model. Distribution, toxicity, and efficacy of pegylated liposomal doxorubicin after CED were evaluated in a U251MG human glioblastoma intracranial xenograft model. CED of pegylated liposomal doxorubicin achieved good distribution in brain tumor tissue and surrounding normal brain tissue. Distribution was not affected by the particle concentration of pegylated liposomal doxorubicin, but tissue toxicity increased at higher concentrations. CED of pegylated liposomal doxorubicin, at a dose not toxic to normal rat brain (0.1 mg/ml doxorubicin), was significantly more efficacious than systemic administration of pegylated liposomal doxorubicin at the maximum tolerated dose. CED of pegylated liposomal doxorubicin resulted in improved survival compared to CED of free doxorubicin at the same dose. Outcomes of this study suggest that CED of liposomal drugs is a promising approach for the treatment of glioblastoma.

Keywords Convection-enhanced delivery · Liposomal doxorubicin · U251MG · Brain tumor

Y. Yamashita · R. Saito · M. T. Krauze · T. Kawaguchi · M. S. Berger · K. S. Bankiewicz (✉)
Department of Neurological Surgery,
University of California, San Francisco,
1855 Folsom Street, Mission Center Building,
Room 226, San Francisco, CA 94103, USA
e-mail: kbank@itsa.ucsf.edu
Tel.: +1-415-5023132
Fax: +1-415-5142177

C. Noble · J. W. Park
Division of Hematology–Oncology,
University of California, San Francisco,
San Francisco, CA, USA

D. C. Drummond · D. B. Kirpotin · J. W. Park
Hermes Biosciences, Inc.,
South San Francisco, CA, USA

Introduction

Despite intensive multimodal treatment such as surgical resection, malignant glioma (e.g., glioblastoma multiforme) remains the most difficult neoplasm to treat. Poor penetration of most anticancer drugs across the blood–brain barrier (BBB) into the central nervous system (CNS), when systemically administered, is one of the major reasons why improvement of survival is limited. Even with drugs that penetrate the BBB, it is difficult to reach sufficient drug concentrations in brain tumor tissue without causing systemic side effects [1].

Convection-enhanced delivery (CED) is a promising local delivery technique. This technique uses bulk flow to deliver small or large molecules directly to targeted sites in clinically significant volumes of tissue and provides wider volumes of distribution compared with simple diffusion techniques [2]. CED of therapeutic agents bypasses the BBB, delivers a high concentration of therapeutic agents within target sites, and minimizes systemic exposure, resulting in fewer side effects. Many investigators are now applying this technique to brain tumors. BCNU [3], topotecan [4], carboplatin, gemcitabine [5], and paclitaxel [6] have been administered with this technique, all with promising outcomes.

Liposomes are nanoscale lipid vesicles with a bilayered membrane structure and hollow core that can encapsulate a variety of small molecules. Liposomes have been shown to provide stable encapsulation for various anticancer drugs and have many advantages over the corresponding free drugs for the systemic treatment of cancer [7–9]. Liposomal formulations of doxorubicin (pegylated liposomal doxorubicin; ALZA/Johnson&Johnson) and daunorubicin (DaunoXome, Gilead) are already approved for the

treatment of cancer [10, 11], and several other liposomal agents are currently being evaluated in various clinical trials [12–14]. In our previous studies, we demonstrated with CED extensive distribution of liposomes in rodent brain tumor xenografts [15, 16]. CED of liposomal chemotherapeutics in brain tumor xenografts has shown extreme prolongation of drug half-life and increased therapeutic margin when compared with CED of the corresponding free drug [17].

Local delivery of liposomal drugs for the treatment of brain tumors, however, still remains largely unexplored. In this study, we evaluate the distribution, toxicity, and efficacy of pegylated liposomal doxorubicin in conjunction with CED into intracranial glioblastoma xenografts.

Materials and methods

Doxorubicin and pegylated liposomal doxorubicin

Pegylated liposomal doxorubicin (doxorubicin hydrochloride liposome for intravenous injection, ALZA Pharmaceuticals, Mountain View, CA, USA) was obtained commercially. The commercial Doxil solution contained 2 mg/ml of doxorubicin. Dilutions to 1 mg/ml of doxorubicin, 0.2 mg/ml of doxorubicin, and 0.1 mg/ml doxorubicin were made with HEPES-buffered saline (HBS), pH 6.5. Free doxorubicin was purchased from Sigma (St. Louis, MO, USA). Stock solutions of free doxorubicin were prepared by diluting doxorubicin in dimethyl sulfoxide (DMSO) to a concentration of 50 mg/ml. The infusion solution of free doxorubicin was made by diluting the stock solution with phosphate-buffered saline. Infusion solution containing 4% DMSO (the maximum concentration used in this study) had no toxicity when 20 μl was infused by CED (preliminary data not shown). $DiIC_{18}(3)$-DS liposomes (control liposomes) were prepared as described in our previous study [15]. Briefly, dioleoyl phosphatidylcholine, cholesterol (molar ratio 3:2), PEG-DSPE (5 mol %), and $DiIC_{18}(3)$-DS (DiI-DS; 0.2 mol%) were co-diluted in chloroform, and dried in a vacuum by rotary evaporation to form a lipid film. The lipid film was hydrated by shaking in HBS and then underwent six successive cycles of freezing at −80°C and thawing at 37°C. The resulting multilamellar liposomes were extruded through polycarbonate membrane filters, yielding liposomes of 77.1±6.6 nm in diameter, as determined by dynamic light scattering. Liposome concentration was measured by means of a standard phosphate assay and was adjusted by diluting with HBS to 20 mM phospholipid.

Tumor cell line, animals, and intracranial xenograft technique

An established human glioblastoma multiforme (GBM) cell line, U251MG, was obtained from the Brain Tumor Research Center Tissue Bank at the University of California San Francisco. Cells were maintained as monolayers in a complete medium consisting of Eagle's minimal essential medium supplemented with 10% fetal calf serum, nonessential amino acids, and 100 U/ml penicillin G. Cells were cultured at 37°C in a humidified atmosphere containing 95% air and 5% CO_2. Male Sprague–Dawley rats, weighing approximately 250 g, were obtained from Charles River Laboratories (Wilmington, MA, USA). Congenitally athymic, male, nude rats (rnu/rnu, homozygous) weighing approximately 150 to 200 g were purchased from the National Cancer Institute (Bethesda, MD, USA) and were housed under aseptic conditions, which included filtered air and sterilized food, water, bedding, and cages. All protocols used in the animal studies were approved by the University of California San Francisco Institutional Animal Care and Use Committee. For the intracranial xenograft tumor model, cells were harvested by trypsinization, washed once with Hanks Balanced Salt Solution without Ca^{++} and Mg^{++} (HBSS) and resuspended in HBSS for implantation. A cell suspension containing 5×10^5 cells/10 μl HBSS was used for implantation into the striatal region of the athymic rat brains. Under deep isoflurane anesthesia, rats were placed in a small-animal stereotactic frame (David Kopf Instrument, Tujunga, CA, USA). A sagittal incision was made through the skin to expose the cranium, and a burr hole was made in the skull at 0.5 mm anterior and 3 mm lateral from the bregma using a small dental drill. At a depth of 4.5 mm from the brain surface, 5 μl of cell suspension was injected. Two minutes later, another 5 μl was injected at a depth of 4 mm, and after a final 2 min, the needle was removed and the wound was sutured.

Convection-enhanced delivery

Throughout this study, CED of free doxorubicin or pegylated liposomal doxorubicin was performed with a volume of 20 μl by the CED method described previously [18]. Briefly, the infusion system consisted of a fused silica needle cannula connected to a loading line (containing liposomes) and an oil infusion line. A 1-ml oil-filled syringe, mounted onto a micro-infusion pump (BeeHive; Bioanalytical Systems, West Lafayette, IN, USA) regulated the flow of fluid through the system. Based on predetermined coordinates, the needle cannula was mounted onto stereotactic holders and guided to targeted region of the brain through burr holes made in the skull (see "Tumor cell lines, animals, and intracranial xenograft technique," above, for details). The following ascending infusion rates were applied to achieve the 20 μl infusion: 0.2 μl/min (15 min) +0.5 μl/min (10 min)+0.8 μl/min (15 min).

Evaluation of distribution

Four rats, bearing U251MG human GBM intracranial xenografts, received CED of 20 μl pegylated liposomal doxorubicin (0.1 mg/ml doxorubicin) 7 days after tumor cell implantation. Rats were euthanized 1 h after CED and

were histologically evaluated. The brains were harvested, frozen in isopentane chilled in dry ice, and cut into serial coronal sections (25 μm) with a cryostat. Because doxorubicin generates fluorescence with UV illumination, areas of distribution were visualized by fluorescence microscopy, and a charged coupled device camera with a fixed aperture was used to capture the image. The volume of distribution was analyzed with a Macintosh-based image analysis system (NIH Image 1.62; NIH Bethesda, MD, USA) as described previously [19].

Evaluation of local toxicity

Fifteen normal Sprague–Dawley rats were used to evaluate local toxicity after CED infusion of pegylated liposomal doxorubicin. Rats were divided into five groups (three rats in each group). One group received 2 mg/ml doxorubicin as pegylated liposomal doxorubicin; a second received 1 mg/ml doxorubicin as pegylated liposomal doxorubicin; a third received 0.2 mg/ml doxorubicin as pegylated liposomal doxorubicin; a fourth received 0.1 mg/ml doxorubicin as pegylated liposomal doxorubicin; and the fifth received 0.1 mg/ml doxorubicin twice as pegylated liposomal doxorubicin at 2-week intervals. Rats were monitored daily for general health (alertness, grooming, feeding, excreta, skin, fur, mucous membrane condition, ambulation, breathing, and posture). Animal weights were reported weekly. Five weeks after the first CED infusion, rats were euthanized and their brains were removed. Brains were fixed in paraffin, and cut into sections 5 μm in thickness. Sections were stained with hematoxylin and eosin (H&E).

Survival study with the U251MG intracranial xenograft model

The first survival studies were conducted to determine whether delivery of pegylated liposomal doxorubicin with CED would improve survival compared with receipt of free doxorubicin with CED and systemic pegylated liposomal doxorubicin through intravenous (i.v.) injection. Twenty-four rats, implanted with U251MG tumor cells, were divided into four groups: (*a*) control group, receiving CED of $DiIC_{18}(3)$-DS fluorescent liposomes (n=6); (*b*) systemic administration of pegylated liposomal doxorubicin (n=6); (*c*) CED of free doxorubicin (0.1 mg/ml) (n=6); and (*d*) CED of pegylated liposomal doxorubicin (0.1 mg/ml doxorubicin) (n=6). Seven days after tumor cell implantation, CED of 20 μl of the specified drug was performed for groups *a*, *c*, and *d*. For the systemic pegylated liposomal doxorubicin group *b*, pegylated liposomal doxorubicin (5.67 mg/kg) was given as three weekly i.v. injections. The cumulative systemic dosage of doxorubicin (17 mg/kg) was the maximum tolerated dose determined in previous studies [20, 21].

The second survival study evaluated the efficacy of repeated administration of low-dose pegylated liposomal doxorubicin with CED. Twenty-four rats, implanted with U251MG tumor cells, were divided into four groups: (*a*) control group (n=6), (*b*) single treatment CED group (n=6), (*c*) double treatment CED group (n=6), and (*d*) triple treatment CED group (n=6). Seven days after tumor cell implantation, the first CED treatment of 20 μl of pegylated liposomal doxorubicin (0.1 mg/ml doxorubicin) was performed in all three treatment groups. In the control group, CED of 20 μl of $DiIC_{18}(3)$-DS fluorescent liposomes was performed. The second and third CED treatments of 20 μl of pegylated liposomal doxorubicin (0.1 mg/ml doxorubicin) were performed 2 weeks after first treatment (on day 21 after tumor cell implantation) and 4 weeks after the first treatment (on day 35 after tumor cell implantation), respectively. In the untreated groups, CED of 20 μl of $DiIC_{18}(3)$-DS fluorescent liposomes was performed as control. Rats were monitored daily for survival and general health (alertness, grooming, feeding, excreta, skin, fur, mucous membrane conditions, ambulation, breathing, and posture). Animal weights were reported weekly. Animals were euthanized at the first sign of large intracranial tumor formation. The following signs were used as euthanasia criteria: motoric deficits, weight loss of more than 10% compared to previous week, and seizures.

Western blotting for P-glycoprotein

U251MG cells, 8×10^5 cells per well, were seeded into a 6-well plate (Corning). After 48 h of incubation, cells were harvested by trypsinization then collected, and protein was extracted in cell lysis buffer (Cell Signaling Technology, Beverly, MA, USA) to avoid degradation of protein. In the second survival study, U251MG xenografts were removed from the euthanized rats that had received liposomes with fluorescent dye, $DiIC_{18}(3)$-DS by CED, or a single dose of 0.1 mg/ml doxorubicin as pegylated liposomal doxorubicin by CED. Xenografts were immediately frozen in liquid nitrogen, and then ground into powder in liquid nitrogen to prevent protein degradation. Protein was extracted in cell lysis buffer (Cell Signaling Technology). Equal amounts of protein were separated on a 3–8% Tris-acetate gel (Invitrogen, CA, USA) and then transferred onto polyvinylidene difluoride (PVDF) membrane. The PVDF membrane was blocked in 5% skim milk solution and then probed with anti-PGP antibody (DakoCytomation, 1:1,000) or anti-α-tubulin antibody (Santa Cruz, 1:2,000) at 4°C overnight. Bound antibody was detected with horseradish peroxidase-conjugated secondary antibodies with ECL Western blotting detection reagents (Amersham, Piscataway, NJ, USA).

Results

Antitumor efficacy of pegylated liposomal doxorubicin treatment

Rats in the control group, which received liposomes tagged with the fluorescent dye $DiIC_{18}(3)$-DS, were all euthanized

36 to 54 days after tumor cell implantation due to neurological symptoms indicative of intracranial tumor growth. Median survival (Ms) for this group was 47.5 days. Rats receiving systemic administration of pegylated liposomal doxorubicin were euthanized due to neurological signs indicative of intracranial tumor growth 41 to 56 days after tumor cell implantation. Ms for this group was 45.5 days. All rats that received CED of 0.1 mg/ml free doxorubicin were euthanized 44 to 64 days after tumor cell implantation. Ms for this group was 50.5 days. Formation of large tumors was verified in all the rats euthanized in these groups [Fig. 1b(i)]. Three of six rats that received single treatment 0.1 mg/ml doxorubicin as pegylated liposomal doxorubicin by CED survived until termination of the study. However, large tumor formations were observed in the other three rats, and they had to be euthanized at 56 to 69 days after tumor cell implantation. However, statistically significant improvement of survival rate was seen in this group (Ms=84.5 days, p=0.0196). One of the surviving rats had no histological sign of tumor [Fig. 1b(ii)]. Although small tumor formations were seen upon postmortem histology in two of the surviving rats, animals did not develop any neurological signs of intracranial tumor growth before termination of the study [Fig. 1b(iii), (iv)]. We conclude that the efficacy of 0.1 mg/ml doxorubicin as pegylated liposomal doxorubicin infused by CED is significantly improved when compared to systemic treatment with pegylated liposomal doxorubicin at the maximum tolerated dose (MTD).

Antitumor efficacy of repetitive pegylated liposomal doxorubicin administration with CED

Rats in the control group, which received liposomes tagged with the fluorescent dye $DiIC_{18}(3)$-DS, were all euthanized 33 to 44 days (Ms=34.5 days) after tumor cell implantation due to symptoms indicative of intracranial tumor growth. Rats that received single or multiple administration of pegylated liposomal doxorubicin by CED lived significantly longer compared to the control group (1× pegylated liposomal doxorubicin, p=0.0026; 2× pegylated liposomal doxorubicin, p=0.0053; and 3× pegylated liposomal doxorubicin, p=0.0041). Just as in the first survival study, three out of six rats that received a single treatment of 0.1 mg/ml doxorubicin as pegylated liposomal doxorubicin by CED survived until termination of the study. In the group that received the double and triple treatments with 0.1 mg/ml doxorubicin as pegylated liposomal doxorubicin infused by CED, two of six rats and three of six rats survived until termination of the study, respectively. Median survival of animals receiving repetitive infusions of 0.1 mg/ml of pegylated liposomal doxorubicin by CED did not improve when compared to single treatment with pegylated liposomal doxorubicin (1× pegylated liposomal doxorubicin, Ms=76 days; 2× pegylated liposomal doxorubicin, Ms=49 days; and 3× pegylated liposomal doxorubicin, Ms=74 days). The surviving rats in these groups had no histological signs of tumor in the brain [Fig. 2b(i), (ii)]. However, increasing tissue damage related to pegylated liposomal doxorubicin accumulation was observed in the triple treatment group receiving pegylated liposomal doxorubicin [Fig. 2b(ii)].

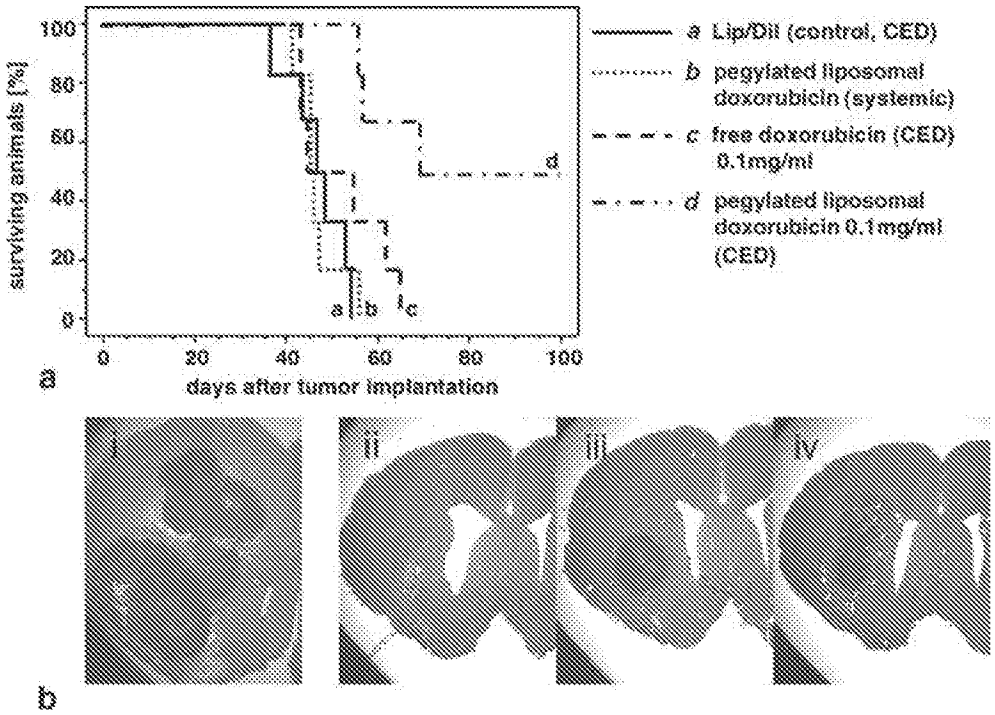

Fig. 1 Survival study. Twenty-four athymic rats intracranially implanted with U251MG human glioblastoma cells were divided into four groups as described in "Materials and methods." **a** Rats were euthanized when they developed neurological symptoms indicative of tumor progression. Results are expressed as Kaplan–Meier curves. **b**(i) Representative H&E section from a rat in the control group. Every rat euthanized in groups *a*, *b*, and *c* developed tumors of similar size. **b**(ii) Three rats in group *d* survived until termination of this study, and one of them had no tumor. **b**(iii)(iv) Although small tumor formations were seen on the postmortem histology in two rats of group *d*, they did not develop any signs of intracranial tumor growth at termination of study

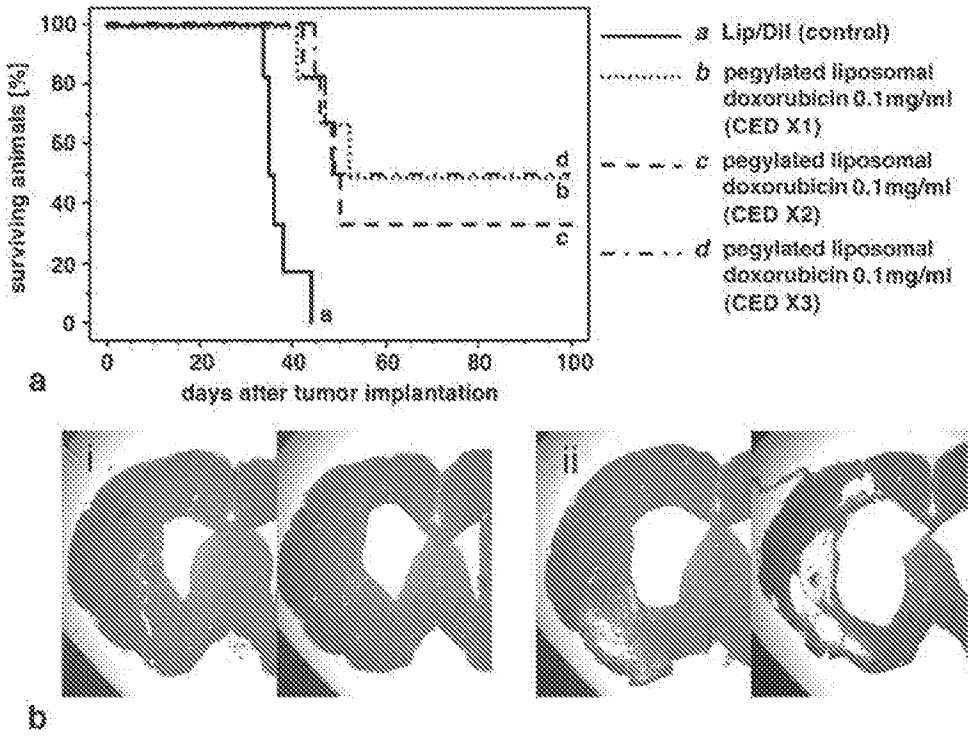

Fig. 2 Survival study. Twenty-four athymic rats intracranially implanted with U251MG human glioblastoma cells were divided into four groups as described in "Materials and methods." **a** Rats were euthanized when they developed neurological symptoms indicative of tumor progression. Results are expressed as Kaplan–Meier curves. **b**(i) Representative H&E section from a rats of group *c*. **b**(ii) Representative H&E section from a rats of group *d*. Although tumor formations were not seen on postmortem histology in both groups, brain damage caused by doxorubicin was observed in rats receiving triple pegylated liposomal doxorubicin *d*

Effect of pegylated liposomal doxorubicin on P-glycoprotein expression

As shown Fig. 3, U251MG monolayer cells had undetectable levels of P-glycoprotein (PGP), whereas a detectable amount of PGP was found in all harvested rodent U251 xenografts after liposome infusion. Increased PGP expression is visible in rodent U251 xenografts receiving 0.1 mg/ml of pegylated liposomal doxorubicin, contrasting with lower PGP expression in animals receiving DiI-Liposomes (control).

Discussion

In preclinical models, pegylated liposomal doxorubicin has produced remission and cure of tumors of the breast, lung, ovaries, prostate, colon, bladder, and pancreas, as well as lymphoma, sarcoma, and myeloma [21]. The tight endothelial junctions of the blood–brain barrier are often disrupted by the presence of a brain tumor. Therefore, the drug was also found to be effective in an orthotopic, parietal sarcoma brain tumor model in rats via systemic administration [20]. Clinical trials evaluating intravenous administration of pegylated liposomal doxorubicin for patients with recurrent high-grade glioblastoma demonstrated that pegylated liposomal doxorubicin has potential application in the treatment of glioblastomas [22–24]. However, efficacy with systemic treatment was limited by systemic toxicity and poor penetration of blood–brain barrier.

In this study, consistent with our previous studies [15, 16], we showed that extensive and effective distribution of pegylated liposomal doxorubicin was achieved with CED in the U251MG intracranial rodent xenograft model, and we could target large portions of the tumor and surrounding brain parenchyma with pegylated liposomal doxorubicin. Glioblastomas usually recur within 2 cm of the resection margin, and it is important for successful therapy for patients with glioblastoma to target, not only the portion of tumor, but

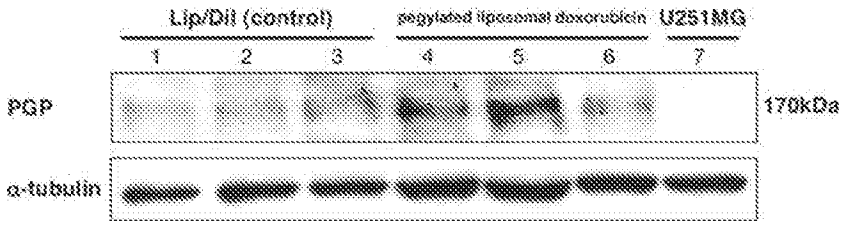

Fig. 3 Effects of pegylated liposomal doxorubicin on PGP expression. Representative Western blot analysis of PGP and alpha-tubulin in U251MG human glioblastoma intracranial xenografts and U251MG monolayer cells are shown. PGP is visible as a 170-kDa band. In the xenografts receiving 0.1 mg/ml pegylated liposomal doxorubicin by CED, significant enhancement of PGP expression was observed (*lanes 4–6*) compared with the PGP expression after CED infusion of liposomes with fluorescent dye, $DiIC_{18}(3)$-DS (*lanes 1–3*). No signal was seen in U251MG monolayer cells

also surrounding normal brain that tumor cells have already invaded [25].

Pegylated liposomal doxorubicin can substantially alter the pharmacokinetic profile of doxorubicin, including the area under the plasma concentration–time curve, the distribution, and the clearance [7]. One potential advantage of liposome-encapsulated cytotoxic drugs over corresponding unencapsulated agents is prolongation of drug half-life when infused systemically [7]. Hence, in conjunction with CED, it was expected that doxorubicin would also be released slowly in the brain to prolong the exposure of brain tumor cells to the drug, and this delivery pattern would thereby provide greater efficacy and less toxicity compared to treatment with free doxorubicin. In this study, we have shown that CED of 0.1 mg/ml pegylated liposomal doxorubicin significantly prolonged survival, when compared with CED of 0.1 mg/ml free doxorubicin.

However, when we evaluated the toxicity of CED of pegylated liposomal doxorubicin in normal rat brain tissue, CED of pegylated liposomal doxorubicin at 2 and 1 mg/ml caused a large lesion in the brain. Although pegylated liposomal doxorubicin at 0.2 mg/ml of doxorubicin was determined to be the MTD after single and multiple CED that did not induce local tissue toxicity, the therapeutic range of pegylated liposomal doxorubicin is narrow, as seen after the triple application of 0.1 mg/ml (cumulative dose of 0.3 mg/ml) of pegylated liposomal doxorubicin in our second survival study. Nevertheless, pegylated liposomal doxorubicin at 0.1 mg/ml showed significantly improved survival when compared to the control group and the same dose of free doxorubicin.

To improve survival, we tried a regimen of repeated CED of pegylated liposomal doxorubicin in this study. However, no increase in efficacy was observed. It is well-known that multiple drug resistance is frequently associated with decreased drug accumulation in tumors. This effect is mediated by induction, upon repetitive doxorubicin treatment, of the multidrug transporter *MDR1* gene and its protein product P-glycoprotein [26]. Indeed, we observed in our study enhancement of PGP expression after CED of pegylated liposomal doxorubicin in U251 xenografts, but not in cells treated in vitro with pegylated liposomal doxorubicin. An explanation for this difference might be that the PGP was expressed by capillaries and not by the tumor cells themselves. It has also been shown that three-dimensional cellular structures, such as spheroids in culture, are more amenable to the development of a multidrug resistant phenotype [27, 28]. These same properties may apply to the U251MG tumor model we used. Possible further enhancement of the therapeutic effect of pegylated liposomal doxorubicin may result from the optimization of the liposomal properties of pegylated liposomal doxorubicin or the use of the PGP inhibitor verapamil to increase efficacy in brain.

In conclusion, we evaluated the efficacy of pegylated liposomal doxorubicin administered by CED into U251MG human glioblastoma intracranial xenografts. Liposome-encapsulated doxorubicin was associated with significantly improved survival when compared to the control group, CED of free doxorubicin, and systemically delivered doxorubicin. pegylated liposomal doxorubicin containing 0.1 mg/ml of doxorubicin was determined to have the potential to treat glioblastoma. However, the therapeutic window of pegylated liposomal doxorubicin was narrow, as seen after three 0.1 mg/ml infusions. As demonstrated in our previous reports [15, 16], liposomal gadolinium constructs can be imaged directly in the CNS during CED by magnetic resonance imaging. It is possible to combine liposomes containing a marker for imaging with liposome-encapsulated drugs, allowing for real-time guidance of CED [29]. CED combined with liposomal chemotherapeutics would very likely enhance current clinical applications by allowing exact perfusion of the critical resection margin or intratumoral infusions in inoperable cases. We believe that the findings presented in this study represent significant progress toward future clinical application of liposomal drugs administered by CED for the treatment of brain tumors.

Acknowledgements Special thanks John Forsayeth Ph.D. for proofreading and editing this work. Grant support: National Cancer Institute Specialized Program of Research Excellence grant (to M. S. Berger, K. S. Bankiewicz, and J. W. Park) and Accelerate Brain Cancer Cure (to K. S. Bankiewicz).

References

1. Groothuis DR (2000) The blood–brain and blood–tumor barriers: a review of strategies for increasing drug delivery. Neuro-oncol 2(1):45–59
2. Bobo RH, Laske DW, Akbasak A, Morrison PF, Dedrick RL, Oldfield EH (1994) Convection-enhanced delivery of macromolecules in the brain. Proc Natl Acad Sci U S A 91(6):2076–2080
3. Bruce JN, Falavigna A, Johnson JP et al (2000) Intracerebral clysis in a rat glioma model. Neurosurgery 46(3):683–691
4. Kaiser MG, Parsa AT, Fine RL, Hall JS, Chakrabarti I, Bruce JN (2000) Tissue distribution and antitumor activity of topotecan delivered by intracerebral clysis in a rat glioma model. Neurosurgery 47(6):1391–1398
5. Degen JW, Walbridge S, Vortmeyer AO, Oldfield EH, Lonser RR (2003) Safety and efficacy of convection-enhanced delivery of gemcitabine or carboplatin in a malignant glioma model in rats. J Neurosurg 99(5):893–898
6. Lidar Z, Mardor Y, Jonas T et al (2004) Convection-enhanced delivery of paclitaxel for the treatment of recurrent malignant glioma: a phase I/II clinical study. J Neurosurg 100(3):472–479
7. Allen TM, Martin FJ (2004) Advantages of liposomal delivery systems for anthracyclines. Semin Oncol 31(6 Suppl 13):5–15
8. Drummond DC, Meyer O, Hong K, Kirpotin DB, Papahadjopoulos D (1999) Optimizing liposomes for delivery of chemotherapeutic agents to solid tumors. Pharmacol Rev 51 (4):691–743
9. Gabizon A, Shmeeda H, Barenholz Y (2003) Pharmacokinetics of pegylated liposomal doxorubicin: review of animal and human studies. Clin Pharmacokinet 42(5):419–436
10. Thigpen JT, Aghajanian CA, Alberts DS et al (2005) Role of pegylated liposomal doxorubicin in ovarian cancer. Gynecol Oncol 96(1):10–18
11. Zucchetti M, Boiardi A, Silvani A, Parisi I, Piccolrovazzi S, D'Incalci M (1999) Distribution of daunorubicin and daunorubicinol in human glioma tumors after administration of liposomal daunorubicin. Cancer Chemother Pharmacol 44 (2):173–176
12. Gelmon KA, Tolcher A, Diab AR et al (1999) Phase I study of liposomal vincristine. J Clin Oncol 17(2):697–705

13. Selden MV, Muggia F, Astrow A et al (2004) A phase II study of liposomal lurtotecan (OSI-211) in patients with topotecan-resistant ovarian cancer. Gynecol Oncol 93(1):229–232
14. Zamboni WC, Ramalingam S, Friedland DM et al (2005) Phase I and Pharmacokinetic (PK) study of STEALTH liposomal CKD-602 (S-CKD602) in patients with advanced solid tumors. J Clin Oncol 23:2069 (Meeting abstracts)
15. Mamot C, Nguyen JB, Pourdehnad M et al (2004) Extensive distribution of liposomes in rodent brains and brain tumors following convection-enhanced delivery. J Neurooncol 68(1):1–9
16. Saito R, Bringas JR, McKnight TR et al (2004) Distribution of liposomes into brain and rat brain tumor models by convection-enhanced delivery monitored with magnetic resonance imaging. Cancer Res 64(7):2572–2579
17. Noble CO, Krauze MT, Drummond DC et al (2006) Novel nanoliposomal CPT-11 infused by convection-enhanced delivery in intracranial tumors: pharmacology and efficacy. Cancer Res 66 (5):2801–2806
18. Bankiewicz KS, Eberling JL, Kohutnicka M et al (2000) Convection-enhanced delivery of AAV vector in parkinsonian monkeys; in vivo detection of gene expression and restoration of dopaminergic function using pro-drug approach. Exp Neurol 164(1):2–14
19. Hamilton JF, Morrison PF, Chen MY et al (2001) Heparin co-infusion during convection-enhanced delivery (CED) increases the distribution of the glial-derived neurotrophic factor (GDNF) ligand family in rat striatum and enhances the pharmacological activity of neurturin. Exp Neurol 168(1):155–161
20. Sharma US, Sharma A, Chan RI, Straubinger RM (1997) Liposome-mediated therapy of intracranial brain tumors in a rat model. Pharm Res 14(8):992–998
21. Zhou R, Mazurchuk R, Straubinger RM (2002) Antivasculature effects of doxorubicin-containing liposomes in an intracranial rat brain tumor model. Cancer Res 62(9):2561–2566
22. Fabel K, Dietrich J, Hau P et al (2001) Long-term stabilization in patients with malignant glioma after treatment with liposomal doxorubicin. Cancer 92(7):1936–1942
23. Hau P, Fabel K, Baumgart U et al (2004) Pegylated liposomal doxorubicin efficacy in patients with recurrent high-grade glioma. Cancer 100(6):1199–1207
24. Koukourakis MI, Koukouraki S, Fezoulidis I et al (2000) High intratumoural accumulation of stealth liposomal doxorubicin (Caelyx) in glioblastomas and in metastatic brain tumours. Br J Cancer 83(10):1281–1286
25. Barker FG 2nd, Chang SM, Gutin PH et al (1998) Survival and functional status after resection of recurrent glioblastoma multiforme. Neurosurgery 42(4):709–720 (Discussion 20–23)
26. Gottesman MM, Fojo T, Bates SE (2002) Multidrug resistance in cancer: role of ATP-dependent transporters. Nat Rev Cancer 2(1):48–58
27. Desoize B, Gimonet D, Jardillier JC (1998) Cell culture as spheroids: an approach to multicellular resistance. Anticancer Res 18(6A):4147–4158
28. Kolchinsky A, Roninson IB (1997) Drug resistance conferred by MDR1 expression in spheroids formed by glioblastoma cell lines. Anticancer Res 17(5A):3321–3327
29. Saito R, Krauze MT, Bringas JR et al (2005) Gadolinium-loaded liposomes allow for real-time magnetic resonance imaging of convection-enhanced delivery in the primate brain. Exp Neurol 196(2):381–389

Available online at www.sciencedirect.com

ScienceDirect

journal homepage: www.elsevier.com/locate/AJPS

Original Research Paper

Development of a method to quantify total and free irinotecan and 7-ethyl-10-hydroxycamptothecin (SN-38) for pharmacokinetic and bio-distribution studies after administration of irinotecan liposomal formulation

Wenqian Yang[a], *Zimeng Yang*[a], *Jieru Liu*[a], *Dan Liu*[b,*], *Yongjun Wang*[a,*]

[a] *Wuya College of Innovation, Shenyang Pharmaceutical University, Shenyang 110016, China*

[b] *Key Laboratory of Structure-Based Drugs Design & Discovery of Ministry of Education, Shenyang Pharmaceutical University, Shenyang 110016, China*

ARTICLE INFO

Article history:
Received 20 March 2018
Revised 22 June 2018
Accepted 10 August 2018
Available online 11 September 2018

Keywords:
Irinotecan
Liposome
UPLC-MS-MS
SPE
Pharmacokinetics
Bio-distribution

ABSTRACT

In 2015, liposomal formulation of irinotecan (ONIVYDE) has been approved by FDA and widely applied in the treatment of pancreatic cancer. ONIVYDE is a novel liposome formulation, entrapping CPT-11 in the aqueous core of vesicles using a modified gradient loading method. Due to toxicity concerns, it is essential to explore a rapid and reliable method to effectively isolate and quantify the non-liposomal, namely, free CPT-11and total CPT-11 in plasma. This study focuses on separation of non-liposomal CPT-11, evaluation of the pharmacokinetics of free CPT-11 and total CPT-11 and bio-distribution after intravenous administration of CPT-11 liposome. Free CPT-11 in plasma was separated by solid-phase extraction (SPE). The amount of total CPT-11 and main metabolite 7-ethyl-10-hydroxycamptothecin (SN-38) in plasma was quantified by ultra-performance liquid chromatography–MS/MS. The calibration curves fitted well and lower limit of quantitation for SN-38, free CPT-11, total CPT-11 and CPT-11 in tissue and were 5 ng/ml, 10 ng/ml, 4.44 ng/ml and 25 ng/ml respectively. The recoveries, precision and accuracy of the method appear satisfactory. Using this method, the pharmacokinetics and bio-distribution of CPT-11 liposome formulation after an intravenous dose of 2.5 mg/kg were then investigated.

* Corresponding authors. Shenyang Pharmaceutical University, No. 103, Wenhua Road, Shenyang 110016, China. Tel.: +86 24 23986325.
E-mail addresses: liudan@syphu.edu.cn (D. Liu), wangyongjun@syphu.edu.cn (Y. Wang).
Peer review under responsibility of Shenyang Pharmaceutical University.

https://doi.org/10.1016/j.ajps.2018.08.003

1. Introduction

Nanoparticles like small unilamellar liposome have shown their promise for improving the pharmacokinetics and tumor localization of encapsulated anticancer drugs [1]. In 2015, FDA approved ONIVYDE (irinotecan liposome injection) in combination with fluorouracil/folinic acid based on the result of clinical study. Compared with fluorouracil/folinic acid, this dosage regimen significantly pro-longed overall survival of patients with advanced and metastatic pancreatic cancer [2]. ONIVYDE was prepared by a modified active loading method, was able to entrap irinotecan (CPT-11) at an extreme high drug to lipid ratio, retain encapsulated CPT-11 stable in vesicles, and also protect CPT-11 from hydrolysis and metabolic conversion to 7-ethyl-10-hydroxycamptothecin (SN-38) during the systemic circulation [3]. For CPT-11 is an ionizable drug, loaded by active loading method, drug release rate and circulation half-life determined the therapeutic activity of liposomal drug delivery systems. And only if liposomes retain CPT-11 over several hours to days will achieve high drug accumulation in tumor [4]. Therefore, it is important to control the ratio of free drug, monitor the pharmacokinetics (PK) and tissue distribution properties to fully understand and the therapeutic efficacy and side effects of liposome formulation.

To get a clear relationship of pharmacokinetics between total drug and non-liposomal drug, namely the free drug, there is an insistent demand of a sophisticated analytical technique to separate free CPT-11 from liposome in plasma. Meanwhile, the developed separation method should have a consistent recovery and extraction efficiency of free CPT-11. Moreover, formulation integrity should be maintained without leakage or breaking of the liposome during sample preparation and storage. Up to now, there are several methods have been reported to achieve this end for vincristine liposome, amphotericin B liposome and doxorubicin liposome, such as solid-phase extraction (SPE) [5–10], ultrafiltration [11], ion-exchange chromatography [12], and capillary electrophoresis [13,14]. Nevertheless, no method has been observed for the separation and detection of free CPT-11 and liposomal CPT-11. Furthermore, as high risk of liposome leakage using ultrafiltration and high sample dilution during gel chromatography, these methods have obvious limitations in applying for CPT-11 liposome determination from biological samples.

Based on previous reports [5–10,15], SPE is the most feasible method for separation of non-liposomal CPT-11 and liposome-encapsulated CPT-11 due to better security and relative rapidness. However, the separation and quantification of non-liposomal, liposomal CPT-11 and metabolite SN-38 was still challenging because carboxylesterase in rat plasma is highly active. Considering that the catalysis of carboxylesterase is related to protein concentration, pH, ionic strength, and these conditions are easily changed under SPE processing [16,17], the working process especially the solution involved in SPE should be controlled properly. In the present study, we build a method to (i) separate free CPT-11 (F-CPT-11) from liposome by SPE without damaging liposome (ii) achieve total release of encapsulated CPT-11 and extract total CPT-11(T-CPT-11) from liposome using protein precipitation extraction (iii) detect CPT-11 in liver (L-CPT-11), heart, spleen, lung and kidney (OT-CPT-11) of mouse using protein precipitation extraction. And the developed method had been proved to be valid for the separation and quantitation of non-liposomal drug and total drug in plasma and tissue samples according to the FDA guidelines on bioanlytical method [18], allowing the study of pharmacokinetics and bio-distribution after administration of CPT-11 loaded liposome.

2. Materials and methods

2.1. Chemicals reagents

Irinotecan was kindly supported by Jiangsu Hengrui Medicine Co., Ltd. (China). Sucrose octasulfate was obtained from Wuhan Hengruikang Reagent Co., Ltd. (China). Methanol, acetonitrile and dichloromethane (HPLC grade) was purchased from Tianjin Kemer Chemical Reagent Co., Ltd. (Tianjin, China). Disaturated phosphatidylcholine (DSPS), cholesterol (chol) and 2-Distearoyl-snglycero-3-phosphoethanolamine-N-[methoxy (polyethylene glycol)-2000] (mPEG2000-DSPE) were obtained from Shanghai Advanced Vehicle Technology L.T.D. Co. Sephadex G-75 size exclusion resins were procured from Sigma Chemical Company (St Louis, USA). All other reagents and solvents mentioned were of analytical grade.

2.2. Instrumentations and UPLC–MS/MS conditions

Mass spectrometric detection was conducted in a Xevo-TQS triple quadrupole mass spectrometer (Waters, Milford, MA, USA) equipped with an electrospray ionization (ESI) source in the positive mode. And the quantification of analytes were operated in the multiple reaction monitoring (MRM) mode. Camptothecin (CPT) which has similar physicochemical properties as CPT-11, was selected as internal standard (IS). The MS operational conditions were optimized, MRM transitions of SN-38, CPT-11and IS were m/z 393.2 → 349, m/z 587.4 → 167.1 and m/z 349.2 → 249.0 respectively. Capillary voltage was 3.5 kV. And cone voltage was 30 V for both IS and CPT-11, and 35 V for SN-38. The collision energies of CPT-11, SN-38 and the IS were 37, 34 and 35 eV, respectively.

LC separations were performed on an ACQUITY UPLC system (Waters Corp., Milford, MA, USA) with UPLC BEH C18 column (2.1 mm × 50 mm, 1.7 μm; Waters Co., Ltd., USA). Acetonitrile (A) and water containing 0.1% formic acid (B) were used as the mobile phase, and the elution was performed by 27% (A): 73% (B) (v/v) at a flow rate of 0.3 ml/min. The injection volume was controlled at 20 μl. The column temperature and the auto sampler temperature was set to 60 °C and 4 °C respectively.

MassLynx™ Version 4.1 software was applied for data acquisition and analysis.

2.3. Preparation of calibration standards and quality control (QC)

Stock solutions of CPT-11 (500 μg/ml), IS (500 μg/ml) and SN-38 (500 μg/ml) were prepared by dissolving weighed corresponding analytes into volumetric flasks and stored at −20 °C before analyze. CPT-11, IS were dissolved in methanol,

and SN-38 was dissolved in dimethyl sulfoxide. To provide intermediate working solutions, the stock solutions were further diluted with methanol /water mixture (50:50, v/v). The calibration standard for all plasma samples were prepared at 7 concentrations, ranging from 10 ng/ml to 10 000 ng/ml for F-CPT-11, from 4.4 ng/ml to 20 000 ng/ml for T-CPT-11 and from 5 ng/ml to 1000 ng/ml for SN-38. Corresponding QC concentrations were 10, 50, 500, 8000 ng/ml for F-CPT-11, 4.4, 11.1, 1778, 8888 ng/ml for T-CPT-11, and 5, 10, 200, 800 ng/ml for SN-38. Liver QC samples and other tissue QC samples were prepared at 25, 62.5, 500 and 800 ng/ml, and corresponding calibration standards were prepared ranging from 25 to 1000 ng/ml.

2.4. Sample preparation

2.4.1. Plasma sample preparation for CPT-11 and SN-38

Part A: SPE for F-CPT-11

F-CPT-11 in plasma was separated from CPT-11 liposome using SPE with an Oasis HLB column (1 cc/30 mg, Waters Corp., Milford, Massachusetts, USA) connected with a vacuum air pump. Previous study has shown that chilling samples at 4 °C could probably sustain the stability of lactone form [18]. Thus, all solvent involved in SPE process was maintained at 4 °C. Firstly, SPE cartridge was preconditioned with 1.0 ml methanol and 1.0 ml water. Then, 75 μl 5% glucose solution were added to 50 μl CPT-11 spiked plasma, the mixture were passed through cartridges without vacuum. Then, 20 μl $ZnSO_4$, 75 μl 5% glucose solution and 50 μl IS working solution (5 μg /ml) were added to 50 μl plasma. Samples were mixed by vortex for 1 min and then centrifuged at 7500 rpm for 3 min. Supernatants were then collected, and passed through the conditioned cartridges with vacuum. After complete passage of samples, each cartridge was further rinsed with 2 ml of PBS, 1 ml of 3.75% ammonia. Finally, each cartridge was washed with 1 ml methanol containing 2% acetic acid, target analyte in the rinsed cartridge was collected and evaporated under a stream of nitrogen at 37 °C. Residues were then dissolved with 200 μl methanol/water containing 0.1% acetic acid (70:30, v/v) and centrifuged at 13,000 rpm for 5 min. 20 μl of the supernatant were injected into the UPLC separation system.

Part B: Protein precipitation extraction for T-CPT-11 and SN-38

Fifty microliter of IS solution (5 μg/ml in methanol) was firstly added to 50 μl plasma (QC samples and calibration standards were spiked with corresponding working solutions) and vortex mixed for 30 s. Then, 400 μl of methanol containing 0.1% acetic acid was added to the plasma samples, after mixing by vortex for 5 min, the mixture was centrifuged at 15 000 rpm for 10 min. Finally, a 20 μl sample of supernatant were injected into the UPLC column for analysis.

2.4.2. Tissue sample preparation for CPT-11

Firstly, 50 μl IS solution (5 μg /ml in methanol) and 850 μl of methanol /acetonitrile (50:50, v/v) were added to 50 μl tissue samples (QC samples and calibration standards were spiked with corresponding working solutions). Samples were then mixed by vortex for 1 min, and centrifuged at 15,000 rpm for 10 min to precipitate possible particulate matter, and the supernatant was collected and then evaporated under a stream of nitrogen at 37 °C. Residues were then reconstituted in 100 μl of methanol /water containing 0.1% acetic acid (70:30, v/v) and centrifuged at 13 000 rpm for 5 min. Finally, a 20 μl sample of supernatant were injected into the UPLC column for analysis.

2.5. Method feasibility

It is necessary to assess the feasibility of SPE method before the method validation, and prove that the separation and quantitation method could be used for pharmaceutical and bio-distribution study. Moreover, the sample preparation methods (both SPE and protein precipitation extraction) must be appropriate for the separation of F-CPT-11 from liposome. Meanwhile, liposome integrity must be ensured. In this research, method feasibility was performed by determining the part of F-CPT-11(F %) and T-CPT-11 (T%) in QC samples (QC samples were spiked with CPT-11 liposomes). And F-CPT-11 (F %) was calculated by the formula: $F\% = C_P/C_N \times 100$, here C_P is the F-CPT-11 concentration detected in QC samples and C_N is the nominal concentration of the CPT-11 added in QC samples. And C_P may compose of originally present F-CPT-11 in liposome formulations as well as the part of released CPT-11 during mixing and SPE separation process. If SPE method could separate F-CPT-11 from liposome, the value of F_1% after the first SPE process should equal to the encapsulation rate. To further prove the liposome integrity throughout the SPE process, liposome fraction in the first SPE process were collected. The collected liposome fraction was then re-run through a new preconditioned cartridge. Theoretically, if the liposomes remain intact and the CPT-11 was not released from the collected liposome fraction during the second SPE process, the value of F_2% after the second SPE process should equal to zero.

Moreover, the value of T-CPT-11 (T%) could be used to verify the feasibility of protein precipitation extraction process. In the equation: $T\% = C_T/C_N \times 100$, C_T is the T-CPT-11 concentration detected in QC samples, and C_N is the nominal concentration of the T-CPT-11 added in QC samples. If protein precipitation process could deposit protein completely and ensure a total release of drug molecular from liposomes, the value of T% should be within 85%–115%.

2.6. Method validation

In this study, analytical methodology of analytes were built for pharmacokinetics studies of CPT-11 liposome. As liver plays an essential role in drug metabolism and excretion when doing bio-distribution studies, so we build analytical methodology for liver and mixture of other tissues (heart, spleen, lung, kidney) respectively. Moreover, selectivity, linearity of calibration curves, lower limit of quantitation (LLOQ), precision and accuracy, recovery and matrix effect and stability of the analytical methodology were validated. And analytical methodology was run on three consecutive days.

2.6.1. Specificity

Specificity of the methodology was evaluated by comparing the chromatograms of blank plasma, blank liver homogenates, and homogenates mixture of blank tissue (heart, spleen, lung and kidney) with the corresponding analytes spiked plasma or tissue homogenates.

2.6.2. *Linearity of calibration curves and LLOQ*
Calibration curves of plasma samples were prepared by diluting corresponding stock solutions to seven final concentrations, ranging from 5 ng/ml to 2000 ng/ml for SN-38, 10 ng/ml to 10 000 ng/ml for F-CPT-11, and 4.4 ng/ml to 20 000 ng/ml for T-CPT-11. As for tissue samples, calibration curves achieved by using seven nonzero liver homogenates and seven nonzero tissue homogenates calibration standards from 25 ng/ml to 1000 ng/ml for CPT-11. Calibration curves linearity was analyzed by plotting peak area ratios of CPT-11 and SN-38 versus the nominal concentration. Moreover, least-square regression using a $1/(\text{concentration})^2$ weighting was applied to evaluate linearity relationship. The correlation coefficients (r^2) needed to be above 0.99. The LLOQ of the calibration curve was defined by using six lots of blank plasma samples and blank tissue homogenates. Both precision and accuracy are required to be less than 20%.

2.6.3. *Precision and accuracy*
For all analytes, intra-day precision, inter-day precision and accuracy were estimated by analyzing QC (low, middle and high) samples on three separated days in six replicates. The precision and accuracy was defined as the relative standard deviation (RSD%) and the relative error (RE%). Moreover, the acceptability for precision was within 15% RSD and that of accuracy was within 15% RE of the theoretical values.

2.6.4. *Extraction recovery and matrix effect*
The extraction recovery of CPT-11 and SN-38 were analyzed by comparing the peak areas of the extracted QC (low, middle and high) samples with average peak area of CPT-11/SN-38 added blank samples after extraction. Moreover, at each QC concentration six replicates were determined. And matrix effect was determined as the ratio of the peak area from extracted with blank plasma/ tissue homogenates to the mean peak area from extracted without plasma/ tissue homogenates at QC concentrations.

2.6.5. *Stability*
Stability of plasma samples and tissue samples were tested including auto-sampler storage, freeze-thaw cycles, and short-term, long-term storage stability at three different levels (QC samples). The auto-sampler stability was evaluated by placing the extracted QC samples in the auto-sampler, and keeping them at 4 °C for 24 h. Freeze–thaw stability was evaluated by comparing peak areas of QC samples after 3 cycles of freeze-thaw (−20 °C to ambient temperature) with peak areas of newly prepared QC samples. Short-term stability of F-CPT-11was invested by keeping the QC samples at 4 °C for 6 h, and that of T-CPT-11, L-CPT-11, OT-CPT-11 and SN-38 was conducted at 25 °C for 12 h for. And the long-term stability was evaluated by comparing the concentration of newly prepared QC samples with that of QC samples stored at −80 °C for 1 months. Moreover, robustness study of the developed method against small variations of column temperature (from 59 °C to 61 °C) was also conducted.

2.6.6. *Dilution effect*
Stock solutions of CPT-11 (120 μg/ml) and SN-38 (8 μg/ml) were prepared by dissolving weighed corresponding analytes into volumetric flasks. Then, CPT-11 stock solution and SN-38 stock solutions were further diluted with blank plasma for 20-fold and 10-fold (v/v), respectively. CPT-11/SN-38 were then extracted as protocol in 2.4.1

2.7. Preparation and characterization of CPT-11 liposome

2.7.1. *Preparation of CPT-11 liposome formulation*
First, solution of triethylammonium salt sucrose octasulfate (TEA_8SOS) was prepared. The concentration was adjusted to 0.65 mol/l, and the pH was 5.5–6.0. Then, the mixture of DSPC (6.81 mg/ml), chol (2.22 mg/ml) and mPEG2000-DSPE (0.12 mg/ml) were combined in 50% (w/v) ethanoic solution and then mixed with TEA_8SOS solution at 65 °C for 30 min. The lipid suspension was then extruded 20 times at 65 °C. Unentrapped TEA_8SOS were then removed by Sephadex G-75 gel filtration chromatography, and the gel filtration was eluted with pH 6.5 HEPES /NaCl (17/144, mM /mM) buffer. After buffer exchange, CPT-11 HCl was then added to liposome at 4.3 mg/ml. The solution was then incubated at 65 ± 5 °C for 1 h and immediately chilled on ice for 20 min.

2.7.2. *Characterization of CPT-11 liposome formulation*
The average size and zeta potential of prepared liposomes was analyzed by dynamic light scattering (Zetasizer Nano ZS90; Malvern Instruments Ltd., Malvern, UK). Each sample was measured in triplicate for 14 cycles at 25 °C. Then, ultrafiltration centrifugal method was used to assess the entrapment efficiency of liposome. In this method, 100 μl liposome was added into the ultrafiltration concentrator (10 kDa) and then centrifuged (3000 rpm) for 30 min to make sure the unentrapped CPT-11 follow to the bottom, and the content was the part of the entrapped liposome. The content of F-CPT-11 and liposomal fraction of CPT-11 were then determined by high-performance liquid chromatography (HPLC) on a reverse Agilent 5 TC-C_{18} (2) column (250 mm × 4.6 mm, 4.5 μm). The entrapment efficiency was then calculated by the equation: entrapment efficiency % = liposome fraction of CPT-11/ (liposome fraction of CPT-11 + F-CPT-11) * 100.

2.8. Pharmacokinetic analysis and bio-distribution study

The developed method was finally applied in the quantification of SN-38, F-CPT-11 and T-CPT-11 for pharmacokinetic study in rat plasma and bio-distribution study (including heart, liver, spleen, lung and kidney) in mice. Animal experiments involved were performed according to the "Guidelines for the Care and Use of Laboratory Animals", and were approved by the Animal Ethics Committee of Shenyang Pharmaceutical University (Shenyang, China).

Each rat was given at 2.5 mg/kg CPT-11 liposome by intravenous administration. Then, at 0.083, 0.25, 0.5,1, 2, 4, 6, 8, 12, and 24 h, 0.2–0.3 ml blood samples was obtained through orbital venous plexus and collected in polyethylene tubes. Collected blood samples was immediately centrifuged at 10 000 rpm for 5 min, upper plasma was then stored at −80 °C until analysis.

In bio-distribution study, each mouse (22 ± 2 g) was given 2.5 mg/kg CPT-11 liposome formulation by intravenous administration. Vital organs (heart, liver, spleen, lung and

kidney) were then removed at 6 h, 24 h and 48 h and washed with saline thoroughly to remove blood. Then, tissues were dried, weighed and diluted 1:1 by saline and homogenized with saline carefully in an ice bath and stored at −80 °C until analysis.

In this study, the DAS 2.1.1 was used for pharmacokinetic parameters analysis. All values were expressed as mean ± SD.

3. Results and discussion

3.1. Method optimization

As carboxylesterase is in a high active state in rat plasma, inactivating carboxylesterase and preventing the transformation of CPT-11 into metabolite SN-38 during sample processing was a major concern. The lactone forms CPT-11 and SN-38 have a closed α-hydroxy-δ-lactone ring, which play a key role in the interaction between CPT-11 / SN-38 with topoisomerase I [16]. However, it should be noted that this functional lactone ring was liable and probably hydrolyzed to the carboxylate form [20]. The hydrolysis of the lactone ring occurred under a pH-dependent equilibrium, and the rate is dependent on pH [17], ionic strength [16], and protein concentration [17]. In the current study, liposome could stabilize entrapped CPT-11 as active lactone form. And it was also possible to ensure that CPT-11 and SN-38 were quantified as total lactone form by adjusting the pH during pre-treatment and chromatographic separation process [21].

The SPE separation process of F-CPT-11 has to be achieved without breaking the liposome integrity. Previous study has shown that chilling samples at 4 °C could probably sustain the stability of lactone form [19]. Thus, all solvent involved in SPE process was maintained at 4 °C. Moreover, zinc sulfate which has strong capacity of enzyme inactivation and compatibility of mass analyses was added to plasma to inactivate carboxylesterase [22,23]. Mass spectroscopy parameters were optimized in positive ion mode to achieve sensitivity and selectivity. CPT-11, IS and SN-38 spectrometric analysis were scanned in ESI positive, and MRM mode was used for signal acquisition. It was found that CPT-11, IS and SN-38 were more sensitive in positive ion mode, were able to accept proton and generate $[M+H]^+$ ions. And the base peak of CPT-11, IS and SN-38 (Fig. 1) was selected at m/z 587.4, 393.2 and 349.2 respectively. In addition, collision energy was further optimized to acquire more abundant product ions of three analytes. The most prominent and stable fragments of CPT-11, SN-38 and IS were selected at m/z 167.1, 349.2 and 305.1 at a collision energy of 37 eV, 34 eV and 35 eV respectively. And the source temperature was set at 120 °C.

3.2. Method validation

3.2.1. Specificity

The specificity of SPE method and protein precipitation extraction were evaluated by analyzing six different batches of blank plasma/tissue versus the corresponding analytes spiked plasma/tissue. The typical chromatograms are shown in Fig. 2 and Fig. S1. The chromatographs demonstrate the sensitivity, selectivity and specificity of both methods. Retention time of 0.67, 1.63, and 1.28 min were observed for CPT-11, IS and SN-38 respectively. Moreover, there was no obvious interference from blank plasma and blank tissue at corresponding retention times.

3.2.2. Linearity calibration curves and LLOQ

The current assay offered LLOQ of 10 ng for quantitation of F-CPT-11, 4.44 ng for T-CPT-11, 25 ng for L-CPT-11 and OT-CPT-11, and 5 ng for SN-38. These limit of quantitation were sufficient enough for further studies. And these standard calibration curves exhibited excellent linearity in the linear range. The typical regression equations were $y = 9.04 \times 10^{-3}x + 4.32 \times 10^{-3}$ ($r^2 = 0.99$) for F-CPT-11, $y = 1.05 \times 10^{-3}x - 2.77 \times 10^{-2}$ ($r^2 = 0.99$) for T-CPT-11, $y = 2.55 \times 10^{-3}x - 3.08 \times 10^{-2}$ ($r^2 = 0.99$) for L- CPT-11, $y = 3.05 \times 10^{-3}x + 6.51 \times 10^{-2}$ ($r^2 = 0.99$) for OT-CPT-11, and $y = 2.57 \times 10^{-3}x - 7.58 \times 10^{-3}$ ($r^2 = 0.99$) for SN-38.

3.2.3. Precision and accuracy

The intra-day and inter-day precision and accuracy of three analytes were validated by analyzing LLOQ ($n = 6$) and QC samples ($n = 6$,) at three levels in plasma and tissue. As shown in Table 1, the established method was accurate and repeatable, tested samples were within the acceptable criteria (RSD% < 15%).

3.2.4. Recovery and matrix effect

SPE and protein precipitation extraction were applied in this study for extracting F-CPT-11 and T-CPT-11 from plasma and tissue. The mean extraction recoveries and matrix effect for two methods were shown in Table 2. Considering that the extraction recoveries of tissue samples were still reproducible and compatible, the developed method remain sufficient within the detection limit. Moreover, as the matrix effect was also within the acceptable range (below 115%), reproducible and did not alter the precious or accuracy.

3.2.5. Stability

The stability of CPT-11 and SN-38 in plasma and tissue was investigated under a variety of conditions: short-term stability, long-term stability, freeze-thaw stability and auto sampler stability. The results were shown in Table S1. Here, the short-term stability of the F-CPT-11 samples was investigated at 4 °C to reduce likely occurrence of liposome leakage. As shown, the results indicated that F-CPT-11 was stable at 4 °C for 6 h and at −30 °C for 2 weeks. Other samples were stable under analysis, all RE values were less than 15%. The stability of this UPLC-MS/MS method against column temperature were also evaluated. As shown in Table S2, tested samples were within the acceptable criteria (all RE and RSD values were less than 15%). Moreover, RSD for inter- and intra-batch were 12.32% and 5.04% respectively, all less than 15%. The results indicated that CPT-11 was stable for against small variations of column temperature.

3.2.6. Dilution effect

To ensure the accuracy of quantitation, plasma samples with high concentration of T-CPT-11/SN-38 must be diluted before processing. Therefore, the dilution effect of T-CPT-11 and SN-38 in rat plasma were measured. As shown in Table S1, the established dilution method was accurate and repeatable, tested

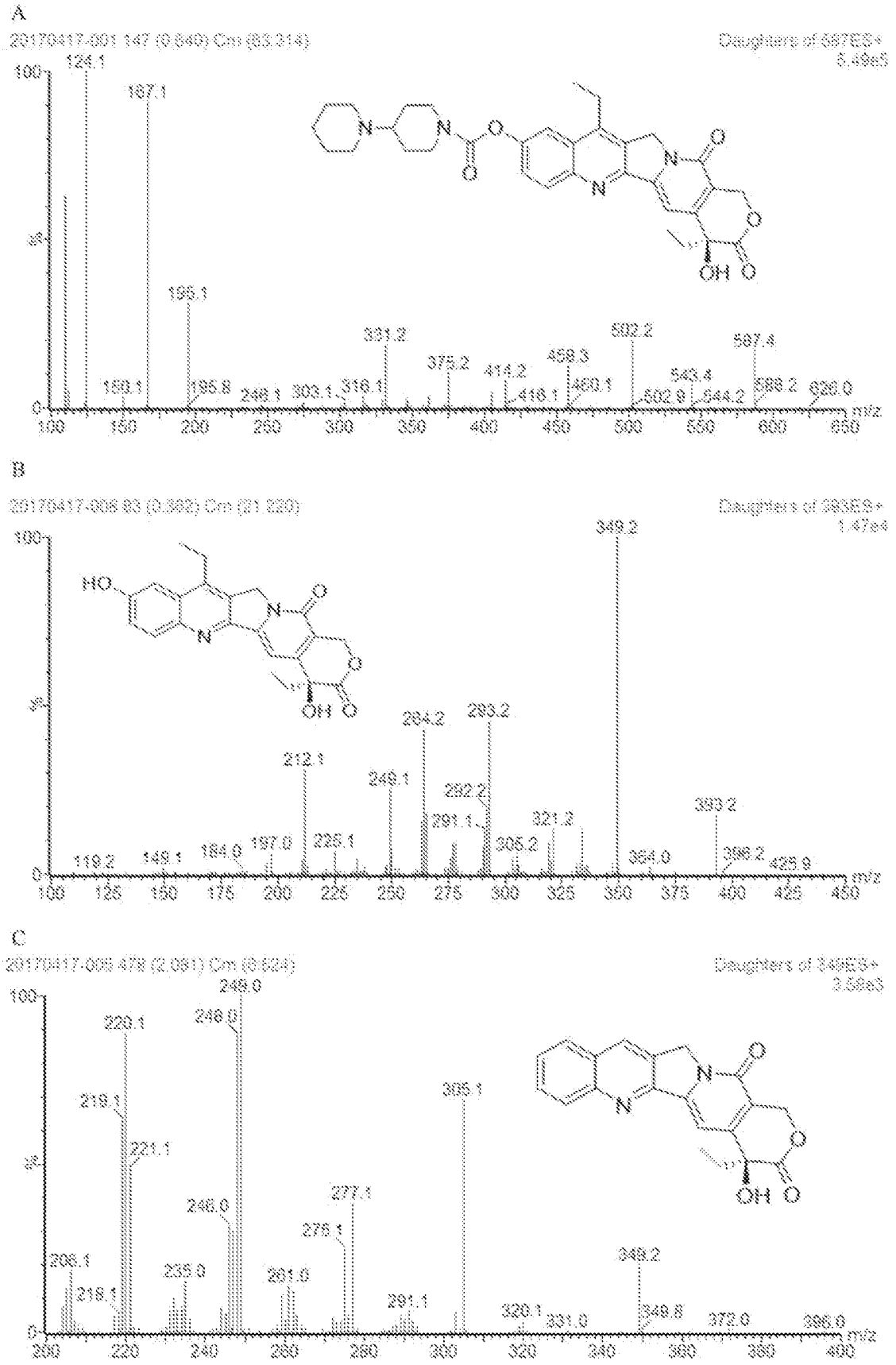

Fig. 1. – Product ion mass spectra of CPT-11(A), SN-38(B), and CPT(C).

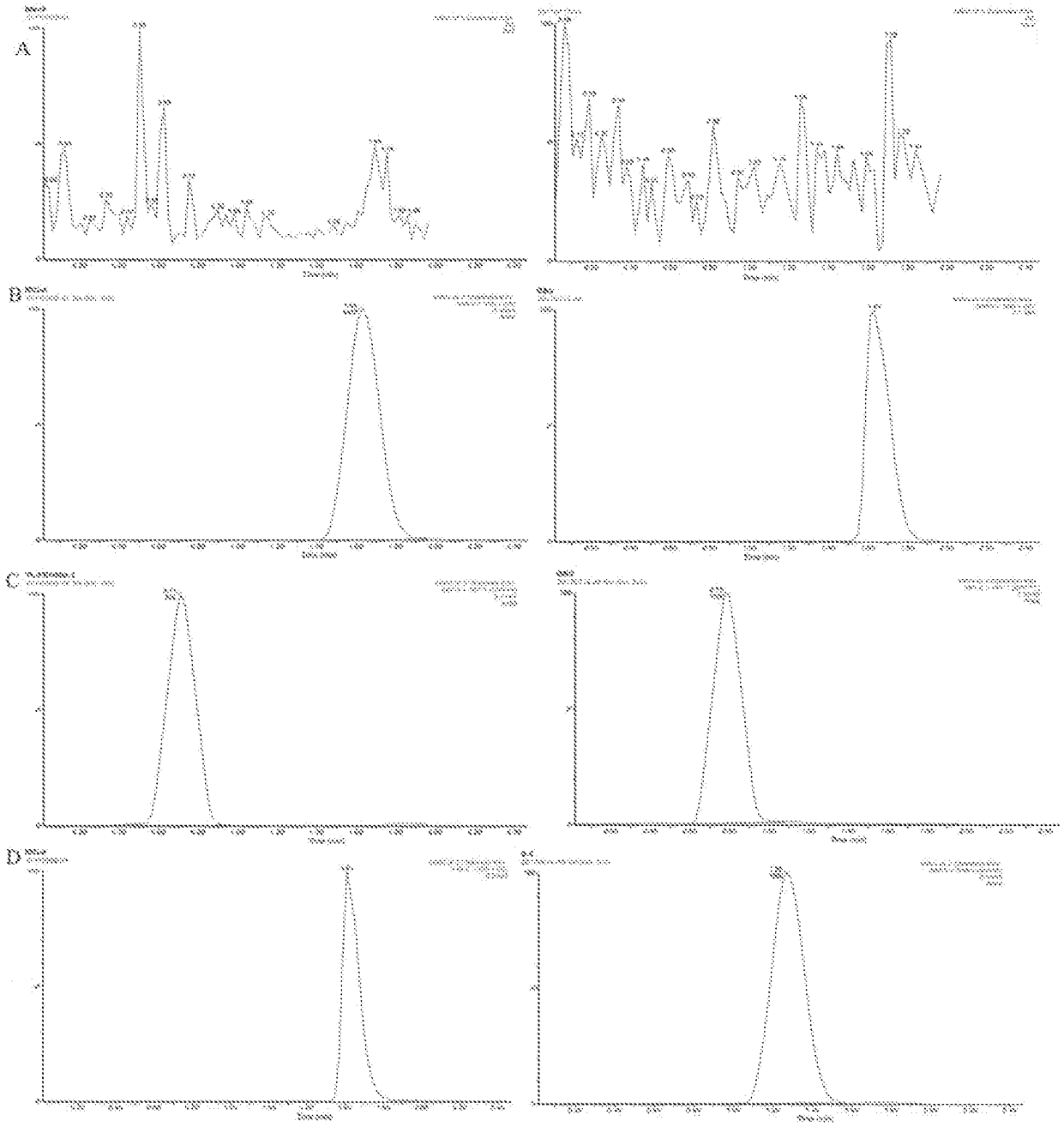

Fig. 2. – Typical UPLC chromatograms of blank plasma samples, blank tissue samples (A), UPLC chromatograms of plasma samples and blank tissue samples spiked with the IS (B), UPLC chromatograms of CPT-11 in plasma samples from a rat at 1 h and tissue sample from a mice at 6 h after intravenous administration of CPT-11 liposome (C), UPLC chromatograms of IS and SN-38 in plasma samples from a rat at 1 h after intravenous administration of CPT-11 liposome (D).

samples were within the acceptable criteria (RSD% < 15%, RE % < 15%).

3.3. *Method feasibility*

Protocol for separating F-CPT-11 from plasma was shown in Fig. 3. And the feasibility results for both SPE and protein precipitation extraction were summarized in Table 3. To quantify the released F-CPT-11 during the extraction process, QC samples spiked with CPT-11 liposome solution ($n = 3$) were extracted at three concentrations by using SPE. After one-step extraction, F-CPT-11 (F_1%) in LOQ, MOQ, and UOQ were 0, 4.90% and 1.59% respectively. And the corresponding F_2% value in three QC levels were 0%, 0.92%, 1.34% respectively. Compared with the amount of F-CPT-11 originally present in CPT-11 liposome solution, the value of F_1% and F_2% in QC samples were below than 5% and negligible. Thus, this result showed that SPE method could separate the F-CPT-11 from liposomes without changing its percentage and causing liposome damage during the extraction. And the

Table 1. – Precision and accuracy for assay of F-CPT-11, T-CPT-11, SN-38 in rat plasma and L-CPT-11, OT-CPT-11 in mouse at QC concentrations on three consecutive days (mean ± SD, $n = 6$).

		Concentration (ng/ml)		RSD (%)		RE (%)
		Added	Measured Conc	Intra-day	Inter-day	
F-CPT-11	LLOQ	10.00	10.14 ± 1.23	12.92	1.63	1.39
	LOQ	50.00	48.61 ± 1.14	8.36	9.56	−2.78
	MOQ	500.00	498.79 ± 41.08	7.98	9.93	−0.24
	UOQ	8000.000	8396.04 ± 566.38	5.81	11.54	4.95
T-CPT-11	LLOQ	4.44	4.06 ± 0.58	14.9	7.50	−8.50
	LOQ	11.10	10.11 ± 0.84	8.13	9.45	−8.93
	MOQ	1778.00	1973.66 ± 53.86	2.68	3.04	11.00
	UOQ	8888.00	8590.71 ± 982.39	10.80	15.38	−3.34
L-CPT-11	LLOQ	25.00	25.34 ± 3.14	12.37	11.62	1.40
	LOQ	62.50	63.69 ± 9.81	15.55	14.22	1.91
	MOQ	522.71	522.71 ± 39.22	7.92	2.79	4.54
	UOQ	863.90	863.90 ± 50.90	6.16	3.18	7.99
OT-CPT-11	LLOQ	25.00	25.49 ± 3.77	12.54	26.13	2.00
	LOQ	62.50	63.69 ± 6.80	7.68	22.94	−2.76
	MOQ	522.71	501.04 ± 41.64	6.42	16.67	0.21
	UOQ	863.90	848.11 ± 54.36	6.47	5.96	6.01
SN-38	LLOQ	5.00	4.86 ± 0.75	11.75	31.25	−2.90
	LOQ	10.00	10.03 ± 0.97	6.82	21.20	0.28
	MOQ	200.00	212.48 ± 14.98	4.74	15.93	6.24
	UOQ	800.00	810.86 ± 63.96	7.08	12.37	1.35

Table 2. – Matrix effect and extraction recovery of F-CPT-11, T-CPT-11, L-CPT-11, SN-38 in rat plasma and L-CPT-11, OT-CPT-11 in mouse at QC concentrations (mean ± SD, $n = 18$).

Analyte	Concentration (ng/ml)	Extraction recovery (%)	Matrix effect (%)
F-CPT-11	50.00	99.67 ± 13.37	103.72 ± 13.89
	500.00	96.54 ± 8.43	87.16 ± 11.77
	8000.000	100.00 ± 7.91	82.29 ± 5.35
T-CPT-11	11.10	78.54 ± 13.14	89.22 ± 11.98
	1778.00	78.76 ± 2.33	109.82 ± 3.25
	8888.00	100.00 ± 5.73	112.65 ± 6.39
L-CPT-11	62.50	83.23 ± 10.43	105.14 ± 13.18
	522.71	85.51 ± 4.19	98.99 ± 4.86
	863.90	95.85 ± 5.34	101.95 ± 5.68
OT-CPT-11	62.50	99.95 ± 8.59	113.30 ± 9.73
	522.71	78.44 ± 9.78	92.61 ± 11.55
	863.90	82.14 ± 4.47	76.44 ± 4.16
SN-38	10.00	99.67 ± 13.37	89.33 ± 12.60
	200.00	96.54 ± 8.43	86.31 ± 7.54
	800.00	100.00 ± 7.91	87.49 ± 6.27

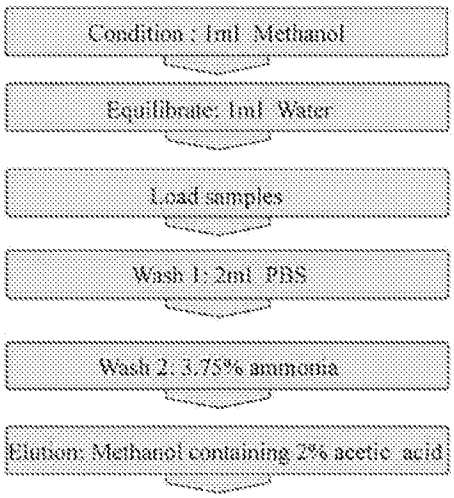

Fig. 3. – Protocol for separating F-CPT-11 from plasma by SPE.

concentrations of three QC samples spiked with liposomal CPT-11 were determined after extraction using protein precipitation, indicating that the protein precipitation extraction could achieve complete release of encapsulated CPT-11 from liposome.

Table 3. – Method feasibility of QC samples for SPE process.

	LOQ	MOQ	UOQ
F-CPT-11			
C_N (Nominal conc, ng/ml)	50	500	8000
C_{E1} (after one-step extraction, ng/ml)	0	24.48 ± 10.05	127.53 ± 38.59
F_1%	0	4.90	1.59
C_{E2}(after one-step extraction, ng/ml)	0	4.58 ± 6.67	107.56 ± 45.19
F_2%	0	0.92	1.34
C_F	39.31 ± 14.28	520.71 ± 145.08	8855.63 ± 488.45
T%	78.61	104.14	110.69

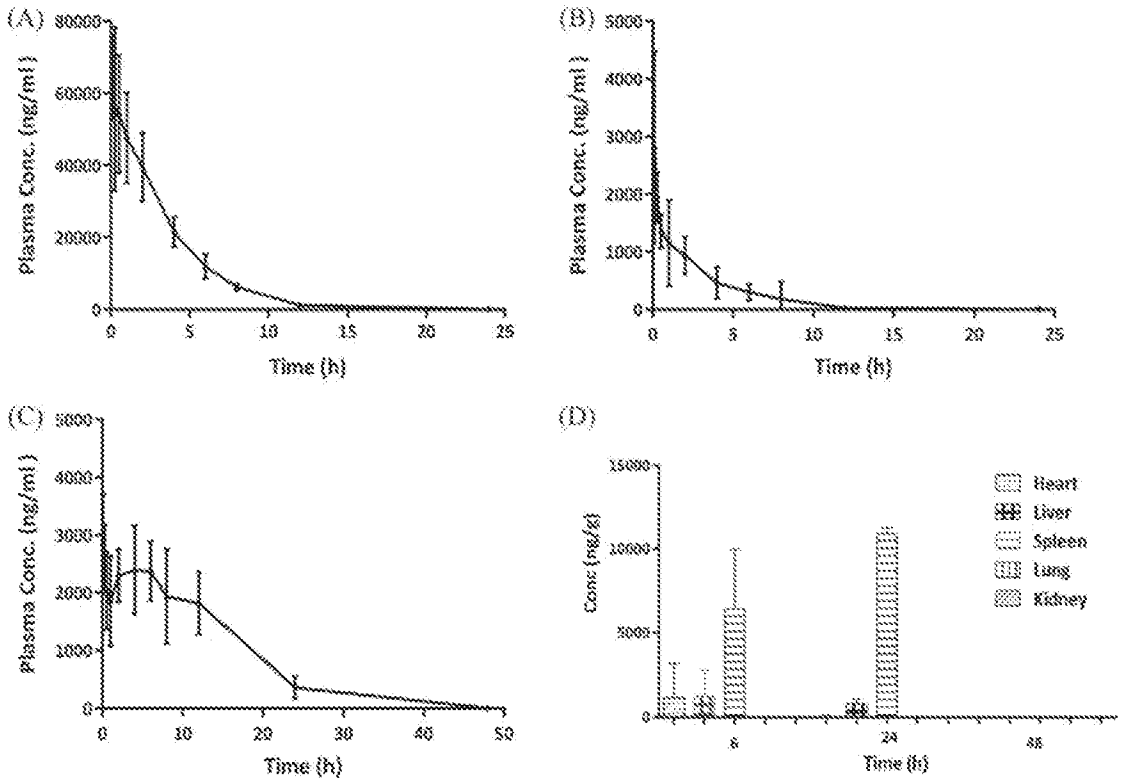

Fig. 4. – Plasma concentration profiles of T-CPT-11 (A), F-CPT-11 (B), SN-38 (C) after intravenous administration of 2.5 mg/kg CPT-11 liposome to rats and tissue distribution of CPT-11 after intravenous administration of 2.5 mg/kg CPT-11 liposome to mice (D).

3.4. *Preparation and characterization of CPT-11 liposome*

For CPT-11 liposome formulation, the entrapment efficiency was 98.23%. The mean diameter and zeta potential of CPT-11 liposomes measured by DLS were 131.4 ± 0.14 nm and – 18.5 ± 8.5 mV, respectively.

3.5. *Pharmacokinetic and bio-distribution study*

The method described above was then used for pharmacokinetic and bio-distribution study after intravenous dose of 2.5 mg/kg CPT-11 liposome. The plasma concentrations-time curves of F-CPT-11, T-CPT-11 and SN-38 were presented in Fig. 4. And main pharmacokinetic parameters of the analytes were shown in Table 4. After injection of CPT-11 liposomes, it was anticipated that most of the CPT-11 measured in rat plasma was encapsulated in the liposomal carrier to avoid system toxicity [11]. In this study, the C_{max} of F-CPT-11, T-CPT-11 were 1979.37 ng/ml and 45 812.62 ng/ml respectively, while the latter is about 23 times higher than the former. At 30 min after intravenous administration of CPT-11 liposome, the plasma concentration of F-CPT-11 was 1359.5 ng/ml, and that of T-CPT-11 was 54 207.36 ng/ml. This result indicated that F-CPT-11 represented 2.5% of the total CPT-11 in the plasma at this time point. As the result of method fea-

Table 4 – Pharmacokinetic parameters of F-CPT-11, T-CPT-11, L-CPT-11 and main metaboliteSN-38 in rat plasma after intravenous administration of 2.5 mg/kg CPT-11 liposome, (mean ± SD, $n = 5$ for T-CPT-11 and SN-38, $n = 3$ for F-CPT-11).

Pharmacokinetic parameters	F-CPT-11	T-CPT-11	SN-38
C_{max} (ng/ml)	1979.37 ± 373.47	45 812.62 ± 10 217.33	5864.599 ± 1266.643
$T_{1/2}$ (h)	1.93 ± 1.71	3.042 ± 0.83	4.42 ± 1.76
$MRT_{(0-48\ h)}$ (h)	3.10 ± 1.42	4.83 ± 0.90	8.31 ± 1.21
$MRT_{(0-\infty)}$ (h)	3.18 ± 1.57	4.94 ± 0.99	8.42 ± 1.25
$AUC_{0-48\ h}$ (ng/ml·h)	5864.599 ± 1266.643	241 352.36 ± 60 229.75	27 057.14 ± 5511.56
$AUC_{0-\infty}$ (ng/ml·h)	5888.45 ± 1295.67	242 452.99 ± 60 288.23	27 130.35 ± 5515.50

sibility above, we believe that leakage of liposome (below 5%) during the SPE process was acceptable, and SPE could be used to separate F-CPT-11 from liposome without changing the percentage of liposome artificially. The proportion of F-CPT-11 in plasma was also assessed by comparing the AUC values for both drug forms. The exposure amount ($AUC_{0-48\ h}$) of T-CPT-11 was found about 42 times higher than that of F-CPT-11 plasma, which means liposomalization and PEG modification significantly increased the circulation time of CPT-11. Previous study have shown that enzyme in rats plasma can catalyze the conversion of CPT-11 to SN-38 [24]. And $MRT_{(0-48\ h)}$ of SN-38 to that of F-CPT-11 ratio in this study was found to be 2.68 and long retention time of SN-38 could be explained by (1) entrapped CPT-11 in liposomes were stable in rat serum (2) CPT-11 was slowly released from liposomes, and then rapidly converted into SN-38 with catalysis of enzyme.

CPT-11 levels in tissues determined at 6 h, 24 h and 48 h were shown in Fig. 4D. The highest concentration of CPT-11 were observed in spleen and followed by liver. And in heart, the concentration of CPT-11 fell off quickly during 6 h to 24 h after administration. The bio-distribution results indicated that CPT-11 liposome was more efficient in delivering CPT-11 to spleen and liver compared with other tissues.

4. Conclusion

In this study, a selective and sensitive UPLC–MS/MS method coupled with SPE technique was developed to quantify the F-CPT-11 and T-CPT-11 in rat plasma. And SPE method was feasible for separating F-CPT from liposome. The UPLC–MS/MS method was then successfully applied for pharmacokinetic and bio-distribution studies of CPT-11 liposome. The result showed that the validated method would be helpful for toxicity assessment of CPT-11 loaded-liposome.

Conflicts of interest

The authors declare no competing financial interest.

Supplementary materials

Supplementary material associated with this article can be found, in the online version, at doi:10.1016/j.ajps.2018.08.003.

REFERENCES

[1] Allen TM, Cullis PR. Liposomal drug delivery systems: from concept to clinical applications. Adv Drug Deliv Rev 2013;65(1):36–48.

[2] Passero FC Jr, Grapsa D, Syrigos KN, Saif MW. The safety and efficacy of Onivyde (irinotecan liposome injection) for the treatment of metastatic pancreatic cancer following gemcitabine-based therapy. Expert Rev Anticancer Ther 2016;16(7):697–703.

[3] Drummond DC, Noble CO, Guo Z, Hong K, Park JW, Kirpotin DB. Development of a highly active nanoliposomal irinotecan using a novel intraliposomal stabilization strategy. Cancer Res 2006;66(6):3271–7.

[4] Charrois GJ, Allen TM. Drug release rate influences the pharmacokinetics, biodistribution, therapeutic activity, and toxicity of pegylated liposomal doxorubicin formulations in murine breast cancer. Biochim Biophys Acta 2004;1663(1-2):167–77.

[5] Mayer LD, St-Onge G. Determination of free and liposome-associated doxorubicin and vincristine levels in plasma under equilibrium conditions employing ultrafiltration techniques. Anal Biochem 1995;232(2):149–57.

[6] Thies RL, Cowens DW, Cullis PR, Bally MB, Mayer LD. Method for rapid separation of liposome-associated doxorubicin from free doxorubicin in plasma. Anal Biochem 1990;188(1):55–71.

[7] Deshpande NM, Gangrade MG, Kekare MB, Vaidya VV. Determination of free and liposomal amphotericin B in human plasma by liquid chromatography-mass spectroscopy with solid phase extraction and protein precipitation techniques. J Chromatogr B Anal Technol Biomed Life Sci 2010;878(3-4):315–26.

[8] Yamamoto E, Ryodo K, Ohuchi N, et al. Direct, simultaneous measurement of liposome-encapsulated and released drugs in plasma by on-line SPE-SPE-HPLC. J Chromatogr B Anal Technol Biomed Life Sci 2011;879(30):3620–5.

[9] Yang F, Wang H, Liu M, Hu P, Jiang J. Determination of free and total vincristine in human plasma after intravenous administration of vincristine sulfate liposome injection using ultra-high performance liquid chromatography tandem mass spectrometry. J Chromatogr A 2013;1275:61–9.

[10] Xie Y, Shao N, Jin Y, et al. Determination of non-liposomal and liposomal doxorubicin in plasma by LC-MS/MS coupled with an effective solid phase extraction: in comparison with ultrafiltration technique and application to a pharmacokinetic study. J Chromatogr B Anal Technol Biomed Life Sci 2017;1072:149–60.

[11] Krishna R, Webb MS, St Onge G, Mayer LD. Liposomal and nonliposomal drug pharmacokinetics after administration of liposome-encapsulated vincristine and their contribution to drug tissue distribution properties. J Pharmacol Exp Ther 2001;298(3):1206–12.

[12] Druckmann S, Gabizon A, Barenholz Y. Separation of liposome-associated doxorubicin from non-liposome-associated doxorubicin in human plasma: implications for pharmacokinetic studies. Biochim et Biophys Acta 1989;980(3):281–4.
[13] Griese N, Bisschke G, Boos J, Hempel G. Determination of free and liposome-associated daunorubicin and daunorubicinol in plasma by capillary electrophoresis. J Chromatogr A 2002;979(1):379–88.
[14] Kim HS, Wainer IW. Simultaneous analysis of liposomal doxorubicin and doxorubicin using capillary electrophoresis and laser induced fluorescence. J Pharmaceut Biomed Anal 2010;52(3):372–6.
[15] Wang G, Zhao DY, Chen HX, et al. Development and validation of a UPLC-MS/MS assay for the determination of gemcitabine and its L-carnitine ester derivative in rat plasma and its application in oral pharmacokinetics. Asian J Pharmaceut Sci 2017;12(5):478–85.
[16] Fassberg J, Stella VJ. A kinetic and mechanistic study of the hydrolysis of camptothecin and some analogues. J Pharmaceut Sci 1992;81(7):676–84.
[17] Burke TG, Mi Z. Preferential binding of the carboxylate form of camptothecin by human serum albumin. Anal Biochem 1993;212(1):285–7.
[18] https://www.fda.gov/Drugs/DevelopmentApprovalProcess/Manufacturing/ucm606333.htm.
[19] Boyd G, Smyth JF, Jodrell DI, Cummings J. High-performance liquid chromatographic technique for the simultaneous determination of lactone and hydroxy acid forms of camptothecin and SN-38 in tissue culture media and cancer cells. Anal Biochem 2001;297(1):15–24.
[20] Ramesh M, Ahlawat P, Srinivas NR. Irinotecan and its active metabolite, SN-38: review of bioanalytical methods and recent update from clinical pharmacology perspectives. Biomed Chromatogr BMC 2010;24(1):104–23.
[21] Goldwirt L, Lemaire F, Zahr N, Farinotti R, Fernandez C. A new UPLC-MS/MS method for the determination of irinotecan and 7-ethyl-10-hydroxycamptothecin (SN-38) in mice: application to plasma and brain pharmacokinetics. J Pharm Biomed Anal 2012;66:325–33.
[22] Zhang Z, Yao J, Wu X, Zou J, Zhu J. An accurate assay for simultaneous determination of irinotecan and its active metabolite SN-38 in rat plasma by LC with fluorescence detection. Chromatographia 2009;70(3-4):399–405.
[23] Kurita A, Kaneda N. High-performance liquid chromatographic method for the simultaneous determination of the camptothecin derivative irinotecan hydrochloride, CPT-11, and its metabolites SN-38 and SN-38 glucuronide in rat plasma with a fully automated on-line solid-phase extraction system, PROSPEKT. J Chromatogr B Biomed Sci Appl 1999;724(2):335–44.
[24] Tsuji T, Kaneda N, Kado K, Yokokura T, Yoshimoto T, Tsuru D. CPT-11 converting enzyme from rat serum: purification and some properties. J Pharmacobio-Dyn 1991;14(6):341–9.

Biomaterials Science

PAPER

View Article Online
View Journal | View Issue

Cite this: *Biomater. Sci.*, 2019, 7, 419

The influence of trapping agents on the antitumor efficacy of irinotecan liposomes: head-to-head comparison of ammonium sulfate, sulfobutylether-β-cyclodextrin and sucrose octasulfate

Wenqian Yang,[a] Zimeng Yang,[a] Jingru Fu,[a] Mengran Guo,[a] Bingjun Sun,[a] Wei Wei,[a] Dan Liu*[b] and Hongzhuo Liu*[a]

Remote loading technology is an outstanding achievement in liposome-based drug delivery systems. Compared with conventional passive loading, remote loading technology exhibits unique superiority in terms of high drug loading efficiency, low leakage rate and adequate drug accumulation. In the intra-liposome aqueous phase, the counterion of the trapping agent can control the state of aggregation/crystallization of the drug-counterion salt, and thereby contribute to control the efficiency of remote loading. Herein, irinotecan (CPT-11)-loaded liposomes were developed using three trapping agents: ammonium sulfate (AS), sulfobutylether-β-cyclodextrin (SBE-β-CD) and sucrose octasulfate (SOS). The corresponding formulations were named as AS liposomal CPT-11, TEA-SBE-β-CD liposomal CPT-11 and TEA-SOS liposomal CPT-11, respectively. Cryo-transmission electron micrographs showed that bundles of CPT-11 fibers were gathered inside TEA-SOS liposomal CPT-11. Furthermore, compared with AS liposomal CPT-11 and TEA-SBE-β-CD liposomal CPT-11, TEA-SOS liposomal CPT-11 demonstrated slower drug release, prolonged circulation time and significantly improved antitumor efficiency. To avoid the protection of ONIVYDE®-related patents, a number of other liposomal CPT-11 formulations are under preclinical investigation or even in clinical trials. Our study gives new insights into the impact of the trapping agent on remote loading, and provides valuable information to evaluate the development of CPT-11 loaded liposomes.

Received 23rd September 2018,
Accepted 10th November 2018

DOI: 10.1039/c8bm01175c

rsc.li/biomaterials-science

Introduction

In 1972, Deamer and coworkers first introduced a remote loading liposomes system.[1,2] Analyses of current loading approaches have revealed that the remote loading approach is the only option to achieve liposomal formulation with high drug encapsulation, enhanced safety and increased efficacy.[3–5]

Inside liposomes, drugs can form an aggregation state with a specific trapping agent such as ammonium sulfate (AS), chloride ammonium, calcium acetate or sodium acetate.[6–9] Moreover, polyanions such as polyphosphate, sulfobutylether-β-cyclodextrin (SBE-β-CD) or sucrose octasulfate (SOS), in conjunction with a transmembrane triethylammonium (TEA) gradient, could also mediate effective drug loading.[10,11]

It is noteworthy that encapsulated drugs are themselves not bioactive; only when the drugs are released from the liposomes, delivered to the disease site and exceed the minimum effective concentration, can optimal therapeutic activity be anticipated.[12,13] The drug-trapping-agent complex, which determines the drug loading ability and encapsulated drug release kinetics,[6,14] influences the therapeutic activity and toxicity of liposomal drug delivery systems.[15,16] The solubility of the drug-trapping-agent complex is important,[17,18] with very low solubility leading to slow drug release. In some cases, slow release of the encapsulated drug is advantageous, with a low leakage rate *in vivo*.[19] However, slow release and a low leakage rate in turn cause low drug availability in inflammatory tissues.[20–22] This is a clear indication of the importance of the drug-trapping agent complex. However, the influence of the trapping agent on drug loading, release and retention properties, as well as toxicity and efficacy, still needs to be evaluated.

[a]*School of Pharmacy, Shenyang Pharmaceutical University, Shenyang 110016, China. E-mail: liuhongzhuo@syphu.edu.cn; Fax: +86-24-43520586; Tel: +86-24-43525865*

[b]*Key Laboratory of Structure-Based Drugs Design & Discovery of Ministry of Education, Shenyang Pharmaceutical University, Shenyang 110016, China. E-mail: sammyld@163.com*

To see how the encapsulation method can influence drug retention properties, we used irinotecan (CPT-11) as the model drug. CPT-11 is a water-soluble derivative of camptothecin.[23] However, the therapeutic efficiency of CPT-11 is severely restricted by its stability and non-specific toxicity. The terminal lactone ring of CPT-11 is easily hydrolyzed in physiological conditions and then converted to the inactive carboxylate form.[24] To overcome these problems, ONIVYDE®, which was developed by encapsulating CPT-11 into liposomes using sucrose octasulfate triethylammonium as a trapping agent, was approved by the Food and Drug Administration (FDA) in 2015 for the clinical treatment of advanced pancreatic cancer.[25] In order to bypass ONIVYDE®-related patents, other liposomal CPT-11 formulations prepared with different trapping agents are currently under investigation. Therefore, it is necessary to directly compare and evaluate the effectiveness of these formulations in order to direct the development of liposomal CPT-11 formulations. In this study, three trapping agents containing different numbers of sulfate groups were selected. AS is a widely used trapping agent in remote loading techniques. SBE-β-CD is one of the most popular β-CD derivatives, with a lipophilic cavity containing a mean of 6.5 sulfates per cyclodextrin (CD). Due to its improved toxicity profile, SBE-β-CD has been widely used to solubilize poorly water-soluble drugs. Moreover, as one SBE-β-CD molecular could bind multiple drug molecules,[11] SBE-β-CD could improve drug retention. Finally, SOS is a highly charged polyanionic moiety with eight sulfonic groups. As expected, the number of sulfates has a profound impact on the physicochemical properties of the trapping agent. In this study, the influence of the trapping agent on the retention properties and kinetics of the encapsulated drug in a remote loading system were evaluated.

Materials and methods

Materials

Irinotecan was kindly provided by Jiangsu Hengrui Medicine Co., Ltd (China). SOS was obtained from Wuhan Hengruikang Reagent Co., Ltd (China). Methanol, acetonitrile and dichloromethane (high-performance liquid chromatography [HPLC] grade) were purchased from Tianjin Kemer Chemical Reagent Co., Ltd (Tianjin, China). Disaturated phosphatidylcholine (DSPS), cholesterol (Chol) and 2-distearoyl-snglycero-3-phosphoethanolamine-*N*-[methoxy (polyethylene glycol)-2000] (mPEG2000-DSPE) were purchased from Shanghai Advanced Vehicle Technology Ltd Co. Sephadex G-75 size exclusion resins were procured from Sigma Chemical Company (St Louis, USA). All other reagents and solvents described were of analytical grade.

The HT-29 tumor cell line was originally obtained from the Institute of Biochemistry and Cell Biology, Chinese Academy of Science (Shanghai, China). Nude mice (8–10 weeks old), Kunming (KM) mice (20 ± 2 g) and Sprague Dawley (SD) rats (250 ± 20 g) were obtained from Shenyang Pharmaceutical University.

Preparation of SBE-β-CD and SOS salts

TEA salt solutions of SBE-β-CD and SOS were prepared from commercially acquired sodium salts by ion-exchange chromatography on 732 cation exchange resin, immediately followed by titration with TEA. The sodium salt was then determined by an Na^+ selective electrode; residual sodium salt in either solution was less than 1% of the cation content. The concentration was adjusted to 0.65 mol L^{-1} for the TEA-SOS solution and 0.2 mol L^{-1} for the TEA-SBE-β-CD solution. For both solutions, the final pH was 5.5 to 6.0. AS solution (0.25 mol L^{-1}) was prepared by dissolving commercial ammonium sulfate salt in water.

Preparation of liposomes

A mixture including DSPC (3 mol. parts), Chol (2 mol. parts) and mPEG2000-DSPE (0.015 mol. parts) was dissolved and mixed in dichloromethane, dried to a thin lipid film, and then subsequently hydrated with TEA-SOS solution, TEA-SBE-β-CD solution and AS solution, respectively. Hydration was performed under continuous shaking at 65 °C for 30 min to form multilamellar vesicles. To obtain large unilamellar vesicles, lipid suspensions were then gradually extruded 20 times through polycarbonate membranes with 0.8 μm, 0.4 μm and 0.2 μm pore sizes at 65 °C. The corresponding formulations were named as AS liposomal CPT-11, TEA-SBE-β-CD liposomal CPT-11 and TEA-SOS liposomal CPT-11, respectively.

Drug loading

Unentrapped salts of TEA-SOS, TEA-SBE-β-CD and AS were removed by column chromatography using Sephadex G-75 columns. Sephadex G-75 columns were equilibrated in pH 6.5 HEPES/NaCl (17/144, mM/mM) buffer to exchange the unentrapped TEA-SOS and AS. pH 6.5 sucrose/histidine (300/20, mM/mM) buffer was used to exchange the unentrapped TEA-SBE-β-CD. Upon buffer exchange, CPT-11 HCl was then added to the empty preformed liposomes at the desired ratio. The loading process was then optimized and performed above the phase transition temperature (T_m) of the lipids. The resulting mixture was incubated at 65 ± 5 °C for 1 h to realize drug loading, and then the mixture was chilled on ice for 20 min. In the TEA-SBE-β-CD gradient remote loading process, drug loading was performed in the presence of nigericin (20 ng mg^{-1} DSPC), and empty liposomes were incubated with nigericin for 15 min before drug loading.

The entrapment efficiency (EE) of the preformed liposomes was determined by a centrifugal ultrafiltration method. Briefly, liposomes (100 μL) were added to an ultrafiltration centrifuge tube (10 kDa), then centrifuged (3000 rpm) for 30 min to allow the free drug to flow to the bottom. To determine the CPT-11 concentration of the liposomes, 100 μL liposomes were solubilized in 10% Triton X-100, followed by a mixture of methanol and 0.001 M citric acid. Drug concentration was determined by HPLC on a reverse Agilent 5 TC-C18 (2) column (250 mm × 4.6 mm, 4.5 μm). Ultraviolet (UV) detection was set at 255 nm, with a mixture of anhydrous sodium dihydrogen phosphate

and sodium octane sulfonate/methanol/acetonitrile (57 : 25 : 18) as the eluent at a flow rate of 1.5 ml min^{-1}. The EE was calculated using the following equation: EE% = liposomes fraction/(liposomes fraction + free drug fraction) × 100.

Characterization of CPT-11 liposome

Particle size and zeta potential. The average size and zeta potential of the liposomes was analyzed using dynamic light scattering (Zetasizer Nano ZS90; Malvern, UK). All samples were diluted 100-fold in water before analysis and measured at 25 °C. Each sample was measured in triplicate over 14 cycles.

Cryo-TEM

An aliquot of 3.5 μL liposomes was added to negatively glow discharged R1.2/1.3 100 holey carbon films grids (Cu 200 mesh) (Quantifoil, Jena, Germany), blotted to remove the excess, and plunge-frozen in a liquid ethane–propane mixture in a chamber at 100% humidity with a Vitrobot Mark IV (FEI, Hillsboro, OR). Data were acquired using a FEI Talos F200C electron microscope at an operating voltage of 200 kV. Images were collected with a charge-coupled device operating at an absolute magnification of 36 000×. The dose rate of 35 e $Å^{-2}$ s^{-1} was used during data collection. Data were collected using Serial EM software with a nominal defocus value of −5 μm.

In vitro drug release study

The release behavior of CPT-11 liposomes formulations was investigated at 37 °C with a solution of glucose–histidine–NH_4Cl (250 mm/10 mm/20 mm, pH 7.5). Typically, liposomes containing 0.4 mg CPT-11 were dispersed in 50 mL of release media with shaking (100 rpm). At 1, 2, 4, 8, 12, 48, 96 and 144 h, 2 mL of solution was withdrawn. The sample was then passed through a 0.22 μm membrane filter. The CPT-11 concentration was determined by HPLC with Waters e2695 Separations Module and Waters 2489 UV/Visible Detector on a reverse Agilent 5 TC-C18 (2) column (250 mm × 4.6 mm, 4.5 μm). The column was maintained at 40 °C, and UV detection was set at 255 nm. A mixture of anhydrous sodium dihydrogen phosphate and sodium octane sulfonate/methanol/acetonitrile (57 : 25 : 18) was used as the eluent at a flow rate of 1.5 mL min^{-1}. The results were expressed as mean ± standard deviation (SD).

Pharmacokinetics study

The animal experiments were approved by the Animal Ethics Committee of Shenyang Pharmaceutical University (Shenyang, China), in accordance with the "Guideline for the Care and Use of Laboratory Animals". Male SD rats (250 ± 20 g) were randomly assigned to three groups (n = 5). Each rat was injected with a liposomes formulation (5 mg kg^{-1} CPT-11 equivalent) *via* the tail vein. At 5, 15 and 30 min, and 1, 2, 4, 6, 8, 12 and 48 h, blood samples (0.2 mL to 0.3 mL) were drawn from the suborbital venous plexus and immediately transferred to heparinized tubes. Blood samples were then centrifuged at 10 000 rpm for 5 min to separate the plasma, and the stored at −20 °C until further analysis.

To access the pharmacokinetic profiles of the CPT-11 liposomes formulations, released CPT-11 (F-CPT-11) and total CPT-11 (T-CPT-11) (released CPT-11 + encapsulated CPT-11) in plasma were separated and quantified.[26]

Bio-distribution study

Bio-distribution experiments were performed on male KM mice. Mice (22 ± 2 g) were randomly assigned to three groups (n = 3) and administered with CPT-11 liposomes at 5 mg kg^{-1} *via* the tail vein. At 6, 24 and 48 h after dosing, mice were sacrificed, and the main tissues (heart, liver, spleen, lung and kidney) were immediately harvested. Tissues were then rinsed in saline, dried, weighed and diluted 1 : 1 by saline, and the homogenized in an ice bath. Samples were then centrifuged at 3000 rpm and supernatants were stored at −20 °C until analysis. To access tissue distribution profiles of CPT-11 liposome formulations, released CPT-11 (F-CPT-11) and total CPT-11 (T-CPT-11) (released CPT-11 + encapsulated CPT-11) in liver and spleen were separated and quantified.[26]

In vivo antitumor activity

HT-29 cells bearing male nude mice were used to evaluate the *in vivo* antitumor efficacy of preformed CPT-11 liposomes. Briefly, HT-29 cells (approximately 2 × 10^6 cells per 100 μL) were inoculated subcutaneously in the right flank region of the mice. When the tumor size reached approximately 200 mm^3, HT-29 xenografts nude mice were randomly divided into six groups (n = 5): untreated control (Saline), 25 mg kg^{-1} TEA-SOS liposomal CPT-11, 25 mg kg^{-1} TEA-SBE-β-CD liposomal CPT-11, 10 mg kg^{-1} TEA-SOS liposomal CPT-11, 10 mg kg^{-1} TEA-SBE-β-CD liposomal CPT-11 and 10 mg kg^{-1} AS liposomal CPT-11. These formulations were administrated every 6 days through the tail veins for a total of five injections. Tumor volume and body weight were measured every 2 or 4 days after the first injection. Mice were sacrificed 4 days after the final injection, then the tumor and major organs were collected and fixed in formalin at room temperature for hematoxylin and eosin (H&E) analysis. In addition, tumors were weighed for the calculation of tumor burden. 0.2 mL serum was also collected to determine the activities of aspartate transaminase (AST), alanine transaminase (ALT), blood urea nitrogen (BUN) and creatinine.

Data analysis

In this research, all data were expressed as mean ± SD. Statistical differences were verified by Student's t-test or one-way analysis of variance (ANOVA).

Results and discussion

Preparation of CPT-11 liposomes

Fig. 1 and 2 describe the overall mechanism of the loading process. In AS liposomal CPT-11 (Fig. 2A), liposomes were prepared in 250 mM ammonium sulfate, then the ammonium sulfate was removed and replaced by HEPES/NaCl solution.

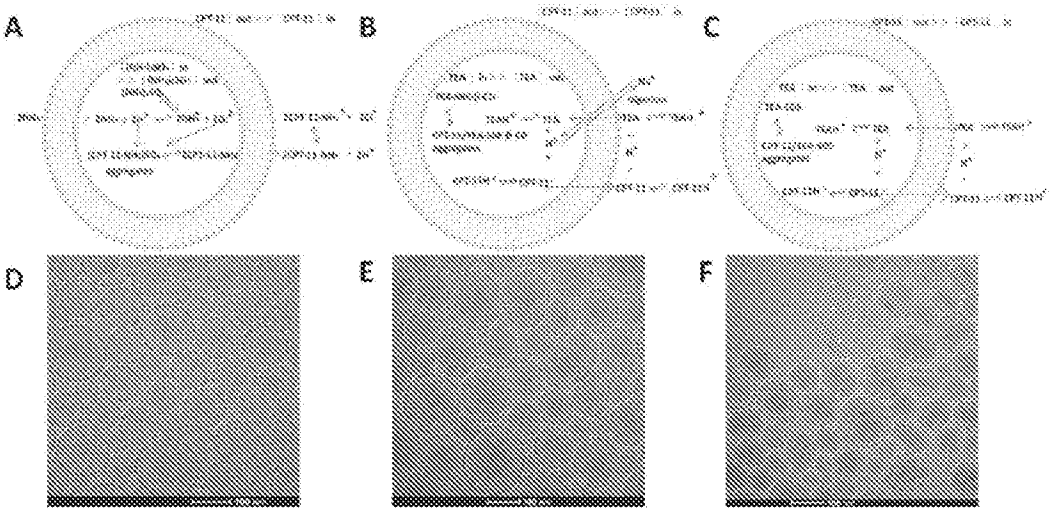

Fig. 1 Remote loading mechanism of AS liposomal CPT-11 (A), TEA-SBE-β-CD liposomal CPT-11 (B), (empty liposomes was incubated with nigericin) (C), Cryo-TEM of AS liposomal CPT-11 (D), TEA-SBE-β-CD liposomal CPT-11 (E) and TEA-SOS liposomal CPT-11 (F).

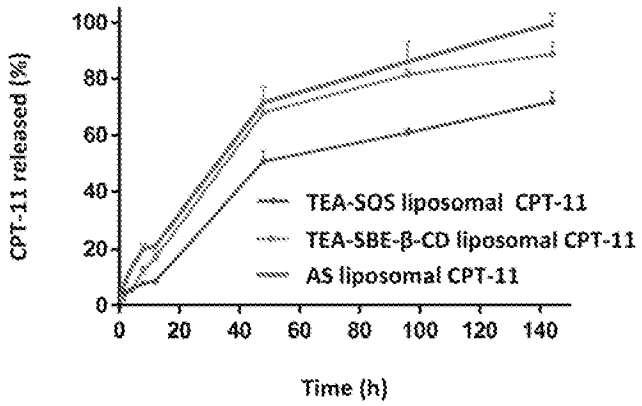

Fig. 2 *In vitro* release of CPT-11 liposomes with release buffer (250 mm glucose, 10 mm histidine, 20 mm NH_4Cl, pH 7.5); incubation temperatures were 37 °C.

The higher ammonium concentration inside AS liposomal CPT-11 induced the diffusion of neutral NH_3, and thus a pH gradient was formed. The magnitude of this AS gradient is derived by the ratio $[NH_4^+]_{extra}/[NH_4^+]_{inter}$. Next, the protonated NH_4^+ leads to an increase of pH, promoting the internalization of CPT-11 molecules. This effect accelerates the flocculation of CPT-11, further improving the drug encapsulation. As TEA is a weak base (pK_a of TEA is 10.75), in the case of TEA-SOS liposomal CPT-11 and TEA-SBE-β-CD liposomal CPT-11 (Fig. 2B and C), they dissociate to produce protons, and neutral TEA can freely permeate lipid bilayer, resulting in the acidification of intra-liposomal media and further improving the accumulation and encapsulation of CPT-11. Nevertheless, the drug-to-lipid (D/L) ratio for the different trapping agents differed, with the different D/L ratios possibly ascribed to different physico-chemical properties of the drug-trapping agent complex. In the AS gradient, AS could mediate stable encapsulation with a D/L ratio of 0.1. In contrast, each of SBE-β-CD and SOS could bind multiple CPT-11 molecules *via* electrostatic effects, such that D/L ratios of 0.40 and 0.63 were obtained. In the TEA-SBE-β-CD gradient remote loading process, nigericin was added to further improve the loading efficacy of the TEA-SBE-β-CD gradient. Nigericin, as a proton ionophore, was used to exchange Na^+ with proton to facilitate the pH gradient.[27,28] Accordingly, CPT-11 could be effectively loaded into liposomes by the TEA-SBE-β-CD gradient, and >99% drug encapsulation was obtained in the presence of nigericin.

Characterization of CPT-11 liposomes

After preparation of the CPT-11 liposomes, the particle size, zeta potential and encapsulation efficiency were investigated (Table 1). The particle sizes of the three formulations were approximately 130 nm. For the three formulations, >99% CPT-11 encapsulation was obtained.

Cryo-TEM was applied to visualize the physical state of the encapsulated CPT-11; representative images are shown in Fig. 1. The results confirm the size distribution determined in dynamic light scattering. Further, the interior of the liposomes appear highly electron-dense, indicating the existence of entrapped CPT-11. Bundles of fibers are clearly shown in the TEA-SOS liposomal CPT-11. In comparison, intra-liposomal CPT-11 gathers into an amorphous/gel precipitate, with no clearly defined structural organization in TEA-SBE-β-CD liposomal CPT-11 or AS liposomal CPT-11.

Intra-liposomal precipitation results from the drug self-association and interaction between the drug and counterion. Indeed, nano-crystal formation occurs only at drug concentrations in excess of its aqueous solubility limit. Furthermore, the property of precipitation (crystalline or non-crystalline form) is affected by many factors including the physico-chemical properties of the drug, intra-liposomal pH and the

Table 1 Characterization of CPT-11 liposomes

Formulation	Particle size (nm)	PDI	Zeta potential (mV)	EE (%)	D/L
TEA-SOS liposomal CPT-11	137.8 ± 3.477	0.096 ± 0.038	−11.30 ± −0.884	99.40	0.63
TEA-SBE-β-CD liposomal CPT-11	132.4 ± 2.460	0.045 ± 0.022	−17.30 ± −1.356	99.16	0.40
AS liposomal CPT-11	133.3 ± 1.484	0.030 ± 0.010	−18.80 ± −1.474	99.00	0.10

counterion of the gradient-forming ion. In a previous study, the physical state of doxorubicin inside the liposomes was examined. Doxorubicin loaded *via* an AS gradient existed in straight rods, while doxorubicin loaded *via* a citrate gradient existed as curved and circular bundles of fibers. However, doxorubicin aggregates appeared as uncondensed fibers in a liposomal formulation containing lactobionic acid. This suggests that the physical state of doxorubicin is related to the trapping agent.[29] In this study, AS could only interact with two CPT-11 molecules. In comparison, the polyanionic SBE-β-CD molecule (with a mean 6.5 sulfates) could bind more CPT-11 molecules. Moreover, SOS (with eight sulfates) carries multiple negative charges, and could interact with multiple CPT-11 molecules and facilitate inter-fiber crosslinking *via* an electrostatic effect. Hence, bundles of CPT-11 fibers could be observed in TEA-SOS liposomal CPT-11.

In vitro drug release

To quantitatively compare the role of the trapping agent in drug retention, *in vitro* release was performed in NH_4Cl-containing release media. NH_3 could freely permeate the lipid bilayer and elevate intra-liposomal pH, and thus induce CPT-11 release.[30] The *in vitro* profiles are shown in Fig. 2. Based on these results, TEA-SOS mediated the most stable CPT-11 encapsulation and showed reduced CPT-11 release. In TEA-SOS liposomal CPT-11, the amount of CPT-11 released was 60.96% over 96 h, which was lower than the amount released in both TEA-SBE-β-CD liposomal CPT-11 and AS liposomal CPT-11.

The difference between the release rates may be attributed to the difference in the extent of precipitation with different trapping agents. In other words, the higher the fraction precipitated, the slower the release rate. In TEA-SBE-β-CD liposomal CPT-11 and AS liposomal CPT-11, CPT-11 exists in a non-crystalline form. However, in TEA-SOS liposomal CPT-11, this is not the case, as CPT-11 exists in a crystalline form. Under this condition, the release property is governed by Fick's law relationship.[31,32]

$$d[C]_o^{ex}/dt = -pA([C]_o - [C]_i)/V_o$$

where $[C]_o^{ex}$ is the total exterior CPT-11 concentration, A is the membrane area, p is the permeability parameter of neutral CPT-11, and $[C]_i$ and $[C]_o$ are the concentrations of neutral CPT-11 inside and outside the liposomes.

Based on this formula, the release rate is proportional to the membrane area of the liposomes and the concentration of CPT-11 between the inner and outer liposome membrane. As the outer volume of the liposome is infinitely larger than the inner volume, thus $[C]_i \gg [C]_o$. The formula was then converted to $d[C]_o^{ex}/dt = pA[C]_i$, which suggests that the rapid release of CPT-11 relies on higher CPT-11 accumulation in the intra-liposome aqueous phase. Inside TEA-SOS liposomal CPT-11, the crystalline form of CPT-11 was in equilibrium with the small amount of the soluble and neutral form; therefore, solubility of the crystal aggregates is limited. Accordingly, if the dissolution of encapsulated CPT-11 crystals is a rate-limiting step, TEA-SOS liposomal CPT-11 would lead to a slower CPT-11 release than TEA-SBE-β-CD liposomal CPT-11 and AS liposomal CPT-11.

Pharmacokinetics study

The pharmacokinetics of TEA-SOS liposomal CPT-11, TEA-SBE-β-CD liposomal CPT-11 and AS liposomal CPT-11 after intravenous injection were investigated in SD rats. The plasma concentration-time curves of total CPT-11 (T-CPT-11), released CPT-11 (F-CPT-11) and the main metabolite 7-ethyl-10-hydroxycamptothecin (SN-38) are shown in Fig. 3, and the main pharmacokinetic parameters are presented in Tables 2–4.

After liposomes were injected into the systemic circulation, the clearance of the liposomal drug was dependent on: (i) the clearance of the liposomal nanocarrier due to interaction with plasma proteins or phagocytosis of reticuloendothelial system; (ii) the disassociation of the entrapped drug in the liposomes inner; (iii) the clearance and metabolism of the released drug.[33,33,34] Despite having the same lipid components, TEA-SOS was more supportive in constructing a sterically stabilized liposomes system, as shown in Fig. 4 and Tables 2–4. The half-lives of T-CPT-11 for TEA-SOS liposomal CPT-11 and TEA-SBE-β-CD liposomal CPT-11 were 5.52 and 6.32 h; significantly longer than that of AS liposomal CPT-11 (2.328 h) ($p < 0.01$ and $p < 0.001$). Moreover, the $AUC_{(0-t)}$ values were 645 543.45, 468 465.57 and 278 006.44 ng L^{-1} h^{-1} for TEA-SOS liposomal CPT-11, TEA-SBE-β-CD liposomal CPT-11 and AS liposomal CPT-11, respectively.

To fully understand the therapeutic efficacy and side effects of the liposomal formulation, the pharmacokinetics of the released CPT-11 were further evaluated. The ratio of F-CPT-11 concentration to T-CPT-11 concentration in plasma was then calculated. We observed that the percentage of F-CPT-11 between the three formulations were different. In the case of TEA-SOS liposomal CPT-11, 95.33% of detected CPT-11 was encapsulated in liposomes, and only 4.67% was present in F-CPT-11 at 6 h after intravenous administration. In contrast, CPT-11 cannot form a precipitate with SBE-β-CD and AS inside liposomes, and the amount of free drug outside the liposomes was relatively high, with 19.09% of detected CPT-11 present in

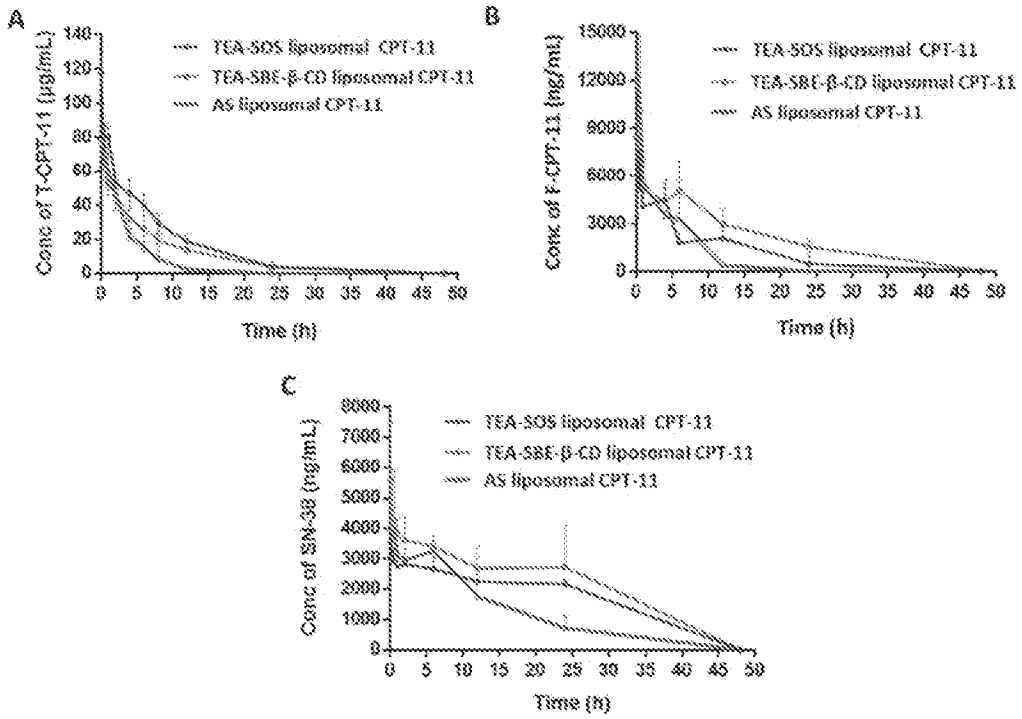

Fig. 3 Plasma concentrations of total CPT-11 levels (A), free CPT-11 levels (B), and main metabolite SN-38 levels (C) in SD rats injected with AS liposomal CPT-11, TEA-SBE-β-CD liposomal CPT-11 and TEA-TEA-SOS liposomal CPT-11. The CPT-11 dose was 5 mg kg^{-1}. CPT-11 levels and SN-38 levels were assayed using the ultra-performance liquid chromatography – tandem mass (UPLC-MS-MS) method. Data are shown as mean ± SD (n = 5).

Table 2 Summary of pharmacokinetic parameters of T-CPT-11

Pharmacokinetic parameters	AS liposomal CPT-11	TEA-SBE-β-CD liposomal CPT-11	TEA-SOS liposomal CPT-11
$AUC_{(0-t)}$ (ng L^{-1} h^{-1})	278 006.44 ± 22 516.72	463 465.57 ± 46 623.90★★★	645 543.45 ± 98 561.19★★★*
$AUC_{(0-\infty)}$ (ng L^{-1} h^{-1})	287 201.85 ± 25 973.99	503 789.36 ± 54 035.14★★★	682 368.64 ± 127 510.22★★★
$MRT_{(0-t)}$ (h)	2.99 ± 0.18	6.60 ± 0.39★★★	6.45 ± 0.52★★★
CLz (L h^{-1} kg^{-1})	0.058 ± 0.012	0.01 ± 0.001★★★	0.007 ± 0.001★★★**
$t_{1/2}$ (h)	2.33 ± 0.53	6.32 ± 1.33★★★	5.52 ± 1.38★★

Pharmacokinetic parameters were calculated for T-CPT-11 after the intravenous injection of CPT-11 liposomes at 5 mg kg^{-1}. Values represent the mean ± SD (n = 5). $p < 0.05$ (★), $p < 0.01$ (★★) and $p < 0.001$ (★★★) *versus* AS liposomal CPT-11 as the control; $p < 0.05$ (*) and $p < 0.01$ (**) and $p < 0.001$ (***) *versus* TEA-SBE-β-CD liposomal CPT-11 as the control.

Table 3 Summary of pharmacokinetic parameters of F-CPT-11

Pharmacokinetic parameters	AS liposomal CPT-11	TEA-SBE-β-CD liposomal CPT-11	TEA-SOS liposomal CPT-11 LPs
$AUC_{(0-t)}$ (ng L^{-1} h^{-1})	44 968.31 ± 11 775.20	96 506.50 ± 22 702.21★★	67 177.53 ± 32 943.54
$AUC_{(0-\infty)}$ (ng L^{-1} h^{-1})	45 152.20 ± 12 006.30	104 630.83 ± 28 683.36★★	67 788.94 ± 32 956.49
$MRT_{(0-t)}$ (h)	5.03 ± 0.63	13.28 ± 1.31★★★	9.72 ± 3.18★
CLz (L h^{-1} kg^{-1})	0.12 ± 0.031	0.27 ± 0.41★★	0.089 ± 0.039
$t_{1/2}$ (h)	4.29 ± 1.46	8.67 ± 2.72★	6.73 ± 1.86★

Pharmacokinetic parameters were calculated for F-CPT-11 after the intravenous injection of CPT-11 liposomes at 5 mg kg^{-1}. Values represent the mean ± SD (n = 5). $p < 0.05$ (★), $p < 0.01$ (★★) and $p < 0.001$ (★★★) *versus* AS liposomal CPT-11 as the control.

F-CPT-11 in TEA-SBE-β-CD liposomal CPT-11 and 20.92% in AS liposomal CPT-11. Accordingly, TEA-SOS liposomal CPT-11 prepared by a remote loading method with TEA-SOS gradient showed different *in vivo* release behavior. TEA-SOS gradient resulted in a close interaction between the SOS and CPT-11 and a lower release rate in the systemic circulation. Moreover, TEA-SOS liposomal CPT-11 showed the lowest F-CPT-11 levels, which could reduce the gastrointestinal toxicity.

Table 4 Summary of pharmacokinetic parameters of SN-38

Pharmacokinetic parameters	AS liposomal CPT-11	TEA-SBE-β-CD liposomal CPT-11	TEA-SOS liposomal CPT-11
$AUC_{(0-t)}$ (ng L^{-1} h^{-1})	499 50.66 ± 14 203.54	72 878.63 ± 17 371.80	59 743.30 ± 7,925.85
$AUC_{(0-\infty)}$ (ng L^{-1} h^{-1})	61 337.22 ± 22 224.52	191 025.44 ± 140 791.81	252 664.79 ± 80 033.28★★★
$MRT_{(0-t)}$ (h)	7.84 ± 1.86	10.91 ± 1.40★	11.08 ± 0.42★★
CLz (L h^{-1} kg^{-1})	0.092 ± 0.038	0.036 ± 0.019★	0.022 ± 0.008★★
$t_{1/2}$ (h)	9.57 ± 3.00	28.33 ± 14.35★★★	63.02 ± 24.52★★★

Pharmacokinetic parameters were calculated for SN-38 after the intravenous injection of CPT-11 liposomes at 5 mg kg^{-1}. Values represent the mean ± SD (n = 5). p < 0.05 (★), p < 0.01 (★★) and p < 0.001 (★★★) *versus* AS liposomal CPT-11 as the control.

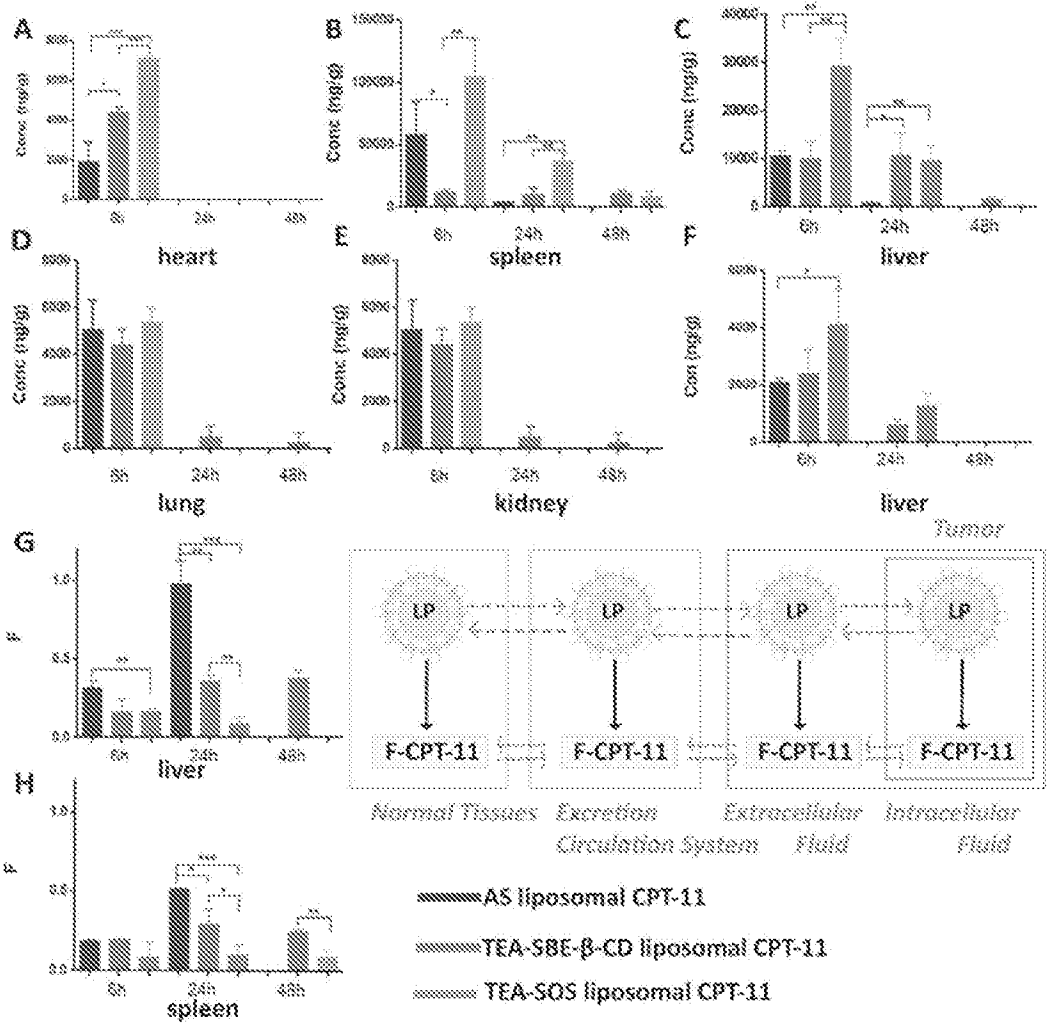

Fig. 4 Bio-distribution of T-CPT-11 levels in the main tissues including the heart (A), spleen (B), liver (C), lung (D) and kidney (E), and metabolite SN-38 levels in the liver (F) in KM mice injected with AS liposomal CPT-11, TEA-SBE-β-CD liposomal CPT-11 and TEA-SOS liposomal CPT-11 at 5 mg kg^{-1}, and F-CPT-11/T-CPT-11 ratio, namely F in the liver (G) and spleen (H). Data are shown as mean ± SD (n = 3).

Bio-distribution study

Tissue distribution (including heart, liver, spleen, lung and kidney) was evaluated at 6, 24 and 48 h after an intravenous injection of 5 mg kg^{-1} of TEA-SOS liposomal CPT-11, TEA-SBE-β-CD liposomal CPT-11 and AS liposomal CPT-11. The results are shown in Fig. 4.

In the liver, CPT-11 concentration at 6 h after administration of TEA-SOS liposomal CPT-11 was approximately 3-fold higher than that of TEA-SBE-β-CD liposomal CPT-11 and AS

liposomal CPT-11. At 24 h, CPT-11 concentration in TEA-SBE-β-CD liposomal CPT-11 was about the same as that at 6 h. However, the accumulation of CPT-11 in the spleen after injection of AS liposomal CPT-11 and TEA-SOS liposomal CPT-11 was 5-fold and 9-fold higher than that of TEA-SBE-β-CD liposomal CPT-11, respectively. Similarly, the accumulation of CPT-11 in the heart also showed a significant difference between groups. To further detect the drug state (encapsulated or released), F-CPT-11 in the liver and spleen was quantified, and the F-CPT-11/T-CPT-11 ratio, namely F (Fig. 3G, H) was calculated. In the liver, 99.3% of the encapsulated CPT-11 was released from the AS liposomal CPT-11 at 24 h after intravenous administration. In contrast, 30.3% CPT-11 was released from TEA-SBE-β-CD liposomal CPT-11, and almost no CPT-11 was released from TEA-SOS liposomal CPT-11. In the spleen, the *F* value also showed a significant difference between the three liposomal formulations.

In this study, AS was unable to form a stable physical state to retain CPT-11, and indeed a transmembrane gradient might be generated. The encapsulated CPT-11 in AS liposomal CPT-11 underwent rapid and total release in the liver. Unlike AS, as polyanions, SOS and SBE-β-CD were able to cross-link drug molecules at the intra-liposomal phase; therefore, this could reduce the leakage of CPT-11 both *in vitro* and *in vivo*. Stable drug entrapment of TEA-SOS liposomal CPT-11 could reduce premature drug release from liposomes to normal tissues, resulting in a lower F-CPT-11 percentage and reducing the conventional hepatotoxicity associated with F-CPT-11. As mentioned above, polyanions are indispensable to improve drug retention and achieve stable drug encapsulation.

In vivo antitumor activity

Male nude mice bearing HT-29 cells were used to evaluate the *in vivo* antitumor efficacy of AS liposomal CPT-11, TEA-SBE-β-CD liposomal CPT-11 and TEA-SOS liposomal CPT-11, the results are summarized in Fig. 5. Hepatorenal function parameters and H&E staining of the major organs, tumors after treatment were shown in Fig. 6. CPT-11 liposomes were administered to mice at two dosages: 10 mg kg^{-1} for three formulations and 25 mg kg^{-1} for TEA-SOS liposomal CPT-11 and TEA-SBE-β-CD liposomal CPT-11. As shown in Fig. 5A, the results revealed that (1) the therapeutic effect was dose-dependent; (2) TEA-SOS liposomal CPT-11 at 25 mg kg^{-1} was the most efficacious of all the formulations, and the tumor completely disappeared; (3) AS liposomal CPT-11 exhibited poor antitumor efficacy; (4) for treatment with TEA-SOS liposomal

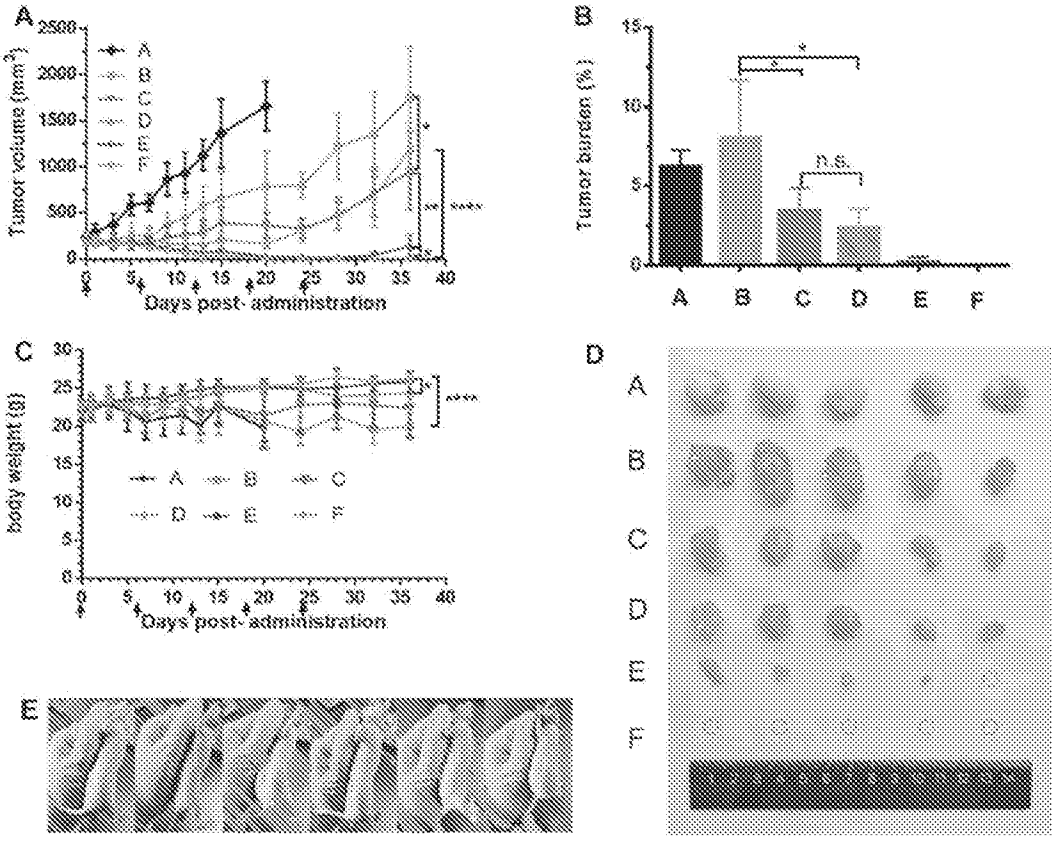

Fig. 5 *In vivo* antitumor activity of CPT-11 liposomes against HT 29 tumors (n = 5). (Group A: Saline, Group B: AS liposomal CPT-11 at 10 mg kg^{-1}, Group C: TEA-SBE-β-CD liposomal CPT-11 at 10 mg kg^{-1}, Group D: TEA-SOS liposomal CPT-11 at 10 mg kg^{-1}, Group E: TEA-SBE-β-CD liposomal CPT-11 at 25 mg kg^{-1}, Group F: TEA-SOS liposomal CPT-11 at 25 mg kg^{-1}). Tumor growth profiles treated with different CPT-11 liposomes formulations (A), tumor burden after the last treatment (B), body weight variations during treatment (C), images of tumors at day 36 (D), images of nudes injected with TEA-SOS liposomal CPT-11 at 25 mg kg^{-1} at day 36 (E).

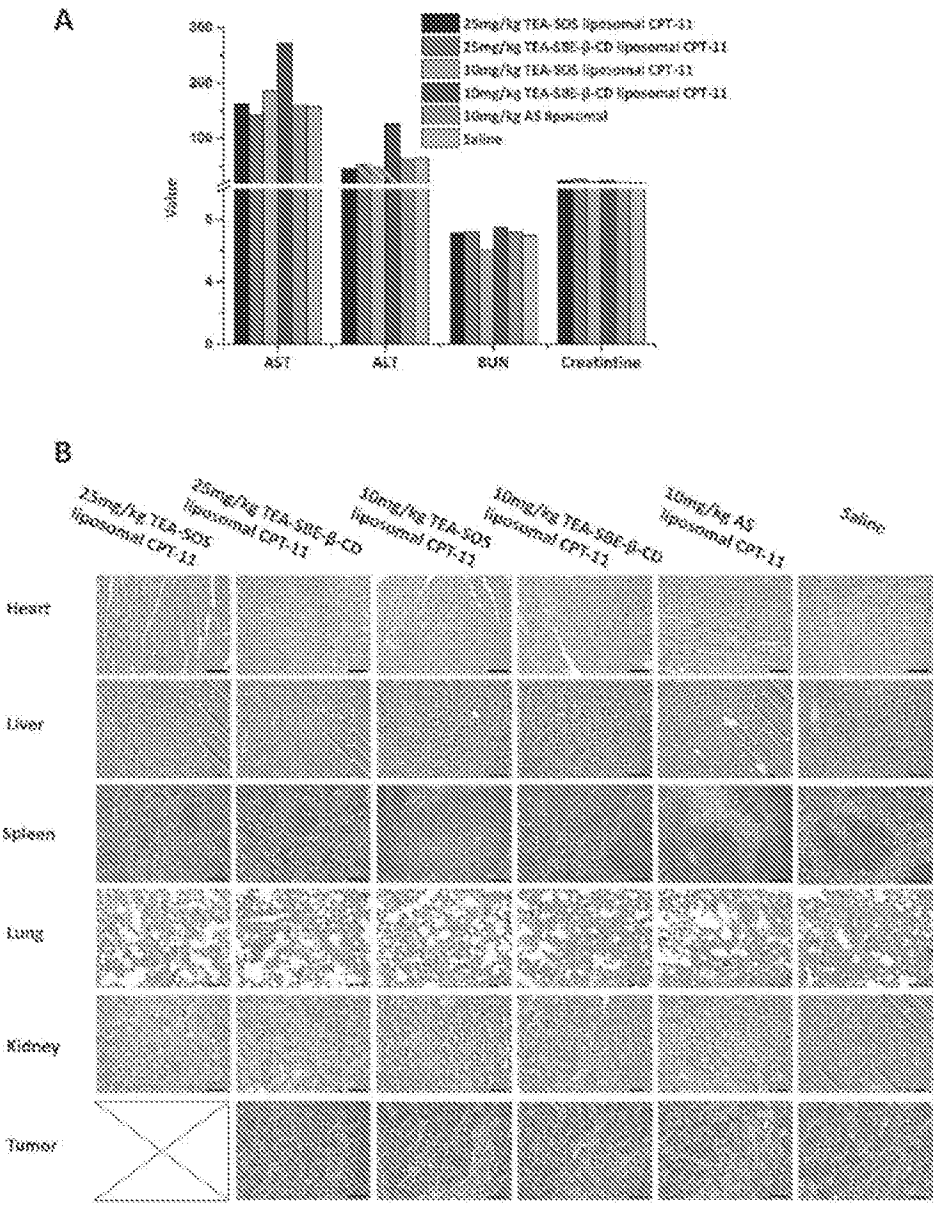

Fig. 6 Liver and kidney functional parameters at day 36 after scarified (A). Images of the different organ sections and tumors stained with H&E after various treatments (B).

CPT-11 and TEA-SBE-β-CD liposomal CPT-11 at 10 mg kg^{-1}, the antitumor activity was only maintained for 24 days, and regrowth of the tumor occurred after the final administration. H&E-stained pathological sections showed different levels of apoptosis in the tumor sections of TEA-SOS liposomal CPT-11, TEA-SBE-β-CD liposomal CPT-11 and AS liposomal CPT-11. Moreover, compared with mice treated with TEA-SOS liposomal CPT-11 at 25 mg kg^{-1}, mice treated with AS liposomal CPT-11 at 10 mg kg^{-1} exhibited significant weight loss ($p < 0.001$). The weight loss may be connected with massive drug leakage of AS liposomal CPT-11 in systemic circulation, as released drug contributes significant toxicity.

As can be seen from the rapid *in vitro* and *in vivo* release profiles, the AS gradient results in a weak interaction between the AS molecule and the CPT-11 molecule, and a lower ability to retain CPT-11 inside the liposomes. Thus, more CPT-11 may escape to the blood circulation before AS liposomal CPT-11 reaches the tumor sites, so the antitumor efficacy of AS liposomal CPT-11 *in vivo* may be less than that of TEA-SBE-β-CD liposomal CPT-11 and TEA-SOS liposomal CPT-11. Accordingly, the superior antitumor efficacy of TEA-SOS liposomal CPT-11 was attributed to several aspects: (i) improved stability and enhanced circulation time *in vivo* by PEGylation, (ii) high D/L ratio and crystallization inside liposomes which further improves the benefits of liposomal formulation and produces an adequate drug concentration, (iii) stable drug entrapment which can reduce premature drug release from liposomes. These aspects cover all stages influencing the biological

activity of the liposomal drug, resulting in superior chemotherapeutic efficacy of TEA-SOS liposomal CPT-11.

Conclusion

It is known that remote loading is an excellent technology for preparing sterically stabilized liposomes. In this study, intraliposomal trapping agents including AS, SBE-β-CD and SOS were used for remote loading of CPT-11 liposomes. Bundles of crystal fibers were observed inside TEA-SOS liposomal CPT-11 using cryo-TEM. Additionally, retention properties of encapsulated CPT-11 in the three liposomes formulations were also evaluated. TEA-SOS liposomal CPT-11 showed measurably slower drug release, a longer circulation time and more potent antitumor efficacy. By contrast, AS liposomal CPT-11 resulted in a rapid release and poor antitumor efficacy. This research confirmed that CPT-11 liposome prepared using a TEA-SOS gradient, with a higher drug-lipid ratio, provides the best antitumor efficacy. To the best of our knowledge, this study is the first deep investigation into how the trapping agents influence the effectiveness of a remote loading liposomes system.

Conflicts of interest

The authors declare that they have no conflicts of interest to disclose.

References

1 D. W. Deamer, R. C. Prince and A. R. Crofts, *Biochim. Biophys. Acta*, 1972, **274**, 323–335.
2 E. Maybew, D. Papahadjopoulos, Y. M. Rustum and C. Dave, *Ann. N. Y. Acad. Sci.*, 1978, **308**, 371–386.
3 Y. Barenholz, *J. Liposome Res.*, 2003, **13**, 1–8.
4 Y. Barenholz, *J. Controlled Release*, 2012, **160**, 117–134.
5 G. Batist, J. Barton, P. Chaikin, C. Swenson and L. Welles, *Expert Opin. Pharmacother.*, 2002, **3**, 1739–1751.
6 D. D. Lasic, B. Ceh, M. C. Stuart, L. Guo, P. M. Frederik and Y. Barenholz, *Biochim. Biophys. Acta*, 1995, **1239**, 145–156.
7 V. Wasserman, P. Kizelsztein, O. Garbuzenko, R. Kohen, H. Ovadia, R. Tabakman and Y. Barenholz, *Langmuir*, 2007, **23**, 1937–1947.
8 S. Clerc and Y. Barenholz, *Biochim. Biophys. Acta*, 1995, **1240**, 257–265.
9 Y. Avnir, R. Ulmansky, V. Wasserman, S. Even-Chen, M. Broyer, Y. Barenholz and Y. Naparstek, *Arthritis Rheum.*, 2008, **58**, 119–129.
10 D. C. Drummond, C. O. Noble, Z. X. Guo, K. Hong, J. W. Park and D. B. Kirpotin, *Cancer Res.*, 2006, **66**, 3271–3277.
11 C. Li, J. Cui, C. Wang, Y. Li, L. Zhang, X. Xiu, Y. Li, N. Wei, L. Zhang and P. Wang, *J. Pharm. Pharmacol.*, 2011, **63**, 765–773.
12 K. M. Laginha, S. Verwoert, G. J. R. Charrois and T. M. Allen, *Clin. Cancer Res.*, 2005, **11**, 6944–6949.
13 M. J. W. Johnston, S. C. Semple, S. K. Klimuk, K. Edwards, M. L. Eisenhardt, E. C. Leng, G. Karlsson, D. Yanko and P. R. Cullis, *Biochim. Biophys. Acta, Biomembr.*, 2006, **1758**, 55–64.
14 G. Haran, R. Cohen, L. K. Bar and Y. Barenholz, *Biochim. Biophys. Acta*, 1993, **1151**, 201–215.
15 T. M. Allen, T. Mehra, C. Hansen and Y. C. Chin, *Cancer Res.*, 1992, **52**, 2431–2439.
16 M. B. Bally, R. Nayar, D. Masin, P. R. Cullis and L. D. Mayer, *Cancer Chemother. Pharmacol.*, 1990, **27**, 13–19.
17 M. J. Johnston, S. C. Semple, S. K. Klimuk, K. Edwards, M. L. Eisenhardt, E. C. Leng, G. Karlsson, D. Yanko and P. R. Cullis, *Biochim. Biophys. Acta*, 2006, **1758**, 55–64.
18 C. Li, J. Cui, Y. Li, C. Wang, Y. Li, L. Zhang, L. Zhang, W. Guo, J. Wang, H. Zhang, Y. Hao and Y. Wang, *Eur. J. Pharm. Sci.*, 2008, **34**, 333–344.
19 C. Li, J. Cui, C. Wang, J. Cao, L. Zhang, Y. Li, M. Liang, X. Xiu, Y. Li, N. Wei and C. Deng, *J. Liposome Res.*, 2012, **22**, 42–54.
20 C. Li, J. Cui, Y. Li, C. Wang, Y. Li, L. Zhang, L. Zhang, W. Guo, J. Wang, H. Zhang, Y. Hao and Y. Wang, *Eur. J. Pharm. Sci.*, 2008, **34**, 333–344.
21 J. Cui, C. Li, W. Guo, Y. Li, C. Wang, L. Zhang, L. Zhang, Y. Hao and Y. Wang, *J. Controlled Release*, 2007, **118**, 204–215.
22 A. L. Seynhaeve, S. Hoving, D. Schipper, C. E. Vermeulen, G. de Wiel-Ambagtsheer, S. T. van Tiel, A. M. Eggermont and T. L. Ten Hagen, *Cancer Res.*, 2007, **67**, 9455–9462.
23 M. Ramesh, P. Ahlawat and N. R. Srinivas, *Biomed. Chromatogr.*, 2010, **24**, 104–123.
24 J. Fassberg and V. J. Stella, *J. Pharm. Sci.*, 1992, **81**, 676–684.
25 F. C. Passero Jr., D. Grapsa, K. N. Syrigos and M. W. Saif, *Expert Rev. Anticancer Ther.*, 2016, **16**, 697–703.
26 W. Yang, Z. Yang, J. Liu, D. Liu and Y. Wang, *Asian J. Pharm. Sci.*, 2018, DOI: 10.1016/j.ajps.2018.08.003.
27 D. B. Fenske and P. R. Cullis, in *Liposomes, Pt E*, ed. N. Duzgunes, Elsevier Academic Press Inc., San Diego, 2005, vol. 391, pp. 7–40.
28 D. B. Fenske, K. F. Wong, E. Maurer, N. Maurer, J. M. Leenhouts, N. Boman, L. Amankwa and P. R. Cullis, *Biochim. Biophys. Acta*, 1998, **1414**, 188–204.
29 X. Li, D. J. Hirsh, D. Cabral-Lilly, A. Zirkel, S. M. Gruner, A. S. Janoff and W. R. Perkins, *Biochim. Biophys. Acta*, 1998, **1415**, 23–40.
30 J. Cui, C. Li, W. Guo, Y. Li, C. Wang, L. Zhang, L. Zhang, Y. Hao and Y. Wang, *J. Controlled Release*, 2007, **118**, 204–215.
31 J. X. Cui, C. L. Li, W. M. Guo, Y. H. Li, C. X. Wang, L. Zhang, L. Zhang, Y. L. Hao and Y. L. Wang, *J. Controlled Release*, 2007, **118**, 204–215.
32 P. R. Harrigan, K. F. Wong, T. E. Redelmeier, J. J. Wheeler and P. R. Cullis, *Biochim. Biophys. Acta*, 1993, **1149**, 329–338.
33 D. C. Drummond, O. Meyer, K. Hong, D. B. Kirpotin and D. Papahadjopoulos, *Pharmacol. Rev.*, 1999, **51**, 691–743.
34 A. Gabizon, H. Shmeeda and Y. Barenholz, *Clin. Pharmacokinet.*, 2003, **42**, 419–436.

BMC Biotechnology

RESEARCH ARTICLE Open Access

Oxaliplatin long-circulating liposomes improved therapeutic index of colorectal carcinoma

Chuang Yang[1,2], Hai Z Liu[3], Zhong X Fu[1*], Wei D Lu[1]

Abstract

Background: Cytotoxic drugs are non-selective between normal and pathological tissue, and this poses a challenge regarding the strategy for treatment of tumors. To achieve sufficient antitumor activity for colorectal carcinoma, optimization of the therapeutic regimen is of great importance. We investigated the ability of oxaliplatin long-circulating liposomes (PEG-liposomal L-oHP) to provide an improved therapeutic index of colorectal carcinoma.

Results: We determined that PEG- liposomes conjugated with cells at 2 h, with a mean fluorescence intensity that was enhanced upon extended induction time. The PEG-liposomal L-oHP induced a significant apoptotic response as compared with free L-oHP, 23.21% ± 3.38% vs. 16.85% ± 0.98%, respectively. Fluorescence imaging with In-Vivo Imaging demonstrated that PEG- liposomes specifically targeted tumour tissue. After intravenous injections of PEG-liposomal L-oHP or free L-oHP, the tumour volume suppression ratio was 26.08% ± 12.43% and 18.19% ± 7.09%, respectively, the percentage increased life span (ILS%) was 45.36% and 76.19%, respectively, and Bcl-2, Bax mRNA and protein expression in tumour tissue was 0.27-fold vs. 0.88-fold and 1.32-fold vs. 1.61-fold compared with free L-oHP, respectively.

Conclusion: The PEG-liposomal L-oHP exhibited a tendency to target tumour tissue and demonstrated a significantly greater impact on apoptosis compared to free oxaliplatin.

Background

Colorectal carcinoma (CRC) is the third most common form of cancer in the world, and the rectum exhibits common internal malignancies [1]. Oxaliplatin (L-oHP) is a third generation platinum antitumor compound. Clinically, it is now approved as first-line chemotherapy in combination with other antitumor drugs for the treatment of advanced colorectal cancer [2,3]. It contains a bulky carrier ligand within its structure, and forms DNA adducts that more effectively inhibit DNA synthesis; however, these adducts are generally considered to be more cytotoxic than those of either cisplatin or carboplatin [4,5]. Cytotoxic drugs exhibit obvious toxicity on the human body, affecting neurotoxicity, gastrointestinal reaction, and cardiotoxicity, etc. [6]; moreover, the non-selective nature of cytotoxic drugs regarding normal and pathological tissue poses a challenge for the treatment of tumors. Conventional chemotherapy is not as effective in colorectal cancer as it is in other cancers since the drug does not reach the target site in an effective concentration [7,8]. Thus, effective treatment demands an increased dose, which may lead to negative side effects. If drugs were targeted to the tumor cells, these limitations would be overcome, and this in turn would be advantageous for the cancer treatment.

Liposomes are small, spherically shape vesicles that can be produced from cholesterols, non-toxic surfactants, sphingolipids, glycolipids, long chain fatty acids and even membrane proteins. Liposomes were among the first nanomolecular drug delivery systems to demonstrate the increased delivery of small molecular weight anticancer drugs to solid tumors by altering the biodistribution of associated drugs [9,10]. It has been previously reported that liposomes attach to cellular membranes and appear to fuse with them, thus releasing their contents into the cells [11]. Alternatively, liposomes are taken up by the cell, their phospholipids are incorporated into the cell membrane, and the drug

* Correspondence: fzx990521@sina.com
[1]Department of Gastrointestinal Surgery, First Affiliated Hospital, Chongqing Medical University, Chongqing 400016, Chongqing, China
Full list of author information is available at the end of the article

trapped inside is then released [12]. Common liposomes, though, were in the body for only a short duration, and many were phagocytized by the reticuloendothelial system (RES). However, the 1,2-distearoyl-sn-glycero-3-phosphoethanolamine-N-[maleimide(polyethylene glycol)-2000] (DSPE-PEG2000) modification to the surface of a liposome potentially prevents interactions *in-vivo*, thus extending the circulation lifetime of the liposome [13-15]. In tumor tissue, because tumor cells grow so quickly, newly formed tumor vessels are comprised of poorly-aligned and defective endothelial cells with wide fenestrations that lack a smooth muscle layer and innervation with the wider lumen. Furthermore, tumor tissues usually lack effective lymphatic drainage [16]. Tumor microvessel permeability is 400~600 nm with permeability for macromolecules having a molecular weight of 2.5×10^4~16×10^4 Da [17]. These factors lead to abnormal molecular and fluid transport dynamics. Therefore, enhancement of the extravasation of certain sizes of molecules, such as macromolecular drugs or liposomes, leads to a much greater accumulation in tumour tissue versus normal tissue. Due to the tumor selective enhanced permeability and retention effect (EPR), this results in extensive extravasation of the liposomes [16,18]. In solid tumours, the EPR effect is a universal phenomenon in which liposomes are passively targeted to tumour tissue, ultimately leading to enhanced accumulation of the liposomes in the tumor interstitium [19].

Recently, FAD of USA approved a few liposomal products, such as Evacet, AM Bison, and doxorubicin in a long-circulating PEG-coated liposome. There have been initial reports indicating that the use of individual functionalities has been demonstrated to be associated with highly positive clinical outcomes [20-22]. However, there is currently no commercially available PEG-liposomal L-oHP product, and studies are still in the experimental stage. There are few reports published regarding PEG-liposomal L-oHP treatment of colorectal cancer. Here, we investigated the therapeutic tumour targeting activity of PEG-liposomal L-oHP *in-vitro* in SW480 cells and *in-vivo* in a nude mice solid tumour model.

Results

Characteristics of long-circulating liposomes (PEG-liposomes) and cellular uptake

We selected an increased particle size of PEG-liposomes through a series of filtration steps using a polycarbonate membrane filter at a pore size of 100 nm. PEG-liposomes with a particle size of 151.56 ± 15.57 nm and zeta-potential of -23.68 ± 2.35 mv were obtained, as determined by laser grain size analysis. The entrapment efficiency of the liposomes was (42.96 ± 6.45)% as determined by HPLC. These values are higher than those reported recently by another group. Flow cytometry demonstrated that after incubation in medium containing Dio-labeled liposomes for 2 h, the PEG-liposomes conjugated with cells, and exhibited an enhanced mean fluorescence intensity upon extended induction time; the mean fluorescence intensity at 24 h was 3.28-fold greater than the intensity measured at 2 h. The immunofluorescence assay revealed considerable aggregation of liposomes within cells at 24 h (Figure 1).

In-vitro drug release and cell viability assay

We used the dialysis method to evaluate L-oHP release from encapsulated PGE-liposomes *in-vitro*, and the drug concentration was then analyzed by HPLC. The cumulative percentage release demonstrated that the amount of drug released from PEG-liposomes was gradually increased over time, and after 120 h there was an increase of over 89%. The free drug exhibited the highest level (94%) at 2 h, confirming the fact that PEG-liposomes act as a barrier against diffusion of hydrophilic drugs.

The viability of cells was analyzed by the MTT colorimetric assay after treatment with empty PEG-liposomes (2.6 μmol/ml), free L-oHP (28 μg/ml) and PEG-liposomal L-oHP (containing L-oHP 28 μg/ml), respectively. Cell viability was decreased with the length of exposure, with a maximum reduction occurring at 12 h. The empty PEG-liposomes exhibited significantly less cytotoxicity.

Analysis of apoptosis

Upon exposure of SW480 cells to free L-oHP or PEG-liposomal L-oHP, cellular apoptosis was assessed by flow cytometry, which demonstrated that PEG-liposomal L-oHP induced SW480 apoptotic incidence of (23.21 ± 3.38)% (Figure 2A). The gel electrophoretic analysis of internucleosomal DNA fragmentation demonstrated the presence of primarily high molecular weight DNA as seen with the untreated control. A DNA ladder pattern, the typical feature of apoptosis, was distinctly observed (Figure 2B).

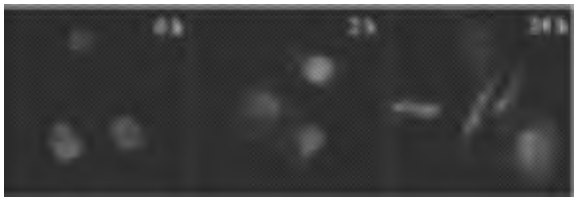

Figure 1 Cellular uptake of liposomes The liposomes conjugated with cells after 2 h, and cellular uptake of liposomes increased over time. Cells were incubated with PI, which stained nuclei red, and Dio-labelled liposomes, which were green in colour. A considerable number of liposomes aggregated within cells at 24 h (× 400).

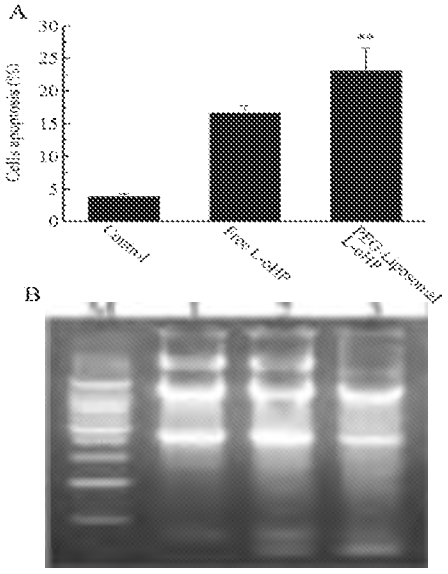

Figure 2 Apoptosis of SW480 cells. SW480 cells treated with free L-oHP (28 μg/ml) or PEG-Liposomal L-oHP (containing L-oHP 28 μg/ml), PEG-Liposomal L-oHP induced marked apoptosis compared with free L-oHP ($P < 0.01$). A, flow cytometery; B, DNA fragmentation. M: marker (4000 bp). 1: Control. 2: Free L-oHP. 3: PEG-liposomal L-oHP.

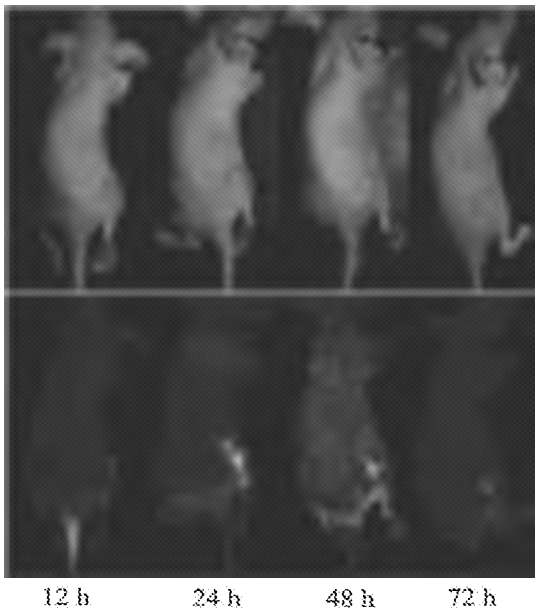

Figure 3 Control mice intravenously injected with Dio-labeled liposomes at 12 h, 24 h, 48 h, and 72 h. On day 10 after tumor inoculation mice received an intravenous injection of fluorescently (Dio) labeled empty PEG-liposomes (no drug) at a dose of 0.5 μmol lipid/g. At 12, 24, 48, and 72 h post-injection, *in-vivo* images were created.

Tumour tissue and Dio-labeled liposomes

Dio-labeled liposomes were intravenously injected via the tail vein (after injection, all mice survived), and then visualized in the tumour tissue by an *in-vivo* imaging system. After 12 h, 24 h, 48 h, and 72 h, typical representative images were captured (Figure 3). The fluorescence intensity distribution of tumour tissue in the animals was indicated by green fluorescence. The fluorescence intensity was maintained at a high level for an extended period of 24 h. However, immediately following intravenous injections, little fluorescence was observed, excluding part of the tail. The fluorescence was observed through 72 h, indicating that PEG-liposomes may continue accumulation.

In-vivo antitumor effect of PEG-liposomal L-oHP

Rapid tumour growth was observed in the mouse control group; however, significant tumor growth suppression was demonstrated in mice treated with PEG-liposomal L-oHP (Figure 4A). The tumour suppression was (26.08 ± 12.43)%, and PEG-liposomal L-oHP demonstrated the strongest effect on the survival time - all of the mice treated with PEG-liposomal L-oHP became long-term survivors (Figure 4B) ($p < 0.01$). Throughout the therapeutic experiment, a noticeable cachexia condition was observed in the control group, and although no bodyweight loss was observed in any of the treated groups, weight loss was significant in the control group (data not show). These results suggest that treatment with PEG-liposomal L-oHP improves the median survival time (MST) of tumor-bearing mice without causing remarkable toxicity.

Bcl-2, Bax mRNA and protein expression in tumour tissue

To elucidate whether the growth inhibitory effect of PEG-liposomal L-oHP was attributable to the induction of apoptosis, Bcl-2 and Bax were analyzed by RT-PCR or Western blot in tumour tissue. On day 15 after treatment, tumours were resected and total RNA and protein were extracted from the tumour tissue. Our experiments demonstrated that mRNA expression levels of Bcl-2 were remarkably decreased in the PEG-liposomal L-oHP group; 0.27-fold compared with free L-oHP, whereas, Bax mRNA increased 1.32-fold compared with free L-oHP (Figure 5A). Protein expression tendency of Bcl-2 and Bax were 0.88-fold and 1.61-fold in comparison, respectively (Figure 5B). These results indicated that apoptosis was strongly induced by PEG-liopsomal L-oHP.

Discussion

The non-selectivity of cytotoxic drugs between normal tissue and the pathological site poses a tumor treatment strategy challenge. To obtain increased therapeutic efficacy, a drug carrier must achieve increased delivery of

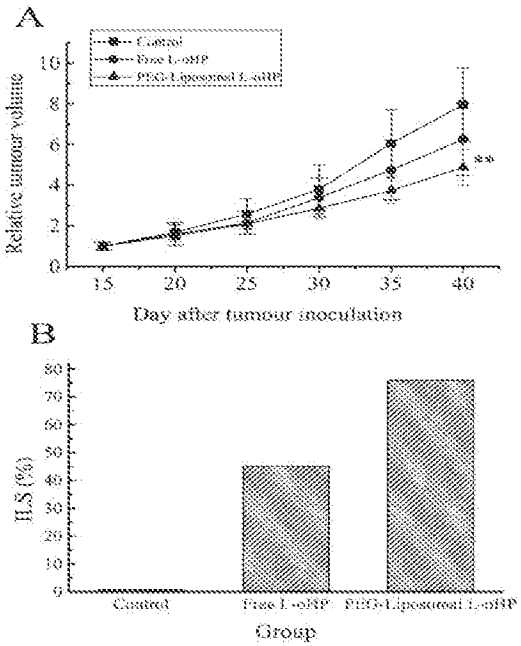

Figure 4 Tumor growth suppression and survival time. On day 12 after tumour inoculation, mice were treated ith free L-oHP (5 μg/g), PEG-liposomal L-oHP (containing L-oHP 5 μg/g), or 5% dextrose solution. Antitumor activity as assessed by tumour size and survival of tumour-bearing mice. A, Relative tumor volume (RTV), data represent mean ± SD (n = 6). ** P < 0.01 compared with the other group. B, The percentage increase in life span (ILS%).

the drug to the tumor tissue, while also allowing for enhanced interaction of the drug with, and subsequent internalization by, tumor cells. Liposomes, as carriers of chemotherapeutic agents, are able to change the distribution of these agents within the body and decrease their toxicity [23,24]. Therefore, drug-loaded liposomes offer a new approach for the treatment of colorectal cancer.

Polyethylene glycol (PEG)-coated liposomes (PEG-liposomes), are stable and not easy to be taken up by cells of the reticuloendothelial system (RES), and exhibit reduced drug leakage compared with conventional liposomes [25]. It has been previously reported that PEG modification of liposomes increases their affinity to cancer cells and increases the cellular uptake of drugs [26-28]. The toxicity of PEG-liposomes for cells should be taken into consideration, and some previous reports have indicated that the toxicity is indeed lower [29,30]. In our experiment, the empty PEG-liposomes *in-vitro* exhibited significantly less cytotoxicity for SW480 cells. The tumour cells took up large numbers of PEG- liposomes, which is in concordance with reports by other groups [31]. However, PEG-liposomes containing a drug increase toxicity. Our MTT assays showed that PEG-liposomal L-oHP (containing L-oHP 28 μg/ml) had significantly greater cytotoxic effects than free oxaliplatin (28 μg/ml). When we assessed their effects on apoptosis, as determined by flow cytometry and the DNA Ladder method, we observed that, at an identical dose, PEG-liposomal L-oHP demonstrated a significantly greater effect on apoptosis than did free L-oHP. PEG-liposomes exhibited tumour-targeted delivery in these cells.

Previous studies have demonstrated that PEG-modified liposomes act primarily through vesicular organelles, and are preferentially taken up by angiogenic tumour endothelium [32]. To obtain sufficient antitumor activity with liposomal anticancer drugs, optimization of the therapeutic regimen is of great importance.

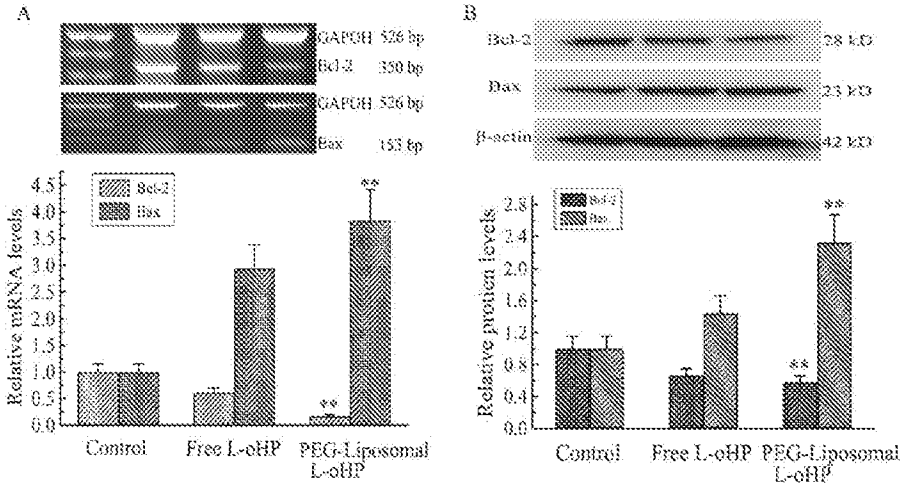

Figure 5 The mRNA and protein expression of Bcl-2 and Bax in tumour tissue. On day 15 after treatment, the total mRNA and protein was extracted from tumour tissue. A, The mRNA expression. Agarose gel electrophoresis result shown in which expression of Bcl-2 is down-regulated and expression of Bax is up-regulated; B, The protein expression. Cell lysates were separated on 12% SDS-PAGE gels, Bcl-2 was down-regulated, whereas Bax was up-regulated. Data are expressed as mean ± SD (n = 3). ** P < 0.01 compared with the other group.

In solid tumours (during the rapid growth of the tumour in particular), the permeability of the vasculature is generally increased compared to normal tissues [32,33]. Therefore, these may provide a channel allowing liposomes to more easily target tumour tissue. After receiving intravenous injections of Dio-labeled PEG-liposomes, mice were able to survive. Experiments presented in this study indicate that PEG-liposomes efficiently accumulate in tumor tissue (Figure 3), and maintain a high level over 24 h, which is in concordance with previous reports from other groups [31,34]. Furthermore, the fluorescence remained detectable even after 72 h. The plasma clearance of anionic molecules occurred more slowly than for cationic molecules [35]. Based upon evidence from the *in-vitro* cell experiments and the mouse tumour model, a higher concentration and longer blood residence time of liposomes would result in greater efficiency of extravasation per unit volume of convective transport [36,37], and this would explain the fact that liposomes remain in the tumor tissue.

Additionally, to investigate the treatment availability of PEG-liposomal L-oHP, Bcl-2 and Bax were evaluated. Bcl-2 and Bax are members of the Bcl-2 family, Bax is a proapoptotic protein that induces mitochondrial outer membrane permeabilization (MOMP), causing the release of caspase activating proteins. In contrast, Bcl-2 is an anti-apoptotic protein and guardian of the outer membrane and it preserves its integrity by opposing Bax; they are associated with apoptosis necrosis, and autophagy, and regulate all major types of cell death [38,39]. We used the level of genes and protein to indicate treatment results. After treatment with PEG-liposomal L-oHP, tumour cell predominance of apoptosis in tumor-bearing nude mice was induced, and Bcl-2 mRNA and protein expression were down-regulated, whereas Bax was up-regulated (Figure 5). This demonstrated that such liposomal L-oHP formulation exhibits potent *in-vivo* antitumor activity, presumably via a dual targeting approach against both tumour endothelial cells and tumour cells [40,41].

The PEG-liposomal L-oHP accumulated in the tumour tissue, following uptake by endothelial cells as well as tumor cells, and liposomes were then degraded, while intracellular drug delivery increased the concentration of drug within cells and slowed drug efflux [42-44]. These findings indicate that liposome encapsulation of chemotherapeutic drugs enhances their damaging effects on tumour cells. At present, FDA approved liposomal products (Evacet, doxorubicin liposomes, etc.) have the advantage of high encapsulation efficiency, rapid release rate, and so forth. As to our study, further research is needed in order to improve drug encapsulation efficiency and stability, as well as further studies involving dynamic research in a clinical setting.

Conclusion

The experiments presented in this report indicate that PEG-liposomal L-oHP achieves a better therapeutic response than the equivalent dose of free L-oHP, and it indicates the potentially wide application for this type of drug target for tumors and other tissues, with the advantage of the ability to overcome some major limitations in conventional anticancer chemotherapy. This study may provide the rationale for the clinical application of CRC. Nevertheless, further studies are warranted to elucidate the underlying molecular mechanism.

Methods

Animals and tumor cell line

Female BALB/c nude mice, 3 weeks old, were obtained from Center of Laboratory Animals, Chongqing Medical University (Permit Number: SCXK(jing) 2009-0004). All animal experiments were evaluated and approved by the Animal and Ethics Review Committee. The human colorectal carcinoma cell line (SW480) was obtained from the Institute of Life Science of Chongqing Medical University, and it was maintained in RPMI 1640 (Sigma, St. Louis, MO) supplemented with 10% fetal bovine serum (FBS) (HyClone, Logan, UT) in a 5% CO_2 incubator at 37°C.

Preparation of liposomes

PEG-liposomes were prepared using lecithin (Sigama Co., US), cholesterol (Sigama Co., US), and DSPE-PEG2000 (Avanti Polar Lipids Inc. US) as previously described [31]. The molar ratio was 2.0:1.0:0.2. In the targeting experiments, 2 nmol/ml of the fluorescent lipid membrane marker, Dio (Vigorous Biotech Co. Ltd. China), was added to the lipid mixture. The liposomes were prepared using the reverse-phase evaporation method. Briefly, lipids (50 mmol) were dissolved in 15 ml of chloroform and then 5 ml of L-oHP solution (1 mg/ml) in 5% (w/v) dextrose was dropped into the lipid mixture to form W/O emulsion. For preparation of no drug-containing liposomes, 5% dextrose solution was added instead of L-oHP solution. The volume ratio of the aqueous to the organic phase was maintained at 1:3. The emulsion was sonicated for 10 min (40 W) and then the organic phase was removed to form the liposomes by evaporation in a rotary evaporator at 40°C under vacuum at 0.045 mPa for 2 h. The resulting liposomes were extruded through a polycarbonate membrane (Millipore, US. 100 nm pore size).

The grade size and zeta-potential were detected by Laser Particle Size Analyzer (Zetasizer, Malvern). Using a transmission electron microscope (Hitachi S-3000N,

japan), the form feature of PEG-liposomes was determined. The free L-oHP was removed by ultrafiltration (MW 100 kDa, 12,000 r/min 20 min). The entrapment efficiency of the liposomes was determined by high-performance liquid chromatography (HPLC, SY-8100, Beijin, China). *In-vitro* drug release from PEG-liposomes was studied using a dialysis method as described by Zhang et al. [45].

Cellular uptake of Dio-labeled PEG-liposomes

SW480 cells were seeded onto 6-well plates in 1 ml of RPMI 1640 medium containing 10% FBS and pre-incubated for 24 h. After removal of culture medium, 1 ml of fresh medium containing the Dio-labeled PEG-liposomes (2 μmol/ml) was added, followed by incubation at 37°C. At 0, 2, 4, 8, 12 and 24 h post-incubation, the cells were trypsinized, followed by two washes with cold phosphate buffered saline (PBS). The cells were re-suspended in 400 μl of PBS (1×10^6/ml). The cellular uptake of Dio-labeled liposomes was quantified using a flow cytometer (FACS Aria, Becton, Dickinson and Company), equipped with an argon-ion laser and 488 nm band pass filters for emission measurements. Approximately 10,000 events were acquired per sample. Cells were also plated onto glass slides and incubated with Dio-labeled liposomes, and the cellular uptake of liposomes was determined by measuring fluorescence.

Cytotoxicity assay

Cytotoxicity of L-oHP formulations was determined by the 3-(4,5-dimethylthiazol-2-yl)-2,5 diphenyl tetrazolium bromide (MTT) assay, as described previously [33]. Briefly, cells in the logarithmic growth phase (5×10^3 per well) were placed in wells of a 96-well plate and incubated for 24 h. The culture medium was replaced with fresh medium containing various concentrations of blank liposomes, free oxaliplatin, or PEG-liposomal L-oHP. After treatment, the culture medium was removed and the cells were incubated with MTT (final concentration 10%) for 4 h at 37°C. Then 150 μl DMSO was added to each well to dissolve formazan crystals. The absorbance of each well was read at 570 nm on a microplate reader, and used to determine IC50 values (IC50 values represent L-oHP concentrations that cause 50% cell death). The concentration of oxaliplatin liposomes was expressed as 1/2 the IC50 of the working concentration of oxaliplatin.

Detection of apoptosis by flow cytometry

SW480 cells cultured in 6-well plates were treated with free oxaliplatin (28 μg/ml) or PEG-liposomal L-oHP (containing L-oHP 28 μg/ml) for 12 h, along with a blank control with no drug treatment. The cells were trypsinized, followed by two washes with cold PBS, re-suspended in 400 μl of PBS (1×10^6/ml), and incubated in the dark for 15 min following addition of Annexin V-FITC (5 μl). Cells were subsequently treated with PI (10 μl) and incubated in the dark for 5 min prior to detection by flow cytometry. Approximately 10,000 events were acquired per sample.

DNA fragmentation analysis for detecting apoptosis

For DNA fragmentation assay, cells were treated as described above. Adherent and floating cells were recovered and DNA was isolated and evaluated for fragmentation as described previously [46]. DNA samples were applied on 1.5% agarose gel containing 1% GoldView™. The gel was examined and photographed using an ultraviolet gel documentation system (Bio-Rad, Hercules, CA, USA).

Targeting of Dio-labeled liposomes in tumor-bearing nude mice

Female BALB/c nude mice were inoculated subcutaneously at the inguen region with SW480 Cells (2×10^7/mouse) in a volume of 200 μl (PBS). On day 15 after tumor inoculation, the tumor volume reached approximately 100 mm^3. Next, intravenous injections of Dio-labeled PEG-liposomes (0.5 μmol/g) were performed via the tail vein. At 12 h, 24 h, 48 h, and 72 h post-injection, nude mice were anesthetized with isoflurane, and fluorescence imaging was performed using the In-Vivo Imaging System (Mastro Ex, USA) which has an affiliated anesthesia device.

Therapeutic efficacy of PEG-liposomal L-oHP in tumor-bearing nude mice

After successful subcutaneously inoculated tumor transplantation, the nude mice were randomly divided into three groups. Control (n = 6): Received intravenous injections of 5% dextrose solution; Free L-oHP (n = 6): Received intravenous injections of 5 μg L-oHP/g; PEG-liposomal L-oHP (n = 6): Received intravenous injections of PEG-liposomal L-oHP (containing L-oHP 5 μg/g). Treatments occurred once every four days, and the antitumor activity was evaluated in terms of both relative tumor volume (RTV) and the percentage of increased life span (ILS%). Tumor volume was calculated using the method described by Kim [47] and the ILS was calculated using the method described by Kviecinski [48]. The median survival time (MST) of each group was recorded.

Reverse transcription-polymerase chain reaction (RT-PCR)

On day 15 after treatment, the nude mice were sacrificed by deep anesthesia, and the tumours were immediately placed in liquid nitrogen for further experiments. Total RNA was extracted using TRIZOL (Takara,

Dalian, China). Reverse transcription was carried out in 10 μl of reaction mixture containing 1 μg of total RNA, 25 pmol of oligo-dT primer, 10 nmol of dNTP mixture, 20 units of RNase inhibitor, and 2.5 units of AMV reverse transcriptase (Takara, Dalian, China) at 37°C for 15 min, 85°C for 5 s. PCR amplification was performed in 25 μl PCR reaction mixture. PCR amplification was conducted to detect differences among the samples as follows: 4 min at 94°C for initial denaturation; 30 cycles × 30 s at 94°C, 30 s at 59°C, and 30 s at 72°C for Bcl-2, Bax; 30 cycles × 30 s at 94°C, 30 s at 60°C, and 30 s at 72°C for GAPDH. The following primer pairs were used: Bax (153 bp): 5'-GAT CGA GCA GGG CGA ATG GG-3' (ForwardPrimer); 5'-CAC GGC GGC AAT CAT CCT CT-3' (ReversePrimer); Bcl-2 (350 bp): 5'-CAG ATG GCA AAT GAC CAG CAGA-3' (ForwardPrimer), 5'-TGG CAG GAT AGC AGC ACA GGAT-3' (ReversePrimer); GAPDH (526 bp): 5'-AGG TCG GAG TCA ACG GAT TTG-3' (ForwardPrimer), 5'-GTG ATG GCA TGG ACT GTG GT-3' (ReversePrimer). For the analysis of PCR products, 6 μl of each PCR reaction was electrophoresed on 1.5% agarose gel containing 1% GoldView™. Band intensity was analyzed with Image system (NIH, USA) and GAPDH was used as an internal control to evaluate the relative expression of Bcl-2 and Bax.

Western blot analysis

For isolation of total protein extract, tumour tissues were washed with ice-cold PBS and lysed in RIPA lysis buffer (50 mM Tris with pH 7.4, 150 mM NaCl, 1% Triton X-100, 1% sodium deoxycholate, 0.1% sodium dodecyl sulphate, and 0.05 mM EDTA) for 30 min on ice, and then the cell lysate was centrifuged (12,000 revs/min, at 4°C) for 10 min. The supernatant was collected and protein content of the extracted samples was measured using the Bradford protein assay kit (BestBo-BeiBo, Beijing, China). All samples were kept at -80°C for further experiments.

Levels of target proteins including Bcl-2, Bax (Santa Cruz Biotechnology, Inc. 1:200), and β-actin (Bioscience Company of America, 1:500) were determined by Western blot analysis using their respective antibodies. Briefly, total cell lysate was boiled in 5 × loading buffer (125 mM Tris-HCl, pH 6.8, 10% SDS, 8% dithiothreitol, 50% glycerol, and 0.5% bromchlorphenol blue) for 10 min. Equal amounts of proteins (50 μg) were subjected to 12% SDS-polyacrylamide gel electrophoresis and transferred to polyvinylidene fluoride membranes (PVDF). The membranes were blocked with 5% skim milk in PBS with 0.1% Tween 20 (PBST) for 1 h, and incubated with primary antibodies overnight at 4°C. Antibodies were detected by means of HRP-conjugated secondary antibody (Bioscience Company of America, 1:2000) for 1 h at room temperature. Immunoreactive bands were visualized using Immobilon™ Western Chemiluminescent HRP Substrate (Millipore, USA), and densitometric analysis was performed using the PDI Imageware System (Bio-Rad, Hercules, CA, USA).

Abbreviations

CRC: Colorectal carcinoma; SDS-PAGE: Sodium Dodecyl Sulfate-Polyacrylamide Gel Electrophoresis; L-oHP: Oxaliplatin; DSPE-PEG2000: 1,2-distearoyl-sn-glycero-3-phosphoethanolamine- N-[maleimide(polyethylene glycol)-2000]; MTT: 3-(4,5)-dimethylthiahiazo (-z-y1)-3,5-di-Phenyltetrazoliumromide; HPLC: High-performance liqued chromatography; DAB: 3,3'-diaminobenzidine; Dio: $DIOC_{18}(3)$, 3,3' dioctadecyloxacarbocyanine perchlorate; RES: Reticuloendothelial system EPR: Enhanced permeability and retention; MOMP: Mitochondrial outer membrane permeabilization; FBS: Fetal bovine serum; RTV: Relative tumor volume; ILS: Increased life span; MST: Median survival time; PVDF: Polyvinylidene fluoride membranes.

Acknowledgements

This work was supported by a grant (No. 09-2-12) from the Health Administration of Chongqing. We thank Xin H Jiang for the expert technical assistance with HLPC, and we are grateful to the Central Lab, the Ophthalmological Lab of Chongqing Medical University First Affiliated Hospital, and the College of Life Science of Chongqing Medical University for the technical support.

Author details

[1]Department of Gastrointestinal Surgery, First Affiliated Hospital, Chongqing Medical University, Chongqing 400016, Chongqing, China. [2]Department of Hepatobiliary Surgery, Mianyang Third People's Hospital, Mianyang 621000, Sichuan Province, China. [3]Departments of Gynecology and Obstetrics, Second Affiliated Hospital, Chongqing Medical University, Chongqing 400016, Chongqing, China

Authors' contributions

CY was responsible for most of the experimental work and drafted the manuscript. ZF participated in the design, supervised this study, and was involved in revising the manuscript. HL participated in culturing cells, performing Western blot detection, and assisting in the statistical analysis. WL was involved with the animal model experiment. All authors read and approved the final manuscript.

Received: 28 September 2010 Accepted: 15 March 2011
Published: 15 March 2011

References

1. Nobili S, Checcacci D, Filippelli F, Del Buono S, Mazzocchi V, Mazzei T, Mini E: Bimonthly chemotherapy with oxaliplatin, irinotecan, infusional 5-fluorouracil/folinic acid in patients with metastatic colorectal cancer pretreated with irinotecan-or oxaliplatin-based chemotherapy. *J Chemother* 2008, 20:622-631.
2. Ibrahim A, Hirschfeld S, Cohen MH, Griebel DJ, Williams GA, Pazdur R: FDA drug approval summaries: oxaliplatin. *Oncologist* 2004, 9:8-12.
3. Persino A, Sobrero A: Optimal treatment of metastatic colorectal cancer, Expert Rev. *Anticancer Ther* 2006, 6:801-812.
4. Basaki Y, Chikahisa L, Aoyagi K, Miyadera K, Yonekura K, Hashimoto A, Okabe S, Wierzba K, Yamada Y: Gamma-hydroxybutyric acid and 5-fluorouracil, metabolites of UFT, inhibit the angiogenesis induced by vascular endothelial growth factor. *Angiogenesis* 2001, 4:163-173.
5. Tashiro T, Kawada Y, Sakurai Y, Kidani Y: Antitumor activity of a new platinum complex, oxalato (trans-l-1,2-diaminocyclohexane)platinum (II): new experimental data. *Biomed Pharmacother* 1989, 43:251-260.
6. Pasetto LM, D'Andrea MR, Rossi E, Monfardini S: Oxaliplatin-related neurotoxicity: how and why? *Crit Rev Oncol Hematol* 2006, 59:159-168.
7. Michor F, Iwasa Y, Lengauer C, Nowak NA: Dynamics of colorectal cancer. *Semin Cancer Biol* 2005, 15:484-493.
8. Pietrangeli A, Leandri M, Terzoli E, Jandolo B, Garufi C: Persistence of high-dose oxaliplatin-induced neuropathy at long-term follow-up. *Eur Neurol* 2006, 56:13-16.

9. Hussain S, Pluckthun A, Allen TM, Zangemeister-Wittke U: Antitumor activity of an epithelial cell adhesion molecule targeted nanovesicular drug delivery system. *Mol Cancer Ther* 2007, 6:3019-3027
10. Sun W, Zou W, Huang G, Li A, Zhang N: Pharmacokinetics and targeting property of TFu-loaded liposomes with different sizes after intravenous and oral administration. *J Drug Target* 2008, 16:357-365.
11. Dunnick JK, Rooke JD, Aragon S, Kriss JP: Alteration of mammalian cells by interaction with artificial lipid vesicles. *Cancer Res* 1976, 36:2385-2389.
12. Poste G, Papahadjopoulos D: Lipid vesicles as carriers for introducing materials into cultured cells: influence of vesicle lipid composition on mechanism(s) of vesicle incorporation into cells. *Proc Natl Acad Sci USA* 1976, 73:1603-1607.
13. Allen TM, Hansen C, Martin F, Redemann C, Yau-Young A: Liposomes containing synthetic lipid derivatives of poly(ethylene glycol) show prolonged circulation half-lives in vivo. *Biochim Biophys Acta* 1991, 1066:29-36.
14. Klibanov AL, Maruyama K, Beckerleg AM, Torchilin VP, Huang L: Activity of amphipathic poly(ethylene glycol) 5000 to prolong the circulation time of liposomes depends on the liposome size and is unfavorable for immunoliposome binding to target. *Biochim Biophys Acta* 1991, 1062:142-148.
15. Allen C, Dos Santos N, Gallagher R, Chiu GN, Shu Y, Li WM, Johnstone SA, Janoff AS, Mayer LD, Webb MS, Bally MB: Controlling the physical behavior and biological performance of liposome formulations through use of surface grafted poly(ethylene glycol). *Biosci Rep* 2002, 22:225-250.
16. Greish K: Enhanced permeability and retention (EPR) effect for anticancer nanomedicine drug targeting. *Methods Mol Biol* 2010, 624:25-37.
17. Yuan F, Dellian M, Fukumura D: Vascular perme-ability in a human tumor xenograft: molecular size dependence and cutoff size. *Cancer Res* 1995, 55:3752-3756.
18. Maeda H, Bharate GY, Daruwalla J: Polymeric drugs for efficient tumor-targeted drug delivery based on EPR-effect. *Eur J Pharm Biopharm* 2009, 71:409-419
19. Fang J, Sawa T, Maeda H: Factors and mechanism of "EPR" effect and the enhanced antitumor effects of macromolecular drugs including SMANCS. *Adv Exp Med Biol* 2003, 519:29-49.
20. HHarrington KJ, Lewanski C, Northcote AD, Whittaker J, Peters AM, Vile RG, Stewart JS: Phase II study of pegylated liposomal doxorubicin (Caelyx) as induction chemotherapy for patients with squamous cell cancer of the head and neck. *Eur J Cance* 2001, 37:2015-2022.
21. Seiden MV, Muggia F, Astrow A, Matulonis U, Campos S, Roche M, Sivret J, Rutk J, Barrett E: A phase II study of liposomal lurtotecan (OSI-211) in patients with topotecan resistant ovarian cancer. *Gynecol Oncol* 2004, 93:229-232.
22. Torchilin VP: Recent advances with liposomes as pharmaceutical carriers. *Nat Rev Drug Discov* 2005, 4:145-160.
23. Desai SK, Naik SR: Preparation, relative toxicity, chemotherapeutic activity, and pharmacokinetics of liposomal SJA-95: a new polyene macrolide antibiotic. *J Liposome Res* 2008, 18:279-92
24. Rouf MA, Vural I, Bernoi JM, Hincal AA: Development and characterization of liposomal formulations for rapamycin delivery and investigation of their antiproliferative effect on MCF7 cells. *J Liposome Res* 2009, 19:322-31.
25. Gabizon A, Papahadjopoulos D: Liposome formulations with prolonged circulation time in blood and enhanced uptake by tumors. *Proc Natl Acad Sci USA* 1988, 85:6949-6953
26. Gabizon AA: Stealth liposomes and tumor targeting: a step further in the quest for the magic bullet. *Clin Cancer Res* 2001, 7:223-225.
27. Zalipsky S, Brandeis E, Newman MS, Woodle MC: Long circulating, cationic liposomes containing amino-PEG-phosphatidylethanolamine. *FEBS Lett* 53:71-74, 994.
28. Cheong I, Zhou S: Tumor-specific liposomal drug release mediated by liposomase. *Methods Enzymol* 2009, 465:251-265.
29. Singh S: Nanomedicine-nanoscale drugs and delivery systems. *J Nanosci Nanotechnol* 2010, 10:7906-1918.
30. Abu Lila AS, Kizuki S, Doi Y, Suzuki T, Ishida T, Kiwada H: Oxaliplatin encapsulated in PEG-coated cationic liposomes induces significant tumor growth suppression via a dual-targeting approach in a murine solid tumor model. *J Control Release* 2009, 137:8-14.
31. Zhang G, Yang Z, Lu W, Zhang R, Huang Q, Tian M, Li L, Liang D, Li C: Influence of anchoring ligands and particle size on the colloidal stability and in vivo biodistribution of polyethylene glycol-coated gold nanoparticles in tumor-xenografted mice. *Biomaterials* 2009, 30:1928-1936.
32. Thurston G, Mclean JW, Rizen M, Baluk P, Haskell A, Murphy TJ, Hanahan D, Mcdonald DM: Cationic liposomes target angiogenic endothelial cells in tumours and chronic inflammation in mice. *J Clin Invest* 1998, 101:1401-1413.
33. Yuan F, Dellian M, Fukumura D: Vascular perme-ability in a human tumor xenograft: molecular size dependence and cutoff size. *Cancer Res* 1995, 55:3752-3756.
34. Doi Y, Okada T, Matsumoto H, Ichihara M, Ishida T, Kiwada H: Combination therapy of metronomic S-1 dosing with oxaliplatin-containing polyethylene glycol-coated liposome improves antitumor activity in a murine colorectal tumor model. *Cancer Sci* 2010, 101:2470-2475.
35. Dellian M, Yuan F, Trubetskoy VS, Torchilin VP, Jain RK: Vascular permeability in a human tumour xenograft: molecular charge dependence. *British Journal of Cancer* 2000, 82:1513-1518.
36. Alexis F, Pridgen E, Molnar LK, Farokhzad OC: Factors affecting the clearance and biodistribution of polymeric nanoparticles. *Mol Pharm* 2008, 5:505-515.
37. Grant DS, Williams TL, Zahaczewsky M, Decker AP: Comparison of antiangiogenic activities using paclitaxel (taxol) and docetaxel (taxotere). *Int J Cancer* 2003, 104:121-129.
38. John C, Reed: Bcl-2-family proteins and hematologic malignancies: history and future prospects. *Blood* 2008, 111:3322-3330.
39. Chipuk JE, Fisher JC, Dillon CP, Kriwacki RW, Kuwana T, Green DR: Mechanism of apoptosis induction by inhibition of the anti-apoptotic BCL-2 proteins. *PNAS* 2008, 105:20327-20332.
40. Lee CM, Tanaka T, Murai T, Kondo M, Kimura J, Su W, Kitagawa T, Ito T, Matsuda H, Miyasaka M: Novel chondroitin sulfate-binding cationic liposomes loaded with cisplatin efficiently suppress the local growth and liver metastasis of tumor cells in vivo. *Cancer Res* 2002, 62:4282-4288.
41. Jain A, Jain SK, Ganesh N, Barve J, Beg AM: Design and development of ligand-appended polysaccharidic nanoparticles for the delivery of oxaliplatin in colorectal cancer. *Nanomedicine: NBM* 2010, 6:179-190.
42. Abu-Lila A, Suzuki T, Doi Y, Ishida T, Kiwada H: Oxaliplatin targeting to angiogenic vessels by PEGylated cationic liposomes suppresses the angiogenesis in a dorsal air sac mouse model. *J Control Release* 2009, 134:18-25.
43. Saito R, Bringas JR, McKnight TR, Wendland MF, Mamot C, Drummond DC, Kirpotin DB, Park JW, Berger MS, Bankiewicz KS: Distribution of Liposomes into Brain and Rat Brain Tumor Models by Convection-Enhanced Delivery Monitored with Magnetic Resonance Imaging. *Cancer research* 2004, 64:2572-2579.
44. Katrilna L, Riitta M, Jari K, Ilpo J, Stina S: Intracellular Distribution of Oligonucleotides Delivered by Cationic Liposomes: Light and Electron Microscopic Study. *The Journal of Histochemistry & Cytochemistry* 1997, 45:265-274.
45. Zhang JA, Anyarambhatla G, Ma L, Ugwu S, Xuan T, Sardone T, Ahmad I: Development and characterization of a novel Cremophor EL free liposome-based paclitaxel (LEPETU) formulation. *Eur J Pharm Biopharm* 2005, 59:177-187.
46. El-Mahdy MA, Zhu Q, Wang QE, Wani G, Wani AA: Thymoquinone induces apoptosis through activation of caspase-8 and mitochondrial events in p53-null myeloblastic leukemia HL-60 cells. *Int J Cancer* 2005, 117:409-417.
47. Kim JH, Kim YS, Park K, Lee S, Nam HY, Min KH, Jo HG, Park JH, Choi K, Jeong SY, Park RW, Kim IS, Kim K, Kwon IC: Antitumor efficacy of cisplatin-loadedglycol chitosan nanoparticles in tumor-bearing mice. *J Control Release* 2008, 127:41-49.
48. Kviecinski MR, Felipe KB, Schoenfelder T, de Lemos Wiese LP, Rossi MH, Gonzalez E, Felicio JD, Filho DW, Pedrosa RC: Study of the antitumor potential of Bidens pilosa (Asteraceae) used in Brazilian folk medicine. *J Ethnopharmacol* 2008, 117:69-75.

doi:10.1186/1472-6750-11-21
Cite this article as: *Yang et al.*: Oxaliplatin long-circulating liposomes improved therapeutic index of colorectal carcinoma. *BMC Biotechnology* 2011, 11:21

Multicenter randomized phase II study of 5-Fluorouracil/leucovorin (5-FU/LV) with or without liposomal irinotecan (nal-IRI) in metastatic bililary tract cancer (BTC) as second-line therapy after progression on gemcitabine plus cisplatin (GemCis): NIFTY trial

Changhoon Yoo[1], Jae Ho Jeong[1], Kyu-pyo Kim[1], Jaekyung Cheon[2], Ilhwan Kim[3], Myoung-Joo Kang[3], Hyewon Ryu[4], Byung Woog Kang[5], Dalnim Seo[1], Baek-Yeol Ryoo[1]
[1]Asan Medical Center, [2]Ulsan University Hospital, [3]Haeundae Paik Hospital, [4]Chungnam National University Hospital, [5]Kyungpook National University Hospital, South Korea

Background

- Patients with BTC have dismal prognosis with 5-year survival of less than 10%.
- GemCis is the globally established first-line therapy based on the phase III ABC-02 trial. However, there is no standard second-line therapy after failure of 1st line GemCis, although 5-FU-based therapy has been widely used.
- Nal-IRI (Onivyde®) comprises irinotecan sucrosofate salt encapsulated in pegylated liposomes that protect the drug from premature conversion in the liver. Nal-IRI plus 5-FU/LV demonstrated the superior survival outcomes compared to 5-FU/LV alone in patients with metastatic pancreatic cancer who progressed on gemcitabine-based therapy.
- This randomized phase 2 trial is designed to compare the clinical outcomes between nal-IRI plus 5-FU/LV with 5-FU/LV alone as 2nd line therapy in patients with BTC who progressed on 1st line Gem/Cis

Preclinical study

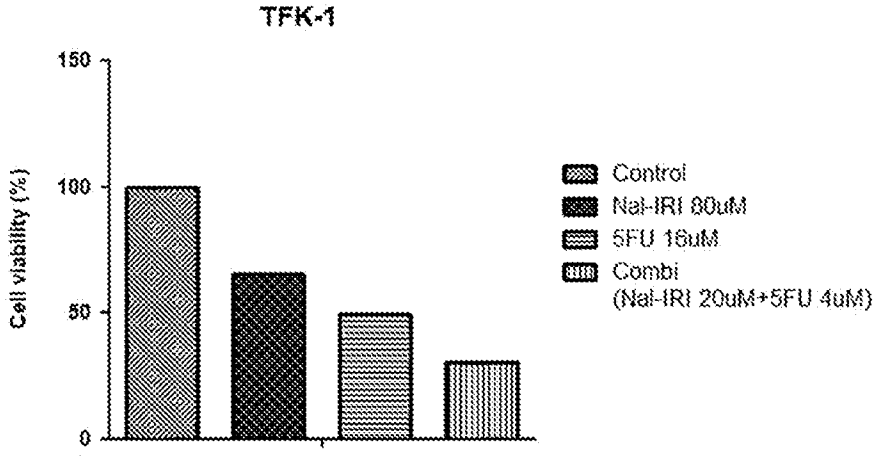

Synergism between nal-IRI and 5-FU in BTC cell line (TFK-1)

Eligibility criteria

Inclusion criteria

- Signed and written informed consent form
- ≥ 19 years of age
- Histologically or cytologically confirmed cholangiocarcinoma
- Documented metastatic disease
- At least one measurable lesion according to the RECIST v1.1
- Disease progression on gemcitabine-cisplatin combination therapy
- For patients whose disease recurred after curative resection (R0 or R1), previous adjuvant 5-FU-based chemotherapy is allowed if there is at least 6 month-interval between the last dose of adjuvant chemotherapy and recurrence of disease.
- Adequate hepatic, renal and hematological function
- Eastern Cooperative Oncology Group (ECOG) Performance status 0-1

Exclusion criteria

- Serum total bilirubin ≥ 2 x ULN (biliary drainage is allowed for biliary obstruction)
- Severe renal impairment (CLcr ≤ 30 ml/min)

- Inadequate bone marrow reserves as evidenced by:
  - ANC ≤ 1,500 cells/μl; or
  - Platelet count ≤ 100,000 cells/μl; or
  - Hemoglobin ≤ 9 g/dL
- Eastern Cooperative Oncology Group performance status 2-4
- Any clinically significant disorder impacting the risk-benefit balance negatively per physician's judgment
- Any clinically significant gastrointestinal disorder, including hepatic disorders, bleeding, inflammation, occlusion, or diarrhea > grade 2
- Severe arterial thromboembolic events (myocardial infarction, unstable angina pectoris, stroke) in last 6 months
- NYHA Class III or IV congestive heart failure, ventricular arrhythmias or uncontrolled blood pressure. Or known abnormal ECG with clinically significant abnormal findings

Study design & treatment

- NIFTY trial is a multicenter, open-label, randomized (1:1), phase II trial and 5 referral cancer centers in Korea participated in this study.

- **Primary endpoint**
  - progression-free survival (PFS) assessed by independent review

- **Secondary endpoints**
  - Overall survival
  - Response rates assessed by RECIST v1.1
  - Quality of life assessed by EORTC QLQ-C30
  - Safety profile assessed by NCI-CTCAE v4.03

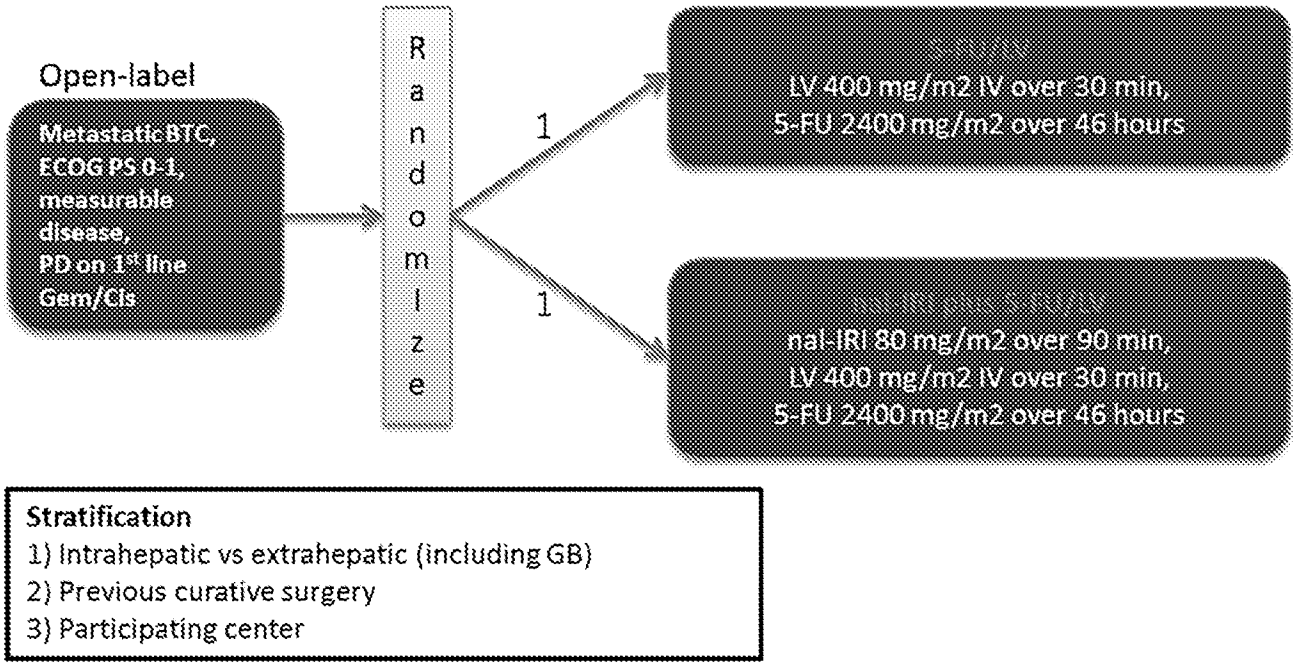

- Study treatment is continued until the disease progression or occurrence of intolerable toxicities

- **Control arm**
  - 400 mg/m^2 LV, 2400 mg/m^2 5-FU over 46 h, every 2 weeks

- **Investigational arm**
  - Nal-IRI 80 mg/m^2, 400 mg/m^2 LV, 2400 mg/m^2 5-FU over 46 h, every 2 weeks

- **Response assessment**
  - Tumor response is assessed using CT or MRI scan every 6 weeks (fixed).

- **Sample size estimation**
  - The addition of nal-IRI to 5-FU/LV would enhance the PFS to median 3.3 months (P1) from median 2.0 (P0) with 5-FU/LV alone. With alpha of 0.05, power of 80%, and drop-out rates of 10%, a total of 174 patients (87 patients per each arm) will be included in this study.

- **Quality of life assessment**
  - EORTC-QLQ C-30 questionnaire is assessed every cycle.

Accrual status

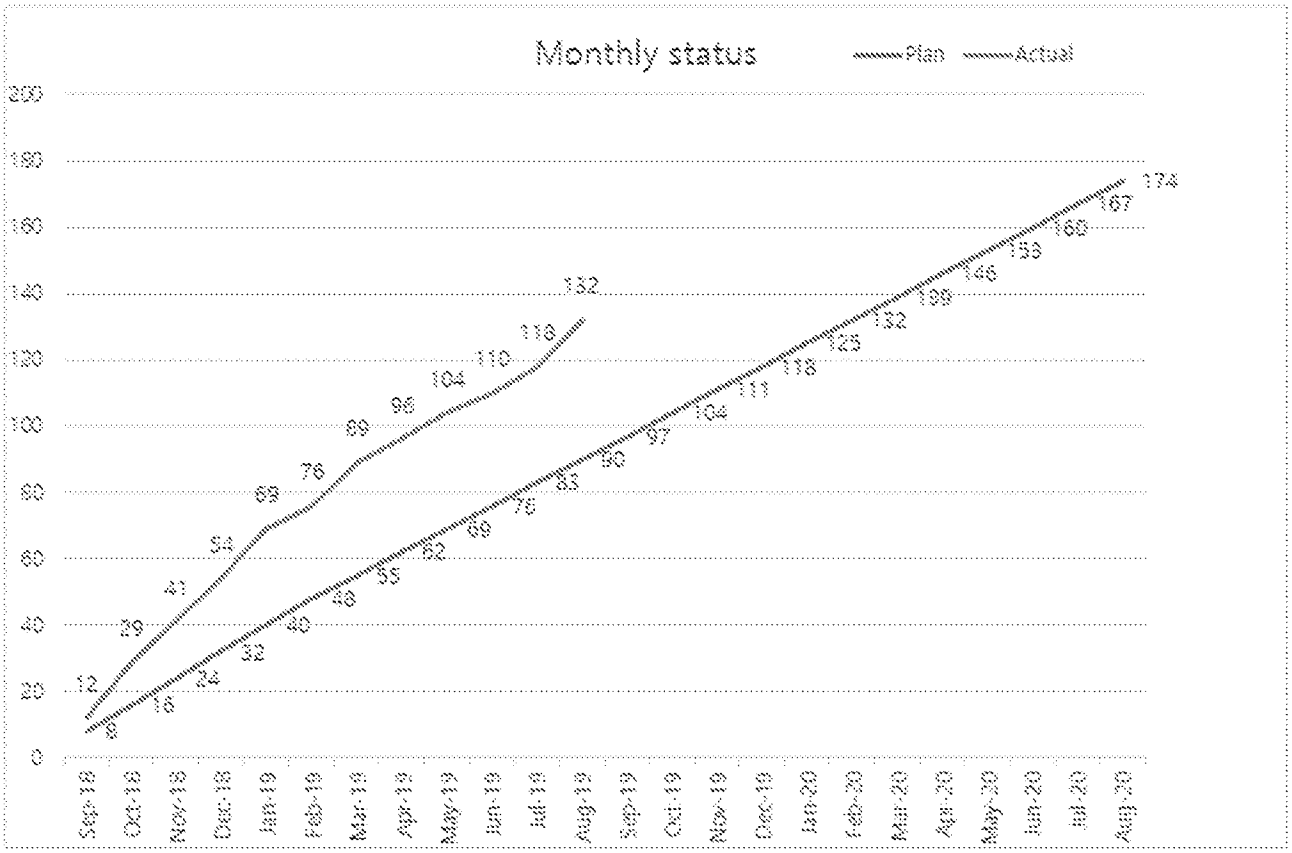

- **Study initiation: SEP-2018**

- **A total of 132 patients are enrolled as of AUG 2019**
  - 75% of target patient number
  - Expected timeline for completion of enrollment: DEC 2019

Multicenter randomized phase II study of 5-Fluorouracil/leucovorin (5-FU/LV) with or without liposomal irinotecan (nal-IRI) in metastatic biliary tract cancer (BTC) as second-line therapy after progression on gemcitabine plus cisplatin (GemCis): NIFTY trial

Chanhoon Yoo[1], Jae Ho Jeong[2], Kyu-pyo Kim[3], Jae-Lyun Cheon[4], Ilhwan Kim[5], Myoung-Joo Kang[6], Hyewon Ryu[6], Byung Wook Kang[6], Dalnim Seo[1], Baek-Yeol Ryoo[1]
[1]Asan Medical Center, [2]Ulsan University Hospital, [3]Incheon Sae Pals Hospital, [4]Chungnam National University Hospital, [5]Kyungpook National University Hospital, South Korea

Background

- Patients with BTC have dismal prognosis with 5-year survival of less than 10%.
- GemCis is the globally established first-line therapy based on the phase III ABC-02 trial. However, there is no standard second-line therapy after failure of 1st line GemCis, although 5-FU-based therapy has been widely used.
- Nal-IRI (Onivyde®) comprises irinotecan sucrosofate salt encapsulated in pegylated liposomes that protect the drug from premature conversion in the liver. Nal-IRI plus 5-FU/LV demonstrated the superior survival outcomes compared to 5-FU/LV alone in patients with metastatic pancreatic cancer who progressed on gemcitabine-based therapy.
- This randomized phase 2 trial is designed to compare the clinical outcomes between nal-IRI plus 5-FU/LV with 5-FU/LV alone as 2nd line therapy in patients with BTC who progressed on 1st line GemCis

Preclinical study

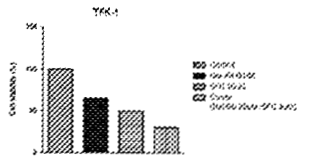

Synergism between nal-IRI and 5-FU in BTC cell line (TFK-1)

Eligibility criteria

Inclusion criteria

- Signed and written informed consent form
- ≥ 19 years of age
- Histologically or cytologically confirmed cholangiocarcinoma
- Documented metastatic disease
- At least one measurable lesion according to the RECIST v1.1
- Disease progression on gemcitabine-cisplatin combination therapy
- For patients whose disease recurred after curative resection (R0 or R1), previous adjuvant 5-FU-based chemotherapy is allowed if there is at least 6 month-interval between the last dose of adjuvant chemotherapy and recurrence of disease.
- Adequate hepatic, renal and hematological function
- Eastern Cooperative Oncology Group (ECOG) Performance status 0-1

Exclusion criteria

- Serum total bilirubin ≥ 2 x ULN (biliary drainage is allowed for biliary obstruction)
- Severe renal impairment (CLcr ≤ 30 ml/min)
- Inadequate bone marrow reserves as evidenced by:
  - ANC ≤ 1,500 cells/μl; or
  - Platelet count ≤ 100,000 cells/μl; or
  - Hemoglobin ≤ 9 g/dl.
- Eastern Cooperative Oncology Group performance status 2-4
- Any clinically significant disorder impacting the risk-benefit balance negatively per physician's judgment
- Any clinically significant gastrointestinal disorder, including hepatic disorders, bleeding, inflammation, occlusion, or diarrhea > grade 2
- Severe arterial thromboembolic events (myocardial infarction, unstable angina pectoris, stroke) in last 6 months
- NYHA Class III or IV congestive heart failure, ventricular arrhythmias or uncontrolled blood pressure. Or known abnormal ECG with clinically significant abnormal findings

Study design & treatment

- NIFTY trial is a multicenter, open-label, randomized (1:1), phase II trial and 5 referral cancer centers in Korea participated in this study.
- **Primary endpoint**
  - progression-free survival (PFS) assessed by independent review
- **Secondary endpoints**
  - Overall survival
  - Response rates assessed by RECIST v1.1
  - Quality of life assessed by EORTC QLQ-C30
  - Safety profile assessed by NCI-CTCAE v4.03

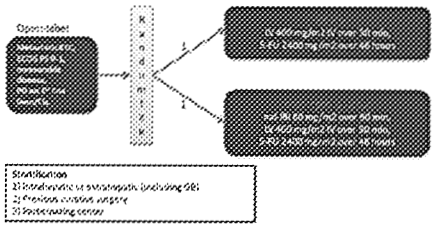

- Study treatment is continued until the disease progression or occurrence of intolerable toxicities
- **Control arm**
  - 400 mg/m² LV, 2400 mg/m² 5-FU over 46 h, every 2 weeks
- **Investigational arm**
  - Nal-IRI 80 mg/m², 400 mg/m² LV, 2400 mg/m² 5-FU over 46 h, every 2 weeks
- **Response assessment**
  - Tumor response is assessed using CT or MRI scan every 8 weeks (fixed).
- **Sample size estimation**
  - The addition of nal-IRI to 5-FU/LV would enhance the PFS to median 3.3 months (P1) from median 2.0 (P0) with 5-FU/LV alone. With alpha of 0.05, power of 80%, and drop-out rates of 10%, a total of 174 patients (87 patients per each arm) will be included in this study.
- **Quality of life assessment**
  - EORTC-QLQ C-30 questionnaire is assessed every cycle.

Accrual status

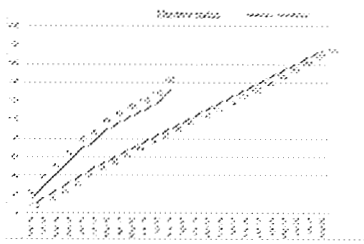

- **Study initiation: SEP-2018**
- **A total of 132 patients are enrolled as of AUG 2019**
  - 75% of target patient number
  - Expected timeline for completion of enrollment: DEC 2019

ClinicalTrials.gov Identifier: NCT03524508 PI: Chanhoon Yoo, MD, PhD email: yoochi@amc.seoul.kr

lesion are key inclusion criteria. Eligible patients are randomized with 1:1 ratio to experimental arm (80 mg/m^2 irinotecan hydrochloride trihydrate salt equivalent to 70 mg/m^2 irinotecan free base over 90 minutes, followed by 400 mg/m^2 LV over 30 min, and then 2400 mg/m^2 5-FU over 46 h, every 2 weeks) and control arm (400 mg/m^2 LV over 30 min, and then 2400 mg/m^2 5-FU over 46 h, every 2 week). Response evaluation is graded by RECIST v1.1 and conducted every 6 weeks. Primary endpoint is progression-free survival and secondary endpoints are overall survival, response rates, quality of life assessed by EORTC QLQ-C30 and safety profile. We hypothesized that the addition of nal-IRI to 5-FU/LV would enhance the PFS to median 3.3 months (P1) from median 2.0 (P0) with 5-FU/LV alone. With alpha of 0.05, power of 80%, and drop-out rates of 10%, a total of 174 patients (87 patients per each arm) are needed based on this hypothesis. As of March 2019, a total of 89 patients (51% of the target number) are enrolled.

Clinical trial identification: NCT03524508.

Legal entity responsible for the study: The authors.

Funding: Shire and Servier.

Disclosure: C. Yoo: Research grant / Funding (self): Shire; Advisory / Consultancy, Research grant / Funding (self): Servier; Honoraria (self): Ipsen. All other authors have declared no conflicts of interest.

829TiP **Multicenter randomized phase II trial of 5-fluorouracil/leucovorin (5-FU/LV) with or without liposomal irinotecan (nal-IRI) in metastatic biliary tract cancer (BTC) as second-line therapy after progression on gemcitabine plus cisplatin (GemCis): NIFTY trial**

C. Yoo[1], J.H. Jeong[1], K-P. Kim[2], J. Cheon[3], I. Kim[3], M. Kang[3], H. Ryu[4], B.W. Kang[5], B-Y. Ryoo[1]

[1]*Department of Oncology, Asan Medical Center, University of Ulsan College of Medicine, Seoul, Republic of Korea,* [2]*Hematology and Oncology, Ulsan University Hospital, Ulsan, Republic of Korea,* [3]*Internal Medicine, Inje University College of Medicine, Busan, Republic of Korea,* [4]*Internal Medicine, Chungnam National University Hospital, Daejeon, Republic of Korea,* [5]*Kyungpook National University, Kyungpook National University, Daegu, Republic of Korea*

Background: Patients with BTC have dismal prognosis with 5-year survival of less than 10%. GemCis is the globally established first-line therapy based on the phase III ABC-02 trial. However, there is no standard second-line therapy after failure of 1st line GemCis, although 5-FU-based therapy has been widely used. Nal-IRI (Onivyde®) comprises irinotecan sucrosofate salt encapsulated in pegylated liposomes that protect the drug from premature conversion in the liver. This randomized phase 2 trial is designed to compare the clinical outcomes between nal-IRI plus 5-FU/LV with 5-FU/LV alone as 2nd line therapy in patients with BTC who progressed on 1st line Gem/Cis.

Trial design: NIFTY trial is a multicenter, open-label, randomized, phase II trial and 5 referral cancer centers in Korea participated in this study. Histologically documented biliary tract cancer (intrahepatic and extrahepatic cholangiocarcinoma, and gallbladder cancer), documented progression on 1st line Gem/Cis, and at least one measurable

Published in final edited form as:
Cancer Chemother Pharmacol. 2009 February ; 63(3): 517–524. doi:10.1007/s00280-008-0769-8.

Enterohepatic recirculation model of irinotecan (CPT-11) and metabolite pharmacokinetics in patients with glioma

Islam R. Younis,
Department of Basic Pharmaceutical Sciences and Mary Babb Randolph Cancer Center, West Virginia University Health Sciences Center, P.O. Box 9300, Morgantown, WV 26506, USA

Samuel Malone,
Duke University Medical Center, Durham, NC, USA

Henry S. Friedman,
Duke University Medical Center, Durham, NC, USA

Department of Surgery, Duke University Medical Center, Durham, NC, USA

Larry J. Schaaf, and
The Ohio State University Comprehensive Cancer Center, Columbus, OH, USA

William P. Petros
Department of Basic Pharmaceutical Sciences and Mary Babb Randolph Cancer Center, West Virginia University Health Sciences Center, P.O. Box 9300, Morgantown, WV 26506, USA, wpetros@hsc.wvu.edu

Abstract

Background—Enterohepatic recirculation of irinotecan and one of its metabolites, SN-38, has been observed in pharmacokinetic data sets from previous studies. A mathematical model that can incorporate this phenomenon was developed to describe the pharmacokinetics of irinotecan and its metabolites.

Patients and methods—A total of 32 patients with recurrent malignant glioma were treated with weekly intravenous administration of irinotecan at a dose of 125 mg/m^2. Plasma concentrations of irinotecan and its three major metabolites were determined. Pharmacokinetic models were developed and tested for simultaneous fit of parent drug and metabolites, including a recirculation component.

Results—Rebound in the plasma concentration suggestive of enterohepatic recirculation at approximately 0.5–1 h post-infusion was observed in most irinotecan plasma concentration profiles, and in some plasma profiles of the SN-38 metabolite. A multi-compartment model containing a recirculation chain was developed to describe this process. The recirculation model was optimal in 22 of the 32 patients compared to the traditional model without the recirculation component.

Conclusion—A recirculation chain incorporated in a multi-compartment pharmacokinetic model of irinotecan and its metabolites appears to improve characterization of this drug's disposition in patients with glioma.

Correspondence to: William P. Petros.

Keywords

Irinotecan; Pharmacokinetics; Enterohepatic recirculation

Introduction

Irinotecan (CPT-11; Camptosar®) is used in the treatment of a variety of malignancies such as ovarian [1, 2], and colorectal cancers [3, 4]. More recently, it has shown activity in the treatment of glioma [5].

Both hydrolysis and metabolism are responsible for elimination of irinotecan (Fig. 1). The hydrolysis pathway is catalyzed by carboxy esterases and results in the formation of the active metabolite 7-ethyl-10-hydroxycamptothecin (SN-38). Although both human carboxy esterase isoenzymes 1 and 2 were identified to be involved in this biotransformation, human carboxy esterase 2 appears to play a more important role in cancer patients [6, 7]. SN-38 is further metabolized in human liver by UDP-glucuronosyl tranferase 1A1 to the inactive metabolite 7-ethyl-10-[3,4,5-trihydroxy-pyran-2-carboxylic acid]-camptothecin (SN-38G) [8, 9]. SN-38 levels are about 100-fold lower than that of irinotecan, with elimination half-life of approximately 10.2 h [10]. SN-38 glucuronide is present in plasma at higher concentrations than SN-38 [11]. The metabolic biotransformation of irinotecan is catalyzed by CYP450 3A4. The major metabolites formed through this pathway are 7-ethyl-10-[4--N-(5-aminopentanoic acid)-1-piperidino)-1-amino]-carbonyloxycamptothecin (APC) and 7-ethyl-10-[4--(1-piperidino)-1-amino]-carbonyloxycamptothecin (NPC) [12]. Only small fractions of irinotecan and its metabolites are eliminated in urine and a higher proportion in the bile.

An apparent enterohepatic recirculation of irinotecan and SN-38 is evident by the rebound in plasma levels at about 0.5--1.0 h following intravenous infusion [13]. We particularly noted this effect in some patients receiving concomitant anticonvulsant medications, however no formal pharmacokinetic model has been published which could describe this complex process in the context of metabolite pharmacokinetics [14].

The pharmacokinetics of irinotecan display high interpatient variation and are typically described by two or three compartment, first order models [15]. We attempted to utilize such models to evaluate parent drug and metabolites in a population of patients with brain tumors, many of which were receiving metabolic enzyme-inducing anticonvulsants [14]. Observable delayed (post-infusion) increases in plasma irinotecan (and to some degree, SN-38) led us to explore alternative approaches for mathematical description of these data. This paper reports use of our published irinotecan pharmacokinetic data to develop a novel enterohepatic recirculation model which incorporates multiple metabolite information. In addition, we have provided data on an additional metabolite (APC) which was not available at the time of the previous publication.

Patients and methods

Inclusion criteria

Patients older than 18 years of age, diagnosed with recurrent primary malignant glioma [glioblastoma multiforme, anaplastic astrocytoma (AA), or anaplastic oligodendroglioma (AO)] and exhibiting a Karnofsky performance status ≥60% were included in this pharmacokinetic study. Other pertinent eligibility criteria included adequate renal function (serum creatinine ≤1.5 mg/dL), adequate hepatic function (blood nitrogen level <25 mg/dL, serum AST and bilirubin levels <1.5 × upper limit of normal), and adequate bone marrow

function (hematocrit concentration >29%, absolute neutrophil count >1,500 cell/μL, platelet count >125,000 cells/μL). Patients who were receiving corticosteroids were required to be on a stable dose for 2 weeks prior to treatment.

Written informed consent was obtained from patients according to the guidelines of the institutional review board prior to initiation of the study. Additional details of the patient eligibility criteria are included elsewhere [14].

Treatment

Irinotecan was diluted with 500 mL of 5% dextrose solution, and administered by a 90 min IV infusion once weekly for 4 weeks, followed by 2 weeks rest. The starting dose of irinotecan was 125 mg/m^2 for all patients. Irinotecan was obtained from the Cancer Therapy Evaluation Program of the National Cancer Institute (NCI) as a sterile solution of 20 mg/mL in 2- or 5-mL vials.

Standard doses of ondansetron and an IV bolus dose of dexamethasone (10–20 mg) were administered before each irinotecan dose to prevent emesis. Patients who exhibited cholinergic affects with 2.5 h of starting of irinotecan infusion were treated with atropine (1 mg, IV). Patients who had late diarrhea were treated with loperamide. Patients already taking anticonvulsants continued treatment as prescribed. Chronic oral administration of corticosteroids was used to reduce tumor produced effects.

Pharmacokinetic studies

Pharmacokinetics of irinotecan and its metabolites, SN-38, SN38-G, and APC were conducted during, and up to 24 h after the first irinotecan infusion. Blood samples (5 mL) were drawn into heparinized tubes before irinotecan infusion at 30, 60, and 90 min (end of infusion), and at 5, 15, and 30 min and 1, 2, 4, 6, 8, and 24 h following the completion of the infusion. Blood samples were immediately placed into slurry of ice and water. Plasma was separated, as soon as possible, by centrifugation at 1,000–1,200×*g* (3,000 rpm) for 20 min, and stored at −70°C until analyzed.

Plasma concentrations of irinotecan and its metabolites (SN-38, SN-38G and APC) were determined using a validated, sensitive, and specific high performance liquid chromatography with fluorescence detection as described previously [14]. The lower limits of quantification were 1.3, 0.5, and 1.0 ng/mL for irinotecan, SN-38, and APC, respectively. Intra- and inter-variability in the assay method was <10% for each analyte.

Pharmacokinetic data analysis

Pharmacokinetic analyses were performed using non-compartmental as well as compartmental pharmacokinetic modeling. Initial parameters were determined by generalized least-square regression of plasma concentration time points, as implemented by the ADAPT program (Biomedical Simulations Resource, University of Southern California) [16]. Irinotecan and its metabolite data were then evaluated by ADAPT using a nonlinear, open, multi-compartment pharmacokinetic model. The model included two compartments for irinotecan, and one compartment each for SN-38 and APC. The data were also evaluated using a model that takes into account the phenomenon of enterohepatic recirculation. This model additionally incorporated a recirculation "chain" stemming off of the irinotecan compartment and leading back into it as depicted in Fig. 2. The recirculation chain consisted of five compartments, each of fixed volume, with a single rate parameter that is equal to the rate constant of flow between each compartment in the chain. This rate parameter also determined the linear rate constants between the primary compartment and the chain compartment, and between the last chain compartment and the primary compartment. The

virtue of having a single parameter is that it allows us to model the recirculation effects while adding minimum complexity to the model. To determine the best number of compartments in the model (five), we ran several informal trials on patients which appeared to display a high qualitative level of recirculation. A four compartment chain worked fairly well for some sets, and our decision to use five reflected our sense that a five compartment chain produced the best fit for the majority of recirculation sets. It should be noted that the five compartments in the chain do not represent any physiological compartment.

A metabolic ratio, estimated as the ratio of each metabolite to irinotecan (AUC_{0-24}), was used to measure the relative ratio of irinotecan conversion to SN-38, SN38 to SN-38G, and irinotecan metabolism to APC.

Model selection

The Akaike Information Criterion (AIC) was utilized to select the best model for each patient data set [17]. Four representative patients were utilized for the determination of appropriate weighing scheme for the analytes. A weighing scheme was selected before running both models. Initially we found that a scheme with a coefficient of 1 for irinotecan, 30 for SN-38, and 5 for APC produced the lowest SSR on average for the patients tested. Improvement in the scheme was evident when coefficients of 1 for irinotecan, 10 for SN-38, and 5 for APC were employed. Like the 1, 30, 5 scheme, the latter scheme produced relatively low SSR for the four representative patients, and the two schemes gave comparable results. In addition, the 1, 10, 5 scheme was chosen because the weights are in keeping with the fact that SN-38 is 10–1,000 times more active than irinotecan, and the activity of APC falls between that of irinotecan and SN-38. Although we experimented with weighting schemes such as 1, 135, 3.5, which is more in line with the relative magnitudes of the analyte activity levels (and which makes the weighted SSR the same order of magnitude for each of the analytes), schemes that gave higher weight to SN-38 inevitably yielded higher total SSRs. Qualitatively, there seemed to be a trade off in some cases between fitting irinotecan well and fitting SN-38 well. In addition, weighting schemes that fit irinotecan well also seemed to fit APC well. After deciding on a weighting scheme, we estimated parameters for each patient using both the standard model and the recirculation model.

The best fit model was selected on a per-patient basis, using analyses of each patient with the recirculation model and the standard four compartment model. In the initial round of inspection, the model corresponding to the lower AIC value was termed the best model. In the second round of inspection, the data set of each patient was rated on a three point scale for the presence of enterohepatic recirculation, a subjective rating of 0, 1, or 2 was assigned to patients of they showed no, possible, or strong recirculation, respectively. This was done via a visual appraisal of the irinotecan and SN-38 concentration-time curves. If the standard model had been selected as best for a patient with a high qualitative degree of recirculation, the data set for that patient was renn with alternative initial parameter estimates and the best model assignments were then finalized.

Results

Blood samples from 32 patients, 20 males and 12 females, were analyzed for irinotecan, SN-38, SN-38G, and APC. All patients received 125 mg/m^2 of irinotecan. Most of the patients (n = 29) were initially diagnosed with glioblastoma multiforme (GBM), two with AA, and one with AO. All the patients except two received enzyme inducing antiepileptic drug treatment.

Pharmacokinetic variables for irinotecan and its metabolites were determined from concentration-time data using non-compartmental and compartmental analysis. Figure 3

shows the plasma concentration-time curve of irinotecan, SN-38, and APC from a representative patient with an apparent recirculation profile. The plasma disposition curves for irinotecan were biphasic, with rapid decrease after the end of the infusion. The descent of the concentration-time curve following the end of infusion was interrupted by a brief upturn before continuing its fall in 22 patients, suggestive of an enterohepatic recirculation pathway. Plasma concentrations of APC displayed first order elimination. Figure 4 depicts the plasma concentration-time curve for irinotecan, SN-38, and APC in a patient with no enterohepatic recirculation. Irinotecan showed a rapid decay after the end of the infusion, with no upturn in irinotecan concentration following the end of the infusion. Table 1 shows the non-compartmental pharmacokinetic parameters for irinotecan, APC, SN-38, SN-38G. The mean ± SD (ng/mL h) AUC_{0-24} were 4,430 ± 1,306 for irinotecan, 1,337 ± 506 for APC, 63.9 ± 39.7 for SN-38, and 359 ± 157 for SN-38G. The AUC_{0-24} accounted for more than 95% of AUC_{0-inf} for irinotecan in all patients. AUC_{0-24} accounted for more than 70% of AUC_{0-inf} in 94, 87, and 100% of the patients for APC, SN-38G, and SN-38, respectively.

The relationship between irinotecan and its metabolites was evaluated by comparing the AUCs. The mean ± SD of the conversion of irinotecan to SN-38 was 0.016 ± 007, while that of the metabolism of irinotecan to APC was 0.3 ± 0.1. The mean ± SD for the conversion of SN-38 to SN-38G was 6.94 ± 3.09.

The best fit model was selected on a per-patient basis, using analyses of each patient with the recirculation model and the standard four compartment model. The final parameters for the best and standard model are shown in Table 2. The recirculation model was best in 22 patients out of the 32 patient data sets, while the standard model was best in 10 patients. Figure 5 shows the relationship between the best model AUC for each analyte to the actual trapezoidal AUC. The regression produced R^2 of 0.971, 0.815, and 0.974 for irinotecan, SN-38, and APC, respectively. The mean precision error (MPE) and root mean squared error (RMSE) were used to quantify the degree of bias and precision of the predicted AUC values. The MPE values for irinotecan, SN-38, and APC were −137, −13.2, and 1.09, respectively. The RMSE values, which measure precision, were 249, 20.82, and 77.95 for irinotecan, SN-38, and APC, respectively.

Discussion

The importance of irinotecan as a chemotherapeutic agent is well established, however approaches to model its plasma disposition and complex metabolite profile are suboptimal for some patients in whom observable enterohepatic recirculation is evident. To our knowledge, this is the first report to incorporate the phenomena of enterohepatic circulation in the pharmacokinetic model used to describe the disposition of irinotecan and its primary metabolites SN-38, SN38G, and APC. We have previously reported the use of irinotecan for the treatment of glioma, and described the pharmacokinetics of irinotecan and its metabolites SN-38, and SN38G using non-compartmental approaches [14]. A majority of previous irinotecan pharmacokinetic studies focus on the parent drug and its active metabolite SN-38 [18–20]. Fewer reports studied the pharmacokinetics of its other metabolites SN-38G, NPC and APC.

Xie et al. [21] introduced a multi-compartment model to describe the population pharmacokinetics of irinotecan and its metabolites. The model consisted of one central and two peripheral compartments for the lactone from of irinotecan, a central and a peripheral compartment for the carboxylate form of irinotecan, the lactone form of SN-38, APC, and NPC. The carboxylate form of SN-38 and SN-38G were accounted for using a single compartment and elimination occurring from the central compartments of the carboxylate form of irinotecan, the carboxylate form of SN-38, APC, NPC, and SN-38G. A three

compartment model was used to describe the pharmacokinetics of irinotecan in patients with metastatic digestive cancer, while a two compartment model was used for SN-38, and one compartment model was used for SN-38G, APC, and NPC [22]. Ma et al. [23] used a four compartment model to describe the pharmacokinetics of irinotecan, SN-38, and APC in children with recurrent solid tumor using low dose of irinotecan. A altered distribution of SN-38 in two patients was observed suggesting enterohepatic recirculation. None of the above models took into account the phenomena of enterohepatic recirculation.

In order to adequately describe the disposition of irinotecan, the mathematical model should have the capacity to simultaneously describe the pharmacokinetics of irinotecan and its metabolites in the body since the SN-38 metabolite is 1,000-fold more potent than the parent drug [24], and enzyme induction could affect the formation of the other metabolites APC and NPC. We explored multi-compartment pharmacokinetic models that take into account the enterohepatic recirculation phenomenon. Unlike the model described by Xie et al. [21], the developed model did not take into account the lactone and carboxylate forms of irinotecan and its metabolites since only total drug concentrations were available on our study. Only the lactone form of irinotecan and its metabolites have antitumor activity [25], and they undergo a pH-dependent equilibrium with carboxylate forms [26]. However, the model simultaneously accounts for irinotecan, its metabolites SN-38 and APC, and the phenomena of enterohepatic recirculation.

Pharmacokinetic data from each patient were first evaluated with a model that included irinotecan, SN-38 and APC. After specifying and selectively testing this model, we realized that some of the patients displayed qualitative evidence supporting the enterohepatic recirculation of irinotecan. In a few cases, patients also displayed evidence for the recirculation of SN-38.

Since the combined model did not appear to fit some data sets very well, we decided to formulate a compartmental model that took into account the recirculation phenomenon. After several attempts, we settled on the model depicted in Fig. 2, which consists of the original combined model with a recirculation "chain" added onto the irinotecan compartment. The idea behind this design is that during the infusion, some of the irinotecan added to the primary compartment is channeled into the recirculation chain. After traveling through the chain, it flows back into the irinotecan compartment. Depending on the specifications of the chain, and the total rate at which irinotecan exits the primary compartment, the reflux of irinotecan from the chain can produce a post-infusion increase in the concentration of irinotecan. In particular, the recirculation chain consists of five compartments, each of fixed volume, with a single rate parameter that equal to the rate constant of flow between each compartment in the chain and between the primary compartment and the first chain compartment and the last chain compartment and the primary compartment. The virtue of having a single parameter is that it allows us to model the recirculation effects while adding a minimum of complexity to the model. The number of compartments in the recirculation does not reflect any physiological setting, the five compartments chain provided a model that can best fit the data and does not add much to the complexity of the model.

Several models that account for enterohepatic recirculation of other drugs, using variable number of compartments in the recirculation chain have been published. Three compartments of fixed volume were used to describe the biliary excretion and enterohepatic recirculation of morphine-3-glucoronide in rats. The recirculation loop was incorporated between the liver compartment and the plasma compartment, and elimination of the drug was assumed to occur partially from the third compartment in the loop [27]. Davis et al. [28] incorporated one compartment to describe the enterohepatic recirculation of gliclazid,

however, this compartment was actually considered to be a series of compartments that delay the release of the drug back into the gastrointestinal tract for reabsorption. Enterohepatic recirculation was incorporated as a secondary input to the systemic circulation in describing the population pharmacokinetics of ezetimibe, a single parameter corresponding to the percentage of the dose was incorporated in the model [29]. A bile compartment was used to account for the enterohepatic recirculation of isoflavone biochanin A in rats. The drug was assumed to be transferred directly from the bile compartment to the plasma compartment at regular intervals, and a sine function was used to describe the transfer [30].

After finalizing the form of the recirculation model, we compared it with the standard compartmental model using the criterion of average AIC value. This was calculated in two stages by estimation of parameters for every other patient using both the standard model and the recirculation model. We found that the average AIC value was slightly lower for the set of patients tested using the recirculation model. Having ascertained that the recirculation model yielded reasonable fits for the data, we tested all patients with both models (recirculation and standard).

The best fit model assignment was further confirmed with the good correlation coefficient obtained when comparing the best fit model trapezoidal AUC, calculated from the model output data, with the corresponding actual trapezoidal AUC for each patient (Fig. 4a–c).

In summary, the introduced model can be used to describe the pharmacokinetic of irinotecan and its metabolites following an IV infusion. This model can simultaneously describe the plasma concentration profile of irinotecan and its metabolites when enterohepatic recirculation is present. We have also demonstrated that the standard compartmental model is adequate only when no evidence of enterohepatic recirculation is present. Given the limited number of samples and patients, the intent of this model is to provide a framework or a prototype that takes into account the enterohepatic recirculation phenomenon obtained in some patients and evident by a secondary peak in plasma profile after the end of the infusion. This consideration should be useful for researchers in designing future studies regarding the pharmacokinetic of irinotecan.

Acknowledgments

This paper is supported in part by the Mylan Chair of Pharmacology at West Virginia University.

References

1. Clamp AR, Maenpaa J, Cruickshank D, Ledermann J, Wilkinson PM, Welch R, Chan S, Vasey P, Sorbe B, Hindley A, Jayson GC. SCOTROC 2B: feasibility of carboplatin followed by docetaxel or docetaxel-irinotecan as first-line therapy for ovarian cancer. Br J Cancer. 2006; 94(1):55–61. [PubMed: 16404360]
2. Matsumoto K, Katsumata N, Yamanaka Y, Yonemori K, Kohno T, Shimizu C, Andoh M, Fujiwara Y. The safety and efficacy of the weekly dosing of irinotecan for platinum- and taxanes-resistant epithelial ovarian cancer. Gynecol Oncol. 2006; 100(2):412–416. [PubMed: 16298422]
3. Pitot HC, Wender DB, O'Connell MJ, Schroeder G, Goldberg RM, Rubin J, Mailliard JA, Kvols LK, Ghosh C, Kirschling RJ, Levitt R, Windschitl HE. Phase II trial of irinotecan in patients with metastatic colorectal carcinoma. J Clin Oncol. 1997; 15(8):2910–2919. [PubMed: 9256135]
4. Conti JA, Kemeny NE, Saltz LB, Huang Y, Tong WP, Chou TC, Sun M, Pulliam S, Gonzalez C. Irinotecan is an active agent in untreated patients with metastatic colorectal cancer. J Clin Oncol. 1996; 14(3):709–715. [PubMed: 8622015]

5. Stupp R, Hegi ME, van den Bent MJ, Mason WP, Weller M, Mirimanoff RO, Cairncross JG. Changing paradigms-an update on the multidisciplinary management of malignant glioma. Oncologist. 2006; 11(2):165–180. [PubMed: 16476837]

6. Slatter JG, Su P, Sams JP, Schaaf LJ, Wienkers LC. Bioactivation of the anticancer agent CPT-11 to SN-38 by human hepatic microsomal carboxylesterases and the in vitro assessment of potential drug interactions. Drug Metab Dispos. 1997; 25(10):1157–1164. [PubMed: 9321519]

7. Humerickhouse R, Lohrbach K, Li L, Bosron WF, Dolan ME. Characterization of CPT-11 hydrolysis by human liver carboxylesterase isoforms hCE-1 and hCE-2. Cancer Res. 2000; 60(5): 1189–1192. [PubMed: 10728672]

8. Iyer L, King CD, Whittington PF, Green MD, Roy SK, Tephly TR, Coffman BL, Ratain MJ. Genetic predisposition to the metabolism of irinotecan (CPT-11). Role of uridine diphosphate glucuronosyltransferase isoform 1A1 in the glucuronidation of its active metabolite (SN-38) in human liver microsomes. J Clin Invest. 1998; 101(4):847–854. [PubMed: 9466980]

9. Rivory LP, Robert J. Identification and kinetics of a beta-glucuronide metabolite of SN-38 in human plasma after administration of the camptothecin derivative irinotecan. Cancer Chemother Pharmacol. 1995; 36(2):176–179. [PubMed: 7767955]

10. Catimel G, Chabot GG, Guastalla JP, Dumortier A, Cote C, Engel C, Gouyette A, Mathieu-Boue A, Maljoubi M, Clavel M. Phase I and pharmacokinetic study of irinotecan (CPT-11) administered daily for three consecutive days every three weeks in patients with advanced solid tumors. Ann Oncol. 1995; 6(2):133–140. [PubMed: 7786821]

11. Canal P, Gay C, Dezeuze A, Douillard JY, Bugat R, Brunet R, Adenis A, Herait P, Lokiec F, Mathieu-Boue A. Pharmacokinetics and pharmacodynamics of irinotecan during a phase II clinical trial in colorectal cancer. J Clin Oncol. 1996; 14(10):2688–2695. [PubMed: 8874328]

12. Santos A, Zanetta S, Cresteil T, Deroussent A, Pein F, Raymond E, Vernillet L, Risse ML, Boige V, Gouyette A, Vassal G. Metabolism of irinotecan (CPT-11) by CYP3A4 and CYP3A5 in humans. Clin Cancer Res. 2000; 6(5) 2012–2020. [PubMed: 10815927]

13. Chabot GG. Clinical pharmacokinetics of irinotecan. Clin Pharmacokinet. 1997; 33(4):245–259. [PubMed: 9342501]

14. Friedman HS, Petros WP, Friedman AH, Schaaf LJ, Kerby T, Lawyer J, Parry M, Houghton PJ, Lovell S, Rasheed K, Cloughsey T, Stewart ES, Colvin OM, Provenzale JM, McLendon RE, Bigner DD, Cokgor I, Haglund M, Rich J, Ashley D, Malczyn J, Elfring GL, Miller LL. Irinotecan therapy in adults with recurrent or progressive malignant glioma. J Clin Oncol. 1999; 17(5) 1516–1525. [PubMed: 10334539]

15. Chabot GG, Abigerges D, Catimel G, Culine S, de Forni M, Extra JM, Maljoubi M, Herait P, Armand JP, Bugat R, Clave M, Marty ME. Population pharmacokinetics and pharmacodynamics of irinotecan (CPT-11) and active metabolite SN-38 during phase I trials. Ann Oncol. 1995; 6(2) 141–151. [PubMed: 7786822]

16. D'Argenio Schumitzky. ADAPT II user's guide: pharmacokinetic/ pharmacodyname systems analysis software. Los Angeles: Biomedical Simulations Resource; 1997.

17. Yamaoka K, Nakagawa T, Uno T. Application of Akaike's information criterion (AIC) in the evaluation of linear pharmacokinetic equations. J Pharmacokinet Biopharm. 1978; 6(2):165–175. [PubMed: 671222]

18. Azrak RG, Yu J, Pendyala L, Smith PF, Cao S, Li X, Shannon WD, Durrani FA, McLeod HL, Rustum YM. Irinotecan pharmacokinetic and pharmacogenomic alterations induced by methylselenocysteine in human head and neck xenograft tumors. Mol Cancer Ther. 2005; 4(5): 843–854. [PubMed: 15897249]

19. Prados MD, Yung WK, Jaeckle KA, Robins HI, Mehta MP, Fine HA, Wen PY, Cloughesy TF, Chang SM, Nicholas MK, Schiff D, Greenberg HS, Junck L, Fink KL, Hess KR, Kuhn J. Phase I trial of irinotecan (CPT-11) in patients with recurrent malignant glioma: a North American Brain Tumor Consortium study. Neuro Oncol. 2004; 6(1):44–54. [PubMed: 14769140]

20. Venook AP, Enders KC, Fleming G, Hollis D, Leichman CG, Hohl R, Byrd J, Budman D, Villalona M, Marshall J, Rosner GL, Ramirez J, Kastrissios H, Ratain MJ. A phase I and pharmacokinetic study of irinotecan in patients with hepatic or renal dysfunction or with prior pelvic radiation: CALGB 9863. Ann Oncol. 2003; 14(12):1783–1790. [PubMed: 14630685]

21. Xie R, Mathijssen RH, Sparreboom A, Verweij J, Karlsson MO. Clinical pharmacokinetics of irinotecan and its metabolites in relation with diarrhea. Clin Pharmacol Ther. 2002; 72(3):265–275. [PubMed: 12235447]

22. Poujol S, Bressolle F, Duffour J, Abderrahim AG, Astre C, Ychou M, Pinguet F. Pharmacokinetics and pharmacodynamics of irinotecan and its metabolites from plasma and saliva data in patients with metastatic digestive cancer receiving Folfiri regimen. Cancer Chemother Pharmacol. 2006; 58(3):292–305. [PubMed: 16369821]

23. Ma MK, Zamboni WC, Radomski KM, Furman WL, Santana VM, Houghton PJ, Hanna SK, Smith AK, Stewart CF. Pharmacokinetics of irinotecan and its metabolites SN-38 and APC in children with recurrent solid tumors after protracted low-dose irinotecan. Clin Cancer Res. 2000; 6(3):813–819. [PubMed: 10741701]

24. Kawato Y, Aonuma M, Hirota Y, Kuga H, Sato K. Intracellular roles of SN-38, a metabolite of the camptothecin derivative CPT-11, in the antitumor effect of CPT-11. Cancer Res. 1991; 51(16): 4187–4191. [PubMed: 1651156]

25. Hertzberg RP, Caranfa MJ, Holden KG, Jakas DR, Gallagher G, Mattern MR, Mong SM, Bartus JO, Johnson RK, Kingsbury WD. Modification of the hydroxy lactone ring of camptothecin: inhibition of mammalian topoisomerase I and biological activity. J Med Chem. 1989; 32(3):715–720. [PubMed: 2537428]

26. Fassberg J, Stella VJ. A kinetic and mechanistic study of the hydrolysis of camptothecin and some analogues. J Pharm Sci. 1992; 81(7):676–684. [PubMed: 1403703]

27. Ouellet DM, Pollack GM. Biliary excretion and enterohepatic recirculation of morphine-3-glucuronide in rats. Drug Metab Dispos. 1995; 23(4):478–484. [PubMed: 7600915]

28. Davis TM, Daly F, Walsh JP, Ilett KF, Beilby JP, Dusci LJ, Barrett PH. Pharmacokinetics and pharmacodynamics of gliclazide in Caucasians and Australian Aborigines with type 2 diabetes. Br J Clin Pharmacol. 2000; 49(3):223–230. [PubMed: 10718777]

29. Ezzet F, Krishna G, Wexler DB, Statkevich P, Kosoglou T, Batra VK. A population pharmacokinetic model that describes multiple peaks due to enterohepatic recirculation of ezetimibe. Clin Ther. 2001; 23(6):871–885. [PubMed: 11440287]

30. Moon YJ, Sagawa K, Frederick K, Zhang S, Morris ME. Pharmacokinetics and bioavailability of the isoflavone biochanin A in rats. AAPS J. 2006; 8(3):E433–E442. [PubMed: 17025260]

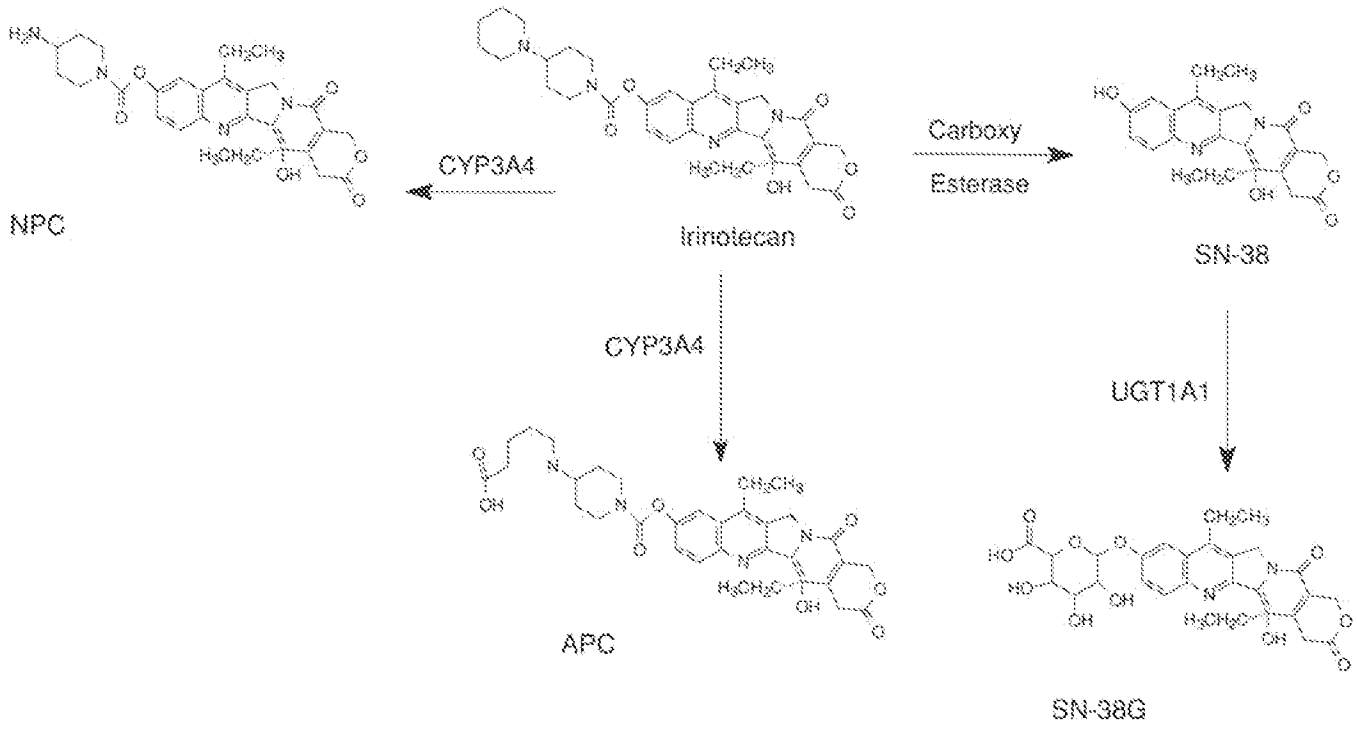

Fig. 1.
Metabolic scheme of irinotecan

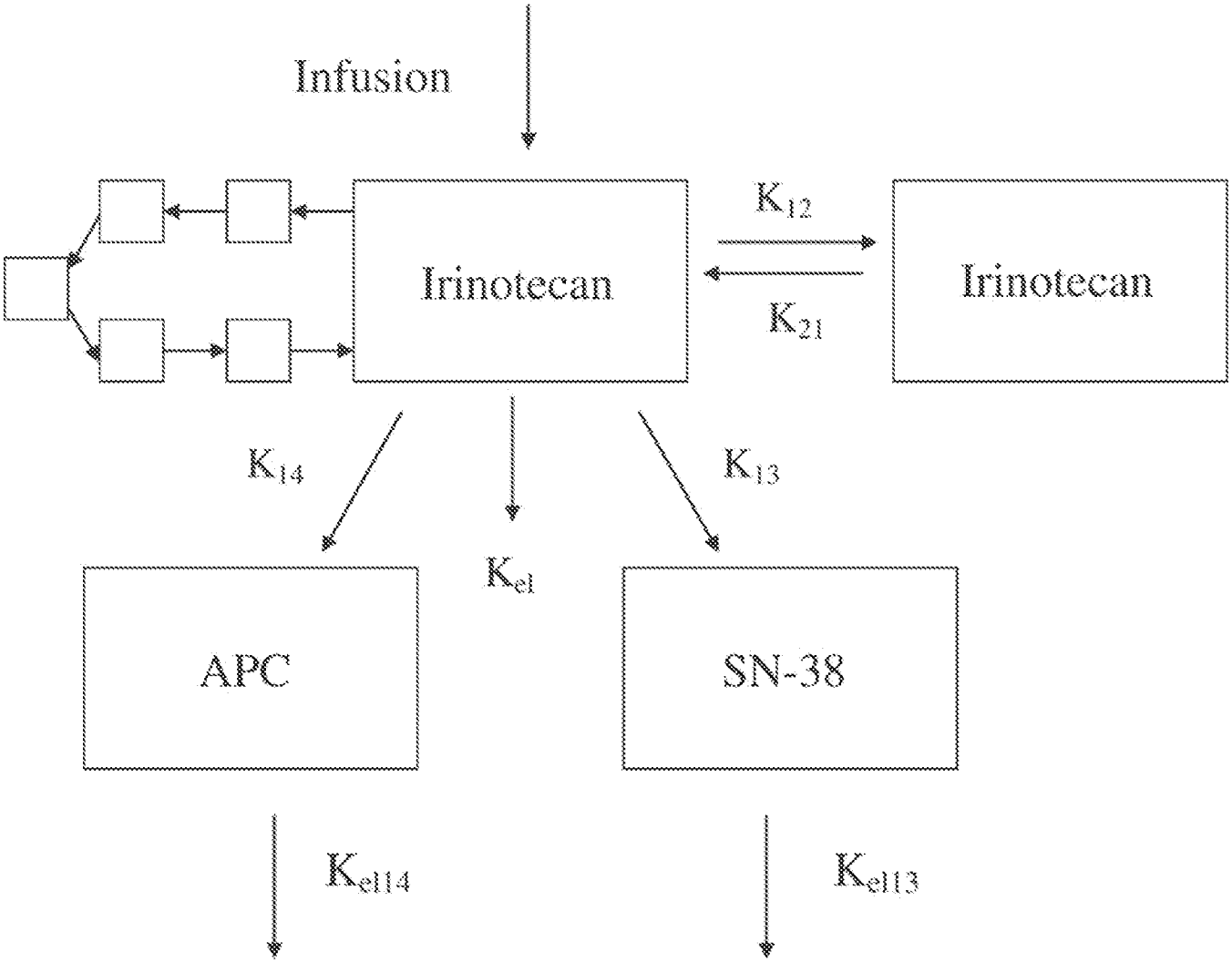

Fig. 2.
The enterohepatic recirculation model consists of irinotecan central compartment, irinotecan peripheral compartment, and SN-38 and APC plasma compartments, and the recirculation chain that consists of five compartments each of fixed volume

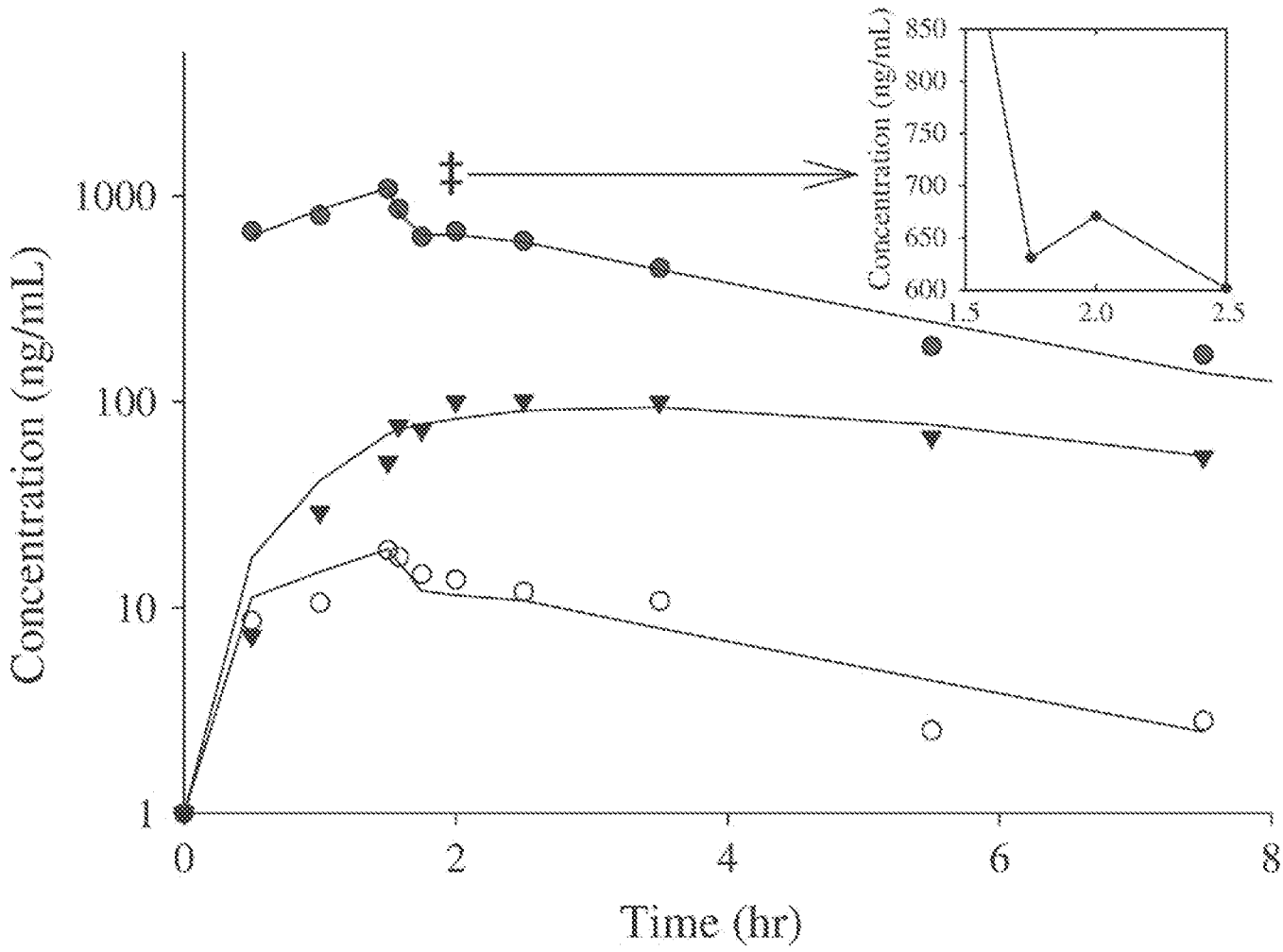

Fig. 3.

Plasma concentration-time profile, in a representative patient of enterohepatic recirculation, for irinotecan (*filled circle*), SN-38 (*open circle*), and APC (*inverted triangle*). Irinotecan *double dagger* secondary peak after the end of the infusion indicative of enterohepatic recirculation. *Symbols* represent measured plasma concentration, and *solid lines* are obtained from predicted concentrations using the recirculation model connected point by point

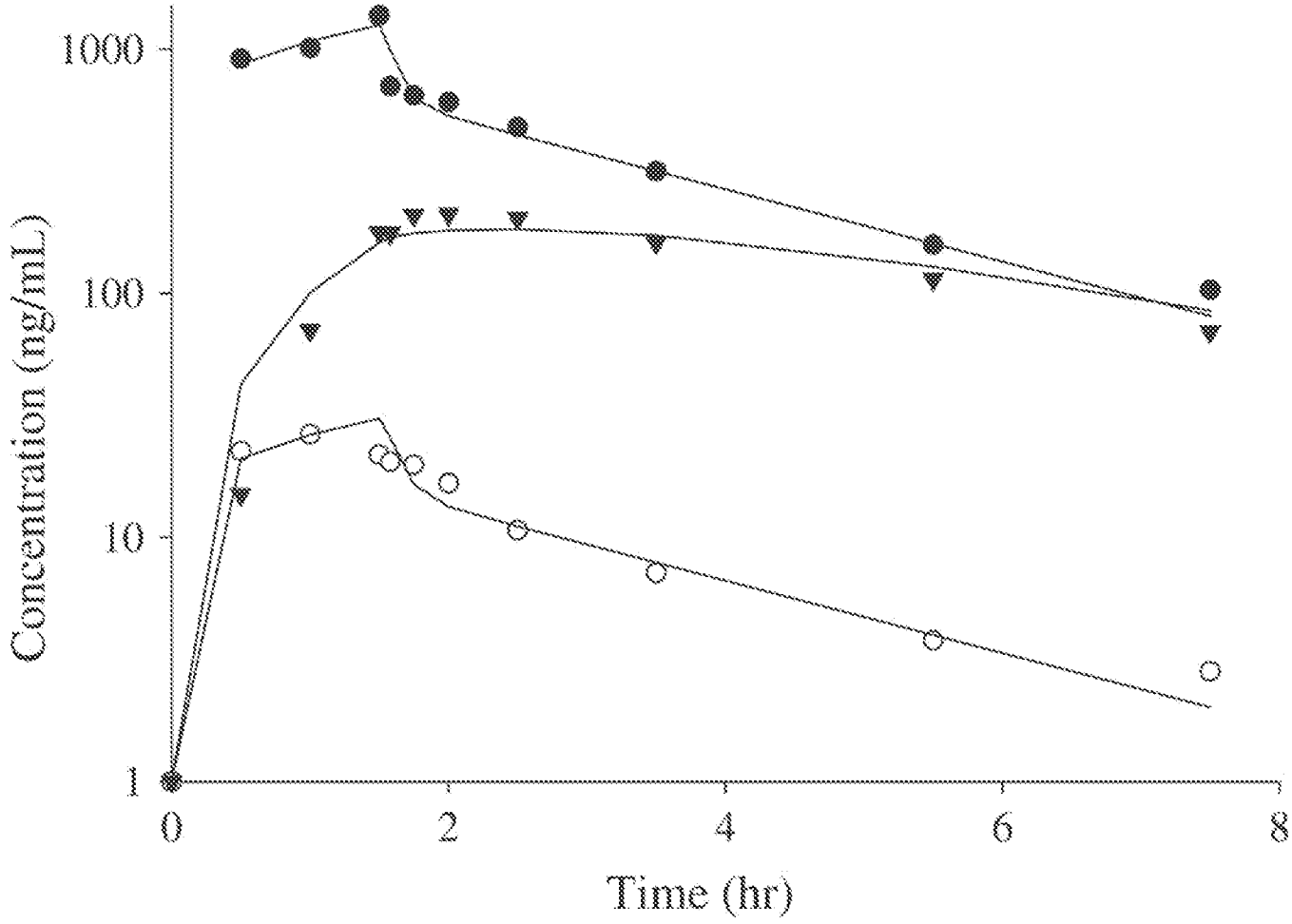

Fig. 4.

Plasma concentration-time profile, in a representative patient of with no evidence of enterohepatic recirculation, for irinotecan (*filled circle*), SN-38 (*open circle*), and APC (*inverted triangle*). Symbols represent measured plasma concentration, and *solid lines* are obtained from point by point connection of the predicted plasma concentrations by the standard model

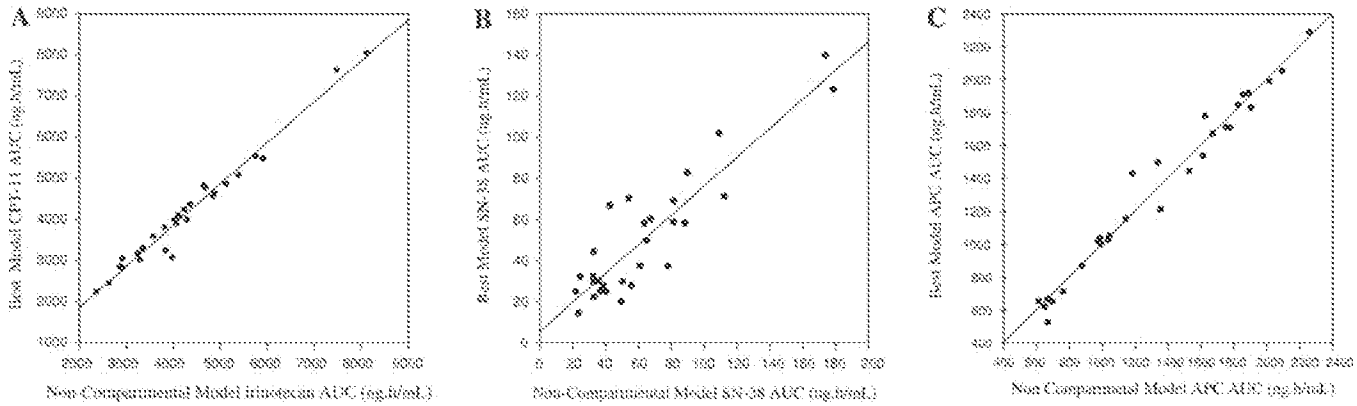

Fig. 5.
Linear regression of the optimal non-compartmental AUCs on the compartmental AUCs for irinotecan (**a**), SN-38 (**b**), and APC (**c**)

Table 1

Comparison of pharmacokinetic parameters for APC, irinotecan, SN-38, and SN-38G using non-compartmental analysis

	APC	Irinotecan	SN-38	SN-38G
Tmax (h)	2.31 ± 0.56	1.3 ± 0.3	1.2 ± 0.4	1.66 ± 0.28
Cmax (ng/mL)	178.6 ± 94.5	1,465 ± 598	12.9 ± 5.5	65.3 ± 25.7
Half-life (h)	5.5 ± 1.08	5.3 ± 0.86	8.5 ± 6.4	10.0 ± 2.9
AUC_{0-24} (ng h/mL)	1,337 ± 506	4,303 ± 1,321	63.9 ± 39.7	359 ± 157
AUC_{0-last} (ng h/mL)	1,423 ± 565	4430 ± 1306	76.7 ± 50.5	440 ± 197
AUC % extrapolated	5.7 ± 5.0	3.1 ± 3.2	19.8 ± 11.1	16.7 ± 9.5

Table 2

Final pharmacokinetic parameters for both the standard and recirculation model

	$V_{IRINOTECAN}$ (L/m^2)	K_{12} (h^{-1})	K_{21} (h^{-1})	K_{el} (h^{-1})	K_{23} (h^{-1})	K_{el3} (h^{-1})	V_{SN-38} (L/m^2)	K_{12} (h^{-1})	K_{el4} (h^{-1})	V_{APC} (L/m^2)
Standard model group (n = 10)										
Mean	24.70	38.25	6.66	6.27	2.55	123.69	394.39	1.14	0.41	40.68
Median	5.42	19.26	1.08	3.83	0.22	15.16	12.28	0.06	0.36	1.45
SD	42.50	58.87	18.29	8.36	6.82	282.12	1165.40	3.07	0.17	72.38
Range	0.77–133.40	0.36–197.70	0.01–58.71	0.00–26.82	0.01–21.90	0.18–905.17	0.50–3710.00	0.00–9.83	0.19–0.67	0.00–209.80
Recirculation model group (n = 22)										
Mean	8.60	6.52	0.55	5.12	0.29	17.30	19.19	0.31	0.44	14.31
Median	8.66	3.22	0.26	4.27	0.11	10.61	8.12	0.08	0.40	4.30
SD	4.60	8.10	0.70	4.45	0.63	25.43	34.40	0.69	0.16	30.76
Range	1.57–16.41	0.03–36.91	0.00–2.77	0.02–19.06	0.00–2.95	0.52–123.20	0.00–164.53	0.00–3.13	0.19–0.84	0.00–146.50

Out of 32 total patients, the standard model was designated as the optimal model for 10 patients and the recirculation model was designated the optimal model for the remaining 22

Phase I and Pharmacokinetic Study of Pegylated Liposomal CKD-602 in Patients with Advanced Malignancies

William C. Zamboni,[1,2] Suresh Ramalingam,[3,4] David M. Friedland,[3] Robert P. Edwards,[5,6] Ronald G. Stoller,[3] Sandra Strychor,[4] Lauren Maruca,[4] Beth A. Zamboni,[7] Chandra P. Belani,[3,4] and Ramesh K. Ramanathan[3,4]

Abstract

Purpose: S-CKD602 is a pegylated liposomal formulation of CKD602, a semisynthetic camptothecin analogue. Pegylated (STEALTH) liposomes can achieve extended drug exposure in plasma and tumor. Based on promising preclinical data, the first phase I study of S-CKD602 was done in patients with refractory solid tumors.

Experimental Design: S-CKD602 was administered i.v. every 3 weeks. Modified Fibonacci escalation was used (three to six patients/cohort), and dose levels ranged from 0.1 to 2.5 mg/m^2. Serial plasma samples were obtained over 2 weeks and total (lactone + hydroxyl acid) concentrations of encapsulated, released, and sum total (encapsulated + released) CKD602 measured by liquid chromatography–tandem mass spectrometry.

Results: Forty-five patients (21 males) were treated. Median age, 62 years (range, 33–79 years) and Eastern Cooperative Oncology Group status, 0 to 1 (43 patients) and 2 (2 patients). Dose-limiting toxicities of grade 3 mucositis occurred in one of six patients at 0.3 mg/m^2, grade 3 and 4 bone marrow suppression in two of three patients at 2.5 mg/m^2, and grade 3 febrile neutropenia and anemia in one of six patients at 2.1 mg/m^2. The maximum tolerated dose was 2.1 mg/m^2. Partial responses occurred in two patients with refractory ovarian cancer (1.7 and 2.1 mg/m^2). High interpatient variability occurred in the pharmacokinetic disposition of encapsulated and released CKD602.

Conclusions: S-CKD602 represents a promising new liposomal camptothecin analogue with manageable toxicity and promising antitumor activity. Phase II studies of S-CKD602 at 2.1 mg/m^2 i.v. once every 3 weeks are planned. Prolonged plasma exposure over 1 to 2 weeks is consistent with STEALTH liposomes and provides extended exposure compared with single doses of nonliposomal camptothecins.

S-CKD602 is a STEALTH liposomal formulation of CKD602, a camptothecin analogue which inhibits topoisomerase I (1–3). The STEALTH liposomal formulation consists of phospholipids covalently bound to methoxypolyethylene glycol on the outside of the lipid bilayer. Nonliposomal CKD602 administered i.v. at 0.5 mg/m^2/d for 5 consecutive days repeated every 21 days is approved in Korea for the treatment of newly diagnosed small cell lung cancer and relapsed ovarian cancer (4–7).

The development of STEALTH liposomes was based on the discovery that incorporation of methoxypolyethylene glycol lipids into liposomes yields preparations with prolonged plasma exposure and superior tumor delivery compared with conventional liposomes composed of natural phospholipids and nonliposomal agents (1, 8, 9). STEALTH liposomal doxorubicin (Doxil) is approved for the treatment of refractory ovarian cancer, Kaposi sarcoma, and multiple myeloma (10, 11). Encapsulation of the CKD602 in the acidic core of a STEALTH liposome should also protect the active lactone form of the drug from being converted to the inactive hydroxy acid form in the blood and allow for release of the active lactone form into the tumor over a protracted period of time, which is ideal for a cell cycle–specific drug (1–3, 12–14). The clearance of nonpegylated and pegylated liposomes is via the reticuloendothelial system (1, 8, 9, 15, 16). Once the drug is released from the liposome, the pharmacokinetic disposition will be the same as after administration of the nonliposomal formulation of the drug (1, 8, 9, 15, 16).

The plasma exposure of S-CKD602 at 1 mg/kg i.v. × 1 was ~25-fold greater than nonliposomal CKD602 at 30 mg/kg

Authors' Affiliations: [1]Division of Pharmacotherapy and Experimental Therapeutics, Eshelman School of Pharmacy, University of North Carolina at Chapel Hill, [2]Molecular Therapeutics, Lineberger Comprehensive Cancer Center, Chapel Hill, North Carolina, [3]Division of Hematology/Oncology, Department of Medicine, School of Medicine, [4]Molecular Therapeutics Drug Discovery Program, University of Pittsburgh Cancer Institute, [5]Department of Obstetrics, Gynecology, and Women's Health, School of Medicine, University of Pittsburgh, [6]Gynecologic Oncology Research and Outreach Program, Magee Women's Hospital, and [7]Department of Mathematics, Carlow University, Pittsburgh, Pennsylvania

Received 5/29/08; revised 8/26/08; accepted 8/26/08; published OnlineFirst 02/03/2009.

Grant support: ALZA Corp., Mountain View, CA, and NIH/NCCR/GCRC #5M01 RR 00056.

The costs of publication of this article were defrayed in part by the payment of page charges. This article must therefore be hereby marked *advertisement* in accordance with 18 U.S.C. Section 1734 solely to indicate this fact.

Presented in part at the 42nd, 43rd, and 44th Annual Meetings of the American College of Clinical Oncology in 2006, 2006, and 2007, respectively.

Requests for reprints: William C. Zamboni, Division of Pharmacotherapy and Experimental Therapeutics, Eshelman School of Pharmacy, University of North Carolina at Chapel Hill, 3308 Kerr Hall, CB 7360, Chapel Hill, NC 27599-7360. Phone: 919-843-6665, Fax: 919-962-0644; E-mail: zamboni@email.unc.edu.

doi:10.1158/1078-0432.CCR-08-1405

Translational Relevance

This study of S-CKD602 is the first phase I study of a pegylated liposomal formulation of a camptothecin analogue and the first pharmacokinetic study evaluating the disposition of the liposomal encapsulated and released drug for a carrier formulation of a camptothecin analogue. Evaluation of the pharmacokinetic disposition of the liposomal encapsulated versus released drug is of the utmost importance because the liposomal encapsulated drug is an inactive prodrug. S-CKD602 showed manageable toxicity and promising antitumor activity, especially in platinum-refractory ovarian cancer. The prolonged plasma exposure of encapsulated and released CKD602 over 1 to 2 weeks is consistent with STEALTH liposomes and provides extended exposure compared with nonliposomal CKD602. S-CKD602 also has pharmacologic advantages over other liposomal camptothecin agents. There is significant interpatient variability in the pharmacokinetic disposition of S-CKD602 and pharmacokinetic disposition of S-CKD is associated with saturable clearance. These pharmacokinetic characteristics may also be associated with all liposomal and nanoparticle carrier agents. The results of our current phase I study of S-CKD602 can be extrapolated to future clinical trials of S-CKD602 and other nanosomal and nanoparticle anticancer agents and can be used to determine if the carrier-mediated anticancer agents provide pharmacologic advantages.

i.v. × 1 in mice (3, 6, 15). In plasma, ~82% of CKD602 was encapsulated inside of the liposome after administration of S-CKD602 (3). In mice bearing human tumor xenografts, the duration of exposure of CKD602 in tumors was 3-fold longer for S-CKD602 compared with nonliposomal CKD602 (3). In addition, the antitumor response and therapeutic index were greater for S-CKD602 compared with nonliposomal CKD602 (3, 6). These results are consistent with reports that the antitumor response to camptothecin analogues is related to the duration of time the drug concentration in tumor is above a critical threshold (3, 6, 12–14, 17).

Therefore, we conducted the first human phase I and pharmacokinetic study of S-CKD602. The objectives in this study were to determine the maximum tolerated dose (MTD) of S-CKD602, determine the toxicity profile of S-CKD602, and evaluate the pharmacokinetics disposition of encapsulated, released, and sum total (encapsulated + released) CKD602.

Patients and Methods

Patients. Patients ≥18 years of age, with a histologically or cytologically confirmed malignancy for which no effective therapy was available, were eligible for this study. Pertinent eligibility criteria included an Eastern Cooperative Oncology Group performance status of 0 to 2, adequate bone marrow, hepatic, and renal function as evidenced by the following: absolute neutrophil count (ANC) ≥1,500/μL, platelets ≥100,000/μL, total bilirubin ≤1.5 times the upper limit of the institutional reference range, aspartate aminotransferase ≤1.5 times the upper limit of the institutional reference range if liver metastases were not present and ≤4 times the upper limit of the institutional reference range if liver metastases were present, and absence of microscopic hematuria (18). Prior treatment with camptothecin analogues other than S-CKD602 or nonliposomal CKD602 was permitted. Written informed consent, approved by the Institutional Review board of the University of Pittsburgh Medical Center, was obtained from all patients prior to study entry.

Table 1. Patient characteristics

Characteristics	
Male/female enrolled (*n*)	21/24
Male/female evaluable (*n*)	21/24
Age (y)	
Median	62
Mean	60.6
Range	33–79
Eastern Cooperative Oncology Group performance status (*n*)	
0	16
1	27
2	2
Tumor type	
Colorectal adenocarcinoma	17
Ovarian cancer	5
Sarcoma	5
Non–small cell lung cancer	4
Pancreatic adenocarcinoma	3
Hepatocellular carcinoma	2
Prostate carcinoma	2
Esophageal, metastatic breast, mesothelioma, renal cell carcinoma, thyroid, appendix, unknown primary	1 patient for each tumor type
Prior treatments	
Median	3
Range	1–9

Dosage and administration. S-CKD602 is a formulation of CKD602 encapsulated in long-circulating STEALTH liposomes. In S-CKD602, the STEALTH liposome bilayer is composed of *N*-(carbonyl-methoxypolyethylene glycol 2000)-1,2-distearoyl-*sn*-glycero-phosphoethanolamine and 1,2-distearoyl-*sn*-glycero-phosphocholine in a molar ratio of approximately 5:95. The mean particle diameter is ~100 nm, and CKD602 encapsulation inside the liposomes exceeds 85%. S-CKD602 was supplied by ALZA Corporation in sterile 10 mL single-use amber

Table 2. Common drug-related adverse events by maximal severity for all cycles

Adverse events*	Grade 1	Grade 2	Grade 3	Grade 4
Anemia	3	6	4	0
Neutropenia	3	2	5	3
Thrombocytopenia	4	1	3	1
Diarrhea	12	0	0	0
Nausea	20	4	1	0
Vomiting	6	2	1	0
Anorexia	5	3	0	0
Fatigue	12	8	3	0
Pyrexia	3	2	0	0

*Patients were counted once per cycle for the most severe of multiple drug-related occurrences of a specific MedDRA preferred term.

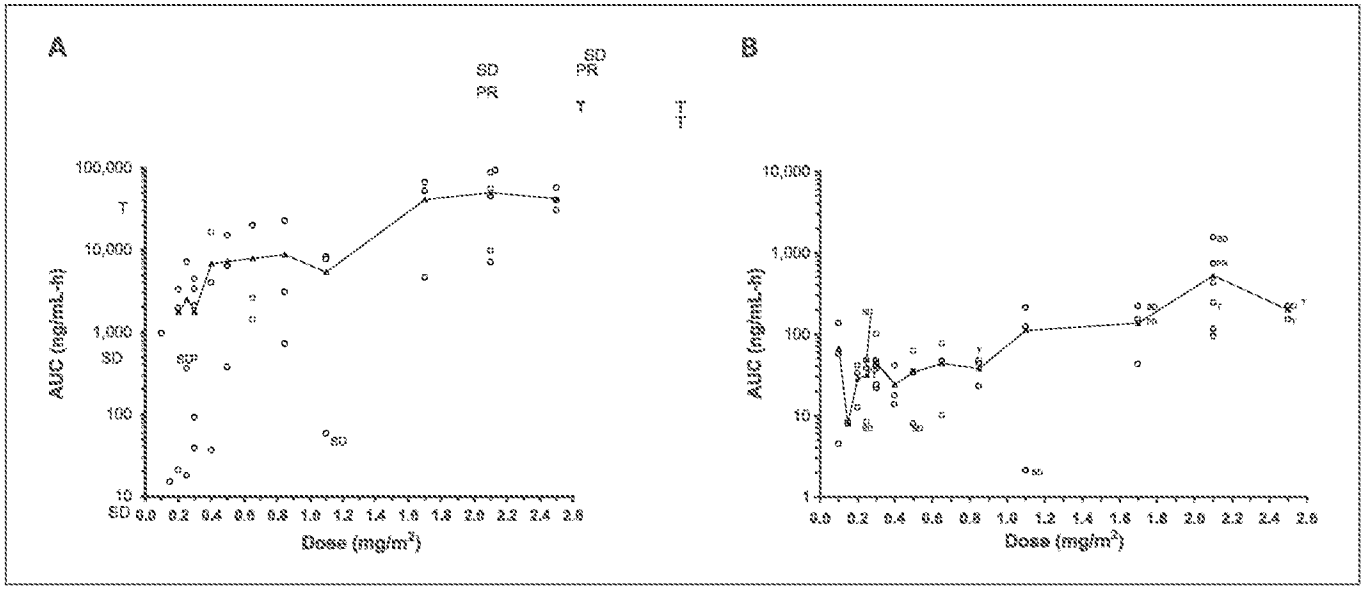

Fig. 1. Relationship between dose of S-CKD602 and encapsulated CKD602 $AUC_{0-\infty}$. *A* and *B*, the encapsulated AUC on a log and linear scale, respectively. S-CKD602 was administered at 0.10, 0.15, 0.20, 0.25, 0.30, 0.40, 0.50, 0.65, 0.85, 1.10, 1.70, 2.10, and 2.50 mg/m^2. Patients with DLT (*T*), partial response (*PR*), and stable disease (*SD*). Two patients in each dose level treated at 0.10, 0.15, and 0.65 mg/m^2 had one to two detectable concentrations of encapsulated CKD602, and thus, an accurate encapsulated CKD602 AUC could not be calculated for these patients. The patients treated at 2.5 mg/m^2 had limited pharmacokinetic sampling due to toxicity and logistical issues. The patients treated at 2.5 mg/m^2 with the highest, medium, and lowest AUCs were calculated from 0 to 96, 0 to 48, and 0 to 96 h, respectively.

vials as a clear to slightly opalescent suspension with a nominal total CKD602 concentration of 0.1 mg/mL. S-CKD602 was diluted 3-fold in 5% dextrose prior to administration. No premedications were administered prior to S-CKD602.

S-CKD602 was administered i.v. over ~1 h every 3 weeks. Doses administered, expressed in milligrams of CKD602 per square meter, were 0.10, 0.15, 0.20, 0.25, 0.30, 0.35, 0.40, 0.45, 0.50, 0.65, 0.85, 1.1, 1.7, 2.1, and 2.5 mg/m^2. This phase I study followed a standard dose escalation design with patients initially enrolled in cohorts of three, with the possibility of extending the cohort to up to six patients depending on the number of dose-limiting toxicities (DLT; ref. 18). No intrapatient dose escalation was permitted. The MTD was defined as the dose below the dose at which two out of up to six patients experienced a DLT. At the 2.5 mg/m^2 dose level, two out of three patients experienced a DLT. Because the next lower dose (1.7 mg/m^2) dose level was associated with minimal toxicity, an additional intermediate dose level of 2.1 mg/m^2 was investigated.

Patient assessment. Radiological response was measured by the Response Evaluation Criteria in Solid Tumors every two cycles (19). Toxicity was assessed according to the National Cancer Institute Common Terminology Criteria for Adverse Events version 3.0[8] and by relationship to study drug. DLTs were assessed during cycle 1. Hematologic DLTs were defined as a platelet count of ≤25,000/mm^3, ANC <500/mm^3 for >7 days, fever (≥38.5°C) accompanied by ANC <1,000/mm^3, and any other grade 3 or 4 hematologic event as listed in the Common Terminology Criteria for Adverse Events version 3.0. Other DLTs included any nonhematologic grade 3 or 4 event that increased by ≥2 grades from baseline, with the exception of nausea, vomiting, alopecia, weight change, fatigue, and infusion reactions. Complete blood counts were obtained weekly and as medically indicated. The nadir and percentage decrease at nadir for the ANC, platelets, RBC, and monocytes were estimated using standard methods (18, 20, 21).

[8] National Cancer Institute Common Terminology Criteria for Adverse Events v3.0 Instructions and Guidelines (updated August 9, 2006) Available from http://www.ida.gov/cder/cancer/toxicityframe.htm.

Sample collection, processing, analytical studies, and pharmacokinetic analysis. Plasma samples for pharmacokinetic assessment were obtained from all patients. On cycle 1, blood (7 mL) was collected in EDTA (purple top) tubes prior to administration, at the end of the infusion (~1 h), and at 3, 5, 7, 24, 48, 72, 96, 168 (day 8), and 336 h (day 15) after the start of the infusion. The blood samples were centrifuged at 1,380 × *g* for 6 min. The plasma for the determination of the encapsulated and released CKD602 was processed via solid phase separation as described previously (3). Plasma for the determination of sum total (encapsulated + released) CKD602 concentrations was placed in a polypropylene screw-top tube and stored at -80°C until processed by acetonitrile extraction as described previously (3). The encapsulated, released, and sum total CKD602 concentrations were measured by a specific liquid chromatography-tandem mass spectrometry assay as previously described (3). The total (lactone + hydroxy acid) form of CKD602 was measured for encapsulated, released, and sum total samples. The lower limit of quantitation (LLQ) of the total form encapsulated, released, and sum total CKD602 were 2, 0.05, and 1 ng/mL, respectively.

The area under the encapsulated, released, and sum total CKD602 plasma concentration versus time curve of the total form of CKD602 from 0 to last measurable sample (AUC_{0-t}) and 0 to infinity ($AUC_{0-\infty}$) were calculated using the log trapezoidal method (22). The ratio of released CKD602 AUC to encapsulated CKD602 AUC for each patient was calculated.

At doses of 1.7, 2.1, and 2.5 mg/m^2, plasma samples for sum total CKD602 were also processed to measure the lactone and carboxylate forms of CKD602 as previously described (12–14, 17). The lactone and carboxylate concentrations of sum total CKD602 were measured via liquid chromatography-tandem mass spectrometry assay and the LLQ was 1 ng/mL for both forms. The percentage of CKD602 lactone in each plasma sample was calculated as: (lactone concentration / lactone concentration + carboxylate concentration) × 100.

Statistical analysis. Comparisons between the nadir and the percentage of decrease at nadir for ANC, platelets, RBC, and monocytes on cycles 1, 2, 4, and 8 were done using ANOVA and multiple comparison *t* test (22). The statistical analysis was done using SAS software.

Results

Patient characteristics. Patient characteristics are summarized in Table 1. Forty-five patients were enrolled on this study from September 29, 2003 to October 17, 2005 at the University of Pittsburgh Cancer Institute. All patients received at least one dose of drug and were evaluable for toxicity. A total of 147 cycles were administered. The mean (range) number of cycles administered was 3.3 (1-12).

Toxicity. Drug-related toxicities are described in Table 2. Hematologic toxicity was the most common adverse event [grades 3 or 4 neutropenia occurred in eight patients (18%), grade 3 anemia occurred in four patients (9%), and grades 3 or 4 thrombocytopenia occurred in four patients each (9%)]. DLT occurred at a dose of 0.3 mg/m^2 (mucositis in one of six patients), 2.1 mg/m^2 (anemia and febrile neutropenia in one of six patients), and 2.5 mg/m^2 (neutropenia, anemia, and thrombocytopenia in two of three patients). The MTD was defined as 2.1 mg/m^2 due to two of three patients experiencing DLT at the dose of 2.5 mg/m^2. The relationship between encapsulated and released CKD602 AUC and DLT is depicted in Figs. 1A and 2A, respectively.

The cumulative toxicity of S-CKD602 as related to ANC, platelets, RBC, and monocytes was evaluated. The nadir and percentage of decrease at nadir for ANC, platelets, RBC, and monocytes are presented in Table 3. The nadir and percentage of decrease at nadir for ANC, platelets, RBC, and monocytes were similar on cycles 1, 2, 4, and 8 ($P > 0.05$).

Response. Partial responses were documented in two (at 1.7 and 2.1 mg/m^2) of five patients with ovarian cancer. The three patients with ovarian cancer who did not respond were treated at 0.3, 2.1, and 2.5 mg/m^2. The patients with ovarian cancer treated at 2.1 and 2.5 mg/m^2 developed DLT in cycle 1 and were not evaluated for response. Six patients [sarcoma ($n = 3$), hepatocellular ($n = 1$), prostate ($n = 1$), and thyroid cancer ($n = 1$)] had stable disease that lasted for six or fewer cycles. The relationship between encapsulated and released CKD602 AUC and response is depicted in Figs. 1A and 2A, respectively.

Pharmacokinetics. Pharmacokinetic sampling was initiated in all 45 patients enrolled on the study. The relationship between S-CKD602 dose and encapsulated CKD602 AUC is presented in Fig. 1A (log scale) and Fig. 1B (linear scale). There was significant variability in the encapsulated AUC at each dose of S-CKD602 and a limited linear relationship between dose and encapsulated AUC. At the MTD of 2.1 mg/m^2, there was a 13.3-fold range in encapsulated CKD602 AUC. The encapsulated CKD602 AUCs were similar from 0.1 to 1.1 mg/m^2 and from 1.7 to 2.5 mg/m^2; however, from 1.1 to 1.7 mg/m^2 there was a 7.7-fold greater increase in the mean encapsulated AUC compared with dose.

The relationship between S-CKD602 dose and released CKD602 AUC is presented in Fig. 2A (log scale) and Fig. 2B (linear scale). There was a significant variability in the released AUC at each dose of S-CKD602 and a poor linear relationship between dose and released AUC. At the MTD of 2.1 mg/m^2, there was a 16.7-fold range in released CKD602 AUC. There is significant variability in the released AUC at each dose of S-CKD602 and a poor linear relationship between dose and released AUC. The released CKD602 AUCs were similar from 0.10 to 0.85 mg/m^2. However, the mean released CKD602 AUC increased 2.1-fold from 0.85 to 1.1 mg/m^2 and 3.8-fold from 1.7 to 2.1 mg/m^2.

The encapsulated, released, and sum total CKD602 AUCs and ratio of released AUC to encapsulated AUC at each S-CKD602 dose are presented in Table 4. The encapsulated CKD602 AUC was similar to the sum total AUC at all doses. In addition, the encapsulated AUC were significantly greater than the released AUC at all doses >0.50 mg/m^2. The ratio of released CKD602 AUC to encapsulated CKD602 AUC decreased as the dose of S-CKD602 was increased. The mean ratio of released CKD602 AUC to encapsulated CKD602 AUC at S-CKD602 doses of 0.10 to 0.40 mg/m^2, 0.50 to 1.10 mg/m^2, and from 1.70 to 2.5 mg/m^2 ranged from 0.14 to 0.71, 0.01 to 0.03, and 0.005

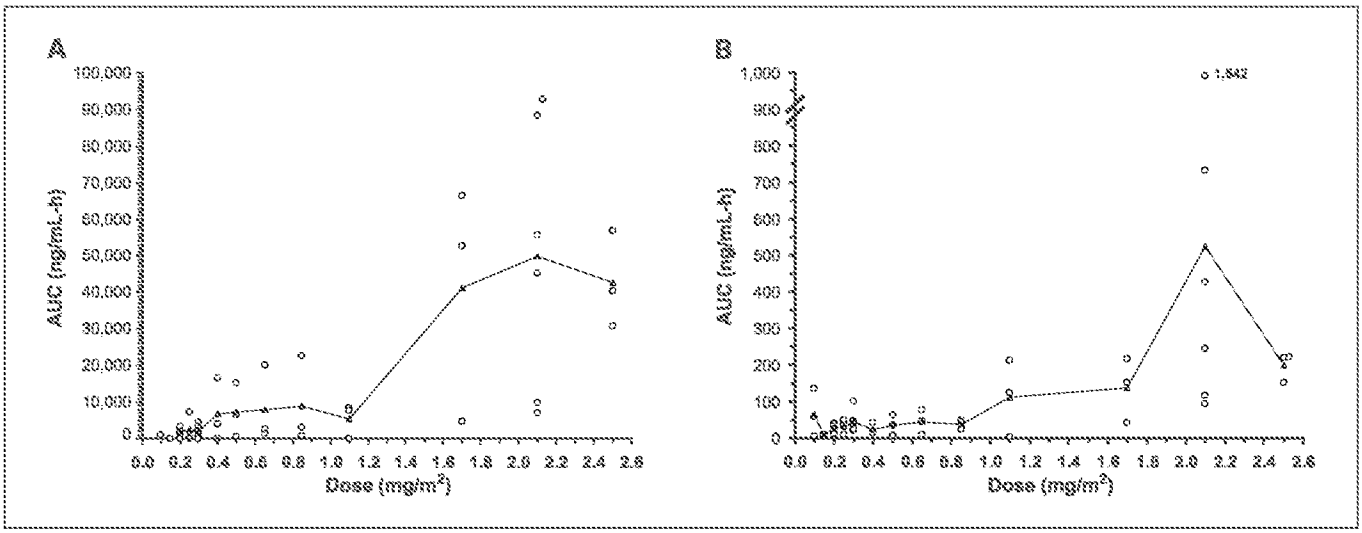

Fig. 2. Relationship between dose of S-CKD602 and released CKD602 $AUC_{0-\infty}$. *A* and *B*, the released AUC on a log and linear scale, respectively. S-CKD602 was administered at 0.10, 0.15, 0.20, 0.25, 0.30, 0.40, 0.50, 0.65, 0.85, 1.10, 1.70, 2.10, and 2.50 mg/m^2. Patients with DLT (*T*), partial response (*PR*), and stable disease (*SD*). The patients treated at 2.5 mg/m^2 had limited pharmacokinetic sampling due to toxicity and logistical issues. The patients treated at 2.5 mg/m^2 with the highest, medium, and lowest AUCs were calculated from 0 to 96, 0 to 48, and 0 to 96 h, respectively.

Table 3. The nadir and percentage decrease at nadir in ANC, platelets, RBC, and monocytes on cycles 1, 2, 4, and 8

	Cycle 1		Cycle 2	
	Percentage of decrease, mean ± SD (range) [n = 45]	Nadir (cells × $10^3/\mu L$) mean ± SD (range) [n = 45]	Percentage of decrease, mean ± SD (range) [n = 36]	Nadir (cells × $10^3/\mu L$) mean ± SD (range) [n = 36]
ANC	33.7 ± 28.4 (0.0-91.2)	3.0 ± 2.2 (0.0-8.7)	24.0 ± 25.3 (0.0-80.0)	2.6 ± 2.4 (0.0-8.0)
Platelets	22.4 ± 25.4 (0.0-93.9)	220.6 ± 119.8 (16.0-570.0)	25.8 ± 27.1 (0.0-90.9)	212.8 ± 97.4 (16.5-427.0)
RBC	11.0 ± 8.5 (0.0-33.0)	3.6 ± 0.57 (2.3-4.6)	8.1 ± 5.7 (0.0-22.9)	3.7 ± 0.47 (2.8-4.7)
Monocytes	43.6 ± 34.6 (0.0-97.4)	0.33 ± 0.28 (0.0-0.88)	40.4 ± 34.0 (0.0-96.7)	0.31 ± 0.26 (0.0-0.94)

to 0.011, respectively. The mean ± SD percentage lactone of sum total CKD602 in each plasma sample at doses of 1.7, 2.1, and 2.5 mg/m^2 were 97.4 ± 1.7%, 97.9 ± 1.4%, and 98.6 ± 0.7%, respectively.

Discussion

Major advances in the use of liposomes, conjugates, and nanoparticles as vehicles to deliver drugs have occurred in the past 10 years (1, 8, 9). STEALTH liposomal doxorubicin (Doxil) and albumin-stabilized nanoparticle formulation of paclitaxel (Abraxane) are now Food and Drug Administration–approved (10, 11, 24). In addition, there are more than 100 liposomal and nanoparticle formulations of anticancer agents currently in development (1). This is the first phase I and pharmacokinetic study of a pegylated liposomal formulation of a camptothecin analogue and also the first to evaluate the pharmacokinetic disposition of the encapsulated and released drug after administration of a liposomal or nanoparticle carrier formulation of a camptothecin analogue (25, 26, 27). Evaluation of the pharmacokinetic disposition of the liposomal encapsulated versus released drug is of the utmost importance because the liposomal encapsulated drug is an inactive prodrug, and thus, only the released drug is active (1, 3).

The prolonged plasma exposure of encapsulated and released CKD602 over 1 to 2 weeks for S-CKD602 is consistent with STEALTH liposomes and provides extended exposure compared with nonliposomal CKD602 and other liposomal formulations of camptothecins (1–3, 25, 27).

S-CKD602 was well tolerated, and the overall incidence of grade 3 or 4 toxicity compared favorably with other camptothecins (7, 12, 20, 21, 23, 25–27). In contrast to irinotecan, patients treated with S-CKD602 did not have grades 3 or 4 diarrhea (12, 20, 28). The incidence of grades 3 or 4 neutropenia and neutropenic fever after administration of S-CKD602 compares favorably to topotecan (12, 20, 29). In addition, the hematologic toxicity associated with S-CKD602 was noncumulative (12, 20, 29).

S-CKD602 exhibited promising antitumor activity with partial responses in two patients with platinum-refractory ovarian cancer and stable disease in six other patients with refractory solid tumors. The two patients with platinum-refractory ovarian cancer were treated at 1.7 and 2.1 mg/m^2. Both patients were heavily pretreated and had previously received STEALTH liposomal doxorubicin (Doxil) and the patient treated at 1.7 mg/m^2 had previously received topotecan. The patient treated at 1.7 mg/m^2 had a partial response confirmed after cycle 4 and was removed from the study after cycle 12 due to increasing CA-125 levels. This patient also received topotecan in addition to other agents. The patient treated at 2.1 mg/m^2 had a partial response confirmed after cycle 6 and was removed from the study after cycle 11 due to increasing CA-125 levels. Thus, studies of S-CKD602 in the treatment of patients with ovarian cancer that is platinum-refractory or sensitive ovarian cancer and in patients with ovarian cancer who have failed Doxil and topotecan are warranted (28, 30). There was no direct relationship between antitumor response and the exposure of encapsulated or released CKD602. However, the two patients with partial responses had encapsulated and released CKD602 AUCs that were greater than the mean AUC for that dose (Figs. 1A and 2A). Moreover, four of the five evaluable patients with encapsulated CKD602 with an AUC of >30,000 ng/mL/h had a partial response (n = 2) or stable disease (n = 2).

The pharmacokinetic disposition of S-CKD602 is consistent with the STEALTH concept (1, 8, 9, 15, 16). After a single dose of S-CKD602 at the MTD of 2.1 mg/m^2, the plasma exposure of sum total CKD602 was 68-fold higher compared with five daily doses of nonliposomal CKD602 at the MTD of 0.5 mg/m^2/d (5, 7). Patients treated at doses of S-CKD602 ≥1.7 mg/m^2 had quantifiable plasma concentrations of encapsulated and released CKD602 from 1 to 2 weeks after administration of a single dose of S-CKD602. The encapsulated CKD602 AUC was similar to the sum total AUC at all doses. In addition, the encapsulated AUC were significantly greater than the released AUC at all doses >0.50 mg/m^2. At a dose of <0.50 mg/m^2, the interpretation of encapsulated and released CKD602 is complicated by the lower LLQ for released CKD602 (0.05 ng/mL) compared with encapsulated CKD602 (2 ng/mL) and that most concentrations of encapsulated and released drug were near or below the LLQ. At the MTD of 2.1 mg/m^2, the mean ± SD ratio of released CKD602 AUC to encapsulated CKD602 AUC was 0.011 ± 0.004. This data suggests that most of the CKD602 remains encapsulated in the plasma after administration of S-CKD602. These results are also consistent with our previous studies of S-CKD602 in mice (3). Encapsulation of the CKD602 in the acidic core of the STEALTH liposome also maintained CKD602 in the active-lactone form with the mean percentage lactone of >97%.

There was significant interpatient variability in the pharmacokinetic disposition of encapsulated and released CKD602 after administration of S-CKD602 (1, 2). There was also a poor relationship between the dose of S-CKD602 and the AUC of encapsulated and released CKD602. At low doses of S-CKD602, the variability of encapsulated CKD602 was greater than at higher doses. At the MTD of 2.1 mg/m^2, there was a 13-fold

Table 3. The nadir and percentage decrease at nadir in ANC, platelets, RBC, and monocytes on cycles 1, 2, 4, and 8 (Cont'd)

Cycle 4		Cycle 8	
Percentage of decrease, mean ± SD (range) [*n* = 12]	Nadir (cells × $10^3/\mu L$) mean ± SD (range) [*n* = 12]	Percentage of decrease, mean ± SD (range) [*n* = 5]	Nadir (cells × $10^3/\mu L$) mean ± SD (range) [*n* = 5]
22.3 ± 32.8 (0.0-100.0)	2.2 ± 2.1 (0.0-6.1)	36.6 ± 42.3 (13.3-99.9)	2.7 ± 1.6 (1.4-5.2)
20.6 ± 25.4 (0.0-83.3)	256.0 ± 86.8 (84.0-386.0)	36.7 ± 23.8 (17.9-76.5)	262.4 ± 79.7 (142.0-355.0)
5.9 ± 5.2 (0.0-16.7)	3.5 ± 0.68 (2.2-4.4)	6.4 ± 4.1 (2.9-11.8)	3.5 ± 0.39 (3.1-3.9)
39.8 ± 30.6 (0.0-89.4)	0.37 ± 0.29 (0.0-0.93)	67.3 ± 33.2 (18.2-90.8)	0.28 ± 0.37 (0.06-0.84)

range in encapsulated CKD602 AUC. There is greater pharmacokinetic variability in encapsulated CKD602 compared with released CKD602. This data suggests that the clearance of the STEALTH liposomal carrier is more variable than the released drug and ultimately determines the overall exposure of drug in each patient (5, 25–27). The high interpatient variability in the pharmacokinetic disposition of S-CKD602 is consistent with other liposomal anticancer agents (5, 25–27). Our data also

Table 4. The total form of encapsulated, released, and sum total CKD602 AUC after administration of S-CKD602 at each dose

Dose (mg/m^2)	Patients	Sum total $AUC_{0-\infty}$ (ng/mL·h)*†	Encapsulated $AUC_{0-\infty}$ (ng/mL·h)†	Released $AUC_{0-\infty}$ (ng/mL·h)†	Ratio of released AUC to encapsulated AUC‡
0.10§	3	180 ± 235 (29 - 451)	962‖	66 ± 66 (4 - 135)	0.141
0.15§	3	49 ± 18 (36 - 70)	15‖	8¶8	0.533
0.20§	3	1,381 ± 1,203 (80 - 2,455)	3,306** 1,972	28 ± 14 (12 - 40)	0.010 0.021
0.25§	3	2,109 ± 3,203 (142 - 5,806)	2,516 ± 4,035 (17 - 7,171)	31 ± 20 (8 - 47)	0.710 ± 1.20 (0.007 - 2.10)
0.30§	6	1,657 ± 1,546 (128 - 3,532)	1,756 ± 1,869 (38 - 4,479)	45 ± 28 (21 - 99)	0.160 ± 0.214 (0.009 - 0.552)
0.40§,††	3	3,592†† 119 14,720	4,007†† 36 16,527	14†† 17 41	0.003†† 0.480 0.002
0.50	3	6,609 ± 5,820 (694 - 12,330)	7,315 ± 7,419 (380 - 15,139)	34 ± 26 (8 - 61)	0.010 ± 0.009 (0.004 - 0.021)
0.65	3	8,600 ± 9,153 (1,897 - 19,030)	8,007 ± 10,408 (1,434 - 20,008)	44 ± 33 (10 - 76)	0.013 ± 0.015 (0.002 - 0.030)
0.85	3	6,700 ± 8,179 (1,053 - 16,080)	8,810 ± 12,026 (718 - 22,630)	38 ± 13 (23 - 48)	0.016 ± 0.015 (0.002 - 0.032)
1.10	3	6,192 ± 5,137 (298 - 9,727)	5,382 ± 4,621 (58 - 8,360)	112 ± 105 (2 - 213)	0.026 ± 0.010 (0.016 - 0.036)
1.70	3	39,814 ± 29,960 (5,933 - 62,810)	41,271 ± 32,462 (4,646 - 66,498)	137 ± 88 (42 - 217)	0.005 ± 0.004 (0.003 - 0.009)
2.10	6	44,639 ± 32,859 (7,358 - 85,875)	49,837 ± 36,968 (7,055 - 92,871)	525 ± 551 (93 - 1,542)	0.011 ± 0.004 (0.005 - 0.017)
2.50‡‡	3	57,126 ± 13,090 (43,300 - 69,330)	42,674 ± 13,212 (30,774 - 56,893)	197 ± 40 (151 - 222)	0.005 ± 0.002 (0.004 - 0.007)

*The sum total (encapsulated + released) CKD602 AUC was based on measured concentrations in plasma and was not calculated based on adding the encapsulated + released concentrations.

†The total (lactone + carboxylate) form of encapsulated, released, and sum total (encapsulated + released) CKD602 AUCs are presented.

‡The ratio of released CKD602 AUC to encapsulated CKD602 AUC was calculated for individual patient values and not the mean of the cohort.

§At a dose of <0.50 mg/m^2, the interpretation of encapsulated and released CKD602 is complicated by the lower LLQ for released (0.05 ng/mL) compared with encapsulated (2 ng/mL) CKD602 and that most concentrations of encapsulated and released drug were near or below the LLQ.

‖Two patients in each dose level treated at 0.10 and 0.15 mg/m^2 had one to two quantifiable concentrations of encapsulated CKD602, and thus, an accurate encapsulated CKD602 AUC could not be calculated for these patients.

¶One patient at 0.15 mg/m^2 had two quantifiable concentrations of released CKD602, and thus, an accurate encapsulated CKD602 AUC could not be calculated for this patient.

**One patient at 0.20 mg/m^2 had two quantifiable concentrations of encapsulated CKD602, and thus, an accurate encapsulated CKD602 AUC could not be calculated for this patient.

††One patient at 0.40 mg/m^2 only had pharmacokinetic samples obtained from 0 to 24 h. Thus, the sum total, encapsulated, and released CKD602 AUC for this patient is from 0 to 24 h because the percentage of the AUC from 0 to infinity that was extrapolated was >15%. The sum total, encapsulated, and released CKD602 AUCs for the other two patients are from 0 to infinity.

‡‡The patients treated at 2.5 mg/m^2 had limited pharmacokinetic sampling due to toxicity and logistical issues. The patients treated at 2.5 mg/m^2 with the highest, medium, and lowest AUCs were calculated from 0 to 96, 0 to 48, and 0 to 96 h, respectively.

suggests that S-CKD602 undergoes nonlinear or saturable clearance at higher doses (1, 3). The clinical significance of these differences and the factors associated with pharmacokinetic variability need to be evaluated for S-CKD602 and other liposomal and nanoparticle anticancer agents (1). As most of the drug remains encapsulated in the pegylated liposome in plasma, it seems that the overall pharmacokinetic variability is associated with the clearance of the liposomal carrier.

S-CKD602 exhibits all of the pharmacologic, antitumor, and cytotoxic advantages of a long-acting, liposomal anticancer agent (1–3, 12, 14, 31). Thus, based on our prior preclinical studies and the phase I study presented here, S-CKD602 warrants evaluation in phase II studies in camptothecin-sensitive tumors, especially in ovarian, gastric, and small cell lung cancer, and potentially, in resistant tumors.

Disclosure of Potential Conflicts of Interest

W.C. Zamboni, commercial research grant and honoraria, ALZA Corp.

Acknowledgments

We thank Jeremy A. Hedges for his detailed work on the submission of the manuscript, and the UPCI Hematology/Oncology Writing Group for their helpful suggestions.

References

1. Zamboni WC. Liposomal, nanoparticle, conjugated formulations of anticancer agents. Clin Cancer Res 2005;11:8230–4.
2. Zamboni WC, Friedland DM, Ramalingam S, et al. Final results of a phase I and pharmacokinetic study of STEALTH liposomal CKD-602 (S-CKD602) in patients with advanced solid tumors. Proc ASCO 2006;24:82s.
3. Zamboni WC, Strychor S, Joseph E, et al. Plasma, tumor, and tissue disposition of STEALTH liposomal CKD-602 (S-CKD602) and non-liposomal CKD-602 in mice bearing A375 human melanoma xenografts. Clin Cancer Res 2007;13:7217–23.
4. Crul M. CKD-602. Curr Opin Investig Drugs 2003;4:1455–9.
5. Lee JH, Lee JM, Lim KH, et al. Preclinical and phase I clinical studies with CKD-602, a novel camptothecin derivative. Ann N Y Acad Sci 2000;922:324–5.
6. Yu NY, Conway CA, Pena RL, Chen JY. STEALTH liposomal CKD-602, a topoisomerase I inhibitor improves the therapeutic index in human tumor xenograft models. Anticancer Res 2007;27:2541–5.
7. Lee D, Kim SW, Suh C, et al. Belotecan, new camptothecin analogue, is active in patients with small-cell lung cancer: results of a multicenter early phase II study. Ann Oncol 2008;19:123–7.
8. Papahadjopoulos D, Allen TM, Gabizon A, et al. Sterically stabilized liposomes: improvements in pharmacokinetics and antitumor therapeutic efficacy. Proc Natl Acad Sci U S A 1991;88:11460–4.
9. Maeda H, Wu J, Sawa T, Matsumura Y, Hori K. Tumor vascular permeability and the EPR effect in macromolecular therapeutics: a review. J Control Release 2000;65:271–84.
10. Markman M, Gordon AN, McGuire WP, Muggia FM. Liposomal anthracycline treatment for ovarian cancer. Semin Oncol 2004;31:91–105.
11. Krown SE, Northfelt DW, Osoba D, Stewart JS. Use of liposomal anthracyclines in Kaposi's sarcoma. Semin Oncol 2004;31:36–52.
12. Sparreboom A, Zamboni WC. Topoisomerase I inhibitors. In: Chabner BA, Longo DL, editors. Cancer chemotherapy and biotherapy: principles and practice. 4th ed. Philadelphia, PA: Lippincott Williams & Wilkins; 2006. p. 371–413.
13. Zamboni WC, Stewart CF, Thompson J, et al. The relationship between topotecan systemic exposure and tumor response in human neuroblastoma xenografts. J Natl Cancer Inst 1998;90:505–11.
14. Stewart CF, Zamboni WC, Crom WR, et al. Topoisomerase I interactive drugs in children with cancer. Invest New Drugs 1996;14:37–47.
15. Zamboni WC, Eiseman JE, Strychor S, et al. Relationship between the plasma and tumor disposition of STEALTH liposomal CKD-602 and macrophages/dendritic cells (MDC) in mice bearing human tumor xenografts. Proc Annu Meet Am Assoc Cancer Res 2006;47:1280–5449.
16. Maruca LJ, Ramanathan RK, Strychor S, et al. Age-related effects on the pharmacodynamic (PD) relationship between STEALTH liposomal CKD-602 (S-CKD602) and monocytes in patients with refractory solid tumors [abstr 2576]. Proc ASCO 2007.
17. Zamboni WC, Gajjar AJ, Houghton PJ, et al. A topotecan 4-hour intravenous infusion achieves cytotoxic exposure throughout the neuroaxis in the nonhuman primate model: implications for the treatment of children with metastatic medulloblastoma. Clin Cancer Res 1998;4:2537–44.
18. Zamboni WC, Ionda ME. New designs of clinical trials. Highlights Oncol Practice 2006;18:2–7.
19. Miller AB, Hoogstraten B, Staquet M, Winkler A. Reporting results of cancer treatment. Cancer 1981;47:207–14.
20. Rowinsky EK, Kaufmann SH, Baker SD, et al. A phase I and pharmacological study of topotecan infused over 30 minutes for five days in patients with refractory acute leukemia. Clin Cancer Res 1996;2:1921–30.
21. Jung LL, Zamboni WC. Cellular, pharmacokinetic, and pharmacodynamic aspects of response to camptothecins: can we improve it? Drug Resist Update 2001;4:273–88.
22. Rowland M, Tozer T. Clinical pharmacokinetics: concepts and applications. Philadelphia: Lea and Febiger; 1989. pp. 9–32.
23. Rosner G. Fundamentals of biostatistics. 5th ed. Pacific Grove (CA): Duxbury; 2000.
24. Gradishar WJ, Tjulandin S, Davidson N, et al. Phase III trial of nanoparticle albumin-bound paclitaxel compared with polyethylated castor oil-based paclitaxel in women with breast cancer. J Clin Oncol 2005;23:7768–71.
25. Kraut EH, Fishman MN, LoRusso PM, et al. Final results of a phase I study of liposome encapsulated SN-38 (LE-SN38): safety, pharmacogenomics, pharmacokinetics, and tumor response. Proc Am Soc Clin Oncol 2005;23:139–139s.
26. Giles FJ, Tallman MS, Garcia-Manero G, et al. Phase I and pharmacokinetic study of a low-clearance, unilamellar liposomal formulation of lurtotecan, a topoisomerase 1 inhibitor, in patients with advanced leukemia. Cancer 2004;100:1449–56.
27. Gelmon K, Hirte H, Fisher B, et al. A phase 1 study of OSI-211 given as an intravenous infusion days 1, 2, and 3 every three weeks in patients with solid cancers. Invest New Drugs 2004;22:263–75.
28. Rowinsky EK, Verweij J. Review of phase I clinical studies with topotecan. Semin Oncol 1997;24:S20.
29. Green AE, Rose PG. Pegylated liposomal doxorubicin in ovarian cancer. Int J Nanomedicine 2006;1:229–39.
30. Innocenti F, Ratain MJ. Irinotecan treatment in cancer patients with UGT1A1 polymorphisms. Oncology 2003;17:52–5.
31. Bookman MA. Developmental chemotherapy and management of recurrent ovarian cancer. J Clin Oncol 2003;21:149–67s.

Correction: Article on Pegylated Liposomal CKD-602

In the article on pegylated liposomal CKD-602 in the February 15, 2009 issue of *Clinical Cancer Research*, there was an error in Figs. 1 and 2. In Fig. 1A, the labels for partial response, stable disease, and dose-limiting toxicity were misaligned. In addition, Figs. 1B and 2A were transposed. The correct figures and legends appear here.

Zamboni WC, Ramalingam S, Friedland DM, et al. Phase I and pharmacokinetic study of pegylated liposomal CKD-602 in patients with advanced malignancies. Clin Cancer Res 2009;15:1466–72.

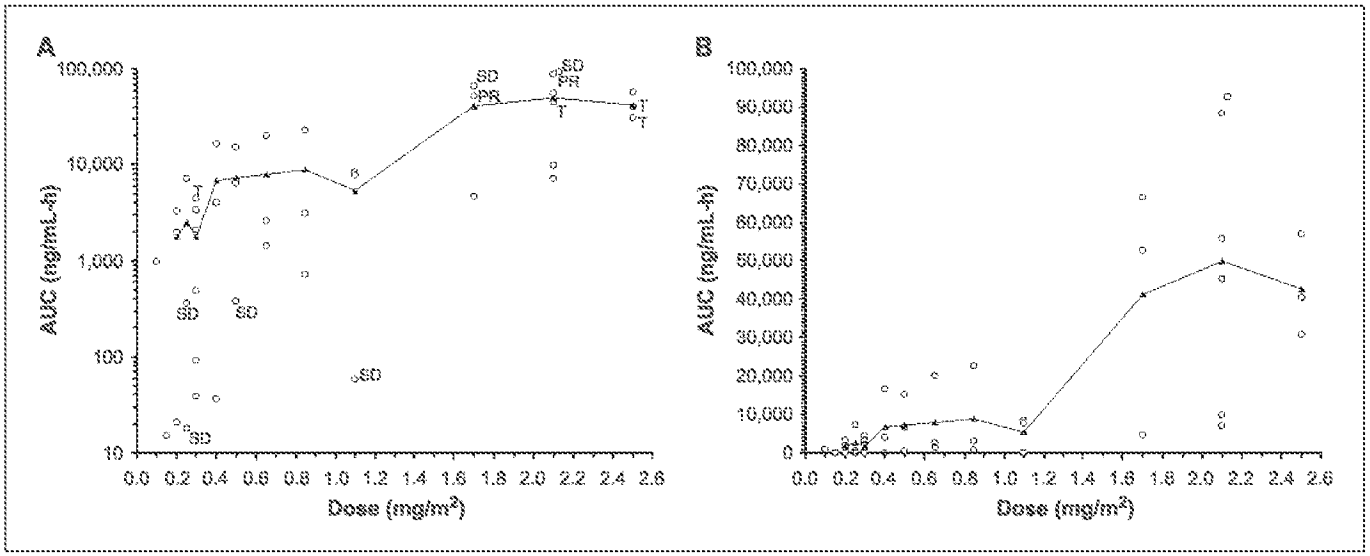

Fig. 1. Relationship between dose of S-CKD602 and encapsulated CKD602 $AUC_{0-\infty}$. *A* and *B*, the encapsulated AUC on a log and linear scale, respectively. S-CKD602 was administered at 0.10, 0.15, 0.20, 0.25, 0.30, 0.40, 0.50, 0.65, 0.85, 1.10, 1.70, 2.10, and 2.50 mg/m^2. Patients with DLT (*T*), partial response (*PR*), and stable disease (*SD*). Two patients in each dose level treated at 0.10, 0.15, and 0.85 mg/m^2 had one to two detectable concentrations of encapsulated CKD602, and thus, an accurate encapsulated CKD602 AUC could not be calculated for these patients. The patients treated at 2.5 mg/m^2 had limited pharmacokinetic sampling due to toxicity and logistical issues. The patients treated at 2.5 mg/m^2 with the highest, medium, and lowest AUCs were calculated from 0 to 96, 0 to 48, and 0 to 96 h, respectively.

doi:10.1158/1078-0432.CCR-15-8-COR

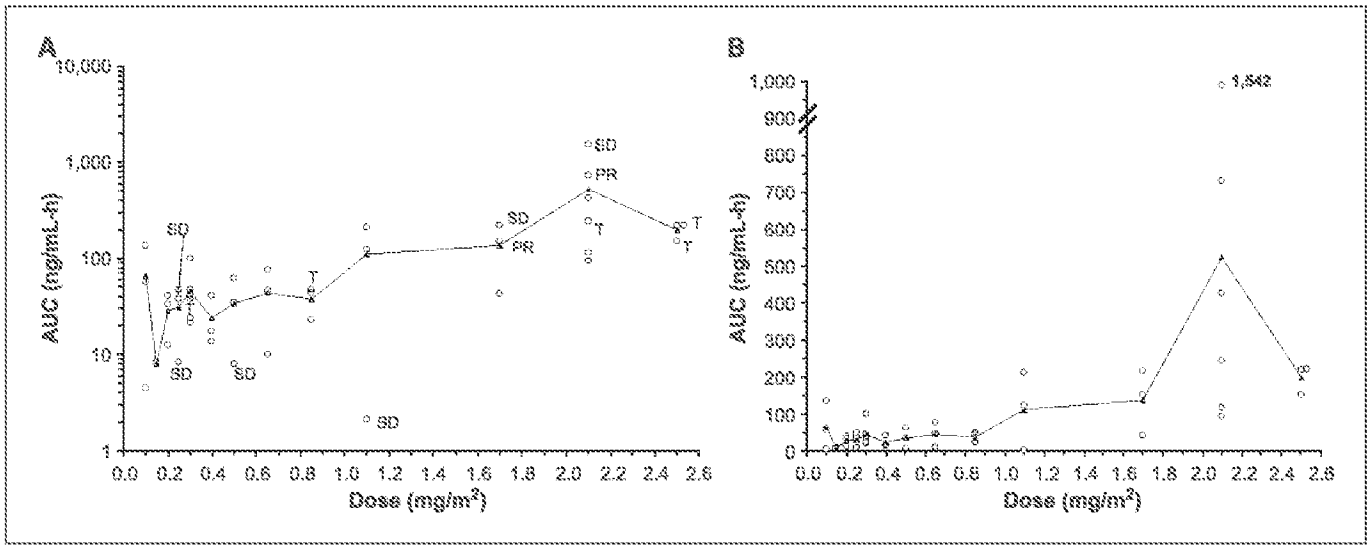

Fig. 2. Relationship between dose of S-CKD602 and released CKD602 $AUC_{0-\infty}$. *A* and *B*, the released AUC on a log and linear scale, respectively. S-CKD602 was administered at 0.10, 0.15, 0.20, 0.25, 0.30, 0.40, 0.50, 0.65, 0.85, 1.10, 1.70, 2.10, and 2.50 mg/m^2. Patients with DLT (*T*), partial response (*PR*), and stable disease (*SD*). The patients treated at 2.5 mg/m^2 had limited pharmacokinetic sampling due to toxicity and logistical issues. The patients treated at 2.5 mg/m^2 with the highest, medium, and lowest AUCs were calculated from 0 to 96, 0 to 48, and 0 to 96 h, respectively.

Clinical Cancer Research

Phase I and Pharmacokinetic Study of Pegylated Liposomal CKD-602 in Patients with Advanced Malignancies

William C. Zamboni, Suresh Ramalingam, David M. Friedland, et al.

Clin Cancer Res 2009;15:1466-1472.

mAbs 7:1, 42–52; January/February 2015; © 2015 Taylor & Francis Group, LLC

Comprehensive optimization of a single-chain variable domain antibody fragment as a targeting ligand for a cytotoxic nanoparticle

Kathy Zhang, Melissa L Geddie, Neeraj Kohli, Tad Kornaga, Dmitri B Kirpotin, Yang Jiao, Rachel Rennard, Daryl C Drummond, Ulrik B Nielsen, Lihui Xu*, and Alexey A Lugovskoy*

Merrimack Pharmaceuticals, Inc.; Cambridge, MA USA

Keywords: antibody fragment, yeast display, stability, manufacturability, nanoparticle, liposome, antibody-drug conjugate

Abbreviations: scFv, single chain variable fragment; CDR, complementarity-determining region; EphA2, ephrin type-A receptor 2; FACS, fluorescence-activated cell sorting; DSF, differential scanning fluorimetry; HTP, high throughput; CLIA, chelated ligand-induced internalization assay

Antibody-targeted nanoparticles have the potential to significantly increase the therapeutic index of cytotoxic anti-cancer therapies by directing them to tumor cells. Using antibodies or their fragments requires careful engineering because multiple parameters, including affinity, internalization rate and stability, all need to be optimized. Here, we present a case study of the iterative engineering of a single chain variable fragment (scFv) for use as a targeting arm of a liposomal cytotoxic nanoparticle. We describe the effect of the orientation of variable domains, the length and composition of the interdomain protein linker that connects VH and VL, and stabilizing mutations in both the framework and complementarity-determining regions (CDRs) on the molecular properties of the scFv. We show that variable domain orientation can alter cross-reactivity to murine antigen while maintaining affinity to the human antigen. We demonstrate that tyrosine residues in the CDRs make diverse contributions to the binding affinity and biophysical properties, and that replacement of non-essential tyrosines can improve the stability and bioactivity of the scFv. Our studies demonstrate that a comprehensive engineering strategy may be required to identify a scFv with optimal characteristics for nanoparticle targeting.

Introduction

Nanoparticle-based drugs have advanced cancer therapy by delivering highly cytotoxic payloads to cancer cells while lowering systemic drug toxicity via sustained release.[1-3] Nanoparticles serve as a carrier to concentrate the encapsulated drug into tumors, thus providing an optimal pharmacological coverage and extending the therapeutic index.[1-3] Paclitaxel and doxorubicin, 2 widely used chemotherapeutic agents, have been incorporated into nanoparticle formulations.[4-6] Albumin-conjugated paclitaxel (nab-paclitaxel; Abraxane®) has been approved by the Food and Drug Administration for the treatment of non-small-cell lung cancer,[7] as well as advanced breast cancer[8] and pancreatic cancer.[9] Pegylated liposomal doxorubicin (Doxil®) is used to treat many cancers including ovarian carcinomas,[6] AIDS-related Kaposi's sarcoma,[10] and refractory multiple myeloma.[11]

The use of antibodies to target cytotoxic drugs can further increase the deposition of the drug into tumors that overexpress aberrant receptors while limiting the exposure of non-cancer cells. This targeted delivery concept has been illustrated by the success of antibody-drug conjugates (ADCs) such as brentuximab vedotin (Adcetris®, Seattle Genetics), an anti-CD30 antibody conjugated with monomethyl auristatin,[12] and ado-trastuzumab emtansine (Kadcyla®, Roche), an anti-HER2 antibody conjugated with emtansine,[13] but has not been broadly applied to nanoparticles.

For nanoparticle targeting, scFvs can be advantageous over full-length antibodies because they have no effector function and do not alter the particle pharmacokinetics and biodistribution in Fc receptor mediated fashion.[14-16] Broad medical application of scFvs has been limited, however, due to numerous biophysical challenges,[17] including the tendency of the molecules to aggregate and their low stability, especially at high concentrations. Moreover, robust conjugation of scFvs to lipid molecules requires incubation at temperatures greater than 60°C, and so high thermal stability of scFvs is highly desirable for nanoparticle targeting. Additionally, other biophysical properties must be optimized, including colloidal, serum, lipid phase and chemical denaturation stability. Finally, in order to be commercially manufactured, expression titers must be high and the scFvs selected should preferably bind to an affinity resin such as protein A.

*Correspondence to: Lihui Xu; Email: lxu@merrimackpharma.com; Alexey A Lugovskoy; Email: alugovskoy@merrimackpharma.com
Submitted: 09/24/2014; Revised: 10/31/2014; Accepted: 11/05/2014
http://dx.doi.org/10.4161/19420862.2014.985933

To generate a ligand for nanoparticle targeting, antibodies or antibody fragments are selected for desired biological properties, including high affinity, cross-reactivity to other preclinical animal species, and internalization rates. scFvs are routinely isolated with in vitro display technologies using libraries that are derived from human repertoire (natural), computationally designed (synthetic), or are hybrid (semi-synthetic) in nature. Analysis of the amino acid distribution of antibodies from the human repertoire have revealed that tyrosine, glycine and serine are overrepresented in complementarity-determining regions (CDRs), [18] with tyrosine alone composing 10% of, and contributing up to 25% of, the antigen contact surface.[19-21] Based on this statistical consideration, designed synthetic antibody libraries composed of a single framework[19] or multiple frameworks[22] often have a high frequency of tyrosines in the CDRs. While these tyrosines can facilitate antigen recognition, we have observed that they can also increase the instability of scFvs by providing a pleiotropic interaction surface for aggregate nucleation.

Here, we present a comprehensive engineering approach to optimize an anti-EphA2 scFv as a targeting ligand for a liposomal nanoparticle. EphA2 is a tyrosine kinase receptor that is selectively expressed on the surface of many solid tumors, but its targeting has shown only limited success in the clinic thus far.[23] Because nanoparticles provide more potent and better tunable delivery of chemotoxic agents toward tumors compared to ADCs, we sought to generate an EphA2-targeted nanoparticle for use as a potential cancer therapy. We isolated an anti-EphA2 scFv, clone 116, from a synthetic scFv library using yeast surface display. The initial hit had the essential functions of a targeting ligand: it internalized into cancer cell lines expressing human EphA2, it was cross-reactive to murine EphA2, and it could be readily conjugated to the lipid anchor and inserted efficiently into the liposomes. However, this clone did not have optimal thermostability and had the propensity to aggregate, which precluded its development into a therapeutic targeting agent. To improve the biophysical properties of this scFv while maintaining the affinity and epitope specificity, we explored the effect of orientation of the variable domains, interdomain protein linker composition, stabilizing mutations, and tyrosine replacements to the biophysical characteristics of clone 116. Ultimately, multiple approaches were required to engineer this scFv into a developable lead. Our studies suggest that a comprehensive optimization strategy is required to develop a scFv with optimal characteristics for nanoparticle targeting.

Results

Anti-EphA2 scFv lead identification and characterization

Anti-EphA2 binders were isolated from a synthetic, yeast-displayed scFv library through 5 rounds of selection consisting of 2 rounds of magnetic-activated cell sorting (MACS) and 3 rounds of quantitative fluorescent-activated cell sorting (FACS). To select specific and thermostable anti-EphA2 binders, progressively more stringent selection pressure was introduced into the last 2 rounds of FACS sorting. In the fourth round, the selected library was depleted with a mixture of biotinylated non-target proteins and streptavidin beads to remove non-specific binders. In the final round, to eliminate binders with low thermostability, the library was heat-shocked at 52.5°C for 5 minutes prior to antigen binding and sorting, and the binders were then picked.

To select scFvs with high thermal stability, these binders were further characterized using a more stringent thermal challenge assay. Specifically, yeast cells expressing individual scFvs were either heat shocked at 65°C or incubated at room temperature for 5 minutes prior to staining and FACS analysis. For every clone, we then calculated the thermal binding index defined as the ratio of the antigen binding signal of the heat shocked cells, compared to the signal of control cells that were not heat-shocked. Out of the 192 scFv binders that were characterized, approximately half showed residual binding between 60% and 110% (Fig. 1A). Clones with residual binding of over 110% were deemed to be non-specific and eliminated from further analysis. DNA sequencing identified 42 unique thermostable clones, which were then characterized as soluble scFvs.

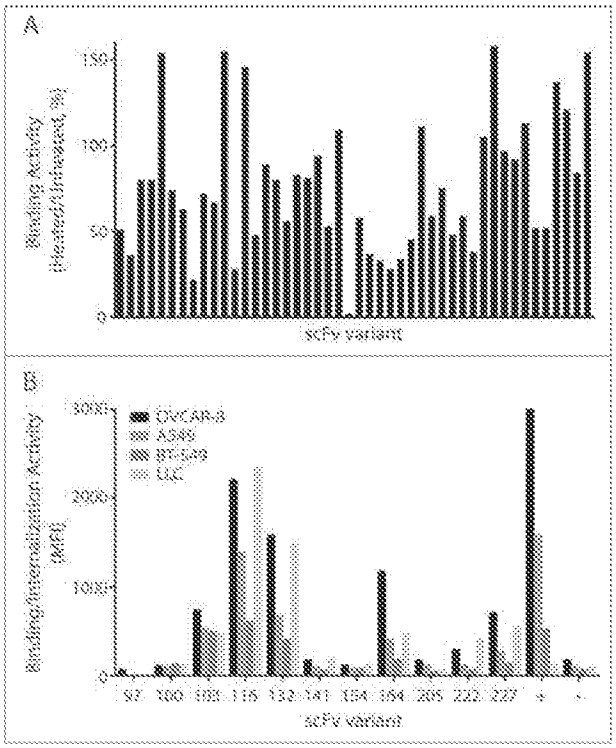

Figure 1. Measurement of thermostability and binding/internalization of anti-EphA2 scFvs. 1A. *Thermal challenge assay of scFvs on the surface of yeast.* EphA2 binders from the final round of library selection were heat shocked prior to binding of EphA2-His6, and the antigen bound cells were evaluated for expression and EphA2 binding. The Y-axis represents the residual binding of the scFvs after incubation at 65°C for 5 minutes as measured by FACS. Mean fluorescent intensity (MFI) of antigen binding was normalized to MFI of expression. 1B. *Chelated ligand-induced internalization assay (CLIA) detects the amount of scFv-conjugated liposomes on the cell surface or internalized.* Soluble scFvs were conjugated to fluorescently labeled liposomes through a Ni (II)-activated nitrotriacetic (NTA) lipid, the fluorescent signal was measured and analyzed on FACS. Two scFvs (D2A6) and liposome without scFv were used as positive and negative control, respectively.

The hexahistidine tagged scFvs were expressed in *S. cerevisiae* and purified using a nickel resin. During purification, varying degrees of visible precipitation was observed for some clones and those with severe precipitation were not characterized further. We then measured the melting temperatures of the scFvs using differential scanning fluorimetry (DSF).[24] The scFvs had melting temperatures between 52.5°C to 65.5°C (Fig. S1). All of the characterized scFvs had melting temperatures equal to or higher than the screened temperature (52.5°C) of the yeast library, suggesting that thermal challenging the scFvs on the yeast surface prior to selection is an effective triage method for more thermostable antibodies.

Selection of internalizing antibodies

For a scFv to effectively target a liposomal nanoparticle, it needs to bind with high specificity and it must be capable of directing the internalization of the liposome. To screen for binding and internalization, we performed a high-throughput internalization screening assay,[25] which measures the amount of liposomal nanoparticles both on the cell surface and within the cell. Hexahistidine-tagged scFvs were conjugated to a fluorescently labeled liposome, added to cells expressing EphA2, and allowed to internalize for 4 hours. Fluorescence was measured both before and after dissociation of the bound antibodies by imidazole, allowing for quantification of the percentage of scFvs internalized. As shown in Fig. 1B, 4 clones (103, 116, 132 and 164) demonstrated strong binding and internalization activity on cell lines expressing human or murine EphA2. Due to its superior internalization and melting temperature, clone 116 was selected as the scFv candidate best suited for further engineering for development into a therapeutic lead.

Engineering strategy for optimization of clone 116

The isolated scFv 116 (shown in Table S1) showed excellent cell binding and internalization activity in human and mouse cell lines expressing EphA2. However, its Tm of 57.5°C was lower than the desired 60°C for liposome conjugation and its partial precipitation during purification suggested that its stability was suboptimal. Before embarking on an engineering campaign, we first removed an aberrant N-linked glycosylation site on CDR-H1 by making a S30A mutation in the third position of NxS motif within CDR-H1. Homology modeling of 116 suggested that the sugar moiety was projected away from the antigen binding site, and, consistent with that model, the binding activity and cross reactivity were not affected after deglycosylation.

To improve the thermostability and solubility of 116 while maintaining its antigen binding, ability to internalize, and murine cross reactivity, a comprehensive engineering and optimization strategy was employed (Fig. 2). We designed a multitude of variants by switching variable domain orientation, optimizing the interdomain protein linkers, stabilizing the framework, CDR tyrosine "sweeping," and the introduction of negatively-charged amino acids. All reengineered scFv variants were transiently expressed in mammalian cells and characterized in biophysical and functional assays.

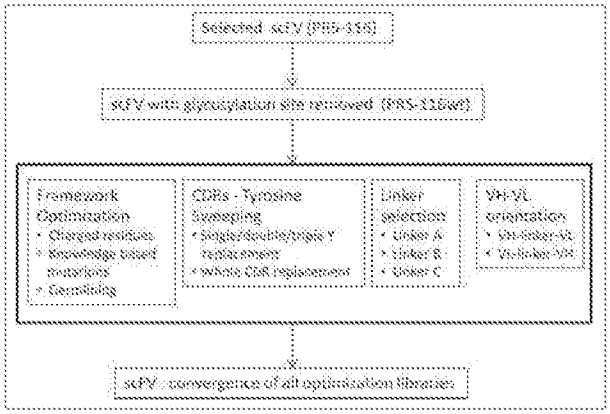

Figure 2. Optimizing anti-EphA2 scFv 116 required several engineering strategies. The N-linked glycosylation site was removed from the parental clone prior to optimization. The iterative engineering approaches include (from left to right): (1) optimizing framework, (2) minimizing tyrosine content in the CDRs, (3) changing the interdomain protein linker, and (4) altering the VH/VL orientation. The best variants resulting from each approach were combined to yield lead candidates.

Initial engineering: stabilization of framework, interdomain protein linker optimization, and domain swapping

Framework optimization

The framework of an antibody plays an important role in stability and affects the affinity by supporting the conformation of the CDRs. We hypothesized that introducing mutations into the framework may improve the biophysical properties of the scFv. The heavy chain is a member of the VH3 family (VH3-23), which is known to be stable[26] and capable of binding to protein A.[27,28] Therefore, we only made one mutation, A49S, to make it more consistent with the VH3 consensus amino acid usage. However, we did extensive engineering to the light chain (VK1-39). We first added charge (S12E, S60D, and F83E) on the surface of the scFv to promote its stability.[29,30] We also changed M4 to L and V58 to I to improve packing of the VL domain core.[31,32] Finally, we ran the protein stability prediction algorithm Eris,[33] and changed R66 to K or to A. We introduced 3 mutations (VH-A49S, VL-R66K and VL-F83E) into the 116v4 framework and 7 mutations (VH-A49S, VL-M4L, VL-S12E, VL-V58I, VL-S60D, VL-R66A and VL-F83E) in the framework of 116v5. As a control, 116v6 had no additional mutations in the framework from the original wild-type clone, but it had both a different domain orientation and interdomain protein linker. The liposome conjugated variants showed comparable binding and internalization activity on human cell lines compared to 116wt clone (Fig. 3A). Interestingly, the binding and internalization of these variants in murine cells line were significantly decreased (Fig. 3B), indicating that their cross-reactivity to murine EphA2 was affected. Unexpectedly, changing the interdomain protein linker and orientation of the variable domains appeared to improve the melting temperature from 58°C to 63°C, but the expression was decreased 10-fold (Table 1). These unanticipated observations prompted us to investigate these engineering parameters more thoroughly.

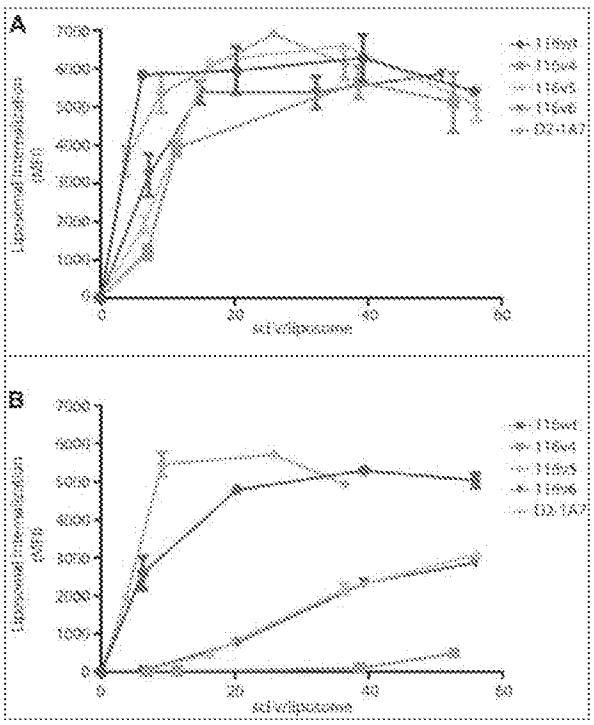

Figure 3. Variable domain or interdomain protein linker composition affect murine cross reactivity of anti-EphA2s. The chelated ligand-induced internalization assay was used to detect the amount of scFv-conjugated liposomes internalized on (**A**) human cancer cell line H-1993 and (**B**) murine cell line LLC-2. A benchmark antibody, 1A7, was used as positive control.

Domain swapping and interdomain protein linker composition variation

We then decided to test the domain orientation and interdomain protein linker composition separately in order to determine which parameter affected the stability and expression titers of the scFvs. To first test the effects of switching the orientation of the variable domains, we compared 116 in both orientations, VH-VL (116v7) and VL-VH (116v9) with the interdomain protein linker from the screened library. We found that the VL-VH orientation yielded 50 mg/L, while the VH-VL yielded 3.8 mg/L (**Table 1**). The melting temperatures were similar (65.4°C for 116v7 and 64°C for 116v9), suggesting that the altering the domain orientation of this scFv mainly affects expression.

We also tested different interdomain protein linkers that tether the variable regions together. Traditionally, these linkers compose low complexity amino acids (such as glycine and serine) to reduce potential immunogenicity.[34,35] In this study, we compared the effect of 3 interdomain protein linkers on the biophysical properties and binding affinity of 116 variants (**Table 2**). Linker A was used in our library throughout the selections. Linker B is similar in composition to linker A, with a high percentage of glycines and serines, but it contains an additional 7 amino acids. Despite this similarity, we found that variants with linker A consistently had much higher expression (**Table 1**). We also tested a less hydrophilic linker, linker C. When comparing this linker (116v18) directly with the linker used in the library (116v7), we found that using linker C increased the melting temperature 4°C, but lowered expression 30-fold (**Table 2**). These results indicate that the choice of interdomain protein linker can affect both the thermal stability and expression yield of an engineered scFv irrespective of CDR composition.

Optimization of CDRs

CDR "tyrosine sweeping"

Tyrosine residues are often highly represented in the CDRs and play a critical role in antibody-antigen interaction by forming multiple types of macromolecular interactions.[36,37] However, we have observed that abundant tyrosines in CDRs can promote instability of scFvs by providing an interaction surface for aggregates to nucleate. Sequence analysis of 116 revealed that 11 tyrosines are in the CDRs, representing 19.7% of their composition (**Fig. 4**). We then compared these tyrosines to a human consensus sequence we generated by compiling antibody repertoires from the National Center for Biotechnology Information (NCBI) protein sequence database, and noting the most common amino acid found at each position. Of these 11 tyrosines, only one, VH-Y59, is present in human consensus sequences at greater than 90% frequency, while the other 10 could have been acquired during the selection process. As shown in **Figure 4**, these non-consensus tyrosine residues were located both in the light chain CDRs (Y27A, Y28, Y30, Y31, Y53 and Y55, Y93) and in the heavy chain CDR-H2 (Y52, Y56, Y58 and Y59). We hypothesized that the high number of tyrosines in clone 116 could be contributing to its overall instability.

To investigate whether these tyrosine residues were essential to the antigen binding of clone 116, 2 dimensional "tyrosine sweeping" was carried out as shown in **Figure 5**. Each tyrosine was individually mutated to the most frequently occurring amino acid based on our human consensus sequence. We also created double mutants to explore pairwise substitution effects. Over 60 scFv variants were made and the binding activity to human EphA2 was assessed on yeast surface by FACS analysis. Mutations in 4 positions, VH-Y52, VH-Y58, VL-Y30 and VL-Y31, significantly affected antigen binding activity, showing that these tyrosines were essential for EphA2 binding. Interestingly, the VH-Y56S mutation improved the antigen binding when combined with certain light chain variants including the wild type, VL-Y27S, and VL-Y55Q (**Fig. 6**).

We next generated variants with triple and quadruple tyrosine mutations to the human consensus sequence. Variants with triple mutations lost over a 100-fold in binding activity (**Fig. 6**) and the quadruple mutations completely lost antigen binding. These results show that it is only possible to remove a single tyrosine from each variable region without loss of at least some affinity. Three variants (VL-Y27AS+VH-Y56S, VL-Y55Q+VH-Y56S and VL-Y53S+VH-Y56S) (116v15, 116v16, 116v17) that still retained wild-type binding affinity were selected for characterization as soluble proteins. After expression, all 3 clones showed no visible precipitation during protein A purification. 116v17 was found to be the superior molecule

Table 1. Sequence comparison and biophysical characterization of 116 and 116 variants

	Order	VL-CDR1	VL-CDR2	VL-CDR3	Interdomain protein linker	VH-CDR1	VH-CDR2	VH-CDR3	Expression (mg/L)	Tm (°C)
116wt	VL-VH	RASQYYSYYGVA	GASYLYS	QQSFYPIT	Linker A	GFNLAGGGVH	GIYSSSGYTYYADSVKG	SSGGFDY	15	58
116v4	VH-VL	RASQYYSYYGVA	GASYLYS	QQSFYPIT	Linker B	GFNLAGGGVH	GIYSSSGYTYYADSVKG	SSGGFDY	2	62.7
116v5	VH-VL	RASQYYSYYGVA	GASYLYS	QQSFYPIT	Linker B	GFNLAGGGVH	GIYSSSGYTYYADSVKG	SSGGFDY	2.8	57.8
116v6	VH-VL	RASQYYSYYGVA	GASYLYS	QQSFYPIT	Linker B	GFNLAGGGVH	GIYSSSGYTYYADSVKG	SSGGFDY	1.5	63.3
116v7	VL-VH	RASQYYSYYGVA	GASYLYS	QQSFYPIT	Linker A	GFNLAGGGVH	GIYSSSGYTYYADSVKG	SSGGFDY	50.0	65.4
116v8	VL-VH	RASQYYSYYGVA	GASYLYS	QQSFYPIT	Linker B	GFNLAGGGVH	GIYSSSGYTYYADSVKG	SSGGFDY	<1	N/D
116v9	VH-VL	RASQYYSYYGVA	GASYLYS	QQSFYPIT	Linker A	GFNLAGGGVH	GIYSSSGYTYYADSVKG	SSGGFDY	3.8	64
116v10	VH-VL	RASQYYSYYGVA	GASYLYS	QQSFYPIT	Linker B	GFNLAGGGVH	GIYSSSGYTYYADSVKG	SSGGFDY	2.7	64
116v11	VH-VL	RASQYYSYYGVA	GASYLYS	QQSFYPIT	Linker B	GFNLAGGGVH	GIYSSSGYTYYADSVKG	SSGGFDY	1.8	58
116v15	VL-VH	RASQSYSYYGVA	GASYLYS	QQSFYPIT	Linker A	GFNLAGGGVH	GIYSSSGSTYYADSVKG	SSGGFDY	2.0	N/D
116v16	VL-VH	RASQYYSYYGVA	GASYLQS	QQSFYPIT	Linker A	GFNLAGGGVH	GIYSSSGSTYYADSVKG	SSGGFDY	4.8	N/D
116v17	VL-VH	RASQYYSYYGVA	GASSLYS	QQSFYPIT	Linker A	GFNLAGGGVH	GIYSSSGSTYYADSVKG	SSGGFDY	7.3	68.6
116v18	VL-VH	RASQYYSYYGVA	GASYLYS	QQSFYPIT	Linker C	GFNLAGGGVH	GIYSSSGYTYYADSVKG	SSGGFDY	1.6	69.5
116v19	VL-VH	RASQYYSYYGVA	GASYLQS	QQSFYPIT	Linker C	GFNLAGGGVH	GIYSSSGSTYYADSVKG	SSGGFDY	2.4	70.5
116v20	VL-VH	RASQYYSYYGVA	GASDLQS	QQSFYPIT	Linker C	GFDLAGGGVH	GIYSSSGSTYYADSVKG	SSGGFDY	1.35	70.5
116v21	VL-VH	RASQYYSYYGVA	DASYLQS	QQSFYPIT	Linker C	GFNLAGDGVH	GIYSSSGSTYYADSVKG	SSGGFDY	2.24	70
116v22	VL-VH	RASQYYSYYGVA	GASDLYS	QQSFYPIT	Linker C	GFDLAGGGVH	GIYSSSGYTYYADSVKG	SSGGFDY	1.4	70
116v23	VL-VH	RASQYYSYYGVA	GASDLQS	QQSFYPIT	Linker A	GFDLAGGGVH	GIYSSSGSTYYADSVKG	SSGGFDY	7.2	69.5
116v24	VL-VH	RASQYYSYYGVA	DASYLQS	QQSFYPIT	Linker A	GFNLAGDGVH	GIYSSSGSTYYADSVKG	SSGGFDY	1.8	69.5
116v25	VL-VH	RASQYYSYYGVA	GASDLYS	QQSFYPIT	Linker A	GFDLAGGGVH	GIYSSSGYTYYADSVKG	SSGGFDY	10.4	65

with the highest level of expression (7.3 mg/L) and a melting temperature of 68.6°C.

Finally, we investigated the role of tyrosines in CDR1 and CDR2 on both the heavy and light chain by changing the loops to the consensus sequence and adding the tyrosines back individually. Interestingly, we found that when the CDR1 or CDR2 were replaced with consensus sequences, these variants lost their binding completely. Although VL-CDR2 had low diversity in our library and was thought not to participate in the antigen binding, it did not tolerate the replacement with a consensus sequence. This suggested that the effect of VL-CDR2 on binding was not negligible and incorporation of targeted VL-CDR2 diversity into synthetic libraries was warranted. Further tyrosine spiked-back-in into consensus VL-CDR2 did not restore the binding ability, suggesting that the effect of tyrosine residues was conformation dependent and that tyrosine-rich loops of the same length adopted different conformation than canonical ones.

Effect of negatively charged residues on the biophysical properties of scFvs

It has been previously shown that adding negative charge, especially aspartate, to the loops of antibodies can improve their biophysical behaviors.[37,38] Therefore, we created 6 scFv variants (116v20 - v25) by introducing negative charge within VH-CDR1 and VL-CDR2. To build on our earlier engineering insight, we also varied the linkers and replaced selected tyrosines with consensus amino acids. We found that the thermostability of many variants was improved by over 5 degrees (Table 1), but that the expression was variable, ranging from 1.4 mg/L to 10.4 mg/L. Our results suggest that increasing the negative charge in the CDRs generally result in an increase in thermostability, but improvements in expression need to be more empirically determined within the context of specific scFv sequences.

Table 2. Composition and comparison of the interdomain protein linkers

Clone	Linker	Amino Acid Sequence	Expression (mg/L)	Tm
116v7	A	GTTAA SGSSG GSSSG A	50	65.4
116v8	B	ASTGG GGSGG GGSGG GGSGG GG5	<1	n/d
116v18	C	RTPSH NSHQV PSAGG PTANS GTSGS	1.6	69.5

Recombination of the best variants to deliver scFvs that support robust liposome conjugation

After comparing properties of the variants generated through framework stabilization, varying the domain orientation, changing the interdomain protein linker, CDR tyrosine replacement

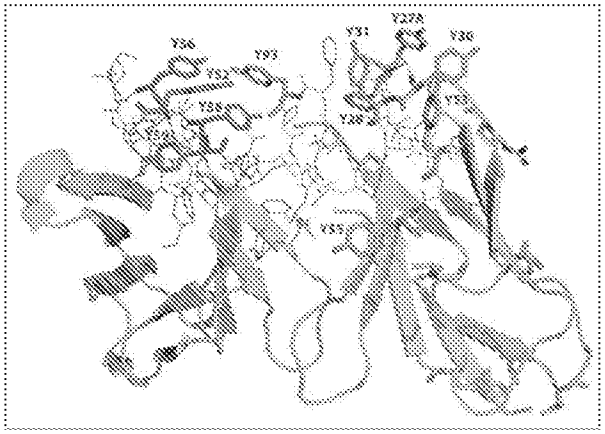

Figure 4. Homology modeling of 116 shows abundance of tyrosines in the CDRs. Tyrosine residues in VL CDRs (Y27, Y28, Y30, Y31, Y53, Y55, Y93) are shown in orange and tyrosine residues in VH CDR2 (Y52, Y56, Y58 and Y59) are purple.

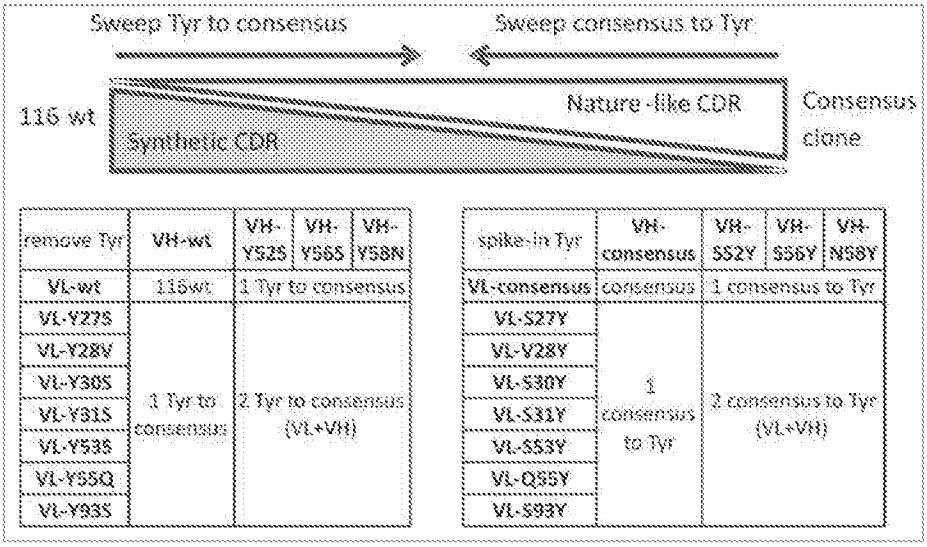

remove Tyr	VH-wt	VH-Y52S	VH-Y56S	VH-Y58N
VL-wt	116wt	1 Tyr to consensus		
VL-Y27S	1 Tyr to consensus	2 Tyr to consensus (VL+VH)		
VL-Y28V				
VL-Y30S				
VL-Y31S				
VL-Y53S				
VL-Y55Q				
VL-Y93S				

spike-in Tyr	VH-consensus	VH-S52Y	VH-S56Y	VH-N58Y
VL-consensus	consensus	1 consensus to Tyr		
VL-S27Y	1 consensus to Tyr	2 consensus to Tyr (VL+VH)		
VL-V28Y				
VL-S30Y				
VL-S31Y				
VL-S53Y				
VL-Q55Y				
VL-S93Y				

Figure 5. Two dimensional tyrosine sweeping scheme. (1) Tyrosines of 116wt are mutated to corresponding consensus residues. (2) A consensus sequence clone was created first, then tyrosine were re-inserted into the CDRs.

and introduction of negatively charged amino acids into CDRs, we identified 4 scFvs (116v7, 116v17, 116v23 and 116v25) as potential leads for nanoparticle targeting. We then performed detailed kinetic analysis of their binding activity to human, cynomolgus monkey, and murine EphA2 (Table 3). We found that all our potential lead molecules had equivalent binding to the 3 antigens to the original 116 scFv, while 116v25 showed slightly improved antigen recognition in all 3 species. Consistent with our earlier findings, these scFvs all featured the same domain orientation (VL-VH) and intervening linker (linker A). However,

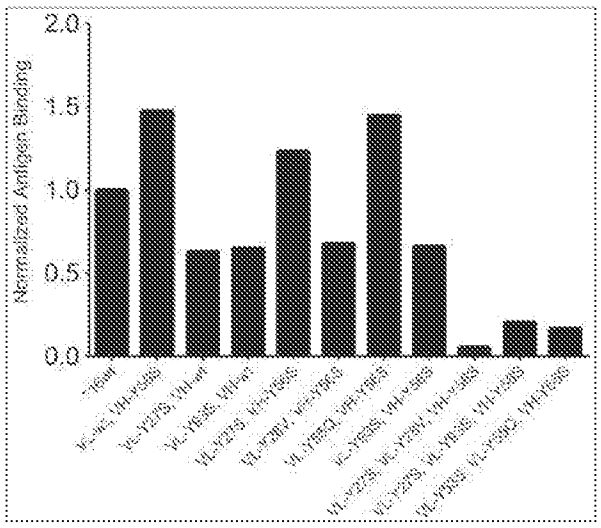

Figure 6. scFv variants with single or double tyrosine mutations to human consensus that retained binding activity to EphA2. Tyrosine sweeping-based identification of tyrosines that are essential for antigen binding. scFv variants with tyrosine to consensus mutations were expressed on yeast surface, the binding activity was measure by FACS.

they contained varying number of tyrosines in the CDRs and varying amounts of negative charge. These molecules were then scaled up to produce 10 mg of scFvs in a transient mammalian system and tested for their ability to be conjugated to liposomes, as well as for biophysical properties.

Liposome conjugation of the selected scFvs

The selected scFvs were conjugated to a liposome using maleimide chemistry and polyethylene glycol (PEG) linkers of varying lengths (2K PEG, 3.4K PEG, and 5K PEG). The reactions were monitored for precipitation, and following an overnight incubation at room temperature, the conjugated liposomes were spun down, and the percent of precipitate was calculated for each scFv and linker combination. The conjugated liposomes were then run on SDS-PAGE to analyze the efficiency of the conjugation. As shown in Figure 7a, 116v7, 116v17, 116v23 and 116v25 were all successfully conjugated using the 5K PEG and 3.4K PEG linkers. However, there was a high level of precipitation (Table S2) when using the 2K PEG linker with all 4 scFvs. When using the 3.4K PEG linker, the amount of precipitation was variable. 116v17 did not precipitate at all, while 116v23 formed 20% precipitate. 116v7 and 116v25 had almost double the amount of precipitate, around 40%.

Final selection of lead molecule

Our 4 lead scFvs, 116v7, 116v17, 116v23, and 116v25 had similar bioactivity as measured by binding and internalization on cells overexpressing EphA2. Additionally, kinetic analysis of binding to recombinant human, cynomolgus monkey, and murine EphA2 revealed their affinities were similar to the parental clone 116, ensuring we maintained both the affinity and cross reactivity of the antibodies. Therefore, we triaged our candidates based on their biophysical characteristics. Given our already significant screening of the scFvs based on purification stability, melting temperature, and expression, all of the selected clones had acceptable profiles for advancement. However, given the higher stability of 116v17 and 116v23 in the liposome conjugation studies, we decided that they were the best candidate anti-EphA2 scFvs for liposome nanoparticle targeting. Our 2 final scFvs, 116v17 and 117v23, kept the bioactivity of the original 116 clone while having much improved biophysical properties over the parental clone, including a melting temperature that was over 10 degrees higher, as well as no precipitation during the scFv purification process. One of these candidates, 116v17, did not precipitate as a liposome conjugate, thus meeting our predefined developability criteria for advancement as therapeutic lead for nanoliposomal targeting.

Table 3. Characterization of potential lead scFvs

Variants	Antigen Binding Affinity (Kd (M))			Tm°C	Expression (mg/L)	Precipitation
	Human EphA2	Cyno EphA2	Rat EphA2			
116wt	1.48E-08	2.44E-08	1.60E-08	58.0	15	Partial
116v7	1.03E-08	1.05E-08	8.54E-09	65.0	30	No
116v17	1.14E-08	1.21E-08	7.05E-09	68.6	7.3	No
116v23	1.07E-08	7.48E-09	9.16E-09	69.5	7.2	No
116v25	6.79E-09	5.14E-09	5.79E-09	65.0	10.4	No

Discussion

scFvs generally require extensive engineering to be used as components of drugs due to their low intrinsic developability.[29,39] To be useful as targeting ligands for nanoparticle delivery, scFvs need to internalize efficiently into antigen expressing cells to release the drug inside the cell, preferably cross-react to the target antigen in rodents and non-human primates to enable in vivo activity, pharmacokinetics and toxicological evaluation, and be highly thermostable to support liposome conjugation. In this study, we applied several engineering approaches to co-optimize these properties in anti-EphA2 scFvs. We introduced framework and CDR mutations, altered the interdomain protein linkers, and changed the orientation of the variable domains. Although scFvs can be found in both orientations, VH-VL is generally favored because the interdomain protein linker is further removed from CDR-H3, which is often a major contributor of antigen binding. However, in our case we found that VL-VH orientation in combination with a low complexity interdomain protein linker favors target binding, internalization capability, and expression of the scFv. Interestingly, in our study the 116v6 variant created in VH-VL orientation had poor cross-reactivity to murine EphA2 while the affinity to human EphA2 was mostly retained. This observation highlights the stress that even a long, low complexity interdomain protein linker can impose on the interface of the variable domains, possibly by introducing a paratope twist. We also observed that the best-expressing molecules featured original VL-VH orientation from the screened library. We also found, consistent with previously published results,[40] that adding negative charge in the CDRs can improve the physical stability of the molecule with one exception of 116V19. In our selected mutants, we found that the melting temperature was typically increased by 5 degrees. Although it is often stated that improving biophysical stability can lead to improved expression, we found that not to be the case for the clones we screened.

Regardless of the origin of the antibody, the abundance of tyrosine and serine residues in CDRs has been well documented. Tyrosine residues constitute 10% of the total CDR composition and up to 25% of the antigen contact surface.[41-43] The tyrosine residues on the CDRs often play critical role in antigen-antibody binding affinity and specificity.[36,42] However, due to their hydrophobic properties, there is concern about the solubility and specificity of scFvs if tyrosine residues are overly represented. This concern may be magnified when biased amino acid repertoire synthetic or semi-synthetic antibody libraries are used.

We applied "tyrosine sweeping" in this study to explore the spectrum of sequences between human consensus and 116 that featured abundant tyrosines in CDRs. We investigated the contribution of CDR tyrosine residues to the antigen binding activity of scFv through tyrosine-to-consensus mutation, or through replacing whole CDR with consensus composition followed by spiking-in tyrosines. By sequence and homology analysis, 10 tyrosines on the CDRs were identified as non-consensus residues while one was highly conserved. Out of these 10 non-canonical CDR tyrosines, only 4 were essential for the antigen binding, and 6 tyrosines were non-essential, suggesting they are "passive," antigen-independent enrichment. Interestingly, when we combined nonessential tyrosine-to-consensus mutations, the binding activity to the antigen was improved, again suggesting that non-essential tyrosines were being selected in a nonspecific fashion.

Our studies suggest that abundant tyrosines can be detrimental to scFv biophysical properties. In another antibody discovery campaign for nanoparticle conjugation, we successfully compiled the concepts of tyrosine replacement from this work into a single step approach of batch scFv optimization. Therefore, the tyrosine

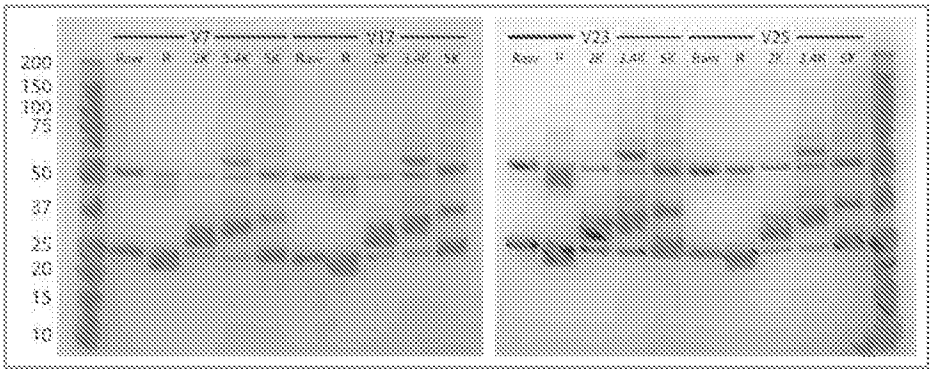

Figure 7. SDS PAGE analysis of scFv and covalently conjugated scFv-liposome (V7, V17, V23 and V25). There are 5 lanes for each variants. (1) raw, scFv; (2) R: reduced scFv; (3) 2K: scFv-Peg(2K)-DSPE conjugate; (4) 3.4K: scFv-Peg(3.4K)-DSPE conjugate; (5) 5K: scFv-Peg(5K)-DSPE conjugate.

sweeping strategy described in this report is antigen independent, and can be applied to optimization of other tyrosine-rich antibodies.

In summary, we have developed a comprehensive iterative engineering strategy to optimize scFvs for targeting of liposome nanoparticles. Our approach is distinct from the strategy used for the generation of targeting ligands for antibody-drug conjugates: it combines high-throughput liposome conjugation, internalization screening and biophysical analysis with rational molecular engineering. This engineering includes optimization of interdomain protein linker composition, variable domain orientation, framework stabilization and CDR mutagenesis toward human consensus. Using the described strategy, we successfully identified 4 developable anti-EphA2 scFv variants with the desired properties for nanoparticle targeting. Our 4 potential targeting scFvs varied in expression, melting temperature, and stability during conjugation, but were all superior to the original clone isolated from our library. Two, antibodies 116v17 and 116v23, showed improved stability during scFv purification and high melting temperature. Clone 116v17, which showed no precipitation during the liposome conjugation process, was nominated as the therapeutic lead for nanoliposomal targeting campaign. This study emphasizes the importance of high-throughput assays to test bioactivity and biophysical properties in order to screen hundreds of antibodies with small amounts of material. It also highlights a primary advantage of pursuing non-redundant focused engineering strategies in parallel, which gives us the ability to rapidly advance antibodies and their ligands from proof-of-concept molecules to viable therapeutic leads.

Materials and Methods:

Materials

Cell culture reagents

F17 media, L-glutamine, pluronic F-68, 5000X Sypro orange solution and pCEP4 vector, RPMI and 10% FBS were purchased from Invitrogen. Dextrose, galactose, raffinose, lithium acetate, salmon sperm DNA (ssDNA) and PEG3500 were obtained from Sigma. Linear Polyethylene imine (PEI, MW, 25 kDa) was acquired from Polysciences. All agar plates were from Teknova. Yeast extract, peptone, yeast nitrogen base and casamino acids were from VWR. RPMI-1640, DMEM and 1x PBS were from Lonza. PenStrep 100X, 0.25% Trypsin-EDTA, Hank's balanced Salt Solution (Ca^{2+}, Mg+) and Hank's balanced Salt Solution (Ca-, Mg-) were from Gibco. The 96-well "V" shaped assay plate was from Axygen Scientific.

Molecular biology reagents

All PCR primers were custom synthesized by IDT. iProof High-Fidelity DNA Polymerase was purchased from Bio-Rad. Zymoprep yeast plasmid miniprep kits were purchased from Zymo Research and DNA MegaPrep kits were from Qiagen. PD-10 disposable columns (Sephadex G-25) were from GE Healthcare. All solutions were prepared in 18MΩ DI water.

Cell lines and other reagents

Human cancer cell lines (H-1993, A549, OVCAR-8) and mouse Lewis lung carcinoma cell line (LL-2) were ordered from ATCC. 293F cells and fluorescent lipid DiIC18(5)-DS (DiI5), M2 anti-Flag antibody, disodium phosphate, monosodium phosphate, Alexa Fluor 647 and 488 and goat-anti-human IgG (Fc specific) were purchased from Invitrogen. EphA2-His and anti-His6 mAb were purchased from R&D Systems. EZ-Link Sulfo-NHSLC-Biotin, Fluorescence Biotin Quantitation Kit and DTT were purchased from Pierce. Streptavidin MicroBeads and LS Columns (MACS columns) were purchased from Miltenyi. TSKgel SuperSW3000 column was purchased from Tosoh Bioscience. Hydrogenated soybean phosphatidylcholine (HSPC) and methoxy-PEG(2000)-distearoyl phosphatidylethanilamine (PEG-DSPE) were from Lipoid AG (Germany). Cholesterol (plant-derived) and maleimido-PEG(2000)-DSPE were from Avanti Polar Lipids (Alabama, USA). Nuclepore PCTE membranes with 100 nm pore size were from Whatman (USA). All chemicals were of analytical or greater purity.

Selection of EphA2 binders from yeast displayed scFv library

The methods of library growth, induction and selection were performed as described previously.[44] In the first 2 rounds of selection, the library was bound to biotinylated anti-EphA2-His6, and captured by Streptavidin MicroBeads using MACS cell separation system. The subsequent 2 rounds of selection were carried out using FACS sorting on the BD Aria system.

Affinity assessment of yeast surface display scFv using FACS

The induced yeast cells were incubated with titrated amounts of EphA2-His6. Cells were washed twice with FACS buffer (1x PBS, 0.5% BSA, pH7.4) to remove unbound antigen. The antigen bound cells were then incubated with 1 μg/mL Alexa647 labeled M2 anti-FLAG antibody and 1 μg/mL Alexa 488 labeled anti-His6 antibody for 30 minutes. After 2 washes, the cells were resuspended in FACS buffer and the fluorescent signals were measured using a BD FACS Calibur. The median fluorescent intensities (MFI) were determined using FlowJo software. Antigen binding MFI (anti-His6-Alexa 488) was normalized to expression MFI (anti-Flag-Alexa 647).

Assessment of thermal stability of selected scFvs on yeast surface using "Cook and Bind" thermal challenge assay

To select for scFvs with high thermal stability, yeast cells expressing individual scFvs were either heat shocked at 65°C or incubated at room temperature for 5 minutes, chilled on ice for 5 minutes, and then incubated with 150 nM EphA2-His6 for 2 hours. These antigen bound cells were stained and analyzed by FACS as described previously.[44] The thermal binding index for each clone was calculated as the ratio of the antigen binding signal of heat shocked cells to the signal of the control cells.

Expression and purification of soluble His6-tagged scFvs in yeast

The plasmid DNA of unique binders was digested to remove both the Flag-tag and fusion gene and co-transformed with a

PCR fragment containing hexahistidine tag into yeast cells to induce ligation via homologous recombination. Transformed yeast colonies were grown in SD-CAA media, induced in YPG media for 2 days at 20°C shaker while shaking at 225 rpm, and the scFvs were purified using Protein A column.

Homology modeling of clone 116 and generation of human consensus sequence

Sequence and structural based analysis was performed as described previously.[44] First, a homology model was created using MolIDE[45] with zero-gapped templates for the variable regions. The model was energy minimized using SCWRL[46-48] and DeepView [49] and Eris.[50] All variants were inspected visually in PyMol for potential steric clashes.

Tyrosine scanning

Databases of VH and VL protein sequences derived from NCBI Entrez Protein database were used to establish the individual amino acid frequencies at each residue position of natural antibody repertoire. The consensus analysis was performed in reference to sets of VH and VL consensus sequences defined by Kabat.[59] Each tyrosine residue in the CDR L1, L2, L3 or H2 of the initial scFv was identified and replaced with the amino acid that occurs most frequently in the natural antibody repertoire. Tyrosines that were found in a position more than 90% of the time were not mutated. The VH and VL variants were synthesized by IDT. The variable domains and interdomain protein linkers were amplified individually and assembled into full-length scFv by overlap PCR. The scFv PCR fragments containing designed mutations were co-transformed with XhoI and NheI digested yeast surface display vector into yeast cells. A few colonies of each transformed variants were grown and induced as described above. The antigen binding of these yeast surface displayed scFv variants were analyzed on FACS.

Expression and production of soluble scFvs in mammalian cells

All the re-engineered variants were expressed using transient transfection in 293F cells. The genes were synthesized at DNA 2.0 and subcloned into a modified pCEP4 vector containing the sequence "GGSGGC" at C-terminus for liposome conjugation. DNA was prepared according to Qiagen MegaPrep kit manual. For transient transfections, 293F cells were grown in cell culture media containing glutamine, pluronic F-68 and F17 media at 37°C, 5% CO2 to a density of 1.5–2.0 million/mL in a baffled shake flask and then transfected with 1 mg/L of DNA. After transfected cells were grown for 6 d, the culture media containing soluble scFv were harvested by centrifuging the cells at 5000 rpm, then filtered using an Akropak filter disc and re-filtered through a 0.22 μm vacuum filter. The soluble scFv was purified through a Protein A column (MAbSelect). Sucrose was added to the dialyzed protein to a final concentration of 5% to keep the scFvs soluble and stable.[35]

Tm measurement by differential scanning fluorescence

The DSF assay was performed using IQ5 real time detection system (Bio-Rad). Briefly, for each measurement, 20 μL of the scFv solution containing 15 μM scFv protein and 1X Sypro Orange in 1X PBS was added to each well on a 96-well plate. The plate was heated from 20°C to 90°C at a rate of 1°C/min and the resulting fluorescence data collected. The data was transferred to GraphPad prism for analysis, and Tm was defined as the temperature of the maximal fluorescent value of the first derivative of the unfolding event.

High-throughput rapid scFv-assisted liposome cell uptake assay

To screen scFvs with good binding and internalization capability, a rapid high-throughput Chelated Ligand-induced Internalization Assay (CLIA)[35] was carried out as described below.

Conjugation of His6-tagged scFv onto fluorescent liposome

The scFv was conjugated to lipophilic fluorescent dye DiI18 (5)-DS containing liposomes through a Ni (II)-activated nitrotriacetic (NTA) lipid. The fluorescent liposome solution was prepared by diluting to 0.4 mM in HBSS then adding 0.1mM NiSO4 with vigorous mixing. His6-tagged scFv solution was prepared by diluting the scFv to a final concentration of 50 μg/mL in 100 μL of RPMI containing 10% FBS, Pen/Strep and glutamine on a 96-well "V" shaped plate. Using a multichannel pipette, 100 μL of the prepared fluorescent liposome solution was added to the 100 μL antibody solution per well on the plate and mixed by pipetting up and down several times.

scFv-mediated liposome internalization

Human cell lines (A-549, OVAR-8, BT-549) and murine cell line (LLC-2) were grown to 90% confluency. The culture media was removed, washed with $Ca^{2+}$and Mg^{2+} free PBS and trypsinized with 0.25% Trypsin. The suspended cell solution was plated at 100 K/well in a 96-well "V" bottom shape polypropylene plate. The cells were washed with 1X PBS to remove any traces of EDTA that may interfere with the conjugate formation. After removal of PBS, 100 μL of the fluorescent liposome/antibody mixture was added into appropriate wells on the 96-well plate. The plate was covered with sealing tape and a piece of aluminum foil and incubated for 4 hrs at 37°C with 5% CO2 on a shaker to allow the scFv-assisted liposome binding to the cell surface target and subsequent internalization. After the liposome and antibody mixture was emptied to discard the unbound scFv-liposome conjugate, the attached cells were washed either with 200 μL/well of PBS to remove any unbound liposomes or with 200 μL/well of PBS containing 0.25 M imidazole (pH7.5) to remove any unbound liposome as well as the bound but not internalized liposomes. The fluorescent signals of these cells were analyzed by FACS.

Mammalian cell uptake of covalently conjugated scFv-liposome

Covalently conjugated scFv-liposome and the mammalian cell uptake assay of these conjugates were carried out as follows:

Activation of terminal thiol of scFv proteins

Isolated scFv proteins were treated with 20 mM cysteine, 5 mM EDTA at 30°C for 1 hour to activate C-terminal cysteine thiol group. Free cysteine was removed by chromatography on PD-10 disposable columns (GE Healthcare, USA) in the conjugation buffer (5 mM citrate, 1 mM EDTA, 140 mM NaCl, pH 6.0). The reduced proteins contained 0.93 - 1.20 free thiol groups per molecule, as determined spectrophotometrically using Ellman's reagent.

Preparation and activation of liposomes

The chloroform solution containing HSPC, cholesterol, PEG-DSPE, and DiIC18(5)-DS mixed at the molar ratio of 3:2:0.24:0.009 was evaporated under reduced pressure to form a lipid film. The film was hydrated in a HEPES-buffered saline (5 mM HEPES, 144 mM NaCl, pH 6.5) at 65°C and 30 mM phospholipid, and the resulting multilamellar vesicles were repeatedly extruded under pressure through stacked 100-nm polycarbonate track-etched membranes (Nuclepore, Whatman, USA) using Lipex extruder (Northern Lipids, Canada). The liposome phospholipid concentration was determined spectrophotometrically after acid digestion using a modified molybdate method.[39] An mal-PEG-DSPE was inserted into the outer layer of the liposome membrane to provide an active group for scFv attachment by an incubation of the liposomes with mal-PEG-DSPE at 60°C for 20 min. The mal-PEG-DSPE and liposome mixture was quenched on ice and the liposomes were then purified from any traces of extraliposomal mal-PEG-DSPE by chromatography on Sepharose 4FF (GE Healthcare) in the conjugation buffer.

Covalent conjugation of scFv to liposome

The fractions containing activated liposome were collected and mixed with the activated scFv (reduced) at varying protein-phospholipid ratios to achieve at average 7.5, 15, 30, and 45 scFv per particle, as estimated using an averaged scFv molecular weight of 26 KD and 8×10^4 HSPC molecules per liposome. After overnight stirring at room temperature, the unreacted maleimide groups were blocked with 0.5 mM cysteine for 5 minutes and the scFv-liposome conjugates were purified by gel-chromatography on Sepharose 4FF, eluted in HEPES-buffered saline, pH 6.5. The amount of scFv molecules per liposome were determined by SDS-PAGE of the liposomes using Bio-Rad Mini-PROTEAN TGX gels and Coomassie G-250 staining according to the supplier's protocol, followed by the densitometry of the protein band. The sample buffer contains 4X SDS amount compared to regular 1X SDS, to achieve complete dissociation of the liposomes for release of conjugated scFvs. Free scFv proteins were run on the gel as reference standards. Control scFv-free liposomes were prepared identically, except that the protein solution was replaced by the conjugation buffer in the conjugation step.

Cell uptake of scFv-conjugated liposomes

Cultured human lung cancer cell line H-1993 and LL-2 mouse Lewis lung carcinoma cells were grown in RPMI containing 10% FBS, 2 mM glutamine and pep/strep and harvested by trypsinization. The cells were suspended in the growth medium and incubated with the liposomes (25 μM phospholipid) at 37°C for 4 hours. The cells were pelleted by centrifugation, re-suspended in PBS, and mean cell fluorescence intensity (MFI) of the DiI5 label was determined using FACScalibur (BD bioscience). The fluorescence signal is the sum of surface-bound and internalized nanoparticles. The MFI of the cells incubated with blank liposomes (no conjugated scFv) was 7.99 ± 1.21 for H-1993 cells and 11.07 ± 1.15 for LL-2 cells.

Disclosure of Potential Conflicts of Interest

No potential conflicts of interest were disclosed.

Acknowledgments

We thank Professor Sachdev S Sidhu, The University of Toronto, for his assistance of generating synthetic antibody library.

Supplemental Material

Supplemental data for this article can be accessed on the publisher's website.

References

1. Drummond DC, Meyer O, Hong K, Kirpotin DB, Papahadjopoulos D. Optimizing liposomes for delivery of chemotherapeutic agents to solid tumors. Pharmacol Rev 1999; 51:691-743; PMID:10581328
2. Drummond DC, Noble CO, Hayes ME, Park JW, Kirpotin DB. Pharmacokinetics and in vivo drug release rates in liposomal nanocarrier development. J Pharm Sci 2008; 97:4696-740; PMID:18351638
3. Allen TM, Cullis PR. Liposomal drug delivery systems: from concept to clinical applications. Adv Drug Deliv Rev 2013; 65:36-48; PMID:23036225; http://dx.doi.org/10.1016/j.addr.2012.09.037
4. Esparza JA, Malik U, Rajdev L, Sarra C, Hopkins U, Wolff AC. Phase I trial of pegylated liposomal doxorubicin and docetaxel in advanced breast cancer. J Clin Oncol 2001; 19:3117-25; PMID:11408509
5. Gaitanis A, Staal S. Liposomal doxorubicin and nab-paclitaxel: nanoparticle cancer chemotherapy in current clinical use. Methods in Mol Biol 2010; 624:385-92; PMID:20217610; http://dx.doi.org/10.1007/978-1-60761-609-2_26
6. Gordon AN, Fleagle JT, Guthrie D, Parkin DE, Gore ME, Lacave AJ. Recurrent epithelial ovarian carcinoma: a randomized phase III study of pegylated liposomal doxorubicin versus topotecan. J Clin Oncol 2001; 19:3312-22; PMID:11454878
7. Socinski MA, Bondarenko I, Karaseva NA, Ananyev M, Makhson AM, Vynnychenko I, Okamoto I, Hon JK, Hirsh V, Bhar P, et al. Weekly nab-paclitaxel in combination with carboplatin versus solvent-based paclitaxel plus carboplatin as first-line therapy in patients with advanced non-small cell lung cancer: final results of a phase III trial. J Clin Oncol 2012; 30:2055-62; PMID:22547591; http://dx.doi.org/10.1200/JCO.2011.39.5848
8. Gradishar WJ, Tjulandin S, Davidson N, Shaw H, Desai N, Bhar P, Hawkins M, O'Shaughnessy J. Phase III trial of nanoparticle albumin-bound paclitaxel compared with polyethylated castor oil-based paclitaxel in women with breast cancer. J Clin Oncol 2005; 23:7794-803; PMID:16172456; http://dx.doi.org/10.1200/JCO.2005.04.937
9. Von Hoff DD, Ervin T, Arena FP, Chiorean EG, Infante J, Moore M, Seay T, Tjulandin SA, Ma WW, Saleh MN, et al. Increased survival in pancreatic cancer with nab-paclitaxel plus gemcitabine. N Engl J Med 2013; 369:1691-703; PMID:24131140; http://dx.doi.org/10.1056/NEJMoa1304369
10. Gill PS1, Wernz J, Scadden DT, Cohen P, Mukwaya GM, von Roenn JH, Jacobs M, Kempin S, Silverberg I, Gonzales G, et al. Randomized phase III trial of liposomal daunorubicin versus doxorubicin, bleomycin, and vincristine in AIDS-related Kaposi's sarcoma. J Clin Oncol 1996; 14:2353-64; PMID:8708728
11. Orlowski RZ, Nagler A, Sonneveld P, Bladé J, Hajek R, Spencer A, Miguel JS, Robak T, Dmoszynska A,

Horvath N, et al. Phase III study of pegylated liposomal doxorubicin plus bortezomib compared with bortezomib alone in relapsed or refractory multiple myeloma: combination therapy improves time to progression. J Clin Oncol 2007; 25:3892-901; PMID:17679727; http://dx.doi.org/10.1200/JCO.2006.10.5860

12. Pro B, Advani R, Brice P, Bartlett NL, Rosenblatt JD, Illidge T, Matous J, Ramchandren R, Fanale M, Connors JM, et al. Brentuximab vedotin (SGN-35) in patients with relapsed or refractory systemic anaplastic large-cell lymphoma: results of a phase II study. J Clin Oncol 2012; 30:2190-6; PMID:22614995; http://dx.doi.org/10.1200/JCO.2011.38.0402
13. Krop IE, Kim SB, González-Martín A, LoRusso PM, Ferrero JM, Smitt M, Yu R, Leung AC, Wildiers H. Trastuzumab emtansine versus treatment of physician's choice for pretreated HER2-positive advanced breast cancer (TH3RESA): a randomised, open-label, phase 3 trial. Lancet Oncol 2014; 15:689-99; PMID:24793816; http://dx.doi.org/10.1016/S1470-2045(14)70178-0
14. Noble CO, Kirpotin DB, Hayes ME, Mamot C, Hong K, Park JW, Benz CC, Marks JD, Drummond DC. Development of ligand-targeted liposomes for cancer therapy. Expert Opin Ther Targets 2004; 8:335-53; PMID:15268628; http://dx.doi.org/10.1517/14728222.8.4.335
15. Koning GA, Morselt HWM, Gorter A, Allen TM, Zalipsky S, Scherphof GL, Kamps JAAM. Interaction of differently designed immunoliposomes with colon cancer cells and Kupffer cells. An in vitro comparison. Pharm Res 2003; 20:1249-57; PMID:12948023; http://dx.doi.org/10.1023/A:1025009300562
16. Kirpotin DB, Drummond DC, Shao Y, Shalaby MR, Hong K, Nielsen UB, Marks JD, Benz CC, Park JW. Antibody targeting of long-circulating lipidic nanoparticles does not increase tumor localization but does increase internalization in animal models. Cancer Res 2006; 66:6732-40; PMID:16818648; http://dx.doi.org/10.1158/0008-5472.CAN-05-4199
17. Wang T, Duan Y. Probing the stability-limiting regions of an antibody single-chain variable fragment: a molecular dynamics simulation study. PEDS 2011; 24:649-57; PMID:21729946
18. Zemlin M, Klinger M, Link J, Zemlin C, Bauer K, Engler JA, Schroeder HW Jr, Kirkham PM. Expressed murine and human CDR-H3 intervals of equal length exhibit distinct repertoires that differ in their amino acid composition and predicted range of structures. J Mol Biol 2003; 334:733-49; PMID:14636599; http://dx.doi.org/10.1016/j.jmb.2003.10.007
19. Birtalan S, Zhang Y, Fellouse FA, Shao L, Schaefer G, Sidhu SS. The intrinsic contributions of tyrosine, serine, glycine and arginine to the affinity and specificity of antibodies. J Mol Biol 2008; 377:1518-28; PMID:18336836; http://dx.doi.org/10.1016/j.jmb.2008.01.093
20. Mian IS, Bradwell AR, Olson AJ. Structure, function and properties of antibody binding sites. J Mol Biol 1991; 217:133-51; PMID:1988675; http://dx.doi.org/10.1016/0022-2836(91)90617-F
21. Wilkinson RA, Piscitelli C, Teintze M, Cavacini LA, Posner MR, Lawrence CM. Structure of the Fab fragment of F105, a broadly reactive anti-human immunodeficiency virus (HIV) antibody that recognizes the CD4 binding site of HIV type 1 gp120. J Virology 2005; vol:13060-69; PMID:16189008; http://dx.doi.org/10.1128/JVI.79.20.13060-13069.2005
22. Prassler J, Thiel S, Pracht C, Polzer A, Peters S, Bauer M, Nörenberg S, Stark Y, Kölln J, Popp A, et al. HuCAL PLATINUM, a synthetic Fab library optimized for sequence diversity and superior performance in mammalian expression systems. J Mol Biol 2011; 413:261-78; PMID:21856311; http://dx.doi.org/10.1016/j.jmb.2011.08.012
23. Barrett NA, Austen FK. Innate cells and T helper 2 cell immunity in airway inflammation. Immunity 2009; 31:425-37; PMID:19766085; http://dx.doi.org/10.1016/j.immuni.2009.08.014
24. Lavinder JJ, Hari SB, Sullivan BJ, Thomas J, Magliery TJ. High-throughput thermal scanning: a general, rapid dye-binding thermal shift screen for protein engineering. J Am Chem Soc 2009; 131:3794-95; PMID:19292479; http://dx.doi.org/10.1021/ja8049063
25. Nielsen UB, Kirpotin DB, Pickering EM, Drummond DC, Marks JD. A novel assay for monitoring intracellularization of nanocarrier coupled antibodies. BMC Immunol 2006; 7:24; PMID:17014727; http://dx.doi.org/10.1186/1471-2172-7-24
26. Ewert S1, Huber T, Honegger A, Plückthun A. Biophysical properties of human antibody variable domains. J Mol Biol 2003; 325:531-53; PMID: 12498801; http://dx.doi.org/10.1016/S0022-2836(02)01237-8
27. Sarvazyan MA1, O'Connell MP, Fairbrother WJ, Kelley RF. Antibody variable region binding by Staphylococcal protein A: thermodynamic analysis and location of the Fv binding site on E-domain. Protein Sci 1999; 8:1423-31; PMID:10422830; http://dx.doi.org/10.1110/ps.8.7.1423
28. Roben PW1, Salem AN, Silverman GJ. VH3 family antibodies bind domain D of staphylococcal protein A. J Immunol 1995;154:6437-45; PMID:7759880
29. Wörn A, Plückthun A. Stability engineering of antibody single-chain Fv fragments. J Mol Biol 2001; 305:989-1010; PMID:11162109; http://dx.doi.org/10.1006/jmbi.2000.4265
30. Jordan JL, Arndt JW, Hanf K, Li G, Hall J, Demarest S, Huang F, Wu X, Miller B, Glaser S, et al. Structural understanding of stabilization patterns in engineered bispecific Ig-like antibody molecules. Protein 2009;77:832-41; PMID:19626705; http://dx.doi.org/10.1002/prot.22502
31. Benhar I, Pastan I. Identification of residues that stabilize the single-chain Fv of monoclonal antibodies B3. J Biol Chem 1995; 270:23572-80; PMID:7559495; http://dx.doi.org/10.1074/jbc.270.40.23572
32. McConnell AD, Spasojevich V, Macomber JL, Krapf IP, Chen A, Sheffer JC, Berkebile A, Horlick RA, Neben S, King DJ, et al. An integrated approach to extreme thermostabilization and affinity maturation of an antibody. Protein Eng Des Sel 2013; 26:151-64; PMID:23173178; http://dx.doi.org/10.1093/protein/gss090
33. Yin S, Ding F, Dokholyan NV. Eris: an automated estimator of protein stability. Nat Methods 2007; 4:466-7; PMID:17538626; http://dx.doi.org/10.1038/nmeth0607-466
34. Alfthan K, Takkinen K, Sizmann D, Söderlund H, Teeri TT. Properties of a single-chain antibody containing different linker peptides. Protein Eng 1995; 8:725-31; PMID:8577701; http://dx.doi.org/10.1093/protein/8.7.725
35. Huston JS1, Levinson D, Mudgett-Hunter M, Tai MS, Novotný J, Margolies MN, Ridge RJ, Bruccoleri RE, Haber E, Crea R, et al. Protein engineering of antibody binding sites: recovery of specific activity in an anti-digoxin single-chain Fv analogue produced in Escherichia coli. PNAS USA 1988; 85:5879-83; PMID: 3045807; http://dx.doi.org/10.1073/pnas.85.16.5879
36. Fellouse FA, Wiesmann C, Sidhu SS. Synthetic antibodies from a four-amino-acid code: a dominant role for tyrosine in antigen recognition. PNAS USA 2004; 101:12467-72; PMID:15306681; http://dx.doi.org/10.1073/pnas.0401786101
37. Perchiacca JM, Lee CC, Tessier PM. Optimal charged mutations in the complementarity-determining regions that prevent domain antibody aggregation are dependent on the antibody scaffold. PEDS 2014; 27:29-39; PMID:24398633
38. Dudgeon K, Rouet R, Kokmeijer I, Schofield P, Stolp J, Langley D, Stock D, Christ D. General strategy for the generation of human antibody variable domains with increased aggregation resistance. PNAS USA 2012; 109:10879-84; PMID:22745168; http://dx.doi.org/10.1073/pnas.1202266109
39. Weaver-Feldhaus JM, Miller KD, Feldhaus MJ, Siegel RW. Directed evolution for the development of conformation-specific affinity reagents using yeast display. PEDS 2005; 18: 527-36; PMID:16186140
40. Perchiacca JM, Lee CC, Tessier PM. Optimal charged mutations in the complementarity-determining regions that prevent domain antibody aggregation are dependent on the antibody scaffold. Protein Eng Des Sel 2014; 27:29-39; PMID:24398633; http://dx.doi.org/10.1093/protein/gzt058
41. Mian IS, Bradwell AR, and Olson AJ. Structure, function and properties of antibody binding sites. J Mol Biol 1991; 217:133-51; PMID:1988675; http://dx.doi.org/10.1016/0022-2836(91)90617-F
42. Wilkinson RA, Piscitelli C, Teintze M, Cavacini LA, Posner MR, Lawrence CM. Structure of the Fab fragment of F105, a broadly reactive anti-human immunodeficiency virus (HIV) antibody that recognizes the CD4 binding site of HIV type 1 gp120. J Virol 2005; 79:13060-9; PMID:16189008; http://dx.doi.org/10.1128/JVI.79.20.13060-13069.2005
43. Collis AV, Brouwer AP, Martin AC. Analysis of the antigen combining site: correlations between length and sequence composition of the hypervariable loops and the nature of the antigen. J Mol Biol 2003; 325:337-54; PMID:12488099; http://dx.doi.org/10.1016/S0022-2836(02)01222-6
44. Xu L, Kohli N, Rennard R, Jiao Y, Razlog M, Zhang K, Baum J, Johnston B, Tang J, Schoeberl B, et al. Rapid optimization and prototyping for therapeutic antibody-like molecules. MABS 2013; 5:337-54; PMID:23392215; http://dx.doi.org/10.4161/mabs.23363
45. Wang Q, Canutescu AA, Dunbrack RL. SCWRL and MolIDE: computer programs for side-chain conformation prediction and homology modeling. Nat Protoc 2008; 3:1832-47; PMID:18989261; http://dx.doi.org/10.1038/nprot.2008.184
46. Canutescu AA, Dunbrack RL. MolIDE: a homology modeling framework you can click with. Bioinformatics 2005; 21:2914-16; PMID:15845657; http://dx.doi.org/10.1093/bioinformatics/bti438
47. Canutescu AA, Dunbrack RL. Cyclic coordinate descent: a robotics algorithm for protein loop closure. Protein Sci 2003; 12:963-72; PMID:12717019; http://dx.doi.org/10.1110/ps.0242703
48. Canutescu AA, Shelenkov AA, Dunbrack RL. A graph-theory algorithm for rapid protein side-chain prediction. Protein Sci 2003; 12:2001-14; PMID:12930999; http://dx.doi.org/10.1110/ps.03154503
49. Guex N, Peitsch MC. SWISS-MODEL and the Swiss-PdbViewer: an environment for comparative protein modeling. Electrophoresis 1997; 18:2714-23; PMID:9504803; http://dx.doi.org/10.1002/elps.1150181505
50. Wu TT, Kabat EA, Bilofsky H. Some sequence similarities among cloned mouse DNA segments that code for lambda and kappa light chains of immunoglobulins. PNAS USA 1979; 76:4617-21; PMID:116235; http://dx.doi.org/10.1073/pnas.76.9.4617

mAbs

ISSN: 1942-0862 (Print) 1942-0870 (Online) Journal homepage: http://www.tandfonline.com/loi/kmab20

Comprehensive optimization of a single-chain variable domain antibody fragment as a targeting ligand for a cytotoxic nanoparticle

Kathy Zhang, Melissa L Geddie, Neeraj Kohli, Tad Kornaga, Dmitri B Kirpotin, Yang Jiao, Rachel Rennard, Daryl C Drummond, Ulrik B Nielsen, Lihui Xu & Alexey A Lugovskoy

To cite this article: Kathy Zhang, Melissa L Geddie, Neeraj Kohli, Tad Kornaga, Dmitri B Kirpotin, Yang Jiao, Rachel Rennard, Daryl C Drummond, Ulrik B Nielsen, Lihui Xu & Alexey A Lugovskoy (2015) Comprehensive optimization of a single-chain variable domain antibody fragment as a targeting ligand for a cytotoxic nanoparticle, mAbs, 7:1, 42-52, DOI: 10.4161/19420862.2014.985933

To link to this article: http://dx.doi.org/10.4161/19420862.2014.985933

European Review for Medical and Pharmacological Sciences 2013; 17: 3347-3361

PEG-coated irinotecan cationic liposomes improve the therapeutic efficacy of breast cancer in animals

L. ZHANG, D.-Y. CAO, J. WANG, B. XIANG, J.-N. DUN, Y. FANG, G.-Q. XUE

Department of Pharmaceutics, School of Pharmaceutical Sciences, Hebei Medical University, Research Center of Chinese Medicine Injection in Hebei Province, Shijiazhuang, China

Abstract. – BACKGROUND: Breast cancer is the most frequently diagnosed cancer and the leading cause of cancer death among females owing.

AIM: This study aimed to construct a kind of PEG-coated irinotecan cationic liposomes for investigating its efficacy and mechanism of action in the treatment of breast cancer in preclinical models.

MATERIALS AND METHODS: Evaluations were performed on the MDA-MB231 breast cancer cells, the xenografted MDA-MB231 cancer cells in Female nude mice and Sprague-Dawley (SD) rat. The liposomes were characterized through assays of cytotoxicity, intracellular uptake, nuclei morphology, antitumor activities, pharmacokinetics and tissue distribution.

RESULTS: The zeta potential of PEG-coated irinotecan cationic liposomes was approximately 23 mV. The PEG-coated irinotecan cationic liposomes were approximately 66nm in diameter, significantly increased the intracellular uptake of irinotecan, and showed strong inhibitory effect on MDA-MB231 breast cancer cells. A significant antitumor efficacy in the xenografted MDA-MB231 breast cancer cells in nude mice was evidenced by intravenous administration of PEG-coated irinotecan cationic liposomes. PEG-coated irinotecan cationic liposomes also improved the irinotecan blood circulation time and showed an enhanced drug concentration in tumor.

CONCLUSIONS: PEG-coated irinotecan cationic liposomes had significant inhibitory effect against breast cancer *in vitro* and *in vivo*, hence providing a new strategy for treating breast cancer.

Key Words:

Breast cancer, PEG-coated irinotecan cationic liposomes, Pharmacokinetics, Tissue distribution, HPLC.

Introduction

Breast cancer is one of the most frequent cancers among women worldwide. It is a disease that can affect women of various ages where the risk of developing breast cancer increases with age[1,2]. Approximately one in eight women will be diagnosed with breast cancer during their lifetime. As a consequence, there is a great need to develop a treatment strategy that can successfully reduce the incidence of breast cancer and prolong the life of affected women[3,4].

Irinotecan (CPT-11), a water-soluble camptothecin, is commonly in clinical used for the cancer treatment. It exerts anti-tumor activity by inhibiting the intranuclear enzyme topoisomerase I[5,6]. In tumor cells, the level of topoisomerase I enzyme is higher than in normal cells. Irinotecan was shown to exert its cytotoxic activity through inhibition of DNA replication while acting upon DNA topoisomerase I enzyme[7,8]. DNA topoisomerase relieves the torsional stress that develops during DNA replication by inducing single strand breaks. The irinotecan binds to the topoisomerase I-DNA complex, thereby leading to replication arrest and the formation of double-strand DNA breaks which, while not repaired, can lead to the cancer cell death. However, the main adverse effects of irinotecan in humans are gastrointestinal toxicity and myelosuppression which limits its usage and administration[9,10].

Liposomes have been widely used in the therapeutic drug delivery to enhance permeability and retention (EPR) effects in tumor tissues and reduce systemic side effect of anticancer agent, including small molecular drugs, proteins, genes (DNA or RNA) and diagnostic contrast reagents[11,12]. PEGylated lipids (PEG_{2000}-DSPE) can inhibit opsonization by plasma proteins and contribute longer circulation for liposome because of the "steric stabilization" effect. With the surface hydrophilic protective layer from PEG chain, PEGylated liposome showed characterizations of more stability, sustained release, prolonged blood circulation time and reduced reticuloendothelial system uptake[13,14].

Although liposomes have been successfully applied in the clinic, further efforts on the component optimization are still a hot topic in the re-

Corresponding Author: De-Ying Cao, Ph.D; e-mail: cao_dy@126.com

search for satisfying requirements from clinic. A change of the liposomes' charge is believed to be one of the key factors affecting cellular adhesion/uptake and drug delivery[15]. Liposomes with cationic charge are prone to binding cells than liposomes with neutral or anionic lipids due to electrostatic interaction with negatively charged molecule on tumor cell membrane (glycoproteins, anionic phospholipids and proteoglycans). This is the reason that cationic liposomes were frequently used to improve *in vitro* and *in vivo* efficacy for drug delivery[16,17].

The objectives of the present study are to prepare polyethylene glycol (PEG)-coated irinotecan cationic liposomes by incorporating octadecylamine into the lipophilic bilayer, as shown in Figure 1A. Irinotecan was entrapped into the aqueous cores by ammonium sulfate gradient method in order to get high encapsulation efficiency[18]. The aim of present study was to explore the preparation of PEG-coated irinotecan cationic liposomes, to define the action mechanisms, to evaluate the efficacy in treating of breast cancer, and to evaluate the pharmacokinetics and distrib-

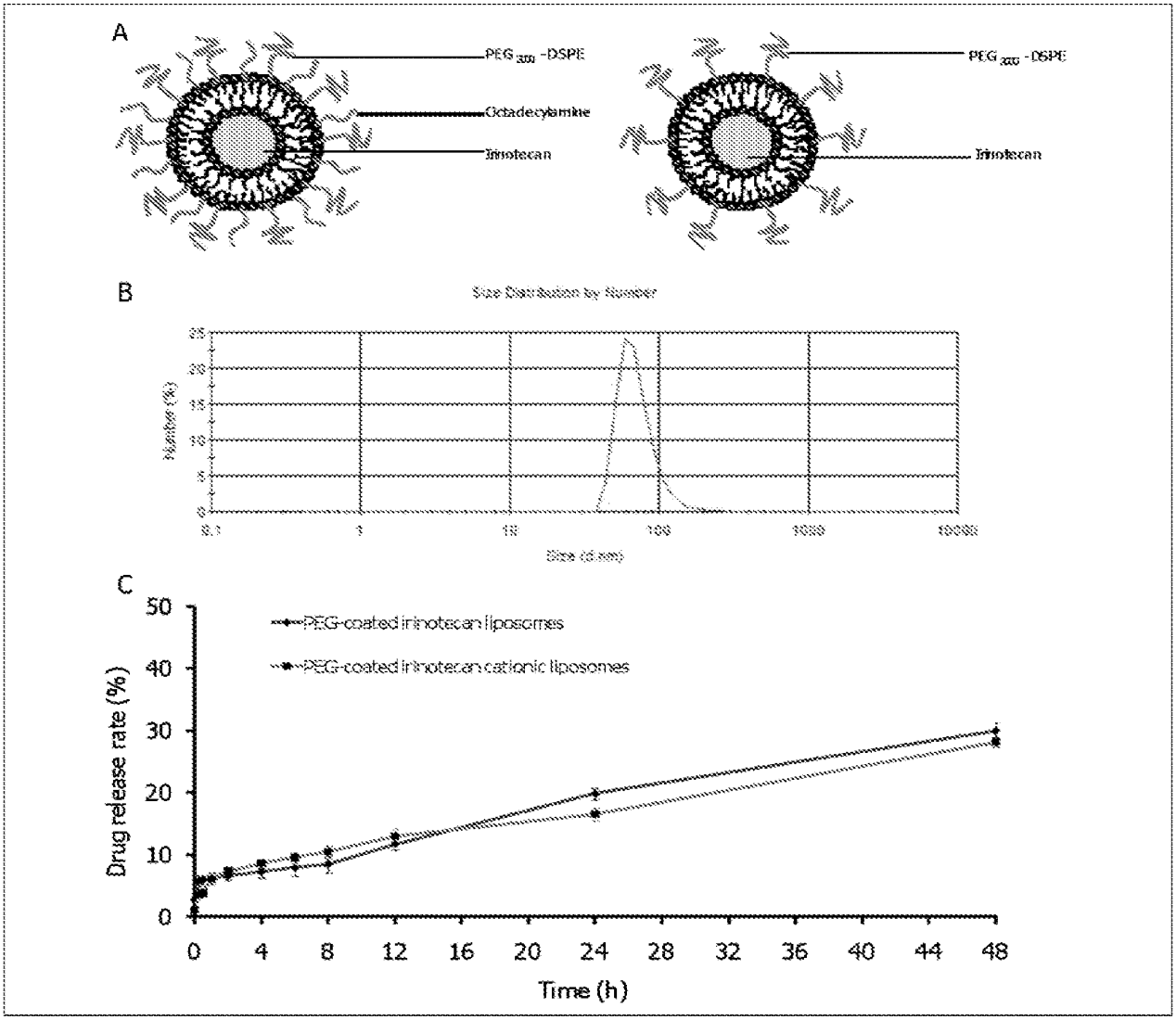

Figure 1. *A,* Schematic representations of two liposomal constructs consisting of PEG-coated irinotecan cationic liposomes and PEG-coated irinotecan liposomes. *B,* Size distribution of PEG-coated irinotecan cationic liposomes by dynamic light scattering (DLS) analysis. *C,* The release profiles of irinotecan from two different liposomes in PBS solution containing 10% serum protein at 37°C respectively. Data are presented as the mean ± SD (n=3).

ution of irinotecan after intravenous administration of PEG-coated irinotecan cationic liposomes.

Materials and Methods

Preparation of PEG-Coated Irinotecan Cationic Liposomes

PEG-coated irinotecan cationic liposomes were prepared as previously described. Soybean phosphatidylcholine (SPC) (Sigma-Aldrich Corporation, Beijing local agent, China), cholesterol (Sigma-Aldrich Corporation, Beijing local agent, China), polyethylene glycol-distearoylphosphatidylethanolamine (PEG_{2000}-DSPE, Avanti Polar Lipids, Alabaster, AL, USA) and octadecylamine (Johnson Matthey Company, London, UK) (54/23/4/2.5, μmol ratio) were dissolved in chloroform in a pear-shaped flask. The chloroform was evaporated to dryness under vacuum with a rotary evaporator, and then the formed lipid film was hydrated with 250 mM ammonium sulfate by sonication in the water bath for 5 min, followed by sonication using a probe-type sonicator for 10 min. The suspensions after hydration were successively extruded through polycarbonate membranes (Millipore, Bedford, MA, USA) with the pore size of 400 nm, and 200 nm for 3 times, respectively. Afterwards, the blank PEG-coated cationic liposomes were obtained[19].

To prepare PEG-coated irinotecan cationic liposomes, the blank PEG-coated cationic liposomes were then dialyzed (8,000-15,000 molecular mass cutoff) (Beijing Dingguo Biotechnology Limited Company, China) in the 500 ml physiological saline (0.9%NaCl) for two times. Irinotecan was loaded using an ammonium sulfate gradient loading method, as reported previously. Appropriate amounts of irinotecan hydrochloride (Jiangsu Henrui Medicine Corporation, China) were added to the blank PEG-coated cationic liposomes. After mixing, the suspensions were incubated at 50 ℃ in water bath, and intermittently shaken for 30 min to produce the PEG-coated irinotecan cationic liposomes.

To prepare PEG-coated irinotecan liposomes, the blank PEG-coated liposomes were made with the same procedures of blank PEG-coated cationic liposomes, excluding the addition of octadecylamine during film forming. Then irinotecan was loaded into the blank PEG-coated liposomes using an ammonium sulfate gradient loading method as above.

Characterization of PEG-coated Irinotecan Cationic Liposomes

PEG-coated irinotecan cationic liposomes and PEG-coated irinotecan liposomes were passed over a Sephadex G-50 column (Sigma-Aldrich Corporation, Beijing local agent, China) to remove the free irinotecan. The encapsulation efficiency of irinotecan was calculated with the formula: $EE = (W_{encap}/W_{total}) \times 100\%$, where EE is the encapsulation efficiency of irinotecan, and W_{encap} is the measured amount irinotecan in the liposomal suspensions after passing over the column. The irinotecan concentration was determined by using fluorospectrophotometer.

In vitro release of irinotecan in the liposomes was performed by the dialysis against the release medium containing serum protein (phosphate buffered saline containing 10% fetal calf serum). A volume of 2.5 ml liposomes plus 2.5 ml of release medium in dialysis tubing was immersed in 30.0 ml of the release medium, and oscillated with a shaker at a rate of 150 times per minute at 37 ℃. A volume of 0.5 ml release medium was taken at 0, 0.25, 0.5, 1, 2, 4, 6, 8, 12, 24 and 48 h, respectively, and immediately replaced with the same volume of fresh release medium after each sampling. The irinotecan content in the release medium was determined by fluorospectrophotometer as above. The release rate was calculated with the formula: $RR = (W_i/W_{total}) \times 100\%$, where RR is the drug release rate (%), W_i is the measured amount of irinotecan at the time-point of ith h in release medium, and W_{total} is the total amount of irinotecan in the equal volume of liposome suspensions prior to dialysis[20].

The particle sizes and zeta potential values of all nanovesicles were measured with Zetasizer 3000HSA (Malvern Instruments Ltd., Malvern, Worcestershire, UK).

Culture of MDA-MB231 Cells

The culture medium was prepared with DMEM (Sigma-Aldrich Corporation, Beijing local agent, China) supplemented with 10% heat-inactivated fetal bovine serum (Sigma-Aldrich Corporation, Beijing local agent, China), 100 units/ml penicillin (Sigma-Aldrich Corporation, Beijing local agent, China), and 100 units/ml streptomycin (Sigma-Aldrich Corporation, Beijing local agent, China). The cells were cultured in the incubator at 37°C and in the presence of 5% CO_2.

Cytotoxicity to MDA-MB231 Cells

MDA-MB231 cells were seeded into 96-well culture plates at a density of 9.0×10^3 cells per well

and grown in culture medium in the incubator at 37°C and in the presence of 5% CO_2 for 24 h. Free irinotecan (0-5 μM), PEG-coated irinotecan liposomes (0-5 μM) and PEG-coated irinotecan cationic liposomes (0-5 μM) were added into 96-well culture plates, respectively. The survival rate was measured at 48 h by the sulforhodamine B (SRB) staining assay, and the absorbance was read on a microplate reader at 540 nm. The survival percentages were calculated using the following formula: Survival % = (A_{540nm} for the treated cells/$A_{540\ nm}$ for the control cells) × 100%, where $A_{540\ nm}$ is the absorbance value. Each assay was repeated in triplicate. Finally, the dose-effect curves were plotted.

Intracellular Uptake of PEG-coated Irinotecan Liposomes

Intracellular uptake of PEG-coated irinotecan liposomes was determined by flow cytometry assay. MDA-MB231 cells were seeded onto six-well plates at 3.0×10^5 per well and cultured for 24 h at 37°C and in the presence of 5% CO_2, followed by adding PEG-coated irinotecan liposomes (2.5 μM) and PEG-coated irinotecan cationic liposomes (2.5 μM). Phosphate buffered saline (PBS) (pH 7.4) was added as a blank control. The cells were further incubated for 5 h and then enzymatically dissociated by adding trypsin (0.25%, g/100 ml). Cells were resuspended in PBS (pH 7.4). The samples were determined by flow cytometry with a FACScan (Becton Dickinson, San Jose, CA, USA). Data were collected of 10,000 gated events and analyzed with the CELL Quest software program.

Morphology of Nuclei Induced by PEG-coated Irinotecan Cationic Liposomes

Hoechst staining of nuclei was performed to observe morphological changes of nuclei in MDA-MB231 cells. Briefly, MDA-MB231 cells were seeded at 3.8×10^4 cells per well in 24-well plates and cultured in the incubator at 37°C and in the presence of 5% CO_2 for 24 h, then treated with free irinotecan (2.5 μM), PEG-coated irinotecan liposomes (2.5 μM) and PEG-coated irinotecan cationic liposomes (2.5 μM), and further incubated for 6 h. Afterwards, cells were fixed with 4% paraformaldehyde for 0.5 h and stained with Hoechst 33342 (120 mg/ml) for 25 min. Cells were examined with a fluorescence microscope (Leica, Heidelberg, Germany) for observing the fragmentation of nuclei. Cells were treated with PBS (pH 7.4) as control.

Animals

For each optimized PEG-coated irinotecan cationic liposomes studied, female BALB/c nude mice and Sprague-Dawley (SD) rats were obtained from Vital Laboratory Animal Center of Hebei Medical University. All of the animal experiments adhered to the principles for care and use of laboratory animals and were approved by the institutional Animal Care and Use Committee of Hebei Medical University.

In vivo Inhibition of the Tumor Growth and Effects on the Indicators of Bone Marrow

Female BALB/c nude mice, initially weighing 18-20 g, were used for investigating the antitumor efficacy *in vivo*. Briefly, approximately 2.0×10^7 MDA-MB231 cells were resuspended in 100 μl of serum-free medium, and injected subcutaneously into the right flanks of the nude mice[21]. When tumors reached 100 to 150 mm^3 in volume, mice were randomly divided into four treatment groups (6 for each group). At day 19, 22, 25, and 28 post inoculation, physiological saline (blank control), free irinotecan (20.00 mg/kg), PEG-coated irinotecan liposomes (20.00 mg/kg), and PEG-coated irinotecan cationic liposomes (20.00 mg/kg) were given intravenously to mice which had been randomly divided into four treatment groups (6 for each) via tail vein, respectively. The presence of each tumor mass was confirmed by necropsy at day 31 since the inoculation. Mice were weighed and tumors were measured with a caliper every one or every two days. Tumor volumes were calculated with the formula (length × $width^2/2$).

At day 31, the mice were sacrificed. Blood specimens of the mice were collected immediately. The blood specimens were used for measuring the indicators of bone marrow in peripheral blood (white blood cells, WBC; hemoglobin, Hb; platelet, PLT).

Pharmacokinetics and Tissue Distribution

Female Sprague-Dawley (SD) rats were used for investigating the pharmacokinetics and randomly divided into three groups (6 for each group). Free irinotecan (20.00 mg/kg), PEG-coated irinotecan liposomes (20.00 mg/kg) and PEG-coated irinotecan cationic liposomes (20.00 mg/kg) were given intravenously to rats via tail vein, respectively. After administrations, a 1ml volume of plasma was collected in a heparinized microcentrifuge tube from retro orbital sinus at the

following time points: 15 min, 30 min, 1h, 2h, 4h, 8h, 12h, 24h and 48h. The plasma was separated by centrifugation at 12,000 rpm for 10 min and stored at –20°C [2]. A 3.0-ml volume of methanol was added to the 100 µl plasma and mixed for 3 min with a vortex, followed by centrifugation at 10,000 rpm for 5 min. The liquid phase was transferred to a clean tube and dried under a gentle N_2 gas stream to obtain residues containing the irinotecan. The irinotecan residue was reconstituted with 100 µl mobile phase and centrifuged at 10,000 rpm for 5 min. Finally, a 20 µl volume of supernatant was injected into the HPLC system.

Female BALB/c nude mice were used for investigating the tissue distribution after xenografting MDA-MB231 breast cancer cells and randomly divided into three groups (6 for each group). Free irinotecan (20.00 mg/kg), PEG-coated irinotecan liposomes (20.00 mg/kg) and PEG-coated irinotecan cationic liposomes (20.00 mg/kg) were given intravenously to mice via tail vein, respectively. After administration, heart, liver, spleen, lung, kidney and tumor were also collected at 1h, 4h, 8h, 24h and 48h after sacrifice by cervical dislocation. The tissues were washed with physiological saline, dried with filter paper, weighted accurately and stored at –20°C [23]. The tissue samples were homogenized with a homogenizer in physiological saline. A 3.0-ml volume of methanol was added to 100 µl tissue homogenate (0.15 g of tissue) and mixed for 3 min with a vortex, followed by centrifugation at 10,000 rpm for 5 min. The liquid phase was transferred to a clean tube and dried under a gentle N_2 gas stream to obtain residues containing the irinotecan. The irinotecan residue was reconstituted with 100 µl mobile phase and centrifuged at 10,000 rpm for 5 min. Finally, a 20 µl volume of supernatant was injected into the HPLC system.

The samples were analyzed by HPLC with fluorescence detection (Waters Technologies Inc., Cotati, CA, USA). Irinotecan was separated by a Diamonsil C_{18} column (200×4.6 mm, 5 µm). The mobile phase consisted of acetonitrile and water containing 2.1% citric acid and 0.2% triethylamine (40/60, v/v) with a flow rate of 1.0 ml/min under isocratic conditions. pH was 3.8 settled by 30% natrium hydroxydatum. The fluorescence detection was set at λ_{ex} 370 nm and λ_{em} 530 nm.

Statistical Analysis

Data are presented as the mean ± standard deviation. One-way analysis of variance was used to determine significance among groups, after which post hoc tests with the Bonferroni correction were used for multiple comparisons between individual groups. A value of $p < 0.05$ was considered to be significant.

Results

Characterization of PEG-coated Irinotecan Cationic Liposomes

Table I represents the characterization results of two liposomes. In two kinds of liposomes prepared, the encapsulation efficiency of irinotecan was ≥ 90%. The mean particle sizes of PEG-coated irinotecan liposomes and PEG-coated irinotecan cationic liposomes were 68.65 ± 5.19 and 66.32 ± 3.06 nm (Figure 1B), respectively. Their corresponding potential val-

Table I. Characterizations of two irinotecan liposomes.

1. Encapsulation efficiency of irinotecan	Results (%)
PEG-coated irinotecan liposomes	93.66 ± 3.12%
PEG-coated irinotecan cationic liposomes	91.39 ± 2.58%
2. Size of irinotecan liposomes	**Results**
	Mean size (nm)
PEG-coated irinotecan liposomes	68.65 ± 5.19
PEG-coated irinotecan cationic liposomes	66.32 ± 3.06
3. Zeta potential of irinotecan liposomes	**Results**
PEG-coated irinotecan liposomes	–15.19 ± 0.68 mv
PEG-coated irinotecan cationic liposomes	23.13 ± 0.59 mv

Each point represents means ± SD (n=3).

ues were -15.19±0.68 mV and 23.13±0.59 mV, respectively.

Figure 1C shows the release rates of irinotecan from two different liposomes in PBS solution containing 10% serum protein oscillated at a rate of 150 times per minute at 37°C. Release rate of irinotecan from the two kinds of liposomes was negligible under the same release condition. The release rates at 48 h of irinotecan from PEG-coated irinotecan liposomes and PEG-coated irinotecan cationic liposomes were 29.92 ± 0.81% and 28.20 ± 1.36%, respectively.

Cytotoxicity to MDA-MB231 Cells

Figure 2A shows the inhibitory effects to MDA-MB231 cells after applying various formulations. As compared to free irinotecan and PEG-coated irinotecan liposomes, PEG-coated irinotecan cationic liposomes showed the strongest inhibitory effects at various dose levels. For example, the rank of survival rates after applying 5 μM irinotecan were PEG-coated irinotecan liposomes (23.77 ± 1.43%) > free irinotecan (5.57 ± 1.14%) > PEG-coated irinotecan cationic liposomes (3.48 ± 1.01%).

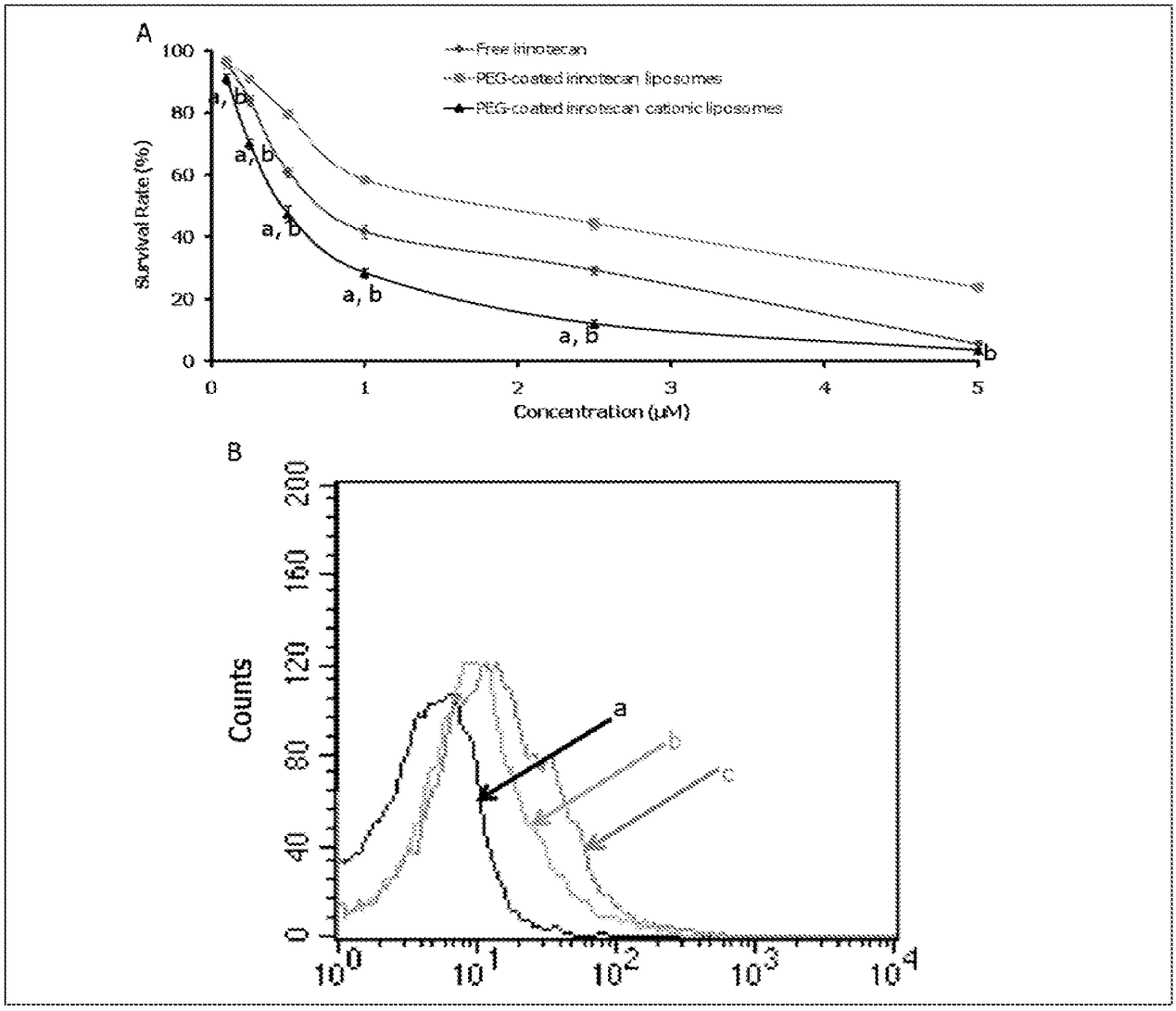

Figure 2. *A,* Survival rates of MDA-MB-231 cells after applying various irinotecan formulations measured by SRB staining assay. Data are presented as the mean ± SD (n=3). a, $p < 0.05$, versus free irinotecan; b, $p < 0.05$, versus PEG-coated irinotecan liposomes. *B,* MDA-MB-231 cellular uptakes after applying various irinotecan formulations measured by FAScan flow cytometry. Notes: a, PBS; b, PEG-coated irinotecan liposomes; c, PEG-coated irinotecan cationic liposomes.

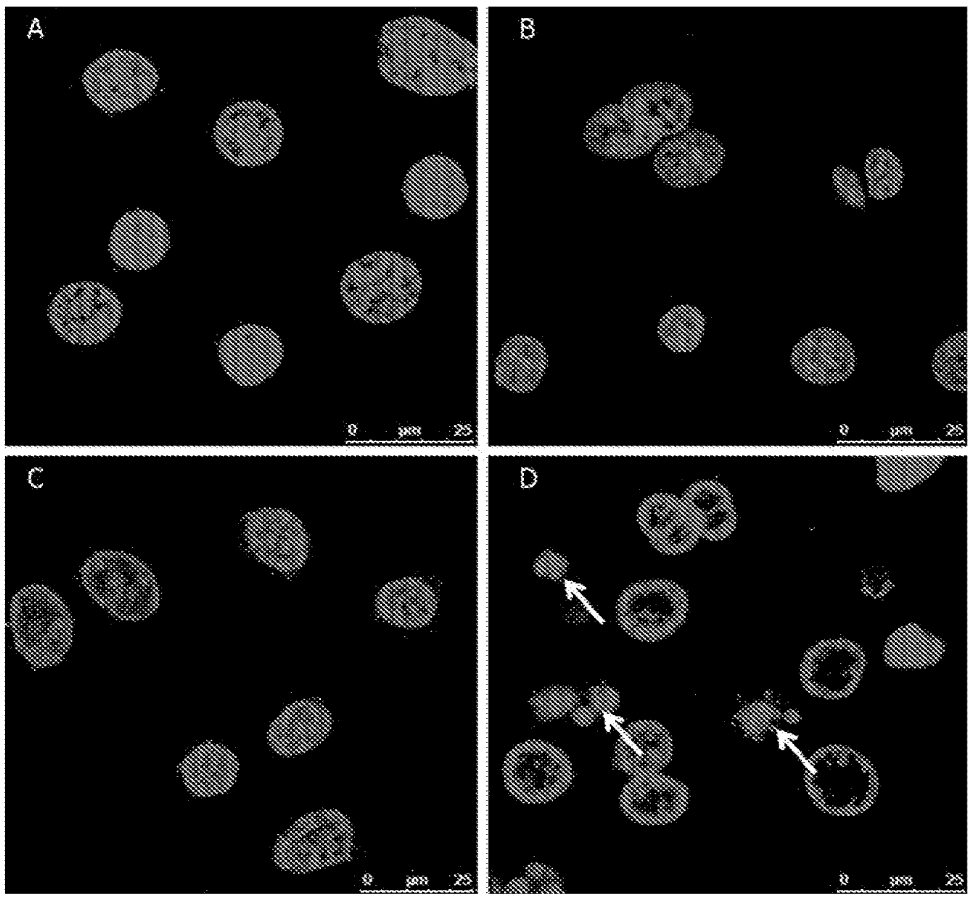

Figure 3. Image of the nuclear morphological changes of MDA-MB-231 induced by applying various formulations, including PBS as blank control *(A)*, Free irinotecan *(B)*, PEG-coated irinotecan liposomes *(C)* and PEG-coated irinotecan cationic liposomes *(D)*, respectively. Arrows: fragmented nuclei.

Intracellular Uptake of PEG-coated Irinotecan Liposomes

Figure 2B shows semi-quantitative drug content observed by flow cytometry in the MDA-MB231 cells after applying PEG-coated irinotecan liposomes and PEG-coated irinotecan cationic liposomes at 5 h.

In quantitative evaluation for ten thousands of events, the geometric mean intensity value was 8.62 for PBS (a) < 15.36 for PEG-coated irinotecan liposomes (b) <22.19 for PEG-coated irinotecan cationic liposomes (c).

Morphology of Nuclei Induced by PEG-Coated irinotecan Cationic Liposomes

Figure 3 shows images for nuclei of MDA-MB231 cells after applying free irinotecan, PEG-coated irinotecan liposomes and PEG-coated irinotecan cationic liposomes.

After applying PEG-coated irinotecan cationic liposomes, nuclei of MDA-MB231 cells became broken and evident fragment occurred as early as 6 h, showing characteristics of nuclei as MDA-MB231 breast cancer cells death. As compared to free irinotecan and PEG-coated irinotecan liposomes, PEG-coated irinotecan cationic liposomes showed the strongest inhibition effect of MDA-MB231 cancer cells.

In vivo Inhibition of the Tumor Growth and Effects on the Indicators of Bone Marrow

Figure 4A shows the efficacy of PEG-coated irinotecan cationic liposomes in treating the MDA-MB231 cells xenografts tumor model. After inoculation of MDA-MB231 cells in nude mice, the tumors reached suitable masses for treatment at day 19. As compared to blank control group, the inhibitory effects of tumor growth were obviously observed in all treatment groups. The rank of inhibitory effects was PEG-coated irinotecan cationic liposomes > PEG-coated irinotecan liposomes > free irinotecan > the blank control.

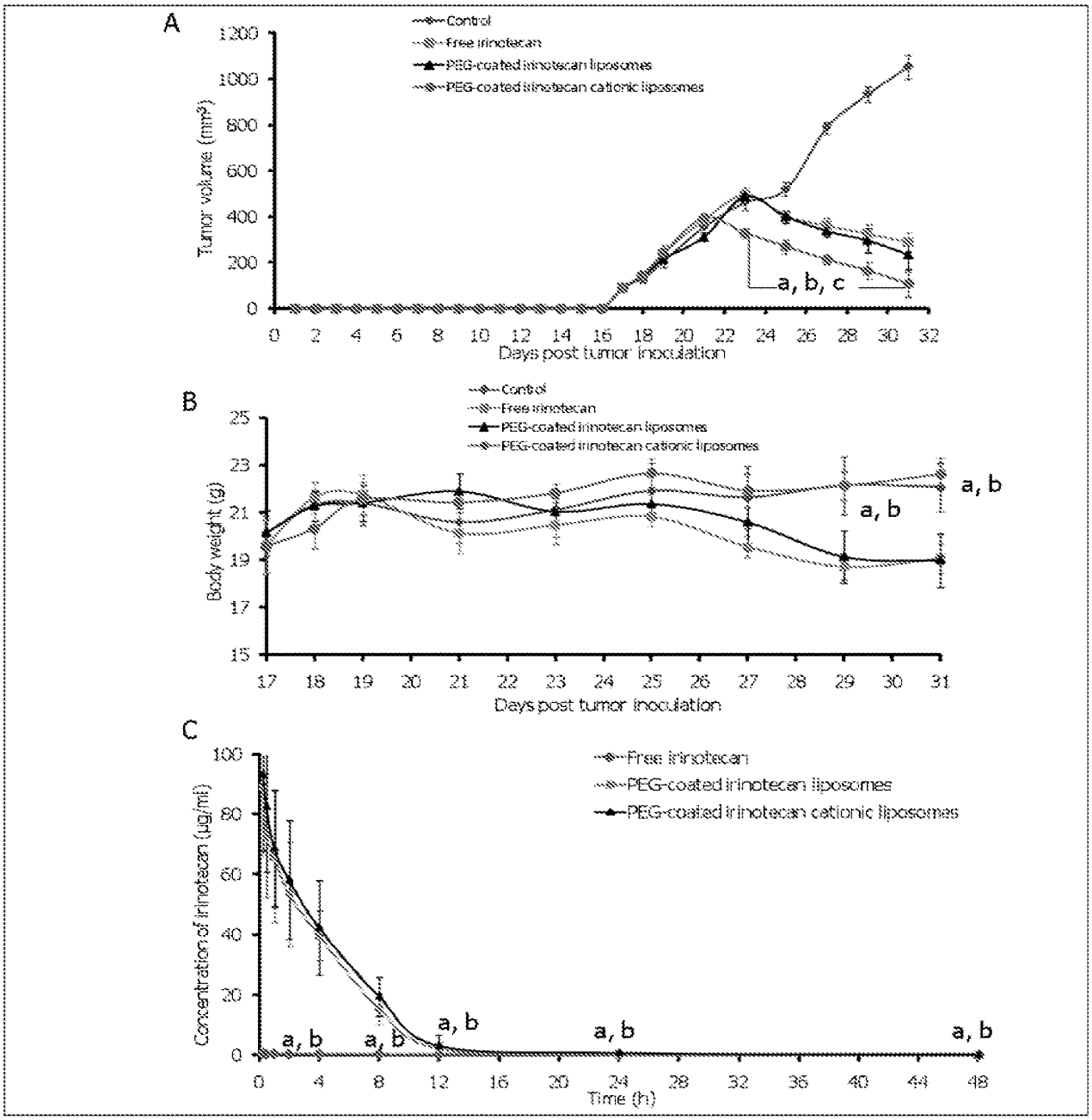

Figure 4. *A,* Effect of PEG-coated irinotecan cationic liposomes on the MDA-MB-231 cells xenografts in female nude mice. At day 19, 22, 25 and 28 after inoculation, physiological saline as control group, free irinotecan (20.00 mg/kg), PEG-coated irinotecan liposomes (20.00 mg/kg), and PEG-coated irinotecan cationic liposomes (20.00 mg/kg) were given intravenously to mice via tail vein, respectively. Data are presented as the mean ± SD (n=6). a, $p < 0.05$, versus physiological saline; b, $p < 0.05$, versus free irinotecan; c, $p < 0.05$, versus PEG-coated irinotecan liposomes. *B,* Body weight changes for the tumor-bearing mice after intravenous administration of physiological saline, free irinotecan, PEG-coated irinotecan liposomes and PEG-coated irinotecan cationic liposomes to mice. Data are presented as the mean ± standard deviation (n=6). a, $p < 0.05$, versus free irinotecan; b, $p < 0.05$, versus PEG-coated irinotecan liposomes. *C,* Time course of irinotecan levels in plasma after intravenous administration of free irinotecan (20.00 mg/kg), PEG-coated irinotecan liposomes (20.00 mg/kg) and PEG-coated irinotecan cationic liposomes (20.00 mg/kg). Each point represents means ± SD (n=6). a, $p < 0.05$, versus PEG-coated irinotecan liposomes; b, $p < 0.05$, versus PEG-coated irinotecan cationic liposomes.

Table II. Effect on the hematological indicators of bone marrow after intravenous administration of physiological saline (blank control), free irinotecan, PEG-coated irinotecan liposomes and PEG-coated irinotecan cationic liposomes in female BALB/c nude mice.

Indicator	Blank control	Free irinotecan	PEG-coated irinotecan liposomes	PEG-coated irinotecan cationic liposomes
WBC (10^9/L)	9.63 ± 0.53	6.01 ± 0.56[a]	8.59 ± 0.72[a]	9.43 ± 0.81
Hb (g/L)	106.33 ± 9.12	75.26 ± 11.13[a]	91.55 ± 10.02[a]	101.29 ± 11.23
PLT (10^9/L)	988.65 ± 35.69	633.61 ± 48.12[a]	901.31 ± 57.42[a]	971.32 ± 39.61

Data are presented as means ± SD (n = 6). WBC: white blood cell; Hb: hemoglobin; PLT: platelets. [a]$p < 0.05$, versus blank control.

Figure 4B shows the body weight changes of the tumor-bearing mice during the study of anti-tumor efficacy. In view of results observed in all treatment groups, body weight loss was not observed significantly in the mice after giving PEG-coated irinotecan cationic liposomes but found in the mice after giving PEG-coated irinotecan liposomes and free irinotecan.

Table II shows the effects of various formulations on the hematological indicators of bone marrow. After administration of PEG-coated irinotecan cationic liposomes, the levels of WBC, Hb, and PLT in blood specimens were slightly decreased, but without significant difference as compared to those in control group. After administration of PEG-coated irinotecan liposomes, the levels of WBC, Hb, and PLT in blood specimens were decreased. However, the levels of WBC, Hb, and PLT were severely lowered after administration of free irinotecan.

Pharmacokinetics of Irinotecan in Plasma

After administration of free irinotecan, the plasma irinotecan level dropped rapidly. While after administration of PEG-coated irinotecan liposomes and PEG-coated irinotecan cationic liposomes, the plasma irinotecan concentration decreased relatively slowly in the initial phase and remained at higher concentration levels in the terminal phase (Figure 4C), resulting in longer blood exposure.

The pharmacokinetic parameters were calculated according to a two-compartment model (Table III).The order of AUC in plasma was: PEG-coated irinotecan cationic liposomes (312.93±62.49 μg·h·ml^{-1}) ≥ PEG-coated irinotecan liposomes (299.79± 58.91 μg·h·ml^{-1}) > free irinotecan (8.97 ± 2.73 μg·h·ml^{-1}). With respect to the elimination half-life in the terminal phase, the rank order of $t_{1/2}$ β values in plasma was: PEG-coated irinotecan cationic liposomes (21.71 ± 5.41h^{-1}) ≥ PEG-coated irinotecan liposomes (19.66 ± 6.35h^{-1}) > free irinotecan (13.29 ± 6.94h-1). The $t_{1/2}$ α value of PEG-coated irinotecan cationic liposomes was longer than that of free irinotecan but similar to that of PEG-coated irinotecan liposomes. The C_{max} and MRT value of free irinotecan were significantly decreased relative to PEG-coated irinotecan liposomes and PEG-coated irinotecan cationic li-

Table III. Pharmacokinetics of irinotecan after intravenous administration of free irinotecan, PEG-coated irinotecan liposomes and PEG-coated irinotecan cationic liposomes in female rats at a dose of 20.00 mg/kg.

Pharmacokinetic parameters	Free irinotecan	PEG-coated irinotecan liposomes	PEG-coated irinotecan cationic liposomes
$t_{1/2}$ α (h)	1.65 ± 0.82	1.93 ± 0.22	1.88 ± 0.39
$t_{1/2}$ β (h)	13.29 ± 6.94	19.66 ± 6.35	21.71 ± 5.41
C_{max} (μg/ml)	0.91 ± 0.33	89.52 ± 18.33	93.26 ± 20.03
CL (ml/h/kg)	1.85 ± 0.29	0.05 ± 0.01	0.04 ± 0.01
$MRT_{0\text{-}48h}$ (h)	9.85 ± 3.51	14.22 ± 0.68	15.86 ± 1.12
$AUC_{0\text{-}48h}$ (μg·h/ml)	8.97 ± 2.73	299.79 ± 58.91	312.93 ± 62.49

Data are presented as means ± SD (n = 6). $t_{1/2}\alpha$ (h), distribution half life; $t_{1/2}$ β (h), elimination half life; C_{max}, peak concentration; CL (ml/h/kg), total body clearance; $MRT_{0\text{-}48h}$, mean residence time; $AUC_{0\text{-}48h}$ (μg/ml·h), area under the plasma concentration-time curve.

posomes. But the CL value of free irinotecan was higher than those of PEG-coated irinotecan liposomes and PEG-coated irinotecan cationic liposomes.

Tissue Distribution of Irinotecan

Figure 5 and Table IV present the irinotecan levels in heart, liver, spleen, lung, kidney and tumor after intravenous administration of free irinotecan, PEG-coated irinotecan liposomes and PEG-coated irinotecan cationic liposomes at 1.0 h, 4.0 h, 8.0 h, 24 h and 48 h.

In heart, lung and kidney tissues, the irinotecan levels were approximately similar treated with free irinotecan, PEG-coated irinotecan liposomes and PEG-coated irinotecan cationic liposomes. But in liver and spleen tissue, the irinotecan level was lower in animals treated with PEG-

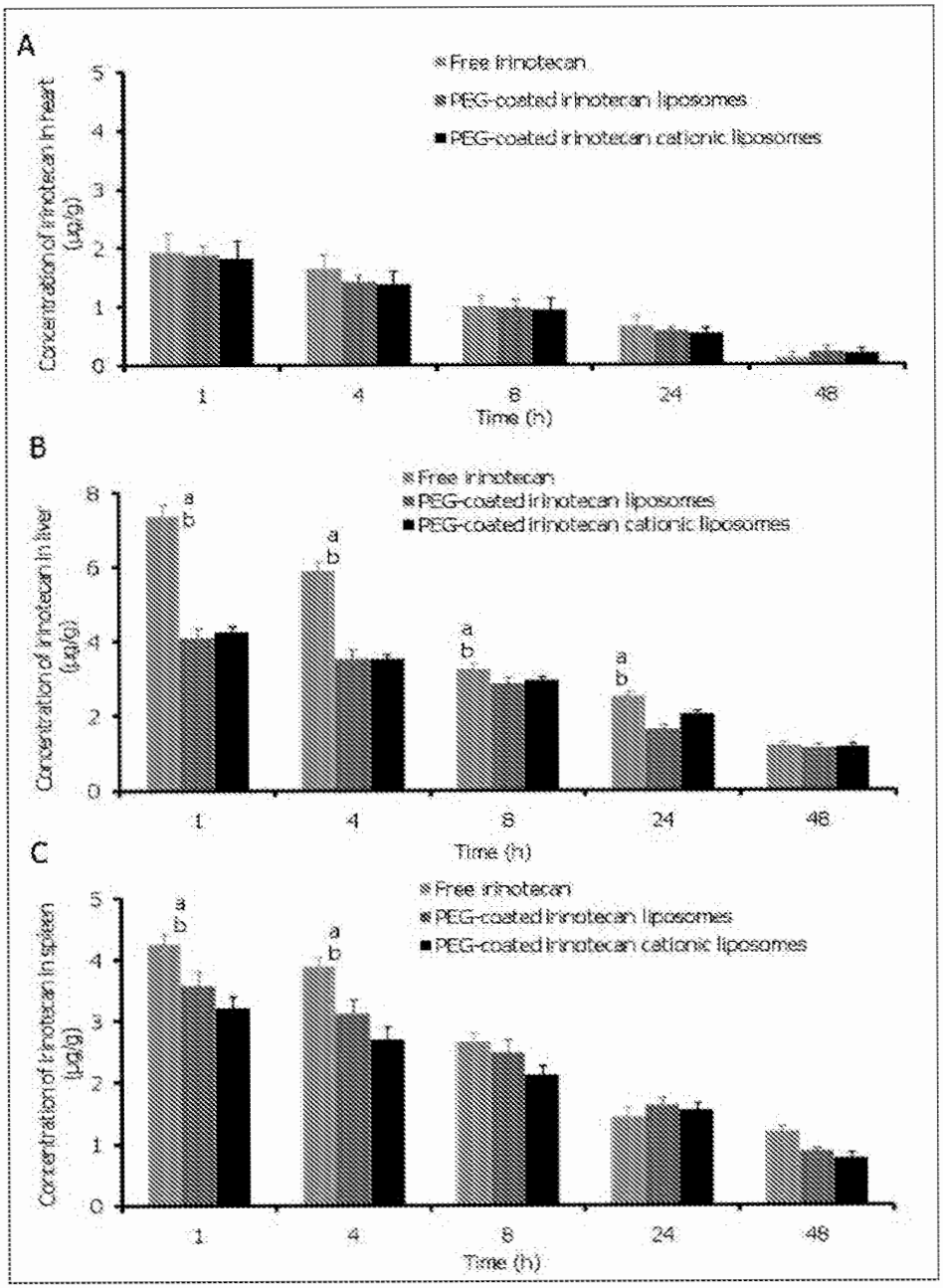

Figure 5. Irinotecan level in heart *(A)*, liver *(B)*, spleen *(C)*, lung *(D)*, kidney *(E)* and tumor *(F)* after intravenous injection of free irinotecan, PEG-coated irinotecan liposomes and PEG-coated irinotecan cationic liposomes in female BALB/c nude mice. Each point represents means ± SD (n = 6). a, $p < 0.05$, versus PEG-coated irinotecan cationic liposomes; b, $p < 0.05$, versus PEG-coated irinotecan liposomes.

Continues in the next page

Figure 5. *Continued.*

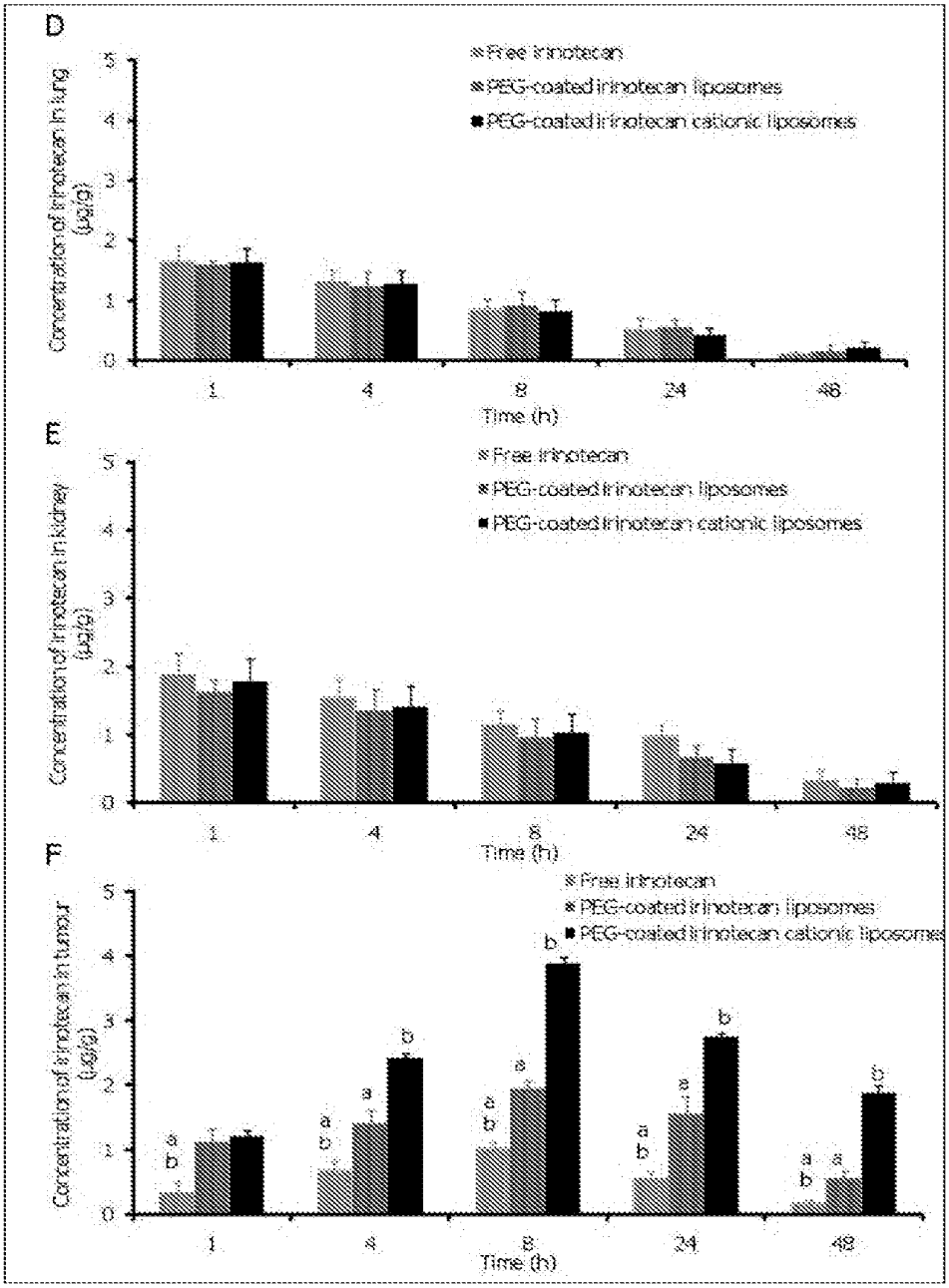

coated irinotecan cationic liposomes and PEG-coated irinotecan liposomes than in those treated with free irinotecan. The rank order of AUC values in liver tissue was: free irinotecan (81.56±3.73 ng·h/g) > PEG-coated irinotecan cationic liposomes (55.21±2.26 ng·h/g) ≥ PEG-coated irinotecan liposomes (49.91±3.51 ng·h/g). The rank order of AUC values in spleen tissue was: free irinotecan (51.82±3.04 ng·h/g) > PEG-coated irinotecan liposomes (45.56±3.89 ng·h/g) ≥ PEG-coated irinotecan cationic liposomes (39.72±3.14 ng·h/g).

In tumor masses (Figure 5F), the irinotecan level was significantly higher in the mice treated with PEG-coated irinotecan cationic liposomes than in those treated with free irinotecan and PEG-coated irinotecan liposomes at the 4, 8, 24 and 48h time points. The rank order of AUC_{0-48h} values in tumor was: PEG-coated irinotecan cationic liposomes (59.24±1.87 ng·h/g) > PEG-

Table IV. AUC0–48h (μg·h/g) after intravenous administration of free irinotecan, PEG-coated irinotecan liposomes and PEG-coated irinotecan cationic liposomes in female BALB/c nude mice at a dose of 20.00 mg/kg (n = 6).

Tissue	Free irinotecan	PEG-coated irinotecan liposomes	PEG-coated irinotecan cationic liposomes
Heart	18.71 ± 4.18	17.63 ± 2.34	16.78 ± 3.39
Liver	81.56 ± 3.73[ab]	49.91 ± 3.51	55.21 ± 2.26
Spleen	51.82 ± 3.04[ab]	45.56 ± 3.89	39.72 ± 3.14
Lung	15.46 ± 3.25	15.80 ± 3.33	14.88 ± 3.41
Kidney	22.72 ± 4.35	16.69 ± 4.64	18.19 ± 3.30
Tumor	12.49 ± 2.08[ab]	30.20 ± 4.17[a]	59.24 ± 1.87[b]

Data are presented as means±SD. [a]$p < 0.05$, versus PEG-coated irinotecan liposomes; [b]$p < 0.05$, versus PEG-coated irinotecan cationic liposomes.

coated irinotecan liposomes (30.20±4.17 ng·h/g) > free irinotecan (12.49±2.08 ng·h/g).

Discussion

Nowadays, research into the rational delivery and targeting of pharmaceutical agents is at the forefront of projects in cancer treatment. These treatments based nanoparticles can improve the specificity and help treatment cancer that cannot be treated with traditional ways, provide more effective and more convenient routes of administration, lower therapeutic toxicity, extend the product life cycle, and ultimately reduce health-care costs[24,25]. In the past few years, a number of nanoparticle-based therapeutic agents have been developed for the treatment of cancer. As a complicated therapeutic delivery system, liposome is one of the most successful nanoparticles in the market approved by FDA for the chemotherapeutic drug loading and delivery[26,27].

In this study, a kind of PEG-coated irinotecan cationic liposomes was developed for treating breast cancer. Polyethylene glycol (PEG_{2000}-DSPE) has been used widely in nanoparticle formulations as a strategy to inhibit opsonization by plasma proteins and to prolong nanoparticle plasma circulation time. The specified uptake of PEG-coated irinotecan cationic liposomes probably relies on electrostatic interaction with negatively charged target structures on MDA-MB231 breast cancer cells membrane[28]. Among the cancer cells associated target structures, there are negatively charged cell surface molecules such as glycoproteins, anionic phospholipids and proteoglycans. These are potential binding sites for cationic liposomes[29,30]. The selectivity of PEG-coated irinotecan cationic liposomes offers the possibility of targeted delivery of irinotecan or other therapeutic agents to tumor cells.

Results demonstrate that PEG-coated irinotecan cationic liposomes have the following physicochemical features: high encapsulation efficiency (Table I), well-distributed particle size (Figure 1B), and delayed drug release (Figure 1C). A lower drug release will be beneficial for preventing the rapid leakage during the process of delivery and blood/lymphatic circulation of PEG-coated irinotecan cationic liposomes, thereby possibly increasing the accumulation of the irinotecan into the tumor masses.

Cytotoxicity results demonstrate that the PEG-coated irinotecan cationic liposomes exhibit strong inhibitory effect to MDA-MB231 cancer cells (Figure 2A). The enhanced inhibitory effects of the PEG-coated irinotecan cationic liposomes are explained by MDA-MB231 cancer cells uptake study in which the PEG-coated irinotecan cationic liposomes are the most strongly endocytosed by MDA-MB231 cancer cells. In a semi-quantification way, flow cytometric measurement gives the relative drug content in the cancer cells. Results show that the PEG-coated irinotecan cationic liposomes evidently increase the irinotecan content in the MDA-MB231 breast cancer cells (Figure 2B).

The morphological studies demonstrate the existence of the nuclei fragment induced by PEG-coated irinotecan cationic liposomes. In view of the fluorescent microscopic images stained by chromatin dye Hoechst 33342 (Figure 3), the irinotecan binds to the topoisomerase I-DNA complex, thereby preventing re-ligation of DNA breaks resulting in the formation of irreversible double-strand breaks and existence of the nuclei fragment after applying PEG-coated irinotecan cationic liposomes, showing the change of nuclei as MDA-MB231 cancer cells death[31].

The inhibitory effects on tumor volume in the MDA-MB231 breast cancer cells xenografted female nude mice demonstrate that, by intravenous injection administration, the PEG-coated irinotecan cationic liposomes exhibit significantly higher antitumor activity as compared to PEG-coated irinotecan liposomes and free irinotecan (Figure 4A). As compared to free irinotecan and PEG-coated irinotecan liposomes, PEG-coated irinotecan cationic liposomes do not cause an appreciable reduction in body weight (Figure 4B).

After administering PEG-coated irinotecan cationic liposomes to the MDA-MB231 breast cancer cells xenografted female nude mice, the bone marrow indicators (WBC, Hb, and PLT) are mildly decreased, suggesting that PEG-coated irinotecan cationic liposomes may have no significant influences on bone marrow (Table II). At least, the potential myelosuppression effect may be no more than those after administering free irinotecan and PEG-coated irinotecan liposomes. Gastrointestinal toxicity (diarrhea) is frequent observed after administration of free irinotecan. It was controlled with the administration of PEG-coated irinotecan cationic liposomes and PEG-coated irinotecan liposomes.

When comparing the concentration-time profile of free irinotecan with that of PEG-coated irinotecan liposomes or PEG-coated irinotecan cationic liposomes, irinotecan blood exposure was clearly extended by the pegylated liposomes, showing a long-circulatory effect[32,33]. Pegylation with PEG_{2000}-DSPE prevents adsorption of opsonin proteins onto the surface of irinotecan liposomes, thereby prolonging the circulation time of the liposomes by avoiding rapid uptake by the reticuloendothelial system (Figure 4C).

The liver and spleen are major sites of drug metabolism and are rich in reticuloendothelial cells[34,35]. No significant difference in irinotecan levels was detected between animals administered PEG-coated irinotecan cationic liposomes and those given PEG-coated irinotecan liposomes. But after administration of PEG-coated irinotecan cationic liposomes or PEG-coated irinotecan liposomes, the irinotecan level in liver and spleen tissue was lower than free irinotecan after administration. This may be explained by the pegylated liposomes escaping rapid uptake by the reticuloendothelial system in the liver and spleen (Figure 5B and C).

Administering PEG-coated irinotecan cationic liposomes resulted in higher drug concentrations in the tumor masses than the other formulations. The higher level of irinotecan in the tumor could be attributed to specificity bind of PEG-coated irinotecan cationic liposomes by electrostatic interaction (Figure 5F). Furthermore, PEG-coated irinotecan cationic liposomes demonstrate a robust anticancer activity against the tumor xenografted with MDA-MB231 breast cancer cells.

Conclusions

In the present work, the PEG-coated irinotecan cationic liposomes were successfully developed with high entrapped efficiency, perfect size distribution, and slow releasing. The efficacies are confirmed *in vitro* and in the breast tumor by xenografting MDA-MB231 breast cancer cells into female nude mice. Mechanism studies demonstrate that PEG-coated irinotecan cationic liposomes improve the circulation time of irinotecan in the blood by escaping rapid uptake by the reticuloendothelial system and specificity bind into tumor masses by electrostatic interaction with negatively charged target structures on breast cancer cells membrane, resulting in enhancing the concentration of irinotecan in tumor area and exhibiting strong inhibitory effect to breast tumor volume. The present study provides a new strategy for treatment of the breast cancer.

Statement of Interest

This study was funded by the Colleges and Universities in Hebei Province Science and Technology Research Project (No. ZD200907).

Conflict of Interest

The Authors declare that there are no conflicts of interest.

References

1) Burns MB, Lackey L, Carpenter MA, Rathore A, Land AM, Leonard B, Refsland EW, Kotandeniya D, Tretyakova N, Nikas JB, Yee D, Temiz NA, Donohue DE, McDougle RM, Brown WL, Law EK, Harris RS. APOBEC3B is an enzymatic source of mutation in breast cancer. APOBEC3B is an enzymatic source of mutation in breast cancer. Nature 2013; 494: 366-370.

2) Montagner M, Enzo E, Forcato M, Zanconato F, Parenti A, Rampazzo E, Basso G, Leo G, Rosato A, Bicciato S, Cordenonsi M, Piccolo S. SHARP1 suppresses breast cancer metastasis by promoting degradation of hypoxia-inducible factors. Nature 2012; 487: 380-384.

3) Jemal A, Bray F, Center MM, Ferlay J, Ward E, Forman D. Global cancer statistics. CA Cancer J Clin 2011; 61:69-90.

4) Rexer BN, Arteaga CL. Optimal targeting of HER2-PI3K signaling in breast cancer: mechanistic insights and clinical implications. Cancer Res 2013; 73: 3817-3820.

5) Heinzel A, Müller D, Langen KJ, Blaum M, Verburg FA, Mottaghy FM, Galldiks N. The use of O-(2-18F-fluoroethyl)-L-tyrosine PET for treatment management of bevacizumab and irinotecan in patients with recurrent high-grade glioma: a cost-effectiveness analysis. J Nucl Med 2013; 54: 1217-1222.

6) Takano M, Goto T, Hirata J, Furuya K, Horie K, Takahashi M, Yokota H, Kino N, Kudoh K, Kikuchi Y. UGT1A1 genotype-specific phase I and pharmacokinetic study for combination chemotherapy with irinotecan and cisplatin: a Saitama Tumor Board study. Eur J Gynaecol Oncol 2013; 34: 120-123.

7) Raciborska A, Bilska K, Drabko K, Chaber R, Pogorzala M, Wyrobek E, Polczyska K, Rogowska E, Rodriguez-Galindo C, Wozniak W. Vincristine, irinotecan, and temozolomide in patients with relapsed and refractory Ewing sarcoma. Pediatr Blood Cancer 2013; 60: 1621-1625.

8) Jones RP, Sutton P, Greensmith RM, Santoyo-Castelazo A, Carr DF, Jenkins R, Rowe C, Hamlett J, Park BK, Terlizzo M, O'Grady E, Ghaneh P, Fenwick SW, Malik HZ, Poston GJ, Kitteringham NR. Hepatic activation of irinotecan predicts tumour response in patients with colorectal liver metastases treated with DEBIRI: exploratory findings from a phase II study. Cancer Chemother Pharmacol 2013; 72: 359-368.

9) Tsubamoto H, Kawaguchi R, Ito K, Shiozaki T, Takeuchi S, Itani Y, Arakawa A, Tabata T, Toyoda S. Phase II study of carboplatin and weekly irinotecan combination chemotherapy in recurrent ovarian cancer: a Kansai clinical oncology group study (KCOG0330). Anticancer Res 2013; 33: 1073-1079.

10) Giessen C, Laubender RP, Fischer von Weikersthal L, Schalhorn A, Modest DP, Stintzing S, Haas M, Mansmann UR, Heinemann V. Early tumor shrinkage in metastatic colorectal cancer: retrospective analysis from an irinotecan-based randomized first-line trial. Cancer Sci 2013; 104: 718-724.

11) Abu Lila AS, Nawata K, Shimizu T, Ishida T, Kiwada H. Use of polyglycerol (PG), instead of polyethylene glycol (PEG), prevents induction of the accelerated blood clearance phenomenon against long-circulating liposomes upon repeated administration. Int J Pharm 2013; 456: 235-242.

12) Tyagi N, Ghosh PC. Folate receptor mediated targeted delivery of ricin entrapped into sterically stabilized liposomes to human epidermoid carcinoma (KB) cells: effect of monensin intercalated into folate-tagged liposomes. Eur J Pharm Sci 2011; 43: 343-353.

13) Abu-Lila A, Suzuki T, Doi Y, Ishida T, Kiwada H. Oxaliplatin targeting to angiogenic vessels by PEGylated cationic liposomes suppresses the angiogenesis in a dorsal air sac mouse model. J Control Release 2009; 134: 18-25.

14) Sonoke S, Ueda T, Fujiwara K, Sato Y, Takagaki K, Hirabayashi K, Ohgi T, Yano J. Tumor regression in mice by delivery of Bcl-2 small interfering RNA with pegylated cationic liposomes. Cancer Res 2008; 68: 8843-8851.

15) Ho EA, Osooly M, Strutt D, Masin D, Yang Y, Yan H, Bally M. Characterization of long-circulating cationic nanoparticle formulations consisting of a two-stage PEGylation step for the delivery of siRNA in a breast cancer tumor model. J Pharm Sci 2013; 102: 227-236.

16) Nie Y, Ji L, Ding H, Xie L, Li L, He B, Wu Y, Gu Z. Cholesterol derivatives based charged liposomes for doxorubicin delivery: preparation, *in vitro* and *in vivo* characterization. Theranostics 2012; 2: 1092-1103.

17) Abu Lila AS, Okada T, Doi Y, Ichihara M, Ishida T, Kiwada H. Combination therapy with metronomic S-1 dosing and oxaliplatin-containing PEG-coated cationic liposomes in a murine colorectal tumor model: synergy or antagonism. Int J Pharm 2012; 426: 263-270.

18) Di Donato L, Cataldo M, Stano P, Massa R, Ramundo-Orlando A. Permeability changes of cationic liposomes loaded with carbonic anhydrase induced by millimeter waves radiation. Radiat Res 2012; 178: 437-446.

19) Lee SM, Ahn RW, Chen F, Fought AJ, O'Halloran TV, Cryns VL, Nguyen ST. Biological evaluation of pH-responsive polymer-caged nanobins for breast cancer therapy. ACS Nano 2010; 4: 4971-4978.

20) Lee SM, Lee OS, O'Halloran TV, Schatz GC, Nguyen ST. Triggered release of pharmacophores from [Ni(HAsO_3)]-loaded polymer-caged nanobin enhances pro-apoptotic activity: a combined experimental and theoretical study. ACS Nano 2011; 5: 3961-3969.

21) He F, Deng X, Wen B, Liu Y, Sun X, Xing L, Minami A, Huang Y, Chen Q, Zanzonico PB, Ling CC, Li GC. Noninvasive molecular imaging of hypoxia in human xenografts: comparing hypoxia-induced gene expression with endogenous and exogenous hypoxia markers. Cancer Res 2008; 68: 8597-8606.

22) Xu M, Wang G, Xie H, Huang Q, Wang W, Jia Y. Pharmacokinetic comparisons of schizandrin after oral administration of schizandrin monomer, Fructus Schisandrae aqueous extract and Sheng-Mai-San to rats. J Ethnopharmacol 2008; 115: 483-488.

23) Lee HJ, Paik WH, Lee MG. Pharmacokinetic and tissue distribution changes of adriamycin and adriamycinol after intravenous administration of adriamycin to alloxan-induced diabetes mellitus rats. Res Commun Mol Pathol Pharmacol 1995; 89: 165-178.

24) Nagarwal RC, Kant S, Singh PN, Maiti P, Pandit JK. Polymeric nanoparticulate system: a potential ap-

proach for ocular drug delivery. J Control Release 2009; 136:2-13.

25) Cuong NV, Hsieh MF. Molecular targeting of liposomal nano-particles to lymphatic system. Curr Cancer Drug Targets 2011; 11: 147-155.

26) Allen T M, Cullis PR. Drug Delivery Systems: Entering the Mainstream. Science 2004; 303: 1818-1822.

27) Peer D, Karp JM, Hong S, Farokhzad OC, Margalit R, Langer R. Nanocarriers as an emerging platform for cancer therapy. Nat Nanotechnol 2007; 2: 751-760.

28) Cuomo F, Mosca M, Murgia S, Avino P, Ceglie A, Lopez F. Evidence for the role of hydrophobic forces on the interactions of nucleotide-monophosphates with cationic liposomes. J Colloid Interface Sci 2013; 410: 146-151.

29) Barichello JM, Kizuki S, Tagami T, Soares LA, Ishida T, Kikuchi H, Kiwada H. Agitation during lipoplex formation harmonizes the interaction of siRNA to cationic liposomes. Int J Pharm 2012; 430: 359-365.

30) Banerjee A, Roychoudhury J, Ali N. Stearylamine-bearing cationic liposomes kill Leishmania parasites through surface exposed negatively charged phosphatidylserine. J Antimicrob Chemother 2008; 61: 103-110.

31) Kontek R, Matlawska-Wasowska K, Kalinowska-Lis U, Marciniak B. Genotoxic effects of irinotecan combined with the novel platinum(II) complexes in human cancer cells. Chem Biol Interact 2010; 188: 66-74.

32) Bothun GD, Lelis A, Chen Y, Scully K, Anderson LE, Stoner MA. Multicomponent folate-targeted magnetoliposomes: design, characterization, and cellular uptake. Nanomedicine 2011; 7: 797-805.

33) Kim JY, Kim JK, Park JS, Byun Y, Kim CK. The use of PEGylated liposomes to prolong circulation lifetimes of tissue plasminogen activator. Biomaterials 2009; 30: 5751-5756.

34) Mager DE, Mody V, Xu C, Forrest A, Lesniak WG, Nigavekar SS, Kariapper MT, Minc L, Khan MK, Balogh LP. Physiologically based pharmacokinetic model for composite nanodevices: effect of charge and size on *in vivo* disposition. Pharm Res 2012; 29: 2534-2542.

35) Cheng SH, Li FC, Souris JS, Yang CS, Tseng FG, Lee HS, Chen CT, Dong CY, Lo LW. Visualizing dynamics of sub-hepatic distribution of nanoparticles using intravital multiphoton fluorescence microscopy. ACS Nano 2012; 6: 4122-4131.

Journal of Cancer Therapy, 2011, 2, 470-474
doi:10.4236/jct.2011.24063 Published Online October 2011 (http://www.SciRP.org/journal/jct)

Scientific Research

Clinical Analysis of Bevacizumab plus FOLFIRI Regimen as Front-Line Therapy for Chinese Patients with Advanced Colorectal Cancer

Xijian Zhou[1], Jun Yang[2,3*], Jinying Liang[2], Peng Li[2], Yuquan Wu[4], Xiaoqiang Fan[1], Xiangyong Li[1]

[1]Department of Hematology & Oncology, 101 Hospital of PLA, Wuxi, China; [2]College of Pharmacy, Xinxiang Medical University, Xinxiang, China; [3]Kamp Institute for Medical Research, Changsha, China; [4]Deaprtment for Senior Cadres, 117 Hospital of PLA, Hangzhou, China.
Email: *bcd2009@126.com

Received July 12th, 2011; revised August 16th, 2011; accepted August 25th, 2011.

ABSTRACT

The study was designed to evaluate the therapeutic and side effects of Bevacizumab plus FOLFIRI regimen as front-line therapy for Chinese patients with advanced colorectal cancer. A total of 15 *previously untreated patients with advanced colorectal cancer received Bevacizumab plus FOLFIRI regimen as font-line therapy, in detail, irinotecan* 180 *mg/m*^{2} *was given intravenously on day1, then calcium folinate* (*CF*) 200 *mg/m*^{2}, *F-fluorouracil* (5-*Fu*) 400 *mg/m*^{2} *given in bolus immediately after CF, day* 1 - 2; 5-*Fu* 600 *mg/m*^{2} *given continuously after bolus for* 22 *hours on day* 1, *day* 2; *Bevacizumab was given intravenously at dosage of* 5 *mg/kg, on day*-1. *Therapeutic and side effects were evaluated at least after four cycles of treatment. The results showed that all the cases among the group were valid for response evaluation, with CR* 0, *PR* 10, *SD* 3, *and PD* 2. *The response rate is* 66.7% *and median time to progression* (*mTTP*) *was* 10.6 *months. The main toxicities were bone marrow suppression, nausea and vomiting, stomach pain and diarrhea; there was no chemotherapy-related death. The data suggested that the combination regimen with Bevacizumab plus FOLFIRI regimen was effective as front-line therapy for Chinese patients with advanced colorectal cancer, and the side effects were tolerable and manageable.*

Keywords: *Bevacizumab, Chinese Patients, FOLFIRI Regimen, Front-Line Therapy, Colorectal Cancer*

1. Introduction

Colorectal cancer is one of the most common types of malignant tumor in China; the rate of new cases has been increasing these years. When found, it turned out to be the advanced colorectal cancer and required systemic treatment. Irinotecan is a topoisomerase I inhibitor, in the United States plus with Fluorouracil as the first-line treatment of advanced colorectal cancer. In our country, the domestic Irinotecan came into market later than domestic Oxaliplatin, so it is now more acceptable to patients with Oxaliplatin-based first-line treatment, Irinotecan-based program for second-line, and gradually become front-line [1].

The combination therapy of Irinotecan and Fluorouracil was previously carried out by giving the Fluorouracil in bolus with the IFL program. With the usage of in-depth study of Fluorouracil, it turned out that the therapeutic index of Fluorouracil continuous infusion is superior to intravenous injection, current clinical multi-Fluorouracil continuous infusion of FOLFIRI regimen was recommended as a way of both combined with the administration program [2,3]. FOLFIRI is a chemotherapy regimen for treatment of colorectal cancer. It is made up of the following drugs: FOL—folinic acid (leucovorin), a vitamin B derivative used as a "rescue" drug for high doses of the drug methotrexate and that modulates/potentiates/reduces the side effects of fluorouracil; F-fluorouracil (5-FU), a pyrimidine analog and antimetabolite which incorporates into the DNA molecule and stops synthesis; and IRI—irinotecan (Camptosar), a topoisomerase inhibitor, which prevents DNA from uncoiling and duplicating. The clinical use of new drugs is one of the most important progressions in advanced colorectal cancer therapy, which obviously ameliorate the prognosis of the patients with advanced colorectal cancer. Cetuximab, a monoclonal antibody to epidermal growth factor receptor, is sometimes added to FOLFIRI.

Bevacizumab is an new vessel anti-tumor drug, which has not been understand well in the combination with other anti-tumor drugs treating Chinese patients with advanced colorectal cancer. The study was designed to study the therapeutic effects after the treatment with Bevacizumab plus FOLFIRI regimen with Irinotecan as the basic drug in 15 Chinese patients with advanced colorectal cancer from December 2005 to December 2007 in our hospitals.

2. Materials and Methods

2.1. General Materials

15 patients, 8 male patients, 7 female patients age 37 - 65, average age 46.7, PS score 0 - 1, 10 colon carcinoma, 5 rectal cancer. The final diagnosis by pathohistological method were as follows: 3 poorly differentiated adenocarcinoma, 5 moderately differentiated adenocarcinoma, 3 mucinous adenocarcinoma, 4 signet-ring cell carcinoma, 5 hepatic metastasis, 2 celiac lymph nodes metastasis, 3 pulmonary metastasis, 1osseous metastasis and 4 multi-organ metastasis were examined by chest x-ray, CT, and type-B ultrasonic. They all had measurable focus of infection and were initial treatment cases. Expect life cycle were more than 3 months. The clinical routine symptoms and signs as: blood, urine and faeces, hepatic and renal function, electrocardiogram, CXR and/or CT were tested before treatment, contraindication were excluded.

2.2. Treatment Programs

Irinotecan hydrochloride (Jiangsu Hengrui Pharmaceutical Company, Trade Name: Aili) 180 mg/m^2 was given intravenously on the first day, then Calcium folinate (CF) 200 mg/m^2; CF 200 mg/m^2 was given intravenously on the first and second day; 5-FU 400 mg/m^2 was given in bolus immediately after CF on the first and second day; 5-FU 600 mg/m^2 was given continuously after bolus for 22 hours on the first and second day. Bevacizumab 5 mg/kg was given intravenously before chemotherapy. 5-HT3 receptors blocking agent were used before chemotherapy to prevent nausea and omit. Atropine 0.1 mg was given subcutaneously once the cholinergic syndrome appeared. Loperamide hydrochloride was given immediately two tablets per time once the delayed diarrhea occurred, and then given one tablet per two hours, till 12 hours after the last looserstools, the total amount of loperamide was no more than 12 tablets. A cycle was two weeks, the evaluation in short result was done after 4 cycles, remission or stable disease need continue treatment until disease progression or intolerance. Before treatment, all patients signed the informed consent, tube PICC was inserted in parallel.

2.3. Evaluation Criteria

The recent results were determined by the short-term effect evaluation criteria of solid tumors by World Health Organization (WHO), the evaluation criteria are as follow: complete remission, CR, partial remission, PR, stable disease, SD, progressive disease, PD. Clinical benefit rate was calculated through the result of CR + PR + SD, Efficacy evaluation was based on physical examination, X ray, CT and other tests, followed regularly and confirmed after 4 weeks. The median time to progression (mTTP) was as the long-term indicator to evaluate the efficacy. The progression time was from the start of treatment until after the time of tumor progression. Adverse reactions were evaluated by NCI-CTC (version 2) standard evaluation, which divided into 0-IVdegrees.

3. Results

3.1. Efficacy Evaluation

All the patients were treated with a total of 93 treatment cycles, with an average of 6.2 treatment cycles for per patient. All the patients can be carried out evaluation of the efficacy and toxicity. Short-term efficacy was evaluated after 4 cycles of therapy, results were as flows: CR 0%, PR 66.7%, SD 20%, PD 13.3%, clinical benefit rate 86.7, mTTP 10.6 months.

3.2. Toxicity

Main toxicity were marrow suppression, cholinergic syndrome and delayed diarrhea, they were all listed in **Table 1**, No treatment-related death occurred to all the patients.

4. Discussion

We have adopted the combination of FOLFIRI program and anti-angiogenesis drugs Bevacizumab, discussed the efficacy and safety of the chemotherapy plus Becacizumab as therapy for Chinese patients with advanced colorectal cancer.

A big step forward in the treatment of advanced colorectal cancer is the emergence and application of monoclonal antibody drugs, which mainly included Bevacizumab for vascular endothelial growth factor (VEGF) and Cetuximab for epidermal growth factor receptor (EGFR). A number of studies have showed that, the over-expression of VEGF is closely related to the tumor invasiveness, vascular density, metastasis and recurrence and prognosis. Bevacizumab is a new anti-VEGF recombinant humanized monoclonal antibody. It plays a role in anti-angiogenesis primarily through neutralizating the VEGF and blocking its receptor-binding of the surface of endothelial

Table 1. The toxicity of Bevacizumab plus FOLFIRI regimen as front-line therapy (case).

Side effects	0 degree	I degree	II degree	III degree	IV degree
Hemoglobin	12	2	1	0	0
Leukocyte	10	3	2	0	0
Platelet	10	4	1	0	0
Liver function	9	4	1	1	0
Cretonne	13	1	1	0	0
Nausea and vomiting	8	5	1	1	0
Cholinergic syndrome	13	1	1	0	0
Delayed diarrhea	10	1	2	2	0
Constipation	12	2	1	0	0
Rash	13	1	1	0	0
Hypertension	10	4	1	0	0
Bradycardia	14	1	0	0	0
Non-infectious fever	13	2	0	0	0

cells. In addition, it can also reduce tumor interstitial fluid pressure in favor of chemotherapy drugs reaching the tumor site to play a role in anti-tumor [4]. Avastin has been approved in combination with chemotherapy for non-small cell lung cancer, colorectal cancer, breast cancer and other patients with advanced by FDA [4]. Eastern Cooperative Oncology Group conducted a randomized controlled phase III study receiving 829 patients with advance colorectal cancer who have experienced the failure treatment of combination of Irinotecan and Fluorouracil previously; they were randomly divided into 3 groups: the combination therapy of FOLFOX4 and Bevacizumab group, FOLFOX4 group and Bevacizumab monotherapy group. Bevacizumab 10 mg/kg was given by intravenous drip one time per 2 weeks, results showed that the median survival time of chemotherapy plus Bevacizumab group was 12.9 months, it was significantly longer than the chemotherapy group the median survival time of which was 10.8 months (HR = 0.75; P = 0.0011). The objective response of recent clinical evaluation also had significant increase (22.7% vs. 8.6%, P < 0.0001) [5]. Bevacizumab can not only improve the second-line treatment effects in combination with chemotherapy, it also further improves the survival of patients in combination with the first-line chemotherapy. Some researchers have evaluated the efficacy and safety of FOLFOX4 regimen combined with Bevacizumab as first-line treatment of metastasis colorectal cancer. Bevacizumab 5 mg/kg was given by intravenous drip one time per 2 weeks, among 53 patients: 8 cases CR (15.1%), 28 cases PR 28 (52.8%), objective response rate 67.9%, 11 cases SD (20.7%), 6 patients (11.3%) disease progression. Median follow-up 13.5 months, TTP 11 months, predicated 1, 2 and 3-year survival rates were 79.8%, 63.8% and 58.3% respectively. 2 patients relapsed during follow-up. 8 patients (15%) achieved RO resection of metastasis [6]. Saltz etc. reported 1401 patients with advanced colorectal cancer were randomly divided into 2 groups, Capecitabine and Oxaliplatin in XELOX group and FOLFOX4 group, then each further divided into 2 groups, plus Bevacizumab group and placebo group, the primary endpoint was PFS. The results showed that the PFS of Bevacizumab group was 9.4 months significantly longer than the placebo group with 8 months PFS (P = 0.0023) [7]. Besides in combination with the Oxaliplatin-based chemotherapy, researchers also explored the joint application of Bevacizumab and Irinotecan-based chemotherapy. In a Phase III clinical study, 923 previously untreated patients with advanced colorectal cancer were randomly divided into IFL/placebo group, IFL/Bevacizumab group and FU/LV/Bevacizumab group, Bevacizumab 5 mg/kg was given intravenously, one time per two weeks. Once the safety of IFL/Bevacizumab group was determined by the interim analysis, FU/LV/Bevacizumab group stopped into the group. Results display that the median survival time of Bevacizumab combined IFL group was significantly longer than the IFL group, and the median survival time trend of Bevacizumab combined FU/LV group was longer IFL group, suggesting that on the basis of IFL adding Bevacizumab can significantly prolong the survival time of initial treatment patients with advanced colorectal. For those patients not suitable for the application of Irinotecan, given Bevacizumab on the basis of FU/LV is also an active choice [8]. However, in this study, Fluorouracil in the combined chemotherapy was given through bolus administration, as mentioned above; this method is not the best way of co-administration. Therefore, we choose the FOLFIRI regimen consist of Irinotecan and continuous infusion of Fluorouracil as first-line chemotherapy program, on this basis, plus this anti-tumor angiogenesis drug Bevacizumab, the results showed better efficacy, recent efficiency reached 66.7%, clinical benefit rate was up to 86.7%, median time to progression was 10.6 months, they were close to the foreign literature [9]. It should be noted that the dosage of Bevacizumab in part of the foreign study was larger, in this study group was 5 mg/kg, and it can also achieved similar clinical efficacy. For the dosage of such anti-tumor angiogenesis drug, it is worth further research [5,10].

As reported in the literature, the main side effects of Irinotecan were abdominal pain, diarrhea, and bone mar-

row suppression. The first two ones can be either part of the cholinergic syndrome or occurred in the form of delayed diarrhea after 24 hours. Acute cholinergic syndrome not only include the early diarrhea and abdominal pain, but also the sweating, contracted pupil, tearing, blurred vision, dizziness and low blood pressure, the incidence of such performances was 9% as reported [11]. The incidence is this group was similar to related report, indicating that the addition of Bevacizumab did not increase the incidence of this adverse reaction. 5 patients in this group suffered from delayed diarrhea, and only 2 patients with III degree adverse reaction, which were much lower than reported in literature abroad [11]. As it will be related with patients and medicines from different sources, the small sample and timely application of Loperamide may also be a factor. The main side effects of Bevacizumab were hypertension, gastrointestinal perforation, and increased risk of bleeding and therefore not recommended for elderly patients with hypertension and the patients proposed to receive recent surgical treatment. During the treatment in this group, blood pressure changes had been closely monitored, hypertension appeared in 2 cases with normal blood pressure, the blood pressure increased further in 3 cases of primary hypertension patients, all presented as diastolic blood pressure, and they all had been controlled through the adjustment of antihypertensive drugs, no gastrointestinal perforation and bleeding occurred in the patients during the treatment.

The present study showed that after 4 cycles of therapy with Bevacizumab plus FOLFIRI regimen treating Chinese patients with advanced colorectal cancer, 1) the short-term efficacy was evaluated as flows: CR 0%, PR 66.7%, SD 20%, PD 13.3%, clinical benefit rate 86.7, and mTTP 10.6 months; 2) there was a little drug toxicity such as marrow suppression, cholinergic syndrome and delayed diarrhea, and no treatment-related death occurred. The data suggested that the therapy with Bevacizumab plus FOLFIRI regimen treating Chinese patients with advanced colorectal cancer was better than only one anticancer drug treatment or the combination treatment with Irinotecan plus Fluorouracil.

In summary, this study showed that anti-tumor angiogenesis drugs Bevacizumab combined with Irinotecan-based FORFIRI regimen as the first-line treatment of advanced colorectal cancer, they can obtain good effect for patients in China, and the side effects of this treatment can be controlled and handled, be worthy of further application.

5. Acknowledgements

This work was supported by Xinxiang Medical University and Kamp Institute for Medical Research.

REFERENCES

[1] H. Y. Luo, Y. H. Li, L. Zhang, W. Q. Jiang, Y. X. Shi, F. Wang, Y. J. He and R. H. Xu, "Efficacy of CPT-11 Combined 5-FU/CF (FOLFIRI) Regimen on Advanced Colorectal Cancer," *Chinese Journal of Cancer*, Vol. 26, No. 8, 2007, pp. 905-908.

[2] J. Li, "Application of Monoclonal Antibody in Combination with Irinotecan in the Treatment of Colorectal Cancer," *Chinese Journal of Oncology*, Vol. 28, No. 10, 2006, pp. 796-797.

[3] J. Ma, S. K. Qin and Q. Y. Zhang, "Album of Chinese Education in Clinical Oncology," Heilongjiang Science and Technology Press, Haerbin, 2007, pp. 302-306.

[4] S. P. Khosravi and P. I. Fernández, "Tumoral Angiogenesis: Review of the Literature," *Cancer Investigation*, Vol. 26, No. 1, 2008, pp. 104-108. doi:10.1080/07357900701662509

[5] B. J. Giantonio, P. J. Catalano, N. J. Meropol, P. J. O'Dwyer, E. P. Mitchell, S. R. Alberts, M. A. Schwartz and A. B. Benson, "Bevacizumab in Combination with Oxaliplatin, Fluorouracil, and Leucovorin (FOLFOX4) for Previously Treated Metastatic Colorectal Cancer: Results from the Eastern Cooperative Oncology Group Study E3200," *Journal of Clinical Oncology*, Vol. 25, No. 12, 2007, pp. 1539-1544.

[6] C. Emmanouilides, G. Sfakiotaki, N. Androulakis, K. Kalbakis, C. Christophylakis, A. Kalykaki, L. Vamvakas, A. Kotsakis, S. Agelaki, E. Diamandidou, N. Tsourouglou, A. Chatzidakis, V. Georgoulias, D. Mavroudis and J. Souglakos, "Front-Line Bevacizumab in Combination with Oxaliplatin, Leucovorin And 5-Fluorouracil (FOLFOX) in Patients with Metastatic Colorectal Cancer: A Multicenter Phase II Study," *BMC Cancer*, Vol. 7, 2007, p. 91.

[7] L. B. Saltz, S. Clarke, E. Díaz-Rubio, W. Scheithauer, A. Figer, R. Wong, S. Koski, M. Lichinitser, T. S. Yang, F. Rivera, F. Couture, F. Sirzén and J. Cassidy, "Bevacizumab in Combination With Oxaliplatin-Based Chemotherapy as First-Line Therapy in Metastatic Colorectal Cancer: A Randomized Phase III Study," *Journal of Clinical Oncology*, Vol. 26, No. 12, 2008, pp. 2013-2019.

[8] H. I. Hurwitz, L. Fehrenbacher, J. D. Hainsworth, W. Heim, J. Berlin, E. Holmgren, J. Hambleton, W. F. Novotny and F. Kabbinavar, "Bevacizumab in Combination with Fluorouracil and Leucovorin: An Active Regimen for First-Line Metastatic Colorectal Cancer," *Journal of Clinical Oncology*, Vol. 23, No. 15, 2005, pp. 3502- 3508.

[9] H. Hurwitz, L. Fehrenbacher, W. Novotny, T. Cartwright, J. Hainsworth, W. Heim, J. Berlin, A. Baron, S. Griffing, E. Holmgren, N. Ferrara, G. Fyfe, B. Rogers, R. Ross and F. Kabbinavar, "Bevacizumab Plus Irinotecan, Fluorouracil, and Leucovorin for Metastatic Colorectal Cancer," *The New England Journal of Medicine*, Vol. 350, 2004, pp. 2335-2342.

[10] D. R. Gandara, R. Sangha and A. M. Davies, "Bevacizu-

mab: Optimal Dose, Schedule, and Duration of Therapy," *Clinical Lung Cancer*, Vol. 8, No. 9, 2007, pp. 522-523.

[11] C. Tournigand, T. André, E. Achille, G. Lledo, M. Flesh, D. Mery-Mignard, E. Quinaux, C. Couteau, M. Buyse, G. Ganem, B. Landi, P. Colin, C. Louvet and A. de Gramont, "FOLFIRI Followed by FOLFOX6 or the Reverse Sequence in Advanced Colorectal Cancer: A Randomized GERCOR Study," *Journal of Clinical Oncology*, Vol. 22, 2004, pp. 229-237.

Electronic Acknowledgement Receipt

EFS ID:	42155033
Application Number:	15809815
International Application Number:	
Confirmation Number:	5137
Title of Invention:	Methods for Treating Metastatic Pancreatic Cancer Using Combination Therapies Comprising Liposomal Irinotecan and Oxaliplatin
First Named Inventor/Applicant Name:	Eliel Bayever
Customer Number:	153749
Filer:	Mary Rucker Henninger/Richard King
Filer Authorized By:	Mary Rucker Henninger
Attorney Docket Number:	263266-421428
Receipt Date:	12-MAR-2021
Filing Date:	10-NOV-2017
Time Stamp:	16:26:22
Application Type:	Utility under 35 USC 111(a)

Payment information:

Submitted with Payment	no

File Listing:

Document Number	Document Description	File Name	File Size(Bytes)/ Message Digest	Multi Part /.zip	Pages (if appl.)
1	Information Disclosure Statement (IDS) Form (SB08)	2021-03-12_01208-0007-01US_SB08_6_OF_6_as_filed.pdf	1057193 385212f8b1cf269c4227083bc6185dfb9a9b8b80	no	8

Warnings:

Information:					
A U.S. Patent Number Citation or a U.S. Publication Number Citation is required in the Information Disclosure Statement (IDS) form for autoloading of data into USPTO systems. You may remove the form to add the required data in order to correct the Informational Message if you are citing U.S. References. If you chose not to include U.S. References, the image of the form will be processed and be made available within the Image File Wrapper (IFW) system. However, no data will be extracted from this form. Any additional data such as Foreign Patent Documents or Non Patent Literature will be manually reviewed and keyed into USPTO systems.					
2	Non Patent Literature	Stathopoulos_2012.pdf	312319 af080d031391b05732c1054ecc940f1a0ec02c71	no	10
Warnings:					
Information:					
3	Non Patent Literature	Stathopoulos_2006b.pdf	138951 c34e7010e543ea699db8b4bd1b8ab04e35ae4215	no	5
Warnings:					
Information:					
4	Non Patent Literature	Stylianopoulos_2013.pdf	287641 0ed55ff27983a31d89e7af4a1e541e3853f176f8	no	6
Warnings:					
Information:					
5	Non Patent Literature	Takano_2010.pdf	203216 0f8742ac09367bba7ae6a931951e5b8171758916	no	9
Warnings:					
Information:					
6	Non Patent Literature	Tardi_2000.pdf	522288 a5fa7ed06d1bd6f2ef296dc680ed593268a644ac	no	5
Warnings:					
Information:					
7	Non Patent Literature	Tardi_2007.pdf	304154 2499cf600e45e5b99bc2720f4ad165dfbd3b9ebd	no	10
Warnings:					
Information:					

8	Non Patent Literature	Toutain_2004.pdf	221745 81bee223ef1c65477106b6bbafd8150b0c7ab4ea	no	13
Warnings:					
Information:					
9	Other Reference-Patent/App/Search documents	US15664976_2019-11-04_OA.pdf	311522 b6603dbb35daf488a52cffe487cfe40e61be9f08	no	9
Warnings:					
Information:					
10	Other Reference-Patent/App/Search documents	US15664976_2020-05-18_OA.pdf	517944 20eab0d8e86eb6d1403d26e9cac77e064de4083e	no	11
Warnings:					
Information:					
11	Other Reference-Patent/App/Search documents	US15664976_2020-10-13_NOA.pdf	1317569 2063811a260879088f47e028aae3a314650afbcb	no	13
Warnings:					
Information:					
12	Other Reference-Patent/App/Search documents	US15809815_2020-02-27_OA.pdf	603129 154a27ee7548404d30093f8e954d7cac5254e0f7	no	16
Warnings:					
Information:					
13	Other Reference-Patent/App/Search documents	US15896389_2020-01-31_OA.pdf	1031092 c96fd9927530ab8e7d83e1b5fb4166383f218f77	no	28
Warnings:					
Information:					
14	Other Reference-Patent/App/Search documents	US15896389_2020-03-26_Int_Sum.pdf	1010771 baebcffd82171f3130cf10eb08f724afccd9240c	no	22
Warnings:					
Information:					

15	Other Reference-Patent/App/Search documents	US15896389_2020-04-09_AA.pdf	141440 b3bb6111d2318b5e4706f6d4611ffe4c280f6360	no	3
Warnings:					
Information:					
16	Other Reference-Patent/App/Search documents	US15896389_2020-06-05_NOA_Int_Sum.pdf	593233 9ec02a44958c7177def5604fb0bae4cf20382b61	no	13
Warnings:					
Information:					
17	Other Reference-Patent/App/Search documents	US16012351_2020-01-07_OA.pdf	324528 d36a5101ee4b89447679644e362b711c81c8f5ab	no	9
Warnings:					
Information:					
18	Other Reference-Patent/App/Search documents	US16012372_2020-01-07_OA.pdf	316850 d889b3b61605ed9c55216f7739975a0a1ce3432b	no	9
Warnings:					
Information:					
19	Other Reference-Patent/App/Search documents	US16012372_2020-07-27_OA.pdf	307104 322ff283c77b081f08e779797d2a86006ddabe21	no	8
Warnings:					
Information:					
20	Other Reference-Patent/App/Search documents	US16302050_2020-01-17_OA.pdf	647464 fea765c8800c405490659057daf8fdd67b116edc	no	17
Warnings:					
Information:					
21	Other Reference-Patent/App/Search documents	US16510394_2020-03-06_OA.pdf	617587 fa01b6876003c57beac90cb296810eeb447e5d28	no	15
Warnings:					
Information:					

22	Other Reference-Patent/App/Search documents	US16567902_2020-04-27_OA.pdf	748411 0b07e346e48596db338aff08c69c54c11628368c	no	20
Warnings:					
Information:					
23	Other Reference-Patent/App/Search documents	US16567902_2020-08-10_OA.pdf	817129 bfb4a42fb4021662753ea15ae336303186129a5c	no	21
Warnings:					
Information:					
24	Other Reference-Patent/App/Search documents	US16586609_2020-10-05_OA.pdf	181689 881e85764b50a96bbebca84adfee800d2e6face6	no	5
Warnings:					
Information:					
25	Non Patent Literature	Vaage_1999.pdf	525688 e4669882341fb6e429cb8bc9d28ba081556cb99e	no	5
Warnings:					
Information:					
26	Non Patent Literature	Veal_2001.pdf	123699 4b9e6677b8f25c16772061b599be2eabf9c83f4c	no	7
Warnings:					
Information:					
27	Non Patent Literature	Venook_2005.pdf	136728 1333cfdacdc77643768de5d65d585814f6cd9376	no	12
Warnings:					
Information:					
28	Non Patent Literature	Ventura_2017_poster.pdf	714366 53e6c113623c2281a66aa26606e9c315de2f8af2	no	6
Warnings:					
Information:					

29	Non Patent Literature	Villalona-Calero_2003.pdf	311875 956b80a43aa81a477b6ce5e3ada196d4fb0b7617	no	10
Warnings:					
Information:					
30	Non Patent Literature	Walker_2005.pdf	137949 69f8d65c13949857e415b9ab75465c1cf276bb03	no	11
Warnings:					
Information:					
31	Non Patent Literature	Wang_1998.pdf	422884 df964f711ac6ab33c845911e70e0ba40eca06f29	no	4
Warnings:					
Information:					
32	Non Patent Literature	Wei_2013.pdf	909603 6e2199d931d8fbbe8e4aa6d80d655e057bf3a87a	no	9
Warnings:					
Information:					
33	Non Patent Literature	Weng_2013.pdf	742681 c203b61f5d7cf9a4cf338da074cc1d587f4364f6	no	13
Warnings:					
Information:					
34	Non Patent Literature	Weng_2008.pdf	341929 6e7dec141ec6f4e99f2d9845f82d2d9e87cc050e	no	7
Warnings:					
Information:					
35	Non Patent Literature	Willett_2004.pdf	369425 6df513aad2033554ec7baa33db8f62346b698817	no	7
Warnings:					
Information:					

36	Non Patent Literature	Wulaningsih_2016.pdf	200746 db127814ab85043808f1bc938f3f1c1ad9a1fd6c	no	36
Warnings:					
Information:					
37	Non Patent Literature	Xeloda_PI_2000.pdf	249337 e14695b15a21fb32e3cde65398008a82221560d2	no	19
Warnings:					
Information:					
38	Non Patent Literature	Yamashita_2007.pdf	430632 7fd9ee065e6b7bd80e216dd1605301fa4448fcc8	no	9
Warnings:					
Information:					
39	Non Patent Literature	Yamashita_2006b.pdf	341891 ff08cbef928ecde7a8f2b009a99df6f2b306eda3	no	7
Warnings:					
Information:					
40	Non Patent Literature	Yang_2019.pdf	399657 b9f0795b8fe732a00a3927ca876e84690efeec78	no	11
Warnings:					
Information:					
41	Non Patent Literature	Yang_2019b.pdf	480873 39beab9d750da7821e678544b32ec9ab9297b4e7	no	10
Warnings:					
Information:					
42	Non Patent Literature	Yang_2011.pdf	386155 1182d063cceda5c56716a7c4406a05b1fcdaf6c9	no	8
Warnings:					
Information:					

43	Non Patent Literature	Yoo_ESMO_2019_poster.pdf	3693854 47d5db4a8540f903d5a6225a8ca5e7e2ca2bd654	no	6
Warnings:					
Information:					
44	Non Patent Literature	Yoo_ESMO_2019_abstract.pdf	48890 4259ca75931151fa64ae6965707e07db1aaf85a0	no	1
Warnings:					
Information:					
45	Non Patent Literature	Younis_2009.pdf	433574 600b566db37bd4055aae66a22bed9b4e26bb2d50	no	16
Warnings:					
Information:					
46	Non Patent Literature	Zamboni_2009.pdf	349766 e421da07366ae3b8ee3a9a2412ae93d2164ea394	no	10
Warnings:					
Information:					
47	Non Patent Literature	Zhang_2015.pdf	433230 424c4a703ab18c31594eba6b403f66f81dfd488	no	12
Warnings:					
Information:					
48	Non Patent Literature	Zhang_2013.pdf	1098552 9d7d6872e2cfb6260c8a1bda031d0d7cdf72aa5f	no	15
Warnings:					
Information:					
49	Non Patent Literature	Zhou_2011.pdf	192061 eb00acd57e6b5a6a42bc9e4a1d8654ef0c7f5039	no	5
Warnings:					
Information:					
			Total Files Size (in bytes):	26011014	

This Acknowledgement Receipt evidences receipt on the noted date by the USPTO of the indicated documents, characterized by the applicant, and including page counts, where applicable. It serves as evidence of receipt similar to a Post Card, as described in MPEP 503.

New Applications Under 35 U.S.C. 111

If a new application is being filed and the application includes the necessary components for a filing date (see 37 CFR 1.53(b)-(d) and MPEP 506), a Filing Receipt (37 CFR 1.54) will be issued in due course and the date shown on this Acknowledgement Receipt will establish the filing date of the application.

National Stage of an International Application under 35 U.S.C. 371

If a timely submission to enter the national stage of an international application is compliant with the conditions of 35 U.S.C. 371 and other applicable requirements a Form PCT/DO/EO/903 indicating acceptance of the application as a national stage submission under 35 U.S.C. 371 will be issued in addition to the Filing Receipt, in due course.

New International Application Filed with the USPTO as a Receiving Office

If a new international application is being filed and the international application includes the necessary components for an international filing date (see PCT Article 11 and MPEP 1810), a Notification of the International Application Number and of the International Filing Date (Form PCT/RO/105) will be issued in due course, subject to prescriptions concerning national security, and the date shown on this Acknowledgement Receipt will establish the international filing date of the application.

CANCERS OF THE COLON AND RECTUM

Phase I study of biweekly liposome irinotecan (PEP02, MM-398) in metastatic colorectal cancer failed on first-line oxaliplatin-based chemotherapy.

Li-Tzong Chen, Her-Shyong Shiah, Peng-Chan Lin, Jeng-Chang Lee, Wu-Chou Su, Yi-Wen Wang, Grace Yeh, Jang-Yang Chang

National Health Research Institutes, Tainan, Taiwan; National Cheng Kung University Hospital, Tainan, Taiwan; PharmaEngine, Inc., Taipei, Taiwan

Show Less

Abstract

613

Background: PEP02 (MM-398) is a nanoliposomal formulation of irinotecan (CPT-11) that has improved pharmacokinetics (PK) and tumor distribution of CPT-11 and its active metabolite, SN-38. PEP02 single agent q3w has shown preliminary efficacy and safety in Phase II pancreatic and gastric cancer studies. Since irinotecan is approved for metastatic colorectal cancer (mCRC) and biweekly regimens are widely used, the aims of this study are to determine the maximum tolerated dose (MTD), characterize the PK and pharmacogenetics (PGx), and explore the efficacy of PEP02 q2w in mCRC.

Methods: Patients (pts) with disease progression after 1st-line oxaliplatin-based chemotherapy, ECOG PS 0-1, and without prior exposure to irinotecan were eligible. PEP02 was given on day 1 and 15 of each 28 day treatment cycle. The starting dose was 80 mg/m^2 and escalated by 10 mg/m^2 to the target dose of 100 mg/m^2. PK was evaluated during the 1st cycle and the tumor response was assessed by RECIST.

Results: A total of 18 pts (M/F 9/9; median age 57.5) were enrolled, with 6 at each dose level. Dose-limiting toxicity manifested as G3 diarrhea was observed in one pt per dose level. The target dose of 100 mg/m^2 was determined to be the MTD. Nine pts had dose delayed (4, 3, 2 at 80, 90, 100 mg/m^2), mostly because of

ARTICLE CITATION

DOI: 10.1200/jco.2012.30.4_sup
Journal of Clinical Oncology 30, no. 4_suppl (February 2012) 613-613.

PMID: 27983424

neutropenia. The PK and PGx are being analysed. As of August 2011, there are 3 pts still on study treatment and 17 pts evaluable for tumor response. Four pts (2 at 80 mg/m^2, 1 each at 90 and 100 mg/m^2) showed partial response (3 after 2 cycles and 1 after 8 cycles) and 8 pts (3 each at 80 and 90 mg/m^2, 2 at 100 mg/m^2) maintained stable disease for at least 2 cycles, which resulted in a response rate (RR) of 23.5% and a disease control rate (DCR) of 70.6%. Current median progression-free survival (PFS) is 4 months and 8 pts (47%) had PFS $\geq$ 6 months.

Conclusions: The MTD of biweekly PEP02 is 100 mg/m^2. As a 2nd-line monotherapy after oxaliplatin-based chemotherapy, the efficacy results indicate the potential benefit of PEP02 for mCRC (FOLFIRI-1 achieved only 4% RR, 34% DCR, and 2.5 months PFS in FOLFOX pretreated pts). A randomized Phase II study evaluating PEP02 plus 5-FU/LV (FUPEP regimen) vs. FOLFIRI is currently ongoing in France.

capecitabine (X) in metastatic colorectal cancer (MCRC) patients (pts)
N. Anderson, J Clin Oncol

Phase I study of weekly oxaliplatin (OXA) + 5-fluorouracil continuous infusion (FU CI) in patients (pts) with advanced colorectal cancer (CRC)
L. M. Pasetto et al., J Clin Oncol

A phase 1b dose-escalation trial of erlotinib, capecitabine and oxaliplatin in metastatic colorectal cancer (MCRC) patients
J. P. Delord, J Clin Oncol

FOLFIRI Plus Bevacizumab as Second-Line Therapy in Patients With Metastatic Colorectal Cancer
PracticeUpdate

FOLFIRI and XELIRI Are Safe, Well-tolerated in Metastatic Colorectal Cancer
Jason Hoffman et al., Cancer Therapy Advisor

FOLFOX4 vs Sequential Dose-Dense FOLFOX7 Followed by FOLFIRI in Patients With Resectable Metastatic Colorectal Cancer
PracticeUpdate

FOLFOXIRI Plus Bevacizumab Is Associated with Superior PFS for Metastatic Colorectal Cancer
Bryant Furlow, Cancer Therapy Advisor

Modified FOLFOX6 With or Without Aflibercept in mCRC

G. Folprecht et al., Medscape

Antiemetics: American Society of Clinical Oncology Clinical Practice Guideline Update
Hesketh et al.

MONARCH 2: Abemaciclib in Combination With Fulvestrant in Women With HR+/HER2– Advanced Breast Cancer Who Had Progressed While Receiving Endocrine Therapy
Sledge et al.

Use of Adjuvant Bisphosphonates and Other Bone-Modifying Agents in Breast Cancer: A Cancer Care Ontario and American Society of Clinical Oncology Clinical Practice Guideline
Dhesy-Thind et al.

Chiang et al. BMC Cancer (2016) 16:907
DOI 10.1186/s12885-016-2933-6

BMC Cancer

RESEARCH ARTICLE Open Access

A phase I dose-escalation study of PEP02 (irinotecan liposome injection) in combination with 5-fluorouracil and leucovorin in advanced solid tumors

Nai-Jung Chiang[1,2], Tsu-Yi Chao[3], Ruey-Kuen Hsieh[4], Cheng-Hsu Wang[5], Yi-Wen Wang[6], C. Grace Yeh[6] and Li-Tzong Chen[1,2,7*]

Abstract

Background: PEP02 (also known as MM-398, nal-IRI) is a novel nanoparticle formulation of irinotecan encapsulated in liposomes. The aims of this study were to investigate the dose-limiting toxicity (DLT), maximum tolerated dose (MTD) and pharmacokinetics (PK) of PEP02 in combination with 5-FU and LV, in patients with advanced refractory solid tumors.

Methods: Patients were enrolled in cohorts to receive PEP02 from 60 to 120 mg/m^2 (dose expressed as the irinotecan hydrochloride trihydrate salt) as a 90-min intravenous infusion on day 1, followed by 24 h infusion of 5-FU 2,000 mg/m^2 and LV 200 mg/m^2 on days 1 and 8, every 3 weeks.

Results: A total of 16 patients were assigned to four dose levels, 60 (three patients), 80 (six patients), 100 (five patients) and 120 mg/m^2 (two patients). DLT was observed in four patients, two at the 100 mg/m^2 dose level (one had grade III infection with hypotension and grade III hemorrhage; the other had grade III diarrhea and grade IV neutropenia), and two at the 120 mg/m^2 dose level (one had grade III diarrhea and grade IV neutropenia; the other had grade III diarrhea). The MTD of PEP02 was determined as 80 mg/m^2. The most common treatment-related adverse events were nausea (81%), diarrhea (75%) and vomiting (69%). Among the six patients who received the MTD, one patient exhibited partial response, four patients had stable disease and one showed progressive disease. Pharmacokinetic data showed that PEP02 had a lower peak plasma concentration, longer half-life, and increased area under the plasma concentration-time curve from zero to time t of SN-38 than irinotecan at similar dose level.

Conclusions: The MTD of PEP02 on day 1 in combination with 24-h infusion of 5-FU and LV on days 1 and 8, every 3 weeks was 80 mg/m^2, which will be the recommended dose for future studies.

Trial registration: The trial was retrospectively registered (NCT02884128) with date of registration: August 12, 2016.

Keywords: Liposomal irinotecan, 5-fluorouracil, Dose-limiting toxicity, Maximum tolerated dose

* Correspondence: leochen@nhri.og.tw; leochen@nhri.org.tw
[1]National Institute of Cancer Research, National Health Research Institutes, 2F, No. 367, Sheng-Li Road, Tainan 704, Taiwan
[2]Division of Hematology/Oncology, Department of Internal Medicine, National Cheng Kung University Hospital, Tainan, Taiwan
Full list of author information is available at the end of the article

Background

PEP02 (also known as MM-398, nal-IRI) is an encapsulated nanoliposomal formulation of irinotecan hydrochloride (CPT-11) [1]. Irinotecan is a water-soluble semi-synthetic analogue of the natural alkaloid, camptothecin. It prevents DNA from unwinding and replication by inhibition of topoisomerase-I, and has already been approved for use worldwide. However, at higher dosage, irinotecan causes severe diarrhea and myelosuppression, which limits its therapeutic index. The therapeutic benefits of encapsulating anti-cancer drugs such as daunorubicin, doxorubicin and cytarabine in liposomes have been documented [2]. An appropriately designed liposome formulation may reduce the toxicity of cytotoxic agents to healthy tissues while maintaining its anti-tumor potency, which in turn improves treatment efficacy.

In our previous study, the maximum tolerated dose (MTD) of PEP02 monotherapy was found to be 120 mg/m^2 at 3-week interval with favorable pharmacokinetic (PK) parameters of the active metabolite, SN-38 [3]. The acceptable toxicity profile explains the beneficial effects of PEP02 in combination with other cytotoxic agents. Irinotecan in combination with 5-fluorouracil (5-FU) and leucovorin (LV) is the first-line or second-line therapy for locally advanced and metastatic colorectal cancer [4]. A synergistic effect was observed upon the sequential administration of irinotecan and 5-FU [5, 6]. On the basis of these results, the combination of PEP02 with 5-FU and LV is considered a reasonable approach to enhance their therapeutic efficacy. This Phase I dose escalation study aimed to investigate the MTD, dose-limiting toxicity (DLT) and recommended dose of PEP02 in combination with 5-FU and LV.

Irinotecan is converted by carboxylesterases to its potent metabolite, SN-38, which is detoxified in part by converting to inactive SN-38 glucuronide (SN-38G) through UDP-glucuronosyl transferase 1A isoforms (UGT1A) [7]. The activity of UGT1A is related to gene polymorphism of *UGT1A* family members. Individuals with genetic mutations of *UGT1A* exhibit reduced glucuronidation of SN-38 and an elevated risk of neutropenia and diarrhea compared with patients with wild-type alleles [8]. The correlation of *UGT1A* polymorphisms and toxicities is discussed.

Methods

Patient eligibility

This trial was a multi-center, open-label, Phase I, dose escalation study of PEP02 (PharmaEngine, Inc., Taipei, Taiwan) in combination with 5-FU and LV in patients with advanced solid tumors. The inclusion criteria were as follows: (1) histologically or cytologically confirmed advanced solid tumor refractory to standard systemic chemotherapy; (2) aged between 20 and 70 years; (3) Eastern Cooperative Oncology Group performance score (ECOG PS) of 0 or 1; (4) life expectancy ≥ 2 months; (5) adequate bone marrow, hepatic and renal functions: white blood cells ≥ 3,000/mm^3, absolute neutrophil count ≥ 1,500/mm^3, platelets ≥ 100,000/mm^3, hemoglobin ≥ 10 g/dL, serum total bilirubin within normal range, AST and ALT ≤ 3× upper limit of normal range, serum creatinine ≤ 1.5 mg/dL and blood urea nitrogen ≤ 25 mg/dL; (6) no prior treatment for at least 4 weeks before study initiation, including major surgery, chemotherapy, any investigational products or radiotherapy (6 weeks for nitrosoureas and mitomycin C); (7) recovered from all treatment-related toxicities or resolved to no greater than grade 1 before enrollment; and (8) written informed consent.

The exclusion criteria were as follows: (1) known or suspicious primary or secondary brain tumors; (2) HBsAg-positive or anti-HCV antibody-positive with splenomegaly (defined as spleen size > 11 cm measured in longest diameter by CT scan); (3) uncontrolled active infection or other concomitant serious disease; (4) pregnancy or breast-feeding; (5) previous exposure to irinotecan; (6) history of allergic reactions to compounds of similar chemical or biologic composition as PEP02, 5-FU, or LV. This trial was approved by the independent ethics committee of each participating institute and the Department of Health, Executive Yuan, Taiwan, and was performed in accordance with International Conference on Harmonization Good Clinical Practice guidelines and Good Clinical Laboratory Practice.

Treatment and dose escalation schedule

The study had a traditional 3 + 3 design with three-patient cohorts for each dose level. Dose escalation was only performed after the successful completion of at least 1 full 3-week cycle by each patient in the dosing cohort. If none of the first three patients experienced DLT, dose escalation was carried out for the next cohort of patients. If one of three patients developed DLT, the cohort was expanded to six patients. If two or more patients experienced any DLT, no more patients were to be entered at the current dose level and the lower dose level was to be declared the MTD. The MTD was the highest dose level with no more than 1 DLT among the accruals. A minimum of six patients were required to be tested at the dose level defined as the MTD. The starting dose of PEP02 was 60 mg/m^2 with dose expressing as the irinotecan hydrochloride trihydrate salt, which was escalated by increments of 20 mg/m^2 between dose levels. Each patient was assigned to a dose level, and no intra-patient dose escalation was allowed. 5-FU and LV were administered at a fixed dose of 2000 and 200 mg/m^2, respectively. PEP02 was administered by intravenous

infusion over 90 min on Day 1, followed by 24-h intravenous infusion of 5-FU and LV on days 1 and 8 every 3 weeks. Pre-medication included dexamethasone and a serotonin-antagonist. Prophylactic anti-cholinergic agent was not administered unless acute cholinergic reaction was observed in prior cycles of treatment. Anti-diarrhea agents were started according to the guideline of American Society of Clinical Oncology. Treatment was continued to a maximum of 6 cycles or until disease progression, unacceptable toxicity, treatment delay > 2 weeks, or patient's refusal or death.

Dose modification on day 1 of subsequent cycles was only applied to PEP02, while the dosage of 5-FU/LV remained unchanged. All dose modifications were to be based on the worst proceeding toxicity. For patients who experienced ≥ grade 3 hematologic or non-hematologic toxicities, the dose of PEP02 was reduced by one dose level. In addition, the dose of 5-FU on day 8 of each cycle could be adjusted according to the laboratory data before the dosing. If the absolute neutrophil count (ANC) is between 1,000 and 1,499/μL, platelet count is between 50,000 and 99,999/μL, or diarrhea of grade 2 severity is observed, the dose of 5-FU could be decreased by 25%. 5-FU was withheld when ANC < 999/μL, platelet count < 50,000/μL or grade 3 diarrhea was observed. The conditions for the administration of the next cycle of treatment were ANC ≥ 1,500/μL, platelet counts ≥ 100,000/μL, serum creatinine ≤ 1.5 mg/dL, and full resolution of gastrointestinal toxicities.

Definition of dose-limiting toxicity (DLT)

Toxicities were assessed according to the National Cancer Institute's CTCAE version 3.0 (CTCAE, v3). DLT was defined as occurrence of 1 or more of the following events attributable to the study drugs during the first cycle: (1) grade III or IV non-hematological toxicity, except grade III nausea, vomiting, or anorexia; (2) grade IV hematologic toxicity lasting for ≥3 days; (3) grade III hematologic toxicity associated with complications (e.g. neutropenic fever or bleeding); (4) dose delay of more than 2 weeks owing to drug-related toxicity. In addition, hematological assessment was performed daily whenever grade IV hematological toxicity occurred.

Patient evaluation

Pretreatment evaluations included medical history, physical examination, performance status, complete blood count, hepatic and renal functions and serology of HBsAg and anti-HCV antibody. Patients were evaluated weekly with complete blood count and biochemistry analysis. Radiologic studies to assess response were performed at baseline and then every 2 cycles of therapy according to the guidelines of Responses Evaluation Criteria in Solid Tumors criteria version 1.0. All complete and partial responses required confirmation by two consecutive observations at least 4 weeks apart.

Pharmacokinetic sampling and analyzing

During the first cycle of treatment, blood samples were collected before treatment, during the infusion at 30 and 60 min, at the end of infusion, at1, 3, 9, 24, 48, 72 and 168 h after the end of infusion, and before the second cycle. Plasma levels of irinotecan and SN-38 were measured by validated LC/MS/MS analytical methods. The peak plasma concentration (C_{max}), time at which C_{max} occurred (T_{max}), elimination half-life ($t_{1/2}$), area under the plasma concentration-time curve from zero to time t ($AUC_{0\to t}$), AUC through infinite time ($AUC_{0\to\infty}$), and clearance (CL) were calculated. Pharmacokinetic parameters of individual data set were analyzed by a non-compartmental model by using WinNonlin™ (Centara, St. Louis, MO).

Pharmacogenetic studies

Additional 5 mL blood sample was collected into a PAXgene vacutainer tube and DNA was extracted using a DNA purification kit. Fragment analysis was used for the detection of short tandem repeat polymorphism. The TaqMan-Allelic discrimination method or direct sequencing was used for the detection of single nucleotide polymorphisms, including *UGT1A1*28* and *UGT1A1*6*.

Statistical analysis

The statistical analysis was descriptive and any inferential statistics was exploratory in nature. Summary statistics were provided for all efficacy, pharmacokinetic, pharmacogenetic, safety and baseline/demographic variables. For categorical variables, frequency tables including percentages were presented. For continuous variables, descriptive statistics such as number of available observations, mean with standard deviation (STD), minimum, and maximum were tabulated.

Results

Patient characteristics, dose escalation, DLT and MTD

Between March 2006 and August 2008, a total of 16 patients (seven men and nine women) were enrolled. The demographics and baseline characteristics of all patients are summarized in Table 1. The median age was 49 years (range: 30–67 years). The most common primary tumors were pancreatic, stomach, and breast carcinomas. Other tumor types included keratinizing squamous cell carcinoma, cervical cancer and nasopharyngeal carcinoma. A total of 66 cycles of treatment were initiated, with an average of 4.1 cycles per patient (range: 1–6 cycles). There were seven patients (43.8%) completed all 6 cycles of treatment.

Table 1 Patient characteristics

Characteristic	Patients, n (%)
Patients enrolled	16
Age (yrs)	
Median	49
Range	30–67
Sex	
Male	7 (44)
Female	9 (56)
ECOG performance status	
0	3 (19)
1	13 (81)
Tumor type	
Breast cancer	4 (25)
Pancreatic cancer	5 (31)
gastric cancer	4 (25)
Other	3 (19)
Previous treatment	
Surgery	14 (88)
Radiotherapy	9 (56)
Chemotherapy	16 (100)

Abbreviation: ECOG Eastern Cooperative Oncology Group

The dose escalation schedule is outlined in Table 2. These patients were assigned to four dose levels, with three, six, five and two patients in dose level I, II, III, and IV, respectively. At first, none of the first three patients experienced DLT at dose level I, II, and III; therefore, the dose level was further escalated to 120 mg/m^2. Because both of the initial two patients at 120 mg/m^2 level experienced DLT during the first cycle of treatment (one had grade III diarrhea and grade IV neutropenia; the other had grade III diarrhea), three additional patients were recruited at the prior dose level, 100 mg/m^2. However, both of the two newly accrued patients at 100 mg/m^2 level experienced DLTs (one had grade III infection with hypotension and grade III hemorrhage; the other had grade III diarrhea and grade IV neutropenia), resulting in 2 episodes of DLT among the five patients at this dose level. Therefore, the tested dose level was further de-escalated to 80 mg/m^2. Since none of the patients experienced any DLT, 80 mg/m^2 of PEP02 by 90-min intravenous infusion was determined as the MTD in combination with weekly infusion of 5-FU/LV on days 1 and 8 of a 21-day cycle.

Table 2 Dose escalation scheme

Dose Level	PEP02 (mg/m^2)	No. patients	No. patients with DLT
I	60	3	0
II	80	3 + 3	0 + 0
III	100	3 + 2	0 + 2
IV	120	2	2

Abbreviation: DLT dose-limiting toxicity

Toxicity

All 16 patients were assessed for toxicity. Table 3 summarizes the therapy-induced toxicity during treatment. There were three (18.4%) patients had grade III or above adverse events (AEs), and 13 and 0.2% of AEs led to dosing delay/reduction and permanent discontinuation of treatment, respectively. No treatment-related death was reported in the study.

The most common treatment-related AEs included nausea (81.3% in incidence), followed by diarrhea (75.0%), vomiting (68.8%), fatigue (43.8%), mucositis (mucosa inflammation, 43.8%), leucopenia (37.5%), neutropenia (37.5%), weight loss (37.5%), anemia (31.3%), and alopecia (31.3%). Acute cholinergic reaction was rarely observed. Compared with the entire safety population, patients who received 80 mg/m^2, the MTD dose of PEP02 experienced less treatment-related AEs (51.1% versus 57.6%), as well as grade III or above AEs (10.6% versus 18.4%).

Pharmacokinetics and exploratory pharmacogenetic studies

The PK of PEP02 is shown in Table 4, Fig. 1a and b. CPT-11 and SN-38 were characterized for PEP02 single dose PK at dose levels of 60, 80, 100, and 120 mg/m^2 by 90-min intravenous infusion. Changes in the plasma concentration of CPT-11 showed almost the same pattern at all levels. All concentration curves of plasma CPT-11 peaked quickly and reached the maximum around 1 h after the end of PEP02 infusion and gradually dropped in a mono-exponential pattern until the last sampling point, which was similar to that observed for PEP02 monotherapy in a previous study [3]. At the MTD of PEP02, the Cmax of SN-38 was lower (7.98 ± 4.39 ng/ml) than that of the conventional formulation of irinotecan at 125 mg/m^2 (26.3 ± 11.9 ng/ml), whereas the AUC of SN-38 was higher than that of irinotecan (AUC0 → t: 343.36 ± 133.24 ng/ml*h vs. 229 ± 108 ng/mL*h). The $t_{1/2}$ of SN-38 at the MTD of PEP02 was 57.54 ± 17.81 h, which was relatively longer than that of the conventional formulation (10.4 ± 3.1 h). No statistically significant difference was observed in the mean values of all pharmacokinetic parameters of SN-38 among the 4 dose levels.

The majority of subjects showed wild type alleles for *UGT1A1*28* (TA6TA6: 88%) and *UGT1A1*6* (GG: 69%). No subject harbored homozygous mutation in *UGT1A1*28* or *UGT1A1*6* allele. Two and five patients had heterozygous *UGT1A1*28* and *UGT1A1*6*, respectively. Of which, one patient with heterozygous

Table 3 Treatment-emergent AEs with maximum CTC grade by dose level (incidence ≥ 20%)

	Total ($N = 16$)	60 mg/m^2 $N = 3$	80 mg/m^2 $N = 6$	100 mg/m^2 $N = 5$	120 mg/m^2 $N = 2$
AE	All grade	Grade 3–4			
Anemia	7 (43.8%)	0	0	2 (40%)	0
Leukopenia	6 (37.5%)	0	0	2 (40%)	1 (50%)
Neutropenia	6 (37.5%)	1 (33.3%)	1 (16.7%)	2 (40%)	1 (50%)
Abdominal pain	7 (43.8%)	0	0	1 (20%)	1 (50%)
Diarrhea	12 (75.0%)	0	1 (16.7%)	2 (40%)	2 (100%)
Nausea	13 (81.3%)	0	1 (16.7%)	0	0
Vomiting	12 (75.0%)	0	1 (16.7%)	0	0
Fatigue	8 (50.0%)	0	0	1 (20%)	0
Infection	6 (37.5%)	0	0	2 (40%)	1 (50%)
Anorexia	4 (25.0%)	0	0	1 (20%)	0
Hypoalbuminemia	4 (25.0%)	0	1 (16.7%)	0	0
Hypokalemia	8 (50.0%)	1 (33.3%)	2 (33.3%)	2 (40%)	1 (50%)
Hyponatremia	4 (25.0%)	0	0	1 (20%)	1 (50%)
Cough	5 (31.3%)	1 (33.3%)	0	0	0

Abbreviation: *AE* adverse event

*UGT1A1*28* and *UGT1A1*6* experienced grade IV neutropenia and grade III diarrhea, and had the largest dose-normalized AUC of SN-38. Four out of the 5 subjects with heterozygous *UGT1A1*6* possessed relatively higher dose-normalized AUC of SN-38 comparing to other subjects; of which 3 patients experienced grade III toxicities.

Antitumor activity

One patient at dose level III, who suffered from DLT did not complete at least one post-treatment tumor assessment. Among the 15 efficacy evaluable patients, two (13.3%) had confirmed partial response (PR) and nine (60%) had stable disease (SD), leading to the overall disease control rate (DCR) of 73.3%. At the MTD of 80 mg/m^2, 1 PR and 4 SD were observed among six patients. The tumor response rate and the disease control rate were 16.7 and 83.3%, respectively. PR was observed in one gastric cancer patient (at the 80 mg/m^2 dose level) and one breast cancer patient (at the 100 mg/m^2 dose level).

Discussion

The current study evaluated the safety profile and preliminary efficacy of PEP02 in combination with 5-FU

Table 4 Pharmacokinetic parameters of PEP02 at each dose level

	Dose of PEP02 (mg/m^2)	C_{max} CPT-11 (μg/mL) SN-38 (ng/mL)	T_{max} (hr)	$AUC_{0\rightarrow 169.5}$ CPT-11 (hr-μg/mL) SN-38 (hr-ng/mL)	$AUC_{0\rightarrow\infty}$ CPT-11 (hr-μg/mL) SN-38 (hr-ng/mL)	V_{ss} (L/m^2)	Cl (mL/hr/m^2)	$t_{1/2}$ (hr)
Total CPT-11	60, $N = 3$	28.9 ± 15.8	2.4 ± 0.7	1047 ± 1210	1047 ± 1210	2.80 ± 1.59	136 ± 116	21.1 ± 11.7
	80, $N = 6$	29.2 ± 5.2	2.1 ± 0.7	1096 ± 834	1151 ± 880	3.39 ± 0.74	124 ± 106	33.3 ± 15.1
	100, $N = 5$	44.1 ± 7.7	4.0 ± 3.8	2237 ± 1090	2289 ± 1119	2.86 ± 0.75	58 ± 37	43.17 ± 4.8
	120, $N = 2$	47.9 ± 16.2	2.3 ± 0.9	1254 ± 553	1254 ± 553	3.95 ± 0.83	106 ± 47	54.4 ± 17.4
SN-38	60, $N = 3$	7.02 ± 5.64	13.1 ± 11.7	364 ± 222	1370 ± 1122	NA	NA	183.8 ± 172.3
	80, $N = 6$	7.98 ± 4.39	13.3 ± 18.3	343 ± 133	505 ± 165	NA	NA	57.5 ± 17.8
	100, $N = 5$	7.39 ± 1.68	12.2 ± 12.3	539 ± 368	840 ± 433	NA	NA	73.4 ± 18.3
	120, $N = 2$	7.26 ± 3.90	37.8 ± 17.2	353 ± 164	305	NA	NA	30.8
	Irinotecan[a]	26.3 ± 11.9	NA	229 ± 108	NA	NA	NA	10.4 ± 3.1

Mean ± STD; C_{max} peak concentration in plasma; T_{max} time to achieve peak plasma concentration; $AUC_{0\rightarrow 169.5}$ and $AUC_{0\rightarrow\infty}$ area under the plasma concentration-time curve from time zero to 169.5 h and infinity, respectively; V_{ss} volume of distribution at steady state; $t_{1/2}$, plasma terminal elimination half-life; Cl, total clearance of drug from plasma; NA, not available

[a]Irinotecan 125 mg/m^2, package inset of Campto®

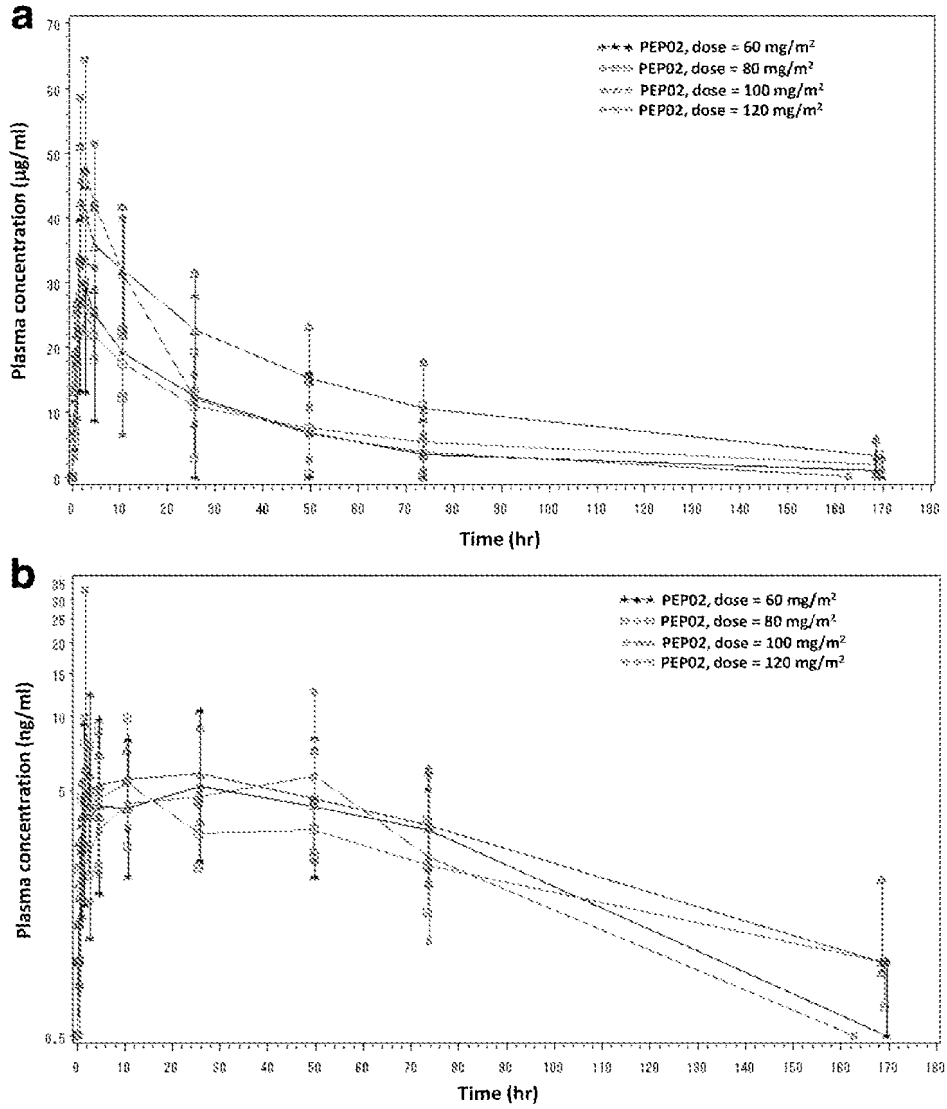

Fig. 1 Plasma concentration-time profiles of **a** CPT-11 and **b** SN-38 at different PEP02 doses

and LV, in patients with refractory advanced malignancy. Gastrointestinal toxicities and myelosuppression were the major DLTs, which were comparable to those of free irinotecan and PEP02 monotherapy [3, 9]. The MTD (80 mg/m^2) of PEP02, in combination with infusion of 5-FU and LV on days 1 and 8 of every-3-week schedule is recommended for the future studies. In a previous study, the MTD of PEP02 monotherapy with a 3-week interval was 120 mg/m^2 [3]. The favorable toxicity profiles of PEP02 made it a better agent to combine with other cytotoxic agents. 5-FU/LV in combination with irinotecan was the first line treatment of colorectal cancer, which explains our interest in the evaluation of PEP02 in combination with 5-FU/LV. The dose of weekly 5-FU in this study was fixed as 2000 mg/m^2, which mimicked the AIO regimen commonly used in Europe and Asia [10, 11]. The percentage of grade III or above AEs or all treatment-related AEs in the MTD group was lower than that in the overall safety population. For hematologic laboratory parameters, nadir was observed between days 13 and 16 after PEP02 administration; however blood biochemistry was mostly unaffected. These tolerable and manageable hematological and non-hematological toxicities indicated that this combination therapy is feasible for further application.

PEP02 affected the PK characteristics of irinotecan. Compared to the data of 125 mg/m^2 free-form irinotecan, 80 mg/m^2 of PEP02 showed lower Cmax (8.0 ± 4.4 ng/mL vs. 26.3 ± 11.9 ng/mL), longer terminal t1/2 (57.5 ± 17.8 h vs. 10.4 ± 3.1 h) and higher AUC (343 ± 133 ng/mL*hr vs. 229 ± 108 ng/mL*hr) of SN-38 [12, 13]. These favorable PK parameters indicated that PEP02

could decrease the influx of SN-38 from the central compartment to the peripheral, leading to less treatment-related toxicities, even in combination with 5-FU/LV. The PK data showed the dose-dependent linear distribution of CPT-11 when study doses were increased from 60 to 120 mg/m^2, but no statistically significant difference was observed in the mean values of pharmacokinetic parameters of CPT-11 and SN-38, including dose-normalized C_{max}, AUC parameters, $t_{1/2}$, CL, and V_{ss}, possibly owning to narrow dose increments, small sample size and high inter-individual variability.

The *UGT1A1* gene encoded a varied spectrum of active enzymes that are responsible for drug metabolism, including UGT. The *UGT1A1*28* allele is characterized by the presence of a 7th dinucleotide repeat in the TATA box of the promoter region, compared to the *UGT1A1*1* allele with 6 repeats. This increased number of repeats results in the reduction in the expression of UGT, leading to decreased SN-38 detoxification and prolonged exposure time of SN-38 in the intestines. Thus, patients with homozygous or heterozygous *UGT1A1*28* and treated with irinotecan commonly developed dose limiting neutropenia and late diarrhea [14]. Similar to *UGT1A1*28* polymorphism, the *UGT1A1*6* allele also can decrease the activity of the enzyme in the heterozygous or homozygous genotype. It has been reported that patients with both *UGT1A1*28* and *UGT1A1*6* heterozygosity were at high risk to develop irinotecan-related toxicities [15, 16]. In our study, owning to the small sample size, a clear correlation cannot be obtained between polymorphism of *UGT1A* family genes and pharmacokinetic parameters or toxicity of PEP02. However, one subject with heterozygous mutation in both *UGT1A1*6* and *UGT1A1*28* had the highest dose-normalized AUC of SN-38 and experienced grade IV neutropenia and grade III diarrhea. To draw any firm conclusions, a PK/PD study according to polymorphism of *UGT1A* family genes should be performed [17].

With the limitation of being a very small sample size study of 15 efficacy evaluable population, two subjects had confirmed PR and nine subjects had SD as their best-ever responses during this study period. The tumor response rate and disease control rate were 13 and 73%, respectively. In a Phase I trial, clinical efficacy cannot be defined accurately because of heterogeneous tumor types and different dose levels. Of the evaluable patients, PR was noted in a heavily treated breast cancer patient and a gastric cancer patient, and four out of five patients with pancreatic cancer had SD, implying that this combination regimen is worthy of further investigation. Indeed, PEP02 either alone or in combination with 5-FU/LV was investigated in a phase II PEP0208 study [18] and a phase III NAPOLI-1 study [19] in metastatic pancreatic cancer patients who progressed after gemcitabine-containing regimen. The NAPOLI-1 study formed the basis for the regulatory approvals of PEP02 (Irinotecan liposome injection) by the Taiwan FDA and US FDA in October 2015.

Conclusions

This is the first trial to apply PEP02 in combination with 5-FU and LV in patients with solid tumors, and major treatment-related DLTs were myelosuppression and diarrhea. PEP02 had a lower C_{max}, longer $t_{1/2}$ and increased $AUC_{0\rightarrow t}$ of SN-38 compared to irinotecan; similar results were observed in another study on PEP02 infusion alone. The dose of 80 mg/m^2 of PEP02 in combination with D1 and D8 infusion of 5-FU/LV with every-3-week schedule is recommended for future studies.

Additional file

Additional file 1: Table S1. Tumor type, dose level, DLT, best response and single nucleotide polymorphisms of UGT1A1*28 and UGT1A1*6. (DOCX 18 kb)

Abbreviations

5-FU: 5-fluorouracil; AEs: Adverse events; ANC: Absolute neutrophil count; $AUC_{0\rightarrow\infty}$: AUC through infinite time; $AUC_{0\rightarrow t}$: Plasma concentration-time curve from zero to time t; CL: Clearance; C_{max}: Peak plasma concentration; CPT-11: Irinotecan hydrochloride; CT: Computed tomography; DLT: Dose-limiting toxicity; ECOG: Eastern Cooperative Oncology Group; FDA: The Food and Drug Administration; LV: Leucovorin; MTD: Maximum tolerated dose; PG: Pharmacogenetics; PK: Pharmacokinetics; PR: Partial response; PS: Performance score; SD: Stable disease; SN-38G: SN-38 glucuronide; STD: Standard deviation; $t_{1/2}$: Elimination half-life; T_{max}: Time at which C_{max} occurred; UGT1A: UDP-glucuronosyl transferase 1A isoforms; V_{ss}: Volume of distribution at steady state

Acknowledgments

We thank the patients and their families who participated in this phase I study, and also thank the medical and nursing staff of the investigational sites for the care and support of the patients in this study.

Funding

This study was supported by PharmaEngine, Inc., Taipei, Taiwan.

Availability of data and materials

The study is an industry-sponsored study. The sponsor, PharmaEngine Inc, Taipei, Taiwan, prefers to keep the raw dataset in-house. However, all the information supporting the conclusions of this article is included within the text and tables of the article and summarized in Additional file 1: Table S1.

Authors' contributions

NJC and LTC wrote the manuscript. TYC, RKH, CHW and LTC enrolled the patients. NJC, YWW, CGY and LTC collected and analyzed data. YWW, CGY and LTC conceived of the study, participated in its design and coordination. All authors contributed to and approved the final version of the manuscript.

Competing interests

NJC, TYC, RKH, JYC, and CHW report no conflicts of interests. YWW and CGY are full-time employees of PharmaEngine. LTC has received an honorarium from PharmaEngine for an advisory board.

Consent for publication

Not applicable.

Ethics approval and consent to participate

The protocol and all recruiting materials and consent foam had been approved by the Joint Institutional Review Board (JIRB), covering all the participating hospitals in the study including Tri-Service General Hospital,

Mackay Memorial Hospital, Linkou Chang Gung Memorial Hospital, National Cheng Kung University Hospital, and Kaohsiung Medical University This study had been performed in accordance with International Conference on Harmonization Good Clinical Practice guidelines, Good Clinical Laboratory Practice, and the Declaration of Helsinki. All participants from each institutions provided written informed consent.

Author details
[1]National Institute of Cancer Research, National Health Research Institutes, 2F, No. 367, Sheng-Li Road, Tainan 704, Taiwan. [2]Division of Hematology/Oncology, Department of Internal Medicine, National Cheng Kung University Hospital, Tainan, Taiwan. [3]Division of Hematology and Oncology, Taipei Medical University-Shuang Ho Hospital, Taipei, Taiwan. [4]Division of Hematology and Oncology, Department of Internal Medicine, Mackay Memorial Hospital, Taipei, Taiwan. [5]Division of Hematology/Oncology, Department of Internal Medicine, Chang Gung Memorial Hospital, Linkou, Taiwan. [6]PharmaEngine, Inc, Taipei, Taiwan. [7]Department of Internal Medicine, Kaohsiung Medical University Hospital, Kaohsiung Medical University, Kaohsiung, Taiwan.

Received: 2 March 2016 Accepted: 28 October 2016
Published online: 21 November 2016

References

1. Drummond DC, Noble CO, Guo Z, Hong K, Park JW, Kirpotin DB. Development of a highly active nanoliposomal irinotecan using a novel intraliposomal stabilization strategy. Cancer Res. 2006;66(6):3271–7.
2. Tsai CS, Park JW, Chen LT. Nanovector-based therapies in advanced pancreatic cancer. J Gastrointest Oncol. 2011;2(3):185–94.
3. Chang TC, Shiah HS, Yang CH, Yeh KH, Cheng AL, Shen BN, Wang YW, Yeh CG, Chiang NJ, Chang JY et al. Phase I study of nanoliposomal irinotecan (PEP02) in advanced solid tumor patients. Cancer Chemother Pharmacol. 2015;75(3):579–86.
4. Saltz LB, Cox JV, Blanke C, Rosen LS, Fehrenbacher L, Moore MJ, Maroun JA, Ackland SP, Locker PK, Pirotta N et al. Irinotecan plus fluorouracil and leucovorin for metastatic colorectal cancer. Irinotecan Study Group. N Engl J Med. 2000;343(13):905–14.
5. Douillard JY, Cunningham D, Roth AD, Navarro M, James RD, Karasek P, Jandik P, Iveson T, Carmichael J, Alakl M et al. Irinotecan combined with fluorouracil compared with fluorouracil alone as first-line treatment for metastatic colorectal cancer: a multicentre randomised trial. Lancet. 2000; 355(9209):1041–7.
6. Kambe M, Kikuchi H, Gamo M, Yoshioka T, Ohashi Y, Kanamaru R. Phase I study of irinotecan by 24-h intravenous infusion in combination with 5-fluorouracil in metastatic colorectal cancer. Int J Clin Oncol. 2012;17(2):150–4.
7. Iyer L, King CD, Whitington PF, Green MD, Roy SK, Tephly TR, Coffman BL, Ratain MJ. Genetic predisposition to the metabolism of irinotecan (CPT-11). Role of uridine diphosphate glucuronosyltransferase isoform 1A1 in the glucuronidation of its active metabolite (SN-38) in human liver microsomes. J Clin Invest. 1998;101(4):847–54.
8. Hoskins JM, McLeod HL. UGT1A and irinotecan toxicity: keeping it in the family. J Clin Oncol. 2009;27(15):2419–21. doi: 24101200/JCO200824209478 Epub.
9. Fuchs CS, Moore MR, Harker G, Villa L, Rinaldi D, Hecht JR. Phase III comparison of two irinotecan dosing regimens in second-line therapy of metastatic colorectal cancer. J Clin Oncol. 2003;21(5):807–14.
10. Kohne CH, Wils J, Lorenz M, Schoffski P, Voigtmann R, Bokemeyer C, Lutz M, Kleeberg C, Ridwelski K, Souchon R et al. Randomized phase III study of high-dose fluorouracil given as a weekly 24-h infusion with or without leucovorin versus bolus fluorouracil plus leucovorin in advanced colorectal cancer: European organization of Research and Treatment of Cancer Gastrointestinal Group Study 40952. J Clin Oncol. 2003;21(20):3721–8.
11. Chen LT, Liu TW, Wu CW, Chung TR, Shiah HS, Jan CM, Liu JM, Whang-Peng J, Chang JY. A phase I study of weekly docetaxel, 24-h infusion of high-dose fluorouracil/leucovorin and cisplatin in patients with advanced gastric cancer. Oncology. 2002;63(3):239–47.
12. Rivory LP, Haaz MC, Canal P, Lokiec F, Armand JP, Robert J. Pharmacokinetic interrelationships of irinotecan (CPT-11) and its three major plasma metabolites in patients enrolled in phase I/II trials. Clin Cancer Res. 1997;3(8):1261–6.
13. Rothenberg ML, Kuhn JG, Burris 3rd HA, Nelson J, Eckardt JR, Tristan-Morales M, Hilsenbeck SG, Weiss GR, Smith LS, Rodriguez GI et al. Phase I and pharmacokinetic trial of weekly CPT-11. J Clin Oncol. 1993;11(11):2194–204.
14. Palomaki GE, Bradley LA, Douglas MP, Kolor K, Dotson WD. Can UGT1A1 genotyping reduce morbidity and mortality in patients with metastatic colorectal cancer treated with irinotecan? An evidence-based review. Genet Med. 2009;11(1):21–34. doi:10.1097/GIM.1090b1013e31818efd31877.
15. Minami H, Sai K, Saeki M, Saito Y, Ozawa S, Suzuki K, Kaniwa N, Sawada J, Hamaguchi T, Yamamoto N et al. Irinotecan pharmacokinetics/pharmacodynamics and UGT1A genetic polymorphisms in Japanese: roles of UGT1A1 6 and 28. Pharmacogenet Genomics. 2007;17(7):497–504.
16. Shimoyama S. Pharmacogenetics of irinotecan: An ethnicity-based prediction of irinotecan adverse events. World J Gastrointest Surg. 2010;2(1): 14–21. doi:10.4240/wjgs.v4242.i4241.4214.
17. Saif MW. MM-398 achieves primary endpoint of overall survival in phase III study in patients with gemcitabine refractory metastatic pancreatic cancer. JOP. 2014;15(3):278–9. doi: 210.6092/1590-8577/2507.
18. Ko AH, Tempero MA, Shan Y, Su W, Lin Y, Dito E, Ong A, Yeh CG, Chen L. A multinational phase II study of liposome irinotecan (PEP02) for patients with gemcitabine-refractory metastatic pancreatic cancer. Br J Cancer. 2013;109: 920–5.
19. Wang-Gillam A, Li CP, Bodoky G, Dean A, Shan YS, Jameson G, Macarulla T, Lee KH, Cunningham D, Blanc JF, et al. NAPOLI-1 Study Group. Nanoliposomal irinotecan with fluorouracil and folinic acid in metastatic pancreatic cancer after previous gemcitabine-based therapy (NAPOLI-1): a global, randomised, open-label, phase 3 trial. Lancet. 2016;387(10018):545–57.

Cancer Medicine

ORIGINAL RESEARCH

PEPCOL: a GERCOR randomized phase II study of nanoliposomal irinotecan PEP02 (MM-398) or irinotecan with leucovorin/5-fluorouracil as second-line therapy in metastatic colorectal cancer

Benoist Chibaudel[1,2,3], Frédérique Maindrault-Gœbel[4], Jean-Baptiste Bachet[5], Christophe Louvet[6], Ahmed Khalil[7], Olivier Dupuis[8], Pascal Hammel[9], Marie-Line Garcia[4], Mostefa Bennamoun[6], David Brusquant[2], Christophe Tournigand[10], Thierry André[4], Claire Arbaud[11], Annette K Larsen[12], Yi-Wen Wang[13], C. Grace Yeh[13], Franck Bonnetain[11] & Aimery de Gramont[1]

[1]Department of Medical Oncology, Franco-British Institute, Levallois-Perret, France
[2]Groupe Coopérateur Multidisciplinaire en Oncologie (GERCOR), Paris, France
[3]Preclinical and Translational Cancer Research Unit, AAREC Filia Research (AFR), Paris, France
[4]Department of Medical Oncology, Saint-Antoine Hospital, Assistance Publique des Hôpitaux de Paris (APHP), Paris, France
[5]Department of Gastroenterology, La Pitié-Salpetrière Hospital, Assistance Publique des Hôpitaux de Paris (APHP), Paris, France
[6]Department of Medical Oncology, Montsouris Mutualiste Institute, Paris, France
[7]Department of Medical Oncology, Tenon Hospital, Assistance Publique des Hôpitaux de Paris (APHP), Paris, France
[8]Department of Medical Oncology, Victor Hugo Clinic, Le Mans, France
[9]Department of Gastroenterology, Beaujon Hospital, Assistance Publique des Hôpitaux de Paris (APHP), Clichy, France
[10]Department of Medical Oncology, Henri Mondor Hospital, Créteil, France
[11]Methodological and quality of life unit in oncology (EA3181) & Quality of life and cancer clinical research platform, CHU Besançon, Besançon, France
[12]Cancer Biology and Therapeutics, INSERM U938 and Pierre and Marie Curie University, Paris, France
[13]PharmaEngine, Inc., Taipei, Taiwan

Keywords
Colorectal cancer, MM398, nanoliposomal irinotecan, PEP02, phase II

Correspondence
Aimery de Gramont, Department of Medical Oncology, Franco-British Institute, 4 rue Kléber, Levallois-Perret 92300, France. Tel: +33(0) 1 47 59 59 16; Fax: +33(0) 1 40 29 85 08; E-mail: aimerydegramont@gmail.com

Funding Information
This study was sponsored by GERCOR and supported by PharmaEngine, Inc. Presented in part to the 2015 American Society of Clinical Oncology (ASCO) Gastrointestinal Cancer Symposium, 15–17 January, 2015, San Francisco, California, USA.

Received: 20 October 2015; Revised: 1 December 2015; Accepted: 11 December 2015

***Cancer Medicine* 2016; 5(4):676–683**

doi: 10.1002/cam4.635

List of the investigators
Benoist Chibaudel, Frédérique Maindrault-Gœbel, Jean-Baptiste Bachet, Christophe Louvet, Ahmed Khalil, Olivier Dupuis, Pascal Hammel, Marie-Line Garcia, Mostefa Bennamoun, Christophe Tournigand, Thierry André, Aimery de Gramont, Ebenezer Christelle, Segura Djezzar Canne, Mansourbakht Touraj.

Abstract

A multicenter, open-label, noncomparative, randomized phase II study (PEPCOL) was conducted to evaluate the efficacy and safety of the irinotecan or PEP02 (MM-398, nanoliposomal irinotecan) with leucovorin (LV)/5-fluorouracil (5-FU) combination as second-line treatment in patients with metastatic colorectal cancer (mCRC). Patients with unresectable mCRC who had failed one prior oxaliplatin-based first-line therapy were randomized toirinotecan with LV/5-FU (FOLFIRI) or PEP02 with LV/5-FU (FUPEP; PEP02 80 mg/m^2 with LV 400 mg/m^2 on day 1 and 5-FU 2400 mg/m^2 on days 1–2). Bevacizumab (5 mg/kg, biweekly) was allowed in both arms. The primary endpoint was 2-month response rate (RR). Fifty-five patients were randomized (FOLFIRI, n = 27; FUPEP, n = 28). In the intent-to-treat population (n = 55), 2-month RR response rate was observed in two (7.4%) and three (10.7%) patients in the FOLFIRI and FUPEP arms, respectively. The most common grade 3–4 adverse events reported in the respective FOLFIRI and FUPEP arms were diarrhea (33% vs. 21%), neutropenia (30% vs. 11%), mucositis (11% vs. 11%), and grade 2 alopecia (26% vs. 25%). FUPEP has activity and acceptable safety profile in oxaliplatin-pretreated mCRC patients.

Introduction

The FOLFIRI regimen, combination of irinotecan with leucovorin (LV) and 5-fluorouracil (5-FU; LV/5-FU)[1] is a standard regimen in first-line or second-line therapy of metastatic colorectal cancer (mCRC) [2, 3].

PEP02 (MM-398) is a highly stable nanoliposomal irinotecan that theoretically has therapeutic advantages over the free form of the drug (irinotecan and its active metabolite SN-38) such as site-specific delivery and extended release of drug. It was found to reduce the toxicity of the encapsulated agent to healthy tissue while maintaining or increasing its antitumor potency [4]. Moreover, as compared to conventional irinotecan, PEP02 was associated with lower maximum concentration, longer elimination half-life, higher area under the curve (AUC) for SN-38, smaller volume of distribution, and slower plasma clearance of total irinotecan [4]. In phase I studies, the maximum tolerated dose (MTD) of PEP02 as a single agent was 120 mg/m^2 once every 3 weeks and 80 mg/m^2 in combination with LV/5-FU [5]. A randomized phase II study of nanoliposomal irinotecan (PEP02) versus irinotecan versus docetaxel was conducted in advanced gastric cancer [6]. The safety profile of PEP02 and irinotecan was similar, however, it was suggested that there may be an improvement of efficacy in a small subset of patients who received a slightly higher dose (150 mg/m^2 every 3 weeks) of PEP02. The longer half-life of PEP02 compared to irinotecan may potentiate the antitumor efficacy of 5-FU.

This phase II study sought to evaluate the efficacy and safety of PEP02 in combination with LV/5-FU, FUPEP regimen, as second-line therapy in patients with mCRC.

Material and Methods

Design

PEPCOL (PEP for PEP02, the other denomination of MM-398, COL for colorectal cancer) is a multicenter, noncomparative, open-label, randomized phase II trial (EudraCT number: 2010–020468–39; ClinicalTrials.gov identifier: NCT01375816) in mCRC patients previously treated with an oxaliplatin-based regimen. The study was conducted according to the International Conference on Harmonization Good Clinical Practice Guidelines, the Declaration of Helsinki, and the local regulatory requirements and laws. Written informed consents were obtained from all patients.

Patients were randomly assigned in a 1:1 ratio to either PEP02 plus LV/5-FU (the FUPEP arm), or irinotecan plus LV5-FU (the FOLFIRI arm), using a minimization technique with the three following stratification criteria: center, GERCOR prognostic score[7] [Eastern Cooperative Oncology Group performance status (ECOG PS) 0, normal lactate dehydrogenase(LDH) value versus ECOG PS $\geq$ 1, and/or LDH > 1 x Upper Normal Limit (ULN)], and first-line time to progression (<9 months vs. ≥ 9 months).

Patient eligibility

Eligible patients were 18–75 years of age, had histologically confirmed adenocarcinoma of the colon or rectum, and documented measurable metastatic disease not suitable for curative surgery. Prior systemic oxaliplatin-based first-line therapy was required. Patients had to have an ECOG PS of 0–2 and adequate organ function (neutrophils 1.5 x 10^9/L, platelets ≥100 x 10^9/L, hemoglobin >9 g/dL, serum creatinine <150 μmol/L, creatinine clearance >30 mL/min, and total bilirubin <1.5 x UNL). Exclusion criteria included preexisting (residual) diarrhea grade >1, total or partial bowel obstruction, prior chemotherapy with irinotecan, history or evidence of brain metastasis, exclusive bone metastasis upon physical examination, uncontrolled hypercalcemia, and pregnant or breast-feeding women (Table S1).

Treatment

The FUPEP regimen was administrated as follows: PEP02 80 mg/m^2 intravenous (IV) over 90 min, with LV 400 mg/m^2 IV over 2-h followed by 5-FU(5-fluorouracil) 2400 mg/m^2 continuous infusion over 46-h. All treatment regimens were given every 14 days until occurrence of progressive disease (PD) or unacceptable toxicity. Two regimens of FOLFIRI were allowed: FOLFIRI-1, irinotecan 180 mg/m^2 IV over 90 min, with LV 400 mg/m^2 IV over 2-h, followed by 5-FU 400 mg/m^2 bolus and 5-FU 2400 mg/m^2 continuous infusion over 46-h, and modified (m) FOLFIRI-3, irinotecan 90 mg/m^2 as 1-h infusion, with LV 400 mg/m^2 over 2-h, followed by 5-FU 2400 mg/m^2 continuous infusion over 46-h on day 1 and irinotecan 90 mg/m^2 as 1-h infusion repeated at the end of 5-FU infusion on day 3. From June 2012, bevacizumab 5 mg/kg was added to the chemotherapy regimen.(Table S2) Premedication with atropine and antiemetics was permitted. Granulocyte colony-stimulating factor was used according to the American Society of Clinical Oncology guidelines [8]. Dose adjustments for each study treatment component individually and/or cycle delays were permitted in the event of toxicity. No crossover to FUPEP was permitted after progression in the FOLFIRI arm.

End points

The primary endpoint was response rate (RR) evaluated at 2 months from randomization (2-month RR) using

RECIST version 1.1 [9]. Secondary endpoints were best objective RR (ORR) defined as the best response recorded from the start of the treatment until treatment failure, disease control rate (DCR) defined as the percentage of patients who have achieved a response or stabilization, overall survival (OS) defined as the time from the date of randomization to the date of patient death (from any cause) or to the last date the patient was known to be alive, progression-free survival (PFS) defined as the time from the date of randomization to the date of progression (local, regional, or distant lesions) or death (from any cause). Alive patients without documented objective PD at the time of the final analysis were censored at the date of their last objective tumor assessment. Toxicity was evaluated according to the NCI-CTCAE version 4.0.

Health-related quality of life (HRQoL) assessments were performed in both arms at baseline, and after 4 and 8 cycles of treatment, using the French version of the EuroQol (EQ-5D) and the Quality of Life QuestionnaireCore 30 (QLQ-C30) [10]. The EQ visual analog scale (VAS) of pain measure was also performed.

Sample size

According to a Simon's Minimax two-stage design [11] with a one-sided 10% type I error, a power of 90% and a 15% improvement in 2-month RR from 10% (H0, considered as uninteresting to pursue any further investigation) to 25% (H1, considered as promising to warrant further investigation in a phase III trial), 27 patients were required for the first stage and more than two responses per arm to proceed to the second stage of 44 patients in each arm, including a 10% drop-out rate.

Statistics

The primary analysis of efficacy used intent-to-treat (ITT) population, that is, including all randomized patients regardless of their eligibility and treatment received. The confirmative analysis was conducted in the modified ITT population of eligible patients and in a per-protocol (PP) population comprising all patients who have received at least 2 cycles of the allocated treatment and without any major protocol deviations. The safety analysis included all patients who received at least one dose of any study drug. Follow-up and survival were estimated using the reverse Kaplan–Meier method [12] and Kaplan–Meier method [13], respectively, and median values were described with 95% confidence intervals (CI).

The main clinical and medical patient characteristics were described based on the completion of at least one baseline HRQoL questionnaire. HRQoL baseline scores were described by treatment arm. Qualitative and continuous variables were described using percent and means (standard deviation) and medians (minimum-maximum), respectively. The Mann–Whitney nonparametric test was used to compare HRQoL scores at baseline according to treatment arm. For exploratory purpose, a linear mixed-effects (repeated measures of variance) model was used to analyze the longitudinal changes of HRQoL at baseline, and after 4 and 8 cycles of treatment. All patients who completed at least one baseline HRQoL assessment were included. Time, treatment, and interaction between time and treatment/performance status effects were explored in multivariate model. An unstructured covariance matrix for the individual random effects (individual deviance from average intercept) and time (individual deviance from average time effect) was employed.

Results

Patient population and treatment characteristics

Fifty-five patients were randomized in six French centers from May 2011 to August 2013. Twenty-seven patients were allocated to the FOLFIRI arm and 28 to the FUPEP arm (Fig. 1). The main patient and tumor characteristics are summarized in Table 1. Mean age was 62 years (range 35–77) in the FOLFIRI arm and 62 years (range 38–80) in the FUPEP arm. Population was balanced between the two arms.

In the FOLFIRI arm, 10 (37%) patients received FOLFIRI-1 and 17 (63%) patients received mFOLFIRI-3. All patients received at least one dose of the allocated study treatment. Bevacizumab was added to chemotherapy in 13 (48.1%) FOLFIRI-treated patients and in 12 (42.9%) FUPEP-treated patients.

The total number of cycles was 268 (range 1–22 cycles) in the FOLFIRI arm and 226 (range 1–25 cycles) in the FUPEP arm. The treatment was postponed by 35 (13.1%) and 18 (8.0%) cycles, in the FOLFIRI arm and FUPEP arm, respectively. The treatment dose was reduced in 33 (12.3%) cycles in the FOLFIRI arm and in 21 (9.3%) cycles in the FUPEP arm.

Response rates

Tumor response rate at 2 months

At the end of the first step of the Simon's design, 2-month RR was evaluated in the first 27 randomized patients in each arm ($n = 54$). A tumor response was

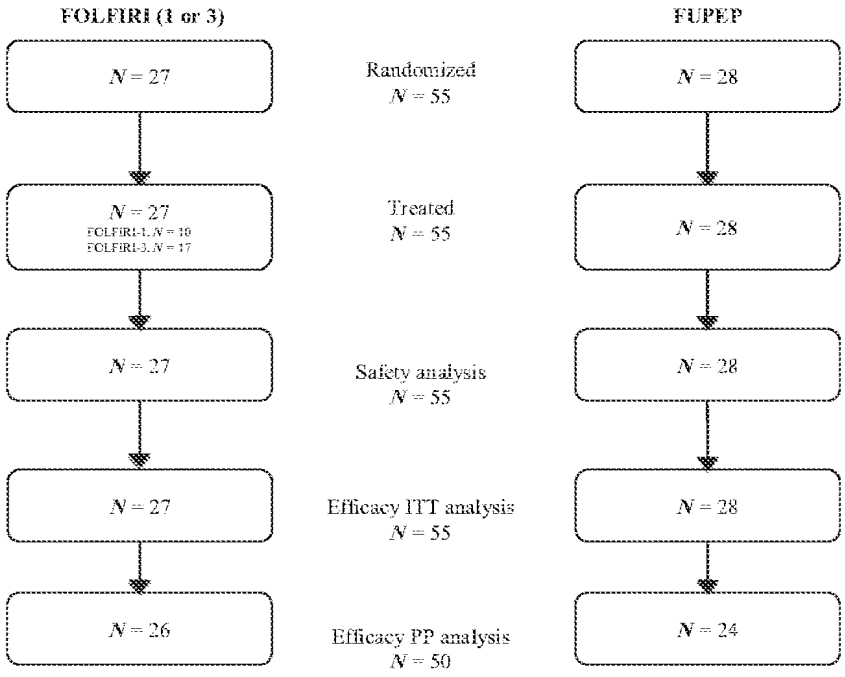

Figure 1. Participant flow.

observed in two (7.4%;95% CI: −2.5–17.3) and three (11.1%;95% CI: −0.7–22.2) patients in the FOLFIRI and FUPEP arms, respectively. In the ITT population, the 2-month RR was 7.4% (n = 2/27) and 10.7% (n = 3/28).

Best overall response rate

In the ITT population (n = 55), three (11.1%, 95% CI: 0.7–22.9) and four (14.3%, 95% CI: 1.3–27.3) patients had PR as the best response in the FOLFIRI and the FUPEP arm, respectively (Table 2). Tumor stabilization was observed in 17 (63.0%;95% CI: 44.8–81.2) patients in the FOLFIRI arm and 13 (46.4%;95% CI: 27.9–64.9) patients in the FUPEP arm. PD at first evaluation was demonstrated in six (22.2%;95% CI: 6.5–37.9) patients in the FOLFIRI arm and seven (25.0%;95% CI: 9.0–41.0) patients in the FUPEP arm. No CR was observed. (Fig. 2) Of note, all responses in the FOLFIRI arm were reported in patients having received the mFOLFIRI-3 regimen (ORR = 0.0% for FOLFIRI-1 vs. ORR = 17.6% for mFOLFIRI-3). The DCR was 74.1% (20/27) in the FOLFIRI arm and 60.7% (17/28) in the FUPEP arm.

Five patients were excluded from PP analysis due to early death (lung infection without neutropenia one patient, cancer one patient), limiting diarrhea (two patients), and PEP02-related allergy (one patient). Of the 50 evaluable patients (26 FOLFIRI-treated patients, 24 FUPEP-treated patients), PR was observed in three (11.5%; 95% CI: 0.7–23.8) patients in the FOLFIRI arm and four (16.7%; 95% CI: 1.8–31.6) patients in the FUPEP arm Table 2.

Survivals

After a median follow-up of 11.6 months (95% CI: 10.2–19.8), 35 patients progressed and 33 patients died. The median PFS was 6.8 months (95% CI: 3.7–8.1) in the FOLFIRI arm and 5.0 months(95% CI: 2.8–6.0) in the FUPEP arm. The median OS was 10.5 months (95% CI: 6.9–21.1) in the FOLFIRI arm and 14.6 months(95% CI: 6.9–16.5) in the FUPEP arm.

Safety

The most frequent grade 3–4 toxicity in the respective FOLFIRI and FUPEP arms were diarrhea (33.3% vs. 21.4%), neutropenia (29.6% vs. 10.7%), grade 2 alopecia (25.9% vs. 25.0%), stomatitis (11.1% vs. 10.7%), and nausea (7.4% vs. 3.6%) (Table 3). There was no toxic-related death in either of the arms. The addition of bevacizumab to both regimens did not significantly increase grade 3–4 toxicities (Table S3).

Twenty-three serious adverse events (SAE) were reported during the study (13 in the FOLFIRI arm and 10 in the FUPEP arm). In the FUPEP arm, six SAEs were related to PEP02 (two severe diarrhea, two allergic reactions, one ileitis, and one general state alteration).

Table 1. Baseline patient and disease characteristics.

	FOLFIRI ($N = 27$)		FUPEP ($N = 28$)	
Variable	*N*	%	*N*	%
Age, years				
<70	22	81.5	22	78.6
≥70	5	18.5	6	21.4
Gender				
Male	14	51.8	19	67.9
Female	13	48.1	9	32.1
KRAS status				
Wild-type	14	51.8	16	57.1
Mutated	10	37.0	10	35.7
Unknown	3	11.1	2	7.1
ECOG performance status				
0	15	55.6	10	35.7
1		40.7	14	50.0
2	111	3.7	4	14.3
BMI				
<25	17	63.0	17	60.7
25–30	9	33.3	6	21.4
≥30	1	3.7	5	17.9
Primary tumor location				
Colon	22	81.5	17	60.7
Rectum	5	18.5	10	35.7
Both	0	0	1	3.6
Primary tumor status				
Resected	21	77.8	19	67.9
Not resected	6	22.2	9	32.1
Metastasis				
Liver				
No	3	11.1	5	17.9
Yes	24	88.9	23	82.1
Lung				
No	12	44.4	17	60.7
Yes	15	55.6	11	39.3
Peritoneal				
No	17	63.0	23	82.1
Yes	10	37.0	5	17.9
Node				
No	23	85.2	20	71.4
Yes	4	14.8	8	28.6
Other tumor sites				
No	20	74.1	26	92.9
Yes	7	25.9	2	7.1
Number of metastatic sites				
1	12	44.4	12	42.9
2	4	14.8	14	50.0
3	10	37.0	0	0
4	1	3.7	2	7.1
Time to metastasis				
Synchronous	19	70.4	19	67.9
Metachronous	8	29.6	9	32.1
Prior adjuvant therapy				
No	22	81.5	22	78.6
Yes	5	18.5	6	21.4
First-line PFS (months)				
>9	14	51.8	14	50.0
<9	13	48.1	14	50.0
Oxaliplatin failure after				
Adjuvant treatment	1	3.7	1	3.6
First-line metastatic treatment	26	96.3	27	96.4
Oxaliplatin reintroduction before second-line				
No	13	50.0	15	53.6
Yes	13	50.0	12	42.9
Missing data	1	3.7	1	3.6
Prior bevacizumab				
No	6	23.1	3	11.1
Yes	20	76.9	24	88.9
Missing data	1	3.7	1	3.6
White blood cell count				
<10000/mm^3	27	100.00	27	96.4
≥10000/mm^3	0	0	1	3.6
Neutrophils				
<4000/mm^3	15	55.6	11	39.3
≥4000/mm^3	12	44.4	17	60.7
Platelet				
<400000/mm^3	25	92.6	24	85.7
≥400000/mm^3	2	7.4	4	14.3
ALP				
Normal	8	29.6	13	46.4
1–3 × ULN	16	59.3	8	28.6
>3 × ULN	3	11.1	7	25.0
AST				
Normal	17	63.0	17	60.7
>1 × ULN	10	37.0	11	39.3
ALT				
Normal	20	74.1	23	82.1
>1 × ULN	7	25.9	5	17.9
Creatinine clearance				
≥60 mL/min	25	92.6	21	80.8
<60 mL/min	2	7.4	5	19.2
Missing data	0	0	2	7.1
CEA				
Normal	8	29.6	7	25.0
>1 × ULN	19	70.4	21	75.0
LDH				
Normal	10	37.0	9	34.6
>1 × ULN	16	59.3	17	65.4
Missing data	1	3.7	2	7.1
GERCOR prognostic model (20)				
Low-risk	15	55.6	10	35.7
Intermediate risk	2	7.4	4	14.3
High-risk	10	37.0	14	50.0
Chemotherapy regimen				
FOLFIRI-1	10	37.0	0	0
mFOLFIRI-3	17	63.0	0	0
FUPEP	0	0	28	100.0
Bevacizumab				
No	14	51.8	16	57.1
Yes	13	48.1	12	42.9

KRAS, Kirsten Rat Sarcoma viral oncogene homolog; BMI, Body mass index; ECOG, Eastern Cooperative Oncology Group; PFS, progression-free survival; ALP, alkaline phosphatase; AST, aspartate aminotransferase; ALT, alanine transaminase; CEA, carcinoembryonic antigen; LDH, lactate dehydrogenase; ULN, upper limit normal.

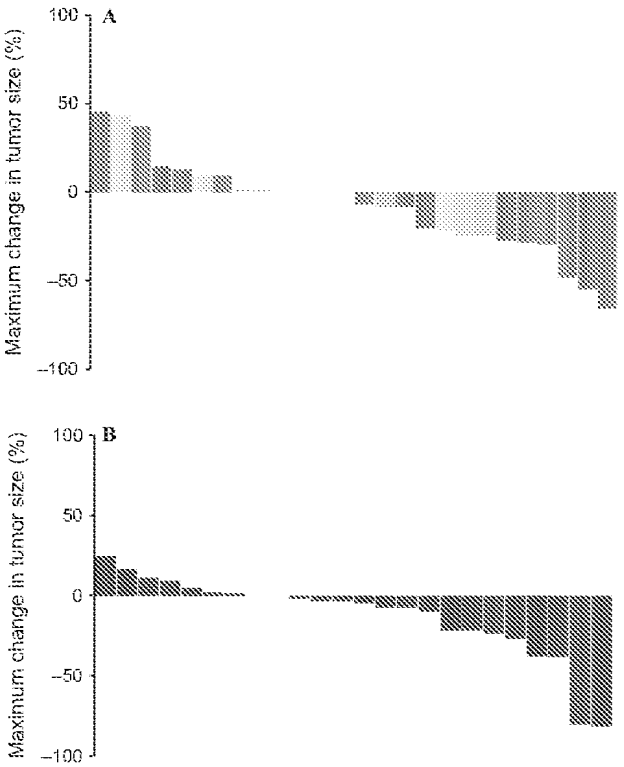

Figure 2. Waterfall plots showing the best response to the FOLFIRI arm (A) and the FUPEP arm (B) [arm A, light: FOLFIRI-1; dark, mFOLFIRI-3].

Table 2. Best overall response rate (ITT population, N = 55; PP population, N = 50).

	FOLFIRI		FUPEP	
	N (%)	95% CI	*N* (%)	95% CI
Best ORR				
ITT	3/27 (11.1)	–0.74–22.97	4/28 (14.3)	1.32–27.25
PP	3/26 (11.5)	–0.74–23.82	4/24 (16.7)	1.76–31.58
2-month ORR				
ITT	2/27 (7.4)	–2.47–17.29	3/28 (10.7)	–0.74–22.17
PP	2/26 (7.7)	–2.55–17.94	3/24 (12.5)	–0.73–25.73

ORR: overall response rate, ITT, intent to treat; PP, per-protocol.

Subsequent therapy

Two (7.4%) patients had salvage surgery for metastasis with complete tumor resection (R0) in the FOLFIRI arm. None of the FUPEP-treated patients underwent surgery.

After study treatment, 44 patients received third-line therapy (19 in the FOLFIRI arm and 25 in the FUPEP arm). Irinotecan-based therapy as third-line treatment after FUPEP was administered in 21 patients, either in combination with fluoropyrimidine (n = 12) or an anti-EGFR agent (n = 9). Two PRs were observed with the combination of panitumumab and irinotecan.

Health-related quality of life

There was no significant difference at baseline between two treatment arms regarding all the dimension of both questionnaires. The mean EQ-5D global health status (GHS)/VAS scores in the FOLFIRI arm were stable between baseline and eight cycles of treatment (scores: 67.7–67.5), but higher compared with the FUPEP arm (scores: 61.5–58.0). The QLQ-C30 GHS/HRQoL scores at baseline were similar between the two treatment arms (65.4 in the FOLFIRI arm and 65.7 in the FUPEP arm).

The FUPEP arm presented a better HRQoL level at baseline compared with the FOLFIRI arm that was characterized by higher scores for three functional scores (emotional, social, and physical functioning), and less pain. On contrary, FUPEP-treated patients had a higher fatigue score compared to those treated with FOLFIRI.

Longitudinal analysis of the EQ-5D and QLQ-C30 scores were performed for 45 and 48 patients, respectively. No significant treatment arm effects on any functional or symptom scores were observed. In the multivariate model, the time effect of emotional functioning, diarrhea, and the time-treatment interaction on physical functioning were significant. FUPEP-treated patients had more diarrhea and less emotional functioning abilities.

No differences were observed for GHS over time between the two arms, but patients in the FUPEP arm presented a higher deterioration of the physical functioning and more fatigue.

Discussion

This is the first randomized phase II study evaluating the effect of adding PEP02 to LV/5-FU when administered in mCRC patients who failed prior oxaliplatin-based first-line therapy. In the ITT population, 2-month RR was similar in both arms (7.4% vs. 10.7%). According to the Simon's Minimax decision rules, the targeted RR was reached only in the FUPEP arm, but not in the FOLFIRI arm. Despite a potential higher antitumor activity than that of the widely used FOLFIRI-1 regimen, it is unlikely that FUPEP could challenge the mFOLFIRI-3 efficacy with the data reported here. This is the main reason why GERCOR (sponsor of the study) decided not to proceed to the second stage of the study, but to make an attempt to optimize the FUPEP regimen. Of note, RR of the FUPEP regimen (14.3%) was closer to that of mFOLFIRI-3 (17.6%) than to FOLFIRI-1 (0%). (Fig. 2) In previous studies which evaluated the FOLFIRI-3 regimen as second-line treatment in mCRC patients, RR has ranged between 7.4% and 23.0% without bevacizumab

and 22.4% and 35.0% when adding bevacizumab (Table S4).

The FUPEP combination safety profile remains similar to that of FOLFIRI, with diarrhea being the most significant SAE (21% in the FUPEP arm, 30% in the FOLFIRI arm) and the incidence of severe neutropenia being around 11% (compared to 30% with free irinotecan). Yet, no unexpected toxicities were observed. Of note, the addition of bevacizumab did not lead to the increased incidence of adverse events.

Based on the preliminary results of the PEPCOL study, the FUPEP regimen was added as the third arm to the positive phase III trial of metastatic pancreatic cancer patients previously treated with gemcitabine-based therapy (NAnoliPOsomaL Irinotecan, NAPOLI-(1). FUPEP was found superior to 5FU [14, 15].

In colorectal cancer, the results of the PEPCOL study suggest that the FUPEP regimen could be as active as the optimized mFOLFIRI3 regimen, but more active than the standard FOLFIRI regimen in oxaliplatin-pretreated mCRC patients with an acceptable safety profile. FUPEP may also safely be combined with bevacizumab. With further ongoing optimization, this regimen has the potential to provide a clinically useful treatment for post-oxaliplatin mCRC patients Table 3.

Acknowldgments

The authors thank Magdalena Benetkiewicz (GERCOR) for editorial assistance in the preparation of the manuscript.

Conflict of Interest

BC has acts as consultant to Sanofi, and has received honoraria from Roche and Sanofi. AdG acts as a consultant to PharmaEngine, Inc, and serves as a consultant on advisory boards to Roche. JBB acts as a consultant to Amgen, Celgene, Merck Serono, and Sanofi, and has received honoraria from Bayer, Lilly, and Roche. AEL has received research funding from Merrimack. FB acts as a consultant to Novartis, Roche, EISAI, Integragen, Invecty, and Nestlé, and has received honoraria from Roche, Celgene, and Merck Serono, and a grant from Roche. CT served as a consultant on advisory board to PharmaEngine Inc. TA acts as a consultant to Roche and has received honoraria from Roche. YWW is employee of PharmaEngine Inc, and has an ownership interest in PhamraEngine Inc. CGY is employee of PharmaEngine Inc., has been compensated for a leadership role by PharmaEngine Inc, and has an ownership interest in PhamraEngine Inc. All remaining authors have declared no conflicts of interest.

Table 3. Incidence of adverse events observed per patient ($N = 55$).

	FOLFIRI ($N = 27$)										FUPEP ($N = 28$)									
NCI-CTCAE grade	0		1		2		3		4		0		1		2		3		4	
	N	%	*N*	%	*N*	%	*N*	%	*N*	%	*N*	%	*N*	%	*N*	%	*N*	%	*N*	%
Neutropenia	9	33.3	4	14.8	6	22.2	6	22.2	2	7.4	15	53.6	6	21.4	4	14.3	2	7.1	1	3.6
Anemia	3	11.1	18	66.7	5	18.5	1	3.7	0	0.0	6	21.4	18	64.3	4	14.3	0	0.0	0	0.0
Thrombocytopenia	18	66.7	8	29.6	1	3.7	0	0.0	0	0.0	20	71.4	8	28.6	0	0.0	0	0.0	0	0.0
Diarrhea	3	11.1	7	25.9	8	29.6	9	33.3	0	0.0	7	25.0	5	17.9	10	35.7	4	14.3	2	7.1
Nausea	7	25.9	13	48.1	5	18.5	2	7.4	0	0.0	6	21.4	10	35.7	11	39.3	1	3.6	0	0.0
Vomiting	18	66.7	5	18.5	3	11.1	1	3.7	0	0.0	13	46.4	4	14.3	10	35.7	1	3.6	0	0.0
Mucositis/stomatitis	12	44.4	8	29.6	4	14.8	3	11.1	0	0.0	13	46.4	11	39.3	1	3.6	3	10.7	0	0.0
Alopecia	7	25.9	13	48.1	7	25.9	–		–		14	50.0	7	25.0	7	25.0	–		–	

NCI-CTCAE, the National Cancer Institute-Common Toxicity Criteria Adverse Events.

References

1. Andre, T., C. Louvet, F. Maindrault-Goebel, C. Couteau, M. Mabro, J. P. Lotz, V. Gilles-Amar, M. Krulik, E. Carola, V. Izrael, and A. de Gramont. 1999. CPT-11 (irinotecan) addition to bimonthly, high-dose leucovorin and bolus and continuous-infusion 5-fluorouracil (FOLFIRI) for pretreated metastatic colorectal cancer. GERCOR. Eur. J. Cancer 35:1343–1347.
2. Tournigand, C., T. Andre, E. Achille, G. Lledo, M. Flesh, D. Mery-Mignard, E. Quinaux, C. Couteau, M. Buyse, G. Ganem, B. Landi, P. Colin, et al. 2004. FOLFIRI followed by FOLFOX6 or the reverse sequence in advanced colorectal cancer: a randomized GERCOR study. J. Clin. Oncol. 22:229–237.
3. Fuchs, C. S., J. Marshall, E. Mitchell, R. Wierzbicki, V. Ganju, M. Jeffery, J. Schulz, D. Richards, R. Soufi-Mahjoubi, B. Wang, and J. Barrueco. 2007. Randomized, controlled trial of irinotecan plus infusional, bolus, or oral fluoropyrimidines in first-line treatment of metastatic colorectal cancer: results from the BICC-C Study. J. Clin. Oncol. 25:4779–4786.
4. Drummond, D. C., C. O. Noble, Z. Guo, K. Hong, J. W. Park, and D. B. Kirpotin. 2006. Development of a highly active nanoliposomal irinotecan using a novel intraliposomal stabilization strategy. Cancer Res. 66:3271–3277.
5. Chang, T. C., H. S. Shiah, C. H. Yang, K. H. Yeh, A. L. Cheng, B. N. Shen, Y. W. Wang, C. G. Yeh, N. J. Chiang, J. Y. Chang, and L. T. Chen. 2015. Phase I study of liposome encapsulated irinotecan (PEP02) in advanced solid tumor patients. Cancer Chemother. Pharmacol. 75:579–586.
6. Roy, A. C., S. R. Park, D. Cunningham, Y. K. Kang, Y. Chao, L. T. Chen, C. Rees, H. Y. Lim, J. Tabernero, F. J. Ramos, M. Kujundzic, M. B. Cardic, et al. 2013. A randomized phase II study of PEP02 (MM-398), irinotecan or docetaxel as a second-line therapy in patients with locally advanced or metastatic gastric or gastro-oesophageal junction adenocarcinoma. Ann. Oncol. 24:1567–1573.
7. Chibaudel, B., F. Bonnetain, C. Tournigand, L. Bengrine-Lefevre, L. Teixeira, P. Artru, J. Desramé, A. K. Larsen, T. André, C. Louvet, and A. de Gramont. 2011. Simplified prognostic model in patients with oxaliplatin-based or irinotecan-based first-line chemotherapy for metastatic colorectal cancer: a GERCOR study. Oncologist 16:1228–1238.
8. Smith, T. J., J. Khatcheressian, G. H. Lyman, H. Ozer, J. O. Armitage, L. Balducci, C. L. Bennett, S. B. Cantor, J. Crawford, S. J. Cross, G. Demetri, C. E. Desch, et al. 2006. 2006 update of recommendations for the use of white blood cell growth factors: an evidence-based clinical practice guideline. J. Clin. Oncol. 24:3187–3205.
9. Eisenhauer, E. A., P. Therasse, J. Bogaerts, L. H. Schwartz, D. Sargent, R. Ford, J. Dancey, S. Arbuck, S. Gwyther, M. Mooney, L. Rubinstein, L. Shankar, et al. 2009. New response evaluation criteria in solid tumours: revised RECIST guideline (version 1.1). Eur. J. Cancer 45:228–247.
10. Aaronson, N. K., S. Ahmedzai, B. Bergman, M. Bullinger, A. Cull, N. J. Duez, A. Filiberti, H. Flechtner, S. B. Fleishman, J. C. de Haes, S. Kaasa, et al. 1993. The European Organization for Research and Treatment of Cancer QLQ-C30: a quality-of-life instrument for use in international clinical trials in oncology. J. Natl Cancer Inst. 85:365–376.
11. Simon, R. 1999. Optimal two-stage designs for phase II clinical trials. Control. Clin. Trials 10:1–10.
12. Schemper, M., and T. L. Smith. 1996. A note on quantifying follow-up in studies of failure time. Control. Clin. Trials 17:343–346.
13. Kaplan, E. L., and P. Meier. 1958. Non parametric estimation from incomplete observations. J. Am. Stat. Assoc. 53:457–481.
14. Von Hoff, D., C. P. Li, A. Wang-Gillam, L. T. Chen, A. Wang-Gillam, G. Bodoky, A. Dean, G. Jameson, K. H. Lee, J. F. Blanc, R. Hubner, and C. F. Chiu, et al. 2014. NAPOLI-1: randomized Phase 3 Study of MM-398 (nal-IRI), With or Without 5-Fluorouracil and Leucovorin versus 5-Fluorouracil and Leucovorin, in Metastatic Pancreatic Cancer Progressed on or following Gemcitabine-Based Therapy. Ann. Oncol. 25(2suppl): ii105–ii117.
15. Chen, L.T., D. D. Von Hoff, C. P. Li, A. Wang-Gillam, G. Bodoky, A. P. Dean, Y. S. Shan, G. S. Jameson, T. Macarulla, K. H. Lee, D. Cunningham, and J. F. Blanc, et al. 2015. Expanded analyses of napoli-1: phase 3 study of MM-398 (nal-IRI), with or without 5-fluorouracil and leucovorin, versus 5-fluorouracil and leucovorin, in metastatic pancreatic cancer (mPAC) previously treated with gemcitabine-based therapy (ASCO abstr 234). J. Clin. Oncol.33(3suppl).

Supporting Information

Additional supporting information may be found in the online version of this article:

Table S1. List of all eligibility criteria.
Table S2. Outline of the study schedule and treatment regimens: FOLFIRI-1 (A), mFOLFIRI-3 (B), and FUPEP (C).
Table S3. NCI grade 3/4 toxicity in the FOLFIRI arm and in the FUPEP arm according to bevacizumab use
Table S4. Trials assessing the efficacy and safety profiles of the FOLFIRI (1 or 3) regimen with and without bevacizumab as second-line therapy in patients with metastatic colorectal cancer.

Cancer Chemother Pharmacol (2011) 67:41–48
DOI 10.1007/s00280-010-1281-5

ORIGINAL ARTICLE

Sequential chemotherapy with dose-dense docetaxel, cisplatin, folinic acid and 5-fluorouracil (TCF-dd) followed by combination of oxaliplatin, folinic acid, 5-fluorouracil and irinotecan (COFFI) in metastatic gastric cancer: results of a phase II trial

Matteo Dalla Chiesa · Gianluca Tomasello · Sebastiano Buti · Rodrigo Kraft Rovere · Matteo Brighenti · Silvia Lazzarelli · Gianvito Donati · Rodolfo Passalacqua

Received: 18 August 2009 / Accepted: 9 February 2010 / Published online: 5 March 2010

Abstract
Purpose To evaluate a new strategy of two sequential, intensified chemotherapy regimens in metastatic gastric cancer.
Patients and methods Chemo-naïve patients with metastatic gastric cancer were enrolled to receive 4 cycles of TCF-dd (docetaxel initially 85 mg/m^2 and cisplatin initially 75 mg/m^2 on day 1 [later modified due to toxicity: 70 and 60 mg/m^2 respectively], l-folinic acid 100 mg/m^2 on days 1 and 2, 5-fluorouracil 400 mg/m^2 bolus and then 600 mg/m^2 as a 22 h continuous infusion on day 1 and 2, every 14 days). Subsequently, patients with CR, PR or SD received 4 cycles of COFFI (oxaliplatin 85 mg/m^2, irinotecan 140 mg/m^2, l-folinic acid 200 mg/m^2, 5-fluorouracil bolus 400 mg/m^2 on day 1 followed by 2,400 mg/m^2 as a 48 h continuous infusion, every 14 days). In both regimens pegfilgrastim 6 mg subcutaneously on day 3 was included.
Results Forty consecutive patients were enrolled. TCF-dd regimen achieved an ORR of 55% (95% CI, 40–70). Twenty-three patients proceeded to COFFI. After this regimen the ORR was then increased to 60% (95% CI, 45–75). Among the 21 patients treated with TCF-dd after the protocol amendments, main grade 3–4 toxicities were: neutropenia (29%), thrombocytopenia (19%), asthenia (24%) and diarrhea (14%). COFFI caused grade 3–4 neutropenia (all not febrile) and diarrhea in 35% and 17% of patients respectively.
Conclusions A sequential strategy with TCF-dd followed by COFFI is very active and may be of special interest in selected patients.

Keywords Sequential chemotherapy · Irinotecan · Oxaliplatin · Docetaxel · Cisplatin · 5-Fluorouracil · Gastric cancer

Introduction

Gastric cancer is the second leading cause of cancer related death in the world [1]. It accounts for more than 20 deaths per 100,000 population annually in East Asia, Eastern Europe, and parts of Central and South America [2]. Surgical resection is the main curative treatment option in the early setting of this disease, with 5-year survival rates of 58% to 78% and 34% reported for stage I and II, respectively [3]. Unfortunately, in the western world, most patients are diagnosed when the tumor is inoperable. In this setting, chemotherapy remains the best treatment option [4].

Many cytotoxic agents, such as platinum compounds, anthracyclines, fluoropyrimidines, taxanes and irinotecan, in various combinations, have demonstrated significant efficacy in patients with metastatic gastric cancer, regarding disease free and overall survival [4–12].

However, in spite of these improvements, most patients with metastatic disease will develop drug resistance in a

Presented in part at 44th annual meeting of the American society for clinical oncology, May 31–June 3, 2008, Chicago, IL (J Clin Oncol 26: 2008 [May 20 Suppl; abstr 4570]).

M. Dalla Chiesa (✉) · G. Tomasello · S. Buti · R. K. Rovere · M. Brighenti · S. Lazzarelli · G. Donati · R. Passalacqua
Departments of Medical Oncology and Biostatistics, Azienda Ospedaliera di Cremona, Cremona, Italy
e-mail: mdallachiesa@yahoo.it

M. Dalla Chiesa
Medical Oncology Division, Azienda Istituti Ospitalieri, Viale Concordia 1, 26100 Cremona, Italy

few months after starting treatment and median survival still remains below 12 months in most trials.

Three decades ago, Norton and Simon reported, in a mathematical model, that the rate of tumor regrowth increases as the tumor shrinks in response to chemotherapy [13].

The Norton-Simon hypothesis [14] predicts either that a rapid reduction of tumor burden could best be achieved by shortening the interval between the cycles, and that the resistance might be overcome by switching from initial chemotherapy to new one.

Based on this hypothesis, many dose-dense regimens and sequential schedules have been developed in various tumors, with mixed results [15–18].

In advanced gastric cancer, studies with intensified weekly or biweekly [19–23] combinations or sequential [24–26] chemotherapies have reported encouraging results.

In the present study we tested a new strategy with the sequence of two intensified biweekly regimens, in order to avoid the emergence of drug resistance.

For the first part of the sequence, a combination of docetaxel, cisplatin and 5-fluorouracil (TCF) was chosen, which is currently considered a valid option in the first-line setting [7].

In order to increase the dose intensity, we have reduced to two weeks the interval between each cycle; furthermore, we have modulated the 5-fluorouracil with folinic acid, according to the studies by de Gramont and colleagues in colorectal carcinoma [27].

For the second part of the sequence, a combination of oxaliplatin, irinotecan, folinic acid and 5-fluorouracil was chosen, based on previous phase II trials that reported high activity in metastatic gastric cancer [22, 23].

Patients and methods

Patients

The inclusion criteria for this study were: histologically confirmed metastatic gastric cancer, at least one measurable metastatic lesion, age $\leq$80 years, an ECOG performance status (PS) $\leq$1, adequate hepatic, renal, haematological and cardiac function and written informed consent.

Prior adjuvant chemotherapy and radiotherapy were allowed, provided that terminated by at least 6 months before the enrollment in the study.

Major exclusion criteria were: prior palliative chemotherapy, either bone metastases or pleural/peritoneal effusion as the sole disease site, pregnancy, breast-feeding, child-bearing potentiality without use of any contraception, any other current or prior malignancy (with the exception of excised cervical carcinoma in situ or squamous cell skin carcinoma) and psychiatric conditions considered as making it difficult or impossible to apply the therapeutic program.

The study was approved by the local ethical committee and was performed in accordance with the Declaration of Helsinki and Good Clinical Practice Guidelines.

Chemotherapy administration and dose reductions

Dose-dense TCF (TCF-dd) regimen consisted of: docetaxel (Taxotere®; Sanofi-Aventis, Paris, France) 85 mg/m^2 over 1-h intravenous (i.v.) infusion on day 1, cisplatin 75 mg/m^2 on day 1 (1 h i.v. infusion), levo-folinic acid 100 mg/m^2 administered in 5% glucose over 2-h i.v. on day 1 and 2, followed by 5-fluorouracil 400 mg/m^2 bolus i.v. on day 1 and 2 and then 5-fluorouracil 600 mg/m^2 as a continuous i.v. infusion over 22 h on day 1 and 2.

Pegfilgrastim (Neulasta®, Amgen, Thousand Oaks, CA, USA) 6 mg was administered on day 3, subcutaneously, at the end of 5-fluorouracil continuous infusion.

As a precaution, we decided per protocol to reduce by 30% all the chemotherapeutic agents for patients aged $\geq$65 years, on the basis of our clinical practice about polichemotherapy regimens in metastatic gastric cancer.

Hematological and non hematological toxicities encountered in the first 6 patients, prompted us to make an amendment to the protocol and thereby we reduced docetaxel dose to 75 mg/m^2.

Because of persistent toxicities, mainly hematological and constitutional symptoms (severe asthenia) we decided, after the 19th patient treated, to further reduce docetaxel (70 mg/m^2) and cisplatin (60 mg/m^2) doses.

Antiemetic treatment (5-hydroxytryptamine receptor antagonist type and dexamethasone), appropriate hydration and premedications were always administered before the infusion of chemotherapy.

In the event of toxicity, the following dose reductions and treatment delays were planned: in case of insufficient hematological function (neutrophil count <1,500/mm^3 and/or platelet count <100,000/mm^3), and/or non-hematological toxicities grade >1 on day 15 of any cycle, treatment was delayed until resolution.

If toxicities lasted longer than two weeks, the treatment was continued, after recovery, with a dose reduction of 20%, but always keeping the 2-week schedule.

In the event of febrile neutropenia, grade 4 not febrile neutropenia lasting longer than five days, grade 4 thrombocytopenia or grade 3 thrombocytopenia with bleeding, there were 25% dose reductions of each drug.

The same dose reduction was indicated for grade 3 and 4 non-hematological toxicity.

Treatment was repeated every 14 days and it was continued for 4 cycles (one cycle = 15 days) in absence of disease

progression, unacceptable toxicity, patient refusal, or at physician's discretion.

At the end of the TCF-dd treatment, patients were re-evaluated and those with complete response (CR), partial response (PR) or stable disease (SD) received COFFI: irinotecan (Campto®, Aventis Pharma, Rainham Road South, Dagenham, UK) 140 mg/m^2 in saline solution over 1-h i.v. infusion on day 1, followed by oxaliplatin (Eloxatin®, Laboratoires Thissen, Braine-L'alleud, Belgium) 85 mg/m^2 and levofolinic acid 200 mg/m^2 administered simultaneously in 5% glucose over 2-h i.v. on day 1, followed by 5-fluorouracil 400 mg/m^2 bolus i.v. on day 1 and then 5-fluorouracil 2,400 mg/m^2 as a continuous i.v. infusion over 48 h.

Also in this case, pegfilgrastim was administered at the end of 5-fluorouracil continuous infusion and patients aged ≥65 years received a 30% dose reduction.

In the event of toxicity, the following dose reductions and treatment delays were planned: in case of insufficient hematological function (neutrophil count <1,500/mm^3 and/or platelet count <100,000/mm^3), and/or gastrointestinal toxicities grade >1 on day 15 of any cycle, treatment was delayed until resolution; if gastrointestinal toxicities lasted longer than two weeks, the treatment was then discontinued.

In the event of febrile neutropenia, grade 4 not febrile neutropenia lasting longer than five days, grade 4 thrombocytopenia or grade 3 thrombocytopenia with bleeding, there were 25% dose reductions of each drug.

The same dose reduction was indicated for grade 3 and 4 gastrointestinal toxicity. For ototoxicity or neurotoxicity grade ≥ 2, oxaliplatin was discontinued.

Treatment was repeated every 14 days and it was continued for 4 cycles (one cycle = 15 days) in absence of disease progression, unacceptable toxicity, patient refusal, or at physician's discretion.

Study assessments

Upon study entry, a medical history was taken, and all of the patients underwent a physical examination, an evaluation of ECOG PS, blood chemistry tests, a chest X-ray and a computed tomography scan of the abdomen and of all measurable and assessable sites. A bone scan, a magnetic resonance imaging scan and an ultrasound endoscopy were carried out only if indicated.

The patients subsequently underwent a physical examination and laboratory tests (blood cell count, serum creatinine, bilirubin, aspartate aminotransferase [ALT], alanine aminotransferase [AST]) before each cycle. The tumor markers carcinoembryonic antigen (CEA) and CA 19.9 were measured at baseline and every month.

Instrumental evaluations of the lesions present at study entry were carried out after 4 cycles of TCF-dd (or at least 2 cycles in case of early stopping), a second time after 4 cycles of COFFI (or at least 2 cycles in case of early stopping) and then every 2 months until disease progression or withdrawal from study medication, on the basis of the RECIST criteria [28].

In addition, survival was monitored every 2 months in each patient leaving the study.

Adverse events, including neurosensory toxicity, were classified according to National Cancer Institute Common Toxicity Criteria (NCI-CTC) version 3.0.

Statistical analysis

This was a monocentric, non-randomized phase II study. The efficacy analyses were based on the intent-to-treat population. The primary objective was the activity evaluated as overall response rate (ORR): CR plus PR. Secondary endpoints were safety, time to progression (TTP) and overall survival (OS).

On the basis of an ORR of 37% for patients who received DCF or TCF regimens in previous recent randomized trials [6, 7] we expected a 50% ORR with the TCF-dd regimen and a further increase of 20% ORR by the addition of COFFI.

We have estimated that 23 evaluable patients receiving both TCF-dd and COFFI were required to accept this hypothesis as being true [29] in order to guarantee a power of the study of 0.80 and significance of 0.05.

We have also projected that an extra amount of 10–15 patients had to be enrolled, considering the expected drop out after TCF-dd regimen, due to progression of disease (per protocol), toxicity and other causes.

Descriptive statistics was reported as proportions and medians. Kaplan-Meier estimates were used in the analysis of time-to-event variable and the 95% confidence interval (CI) for the median time to event was computed.

The dose intensity (DI) was calculated according to Hryniuk method [30]. The relative DI was calculated as the ratio of the DI actually delivered to the DI planned by the protocol.

Results

Patients' characteristics

Forty consecutive patients were enrolled into this study from November 2004 to April 2008.

Patients' characteristics are listed in Table 1. Median age was 64 years (range 40–80 years); the majority were male (73%) and had an ECOG PS of 0 (70%).

All patients had histologically confirmed adenocarcinoma.

Table 1 Patients' characteristics

	No.	%
Enrolled patients	40	100
Sex		
Male	29	73
Female	11	27
Age (years)		
Median	64	
Range	40–80	
ECOG PS		
0	28	70
1	12	30
Primary tumor site		
Esophagogastric junction	8	20
Stomach	32	80
Histological diagnosis		
Adenocarcinoma	40	100
G1	0	0
G2	16	40
G3	18	45
Unknown	6	15
Prior gastrectomy	18	45
Disease sites		
Distant lymph nodes	23	58
Stomach	22	55
Liver	20	50
Peritoneum	15	38
Bone	6	15
Lung	5	13
Prior adjuvant chemotherapy	4	10
Prior adjuvant radiotherapy	2	5

The most common disease sites were distant lymph nodes (58% of patients), liver (50%), peritoneum (38%), bone (15%) and lung (13%).

Eight patients (20%) had their primary tumor at the esophagogastric junction. Forty-five percent of patients underwent prior gastrectomy, the rest had metastatic disease as first diagnosis.

Four patients (10%) had received prior adjuvant chemotherapy. Two patients (5%) had received prior adjuvant radiotherapy.

Chemotherapy delivery

The exposure to study medications is listed in Table 2.

A median of 4 cycles (range 1–4) of TCF-dd per patient were administered.

Sixteen patients (40%) completed the planned 4 cycles without any delay nor dose reductions.

Four patients received less than 4 cycles (see below for further details).

Median actual DI was 42.5 mg/m^2/week (range 21.2–42.5; relative DI = 1.0, range 0.5–1.0) for docetaxel and 37.5 mg/m^2/week (range 18.7–37.5; relative DI = 1.0, range 0.5–1.0) for cisplatin in the first 6 patients treated at the initial doses (docetaxel 85 mg/m^2 and cisplatin 75 mg/m^2). After the protocol amendments, in which the docetaxel dose was reduced to 70 mg/m^2 and cisplatin dose was reduced to 60 mg/m^2, median actual DI was 35 mg/m^2/week (range 14–35; relative DI = 1.0, range 0.4–1) for docetaxel, 30 mg/m^2/week (range 12–30; relative DI = 1.0, range 0.4–1) for cisplatin and 1,000 mg/m^2/week (range 400–1,000; relative DI = 1.0, range 0.4–1) for 5-fluorouracil.

Twenty-three patients were treated with COFFI and a median of 4 cycles (range 2–4) per patient was administered.

Nine patients (39%) completed the planned 4 cycles without any delay nor dose reductions.

Three patients received less than 4 cycles of COFFI: one experienced severe gastrointestinal toxicity after 3 cycles, the second developed clinical progression of disease after 2 cycles and the other refused to continue the treatment after 3 cycles.

Median actual DI was 64 mg/m^2/week (range 43.7–70; relative DI = 0.92, range 0.62–1) for irinotecan, 39 mg/m^2/week (range 26.5–42.5; relative DI = 0.92, range 0.62–1) for oxaliplatin and 1,280 mg/m^2/week (range 875–1,400; relative DI = 0.92, range 0.62–1) for 5-fluorouracil.

Efficacy

Thirty-six patients were evaluable for response to the TCF-dd regimen. There were two treatment related deaths (one patient died after 1 cycle because of bowel perforation and another because of septic shock due to febrile neutropenia) and two early suspensions (one patient discontinued the treatment because of severe allergic reaction to docetaxel in the 2nd cycle and another interrupted after 3 cycles because of severe gastrointestinal and hematological toxicity, without instrumental evaluation of disease).

After 4 cycles of TCF-dd, 2 CR (5%), 20 PR (50%), 9 SD (22%) and 5 disease progressions (12%) were observed, for an ORR of 55% (95% CI, 40–70), as shown in Table 3.

The activity rate achieved after the administration of COFFI is listed in Table 4. The two CR observed after TCF-dd were maintained after COFFI. Among the 20 patients with PR after TCF-dd, 2 achieved CR, 6 had a further improvement of response, 6 maintained PR, 2 progressed and 4 did not start COFFI (1 early death not related to the disease nor to the treatment, 1 protocol violation, 1 patient refusal and 1 for other reasons).

Table 2 Chemotherapy delivery

	TCF-dd	COFFI
No. of treated patients	40	23
No. of patients who completed 4 cycles without delay nor dose reductions (%)	16 (40)	9 (39)
No. of patients who received less than 4 cycles (%)	4 (10)	3 (13)
No. of patients with dose reduction (%)	10 (25)	6 (26)
No. of patients with at least 1 cycle delay (%)	21 (53)	13 (57)
No. of patients with at least 1 cycle delay and dose reduction (%)	9 (23)	5 (22)
Median no. of cycles per patient (range)	4 (1–4)	4 (2–4)
No. of planned cycles	160	92
No. of delivered cycles (%)	151 (94)	88 (96)
No. of delayed cycles (%)	61 (40)	21 (24)
No. of cycles with dose reduction (%)	15 (10)	16 (18)
Median dose intensity[a] (mg/m^2/week)	Docetaxel 35	Irinotecan 64
	Cisplatin 30	Oxaliplatin 39
	5-Fluorouracil 1.000	5-Fluorouracil 1.280
Median relative dose intensity[a] (range)	Docetaxel 1 (0,4-1)	Irinotecan 0,92 (0,6-1)
	Cisplatin 1 (0,4-1)	Oxaliplatin 0,92 (0,6-1)
	5-Fluorouracil 1 (0,4-1)	5-Fluorouracil 0,92 (0,6-1)

[a] Refers to 21 patients treated after the protocol amendments

Table 3 Activity of TCF-dd regimen—intention to treat analysis

	No.	%
CR	2	5
PR	20	50
ORR	22	55 (95% CI, 40–70)
SD	9	22
PD	5	13
NE	4	10

TCF-dd Docetaxel, cisplatin, 5-fluorouracil modulated with folinic acid—dose-dense, *CR* Complete response, *PR* partial response, *SD* stable disease, *ORR* overall response rate (CR + PR), *PD* progressive disease, *NE* not evaluable

Among the 9 patients with SD after TCF-dd, 2 achieved PR, 2 maintained stable disease, 1 progressed and 4 did not start COFFI (1 protocol violation, 1 patient refusal and 2 for other reasons).

The ORR in the 23 patients who received both TCF-dd and COFFI was 60% (95% CI, 45–75).

Two patients with multiple liver metastases maintained CR for 16 and over 36 months respectively. Two patients with peritoneal macrometastases maintained CR for 11 and over 12 months respectively. At a median follow-up of 19 months (95% CI, 16–23), median TTP was 8.6 months (95% CI, 6.2–9.3) and median OS was 10.7 months (95% CI, 8.4–15.6). The 1-year OS was 31%. These survival figures refer to patients who received both regimens.

Table 4 Activity of the sequence TCF-dd followed by COFFI—intention to treat analysis

	No.	%
CR	4	10
PR	20	50
ORR	24	60 (95% CI, 45–75)
SD	7	17
PD	5	13
NE	4	10

TCF-dd docetaxel, cisplatin, 5-fluorouracil modulated with folinic acid—dose-dense, *COFFI* combination of oxaliplatin, folinic acid, 5-fluorouracil and irinotecan, *CR* complete response, *PR* partial response, *SD* stable disease, *ORR* overall response rate (CR + PR), *PD* progressive disease, *NE* not evaluable

Safety

Toxicities experienced during treatment are listed in Tables 5 and 6.

All patients were evaluable for toxicity. Among the 21 patients treated with TCF-dd after the protocol amendments, grade 3–4 neutropenia and thrombocytopenia rates were 29% and 19% respectively. Febrile neutropenia occurred in 10% of patients. Most frequent grade 3–4 non-hematological toxicities were: asthenia (24%), diarrhea (14%) and hypokalemia (14%).

Eight patients (35%) treated with COFFI developed grade 3–4 neutropenia (all not febrile); however, two

Table 5 Toxicity of TCF-dd before and after the protocol amendments according to NCI-CTC version 3.0 criteria

	Before the amendments		After the amendments	
	No. of patients	%	No. of patients	%
Treated	19	100	21	100
Neutropenia				
Grade 1–2	6	32	1	5
Grade 3–4	13	68	6	29
Febrile neutropenia	6	32	2	10
Thrombocytopenia				
Grade 1–2	10	53	3	14
Grade 3–4	7	37	4	19
Anemia				
Grade 1–2	14	74	7	33
Grade 3–4	4	21	1	5
Nausea/vomiting				
Grade 1–2	9	47	9	43
Grade 3–4	2	11	3	14
Diarrhea				
Grade 1–2	9	47	5	24
Grade 3–4	5	26	3	14
Asthenia				
Grade 1–2	2	11	9	43
Grade 3–4	9	47	5	24
Stomatitis				
Grade 1–2	3	16	3	14
Grade 3–4	2	11	1	5
Hypokalemia				
Grade 1–2	6	32	4	19
Grade 3–4	4	2	3	14
Hypocalcaemia				
Grade 1–2	4	21	3	14
Grade 3–4	5	26	0	0
Creatinine elevation				
Grade 1–2	8	42	1	5
Grade 3–4	0	0	0	0

patients did not receive erroneously for the first cycle any primary prophylaxis with granulocyte colony stimulating factors. Grade 3–4 diarrhea occurred in 17% of patients.

Discussion

In this study we have tested for the first time in advanced gastric cancer a strategy consisting of two sequential, intensified chemotherapy regimens.

The ORR of 55%, obtained after 4 cycles of TCF-dd rose to 60% after 4 cycles of COFFI.

This result is interesting and also confirms those of previous phase II trials of sequential chemotherapy in this setting, which have shown an increase of activity by introducing non cross-resistant drugs [24–26].

However the administration of 8 cycles of chemotherapy might have lead to the good response rates registered; for this reason we believe that this issue deserves to be clarified by the means of a randomized study.

Despite the dose reduction of cisplatin and docetaxel after the study started, the activity of the TCF-dd regimen was apparently not compromised: in fact, among the first 19 treated patients, the ORR was 47% compared to 62% observed among the 21 patients subse-

Table 6 Toxicity of COFFI according to NCI-CTC version 3.0 criteria

	No. of patients	%
Treated	23	100
Neutropenia		
Grade 1–2	0	0
Grade 3–4	8*	35[a]
Febrile neutropenia	0	0
Thrombocytopenia		
Grade 1–2	7	30
Grade 3–4	2	9
Anemia		
Grade 1–2	4	17
Grade 3–4	1	4
Nausea/vomiting		
Grade 1–2	4	17
Grade 3–4	1	4
Diarrhea		
Grade 1–2	8	35
Grade 3–4	4	17
Asthenia		
Grade 1–2	3	13
Grade 3–4	1	4
Stomatitis		
Grade 1–2	1	4
Grade 3–4	0	0
Creatinine elevation		
Grade 1–2	0	0
Grade 3–4	0	0

[a] Two patients did not receive erroneously for the first cycle any primary prophylaxis with granulocyte colony stimulating factors

quently treated after the protocol amendments (data not shown).

The increase of activity in our study is less than we expected at the time of the trial design; probably the 70% ORR foreseen was too optimistic.

Moreover we think that the results obtained from this sequential therapy should be balanced with the potential toxicity and financial burden of the heavy regimens administered. It is then of paramount importance the proper selection of patients which may potentially have benefit.

The TTP and OS were not primary end-points, however they deserve some considerations.

A median TTP of 8.6 months is longer than those achieved by other regimens considered among the most effective in advanced gastric cancer, such as ECF [5], DCF [6] and TCF [7].

Notwithstanding, due to a relatively small sample size and a non-randomized design, it is not possible to draw definitive conclusions from this result. Despite the fact that we have found a long TTP, the median OS of 10.7 months was not impressive. This could be explained by the fact that only patients with distant metastases were included in our study. In addition, the 1-year OS was 31%.

It is also important to show the clinical course of the four patients with CR: of the two patients with multiple liver metastases, one is still in CR after 36 months of follow-up and the other has relapsed after 16 months. Of the two patients with peritoneal macrometastases, one is still in CR after 12 months of follow-up and the other has relapsed after 11 months.

Regarding the toxicity, some remarks are deserved. The TCF-dd regimen was unacceptably toxic at the initial dosing schedule, especially concerning the gastrointestinal and hematological toxicities and lethargy.

Undoubtedly it would have been more correct to perform first a dose-escalation phase I study to determine the recommended dose of cisplatin and docetaxel.

After the protocol amendments, the toxicity was significantly reduced in the 21 patients subsequently treated. However, constitutional symptoms and hematological toxicity were still not negligible.

At the reduced doses the TCF-dd regimen was feasible, as 10 patients (48%) completed the planned 4 cycles without any delay nor dose reductions (data not shown).

The toxicity of COFFI, mainly represented by diarrhea and neutropenia, was acceptable and comparable to that found in previous phase II studies with this combination [22, 23]. Another point that must be discussed is that unfortunately, no quality of life questionnaires were responded by the enrolled patients. It would have been undoubtedly additive valuable information, also when considering this approach instead of the "classic" strategies in this disease.

Nevertheless, on the basis of aforementioned considerations, we think that a sequential strategy with TCF-dd for 4 cycles followed by COFFI for 4 cycles is feasible, effective and deserves to be tested in well designed randomized trials. It may be of special interest in patients with symptomatic disease in need of a rapid reduction of tumor burden as well as in the neoadjuvant setting in order to achieve better response rates.

It also may be of special interest the addition of biological agents to enhance the efficacy of this strategy, which will be our next subject of research.

Conflict of interest The author(s) indicated no potential conflicts of interest.

References

1. Kamangar F, Dores GM, Anderson WF (2006) Patterns of cancer incidence, mortality, and prevalence across five continents: defining priorities to reduce cancer disparities in different geographic regions of the world. J Clin Oncol 24:2137–2150

2. Parkin DM, Bray F, Ferlay J et al (2005) Global cancer statistics, 2002. CA Cancer J Clin 55:74–108
3. Lim L, Michael M, Mann GB et al (2005) Adjuvant therapy in gastric cancer. J Clin Oncol 23:6220–6232
4. Wagner AD, Grothe W, Haerting J et al (2006) Chemotherapy in advanced gastric cancer: a systematic review and meta-analysis based on aggregate data. J Clin Oncol 24:2903–2909
5. Webb A, Cunningham D, Scarffe JH et al (1997) Randomized trial comparing epirubicin, cisplatin, and fluorouracil versus fluorouracil, doxorubicin, and methotrexate in advanced esophagogastric cancer. J Clin Oncol 15:261–267
6. Van Cutsem E, Moiseyenko VM, Tjulandin S et al (2006) Phase III study of docetaxel and cisplatin plus fluorouracil compared with cisplatin and fluorouracil as first-line therapy for advanced gastric cancer: a report of the V325 Study Group. J Clin Oncol 24:4991–4997
7. Roth AD, Fazio N, Stupp R et al (2007) Docetaxel, cisplatin, and fluorouracil; docetaxel and cisplatin; and epirubicin, cisplatin, and fluorouracil as systemic treatment for advanced gastric carcinoma: a randomized phase II trial of the Swiss Group for Clinical Cancer Research. J Clin Oncol 25:3217–3223
8. Cunningham D, Starling N, Rao S et al (2008) Capecitabine and oxaliplatin for advanced esophagogastric cancer. N Engl J Med 358:36–46
9. Al-Batran SE, Hartmann JT, Probst S et al (2008) Phase III trial in metastatic gastroesophageal adenocarcinoma with fluorouracil, leucovorin plus either oxaliplatin or cisplatin: a study of the Arbeitsgemeinschaft Internistische Onkologie. J Clin Oncol 26:1435–1442
10. Kang YK, Kang WK, Shin DB et al (2009) Capecitabine/cisplatin versus 5-fluorouracil/cisplatin as first-line therapy in patients with advanced gastric cancer: a randomised phase III noninferiority trial. Ann Oncol 20:666–673
11. Dank M, Zaluski J, Barone C et al (2008) Randomized phase III study comparing irinotecan combined with 5-fluorouracil and folinic acid to cisplatin combined with 5-fluorouracil in chemotherapy naive patients with advanced adenocarcinoma of the stomach or esophagogastric junction. Ann Oncol 19:1450–1457
12. Koizumi W, Narahara H, Hara T et al (2008) S-1 plus cisplatin versus S-1 alone for first-line treatment of advanced gastric cancer (SPIRITS trial): a phase III trial. Lancet Oncol 9:215–221
13. Norton L, Simon R, Brereton HD et al (1976) Predicting the course of Gompertzian growth. Nature 264:542–545
14. Norton L, Simon R (1986) The Norton-Simon hypothesis revisited. Cancer Treat Rep 70:163–169
15. Fizazi K, Zelek L (2000) Is one cycle every three or four weeks' obsolete? A critical review of dose-dense chemotherapy in solid neoplasms. Ann Oncol 11:133–149
16. Vasey PA (2003) Resistance to chemotherapy in advanced ovarian cancer: mechanisms and current strategies. Br J Cancer 89(Suppl 3):S23–S28
17. Grossi F, Aita M, Follador A et al (2007) Sequential, alternating, and maintenance/consolidation chemotherapy in advanced non-small cell lung cancer: a review of the literature. Oncologist 12:451–464
18. Ocana A, Hortobagyi GN, Esteva FJ (2006) Concomitant versus sequential chemotherapy in the treatment of early-stage and metastatic breast cancer. Clin Breast Cancer 6:495–504
19. Cascinu S, Labianca R, Alessandroni P et al (1997) Intensive weekly chemotherapy for advanced gastric cancer using fluorouracil, cisplatin, epi-doxorubicin, 6S-leucovorin, glutathione, and filgrastim: a report from the Italian Group for the Study of Digestive Tract Cancer. J Clin Oncol 15:3313–3319
20. Lordick F, Lorenzen S, Stollfuss J et al (2005) Phase II study of weekly oxaliplatin plus infusional fluorouracil and folinic acid (FUFOX regimen) as first-line treatment in metastatic gastric cancer. Br J Cancer 93:190–194
21. Louvet C, Andre T, Tigaud JM et al (2002) Phase II study of oxaliplatin, fluorouracil, and folinic acid in locally advanced or metastatic gastric cancer patients. J Clin Oncol 20:4543–4548
22. Chiesa MD, Buti S, Tomasello G et al (2007) A pilot phase II study of chemotherapy with oxaliplatin, folinic acid, 5-fluorouracil and irinotecan in metastatic gastric cancer. Tumori 93:244–247
23. Lee J, Kang WK, Kwon JM et al (2007) Phase II trial of irinotecan plus oxaliplatin and 5-fluorouracil/leucovorin in patients with untreated metastatic gastric adenocarcinoma. Ann Oncol 18:88–92
24. Cascinu S, Graziano F, Barni S et al (2001) A phase II study of sequential chemotherapy with docetaxel after the weekly PELF regimen in advanced gastric cancer. A report from the Italian group for the study of digestive tract cancer. Br J Cancer 84:470–474
25. HC Yeh K, Lu Y et al (2006) Phase II study of sequential non-cross-resistant chemotherapy using weekly 24-hour infusion of cisplatin, high-dose 5-fluorouracil and leucovorin (P-HDFL) followed by weekly docetaxel and irinotecan (DI) for recurrent or metastatic gastric cancer: an interim analysis. J Clin Oncol 24:18S (Suppl; abstr 14063)
26. F Loupakis, Masi G, Bursi S et al (2007) Phase II study of sequential chemotherapy with cisplatin (P) in combination with infusional 5FU/LV (PFL) followed by irinotecan (Ir) + 5FU/LV (IrFL) followed by docetaxel (T) + 5FU/LV (TFL) in patients (pts) with metastatic gastric carcinoma (MGC) by the Gruppo Oncologico Nord-Ovest (GONO). J Clin Oncol 25:18S (Suppl; abstr 15059)
27. de Gramont A, Bosset JF, Milan C et al (1997) Randomized trial comparing monthly low-dose leucovorin and fluorouracil bolus with bimonthly high-dose leucovorin and fluorouracil bolus plus continuous infusion for advanced colorectal cancer: a French intergroup study. J Clin Oncol 15:808–815
28. Therasse P, Arbuck SG, Eisenhauer EA et al (2000) New guidelines to evaluate the response to treatment in solid tumors. European Organization for Research and Treatment of Cancer, National Cancer Institute of the United States, National Cancer Institute of Canada. J Natl Cancer Inst 92:205–216
29. A'Hern RP (2001) Sample size tables for exact single-stage phase II designs. Stat Med 20:859–866
30. Hryniuk WM, Goodyear M (1990) The calculation of received dose intensity. J Clin Oncol 8:1935–1937

Pharmaceutical Research, Vol. 7, No. 8, 1990

Research Article

Efficiency of Cytoplasmic Delivery by pH-Sensitive Liposomes to Cells in Culture

Chun-Jung Chu,[1] Jan Dijkstra,[2] Ming-Zong Lai,[3] Keelung Hong,[4] and Francis C. Szoka[1,5]

Received November 30, 1989; accepted February 22, 1990

The intracellular processing of pH-sensitive liposomes composed of cholesterylhemisuccinate (CHEMS) and dioleoylphosphatidylethanolamine (DOPE) by eukaryotic cell lines has been compared to non-pH-sensitive liposomes made of CHEMS and dioleoylphosphatidylcholine (DOPC). The pH-sensitive liposomes can deliver encapsulated fluorescent molecules [calcein, fluoresceinated dextran, fluoresceinated polypeptide, and diphtheria toxin A chain (DTA)] into the cytoplasm. Cytoplasmic delivery can be blocked in the presence of ammonium chloride or EDTA, indicating that the process requires a low-pH environment and the presence of divalent cations. Inhibition of cellular protein synthesis by DTA delivery from the pH-sensitive liposome is orders of magnitude greater than from the non-pH-sensitive liposome composition. The delivery of DTA into the cytoplasm by pH-sensitive liposomes is at least 0.01% of cell-associated liposomal DTA. There is no significant difference in the degradation rate of bovine serum albumin (BSA) or the rate of acidification of pH-sensitive dye, 8-hydroxy-1,3,6-pyrene-trisulfonate (HPTS), when delivered to cells in pH-sensitive and non-pH-sensitive liposomes. Thus the efficiency of cytoplasmic delivery is less than 10% of the cell-associated liposome contents, which is the smallest difference that can be detected by these two assays. Based upon the various assays used to measure liposome content disposition in the cell, we conclude that the efficiency of cytoplasmic delivery by the CHEMS/DOPE liposomes is greater than 0.01% and less than 10% of the cell-associated liposomal contents.

KEY WORDS: cell culture; drug delivery; fluorescence; fusion; *in vitro;* liposomes; pH sensitive.

INTRODUCTION

A variety of macromolecules that can modulate the physiology and metabolism of cells, such as antibodies (1), DNA (2), antisense oligonucleotides (3), and ribozymes (4), have been proposed as novel therapeutic modalities. These molecules cannot readily cross the plasma membrane, hence a delivery system to introduce them into the cytoplasm is essential for their continued development. One possibility is to use liposomes, which have been widely employed as drug carriers, functioning both as a controlled-release system and to deliver encapsulated compounds into cells (5). However, the majority of liposomes internalized by cells enter through an endocytic pathway (6,7) and the ultimate fate of the liposome is the lysosome. Here enzymatic degradation of the lipids and their contents occur (8,9). Compounds that are degraded in or cannot escape the lysosomal compartment would be inactive when delivered by most liposome compositions described to date.

pH-sensitive liposomes have been developed to circumvent delivery to the lysosome. Such liposomes destabilize membranes or become fusogenic when they are exposed to an acidic environment. In the process of endocytosis the pH is reduced in the endosome, a compartment that precedes the lysosome (10). The appropriately designed pH-sensitive liposome might then transfer its contents into the cytoplasm before the liposome can be conveyed to the lysosomes.

Straubinger and co-workers (11) demonstrated that a liposome composed of oleic acid (OA)[6]/phosphatidylethanolamine (PE) can deliver membrane impermeant calcein and fluoresceinated dextran to the cytoplasm. Huang and colleagues (12–14) incorporated monoclonal antibodies with the

[1] Department of Pharmacy and Pharmaceutical Chemistry, School of Pharmacy, University of California, San Francisco, California 94143.

[2] Laboratory of Physiological Chemistry, University of Groningen, 9712 KZ Groningen, The Netherlands.

[3] Department of Immunology, Institute of Molecular Biology, Academia Sinica, Taipei, Taiwan.

[4] Cancer Research Institute, University of California, San Francisco, California 94143.

[5] To whom correspondence should be addressed.

[6] Abbreviations used: BSA, bovine serum albumin; CHEMS, cholesterylhemisuccinate; DMEM, Dulbecco modified Eagle medium; DOPC, dioleoylphosphatidylcholine; DOPE, dioleoylphosphatidylethanolamine; DPX, *N,N'-p*-xylenebis(pyridinium bromide); DTA, diphtheria A chain; EPC, egg phosphatidylcholine; EPE, egg phosphatidylethanolamine; FCS, fetal calf serum; FITC, fluorescein isocyanate; FITC–poly-GL, FITC-labeled poly(D-glutamic acid-D-lysine); Fl 450/413, the ratio of fluorescence emission at excitation wavelengths of 450 and 413 nm; Hepes, *N*-2-hydroxyethylpiperazine-*N'*-2-ethanesulfonic acid; HPTS, 8-hydroxy-1,3,6-pyrene-trisulfonate; IC_{50}, concentration at 50% inhibition; LysoPC, lysophosphatidylcholine; NH_4Cl, ammonium chloride; OA, oleic acid; PBS, phosphate-buffered saline; PC, phosphatidylcholine; PE, phosphatidylethanolamine; poly-GL, poly(D-glutamic acid-D-lysine); TCA, trichloroacetic acid.

0724-8741/90/0800-0824$06.00/0

fatty acid containing pH-sensitive liposomes to construct pH-sensitive immunoliposomes and were able to deliver various chemotherapeutic agents and DNA to the cytoplasm of target cells. Evidence has also been presented that cytoplasmic delivery can occur *in vivo* (15). In these prior studies the efficiency of cytoplasmic delivery via the pH-sensitive liposomes was not quantitated.

We have demonstrated that cholesterylhemisuccinate (CHEMS) behaves like cholesterol and stabilizes PE vesicles at neutral pH (16,17) and that protonated CHEMS accelerates the destabilization of PE vesicles at low pH (<6.0) by catalyzing the formation of the hexagonal H_{II} phase (16,17). Thus the CHEMS/PE composition is sensitive to the pH change which occurs along the endocytic pathway and liposomes composed of CHEMS/PE may become leaky or fuse with the intracellular membrane by this proton-triggering mechanism after they are endocytosed by cells.

In this report, the intracellular processing of pH-sensitive liposomes has been compared to non-pH-sensitive liposomes using a combination of fluorescent pH-sensitive dyes, radiolabeled albumin, and diphtheria toxin A chain (DTA). We show that pH-sensitive liposomes made of CHEMS/DOPE deliver encapsulated fluorescent molecules and biologically active macromolecules into the cytoplasmic compartment. Cytoplasmic delivery from the pH-sensitive liposome is orders of magnitude greater than from the non-pH-sensitive composition. However, cytoplasmic delivery still accounts for less than 10% of the liposome contents that become cell associated.

MATERIALS AND METHODS

Materials

Dioleoylphosphatidylethanolamine, dioleoylphosphatidylcholine (DOPC), egg phosphatidylcholine (EPC), egg phosphatidylethanolamine (EPE), lysophosphatidylcholine (LysoPC), and oleic acid were obtained from Avanti Polar Lipids Inc. (Birmingham, AL). Ammonium chloride (NH_4Cl), guanidine, dithiothreitol, trichloroacetic acid (TCA), *N*-2-hydroxyethylpiperazine-*N'*-2-ethanesulfonic acid (HEPES), Triton X-100, CHEMS, fluorescein isocyanate (FITC), FITC–dextran (MW 4200; 0.0035 mol FITC/mol glucose), and bovine serum albumin (BSA) were purchased from Sigma (St. Louis, MO). Calcein, 8-hydroxy-1,3,6-pyrene-trisulfonate (HPTS), *N,N'-p*-xylenebis-(pyridinium bromide) (DPX) and sulforhodamine 101 were obtained from Molecular Probes (Junction City, OR). Poly(D-glutamic acid-D-lysine) at a 6/4 ratio (poly-GL; MW 69,000) was obtained from Miles (Naperville, IL). Nicked diphtheria toxin was obtained from Calbiochem (San Diego, CA). ^{3}H-Inulin, ^{3}H-leucine, and ^{125}I-NaI were purchased from Amersham (Arlington Heights, IL). ^{125}I-Labeled *p*-hydroxybenzamidine dihexadecylphosphatidylethanolamine was synthesized as described (18). Nuclease-treated rabbit reticulocyte lysate mixture, leucine-deficient amino acid mixture, and Brome mosaic virus RNA were purchased from Promega Biotec Inc. (Madison, WI).

Cell Culture

The macrophage-like cell line RAW 264.7 and P388D1 cells were maintained in Dulbecco modified Eagle medium (DMEM) with 10% heat-inactivated fetal calf serum (FCS) and RPMI 1640 with 10% FCS, respectively. For all the experiments, cells were plated as monolayers in 35-mm or 96-well culture dishes (Costar, Cambridge, MA) 16–20 hr prior to use. Cells were checked and found free from mycoplasma contamination.

Preparations of Liposomes

Liposomes (22 μ*M* lipid) were prepared by the method of reverse-phase evaporation (19) and extruded through 0.2-μm polycarbonate membranes (20). pH-sensitive liposomes were composed of CHEMS/DOPE at molar ratios of 4/6, if not otherwise indicated, while control liposomes were made of CHEMS/DOPC with the corresponding ratio. Compounds to be encapsulated were suspended in an isotonic, pH 7.4 solution with the following concentrations: 50–75 m*M* calcein, 50 m*M* FITC–dextran (FITC/dextran, 0.08/1), 30 m*M* HPTS/50 m*M* DPX, 1 mg/ml BSA/1 m*M* inulin, 0.6 m*M* fluoresceinated poly-GL, and 10 μ*M* DTA. Nonencapsulated calcein, FITC-dextran, and HPTS/DPX were separated by Sephadex G-75 (1 × 20-cm) gel filtration. Nonencapsulated BSA and poly-GL (in 10 m*M* Hepes, 145 m*M* NaCl, pH 7.4 buffer) were separated from encapsulated material by Bio-Gel A 5m (1 × 20-cm) gel filtration. Nonencapsulated DTA was separated from liposome-encapsulated DTA by floating the liposomes through a metrizamide gradient (21). Liposome diameter was determined with a laser light-scattering apparatus (NS-4; Coulter Electronics, Inc., Hialeah, FL). Phospholipid concentration was measured by the method of Bartlett (22).

Stability of Liposomes in Serum

Calcein at 75 m*M*, a self-quenched fluorescence concentration, was encapsulated in liposomes composed of CHEMS/EPE (1/2), CHEMS/EPC (1/2), OA/EPC (3/10), and lysoPC/EPC (3/10). Nonencapsulated calcein was removed from the preparation by column chromatography on Sephadex G-25 and 1 μmol of lipid was placed in 1 ml of a 50% FCS/Hepes, pH 7.4, buffer at 37°C. At intervals, a sample was removed from the incubation mixtures and the percentage of calcein remaining in the liposomes was quantitated from the dequenching of calcein fluorescence (23).

Preparation of FITC–Poly-GL

Poly-GL was labeled with FITC as follows (24). Peptide dissolved in 50 m*M* borate buffer, pH 9, was mixed with FITC in DMSO at a 1/9 (poly-GL/FITC) molar ratio. The reaction mixture was kept in the dark at pH 9, room temperature, with constant stirring for 20 hr. Nonreacted FITC was separated on a Sephadex G/50 (1 × 28-cm) column eluted with water. The FITC–poly-GL complex fractions were lyophilized and redissolved in 10 m*M* Hepes, 145 m*M* NaCl, pH 7.4, at a concentration of 0.6 m*M* before encapsulation. The final product has approximately 6 molecules of FITC conjugated to 1 molecule of poly-GL.

Liposome Uptake by Cells in Culture

Cells (1.5×10^6) in 35-mm culture dishes were rinsed

with FCS-free media before the addition of liposomes. Liposomes containing ^{125}I-*p*-hydroxybenzamidine dihexadecylphosphatidylethanolamine were diluted in serum-free media and incubated with cells for 1 hr at 37°C. At the end of the incubation, cells were washed with cold PBS (6×) and then lysed with 0.5 *N* NaOH. Radioactivity associated with the cell lysate was measured in a Beckman gamma scintillation spectrometer and protein concentrations were assayed by the method of Lowry (25).

Fluorescence Microscopy of Liposomal Cytoplasmic Delivery

P388D1 cells (1×10^6) cultured in 35-mm culture dishes were rinsed with FCS-free media and then incubated with calcein, FITC–dextran or FITC–poly-GL containing liposomes (50–1000 μmol of lipid diluted in FCS-free medium) with or without NH_4Cl (20 m*M*) at 37°C for 1 hr. Cells were then washed three times with 2 ml of phosphate-buffered saline (PBS) (137 m*M* NaCl, 2.7 m*M* KCl, 1.5 m*M* KH_2PO_4, 8.1 m*M* Na_2HPO_4, pH 7.4) and refed with 1 ml of FCS-free medium. A Leitz fluorescence microscope with an excitation filter in the range 450–490 nm (blue band) and a barrier filter for emission fluorescence at wavelengths greater than 515 nm was used to examine cells treated with calcein/FITC liposomes. For cells incubated with HPTS/DPX-containing liposomes, one filter set consisting of a blue-band excitation filter was used to observe the fluorescence from intracellular HPTS in the higher-pH compartment. Fluorescence from HPTS at lower pH (<6) was efficiently filtered using the blue-band filter set. A second set of filters (violet band), excitation 350–410 nm and an emission filter for wavelengths greater than 455 nm, was employed to observe the fluorescence from all HPTS inside of cells. The violet-band filter permitted observation of HPTS in both the low- and the high-pH compartments (26).

To investigate if the endosome/lysosome membrane can be destabilized by the pH-sensitive vesicles, P388D1 cells were incubated with the sulforhodamine 101 (12.5 μg/ml). This fluorescent dye was concentrated in the lysosomes after 3 days of incubation. Empty CHEMS/DOPE liposomes (100 μ*M*) were added to the cell culture in dye-free medium for 4 hr, and then the nonattached vesicles were removed by washing three times with PBS. The cells were examined with a fluorescence microscope using the 530- to 560-nm excitation filters and an emission filter set to pass light at wavelengths greater than 610 nm.

Fluorescence was photographed using Kodak P800/1600 film. Exposure time varied from 5 to 78 sec.

Inhibition of Protein Synthesis by Liposomal DTA

Determination of Encapsulated DTA Concentration

Diphtheria toxin A chain was prepared by a modification of a published method (27). Nicked diphtheria toxin was mixed with dithiothreitol (100 m*M*) and guanidine (500 m*M*) at pH 7.5 for 1 hr at 37°C. Denatured B chain was precipitated by centrifugation at 10,000*g* for 20 min. DTA remaining in the supernatant was dialyzed against 10 m*M* Hepes, 145 m*M* NaCl, pH 7.5, buffer. The DTA-containing liposomes were lysed with 0.4% Triton X-100 and the amount of DTA encapsulated was determined using the reticulocyte lysate assay (28). A standard curve was constructed by assaying known amounts of DTA with lysed empty lipid vesicles. Aliquots (3.5 μl) of lysed liposomes and DTA were mixed with 17.5 μl of reticulocyte lysate mixture, 0.5 μl of 1 m*M* amino acid mixture (minus leucine), 1 μl of Brome mosaic virus RNA (0.5 μg/μl), and 2.5 μl of ^{3}H-leucine (156 mCi/μmol, 1 mCi/ml) and then incubated at 33°C for 1 hr. Amino acid incorporation into protein was assayed in a 3-μl aliquot of the reaction mixture to which 25% TCA and 1% carrier BSA were added. The protein precipitate was collected onto Whatman GF/C filter paper and the radioactivity associated with the filter was measured in a Beckman beta scintillation spectrometer. A standard curve of DTA concentration (10^{-6} to 10^{-9} *M*) versus the percentage inhibition of leucine incorporation to protein by DTA was thus constructed. This standard curve was used to determine the amount of biologically active DTA in the lysate of DTA-containing liposomes.

Inhibition of ^{3}H-Leucine Incorporation to Cellular Protein

P388D1 cells (1×10^5) in a 96-well dish (flat bottom) were incubated with medium, nonencapsulated DTA, empty vesicles, or DTA-encapsulated CHEMS/DOPC (2.5/7.5) or CHEMS/DOPE (2.5/7.5) liposomes for 1 hr at 37°C. In order to obtain a more pronounced effect via pH-sensitive liposomes, the ratio of CHEMS/PE is changed to a lower ratio, which is more likely to become destabilized or fusogenic when encountering the acidic pH (17). After two washes, cells were pulsed with ^{3}H-leucine (1 μCi/well) in fresh medium for 6 hr and then lysed with 20 μl 7 *M* guanidine. Protein precipitated with 100 μl 25% TCA and 50 μl 1% carrier BSA was collected onto glass-fiber disks and washed with 10% TCA using a cell harvester (Skatron Inc., Sterling, VA). The radioactivity associated with the dried disks was determined in a Beckman beta scintillation spectrometer.

Fluorimetry of Cell-Associated HPTS

In order to decrease the fluorescence contributed from noninternalized HPTS-containing liposomes on the cell surface or the background fluorescence from liposomes attached to the culture dish, HPTS was coencapsulated with the collisional quencher DPX at a 1:1.7 ratio (30/50 m*M*) in liposomes. P388D1 cells (1.5×10^6) in 35-mm culture dishes were incubated with vesicles, 50 μ*M* CHEMS/DOPE or 500 μ*M* CHEMS/DOPC, for 1 hr and washed with medium three times. Then incubation was continued in fresh medium without liposomes. At each indicated time point after washing, cells were removed from dishes by exposure to 3 m*M* EDTA/PBS and diluted to $2.5–5 \times 10^5$ cells/ml in PBS. Fluorescence emission was monitored at 510 nm using a SPEX Fluorolog 2 spectrofluorometer (26). Fluorescence intensity associated with the cell suspension irradiated at excitation wavelengths of 413 and 450 nm was measured. The ratio of emitted fluorescence intensity at each excitation wavelength of 450 and 413 nm (Fl 450/413) was calculated.

The excitation spectrum of HPTS is a function of pH. The isobestic point for the excitation wavelength of this pH-dependent phenomenon is 413 nm. When an excitation wavelength of 450 nm is used, the fluorescence signal increases more than 100-fold as the pH increases from 6 to 8.

The ratio of the fluorescence emission for the 450-nm excitation wavelength compared to the 413-nm excitation wavelength (Fl 450/413) can be used as an indicator of the pH of the HPTS solution (29). For instance, a Fl 450/413 of 2.1 indicates that HPTS experiences a neutral pH of 7.4 and a Fl 450/413 of 0.2 represents that HPTS is in an acidic pH (pH < 6) environment. The pH-dependent fluorescent pattern of nonencapsulated HPTS is not affected by the coencapsulation of DPX with HPTS in the liposomes. Since the relationship between the pH and the Fl 450/413 value is almost linear between pH 8 (Fl 450/413 = 3.2) and pH 6.5 (Fl 450/413 = 0.59), this assay permits one to estimate the pH experienced by HPTS molecules when they become cell associated. The measured cell-associated fluorescence included contributions from HPTS in the cytoplasm, HPTS released in acidic vesicles, and to a small extent, HPTS in vesicles that were on the cell surface. The encapsulated HPTS/DPX elicited less than 4% of the maximum unquenched signal at neutral pH, thus the contribution from noninternalized liposomes containing HPTS/DPX to the total cell-associated fluorescence is small. This assumes that there is no leakage of vesicles contents at the cell surface. If 50% of the contents leak, then the residual encapsulated HPTS fluorescence would be 12% of the maximum unquenched signal and the contribution from these HPTS/DPX-containing liposomes on the cell surface is still small. The cell-associated Fl 450/413 would range between 2.1 to 0.2, since the majority of HPTS would be exposed to either an acidic environment in the intracellular compartments or the neutral environment of the cytoplasm, and the ratio would decrease as the fraction of HPTS exposed to an acidic pH increased.

Degradation of Liposomal BSA

Iodinated BSA (300 μCi/mg) was prepared by the chloramine-T method (30) and was coincorporated with ^{3}H-inulin (28 μCi/mg) into liposomes. Mixtures of double-labeled CHEMS/DOPC vesicles (500 μ*M*) plus empty CHEMS/DOPE vesicles (50 μ*M*) and double-labeled CHEMS/DOPE vesicles (50 μ*M*) plus empty CHEMS/DOPC vesicles (500 μ*M*) were incubated with 1.8×10^6 P388D1 cells in serum-free medium for 2 hr at 37°C. Vesicles not associated with cells were removed by washing six times with PBS. Cells were incubated in the fresh medium without FCS or liposomes for the period indicated. At each time point, cells were washed with PBS (six times) and lysed with 0.5 *N* NaOH. Radioactivity (^{125}I or ^{3}H) associated with cell lysates was measured using a Beckman gamma counter and a Beckman beta scintillation spectrometer, respectively. The ratio of cell-associated ^{125}I-BSA/^{3}H-inulin was calculated and normalized to the ratio of ^{125}I-BSA/^{3}H-inulin at the beginning of the experiment.

The iodopeptide product from BSA degradation in the lysosomal compartment is released to the extracellular medium (8). When a nonmetabolizable ^{3}H-labeled compound is encapsulated with the BSA, the ratio of the ^{125}I to ^{3}H is a measure of the metabolism of BSA. Inulin which is not degraded by lysosomal enzymes was selected as the nonmetabolizable marker. The loss of inulin could occur due only to dissociation of vesicles from the cell, release of liposomal contents at the cell surface, and/or regurgitation of lysosomal contents. Thus inulin coencapsulated with BSA serves as an internal standard to normalize the cell-associated liposomal contents and the BSA/inulin ratio is an indicator for the extent of degradation of liposomal BSA in the cells.

RESULTS

Liposome Preparation and Characterization

The charge and head group of phospholipids can influence the physical properties of the resulting liposomes (31). In the case of PE, containing unsaturated acyl chains, a stable liposome cannot be formed at a pH less than 9.0; rather planar sheets of lipid or hexagonal H_{II} phase lipid tubes exist at room temperature. Incorporating a charged lipid with PE, such as CHEMS, results in the formation of liposomes which are stable at pH 7.0 and room temperature but destabilize as the pH is lowered (16).

Liposomes composed of CHEMS/DOPC have a higher encapsulation volume and encapsulation efficiency than pH-sensitive (CHEMS/DOPE) liposomes (Table I). This occurs in spite of their comparable size (diameters, 203 ± 70 nm) and surface charge density. The encapsulation volume is 1.5- to 3-fold higher for the control liposomes than for the pH-sensitive liposomes. This suggests that the pH-sensitive liposomes are oligolamellar.

Table I. Comparison of Control and pH-Sensitive Liposome Preparations

Lipid composition	Encapsulated compound	Encapsulated ratio (μl/μmol lipid)[a]	Encapsulation efficiency (%)
CHEMS/DOPC[b]	Calcein	4.1	ND[c]
CHEMS/DOPE[b]	Calcein	2.8	ND
CHEMS/DOPC[b]	BSA/inulin	5.1	17.7
CHEMS/DOPE[b]	BSA/inulin	3.4	12.5
CHEMS/DOPC[d]	DTA	5.2	20.9
CHEMS/DOPE[d]	DTA	1.8	7.0

[a] Results are values from a single experiment of each preparation. When other preparations were measured, the CHEMS/DOPE encapsulation ratio was within 30% of the given values.
[b] The molar ratio of CHEMS/DOPC or CHEMS/DOPE is 4/6.
[c] Not determined.
[d] The molar ratio of CHEMS/DOPC or CHEMS/DOPE is 2.5/7.5.

Stability of Liposomes in Serum

Incorporation of cholesterol into the lipid bilayer results in a more rigid membrane (32). In the presence of serum, such vesicles are more stable than single-component phospholipid vesicles. Cholesterylhemisuccinate behaves like cholesterol and stabilizes PE liposomes at neutral pH (17). As shown in Table II, the CHEMS/PE composition retains encapsulated calcein as well as the CHEMS/PC formulation and considerably better than formulations that contain oleic acid or lysophospholipid.

Uptake of Liposomes by Cells in Culture

Liposomes composed of CHEMS/DOPE are taken up by P388D1 cells 5–10 times more efficiently than the CHEMS/DOPC vesicles when the same amount of lipid is added to cells in culture (Fig. 1a). The uptake is concentration and time dependent. The kinetics of uptake saturates about 8 hr after the start of incubation (data not shown). The higher uptake of the PE vesicles cannot be due to the negative charge density since the PC vesicles contained the same molar ratio of CHEMS.

Ellens and co-workers showed that the PE/CHEMS vesicles tended to aggregate in the presence of a high concentration of Ca^{2+}/Mg^{2+} (33) and these divalent cations can influence the cellular uptake of certain negatively charged liposomes. The amount of CHEMS/DOPE vesicles taken up by RAW (Fig. 1b) or P388D1 (data not shown) cells is influenced by the Ca^{2+}/Mg^{2+} present in the medium, 1.8 m*M* Ca^{2+}/0.8 m*M* Mg^{2+} in DMEM and 0.5 m*M* Ca^{2+}/0.4 m*M* Mg^{2+} in RPMI, whereas the uptake of CHEMS/DOPC vesicles is not affected by the Ca^{2+} concentration. The reason for the different cell affinities of CHEMS/PE and CHEMS/PC liposomes is not clear. We speculate that the hydration of phospholipids, e.g., PE is less hydrated than the PC, may play a role in the phenomenon observed. Vesicles containing PE are shown to adhere to each other more strongly than do vesicles containing PC because of the difference in hydration (34). This may explain the greater effect of divalent cations, which can promote the dehydration of phospholipid, on the uptake of the CHEMS/PE vesicles than on that of CHEMS/PC vesicles.

The cellular uptake of CHEMS/PE is higher than that of CHEMS/PC vesicles (Fig. 1), and the leakage in serum is comparable, therefore the amount of contents delivered varies accordingly. Based on the data in Fig. 1a, 50 μ*M* CHEMS/DOPE and 500 μ*M* CHEMS/DOPC were selected for the experiments reported below. These respective concentrations result in comparable amounts of cell-associated content delivery by the two liposome compositions.

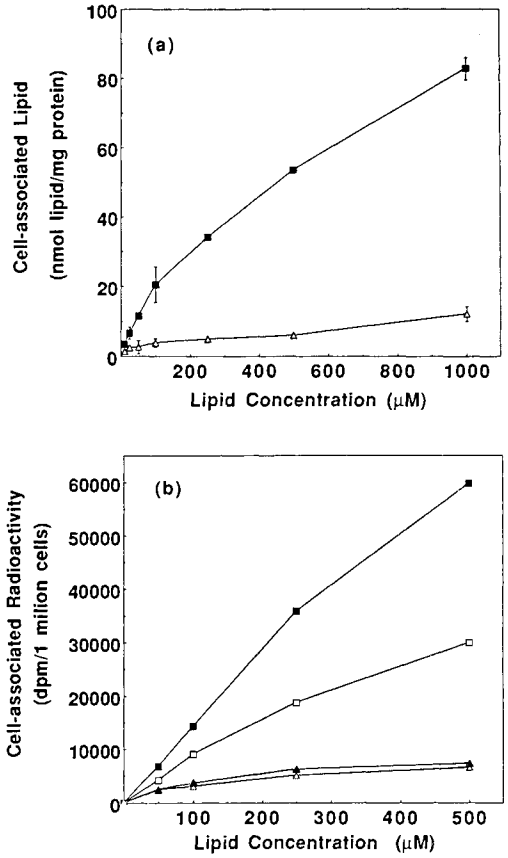

Fig. 1. (a) Concentration-dependent uptake of liposomes by P388D1 cells. Cells were incubated with ^{125}I-labeled liposomes of CHEMS/DOPC (2.5/7.5) (△) or CHEMS/DOPE (2.5/7.5) (■) for 1 hr at 37°C and nonattached liposomes were washed off before the measurement of cell-associated radioactivity. (b) Divalent ion dependent uptake of liposomes by RAW 264.7 cells. Cells were incubated with ^{125}I-labeled CHEMS/DOPC (4/6) (▲, △) or CHEMS/DOPE (4/6) (■, □) liposomes suspended in either DMEM (1.8 m*M* Ca^{2+}/0.8 m*M* Mg^{2+}) (▲, ■) or RPMI1640 (0.5 m*M* Ca^{2+}/0.4 m*M* Mg^{2+}) (△, □) for 1 hr at 37°C. Values are the means of duplicates in a single experiment and the bars represent the range of values from the means.

Table II. Percentage of Calcein Remaining in Liposomes[a]

Time (hr)	CHEMS/EPE (1/2)	CHEMS/EPC (1/2)	OA/EPC (3/10)	LysoPC/EPC (3/10)
0	97[b]	95	95	97
1	95	85	10	29
2	94	81	10	26
3	92	78	11	26
4	91	73	12	29
24	44	29	13	19

[a] Liposomes incubated at 37°C in the presence of serum.
[b] Values are the mean of duplicate measurements from a single experiment that agreed to within 15%.

Fluorescent Microscopy of Cytoplasmic Delivery of Fluorophores

Calcein is a very sensitive indicator for delivering liposome contents into the cytoplasm because it does not readily cross membranes even under mildly acidic conditions (7), and when a 50 m*M* self-quenched solution is diluted into a larger volume, the fluorescence intensity increases more than 20-fold. When encapsulated in control liposomes (CHEMS/DOPC) and incubated with cells, fluorescence is present in a punctate (vacuolar) pattern in the cells (Fig. 2a). If delivered by pH-sensitive liposomes, a diffuse calcein fluorescence is visible throughout the cells (Fig. 2b), indicating that calcein molecules distribute in the cytoplasm. Although the cells shown in Fig. 2b are incubated with liposomes for 1 hr, the diffuse cytoplasmic fluorescence with a lower intensity can be seen at as early as 15 min after addition of the pH-sensitive liposomes.

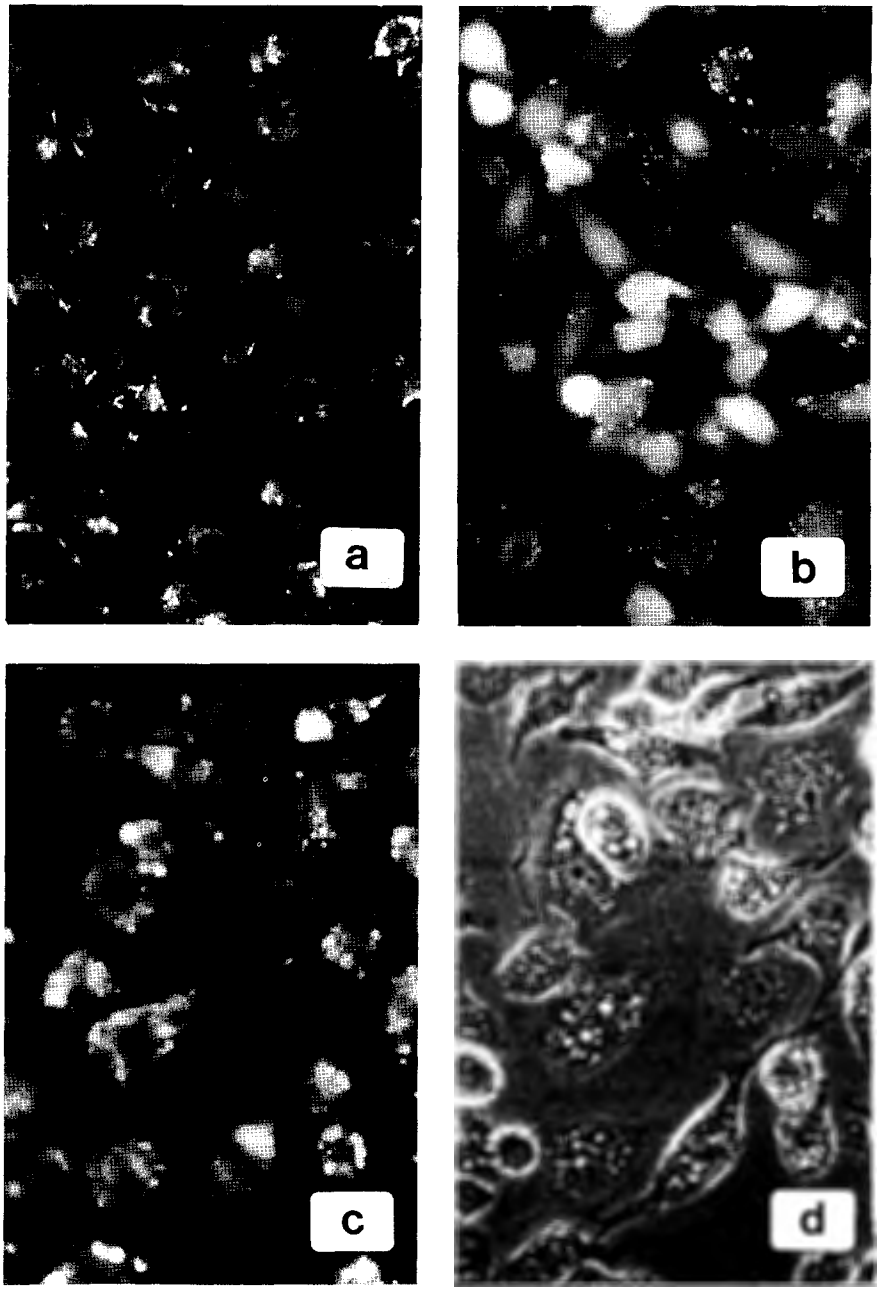

Fig. 2. Fluorescence of RAW264.7 cells after incubation with calcein-containing liposomes for 1 hr. (a) Punctate fluorescence resulting from incubation with 500 μ*M* CHEMS/DOPC (4/6) liposomes. (b) Diffuse (cytoplasmic) fluorescence obtained by incubation with 100 μ*M* CHEMS/DOPE (4/6) liposomes. (c) Vacuolar fluorescence from incubation with 100 μ*M* CHEMS/DOPE (4/6) vesicles in the presence of 20 m*M* NH_4Cl. (d) Phase-contrast image of the field shown in c. Bar indicates 10 μm.

In the presence of 20 m*M* NH_4Cl, a concentration that dissipates the pH gradients in the acidic granules (35), a punctate fluorescence is observed in cells incubated with the pH-sensitive liposomes (Fig. 2c). The brightly fluorescent vacuoles indicate that calcein is released and confined in these compartments. This supports the idea that transfer of calcein to the cytoplasm is a pH-dependent phenomenon.

Divalent cations, Ca^{2+}/Mg^{2+}, are also required for cytoplasmic delivery via pH-sensitive liposomes. When divalent cations were chelated by the addition of 1 m*M* EDTA in DMEM, cytoplasmic calcein fluorescence from pH-sensitive liposomes was not observed (data not shown). Only the punctate fluorescence which was similar to that of cells treated with NH_4Cl was obtained; even the fluorescence intensity observed under these two conditions, NH_4Cl and EDTA treatment, was similar. These findings indicate that both protons and divalent cations are involved in the destabilization/fusion of CHEMS/DOPE vesicles resulting in cytoplasmic delivery. All the phenomena describing the cytoplasmic delivery via CHEMS/DOPE vesicles and the factors altering the outcomes are similar in RAW 264.7 and P388D1 cells. No appreciable differences in their response to the pH-sensitive liposomes were observed.

When either P388D1 or RAW 264.7 cells were incubated with sulforhodamine 101 for 3 days, fluorescence was found to be concentrated in the perinuclear vacuoles (lysosomes) as previously described (36). Incubation of these cells with fresh medium containing empty CHEMS/DOPE or CHEMS/DOPC vesicles does not change the fluorescent distribution in the cell; in other words, fluorescence is observed only in the perinuclear vacuole, and not in the cytoplasm (data not shown). This result indicates that pH-sensitive liposomes are not likely to destabilize the lysosomal membranes and cause release of sulforhodamine 101 from these intracellular compartments into the cytoplasm. The possibility of fusion between pH-sensitive liposomes and the endosomal/lysosomal membrane or destabilization of endosomal membranes by the pH-sensitive liposomes cannot be excluded. Since the intracellular vacuoles are known to become disrupted due to the hypertonicity of a 20% glycerol solution (37), sulforhodamine in the perinuclear vacuoles could be released into the cytoplasm by exposing the cells to 20% glycerol for 5 min. This treatment of glycerol results in a bright cytoplasmic fluorescence in the control cells and the cells incubated with the pH-sensitive or non-pH-sensitive liposomes. The glycerol treatment also serves as a positive control demonstrating the rupture of the intracellular vesicles and redistribution of the dye into the cytoplasm. Whether the effect of hypertonic glycerol treatment is limited only to the disruption of lysosomal or involves other intracellular membranes is not clear, so that other mechanisms that induce redistribution of the dye from the lysosomes to the cytoplasm cannot be ruled out.

When large fluorescent molecules, such as FITC–dextran (MW 4200) and FITC–poly-GL (MW 69,000) are delivered in pH-sensitive liposomes, cytoplasmic fluorescence is observed in the cells, which can be differentiated from punctate fluorescence in the vacuoles. Only punctate fluorescence is observed when these two macromolecules are delivered in the non-pH-sensitive CHEMS/DOPC composition. However, due to the background fluorescence of vesicles containing the nonquenched fluorophore adhering to the cell surface and the substratum, photographs of cells (P388D1 and RAW 264.7) treated with the pH-sensitive liposomes do not conclusively document the phenomenon.

The efficiency of cytoplasmic delivery from one other pH-sensitive composition, oleic acid/DOPE, was also examined on the P388D1 and RAW 264.7 cells using calcein as a fluorescent marker. A very dim diffuse fluorescence, much less than that seen with the CHEMS/DOPE vesicles (Fig. 2b), is observed (data not shown).

In cells (P388D1) incubated with pH-sensitive liposomes containing HPTS/DPX, cytoplasmic fluorescence is observed when the blue-band filter (high-pH form of HPTS) is used (Fig. 3b). When the violet-band filter (both pH forms of HPTS) is used, a punctate and diffuse fluorescence pattern is observed in cells incubated with the pH-sensitive liposomes (Fig. 3a). A similar result is obtained when the RAW 264.7 cell is used (data not shown).

These results indicate that membrane-impermeant fluorophores can reach the cytoplasm when they are delivered by pH-sensitive liposomes but end up predominantly in the perinuclear vacuoles while delivered by non-pH-sensitive liposomes.

Protein Synthesis Inhibition by Liposomal DTA

Diphtheria toxin is a highly potent inhibitor of protein synthesis. Estimates as low as one molecule per cell, under appropriate conditions, can totally inhibit protein synthesis (38). The A chain of diphtheria toxin is unable to cross either the plasma membrane or the endosomal membrane without the assistance of the B chain of the toxin. Hence DTA is not inhibitory to cells. The inhibition of leucine incorporation by DTA delivered by liposomes is shown in Fig. 4. Neither nonencapsulated DTA (up to 10^{-6} *M*) plus empty vesicles, equivalent to the concentration of DTA-containing liposomes, nor DTA-containing control liposomes (up to 5×10^{-8} *M* DTA/10^{-3} *M* lipid) inhibit leucine incorporation into cellular protein. Inhibition is observed only when cells are incubated with DTA-containing pH-sensitive liposomes. A dose-dependent inhibition from DTA encapsulated in pH-sensitive liposomes is observed (Fig. 4a). The concentration of CHEMS/DOPE vesicles that caused a 50% inhibition (IC_{50}) is 40 μM which contain about 7.0×10^{-10} *M* (or 1.4×10^{-13} mol) of DTA. Ammonium chloride blocks the inhibition of protein synthesis elicited by DTA-containing pH-sensitive liposomes (data not shown). This indicates that a low-pH pathway is involved in the introduction of DTA from the pH-sensitive liposomes into the cytoplasm. This inhibition of protein synthesis experiment was not examined in RAW 264.7 cells, although the outcome is expected to be similar to that obtained from P388D1 cells due to the similar behaviors observed in other experiments.

Cell-associated DTA can be calculated based upon the amount of DTA encapsulated in liposomes (17.5×10^{-15} mol DTA/nmol CHEMS/DOPE lipid or 52.1×10^{-15} mol/nmol CHEMS/DOPC lipid) and the measured amount of vesicle uptake per cell (Fig. 1a). This assumes that all the cells take up liposomes, encapsulated molecules do not leak from the liposomes, and 1 million cells corresponds to 0.3 mg of cellular protein. When the dose–response curves are plotted on the basis of the amount of cell-associated DTA (Fig. 4b), the pH-sensitive composition is at least 100 times more ef-

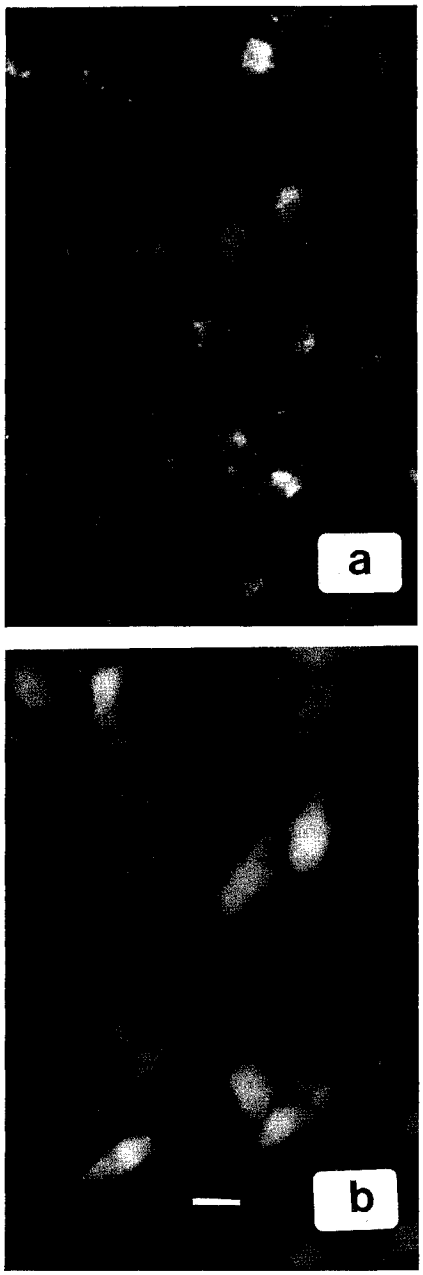

Fig. 3. Cellular location of liposomal HPTS in P388D1 cells. (a) Vacuolar fluorescence and diffuse fluorescence observed under violet-band filter set after incubation with 50 μM CHEMS/DOPE (4/6) vesicles containing HPTS/DPX. (b) Cytoplasmic fluorescence viewed under blue-band filter set after incubation with 50 μM corresponding pH-sensitive liposomes. Bar indicates 10 μm.

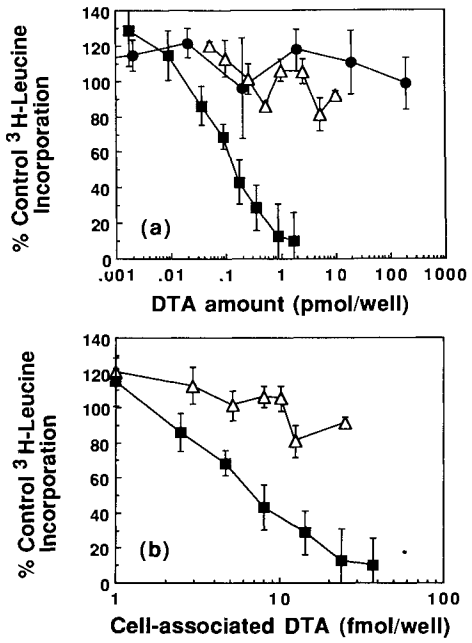

Fig. 4. Inhibition of ^{3}H-leucine incorporation by liposomal DTA in P388D1 cells. (a) Result expressed as amount of DTA in DTA-containing CHEMS/DOPC (2.5/7.5) vesicles (△), in DTA-containing CHEMS/DOPE (2.5/7.5) vesicles (■), or in a nonencapsulated form (●) incubated with 1×10^5 cells for 1 hr. (b) Result expressed as cell-associated DTA after 1 hr of incubation with DTA-containing CHEMS/DOPC (△) or DTA-containing CHEMS/DOPE vesicles (■). The cell-associated amount of DTA was calculated based on the result shown in Fig. 1a and the encapsulation ratio of DTA in the liposomes (moles DTA/moles lipid; see text). Values are the means of quadruplicate measurements in a single experiment and bars represent the standard deviations from the means.

ficient at delivering DTA to the cytoplasm than the non-pH-sensitive composition.

Acidification of HPTS

The fluorescence ratio from cell-associated HPTS/DPX as a function of time after incubation is shown in Fig. 5. Since the Fl 450/413 of cell-associated HPTS correlates with the pH of the environment HPTS is exposed to, this assay is used to estimate the pH of the cell-associated HPTS. In this experiment, the liposomes containing HPTS/DPX have a Fl 450/413 of 2.1 at pH 7.4, which is not significantly different from the value obtained using the nonencapsulated, unquenched HPTS solution at pH 7.4. At the zero-time point, shown in Fig. 5, the P388D1 cells have already been incubated with the HPTS/DPX-containing liposomes for 1 hr at 37°C. Vesicles not firmly attached to the cells are removed using three successive washes at 4°C. At the zero-time point, the assay indicates that the average HPTS molecule experiences a pH 6.6 environment. This is because a fraction of the liposomes has been internalized and they have delivered their contents into a low-pH compartment. As the incubation continues, the Fl 450/413 ratio progressively declines until the Fl 450/413 reaches 0.25 (corresponding to pH 6.1) after 4.5 hr (Fig. 5). The Fl 450/413 ratio remains constant at 0.25 for 24 hr, the last time point measured. There is no significant difference in the rate of acidification of intracellular HPTS whether the fluorophore is delivered in the pH-sensitive or non-pH-sensitive lipid vesicles. The similar result is obtained when RAW 264.7 cells were studied (data not shown). Only the Fl 450/413 ratio is slightly higher at 4.5 hr after washing. The variability of this assay is about 15%. Although fluorescence microscopy indicates cytoplasmic delivery from the pH-sensitive liposomes, the result with the spectrofluorimetric assay suggests that the fraction of HPTS delivered into cytoplasm via the pH-sensitive liposomes is less than 10% of the cell-associated contents.

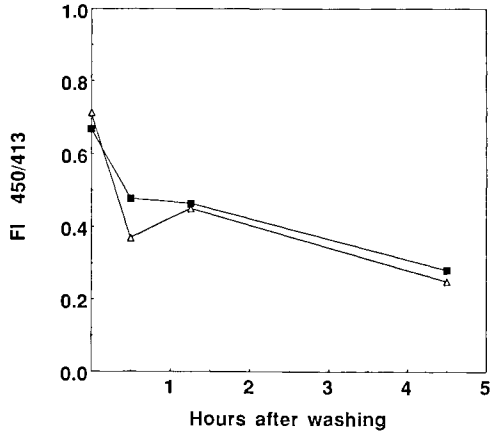

Fig. 5. Time course of acidification of liposomal HPTS in P388D1 cells. Cells were treated with HPTS/DPX-containing CHEMS/DOPC (4/6), 500 μ*M* (△), or CHEMS/DOPE (4/6), 50 μ*M* (■), vesicles for 1 hr. Nonattached vesicles were removed and fresh medium was added to cells at time 0. At the time indicated, cell-associated fluorescence observed at 510 nm when excited at wavelengths of 450 and 413 nm was measured as described under Materials and Methods. Values represent one measurement from a single experiment. The variation between experiments is within 15% of the value reported.

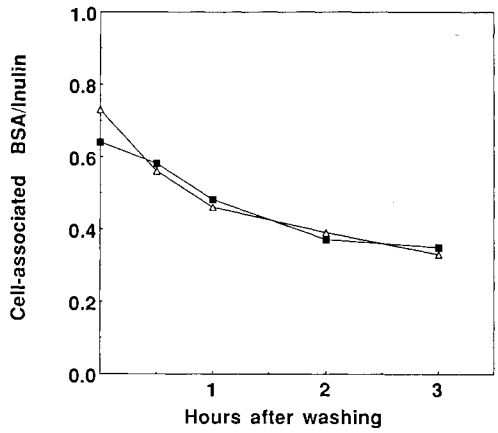

Fig. 6. Time course of degradation of liposomal BSA in P388D1 cells. Empty CHEMS/DOPC (4/6) liposomes (500 μ*M*) plus ^{125}I-BSA/^{3}H-inulin-encapsulated CHEMS/DOPE (4/6) vesicles (50 μ*M*) (■) and empty CHEMS/DOPE (4/6) vesicles (50 μ*M*) plus ^{125}I-BSA/^{3}H-inulin-containing CHEMS/DOPC (4/6) vesicles (500 μ*M*) (△) were incubated with cells for 2 hr. At time 0, nonattached liposomes were washed off and fresh medium was added for continued incubation. Cell-associated radioactivity was measured at the indicated times after washing. Values are the means of duplicates in a single experiment. The ranges of values are within 10% of the means.

Degradation of BSA

The degradation rate of BSA was investigated to estimate the fraction of BSA that escaped the lysosomotropic pathway. This assay is based on the fact that BSA degradation in the cytoplasm (half-life, 20–34 hr) (39,40) is much slower than BSA degradation in the lysosomes (half-life, <1 hr) (8). The degradation products of BSA are released into the extracellular medium, while the inulin is resistant to lysosomal enzymes and remains within the cells. Thus the cell-associated BSA/inulin ratio can be used as an indicator for the extent of degradation of liposomal BSA in the cells. This experiment was conducted so that a similar level of lipid became cell-associated with both the pH-sensitive liposomes and the non-pH-sensitive liposomes. The initial BSA/inulin ratio was 1.0. After a 2-hr exposure to liposomes, the cells were washed and the incubation continued in the absence of liposomes. Immediately after the wash the ratio was 0.73 for control liposomes and 0.65 for pH-sensitive liposomes because the BSA was being degraded inside the cells during the incubation. This ratio progressively declines, regardless of the liposome composition, to 0.34 by 3 hr (Fig. 6). The BSA/inulin ratio in duplicate determinations varied 10% from the mean value. Thus cytoplasmic delivery of less than 10% of the contents would be undetectable by this method. The similarity in the BSA degradation rate between the two compositions indicates that the cytoplasmic delivery from the pH-sensitive composition is less than 10% of the cell-associated contents. A similar conclusion is reached when BSA-containing CHEMS/DOPE and CHEMS/DOPC liposomes were incubated with RAW cells (data not shown).

DISCUSSION

pH-sensitive liposomes were originally developed to release their contents in the pH environment (pH 6.6–7.2) found in the vicinity of certain tumors (41). Since the pH change from the plasma to the tumor is rather modest, investigators turned their attention to the endosome. Liposomes are internalized into cells via the endosome and the pH in this prelysosomal compartment is reduced from 7.4 to between 5.3 and 6.5 within minutes after the endosome is formed. The pH-sensitive liposomes are designed to mimic enveloped viruses which have membrane fusion proteins that undergo a conformational change when the pH is reduced to about 6.0. The change in protein conformation induces fusion between the viral and the endosomal membrane and the viral genetic material is delivered into the cytoplasm. Lipid mixtures composed of PE and a pH-titratable fatty acid or lipid derivative have been developed to achieve this goal (42,43). Biophysical studies have demonstrated that such vesicles either fuse or leak their contents at low pH. Ellens and colleagues have demonstrated that CHEMS/DOPE vesicles, triggered by H^+, become destabilized at pH <5.5 and fuse at pH <5.0 (16,33).

In this work, we demonstrate that CHEMS/DOPE vesicles deliver various fluorophores (calcein, FITC–dextran, FITC–poly-GL) and biologically active DTA into the cytoplasm. The fact that both low and high molecular weight molecules are transferred into the cytoplasm implies that disruption of the intracellular membranes or fusion between the liposomal membrane and the intracellular compartment membranes is the most likely mechanism involved in the cytoplasmic delivery. The destabilization/fusion events are most likely to occur in the endosomes, since these vacuoles are the first compartment where liposomes encounter a low pH. Cytoplasmic fluorescence is not observed in the presence of agents that dissipate the pH gradient in intracellular vacuoles; a pH-sensitive event is necessary for the cytoplasmic delivery from the CHEMS/DOPE vesicles. It is also interesting that calcium/magnesium is required for cytoplasmic delivery since biophysical studies have indicated a re-

quirement of millimolar levels of these divalent cations for fusion to occur in model systems (33).

The inhibition of protein synthesis by DTA-containing CHEMS/DOPE vesicles but not by nonencapsulated DTA, empty liposomes, or DTA-containing CHEMS/DOPC liposomes further confirms that DTA is introduced into the cytoplasm by pH-sensitive liposomes. There is a greater than five order of magnitude difference between the cytotoxicity of CHEMS/DOPE DTA and that of nonencapsulated DTA. Moreover, the CHEMS/DOPE composition is at least 100-fold more efficient in delivering cytotoxic DTA than the CHEMS/DOPC composition. A 50% inhibition was obtained by incubating 7×10^{-10} *M* DTA, encapsulated in 40 μM pH-sensitive liposomes, with cells for 1 hr (Fig. 4).

The calculated amount of DTA which becomes cell associated after 1 hr of incubation with CHEMS/DOPE vesicles is 30,000 molecules per cell, if we assume that no leakage occurs during the incubation. The actual cell-associated DTA is probably lower than the amount calculated due to the leakage of contents induced by cell contact (44). To estimate the fraction of the 30,000 cell-associated DTA molecules that reach the cytoplasm in an active form, we can use data from studies on the efficiency of translocation of intact diphtheria toxin into the cytoplasm of susceptible cells (45). In this work the reciprocal half-time for inhibition of protein synthesis in a cell-free system is a linear function of DTX concentration, with a slope of 1.2 nM^{-1} min^{-1}. If we assume the cytoplasmic volume to be 2 pl and the half-time of inhibition of protein synthesis by 40 μM DTA-containing DOPE/CHEMS liposomes to be 360 min (assay was carried out with a pulse of ^{3}H-leucine for 6 hr after removal of nonattached liposomes), the amount of DTA required to elicit this degree of inhibition is 3 molecules per cell. Thus the cytoplasmic delivery efficiency of the CHEMS/DOPE system is at least 0.01% of the cell-associated contents.

The correlation between diphtheria toxin effects on protein synthesis reported in the cell-free system (45) and DTA effects in the P388D1 cells can only be inferred; thus we emphasize that this estimate is a lower bound on the efficiency of cytoplasmic delivery by the CHEMS/PE system. It is interesting, however, that Moynihan and Pappenheimer (45) conclude that only 0.4% of the diphtheria toxin that becomes cell associated reaches the cytoplasm. Colombatti and co-workers have shown that the cytotoxicity of diphtheria toxin is about 1000 times greater than antibody-linked DTA in target cells (46). This indicates that the CHEMS/DOPE vesicles are about two orders of magnitude more efficient than antibody-linked DTA and within an order of magnitude as efficient as intact toxin at transporting DTA molecules into the cytoplasm.

The CHEMS/DOPE composition seems to be the most efficient liposomal composition reported to date to deliver DTA-inhibitory activity. McIntosh and Heath (47) showed that DTA-containing phosphatidylserine (PS) vesicles did not inhibit protein synthesis in lymphoma cells even after 21 hr of lag time. Ikuta and colleagues (48) demonstrated that DTA-containing liposomes (EPC/cholesterol/PS) could kill HIV-infected leukemia cells but not noninfected cells with continuous incubation for 3 days. The killing resulted from the facilitated transport of DTA through the altered plasma membrane of the infected cells rather than from cytoplasmic delivery by the liposomes. Using a similar lipid composition (DOPC/cholesterol/PS or DOPC/cholesterol/DOPE), Jansons and Panzner (49) reported that approximately 50% inhibition of protein synthesis in human lymphoblastoid cells was obtained by incubating DTA-containing (DTA = 1.2×10^{-8} *M*) vesicles with cells for 2.5 hr. They were not able to get greater than 70% inhibition with longer incubations or higher concentrations. Attaching antibodies to the surface of liposomes, Collins and Huang (13) showed that only the DTA-containing pH-sensitive immunoliposomes could inhibit protein synthesis ($IC_{50} = 1.4 \times 10^{-9}$ *M*) in target cells after 3 hr of incubation, while nontargeted pH-sensitive liposomes or non-pH-sensitive immunoliposomes were ineffective. The cell-associated DTA using the pH-sensitive immunoliposomes was not quantitated, so the efficiency of delivery is unknown. In the absence of targeting, we can obtain a 50% inhibition of protein synthesis at 7.0×10^{-10} *M* of DTA after a 1-hr incubation of CHEMS/DOPE-DTA with P388D1. However, the macrophage-like nature of P388D1 cells may also contribute to the higher apparent delivery efficiency of the CHEMS/DOPE vesicles when compared to results in the other studies.

When the efficiency of cytoplasmic delivery by CHEMS/DOPE was compared with another pH-sensitive composition, OA/DOPE, the CHEMS/DOPE vesicles delivered more calcein to the cytoplasm. Moreover, CHEMS/DOPE seems to be able to deliver macromolecules better than the OA/PE composition as well. Baldwin and coworkers (50) employed OA/PE vesicles to deliver pokeweed antiviral protein, a DTA-like protein synthesis inhibitor which cannot readily cross the cell membrane. They showed that the OA/PE-encapsulated compound was 2500-fold more potent than nonencapsulated molecules in inhibiting CV-1 cell growth after 8 hr of incubation, while CHEMS/DOPE-DTA is at least 10^5 times more potent than nonencapsulated DTA in our system. In addition, the greater stability of CHEMS/DOPE in the presence of serum makes CHEMS/DOPE a more suitable formulation for *in vivo* use.

Both HPTS acidification and BSA degradation experiments clearly show that pH-sensitive liposomes are taken up by cells by an endocytotic pathway. This pathway routes the majority of liposomes and their contents into an acidic environment and eventually into the lysosomes where iodoalbumin is degraded. This is the same as the fate of non-pH-sensitive liposomes. The sensitivity of these two assays to discern the fate of the encapsulated molecules is limited by experimental variation, which is always between 3 and 15%. Since there is no significant difference found in the rates of HPTS acidification and BSA degradation between pH-sensitive and control liposomes, the efficiency of the cytoplasmic delivery is less than the sensitivity of the assays.

In summary, we conclude that the CHEMS/DOPE composition can deliver macromolecules to the cytoplasm of cells. This process requires a low-pH environment and the presence of divalent cations to effect cytoplasmic delivery. Whether a true fusion of the liposomal membrane with the endosomal and/or lysosomal membranes occurs cannot yet be determined. However, cells whose lysosomes have been labeled with sulforhodamine 101 do not show cytoplasmic fluorescence when incubated with the pH-sensitive liposomes. This indicates that the pH-sensitive liposomes do not cause extensive leakage of the endosomal/lysosomal contents. It suggests that leakage from these intracellular com-

partments is probably not a significant delivery pathway as opposed to endosome/lysosome liposome fusion for the CHEMS/DOPE composition. The efficiency of cytoplasmic delivery in the endocytotically active cells studied here is greater than 0.01% and less than 10% of the cell-associated liposomal contents. This is superior to other liposome compositions reported to date but still leaves much room for improvement.

Incorporating ligands onto the surface of pH-sensitive vesicles as has been done with antibodies (12,13) may increase the efficiency of cytoplasmic delivery. This is because cellular uptake of liposomes is more efficient by receptor-mediated endocytosis than by nonspecific adsorptive endocytosis (51) and the receptor–ligand binding may bring the liposome membrane and the endosome membrane into close proximity. The latter can accelerate the fusion between the two membranes (52). An alternative approach is to incorporate viral fusion proteins (53) or synthetic peptides (54) into the liposome bilayer, where they may assume a fusogenic conformation in the acidic endosome and induce fusion between the liposomal and the endosomal membranes (55). At present, we are exploring both approaches to increase the efficiency of cytoplasmic delivery from pH-sensitive liposomes.

ACKNOWLEDGMENTS

We thank Drs. R. Parente, P. Dal Monte, and R. Straubinger for helpful discussions and Dr. L. Huang for the procedure of DTA preparation. The technical assistance of Rick Dovey for setting up the reticulocyte assay is appreciated. This work was supported by Public Health Service Grant GM30163 to F.C.S. from the National Institutes of Health.

REFERENCES

1. D. O. Morgan and R. A. Roth. *Immunol. Today* 9:84–88 (1988).
2. T. Friedman. *Science* 244:1275–1281 (1989).
3. G. Zon. *Pharm. Res.* 5:539–549 (1988).
4. J. Haseloff and W. L. Gerlach. *Nature* 334:585–591 (1988).
5. G. Gregoriadis and A. C. Allison. *Liposomes in Biological Systems,* John Wiley & Sons, New York, 1980.
6. F. C. Szoka, K. Jacobson, Z. Derzko, and D. Papahadjopoulos. *Biochim. Biophys. Acta* 600:1–18 (1980).
7. R. M. Straubinger, K. Hong, D. S. Friend, and D. Papahadjopoulos. *Cell* 32:1069–1079 (1983).
8. J. Dijkstra, J. W. M. van Galen, C. E. Hulstaert, D. Kalicharan, F. H. Roerdink, and G. L. Scherphof. *Exp. Cell Res.* 150:161–176 (1984).
9. F. C. Szoka. In K. Yagi (ed.), *Medical Application of Liposomes,* Japan Scientific Society Press, Tokyo, 1986, pp. 21–30.
10. B. Tycko and F. R. Maxfield. *Cell* 28:642–651 (1982).
11. R. M. Straubinger, N. Duzgunes, and D. Papahadjopoulos. *FEBS Lett.* 179:148–154 (1985).
12. J. Connor and L. Huang. *Cancer Res.* 46:3431–3435 (1986).
13. D. Collins and L. Huang. *Cancer Res.* 47:735–739 (1987).
14. R. J. Y. Ho, B. T. Rouse, and L. Huang. *J. Biol. Chem.* 262:13973–13978 (1987).
15. C.-Y. Wang and L. Huang. *Proc. Natl. Acad. Sci. USA* 84:7851–7855 (1987).
16. H. Ellens, J. Bentz, and F. C. Szoka. *Biochemistry* 23:1532–1538 (1984).
17. M.-Z. Lai, N. Duzgunes, and F. C. Szoka. *Biochemistry* 24:1654–1661 (1985).
18. R. H. Abra, H. Schreier, and F. C. Szoka. *Res. Commun. Pathol. Pharmacol.* 37:199–213 (1982).
19. F. C. Szoka and D. Papahadjopoulos. *Proc. Natl. Acad. Sci. USA* 75:4194–4198 (1978).
20. F. C. Szoka, F. Olson, T. Heath, W. Vail, E. Mayhew, and D. Papahadjopoulos. *Biochim. Biophys. Acta* 601:559–571 (1980).
21. T. D. Heath. *Methods Enzymol.* 149:111–119 (1987).
22. G. R. Bartlett. *J. Biol. Chem.* 234:466–468 (1959).
23. R. L. Magi and J. N. Weinstein. In G. Gregoriadis (ed.), *Liposome Technology, Vol. III,* CRC Press, Boca Raton, FL, 1984, pp. 137–155.
24. R. R. Skelly, P. Munkenbeck, and D. C. Morrison. *Infect. Immun.* 23:287–293 (1979).
25. O. H. Lowry, N. J. Rosebrough, A. L. Farr, and R. J. Randall. *J. Biol. Chem.* 193:265–275 (1951).
26. K. M. Matthay, A. M. Abai, S. Cobb, K. Hong, and R. M. Straubinger. *Cancer Res.* 49:4879–4886 (1989).
27. J. J. Donovan, M. I. Simon, and M. Montal. *J. Biol. Chem.* 260:8817–8823 (1985).
28. M. J. Clemens, E. C. Henshaw, and H. Rahaminoff. *Proc. Natl. Acad. Sci. USA* 71:2946–2950 (1979).
29. O. S. Wolfbeis, E. Furlinger, H. Kroneis, and H. Marsoner. *Fresenius Z. Anal. Chem.* 314:119–124 (1983).
30. T. C. Greenwood, W. M. Hunter, and J. S. Glover. *Biochem J.* 39:114–127 (1963).
31. S. M. Gruner. In M. J. Ostro (ed.), *Liposomes: From Biophysics to Therapeutics,* Marcel Dekker, New York and Basel, 1987, pp. 1–38.
32. P. L. Yeagle. *Biochim. Bipohys. Acta* 882:267–287 (1985).
33. H. Ellens, J. Bentz, and F. C. Szoka. *Biochemistry* 24:3099–3106 (1985).
34. B. Kachar, N. Fuller, and R. P. Rand. *Biophys. J.* 50:779–788 (1986).
35. F. R. Maxfield. *J. Cell Biol.* 95:676–681 (1982).
36. Y. Wang and M. B. Goren. *J. Cell Biol.* 104:1749–1754 (1987).
37. C. Y. Okada and M. Rechsteiner. *Cell* 29:33–41 (1982).
38. M. Yamaizumi, E. Mekada, T. Uchida, and Y. Okada. *Cell* 15:245–250 (1978).
39. N. T. Neff, L. Bourret, P. Miao, and J. F. Dice. *J. Cell Biol.* 91:184–194 (1981).
40. M. Zavortink, T. Thacher, and M. Rechsteiner. *J. Cell. Physiol.* 100:175–186 (1979).
41. M. B. Yatvin, W. Kreutz, B. A. Horwitz, and M. Shinitzky. *Science* 210:1253–1255 (1980).
42. R. Nayar and A. Schroit. *Biochemistry* 24:5967–5971 (1985).
43. N. Duzgunes, R. M. Straubinger, P. A. Baldwin, D. S. Freind, and D. Papahadjopoulos. *Biochemistry* 24:3091–3098 (1985).
44. F. C. Szoka, K. Jacobson, and D. Papahadjopoulos. *Biochim. Biophys. Acta* 551:295–303 (1979).
45. M. R. Moynihan and A. M. Pappenheimer Jr. *Infect. Immun.* 32:575–582 (1981).
46. M. Colombatti, L. Greenfield, and R. J. Youle. *J. Biol. Chem.* 261:3030–3035 (1986).
47. D. P. McIntosh and T. D. Heath. *Biochim. Biophys. Acta* 690:224–230 (1982).
48. K. Ikuta, S. Ueda, T. Uchida, Y. Okada, and S. Kato. *Jap. J. Cancer Res.* 78:1159–1163 (1987).
49. V. K. Jansons and E. A. Panzner. *Biochim. Biophys. Acta* 735:433–437 (1983).
50. P. A. Baldwin, R. M. Straubinger, and D. Papahadjopoulos. *J. Cell Biol.* 103:57a (1986).
51. K. M. Matthay, T. D. Heath, and D. Papahadjopoulos. *Cancer Res.* 44:1880–1886 (1984).
52. F. C. Szoka, K.-E. Magnusson, J. Wojcieszyn, Y. Hou, Z. Derzko, and K. Jacobson. *Proc. Natl. Acad. Sci. USA* 78:1685–1689 (1981).
53. T. Stegmann, H. W. M. Morselt, F. P. Booy, J. L. van Breemen, G. L. Scherphof, and J. Wilschut. *EMBO J.* 6:2651–2659 (1987).
54. F. C. Szoka, N. K. Subbarao, and R. A. Parente. In S. Ohki (ed.), *Molecular Mechanisms of Membrane Fusion,* Plenum Press, New York, 1988, pp. 317–324.
55. R. A. Parente, S. Nir, and F. C. Szoka. *J. Biol. Chem.* 263:4724–4730 (1988).

A phase I trial of intravenous liposomal irinotecan in patients with recurrent high-grade gliomas

Jennifer L. Clarke[1,2], Annette M. Molinaro[1], Ashley A. DeSilva[1], Jane E. Rabbitt[1], Joshua Prey[3], Daryl C. Drummond[4], Susan M. Chang[1], Nicholas A. Butowski[1], Michael D. Prados[1]

[1]Dept of Neurological Surgery, Division of Neuro-oncology, and [2]Dept. of Neurology, University of California, San Francisco; [3]Roswell Park Cancer Institute, Buffalo, NY, [4]Merrimack Pharmaceuticals, Cambridge, MA

Introduction

- Treatment options for recurrent malignant glioma are limited.
- Preclinical activity of irinotecan has been seen in glioma models but only modest efficacy has been noted in clinical studies, perhaps related to drug distribution and/or pharmacokinetic limitations.
- In preclinical testing, liposomal irinotecan (nal-IRI, also MM-398, PEP02, BAX2398) demonstrated prolongation of drug exposure and higher tissue levels of drug due to slower metabolism (Drummond, et al. 2006).
- In preclinical testing, nal-IRI was also found to cross the blood-brain barrier and to accumulate in parenchymal brain tumors, although at lower levels relative to many other solid tumors (Noble, et al. 2014).
- In a phase I study of this drug administered intravenously in advanced solid tumor patients in Taiwan, the MTD was 120 mg/m^2; UGT1A1 genotyping was not prospectively undertaken in that solid tumor study (Chang, et al. 2015).
- Prior to embarking on a trial of convection-enhanced delivery (CED) of this agent, the FDA required a dose finding trial testing safety of systemic drug delivery.

nal-IRI, nanoliposomal irinotecan

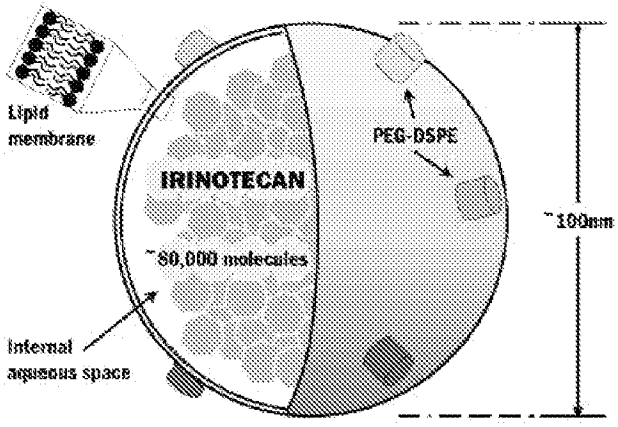

Objectives

- To assess the safety and pharmacokinetics (PK) of nal-IRI
- To determine the maximum tolerated dose (MTD) in patients with recurrent malignant glioma, stratified by UGT1A1*28 genotyping.

Methods

Patient Eligibility

- Patients were assessed during screening, and those who were UGT1A1*28 6/6 (homozygous, "WT") and 6/7 (heterozygous, "HT") were eligible to enroll.
- Other pertinent eligibility criteria:
  - Age ≥ 18 years, KPS ≥ 60
  - Recurrent malignant (grade III or IV) glioma, any recurrence
  - Not on cytochrome P450 enzyme-inducing drugs, including no enzyme-inducing anti-epileptic drugs (EIAEDs)
  - No prior treatment with irinotecan

Trial Design

- A standard 3 + 3 dose escalation design was used. Patients were treated with intravenous infusions every 3 weeks.
- The DLT assessment period was one cycle (21 days).
- Treatment was stratified by UGT1A1*28 status as per the table below, with dose increments of 60 mg/m^2 planned for Arm 1 and 30 mg/m^2 for Arm 2.

	Arm 1: WT	Arm 2: HT
Dose Level -1	60 mg/m^2	30 mg/m^2
Dose Level 0	120 mg/m^2	60 mg/m^2
Dose Level 1	180 mg/m^2	90 mg/m^2
Dose Level 2	240 mg/m^2	120 mg/m^2
Dose Level 3		150 mg/m^2
Dose Level 4		180 mg/m^2

PK Analyses

- PK analyses were undertaken with samples drawn at the following time points:
  - Cycle 1:
    - Pre-dose
    - 2 hours post-infusion
    - 4 hours post-infusion
    - 6 hours post-infusion
    - 24 hours post-infusion
  - Cycle 2:
    - Pre-dose
- Total irinotecan, encapsulated irinotecan, and SN-38 levels were assessed.

Results

Patient Demographics

	Arm 1: WT (n = 16)	Arm 2: HT (n = 18)
Mean Age (range)	50 years (28 – 66)	47 years (28 – 75)
Median KPS at enrollment (range)	80 (60 – 90)	90 (60 – 100)
Tumor Type:		
GBM	12	14
Grade III astro	0	4
Grade III oligo/OA	4	0
Median # of relapses (range)	3 (1 – 5)	3 (1 – 8)

MTD and DLTs

- In the WT cohort, the MTD was 120 mg/m^2.
- In the HT cohort, the MTD was 150 mg/m^2.
- DLTs in both cohorts included diarrhea, some with associated dehydration and/or fatigue.

Efficacy

- Median PFS for all patients treated with initial dose ≥ 120 mg/m^2 was 43 days (95% CI 39-44).
- PFS6 was 0.

PFS for all patients treated with initial dose ≥ 120 mg/m^2

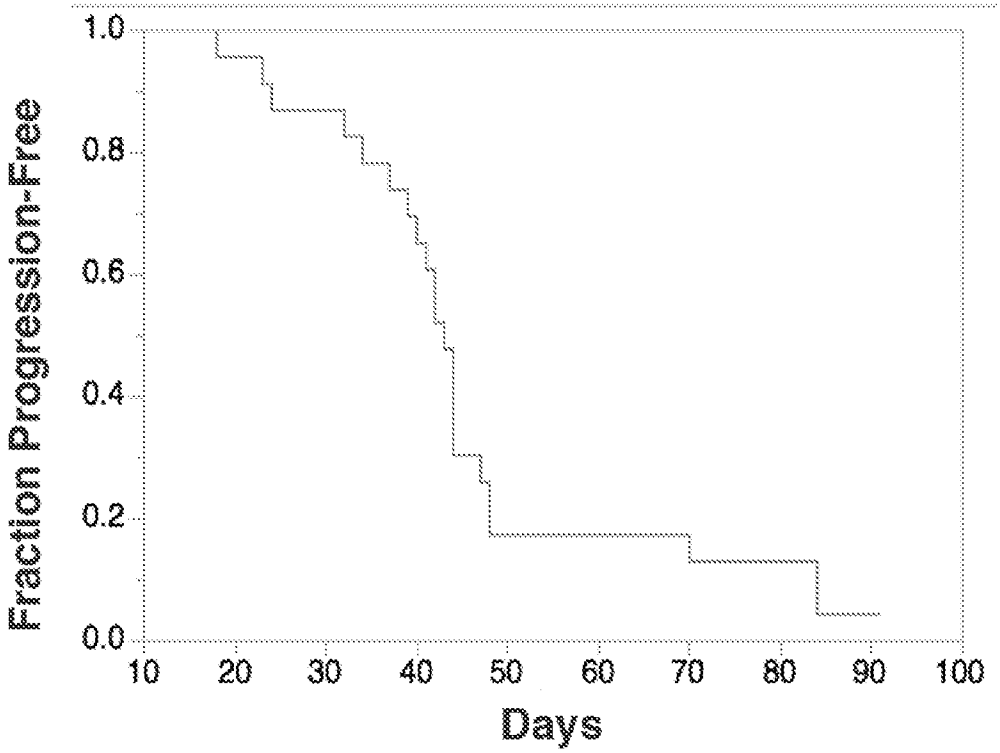

PK Results

- nal-IRI PK is linear; total irinotecan C_{max} and $AUC_{0-\infty}$ proportionally increase with dose.
- Median nal-IRI half life was 28.4 hrs, similar to prior results.
- UGT1A1*28 genotype had no clear effect on nal-IRI PK parameters.

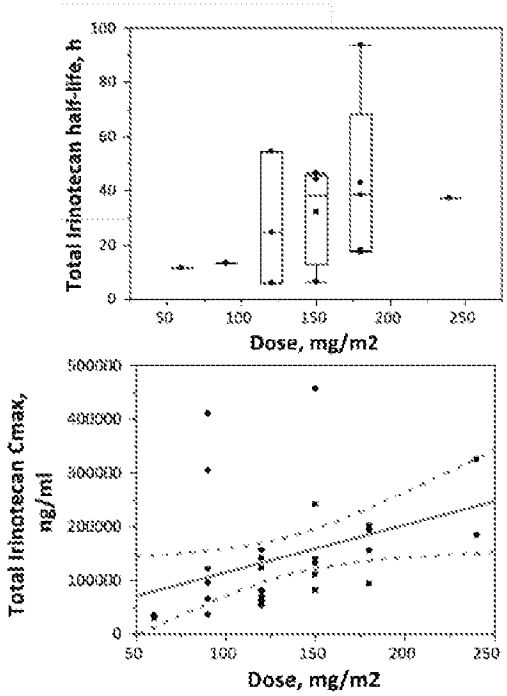

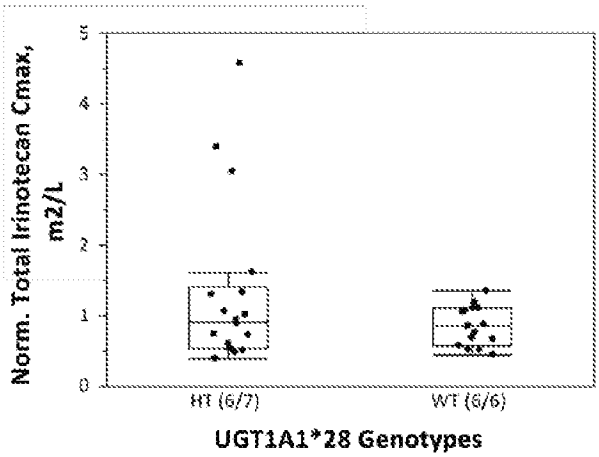

Conclusions and Future Directions

- Nal-IRI had no unexpected toxicities when given intravenously.
- Tolerability was similar between the two study arms, and consistent with that found in the original phase I study in solid tumors.
- As the 150 mg/m^2 dose level was not tested for homozygous (6/6) patients, we would recommend that 120 mg/m^2 be considered the recommended phase II dose going forward for patients with either homozygous (6/6) or heterozygous (6/7) UGT1A1*28 status.
- PK results are comparable to those seen in other PK studies; UGT1A1*28 genotype did not affect PK parameters.
- The toxicity profile of the drug was felt to be acceptable, thus supporting additional testing using CED into intracranial tumors. Such a Phase I study is currently enrolling at UCSF.

References

- Drummond, D. C., et al. (2006). "Development of a Highly Active Nanoliposomal Irinotecan Using a Novel Intraliposomal Stabilization Strategy." Cancer Research **66**(6): 3271-3277.
- Noble, C. O., et al. (2014). "Pharmacokinetics, tumor accumulation and antitumor activity of nanoliposomal irinotecan following systemic treatment of intracranial tumors." Nanomedicine **9**(14): 2099-2108.
- Chang, T. C., et al. (2015). "Phase I study of nanoliposomal irinotecan (PEP02) in advanced solid tumor patients." Cancer Chemotherapy and Pharmacology **75**(3): 579-586.

A phase I trial of intravenous liposomal irinotecan in patients with recurrent high-grade gliomas

Jennifer L. Clarke[1,2], Annette M. Molinaro[1,2], Ashley A. DeSilva[1], Jane E. Rabbitt[3], Joshua Prey[2], Daryl C. Drummond[4], Susan M. Chang[1], Nicholas A. Butowski[1], Michael D. Prados[1]
[1]Dept of Neurological Surgery, Division of Neuro-oncology, and [2]Dept. of Neurology, University of California, San Francisco; [3]Roswell Park Cancer Institute, Buffalo, NY; [4]Merrimack Pharmaceuticals, Cambridge, MA

UCSF University of California San Francisco

Introduction

- Treatment options for recurrent malignant glioma are limited.
- Preclinical activity of irinotecan has been seen in glioma models but only modest efficacy has been noted in clinical studies, perhaps related to drug distribution and/or pharmacokinetic limitations.
- In preclinical testing, liposomal irinotecan (nal-IRI, also MM-398, PEP02, BAX2398) demonstrated prolongation of drug exposure and higher tissue levels of drug due to slower metabolism (Drummond, et al. 2006)
- In preclinical testing, nal-IRI was also found to cross the blood-brain barrier and to accumulate in parenchymal brain tumors, although at lower levels relative to many other solid tumors (Noble, et al. 2014).
- In a phase I study of this drug administered intravenously in advanced solid tumor patients in Taiwan, the MTD was 120 mg/m²; UGT1A1 genotyping was not prospectively undertaken in that solid tumor study (Chang, et al. 2015)
- Prior to embarking on a trial of convection-enhanced delivery (CED) of this agent, the FDA required a dose finding trial testing safety of systemic drug delivery.

nal-IRI, nanoliposomal irinotecan

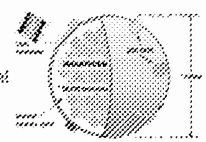

Objectives

- To assess the safety and pharmacokinetics (PK) of nal-IRI
- To determine the maximum tolerated dose (MTD) in patients with recurrent malignant glioma, stratified by UGT1A1*28 genotyping

Methods

Patient Eligibility

- Patients were assessed during screening, and those who were UGT1A1*28 6/6 (homozygous, "WT") and 6/7 (heterozygous, "HT") were eligible to enroll.
- Other pertinent eligibility criteria:
  - Age ≥ 18 years, KPS ≥ 60
  - Recurrent malignant (grade III or IV) glioma, any recurrence
  - Not on cytochrome P450 enzyme-inducing drugs, including no enzyme-inducing anti-epileptic drugs (EIAEDs)
  - No prior treatment with irinotecan

Methods

Trial Design

- A standard 3 + 3 dose escalation design was used. Patients were treated with intravenous infusions every 3 weeks.
- The DLT assessment period was one cycle (21 days).
- Treatment was stratified by UGT1A1*28 status as per the table below, with dose increments of 60 mg/m² planned for Arm 1 and 30 mg/m² for Arm 2.

	[illegible]	[illegible]
Dose Level -1	60 mg/m²	30 mg/m²
Dose Level 0	120 mg/m²	60 mg/m²
Dose Level 1	180 mg/m²	90 mg/m²
Dose Level 2	240 mg/m²	120 mg/m²
Dose Level 3		150 mg/m²
Dose Level 4		180 mg/m²

PK Analyses

- PK analyses were undertaken with samples drawn at the following time points:
  - Cycle 1:
    - Pre-dose
    - 2 hours post-infusion
    - 4 hours post-infusion
    - 6 hours post-infusion
    - 24 hours post-infusion
  - Cycle 2:
    - Pre-dose
- Total irinotecan, encapsulated irinotecan, and SN-38 levels were assessed.

Results

Patient Demographics

	[illegible]	[illegible]
Mean Age (range)	50 years (26 – 66)	47 years (28 – 75)
Median KPS at enrollment (range)	90 (60 – 90)	90 (60 – 100)
Tumor Type: GBM / Grade III astro / Grade III oligo/OA	12 / 0 / 4	14 / 4 / 0
Median # of relapses (range)	3 (1 – 5)	3 (1 – 8)

MTD and DLTs

- In the WT cohort, the MTD was 120 mg/m².
- In the HT cohort, the MTD was 150 mg/m².
- DLTs in both cohorts included diarrhea, some with associated dehydration and/or fatigue.

Efficacy

- Median PFS for all patients treated with initial dose ≥ 120 mg/m² was 49 days (95% CI 39-64).
- PFS6 was 0

PFS for all patients treated with initial dose ≥ 120 mg/m²

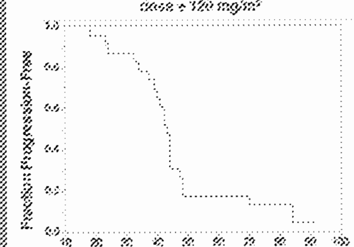

Results

PK Results

- nal-IRI PK is linear; total irinotecan C_{max} and AUC_{0-t} proportionally increase with dose.
- Median nal-IRI half life was 38.4 hrs, similar to prior results.
- UGT1A1*28 genotype had no clear effect on nal-IRI PK parameters.

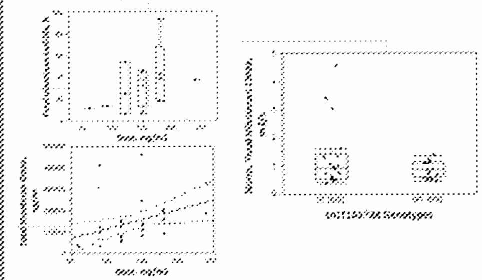

Conclusions and Future Directions

- Nal-IRI had no unexpected toxicities when given intravenously.
- Tolerability was similar between the two study arms, and consistent with that found in the original phase I study in solid tumors.
- As the 150 mg/m² dose level was not tested for homozygous (6/6) patients, we would recommend that 120 mg/m² be considered the recommended phase II dose going forward for patients with either homozygous (6/6) or heterozygous (6/7) UGT1A1*28 status.
- PK results are comparable to those seen in other PK studies; UGT1A1*28 genotype did not affect PK parameters.
- The toxicity profile of the drug was felt to be acceptable, thus supporting additional testing using CED into intracranial tumors. Such a Phase I study is currently enrolling at UCSF.

References

- Drummond, D. C., et al. (2006). "Development of a Highly Active Nanoliposomal Irinotecan Using a Novel Intraliposomal Stabilization Strategy." Cancer Research 66(6): 3271-3277.
- Noble, C. O., et al. (2014). "Pharmacokinetics, tumor accumulation and antitumor activity of nanoliposomal irinotecan following systemic treatment of intracranial tumors." Nanomedicine 9(14): 2099-2108.
- Chang, T. C., et al. (2015). "Phase I study of nanoliposomal irinotecan (PEP02) in advanced solid tumor patients." Cancer Chemotherapy and Pharmacology 75(3): 579-586.

Article Tools

CENTRAL NERVOUS SYSTEM TUMORS

A phase I trial of intravenous liposomal irinotecan in patients with recurrent high-grade gliomas.

Jennifer Leigh Clarke , Annette M Molinaro , Ashley A DeSilva , Jane E Rabbitt , Daryl C. Drummond , Susan Marina Chang...

Show More

Abstract Disclosures

Abstract

2029

Background: Treatment options for recurrent malignant glioma are limited. Preclinical activity of irinotecan has been seen in glioma models but only modest efficacy has been noted in clinical studies, perhaps related to drug distribution and/or pharmacokinetic limitations. In preclinical testing, liposomal irinotecan (nal-IRI, also MM-398, PEP02) demonstrates prolongation of drug exposure and higher tissue levels of drug due to slower metabolism. A Phase I study was undertaken in advanced solid tumor patients in Taiwan, and the MTD was 120 mg/m^2; UGT1A1 genotyping was not prospectively undertaken in that solid tumor study. Objectives: To assess the safety and pharmacokinetics (PK) of nal-IRI and to determine the maximum tolerated dose (MTD) in patients with recurrent malignant glioma stratified based on UGT1A1 genotyping. **Methods:**This Phase I study in recurrent malignant glioma stratified patients by UGT1A1 status, to homozygous WT ("WT") vs heterozygous WT/*28 ("HT"). Patients who were homozygous *28 were ineligible. Eligibility criteria included age > = 18, KPS > = 60, not on enzyme-inducing drugs (including enzyme-inducing seizure medications), and no prior treatment with irinotecan. The design was a standard 3+3 Phase I design. Patients who were WT were started at 120 mg/m^2(the MTD from the Taiwanese study) with dose increases in 60 mg/m^2 increments. Patients who were HT were started at 60 mg/m^2, with dose increases in 30 mg/m^{2}increments. Dosing was given IV every 3 weeks. The DLT assessment period was 1 cycle (21 days). **Results:** In the WT cohort, the MTD was 120 mg/m^2. In the HT cohort, the MTD was 150 mg/m^2. DLTs in both cohorts included diarrhea, some with associated dehydration and/or fatigue. Analysis of PK data is in process, and will be presented at the

meeting.**Conclusions:** Nal-IRI had no unexpected toxicities when given via IV. The toxicity profile of the drug was felt acceptable to move forward with additional testing using convection-enhanced delivery into intracranial tumors, and such a Phase I study is currently enrolling at our institution. Clinical trial information: NCT00734682.

Encapsulation of the Topoisomerase I Inhibitor GL147211C in Pegylated (STEALTH) Liposomes: Pharmacokinetics and Antitumor Activity in HT29 Colon Tumor Xenografts

Gail T. Colbern,[1] Donald J. Dykes, Charles Engbers, Randy Musterer, Alan Hiller, Erik Pegg, Renee Saville, Steve Weng, Michael Luzzio, Paul Uster, Michael Amantea, and Peter K. Working

SEQUUS Pharmaceuticals, Inc., Menlo Park, California 94025 [G. T. C., C. E., R. M., A. H., E. P., R. S., S. W., P. U., M. A., P. K. W.]; Southern Research Institute, Birmingham, Alabama 35246 [D. J. D.]; and Glaxo Wellcome, Inc., Research Triangle Park, North Carolina 27709 [M. L.]

ABSTRACT

The topoisomerase I inhibitor GL147211C {7-[(4-methylpiperazino)methyl]-10,11-(ethylenedioxy)-(20*S*)-camptothecin trifluoroacetate}, a camptothecin analogue, has significant activity in tumor cell cytotoxicity assays *in vitro* and antitumor activity in both animal tumor models and human patients. Its toxicity is significant, however, effectively limiting the amount of drug that can be administered and its clinical utility. To determine whether the therapeutic index of GL147211C could be improved, the drug was encapsulated in long-circulating, pegylated (STEALTH) liposomes (SPI-355). The pharmacokinetics and antitumor activity of SPI-355 were compared to those of nonliposomal GL147211C. The plasma pharmacokinetics of SPI-355 in rats were typical of those of other pegylated liposomal formulations, with significantly increased blood circulation time; the dose-corrected area under the curve and C_{max} of SPI-355 (10 mg/kg) were 1250- and 35-fold higher, respectively, than those of nonliposomal GL14711C (8.72 mg/kg). The comparative antitumor activity of SPI-355 and nonliposomal GL1472211C was evaluated in nude mice implanted with HT29 colon carcinoma xenografts. SPI-355 was 20-fold more effective than GL147211C in inhibiting tumor growth (1 mg/kg SPI-355 and 20 mg/kg GL147211C) and produced durable complete remissions of tumors at well-tolerated dose levels that were >5-fold lower than the maximally tolerated dose of GL147211C, which induced no durable complete responses. Signs of toxicity were similar between the two drugs, but liposome encapsulation increased the toxicity of drug ~4-fold, with increased weight loss and several deaths with SPI-355 (5 mg/kg SPI-355 *versus* 20 mg/kg GL147211C). Despite the increased toxicity seen with SPI-355, the therapeutic index of the liposomal formulation was increased ~5-fold over that of nonliposomal GL147211C, suggesting that such a pegylated liposomal formulation could demonstrate increased therapeutic index in human patients.

INTRODUCTION

The camptothecin analogue GL147211C {7-[(4-methylpiperazino)methyl]-10,11-(ethylenedioxy)-(20S)-camptothecin trifluoroacetate}, provided by Glaxo Research Institute (Research Triangle Park, NC), is a potent and specific inhibitor of DNA topoisomerase I (1, 2). Topoisomerase I inhibitors stabilize the cleavable complex formed by topoisomerase I and DNA and cause single-stranded DNA breaks (1, 3). This DNA damage, however, is not toxic to the cell until DNA synthesis, when DNA replication forks encounter stabilized cleavable complexes and result in double-stranded DNA breaks (3, 4). Because of this significant cell cycle-dependent antitumor activity (1, 3), prolonged exposure to effective drug concentrations is required to maximize the fractional tumor cell kill (3, 5).

The topoisomerase I inhibitor GL147211C has significant activity in both *in vitro* cytotoxicity tests and *in vivo* animal tumor models (2, 6). Phase I clinical trials have been published (7–9) using a 5-day infusion per cycle, with a recommended dose of 1.0–1.5 mg/m^2/day. Toxicity of the nonliposomal drug (marked weight loss in mice at clinically effective doses and myelosuppression and moderate gastrointestinal toxicity in Phase I clinical trials in humans) is significant, limiting the amount of drug that can be administered and restricting exposure of tumor tissue to effective drug concentrations (1, 7–10).

STEALTH liposomes are liposomes that contain surface-bound polyethylene glycol chains (11–13). Pegylated liposomes exhibit prolonged circulation times by avoiding uptake by the organs of the mononuclear phagocyte system (13–15). Molecules that have been successfully incorporated into pegylated liposomes, such as doxorubicin, have shown marked increase in circulation times and improvement in antitumor activity (16, 17).

This report summarizes the results of a pharmacokinetic study in rats and efficacy studies initiated with xenograft tumors in mice to determine the antitumor activity of GL147211C encapsulated in long-circulating, pegylated liposomes (SPI-355).

MATERIALS AND METHODS

Test Material

GL147211C (GG211 or Lurtotecan; supplied by Dr. Michael Luzzio at Glaxo Research Institute, Research Triangle

Received 6/23/98; revised 9/11/98; accepted 9/15/98.
The costs of publication of this article were defrayed in part by the payment of page charges. This article must therefore be hereby marked *advertisement* in accordance with 18 U.S.C. Section 1734 solely to indicate this fact.

[1] To whom requests for reprints should be addressed, at SEQUUS Pharmaceuticals, Inc., 960 Hamilton Court, Menlo Park, CA 94025. Phone: (650) 463-3119; Fax: (650) 617-3080.

Table 1 Lipid components of the pegylated liposomes of SPI-355

More than 90% of drug is encapsulated into average 100-nm-diameter liposomes.

Lipid component	Lipid content,[a] mg/ml (%)	Molar ratio
HSPC[b]	9 (60)	55.4
MPEG-DSPE	3 (20)	5.6
Cholesterol	3 (20)	39

[a] Values shown are the theoretical concentrations in the final formulation.

[b] HSPC, hydrogenated soy phosphatidylcholine; MPEG-DSPE, *N*-(carbamoyl-methoxypolyethylene glycol 2000)-1,2-distearoyl-*sn*-glycero-3-phosphoethanolamine sodium salt.

Park, NC) was formulated in liposomes containing: a pegylated lipid, *N*-(carbamoyl-methoxypolyethylene glycol 2000)-1,2-distearoyl-*sn*-glycero-3-phosphoethanolamine sodium salt; another phospholipid, hydrogenated soy phosphatidylcholine; and cholesterol (Table 1). SPI-355 was formulated at a GL147211C concentration of 2.5 mg/ml, with ~15 mg total lipid/ml. More than 90% of drug was entrapped within liposomes with an average diameter of 100 nm. Both nonliposomal GL147211C and SPI-355 were diluted in 5% dextrose in water as required to achieve appropriate concentrations for injection. Negative control animals received saline in the same volume used to treat test groups.

Pharmacokinetic Study

Animals. Eight male Sprague Dawley rats were obtained from Simonsen Labs (Gilroy, CA) and allowed to acclimate for 5 days prior to study initiation. Rats were housed in conventional hard-bottomed cages with food and acidified water *ad libitum* under a 12-h light/dark cycle. Experiments were conducted under the auspices of the Institutional Animal Care and Use Committee of SEQUUS Pharmaceuticals, following the 1996 Guide for the Care and Use of Animals in Research.

Study Design. SPI-355 and nonliposomal GL147211C were administered as a single bolus via lateral tail vein at 10 and 8.72 mg/kg, respectively (n = 4 rats per formulation). Blood samples were collected at 3–5, 15, and 30 min and 1, 2, 4, 6, and 24 h postdose. Two 0.20-ml samples of whole blood were extracted in 0.40 ml of either 4°C AcN[2] or 25°C acidified AcN (H_3PO_4), immediately vortexed vigorously for 10 s, and then centrifuged at 13,000 rpm for 5 min at room temperature. Supernatant was removed and immediately frozen at −70°C until assay by HPLC (18). Assay results for the acidified AcN extract (lactone form) and the nonacidified AcN extract were essentially equal. Here, we report values obtained from acidified AcN extract (lactone form).

Data Analysis. Mean drug concentrations in whole blood were plotted against time. The apparent half-lives were calculated as $\ln 2/k_{el}$, where k_{el} is the elimination constant of drug from blood. The AUC_{ss} measurement was determined by the linear trapezoidal rule and extrapolated to infinity by dividing the last measured concentration into the slope of the terminal phase. The maximum concentration achieved (C_{max}) was measured directly.

Efficacy Studies

Animals. Two studies were conducted at Southern Research Institute (Birmingham, AL) on a contract basis. For each study, 80 homozygous nude mice were obtained from Taconic Farms (Germantown, NY) and allowed to acclimate for 7 days prior to initiation of the experiment. Animals were housed in appropriate isolated caging with sterile rodent food and acidified water *ad libitum* and a 12-h light/dark cycle. Animals were randomized into treatment groups prior to inoculation of tumors based on body weight. Randomization was confirmed based on tumor size immediately prior to initiation of treatment.

Tumors. Tumors were inoculated s.c. by trochar placement of fragments from rapidly growing tumors on donor animals. The human colon cancer cell line HT-29 was used to initiate xenograft tumors.

Monitoring. All animals were observed daily for general well-being throughout the experiments. Animals were weighed prior to inoculation of tumors and at least weekly thereafter. Tumors were measured twice weekly throughout the experiment, beginning 10 days after tumor inoculation. Any animal with a weight loss of ≥15% of the initial starting weight was immediately euthanized, as was any animal with a tumor volume of >4000 mm^3. Experiments were conducted under the auspices of the Institutional Animal Care and Use Committees of SEQUUS and Southern Research Institute following the 1996 Guide for the Care and Use of Animals in Research.

Treatment. Animals were randomized to one of seven treatment groups (n = 10 animals each) in each experiment (20 animals in negative control group). Treatment was initiated on day 9 or 10 postinoculation, when the average tumor volume was ~75 mm^3 and the tumors were progressively growing. All treatments were administered as i.v. bolus injections, given weekly for 3 consecutive weeks. In study 1, treatment groups were nonliposomal GL147211C at 6, 15, or 24 mg/kg and SPI-355 at the same dose levels. In study 2, treatment groups were nonliposomal GL147211C at 20 mg/kg and SPI-355 at 5, 3, 1, 0.5, and 0.1 mg/kg.

Evaluation. Tumor size during and following each experiment was used as the primary evaluation of therapeutic efficacy. Body weight and survival were evaluated to assess toxicity. All tumor-bearing animals were observed following cessation of treatment until they were euthanized, based on criteria above. Experiments were concluded when a majority of control tumors achieved the maximal allowed volume (4000 mm^3).

Data Analysis. For each individual, tumor size was measured repeatedly at various time points; thus, these measurements were regarded as correlated information. Because the tumor sizes over time after treatment were of interest, repeated measurement analyses were performed for each data set. From examination of the data, a log transformation seemed reasonable. In this transformation, Y denotes the original tumor measurement, and $Z = \log(Y + 1)$. After the data were transformed, repeated measurement analyses were performed for the trans-

[2] The abbreviations used are: AcN, acetonitrile; AUC_{ss}, steady-state area under the curve; CR, complete response; PR, partial response; MTD, maximum tolerated dose.

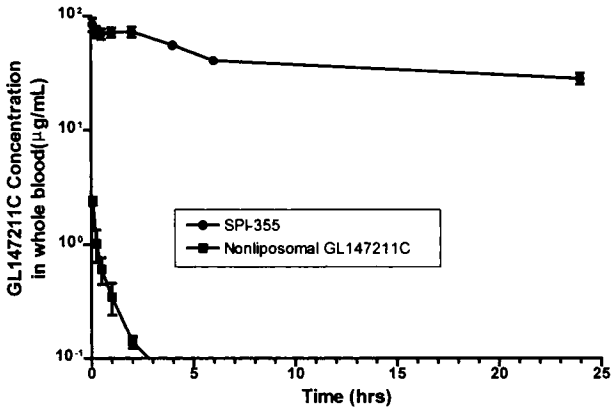

Fig. 1 Blood concentration *versus* time curves of STEALTH liposome encapsulated SPI-355 (●) and nonliposomal GL147211C (■) following a single i.v. bolus of 10 and 8.72 mg/kg, respectively, in rats.

Table 2 Concentration of GL147211C in whole blood after a single i.v. bolus of SPI-355 (10 mg/kg) or nonliposomal GL147211C (8.72 mg/kg) in rats (μg/ml, mean ± SD)

	Formulations	
Time postdose (h)	SPI-355	Nonliposomal GL147211C
0.083	84.2 ± 11.60	2.44 ± 0.23
0.25	72.5 ± 8.27	1.02 ± 0.32
0.50	69.5 ± 7.42	0.61 ± 0.16
1.0	71.6 ± 6.76	0.35 ± 0.11
2.0	72.2 ± 7.56	0.14 ± 0.017
4.0	55.3 ± 2.41	0.060 ± 0.000
6.0	40.4 ± 2.90	0.036 ± 0.016
24.0	28.1 ± 3.17	ND[a]

[a] ND, not detectable.

formed data Z using the SAS procedure PROC MIXED. The log growth rate for each treatment group was calculated and used to compare the different treatment groups. Statistical significance was declared at the 0.05 level, but due to multiple comparisons, adjustment to the type I error was performed, and a P of <0.005 indicated a statistically significant difference in any designated comparison. Response to therapy was also classified as either: CR, defined as complete elimination of tumor mass; or partial response (PR), defined as tumor volume of <50% of the peak tumor volume for an individual animal.

RESULTS

Pharmacokinetic Study

In rats administered nonliposomal GL147211C, blood concentrations declined in a biexponential manner. The concentration (mean ± SD) at 3–5 min postdose was 2.44 ± 0.23 μg/ml and declined to 0.036 ± 0.016 μg/ml by 6 h postdose (Fig. 1 and Table 2). No GL147211C was detected in blood at 24 h postdose. The AUC_{ss} was 1.49 ± 0.175 μg/ml·h, and the apparent half-life was 1.58 ± 0.41 h (Table 3).

In rats administered SPI-355, blood concentrations of GL147211C also declined in a biexponential manner; at 3–5 min postdose, the concentration was 84.2 ± 11.6 μg/ml, and it declined to 28.1 ± 3.17 μg/ml by 24 h postdose (Fig. 1 and Table 2). The AUC_{ss} of SPI-355 was 1853 ± 268 μg/ml·h, and the apparent half-life was 21.1 ± 4.33 h (Table 3).

Table 3 Pharmacokinetic parameters after a single i.v. bolus of SPI-355 (10 mg/kg) or nonliposomal GL147211C (8.72 mg/kg) in rats

	Formulations	
Parameter	SPI-355	Nonliposomal GL147211C
AUC (μg/ml · h)	1853 ± 268	1.49 ± 0.18
Apparent $T_{1/2}$ (h)	21.1 ± 4.33	1.58 ± 0.41
C_{max} (μg/ml)	84.2 ± 11.6	2.44 ± 0.23

Efficacy Studies

Study 1: HT29 Colon Xenograft. There were significantly more deaths in the SPI-355 treatment groups than in animals that received the same doses of nonliposomal GL147211C. All animals in the 15 and 24 mg/kg SPI-355 dose groups died after two doses, with most deaths occurring on day 5 after the first dose. Animals in the 6 mg/kg dose group survived all three doses, but 6 of 10 died within 8 days after the third dose. With the exception of one animal in the 24 mg/kg nonliposomal GL147211C group that died after the third dose, all animals survived in the nonliposomal GL147211C treatment groups. Body weight losses reflected the greater toxicity of liposomal SPI-355 (Fig. 2).

Despite its greater toxicity, the 6 mg/kg dose level of SPI-355 showed substantial antitumor activity (log growth rate of −0.026), significantly greater than that displayed by even the highest dose level of nonliposomal GL147211C (log growth rate of 0.0048; $P = 0.0022$). Tumor growth was significantly inhibited by treatment with 6 mg/kg SPI-355 (Fig. 3), with CR of tumors in all 10 animals by 5 days after the second treatment (Table 4). Tumors did not recur in surviving animals (4 of 10) in this treatment group by the end of study, ~30 days after final treatment.

Nonliposomal GL147211C also caused a significant inhibition of tumor growth (Fig. 3), particularly at a dose of 24 mg/kg, but did not result in as many tumor remissions (three CRs and one PR) as a 4-fold lower dose of SPI-355 (Table 4), and these remissions were not sustained by day 69. At a dose level of 6 mg/kg, free GL147211C caused no tumor remissions and was only minimally effective at inhibiting growth of HT29 tumors (Fig. 3).

Study 2: HT29 Colon Xenograft. Because of drug-related toxicity seen in the first study, a repeat study was conducted in this tumor model using lower dose levels in an effort to define the MTD and antitumor activity of SPI-355. Because the activity profile of nonliposomal GL147211C was well defined in first study, only one dose level was used in this study. Additionally, the dose level was decreased from 24 to 20 mg/kg, because one animal died at the higher dose in the first study.

At lower doses in this study, 4 of 10 animals in the 5 mg/kg SPI-355 dose group died of drug-related toxicity after dose 3; one additional animal died of apparently nonspecific causes after the third dose. One of 10 animals in the 3 mg/kg SPI-355 dose group died after dose 2, but death was not considered due

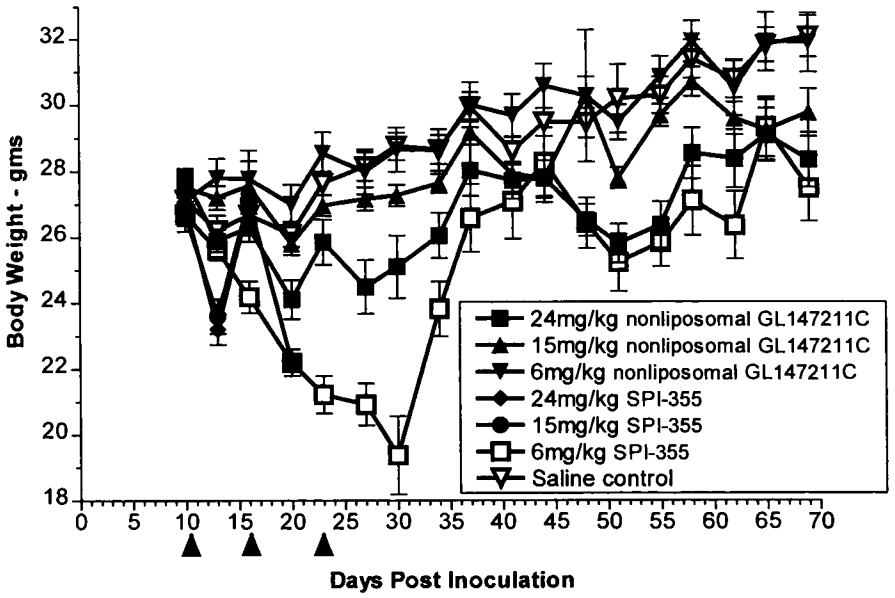

Fig. 2 Body weights of HT29 colon tumor-bearing nude mice from study 1. *Data points*, mean body weights; *bars*, SE. Animals were treated with SPI-355 or nonliposomal GL147211C on days 10, 16, and 23 after tumor inoculation. Treatment-related toxicity was reflected as weight loss during treatment.

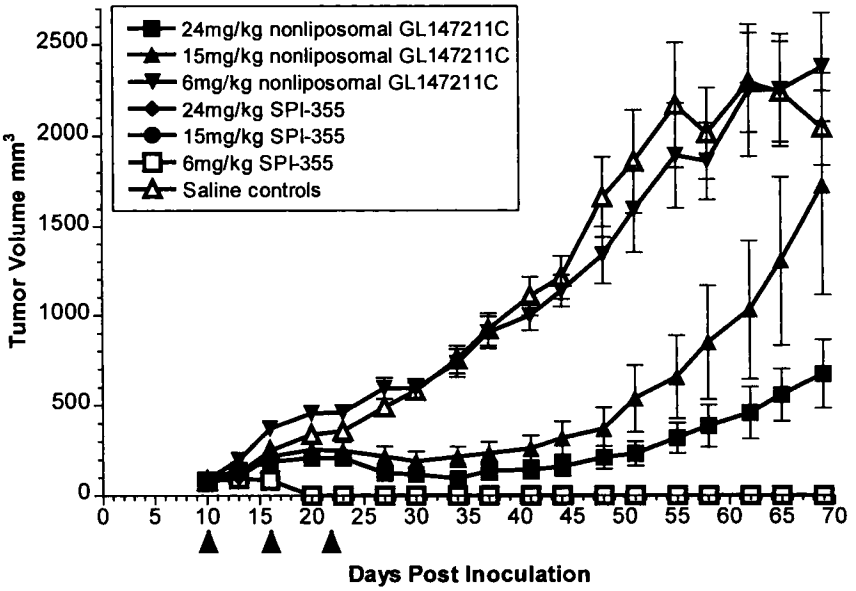

Fig. 3 Volumes of HT29 colon tumors in nude mice from study 1. *Data points*, mean tumor volumes; *bars*, SE. Animals were treated with SPI-355 or nonliposomal GL147211C on days 10, 16, and 23 after tumor inoculation. Moderate- and high-dose nonliposomal GL147211C had substantial antitumor activity, but tumors tended to regrow after cessation of treatment. Low-dose GL147211C had no antitumor activity. Moderate- and high-dose SPI-355 were toxic and could not be evaluated, but low-dose SPI-355 had substantial antitumor activity, and tumors failed to regrow after cessation of treatment during a prolonged posttreatment period.

to drug treatment because of absence of any correlating signs of toxicity. All other animals survived the entire study duration, and there were no deaths in the 20 mg/kg nonliposomal GL147211C dose group. Body weight changes were dose-related and correlated with other observations of toxicity (Fig. 4).

Treatment with 20 mg/kg nonliposomal GL147211C significantly inhibited tumor growth (log growth rate of 0.011) and was approximately equivalent in its antitumor activity to 1 mg/kg SPI-355 (log growth rate of 0.017; $P = 0.091$; Fig. 5). At 3 mg/kg, SPI-355 (log growth rate of −0.029) exhibited significantly greater antitumor activity than 20 mg/kg of nonliposo-

Table 4 Response of HT29 colon cancer xenografts: study 1

Treatment	CR[a]	PR
Saline	0/20	0/20
GL147211C, 24 mg/kg	3/10	1/10
GL147211C, 15 mg/kg	2/10	0/10
GL147211C, 6 mg/kg	0/10	0/10
SPI-355, 24 mg/kg	NA	NA
SPI-355, 15 mg/kg	NA	NA
SPI-355, 6 mg/kg	10/10	NA

[a] CR, elimination of tumor mass until experiment termination; PR, tumor volume of <50% of peak tumor volume for an individual animal; NA, not applicable.

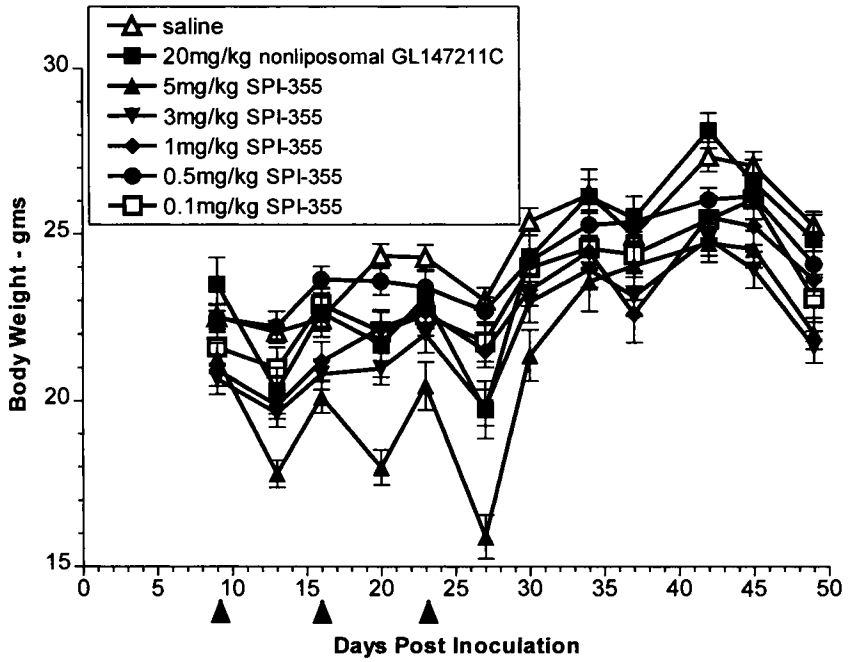

Fig. 4 Body weights of HT29 colon tumor-bearing nude mice from study 2. *Data points*, mean body weights; *bars*, SE. Animals were treated with SPI-355 or nonliposomal GL147211C on days 9, 16, and 23 after tumor inoculation. All treatments were associated with transient weight loss, recovered prior to subsequent treatment, with the most significant weight loss in high-dose SPI-355 treatment group.

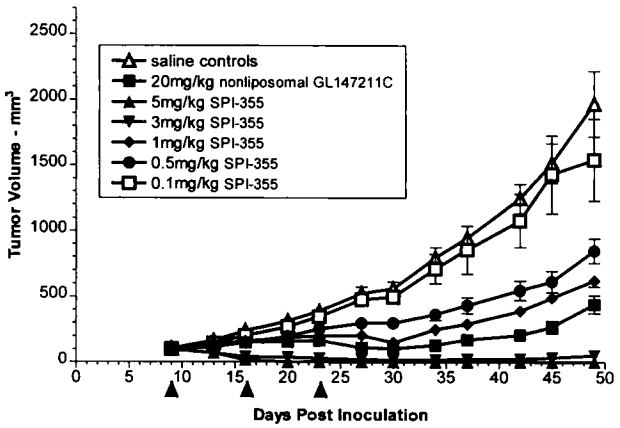

Fig. 5 Volumes of HT29 colon tumors in nude mice from second experiment. *Data points*, mean tumor volumes; *bars*, SE. Animals were treated with SPI-355 or nonliposomal GL147211C on days 9, 16, and 23 after tumor inoculation. The MTD of nonliposomal GL147211C had substantial antitumor activity, but tumors tended to regrow after cessation of treatment. SPI-355 had a significant antituor dose response, with antitumor activity in animals receiving I mg/kg SPI-355, most similar to that seen in animals receiving 20 mg/kg nonliposomal GL147211C.

mal drug ($P = 0.0006$). Both the 1 mg/kg SPI-355 and 20 mg/kg nonliposomal GL147211C groups were significantly more effective than 0.5 mg/kg SPI-355 treatment (log growth rate of 0.024; $P = 0.0041$).

There were no CRs and only 1 of 10 PRs in animals treated with 20 mg/kg nonliposomal GL147211C, compared to 7 of 10 CRs and 1 of 10 PRs in the 3 mg/kg SPI-355 group and 10 of 10 CRs in the 5 mg/kg SPI-355 group (Table 5). CRs were maintained to day 63 in three animals each in the 5 and 3 mg/kg

Table 5 Response of HT29 colon cancer xenografts: study 2

Treatment	CR[a]	PR
Saline	0/20	0/20
GL147211C, 20 mg/kg	0/10	1/10
SPI-355, 5 mg/kg	10/10	NA
SPI-355, 3 mg/kg	7/10	1/10
SPI-355, 1 mg/kg	0/10	0/10
SPI-355, 0.5 mg/kg	0/10	1/10
SPI-355, 0.1 mg/kg	0/10	0/10

[a] CR, elimination of tumor mass until experiment termination; PR, tumor volume of <50% of the peak tumor volume for an individual animal; NA, not applicable.

SPI-355 treatment groups. There was one nonsustained partial tumor remission in the 0.5 mg/kg liposomal SPI-355 group, but no remissions in either the 1 or 0.1 mg/kg group. This latter dose level showed no antitumor activity (log growth rate of 0.028, similar to the saline-treated controls with a log growth rate of 0.030, $P = 0.755$).

DISCUSSION

The pharmacokinetics of SPI-355 observed here are typical of other STEALTH liposome-encapsulated molecules. Encapsulation of GL147211C into STEALTH liposomes significantly increases its blood circulation time compared to nonliposomal GL147211C, allowing prolonged exposure of tumor tissue to significant drug concentrations. In rats administered SPI-355, the dose-corrected C_{max} and AUC_{ss} values were 35- and 1250-fold higher, respectively, compared to nonliposomal GL147211C. The decline in blood concentrations of both SPI-355 and nonliposomal GL147211C was biexponential, and the apparent half-life of SPI-355 was ~13-fold longer than that of nonliposomal GL147211C (21.1 *versus* 1.58 h, respectively).

The first antitumor activity study with HT29 colon xenografts was performed with dose levels selected from previously published data on the MTD of nonliposomal GL147211C (6). Toxicity was evident after the first administration of SPI-355, with death or euthanasia of all animals in the 24 and 15 mg/kg dose groups by the second weekly drug administration. Despite significant toxicity at the lowest dose (6 mg/kg), SPI-355 demonstrated remarkable antitumor activity in surviving animals, with all 10 HT29 colon tumor-bearing animals having a CR, which was sustained for the duration of the study in the survivors.

The second antitumor activity study established that the MTD of SPI-355 for repeated administration is between 3 and 5 mg/kg. The antitumor activity of 1 mg/kg SPI-355 was significant and equivalent to a 20-fold higher dose of nonliposomal GL147211C. Both 3 and 5 mg/kg SPI-355 were significantly more effective than 20 mg/kg nonliposomal GL147211C. These findings suggest that the therapeutic index of SPI-355 is ~4–5-fold higher than that of nonliposomal GL147211C, as confirmed by the large number of complete and partial antitumor responses in the 3 mg/kg (7 of 10 CRs and 1 of 10 PRs) and 5 mg/kg (10 of 10 CRs) SPI-355 groups. Nonliposomal GL147211C, although demonstrating significant tumor growth delay, failed to produce any CRs and produced only one PR. A recently described conventional, nonpegylated liposomal formulation of GL147211C, NX-211 (19), also increased drug AUC and enhanced antitumor activity, but only at dose levels similar to nonliposomal GL147211C; no data on tumor remissions were provided. This report suggests that encapsulation of GL147211C in pegylated liposomes confers an additional therapeutic advantage.

The increased circulation time associated with pegylated liposomal encapsulation of SPI-355 likely allows prolonged exposure of tissues to significant drug concentrations, as seen with other cytotoxic drugs encapsulated in pegylated liposomes (16). The prolonged exposure increases the cell cycle-specific cytotoxicity of the drug and may account for the large number of cures among study animals (3, 5). Although increased toxicity (4-fold) of SPI-355 was observed, the improvement in antitumor activity (20-fold) and therapeutic index (5-fold) of this formulation over the nonliposomal GL147211C warrants further study.

REFERENCES

1. Dancey, J., and Eisenhauer, E. A. Current perspectives on camptothecins in cancer treatment. Br. J. Cancer, *74:* 327–338, 1996.

2. Besterman, J. M. Topoisomerase I inhibition by the camptothecin analog GI147211C: from the laboratory to the clinic. Ann. N. Y. Acad. Sci., *803:* 202–209, 1996.

3. Takimoto, C. H., and Arbuck, S. G. The camptothecins. *In:* B. A. Chabner and D. L. Longo (eds.), Cancer Chemotherapy and Biotherapy, Ed. 2, pp. 463–484. Philadelphia: Lippincott-Raven Publishers, 1996.

4. Hsiang, Y-H., Lihou, M. G., and Lui, L. F. Arrest of replication forks by drug-stabilized topoisomerase I-DNA cleavable complexes as a mechanism of cell killing by camptothecin. Cancer Res., *49:* 5077–5082, 1989.

5. Gerrits, C. J., de Jonge, M. J., Schellens, J. H., Stoter, G., and Verweij, J. Topoisomerase I inhibitors: the relevance of prolonged exposure for present clinical development. Br. J. Cancer, *76:* 952–962, 1997.

6. Luzzio, M. J., Besterman, J. M., Emerson, D. L., Evans, M. G., Lackey, K., Leitner, P. L., McIntyre, G., Morton, B., Myers, P. L., Peel, M., Sisco, J. M., Sternback, D. D., Tong, W-Q., Truesdale, A., Uehling, D. E., Vuong, A., and Yates, J. Synthesis and antitumor activity of novel water soluble derivatives of camptothecin as specific inhibitors of topoisomerase I. J. Med. Chem., *38:* 395–401, 1995.

7. Gerrits, C. J., Creemers, G. J., Schellens, J. H., Wissel, P., Planting, A. S., Kunka, R., Selinger, K., deBoer-Dennert, M., Marijnen, Y., and Verweij, J. Phase I and pharmacological study of the new topoisomerase I inhibitor GL147211, using a daily × 5 intravenous administration. Br. J. Cancer, *73:* 744–750, 1996.

8. Eckhardt, J. R., Rodriguez, G. I., Burris, H. A., Wissel, P. S., Fields, S. M., Rothenberg, M. L., Smith, L., Thurman, A., Kunka, R. L., Depee, S. P., Littlefield, D., White, L. J., and Von Hoff, D. D. A Phase I and pharmacokinetic study of the topoisomerase I inhibitor GG211. Proc. Am. Soc. Clin. Oncol., *14:* 476, 1995.

9. Eckhardt, S. G., Baker, S. D., Eckhardt, J. R., Burke, T. G., Warner, D. L., Kuhn, J. G., Rodriguez, G., Fields, S., Thurman, A., Smith, L., Rothenberg, M. L., White, L., Wissel, P., Kunka, R., DePee, S., Littlefield, D., Burris, H. A., Von Hoff, D. D., and Rowinsky, E. K. Phase I and pharmacokinetic study of GL147211, a water-soluble camptothecin analogue, administered for five consecutive days every three weeks. Clin. Cancer Res., *4:* 595–604, 1998.

10. O'Dwyer, P., Cassidy, J., Kunka, R., Pas-Arez, L., Kaye, S., Depee, S., Littlefield, D., Demaria, D., Selinger, K., Beranek, P., Collis, P., and Wissel, P. Phase I trial of GG211, a new topoisomerase inhibitor, using a 72 hour continuous infusion. Proc. Am. Soc. Clin. Oncol., *14:* 471, 1995.

11. Gabizon, A., Barenholz, Y., and Bialer, M. Prolongation of the circulation time of doxorubicin encapsulated in liposomes containing a polyethylene glycol derivatized phospholipid: pharmacokinetic studies in rodents and dogs. Pharm. Res. (N. Y.), *10:* 703–708, 1993.

12. Gabizon, A., Catane, R., Uziely, B., Kaufman, B., Safra, T., Cohen, R., Martin, F., Huang, A., Barenholz, Y. Prolonged circulation time and enhanced accumulation in malignant exudates of doxorubicin encapsulated in polyethylene-glycol coated liposomes. Cancer Res., *54:* 987–992, 1994.

13. Papahadjopoulos, D., Allen, T. M., Gabizon, A., Mayhew, E., Matthay, K., Huang, S. K., Lee, K. D., Woodle, M. C., Lasic, D. D., Redemann, C., and Martin, F. J. Sterically stabilized liposomes: improvements in pharmacokinetics and antitumor therapeutic efficacy. Proc. Natl. Acad. Sci. USA, *88:* 11460–11464, 1991.

14. Gabizon, A., and Papahadjopoulos, D. Liposome formulations with prolonged circulation time in blood and enhanced uptake by tumors. Proc. Natl. Acad. Sci. USA, *85:* 6949–6953, 1988.

15. Woodle, M. C., Newman, M. S., and Working, P. K. Biological Properties of Sterically Stabilized Liposomes, pp. 103–117. Boca Raton, FL: CRC Press, 1995.

16. Working, P. K., Newman, M. S., Huang, S. K., Mayhew, E., Vaage, J., and Lasic, D. D. Pharmacokinetics, biodistribution and therapeutic efficacy of doxorubicin encapsulated in Stealth liposomes (DOXIL). J. Liposome Res., *4:* 667–687, 1994.

17. Working, P. K., and Dayan, A. D. Pharmacological-toxicological expert report. CAELYX™ (Stealth® liposomal doxorubicin HCl). Hum. Exp. Toxicol., *15:* 752–785, 1996.

18. Stafford, C. G., and St. Claire, R. L. High-performance liquid chromatographic analysis of the lactone and carboxylate forms of a topoisomerase I inhibitor (the antitumor drug GI147211C) in plasma. J. Chromatogr. B, *663:* 119–126, 1995.

19. Emerson, D. L., Amirgahari, N., Bendele, R., Brown, E., Chen, L-S., Chiang, S-M., Gill, S., LeRay, J. D., Moynihan, K., Tomkinson, B., and Luzzio, M. J. NX-211, a liposomal formulation of Lurtotecan, demonstrates enhanced pharmacokinetic and antitumor activity. Proc. Am. Assoc. Cancer Res., *39:* 278, 1998.

British Journal of Cancer (2003) 89, 992–996

www.bjcancer.com

Irinotecan plus leucovorin-modulated 5-fluorouracil I.V. bolus every other week may be a suitable therapeutic option also for elderly patients with metastatic colorectal carcinoma

P Comella*[,1], A Farris[2], V Lorusso[3], S Palmeri[4], L Maiorino[5], L De Lucia[6], F Buzzi[7], S Mancarella[8], F De Vita[9] and A Gambardella[10]

[1]Division of Medical Oncology, National Tumour Institute, Via M. Semmola, 80131 Naples, Italy; [2]Chair of Medical Oncology, University School of Medicine, Viale S. Pietro 8, 07100 Sassari, Italy; [3]Department of Medical Oncology, Oncology Institute, Via G. Amendola 209, 70126 Bari, Italy; [4]Chair of Medical Oncology, University School of Medicine, P.za delle Cliniche 2, 90127 Palermo, Italy; [5]Medical Oncology, San Gennaro Hospital, Via S. Gennaro dei Poveri 5, 80131 Naples, Italy; [6]Medical Oncology, City Hospital, Via G. Tescione 81, 81100 Caserta, Italy; [7]Medical Oncology, City Hospital, Via T. Joannuccio, 05100 Terni, Italy; [8]Medical Oncology, City Hospital, Via Taranto, 73021 Campi Salentino (Lecce), Italy; [9]Chair of Medical Oncology, Second University School of Medicine, Via S. Pansini, 80131 Naples, Italy; [10]Chair of Geriatrics, Second University School of Medicine, Via S. Pansini, 80131 Naples, Italy

The aim of this study was to assess the safety and efficacy of biweekly irinotecan plus leucovorin-modulated 5-fluorouracil i.v. bolus in metastatic colorectal carcinoma according to the age of patients. For this purpose, we have analysed 108 patients randomly allocated to receive irinotecan 200 mg m^{-2} i.v. (1-h infusion) on day 1, and L-leucovorin 250 mg m^{-2} i.v. (1-h infusion) plus 5-fluorouracil 850 mg m^{-2} i.v. bolus on day 2 every 2 weeks (IRIFAFU) in our previous SICOG 9801 trial. According to age, patients were retrospectively divided into three groups: younger ($\leqslant$ 54 years, $n = 37$), middle-aged (55–69 years, $n = 64$), and elderly ($\geqslant$ 70 years, $n = 17$). Apart from gender, pretreatment characteristics were well balanced across the three groups. WHO grade $\geqslant$ 3 neutropenia and diarrhoea affected on the whole 46 and 16 patients, respectively, without any significant difference according to age-grouping. Patients aged $\leqslant$ 54 years stayed on therapy for a longer time (median 24 vs 14–15 weeks), and received more cycles (median 9 vs 7), than the older ones. Only one patient in the young group withdrew consent to therapy as opposed to four patients each in the aged and elderly one. Response rate was 38% for younger patients, 34% for aged, and 35% for the elderly ones. Median time to progression was 7.4, 8.0, and 5.3 months, and median survival time was 13.4, 15.3, and 13.9 months, respectively. We conclude that IRIFAFU given every other week may represent a suitable therapeutic option also for elderly patients with metastatic colorectal carcinoma.

British Journal of Cancer (2003) **89**, 992–996. doi:10.1038/sj.bjc.6601214 www.bjcancer.com

Keywords: colorectal carcinoma; elderly patients; combination chemotherapy; irinotecan; 5-fluorouracil

Colorectal carcinoma is among the most common cancers in western countries. In Italy, about 40 new cases per 100 000 males, and 20 new cases per 100 000 females are diagnosed each year (Zanetti *et al*, 1997). Most of these cases are discovered in patients aged 65 years or more.

In recent years, the postsurgical administration of 5-fluorouracil (FU)-based chemotherapy in high-risk (Dukes' stage C) colon cancer patients has been proven to reduce the recurrence and death rate (Wolmark *et al*, 1999). On the contrary, there is still no agreement about the absolute benefit that could be obtained in patients with more limited (Dukes' stage B) extension (International Multicenter Pooled Analysis of B2 Colon Cancer Trials, 1999; Mamounas *et al*, 1999). Anyway, recently published retrospective studies and meta-analyses have reported no interaction between age of patients and effect of adjuvant chemotherapy, suggesting that elderly patients should also be offered such treatments (Sargent *et al*, 2001a; Sundararajan *et al*, 2002).

*Correspondence. Dr P Comella; E-mail: pasqualecomella@libero.it
Received 16 October 2002; revised 3 June 2003; accepted 29 June 2003

Until recently, the usual management for the recurrent or metastatic disease included leucovorin (LV)-modulated FU chemotherapy (LV-FU), given in a 5-day monthly or in a once-a-week schedule (Buroker *et al*, 1994). These two regimens produced equivalent results, and a meta-analysis has shown that this palliative treatment was associated with a 35% reduction in the risk of death as compared with supportive care alone, which translated in an improvement in median survival of 3.7 months (Colorectal Cancer Collaborative Group, 2000). Also in this case, no age-related difference was found as to the effectiveness of chemotherapy (Chiara *et al*, 1998; Popescu *et al*, 1999).

Despite this observation, the number of elderly patients receiving palliative chemotherapy for colorectal carcinoma is still limited (Hutchins *et al*, 1999). Indeed, there is still a diffuse concern about the compliance and tolerability of chemotherapy in such patients (Daniele *et al*, 1999). On the other hand, some investigators have already stressed that performance status, and associated morbidities, more than age of patients, may adversely affect their outcome (Extermann *et al*, 1998; Yancik *et al*, 2001).

Recently, novel drugs such as irinotecan or oxaliplatin have shown activity in this disease when used either alone or in

combination with FU. Addition of irinotecan to LV-FU has been proven to increase significantly the response rate, the time to progression, and the median survival of patients, in comparison with LV-FU alone (Douillard *et al*, 2000; Saltz *et al*, 2000). Also, oxaliplatin combined with LV-FU has demonstrated to increase significantly the response rate and the time to progression, but not the survival, in comparison with the same regimen without oxaliplatin (de Gramont *et al*, 2000). Therefore, irinotecan plus LV and FU is now considered the gold standard of treatment for metastatic patients. However, because no prospective analysis has been carried out on the tolerability of these new combinations in aged people, a special care has been recommended, in consideration of the early and unpredictable adverse events that may occur in older individuals (Rothemberg *et al*, 2001; Sargent *et al*, 2001b).

In recent years, the Southern Italy Cooperative Oncology Group (SICOG) has devised an original biweekly regimen, including irinotecan plus LV-modulated FU given as i.v. bolus (IRIFAFU) for metastatic colon cancer patients (Comella *et al*, 2000). The IRIFAFU combination has been compared in a randomised multicentre study (SICOG trial 9801) with FU modulated by methotrexate and LV. In that trial, the IRIFAFU regimen produced a greater response rate, and a longer time to progression, than the control treatment (Comella *et al*, 2002). Here we report the results of a retrospective analysis we have carried out on the patients randomly allocated to receive the combination regimen, with the aim of having a deeper insight on the interaction between age of patients, their tolerability to chemotherapy, and outcome.

PATIENTS AND METHODS

Patient population

Patients affected by metastatic colorectal cancer, enrolled into the SICOG trial 9801, and randomly allocated to receive the IRIFAFU regimen (experimental arm), were the object of this retrospective analysis. Briefly, eligibility criteria for SICOG trial 9801 were: histologically proven adenocarcinoma of the colon or rectum; presence of bidimensionally measurable lesion(s); age $\geqslant 18$ years; performance status $\leqslant 2$ of the Eastern Cooperative Oncology Group (ECOG) scale; adequate liver, renal, and bone marrow reserve. Patients previously treated with FU-based adjuvant chemotherapy were also included, provided that at least 6 months had elapsed from treatment discontinuation.

Treatment

Patients in the experimental arm received the IRIFAFU regimen: irinotecan 200 mg m^{-2} given i.v. over 1-h on day 1, and L-leucovorin 250 mg m^{-2} given as 1-h i.v. infusion, followed by FU 850 mg m^{-2} as i.v. bolus, on day 2. Cycles were repeated every other week until progression, or for a maximum of 6 months. Attending physicians were required to specify the reason for an earlier treatment discontinuation. Disease status was checked every 2 months, and classified according to the World Health Organization (WHO) criteria (Miller *et al*, 1981). Adverse events of each treatment cycle were scored according to WHO scale (Miller *et al*, 1981), and the worst grade for each patient during treatment was recorded. Haematological toxicity was checked weekly. The actual dose intensity of cytotoxic drugs over 4 and 8 cycles (DI_4 and DI_8, respectively) was calculated as previously reported. Patients were followed every 2 months for assessing tumour progression and survival, and the cause of death (disease- or treatment-related, or due to other reasons) was recorded.

Analysis of safety and activity

According to their age, patients were divided into three groups: younger ($\leqslant 54$ years), middle-aged (55–69 years), and elderly ($\geqslant 70$ years). Differences in distribution of pretreatment characteristics among the three groups were assessed by the χ^2 test. Comparison of treatment in the three age groups (i.e., number of cycles, duration of therapy, and dose intensities) was made by the Kruskal–Wallis test. The difference in reasons for going off-study was assessed for significance by the Pearson χ^2-test. For exploring the interaction between pretreatment characteristics and treatment activity, patients achieving a complete or partial response were classified as 'responders', while patients showing a stable or progressive disease, as well as those not assessed for response, were classified as 'failures' according to intent-to-treat analysis. The following characteristics were explored for correlation with activity: age, sex, primary site, previous radical surgery, previous adjuvant chemotherapy, time to occurrence of metastatic disease, performance status, presence of symptoms, significant loss of body weight, number of disease sites, and basal carcinoembryonic antigen (CEA) serum level. For statistical analysis, the following variables were coded as dichotomous: primary site (colon or rectum), performance status (0 or $\geqslant 1$), timing of metastasis (synchronous or metachronous), number of disease sites (1 or $\geqslant 2$), and CEA basal value (< 100 or $\geqslant 100$ ng ml^{-1}).

Analysis of outcome

Progression-free survival (PFS) was calculated for each patient from the date of registration to the date of documented tumour progression, or death. Patients who discontinued the treatment early because of toxicity, refusal, or reason other than progression, were considered as censored at that time interval. Overall survival (OS) time was calculated for all patients from the date of registration to the date of death for any cause, or to patients last follow-up. Survival curves were generated by actuarial method (Kaplan and Meier, 1958), and compared by the log-rank test (Peto *et al*, 1977).

A logistic regression analysis was performed to identify the interaction between probability of response and pretreatment characteristics, while the Cox multivariate analysis (Cox, 1972) was carried out to assess their effect on time to progression and survival.

RESULTS

Patients and treatment

Patient main characteristics are listed in Table 1, according to age grouping. An imbalance in gender distribution was observed, given that elderly patients were more likely to be male ($P = 0.004$). Other baseline characteristics were well matched across the three groups.

Younger patients stayed somewhat longer on treatment, while a similar length of treatment (and number of cycles) was administered to middle-aged or elderly patients (Table 2). Analysis of reasons for treatment discontinuation revealed that younger patients were less likely to refuse chemotherapy as compared to the middle-aged or elderly ones ($P = 0.016$), while other causes were evenly distributed among the three groups.

A greater (although not statistically significant) proportion of elderly patients (35%) had a dose reduction along the first four cycles, in comparison with the middle-aged (25%), and younger patients (19%). In addition, a >2-week delay during the administration of the first four cycles was applied in 40% of elderly, in 25% of middle-aged, and in 26% of younger patients. During the four subsequent cycles, such a delay was applied in 62% of elderly, in 64% of middle-aged, and in 65% of younger patients. As a consequence, the median DI_4 of cytotoxic drugs was slightly lower for elderly patients, but DI_8 was substantially comparable in all groups (Table 3).

Table 1 Main patient characteristics according to age grouping

Characteristics	Age groups (years) ≤54 n = 37	55–69 n = 64	≥70 n = 17	Total N = 118
Median age in years (range)	48 (28–54)	64 (55–69)	68 (65–79)	62 (28–79)
Males	14	41	14	69
Females	23	23	3	49
Primary				
Colon or recto–sigmoid	27	48	13	88
Rectum	10	16	4	30
Previous surgery				
No	5	11	1	17
Yes	32	53	16	101
Previous adjuvant CT				
No	26	50	13	89
Yes	11	14	4	29
Synchronous metastasis				
No	18	28	9	55
Yes	19	36	8	63
Performance status				
0	20	38	12	70
1	15	24	5	44
2	2	2	0	4
Presence of symptoms				
No	20	43	13	76
Yes	17	21	4	42
Weight loss ≥5%				
No	28	53	12	93
Yes	9	11	5	25
No. disease sites				
1	20	36	10	66
>1	17	28	7	52
Liver involvement				
No	12	14	8	34
Yes	25	50	9	84
Single	4	12	0	16
<25%	12	23	4	39
>25%	9	15	5	29
Lung involvement				
No	31	49	13	93
Yes	6	15	4	25
CEA basal value ≥100				
No	24	42	11	85a
Yes	11	22	6	20a

[a]No available basal values in 13 patients.

Table 2 Duration of treatment, number of delivered cycles, and reason for discontinuation of therapy according to age grouping

Age groups (years)	≤54 n = 37	55–69 n = 64	≥70 n = 17	
Stay on treatment (weeks)				
Median	24	15	14	$P^a = 0.091$
Range	2–42	2–45	2–35	
Administered cycles				
Median	9	7	7	$P^a = 0.045$
Range	2–16	1–20	1–12	
Reasons for treatment discontinuation				
As for protocol	32	40	13	
Toxicity	0	7	0	
Refusal	1	4	4	$P^b = 0.016$
Disease complications	1	5	0	
Death	0	5	0	
Physician's decision	3	3	0	

[a]Kruskal–Wallis test. [b]Pearson's χ^2 test.

Table 3 Absolute dose intensity ($mg\,m^{-2}\,week^{-1}$) over the first four (DI_4) and eight (DI_8) cycles according to age grouping

Dose intensity	Age-groups (years) ≤54 n = 37	55–69 n = 64	≥70 n = 17	P^a
DI_4				
IRI				
Median	86	82	66	0.230
Range	55–100	52–100	41–100	
5FU				
Median	366	361	270	0.131
Range	231–425	249–458	175–426	
DI_8				
IRI				
Median	85	75	81	0.532
Range	58–98	50–100	50–100	
5FU				
Median	366	322	345	0.449
Range	230–410	230–41	209–425	

[a]Kruskal–Wallis test.

After discontinuation of study treatment, 55 patients (47% of the whole series) received second-line therapy: 19 (51%) younger patients, 28 (44%) middle-aged patients, and 7 (41%) elderly patients (χ^2 for trend not significant).

Safety

Main severe haematological toxicity of this regimen was neutropenia, which occurred in 46 patients on the whole: grade ≥3 neutropenia was detected in 43% of younger, in 41% of middle-aged, and in 31% of elderly group. Only four patients suffered from neutropenic fever or infection: their age ranged between 45 and 64 years. Among nonhaematological side effects, grade ≥3 diarrhoea was reported in 11% of younger, 18% of aged, and 6% of elderly patients (χ^2-test not significant). Severe stomatitis occurred in three patients on the whole: one patient in each age-group. Occurrence of other adverse events was not different in the three age groups (Table 4). Interestingly, a lower proportion of elderly patients suffered from at least one episode of grade ≥3 toxicity of any type (excluding alopecia) in comparison with aged or younger patients. However, seven patients, all belonging to the *middle-aged group*, went off-study for toxicity (diarrhoea, six cases; severe bone marrow suppression, one case). Treatment-induced or treatment-exacerbated early death (as defined by Rothemberg *et al*, 2001) occurred in three of 118 (2.5%) patients: a 62-year-old woman, completely asymptomatic at study entry), died of severe diarrhoea and dehydration after two courses; another woman, aged 63 years, and with initial PS = 1, suffered from deep phlebitis with subsequent pulmonary embolism and acute cardiac failure after three cycles; and a 69-year-old man, entered into the study in good PS and no cardiac contraindications, had a fatal myocardial infarction after three cycles.

Table 4 Severe (WHO grade ⩾3) toxicity according to age grouping

	Age groups (years)		
Toxicity WHO grade ⩾3	**⩽54 n=37**	**55–69 n=64**	**⩾70 n=17**
Neutropenia	43	41	31
Anaemia	0	2	6
Thrombocytopenia	0	3	6
Neutropenic fever/infection	5	3	0
Diarrhoea	11	18	6
Stomatitis	3	2	6
Nausea/vomiting	5	0	6
Alopecia	51	36	12
Hepatic	0	2	0
Cholinergic syndrome	2	1	
Any type (except for alopecia)	68	70	50

Numbers are percent of patients.

Activity

As already reported, the IRIFAFU regimen produced nine complete plus 33 partial responses, for an overall response rate (RR) of 36% (95% confidence interval, 28–44%), according to intent-to-treat analysis. In addition, 12 patients showed a tumour shrinkage that did not qualify for a major response. RR was comparable in all age groups: it was 38% in the younger, 34% in the middle-aged, and 35% in the elderly patients. Similarly, no statistically significant difference in RR was observed according to gender (males, 36%; females, 35%); primary site (colon, 37%; rectum, 36%); previous adjuvant chemotherapy (yes, 41%; no, 34%); onset of metastasis (synchronous, 35%, metachronous, 36%); basal CEA serum level ($<100\,ng\,ml^{-1}$, 36%; $\geqslant 100\,ng\,ml^{-1}$, 40%). Some baseline characteristics, although not reaching a significant *P*-value, seemed affecting more the probability of response. This holds true for number of disease sites (single, 42%; multiple, 27%), performance status (0, 41%; ⩾1, 27%), disease symptoms (absent, 41%; present, 26%), previous loss of body weight (absent, 39%; present, 24%), previous radical surgery (yes, 38%; no, 23%). Keeping these last variables together with the age grouping into a logistic regression analysis, no significant interaction was reported with the activity rate.

Long-term outcome

After a median follow-up of 30 months, 91 (77%) patients had progressed, and 75 (64%) had died. Besides the already mentioned three early deaths, two other patients died for a disease- and treatment-unrelated reason: a 66-year-old man committed suicide after 4 months from initial treatment, and a 36-year-old patient affected by insulin-dependent diabetes died of uncontrolled metabolic coma after 3 months from the start of therapy. Median PFS was 7.4, 8.0, and 5.3 months, for younger, middle-aged and elderly patients (log-rank test not significant also when adjusted by gender). In the multivariate analysis, taking into account all pretreatment characteristics, the presence of disease-related symptoms was the only variable significantly associated with a shorter PFS ($P=0.053$), while age group was of borderline significance ($P=0.099$). Survival, which at the Cox analysis resulted significantly affected by number of disease sites and previous loss of body weight, was unrelated to the age of patients: indeed, median OS was 13.4, 15.3, and 13.9 months, respectively, for the three age groups.

DISCUSSION

In this paper, we have retrospectively reported on a series of patients affected by advanced colorectal carcinoma, randomly allocated to receive the IRIFAFU regimen, with the aim to ascertain whether the safety and activity of this regimen could have been affected by the age of patients. For this purpose, patients were divided in three age groups. Apart from sex, other baseline characteristics were evenly distributed across the three groups.

Considering the occurrence of treatment-related adverse events, as registered by the investigators, it appeared that severe toxicity was not greater in elderly as compared with other patients. An usually uncomplicated neutropenia affected a similar proportion of patients, regardless of age. Occurrence of severe diarrhoea was even lower among elderly patients. On the whole, a smaller proportion of elderly patients suffered from any type of severe toxicity. However, delays or dose reductions were applied during the initial treatment more frequently for elderly than for remaining patients. This apparent discrepancy may be explained by an earlier onset of side effects in elderly patients. Indeed, dose intensity over eight cycles was not different across the age groups, which is an indirect evidence that, with a cautious and tailored approach, our regimen was feasible also in elderly patients.

As for treatment discontinuation, it is worth noting that no young patient refused the study treatment, in contrast with four patients each in the two other groups. This observation may suggest that, despite toxicity was not more pronounced among these patients, the subjective perception of treatment-related physical and/or psychological distress was in these cases no longer tolerable. At this proposal, we would remember that a mental depression, which is a common psychiatric syndrome in elderly subjects, may be even more frequent in cancer patients. The presence and severity of this syndrome, when not sought and properly managed by the attending physicians, may adversely affect the compliance of patients to the anticancer treatment.

Although the results reported here were generated by a retrospective analysis, which was not powered to reveal significant differences according to age of patients, we believe meaningful that the proportion of responders was similar in all age groups. In addition, while a slightly poorer median PFS was registered for elderly, no difference at all in OS was noted for these patients as compared to middle-aged and younger ones. In this respect, a careful check for the presence of disease-related symptoms, or for a recent loss of body weight, together with an appropriate assessment of disease extent, showed a greater prognostic significance than the ECOG PS score.

Of course, this basically descriptive analysis cannot permit to draw firm conclusions, but it could help in generating hypotheses for future studies, in which the clinical benefit for elderly patients should be prospectively outweighed against the occurrence of side effects. Indeed, we have to admit that patients aged ⩾70 years were under-represented also in our trial. Although we may confirm that all eligible patients were offered to entry into this study, we cannot exclude a systematic selection bias, due to some reluctance of attending caregivers in referring elderly patients to cancer centres, or because of a poor willingness of patients themselves to take part in a randomised trial, or to undergo chemotherapy at all.

Moreover, in our case series no information was collected about the number and types of associated diseases, which may adversely affect the long-term outcome of patients (Extermann *et al*, 1998; Yancik *et al*, 1998). This was mainly due to the lack of a standard scoring system for co-morbidities in cancer patients (Repetto *et al*, 2002). Furthermore, a comprehensive geriatric assessment, including an evaluation of functional, cognitive and psychological status, has been strongly recommended for aged patients, in order to anticipate the acceptance and tolerability of a cytotoxic treatment (Balducci and Yates, 2000; Kearney *et al*, 2000; Köhne *et al*, 2001).

In conclusion, we suggest that geriatrics and medical oncologists should tightly cooperate in carefully evaluating elderly colon cancer patients, in order to identify those who may benefit from irinotecan plus FU combinations, and excluding patients with

medical contraindications, or with an impairment of their physical, cognitive and/or psychological status. Furthermore, we strongly recommend the implementation of prospective trials to assess properly the quality of life of elderly patients undergoing chemotherapy. In this way, it could be possible to counteract an unjustified 'ageism', a prejudice that denies opportunities of treatment or even cure for patients that, as far as we know, may have the same chance as younger people (Potosky *et al*, 2002). Apart from the obvious ethical and juridical implications of such a negative attitude, we would remember that a recent economic evaluation of healthcare intervention has quantified an additional yearly cost of about $1200 for elderly cancer patients receiving specific treatments (Hayman *et al*, 2001). In our opinion, this extra expense is by far included in the costs that a developed country can effort to manage these individuals.

ACKNOWLEDGEMENTS

We thank Dr Maurizio Montella and Dr Anna Crispo (Unit of Epidemiology and Biostatistics, National Tumour Institute, Naples, Italy) for their assistance in data management and statistical analysis of this study.

REFERENCES

Balducci L, Yates J (2000) General guidelines for the management of older patients with cancer. *Oncology (Huntington)* **14:** 221 – 227

Buroker TR, O'Connel MJ, Wieand HS, Krook JE, Gerstner JB, Mailliard JA, Schaefer PL, Levitt R, Kardinal CG, Gesme DH (1994) Randomized comparison of two schedules of fluorouracil and leucovorin in the treatment of advanced colorectal cancer. *J Clin Oncol* **12:** 14 – 20

Chiara S, Nobile MT, Vincenti M, Lionetto R, Gozza A, Barzacchi MG, Sanguineti O, Repetto L, Rosso R (1998) Advanced colorectal cancer in the elderly: results of consecutive trials with 5-fluorouracil-based chemotherapy. *Cancer Chemother Pharmacol* **42:** 336 – 340

Colorectal Cancer Collaborative Group (2000) Palliative chemotherapy for advanced colorectal cancer: systematic review and meta-analysis. *BMJ* **321:** 531 – 535

Comella P, De Vita F, Mancarella S, De Lucia L, Biglietto M, Casaretti R, Farris A, Iannello GP, Lorusso V, Avallone A, Carteni G, Leo S, Catalano G, De Lena M, Comella G (2000) Biweekly irinotecan or raltitrexed plus 6S-leucovorin and bolus 5-fluorouracil in advanced colorectal carcinoma. A Southern Italy Cooperative Oncology Group phase II/III randomized trial. *Ann Oncol* **11:** 1323 – 1333

Comella P, Crucitta E, De Vita F, De Lucia L, Farris A, Del Gaizo F, Palmeri S, Iannelli A, Mancarella S, Tafuto S, Maiorino L, Buzzi F, De Cataldis G (2002) Addition of either irinotecan or methotrexate to bolus fluorouracil and high-dose leucovorin every two weeks in advanced colorectal carcinoma: a randomized study of the Southern Italy Cooperative Oncology Group. *Ann Oncol* **13:** 866 – 873

Cox DR (1972) Regression models and life tables. *J Roy Stat Assoc* **34:** 187 – 220

Daniele B, Simmonds PD, Best LY, Ross PJ, Cunningham D (1999) Should chemotherapy be used as a treatment of advanced colorectal carcinoma (ACC) in patients over 70 years of age? *Eur J Cancer* **35:** 1640 – 1649

de Gramont A, Figer A, Seymour M, Homerin M, Hmissi A, Cassidy J, Boni C, Cortes-Funes H, Cervantes A, Freyer G, Papamichael D, Le Bail N, Louvet C, Hendler D, de Braud F, Wilson C, Morvan F, Bonetti A (2000) Leucovorin and fluorouracil with or without oxaliplatin as first-line treatment in advanced colorectal cancer. *J Clin Oncol* **18:** 2938 – 2947

Douillard JY, Cunningham D, Roth AD, Navarro M, James RD, Karasek P, Jandik P, Iveson T, Carmichael J, Alaki M, Gruia G, Awad L, Rougier P (2000) Irinotecan combined with fluorouracil compared with fluorouracil alone as first-line treatment for metastatic colorectal cancer. *A multicentre randomised trial. Lancet* **355:** 1041 – 1047

Extermann M, Overcash J, Lyman GH, Parr J, Balducci L (1998) Comorbidity and functional status are independent in older cancer patients. *J Clin Oncol* **16:** 1582 – 1587

Hayman J, Langa KM, Kabeto MU, Katz SJ, DeMonner SM, Chernew ME, Slavin MB, Fendrick AM (2001) Estimating the cost of informal caregiving for elderly patients with cancer. *J Clin Oncol* **19:** 3219 – 3225

Hutchins LF, Unger JM, Crowley JJ, Coltman CA, Albain KS (1999) Underrepresentation of patients 64 years of age or older in cancer-treatment trials. *N Engl J Med* **341:** 2061 – 2067

International Multicenter Pooled Analysis of B2 Colon Cancer Trials (1999) Efficacy of adjuvant fluorouracil and folinic acid in B2 colon cancer. *J Clin Oncol* **17:** 1356 – 1363

Kaplan EL, Meier P (1958) Non-parametric estimation from incomplete observations. *J Am Stat Assoc* **53:** 457 – 481

Kearney N, Miller M, Paul J, Smith K (2000) Oncology healthcare professionals' attitude towards elderly people. *Ann Oncol* **11:** 599 – 601

Köhne CH, Grothey A, Bokemeyer C, Bontke N, Aapro M (2001) Chemotherapy in elderly patients with colorectal cancer. *Ann Oncol* **12:** 435 – 442

Mamounas E, Wieand S, Wolmark N, Bear HD, Atkins JN, Song K, Jones J, Rockette H (1999) Comparative efficacy of adjuvant chemotherapy in patients with Dukes' B versus Dukes' C colon cancer: results from four National Surgical Adjuvant Breast and Bowel Project adjuvant studies (C-01, C-02, C-03, and C-04). *J Clin Oncol* **17:** 1349 – 1355

Miller AB, Hoogstraten B, Staquet M, Winkler V (1981) Reporting results of cancer treatment. *Cancer* **47:** 207 – 214

Peto R, Pike C, Armitage P, Breslow NE, Cox DR, Howard SV, Mantel N, McPherson K, Peto J, Smith PG (1977) Design and analysis of randomised clinical trials requiring prolonged observation on each patient. *Br J Cancer* **35:** 1 – 39

Popescu RA, Norman A, Ross PJ, Parikh B, Cunningham D (1999) Adjuvant or palliative chemotherapy for colorectal cancer in patients 70 years or older. *J Clin Oncol* **17:** 2412 – 2418

Potosky AL, Harlan LC, Kaplan RS, Johnson KA, Lynch CF (2002) Age, sex, and racial differences in the use of standard adjuvant therapy for colorectal cancer. *J Clin Oncol* **20:** 1192 – 1202

Repetto L, Fratino L, Audisio RA, Venturino A, Gianni W, Vercelli M, Parodi S, Dal Lago D, Gioia F, Monfardini S, Aapro MS, Serraino D, Zagonel V (2002) Comprehensive geriatric assessment adds information to Eastern Cooperative Oncology Group Performance Status in elderly cancer patients: an Italian Group for Geriatric Oncology study. *J Clin Oncol* **20:** 494 – 502

Rothemberg ML, Meropol NJ, Poplin EA, Van Cutsem E, Wadler S (2001) Mortality associated with irinotecan plus bolus fluorouracil/leucovorin: summary findings of an independent panel. *J Clin Oncol* **19:** 3801 – 3807

Saltz LB, Cox JV, Blanke C, Rosen LS, Fehrenbacher L, Moore MJ, Maroun JA, Ackland SP, Locker PK, Pirotta N, Elfring JL, Miller LL (2000) Irinotecan plus fluorouracil and leucovorin for metastatic colorectal cancer. *N Engl J Med* **343:** 905 – 914

Sargent DJ, Goldberg RM, Jacobson SD, MacDonald JC, Labianca R, Haller DG, Shepherd LE, Seitz JF, Francini G (2001a) A pooled analysis of adjuvant chemotherapy for resected colon cancer in elderly patients. *N Engl J Med* **345:** 1091 – 1097

Sargent DJ, Niedzwiecki D, O'Connel MJ, Schilsky RL (2001b) Recommendation for caution with irinotecan, fluorouracil, and leucovorin for colorectal cancer. *N Engl J Med* **345:** 144 – 145

Sundararajan V, Mitra N, Jacobson JS, Grann VR, Heitjan DF, Neugut AI (2002) Survival associated with 5-fluorouracil-based adjuvant chemotherapy among elderly patients with node-positive colon cancer. *Ann Intern Med* **136:** 349 – 357

Wolmark N, Rockette H, Mamounas E, Jones J, Wieand S, Wickerham DL, Bear HD, Atkins JN, Dimitrov NV, Glass AG, Fisher ER, Fisher B (1999) Clinical trial to assess the relative efficacy of fluorouracil and leucovorin, fluorouracil and levamisole, and fluorouracil, leucovorin, and levamisole in patients with Dukes' B and C carcinoma of the colon: results from National Surgical Adjuvant Breast and Bowel Project C-04. *J Clin Oncol* Nov; **17(11):** 3553 – 3559

Yancik R, Ganz PA, Varricchio CG, Conley B (2001) Perspectives on comorbidity and cancer in older patients: Approaches to expand the knowledge base. *J Clin Oncol* **19:** 1147 – 1151

Yancik R, Wesley MN, Ries LA, Havlik RJ, Long S, Edwards BK, Yates JW (1998) Comorbidity and age as predictors of risk for early mortality of male and female colon carcinoma patients: A population-based study. *Cancer* **82:** 2123 – 2134

Zanetti R, Crosignani P, Rosso S, Vigane C (1997) *Cancer in Italy: Incidence data from Cancer Registries. Vol. 2, 1988 – 1992.* Roma: Il Pensiero Scientifico Editore

CANCER RESEARCH

Clinical Trials

Abstract CT154: Multicenter open-label, phase II trial, to evaluate the efficacy and safety of liposomal irinotecan (nal-IRI) for progressing brain metastases in patients with HER2-negative breast cancer (The Phenomenal Study)

Javier Cortés, David Paez, José Manuel Pérez García, Salvador Blanch Tormo, Kepa Amillano Parraga, Manuel Ruiz Borrego, Antonio Antón Torres, María Fernández, Emilio Alba Conejo, Miguel Ángel Seguí Palmer, Joan Dorca Ribugent, Rafael López López, Mireia Margelí Vila, Elena Aguirre, and Antonio Llombart

DOI: 10.1158/1538-7445.AM2018-CT154 Published July 2018

Proceedings: AACR Annual Meeting 2018; April 14-18, 2018; Chicago, IL

Abstract

Background: HER2-negative metastatic breast cancer (MBC) patients with central nervous system (CNS) involvement previously treated with a local therapy had very few possibilities of disease response with conventional systemic treatments. Liposomal irinotecan (nal-IRI) is a novel formulation of irinotecan. It has shown promising activity in patients with CNS involvement. The aim of this trial is to evaluate the efficacy of nal-IRI as single agent in HER2-negative MBC patients with CNS progression following local treatment with surgery, stereotactic radiosurgery or whole-brain radiotherapy.

Trial design: This is an open label, non-randomized, multicenter two-stage phase IIA clinical trial. Patients will receive intravenous nal-IRI in a fixed dose of 60 mg/m^2 expressed as irinotecan hydrochloride trihydrate salt on day 1 of a 14-day cycle until progression or unacceptable toxicity. The principal selection criteria are: (1) HER2-negative inoperable MBC with CNS involvement; (2) prior local treatment with surgery, stereotactic radiosurgery or whole-brain radiotherapy; (3) prior treatment with taxanes; (4) at least one measurable brain lesion according to RECIST v1.1 criteria. The primary objective is to evaluate the efficacy of nal-IRI monotherapy. Primary endpoint is the CNS overall response rate (ORR), defined as the percentage of patients who experienced complete (CR) and partial response (PR) (as best response). It will be assessed in accordance with the Response Assessment in Neuro-Oncology Brain Metastases (RANO-BM) criteria. The trial uses a Simon's minimax two-stage design. We hypothesized that excluding a CNS ORR ≤5% while targeting an improvement of the CNS ORR to ≥15% would be an optimal approach for evaluating the study strategy. At least 2 responders among 23 patients will be necessary to proceed to the second stage. At the study end, ≥6 responders out of 56 evaluable subjects are required to justify this strategy in further clinical trials. Considering a drop-out rate of 10%, a sample size of 63 patients will be needed to attain 80% power at nominal level of one-sided alpha of 0.05. The secondary objectives include safety-related outcomes and efficacy measures: CNS clinical benefit rate (CR, PR and stable disease [SD] ≥12 weeks), ORR according to a CNS volumetric parameter (CR, PR and >65% reduction of CNS lesion), clinical benefit rate (CR, PR and SD ≥24 weeks), progression-free survival and overall survival. **Trial registration**: NCT03328884. **Date of registration**: November 1st, 2017. **First patient included**: July, 05th 2017.

Citation Format: Javier Cortés, David Paez, José Manuel Pérez García, Salvador Blanch Tormo, Kepa Amillano Parraga, Manuel Ruiz Borrego, Antonio Antón Torres, María Fernández, Emilio Alba Conejo, Miguel Ángel Seguí Palmer, Joan Dorca Ribugent, Rafael López López, Mireia Margelí Vila, Elena Aguirre, Antonio Llombart. Multicenter open-label, phase II trial, to evaluate the efficacy and safety of liposomal irinotecan (nal-IRI) for progressing brain metastases in patients with HER2-negative breast cancer (The Phenomenal Study) [abstract]. In: Proceedings of the American Association for Cancer Research Annual Meeting 2018; 2018 Apr 14-18; Chicago, IL. Philadelphia (PA): AACR; Cancer Res 2018;78(13 Suppl):Abstract nr CT154.

Previous

Cancer Research Online ISSN: 1538-7445
Cancer Research Print ISSN: 0008-5472
Journal of Cancer Research ISSN: 0099-7013
American Journal of Cancer ISSN: 0099-7374

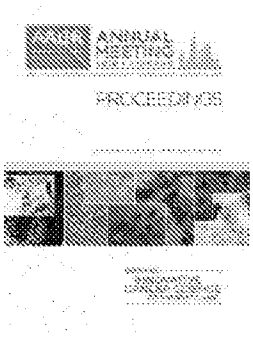

July 2018
Volume 78, Issue 13 Supplement
Table of Contents

Biochimica et Biophysica Acta, 1024 (1990) 352–366
Elsevier

BBAMEM 74883

Endocytosis of liposomes by macrophages: binding, acidification and leakage of liposomes monitored by a new fluorescence assay

David L. Daleke [1,*], Keelung Hong [1] and Demetrios Papahadjopoulos [1,2]

[1] *Cancer Research Institute and* [2] *Department of Pharmacology, University of California, San Francisco, CA (U.S.A.)*

(Received 18 October 1989)
(Revised manuscript received 25 January 1990)

Key words: Endocytosis; Macrophage; Liposome; pH; Drug delivery

The interaction of liposomes with macrophage cells was monitored by a new fluorescence method (Hong, K., Straubinger, R.M. and Papahadjopoulos, D., J. Cell Biol. 103 (1986) 56a) that allows for the simultaneous monitoring of binding, endocytosis, acidification and leakage. Profound differences in uptake, cell surface-induced leakage and leakage subsequent to endocytosis were measured in liposomes of varying composition. Pyranine (1-hydroxypyrene-3,6,8-trisulfonic acid, HPTS), a highly fluorescent, water-soluble, pH sensitive dye, was encapsulated at high concentration into the lumen of large unilamellar vesicles. HPTS exhibits two major fluorescence excitation maxima (403 and 450 nm) which have a complementary pH dependence in the range 5–9: the peak at 403 nm is maximal at low pH values while the peak at 450 nm is maximal at high pH values. The intra- and extracellular distribution of liposomes and their approximate pH was observed by fluorescence microscopy using appropriate excitation and barrier filters. The uptake of liposomal contents by cells and their subsequent exposure to acidified endosomes or secondary lysosomes was monitored by spectrofluorometry via alterations in the fluorescence excitation maxima. The concentration of dye associated with cells was determined by measuring fluorescence at a pH independent point (413 nm). The average pH of cell-associated dye was determined by normalizing peak fluorescene intensities (403 nm and 450 nm) to fluorescence at 413 nm and comparing these ratios to a standard curve. HPTS-containing liposomes bound to and were acidified by a cultured murine macrophage cell line (J774) with a $t_{1/2}$ of 15–20 min. The acidification of liposomes exhibited biphasic kinetics and 50–80% of the liposomes reached an average pH lower than 6 within 2 h. A liposomal lipid marker exhibited a rate of uptake similar to HPTS, however the lipid component selectively accumulated in the cell; after an initial rapid release of liposome contents, 2.5-fold more lipid marker than liposomal contents remained associated with the cells after 5 h. Coating haptenated liposomes with antibody protected liposomes from the initial release. The leakage of liposomal contents was monitored by co-encapsulating HPTS and *p*-xylene-bis-pyridinium bromide, a fluorescence quencher, into liposomes. The time course of dilution of liposome contents, detected as an increase in HPTS fluorescence, was coincident with the acidification of HPTS. The rate and extent of uptake of neutral and negatively charged liposomes was similar; however, liposomes opsonized with antibody were incorporated at a higher rate (2.9-fold) and to a greater extent (3.4-fold). In addition, the rate and extent of incorporation of liposome encapsulated HPTS was dependent on temperature and the metabolic state of the cell, consistent with uptake of liposomes by endocytosis. The use of HPTS allowed accurate and simultaneous quantitation of liposome uptake, acidification, cell-induced leakage of liposomes, and regurgitation of liposome contents. In addition to cell-surface induced leakage, liposomes leaked extensively during endocytosis coincident with acidification; half of the cell-induced dilution of liposome contents was accounted for by leakage at the cell surface, while the remainder occurred coincident with acidification. Liposome contents labeled the aqueous space of endosomes and lysosomes and were regurgitated rapidly as liposomal lipid accumulated selectively. Opsonization of liposomes, to induce Fc-mediated endocytosis, afforded protection to the initial dilution of liposome contents, but not the rate of leakage, after endocytosis. Implications of these studies for the use of liposomes as drug delivery vehicles are discussed.

Abbreviations: HPTS, 1-hydroxypyrene-3,6,8-trisulfonic acid; PC, egg phosphatidylcholine; PS, bovine brain phosphatidylserine; [^{3}H]DPPC, di-[9,10-^{3}H]palmitoylphosphatidylcholine; DNP-PE, *N*-dinitrophenyl phosphatidylethanolamine; DPX, *p*-xylene-bis-pyridinium bromide; DMEM, Dulbecco's modified Eagle's medium; EDTA, ethylenediaminetetraacetic acid; FD, fluorescein isothiocyanate conjugated dextran; Hepes, *N*-2-hydroxyethylpiperazine-*N'*-2-ethanesulfonic acid; λ_{ex}, excitation wavelength; λ_{em}, emission wavelength.

* Correspondence: D.L. Daleke (present address): Department of Chemistry, Indiana University, Bloomington, IN 47405, U.S.A.

Introduction

The endocytotic capabilities of macrophages have been exploited in the design of systems for the enhanced delivery of drugs, activating agents, and antigens. Liposomes provide an ideal vehicle for the delivery of macromolecules to macrophages. Once injected into the circulatory system, liposomes are removed rapidly by macrophages of the reticuloendothelial system [1–3] resulting in specific, passive delivery of liposomes and their contents. Liposome encapsulated macrophage activating agents such as *N*-acetyl-muramyl-L-alanyl-D-isoglutamine (muramyl dipeptide) and a lipophilic derivative of muramyl dipeptide induce significant tumoricidal activity in vitro [4] or in vivo [5–7]. Other lymphokines encapsulated in liposomes similarly induce an in vivo tumoricidal response [8]. Antibiotics encapsulated in liposomes are more effective than unecapsulated drug in the treatment of several intracellular infections of macrophages [9–11]. Finally, liposomes are effective adjuvants for vaccine production [12,13].

The use of liposomes as a delivery system offers several advantages over unencapsulated compounds. Liposomes act as a depot, increasing the effective time of administration of drugs [14,15] and reducing nonspecific toxicity [10,11,16–18]. Encapsulation of labile compounds in liposomes offers protection against their clearance from the bloodstream or degradation before delivery to the target site. Furthermore, by conjugation to appropriate ligands, liposomes can be targeted to specific cells [19–22].

However, the general use of liposomes as a drug delivery system has been hindered by several problems. Among these are leakage of liposomal contents mediated by serum proteins [2,23–26] and cells [27–29], slow extravisation of liposomes from the bloodstream to target cells [30,31] and, if the target cells are not macrophages, clearance of liposomes from the vasculature by cells of the reticuloendothelial system [1–3]. Some of these problems may be circumvented by utilizing the natural targeting to cells of the reticuloendothelial system [5,32] or by developing liposomes which avoid uptake by macrophages [33–35]. Nonetheless, clearance of liposomes from the vasculature by macrophages of the reticuloendothelial system remains a major factor affecting their in vivo disposition to various tissues. A further understanding of the mechanisms by which macrophages recognize and incorporate liposomes and a simple method to measure liposome-cell interactions will aid in the design of liposomes for in vivo delivery.

Previous work has shown that the primary mode by which liposomes are incorporated into cells is endocytosis [36,37] via the coated pit pathway [37]. Once endocytosed, liposomes come in contact with low pH compartments [37] within the cell, presumably endosomes and lysosomes [38,39]. The location of liposomes within cells and the kinetics of liposome uptake are difficult to measure accurately. Commonly used pH-dependent fluorescent probes in the study of liposome-cell interactions are membrane permeant (carboxyfluorescein, [37]), are quenched at low pH, precluding direct pH measurement (fluorescein and calcein, [40]), or have a pH dependence outside the physiological range [41].

Recently an assay utilizing the fluorophore pyranine (1-hydroxypyrene-3,6,8-trisulfonic acid, HPTS), has been developed to accurately measure the pH of liposomes endocytosed by CV-1 fibroblasts [42,43]. HPTS is a highly water-soluble, pH-dependent fluorophore with properties well suited to pH measurement. The fluorophore is readily encapsulated in liposomes, is non-permeant, and responds to intraliposomal changes in pH [44–46]. The excitation spectrum of HPTS exhibits two major peaks, one which is maximal at low pH (403 nm) and one which is maximal at high pH (450 nm), as observed at its broad emission maximum centered at 510 nm. A pH-independent isosbestic point at 413 nm permits the normalization of fluorescence intensities to the total amount of HPTS.

The use of HPTS has made it possible to simultaneously and directly measure liposome binding, leakage of liposomes induced by cells, the average pH of endocytosed liposomes, and, by fluorescence microscopy, the intracellular location of the dye. In combination with a fluorescence quenching agent, liposome-encapsulated HPTS is used to monitor the leakage of liposome contents within endosomal compartments. This fluorophore uniquely provides simultaneous quantitation of parameters associated with the endocytosis of liposomes.

Materials and Methods

Materials. Egg phosphatidylcholine (PC), bovine brain phosphatidylserine (PS), and *N*-dinitrophenyl-phosphatidylethanolamine (DNP-PE) were purchased from Avanti Polar Lipids. Fluorescein isothiocyanate dextran (FD, mol. wt. 20000) and cholesterol were obtained from Sigma Chemical Co. Cholesterol was recrystalized once from methanol before use. 1-Hydroxypyrene-3,6,8-trisulfonic acid (trisodium salt, HPTS) and *p*-xylene-bis-pyridinium bromide (DPX) were obtained from Molecular Probes. [^{3}H]Dipalmitoylphosphatidylcholine ([^{3}H]DPPC, approx. 5 Ci $\cdot$ μmol^{-1}) was obtained from Amersham Corp., and purified (> 98%) by CM-52 cellulose chromatography [47]. Anti-dinitrophenol antibody was kindly provided by Dr. T. Heath. Protein concentration was determined by the method of Lowry et al. [48]. The scintillation cocktail Liquiscint was obtained from National Diagnostics. All other chemicals were reagent grade.

Cell culture. The macrophage-like cell lines J774, RAW 264.7, and P388D1 were maintained in mono-

layer culture in Dulbecco's modified Eagle's medium supplemented with 3 $g \cdot l^{-1}$ glucose and 10% calf serum (DMEM) and incubated under 7% humidified CO_2. Cells were plated at a concentration of 10^6 cells per 9.6 cm^2 plastic culture dish 24 h prior to use.

Liposome preparation. Lipid mixtures (PC/cholesterol (3 : 1); PC/PS/cholesterol (2 : 1 : 1), PC/PS/DNP-PE/cholesterol (2 : 1 : 0.04 : 1), in some experiments containing [^{3}H]DPPC (1.9 $\mu Ci \cdot \mu mol^{-1}$ lipid)) were prepared in chloroform and the solvent was removed under reduced pressure. Solutions of HPTS (35 mM) in 2.5 mM Hepes, 75 mM NaCl, 50 μM EDTA (pH 7.4) or HPTS (35 mM) + DPX (50 mM) in 2.5 mM Hepes, 50 μM EDTA (pH 7.4; adjusted to approx. 300 mOsm with 1 M NaCl) were added and liposomes were prepared by the reverse-phase evaporation procedure [49]. Liposomes were extruded through 0.4 μm, then 0.2 μm polycarbonate filters [50] and unencapsulated material was separated from liposomes by gel filtration on a Sephadex G-75 column (1 × 15 cm) equilibrated with 5 mM Hepes, 150 mM NaCl, pH 7.4 (HBS). Phospholipid concentration was determined by the method of Bartlett [51]. The liposomes averaged 165 nm in diameter as measured by laser light scattering and entrapped an aqueous volume of 2.9 $\mu l \cdot \mu mol^{-1}$ lipid. The liposomes were 44% unilamellar and 56% bilamellar as calculated from the measured trapped volume and theoretical trapped volumes of 165 nm diameter, uni- and bi-lamellar liposomes (4.3 $\mu l \cdot \mu mol^{-1}$ lipid and 1.88 $\mu l \cdot \mu mol^{-1}$ lipid, respectively). This corresponded to $1.6 \cdot 10^9$ liposomes $\cdot$ $nmol^{-1}$ phospholipid.

Multilamellar liposomes were used for the calibration of quenching by DPX. Solutions of HPTS (35 mM) with increasing DPX concentration (0–50 mM) were constructed by mixing appropriate volumes of the HPTS and the HPTS/DPX solutions described above. In addition, solutions of decreasing HPTS/DPX concentration were made by diluting the HPTS (35 mM) + DPX (50 mM) solution with HBS. Lipid mixtures (PC/cholesterol, 3 : 1) were prepared as described above. The HPTS/DPX solutions were added, vortexed for 5 min and extruded three times through a 0.2 μm polycarbonate filter. Unencapsulated material was separated from liposomes by gel filtration as described above.

Liposome-cell incubations. DMEM was removed from cells and the cells were washed twice with 2 ml 137 mM NaCl, 2.7 mM KCl, 1.5 mM KH_2PO_4, 8.1 mM Na_2HPO_4, pH 7.4 (PBS) supplemented with 0.4 mM calcium, 0.4 mM magnesium, and 5 mM glucose (PBS-CMG). Liposomes were diluted to 80 μM phospholipid in PBS-CMG and 0.5 ml was added to each culture dish (approx. $(2–3) \cdot 10^6$ cells). In experiments with HPTS/DPX liposomes, 1 ml of 100 μM phospholipid was added to each culture dish. In experiments with DNP-PE-containing liposomes, anti-DNP antibody was diluted to a final concentration of 50 nM in the liposome suspension. Cells were incubated with liposomes at 37°C in a humidified incubator or on ice. To effect energy depletion, cells were incubated with NaN_3 (5 mM) + deoxyglucose (50 mM) in PBS-CM for 30 min at 37°C prior to exposure to liposomes.

Fluorescence microscopy. After incubation with HPTS-containing liposomes, cells were washed twice with 2 ml PBS-CMG and viewed in PBS-CMG with a Leitz fluorescence microscope equipped with epifluorescence, a Zeiss 25 × phase contrast water immersion objective, and a Nikon camera with an automatic exposure meter. Cells were viewed by phase contrast or epifluorescence with two excitation filter sets; either with a set that produces excitation in the range 350–410 nm, and allows observation of fluorescence emission above 455 nm with a long wave pass dichroic mirror and barrier filter, or with a set that produces excitation in the range 450–490 nm, and allows observation of fluorescence emission at wavelengths greater than 515 nm with a long wave pass dichroic mirror and barrier filter. Fluorescence micrographs were automatically corrected for intensity with an exposure meter. Exposure times were typically 1 s for phase contrast, 1 min for λ_{ex} 350–410 nm fluorescence, and 5 min for λ_{ex} 450–490 nm fluorescence.

Fluorometry. After incubation with liposomes for various times, cells were washed twice with PBS-CMG and incubated for 5 min at 37°C with 1.5 ml PBS containing 3 mM EDTA. Cells were dislodged and diluted to $(2.5–5) \cdot 10^5$ cells/ml in PBS. Corrected fluorescence excitation spectra (λ_{ex} 395–465 nm, 1.8 nm bandwidth) were measured at 510 nm emission with a wide (4.5 nm) emission bandwidth using a SPEX Fluorolog 2 fluorometer outfitted with a stirred, temperature controlled cuvette (20°C). For calibration of HPTS quenching by DPX as described above, liposomes were diluted to 5 μM in PBS, and fluorescence was measured as described above. In some experiments, Triton X-100 (0.1%) was added and fluorescence was remeasured after 1 min. Spectra were smoothed using a 13 point smoothing routine [52], peak heights (λ_{ex} 403, 413, 450 nm) were measured and the fluorescence excitation ratios 403/413 nm and 450/413 nm were calculated. Fluorescence units are expressed as photon counts per second per 10^6 cells.

Pinocytosis of fluorescein dextran and free HPTS. DMEM was removed from cells, replaced with media containing 0.1 $mg \cdot ml^{-1}$ FD or 100 μM HPTS and cells were incubated for 24 h at 37°C. HPTS-treated cells were washed with PBS-CMG, resupplied with fresh media and incubated for 5 h at 37°C. Cells were washed with PBS-CMG, dislodged as described above, counted, and resuspended in PBS ($(2.5–5) \cdot 10^5$ cells/ml). HPTS fluorescence was measured as described above. Fluorescence excitation spectra (λ_{ex} 425–500 nm) of FD treated cells were obtained at λ_{em} 520 nm and the pH-depen-

dent fluorescence ratio λ_{ex} 495/450 was calculated [39]. Average pH values were calculated from standard curves of HPTS or FD generated from solubilized (0.1% Triton X-100) samples.

Scintillation counting. Samples were prepared for scintillation counting by dissolving in Liquiscint scintillation fluid and radioactivity was measured in a Beckman LS-3801 scintillation counter. The number of liposomes associated with cells was calculated from the specific activity of liposomal lipid (3.8 Ci [^{3}H]DPPC/mol phospholipid) and the number of liposomes per mole of phospholipid ($1.6 \cdot 10^9$ liposomes/nmol phospholipid).

Results

Properties of HPTS in relation to endocytosis

When incubated with cells, liposomes bind to the plasma membrane and, depending on the cell type and liposome composition, a portion is taken up into the cell where the local pH within endosomal and lysosomal compartments is expected to be low [36,37,53]. The spectral shifts of HPTS with changes in pH make it a powerful new marker of the fate of liposome contents following endocytosis [42,43]. The excitation spectrum of HPTS measured at λ_{em} 510 nm exhibits two complementary pH-dependent peaks (λ_{ex} 403 nm and 450 nm) and a pH-independent point at λ_{ex} 413 nm that can be used to normalize measurements for changes in dye content (Fig. 1A). The fluorescence excitation ratio 450/413 nm (Fig. 1B, squares) is linear over a greater range of pH and shows a greater magnitude of change in the range pH 6–8 than the 403/413 nm ratio (Fig. 1B, circles). The 450/413 nm ratio becomes insensitive to pH below pH 6.0.

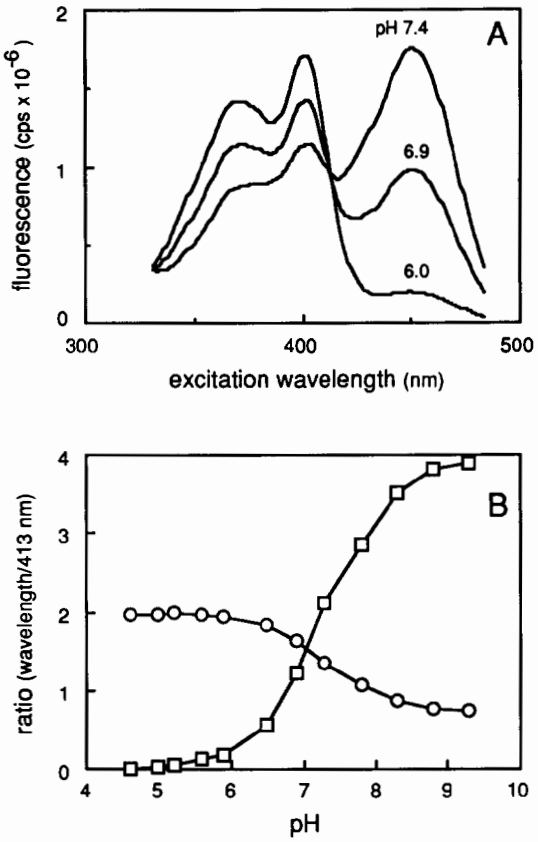

Fig. 1. The pH-dependent properties of HPTS. (A) Excitation spectra of HPTS. HPTS (1 μM) in PBS was adjusted to various pH values (as noted) and excitation spectra (1.8 nm bandwidth) were measured at λ_{em} 510 nm with a 4.5 nm bandwidth. Fluorescence is expressed as photon counts per sec (cps). (B) Fluorescence emission intensities at λ_{ex} 403 nm and λ_{ex} 450 nm normalized to intensity at λ_{ex} 413 nm; 403/413 nm (○), 450/413 nm (□).

Fluorescence microscopy

Fluorescence micrographs of J774 cells treated with HPTS-containing PC/PS/cholesterol liposomes from a typical experiment are shown in Fig. 2. Cells were treated with liposomes for 1 h at 37°C, washed twice in PBS-CMG and were viewed by phase contrast and fluorescence microscopy using λ_{ex} 350–410 nm and λ_{ex} 450–490 nm filters. A phase contrast light micrograph of a typical field of cells is shown in Fig. 2a. When viewed with the λ_{ex} 350–410 nm filter, resulting in excitation of the relatively pH-insensitive region, the cells fluoresce brightly wherever HPTS is located (Fig. 2b). Under excitation with longer wavelengths (λ_{ex} 450–490 nm) the pH-sensitive 450 nm peak is excited, thus fluorescence results only from dye that is at high pH (pH 7.4, Fig. 2c). Therefore, fluorescence apparent under both excitation filters is from HPTS at high pH and fluorescence with the λ_{ex} 350–410 nm filter only is from HPTS at low pH. At early times (1 h), the short λ_{ex} fluorescence (λ_{ex} 350–410 nm, Fig. 2b) is on the cell periphery as well as in punctate intracellular compartments under short wavelength excitation, however the pattern is mostly peripheral under long wavelength illumination (λ_{ex} 450–490 nm, Fig. 2c). At later times (4 h) both the pattern and the intensity of fluorescence changes; the peripheral pattern is diminished and the fluorescence is in perinuclear vacuoles under both short (Fig. 2e) and long (Fig. 2f) wavelength excitation, though the intensity of fluorescence under long wavelength excitation is diminished. The corresponding phase contrast micrograph is shown in Fig. 2d. This indicates that at early times liposomes bind to the cell surface, where they are at a high pH, and with continued incubation they accumulate in low pH intracellular compartments. At all times fluorescence with λ_{ex} 450–490 nm illumination was less intense than with λ_{ex} 350–410 nm; the micrographs in Figs. 2c and 2f were exposed 5 times longer than the micrographs in Figs. 2b and 2e. In separate experiments, the pattern of fluorescence observed after treatment with acridine orange, a lysosomotropic agent [54], is similar to that observed with HPTS

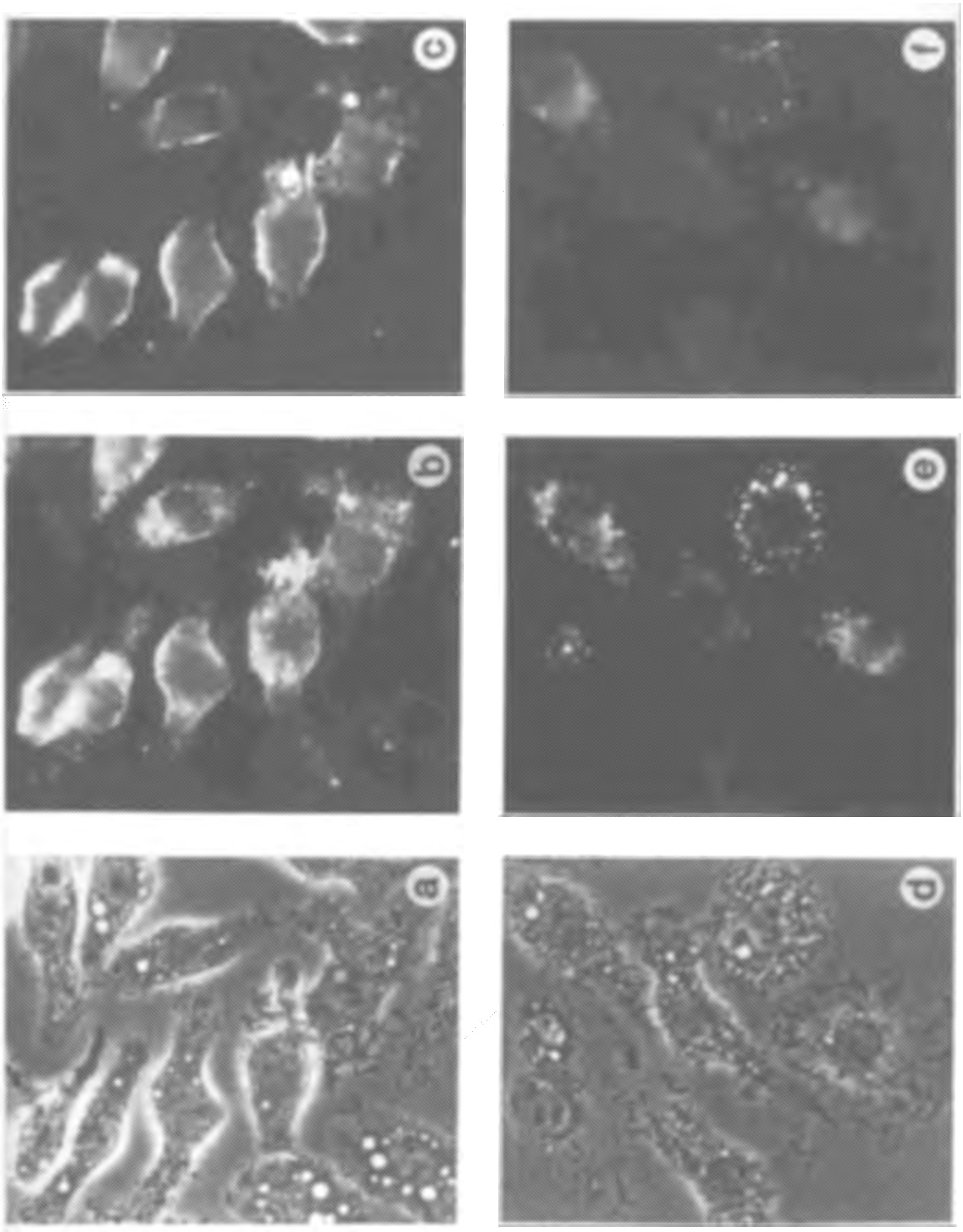

Fig. 2. Fluorescence micrographs of J774 macrophages treated with HPTS-containing PC/PS/cholesterol (2:1:1) liposomes. Cells were treated with liposomes for 1 h (a–c) or for 4 h (d–f) at 37 °C, washed, and viewed with a water immersion objective by: phase contrast (a, d), or epifluorescence with λ_{ex} 350–410 (b, e) or λ_{ex} 450–490 (c, f) filters.

indicating that these probes accumulate in similar intracellular compartments (not shown).

The uptake of liposomes by macrophages is energy- and temperature-dependent. Fluorescence patterns observed after incubating HPTS-containing liposomes with J774 cells subsequent to azide (5 mM) + deoxyglucose (50 mM) pretreatment (30 min) or by incubation at 4°C is peripheral and bright under both excitation filter sets (not shown), indicating that the liposomes are on the cell surface at a high pH.

Quantitation of HPTS incorporation by spectrofluorometry

The fraction of dye taken up by endocytosis can be calculated using the 450/413 nm ratio. Because endosomal and lysosomal compartments are acidic (pH < 6), the measured 450/413 nm ratio will lie between the ratio at pH 7.4 (approx. 2.0) and at pH 6 (approx. 0.2). The pK_a of HPTS varied between 7.0 and 7.5, depending on the presence of protein, detergent, buffer strength and ionic strength of the medium (Table I). Isotonic concentrations of salt slightly increased pK_a, while 15 mM phosphate increased pK_a by half a pH unit. Detergent (0.1% Triton X-100) and protein (0.1% albumin) decreased the pK_a. A decrease in pK_a would cause an increase in the observed 450/413 ratio and result in an apparent increase in pH. Changing salt, buffer, and protein concentrations during endocytosis may alter the apparent pK_a of HPTS. Thus, a direct measure of the lowest 450/413 nm ratio obtainable for HPTS pinocytosed by J774 cells was made. Cells were incubated with free HPTS (100 μM) in DMEM for 24 h at 37°C, washed and reincubated in fresh DMEM for 5 h at 37°C to concentrate HPTS in lysosomal compartments. The 450/413 nm ratio obtained ($ratio_{low}$), 0.5, corresponds to an average pH of 6.5 (Fig. 1B). Other macrophage cell lines yielded lower 450/413 nm ratios of 0.20 (RAW 264.7) and 0.28 (P388D1), corresponding to lower average pH values of 6 (RAW 264.7) and 6.1 (P388D1). Measurements of endosomal/lysosomal pH using pinocytosed FD (Table II) gave similar values for RAW 264.7 cells (5.76 ± 0.13) and P388D1 cells (5.88 ± 0.14), but a lower value for J774 cells (5.59 ± 0.20) compared with HPTS measurements. Some shift in the pK_a of HPTS may have occurred or HPTS may be accumulating in another compartment with a higher pH (see Discussion). The HPTS $ratio_{low}$ for J774 cells was used to calculate the fraction of HPTS endocytosed in liposome experiments:

$$\text{fraction endocytosed} = \frac{(\text{ratio}_{\text{pH 7.4}} - \text{ratio}_{\text{measured}})}{(\text{ratio}_{\text{pH 7.4}} - \text{ratio}_{\text{low}})} \quad (1)$$

where $ratio_{measured}$ is the 450/413 nm ratio of liposome-treated cells and $ratio_{pH\ 7.4}$ is the 450/413 nm ratio of liposomes in PBS.

The uptake of a variety of different liposomes (PS/PC/cholesterol (1 : 2 : 1), PC/cholesterol (3 : 1) or PC/PS/DNP-PE/cholesterol (2 : 1 : 0.04 : 1) liposomes in the presence or absence of anti-DNP antibody) by J774 macrophages was measured during continuous incubation at 37°C. HPTS uptake was measured directly as fluorescence intensity at λ_{ex} 413 nm. The rate and extent of incorporation of HPTS into cells was similar for negative (PS-containing) and neutral (PC) liposomes (Fig. 3A); approx. 0.26 and 0.44%, respectively, of the HPTS dose became associated with the cells within 2 h. Coating DNP-PE-containing liposomes with antibody resulted in an 8-fold increase in the amount of HPTS incorporated and a 5-fold increase in the rate of uptake compared with DNP-PE-containing liposomes not exposed to antibody. HPTS encapsulated in antibody coated liposomes was taken up at a greater rate (2.5-fold) and to a greater extent (4-fold) than in negative (PS-containing) or neutral (PC) liposomes.

The fluorescence excitation spectrum of HPTS was altered during the time-course of incubation of cells with vesicles. The peak at 450 nm progressively decreased while the peak at 403 nm increased. The normalized 450 nm values (450/413 nm ratio) from J774 cells exposed to PC, PS-containing, or DNP-PE-containing liposomes (in the presence or absence of anti-DNP antibody) are shown in Fig. 3B. A decrease in the 450/413 nm ratio is indicative of a decrease in pH. Assuming that HPTS is in one of two compartments, outside the cell at pH 7.4 (high pH) or within endosomes or lysosomes at low pH, then the fraction of dye endocytosed can be calculated using eqn. (1). Approx. 60% of the PC or PS-containing liposomes associated with the cells within 30 min were at low pH (Fig. 3C).

TABLE I

pK_a values for HPTS in aqueous solutions

Conditions	pK_a
water	7.01
0.15 M NaCl	7.09
PBS+0.1% Triton X-100	7.32
PBS+0.1% albumin	7.40
PBS	7.52

TABLE II

Average pH of HPTS or fluorescein dextran (FD) pinocytosed by macrophages

Macrophage	HPTS	FD
J774	6.5	5.59 ± 0.20
P388D1	6.1	5.88 ± 0.14
RAW 264.7	6.0	5.76 ± 0.13

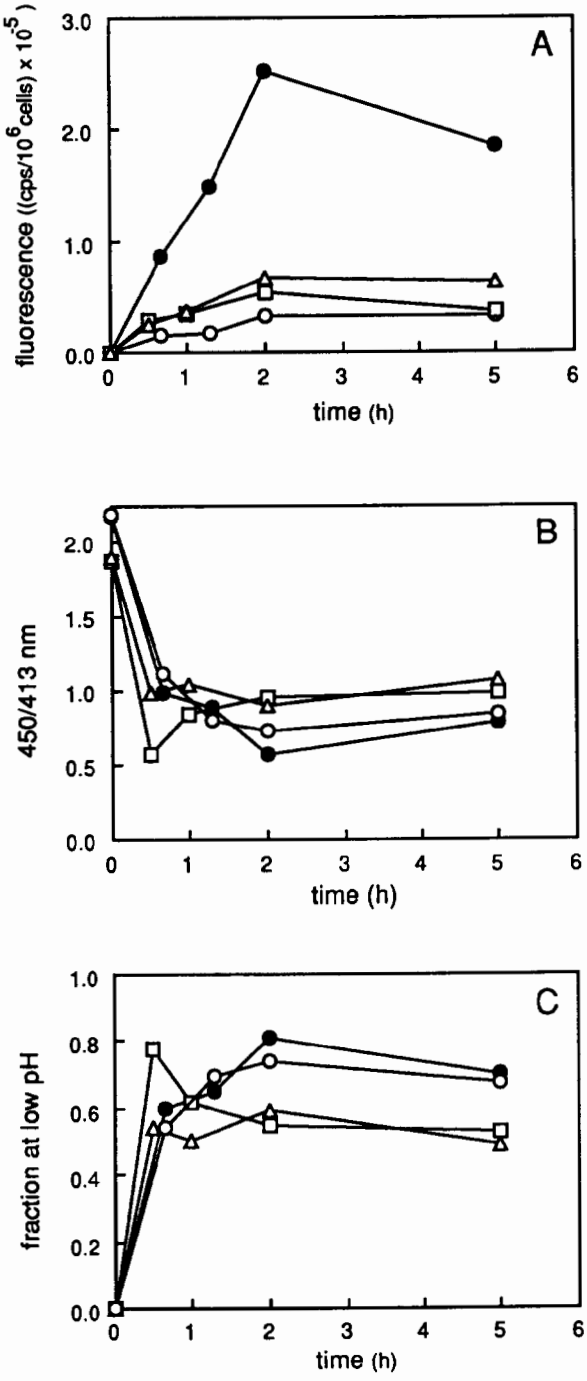

Fig. 3. Time-course of uptake of HPTS-containing liposomes by J774 macrophages. Cells were treated with PC/cholesterol (3 : 1) liposomes (□), PC/PS/cholesterol (2 : 1 : 1) liposomes (△), or PC/PS/DNP-PE/cholesterol (2 : 1 : 0.04 : 1) liposomes in the presence (●) or absence (○) of anti-DNP antibody. Fluorescence at λ_{ex} 413 and 450 nm was measured, the ratio 450/413 nm was calculated, and the amount of HPTS incorporated into the cells was calculated using equation (1): (A) Fluorescence intensity at λ_{ex} 413 nm (photon cps/(10^6 cells)), (B) 450/413 nm ratio, and (C) fraction of HPTS endocytosed (at low pH).

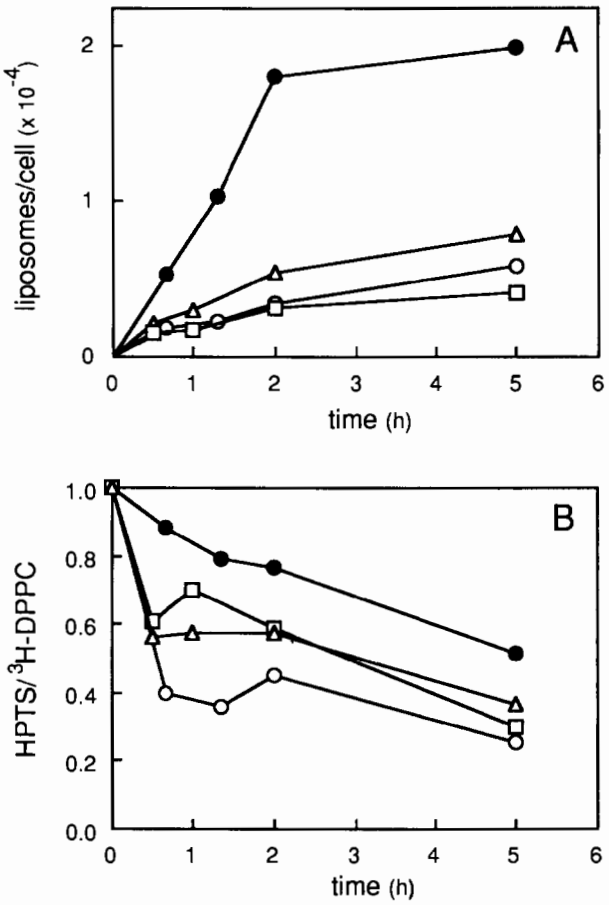

Fig. 4. Time-course of uptake of [^{3}H]DPPC containing liposomes by J774 macrophages. Liposomes from the experiment described in Fig. 3 also contained (3.5–4)·10^3 cpm [^{3}H]DPPC per nmole phospholipid. Cells were treated with PC/cholesterol (3 : 1) liposomes (□) PC/PS/cholesterol (2 : 1 : 1) liposomes (△), or PC/PS/DNP-PE/cholesterol (2 : 1 : 0.04 : 1) liposomes in the presence (●) or absence (○) of anti-DNP antibody, as described in Fig. 3. Radioactivity of aliquots of samples was determined after fluorescence measurements: (A) number of liposomes per 10^6 cells, (B) ratio of HPTS/[^{3}H]DPPC (photon cps/[^{3}H]DPPC cpm) normalized to the ratio in the absence of cells. Starting ratios: PC/cholesterol liposomes, 22.4; PC/PS/cholesterol liposomes, 18.5; and PC/PS/cholesterol/DNP-PE liposomes, 18.1.

DNP-PE-containing liposomes, in the presence or absence of antibody, were acidified to a greater extent (80%), though the rate of acidification of HPTS was similar for all liposomes.

Comparison of uptake of lipid and aqueous contents

The uptake of liposomal lipid was measured using [^{3}H]DPPC as a tracer (Fig. 4, Table III). [^{3}H]DPPC in PC and PS-containing liposomes was incorporated into cells at approximately the same initial rate; however, PS-containing liposomes were incorporated to a greater extent than PC liposomes. These observations are consistent with measurements of liposome uptake by J774 cells by Stevenson et al. [55]. The initial rate of incorporation of radiolabelled lipid from DNP-PE-containing

liposomes was similar to that observed for PC and PS-containing liposomes; however, the rate increased in the presence of antibody. The extent of incorporation of radiolabel from antibody-treated DNP-PE-containing liposomes was approx. 3.4-fold greater than for non-antibody coated DNP-PE-containing liposomes. Compared with HPTS uptake (Fig. 3A), [^{3}H]DPPC was incorporated at similar relative rates and extents (Fig. 4A); however, the absolute amount of incorporation of liposomal lipid and contents markers was not equivalent. As shown in Fig. 4B, the ratio of liposomal contents to liposomal lipid (HPTS/[^{3}H]DPPC) decreased during the course of incubation for all types of liposomes, indicating selective accumulation of liposomal lipid with respect to contents. Within the first hour of incubation cells treated with PC, PS-containing, or DNP-PE-containing liposomes (in the absence of antibody) accumulated 40–60% more lipid than contents label. Upon further incubation cells continued to selectively accumulate liposomal lipid at a slower rate ($11–18\% \cdot h^{-1}$), as evinced by the decrease in the HPTS/[^{3}H]DPPC ratio. The initial loss of liposomal contents within the first hour of incubation was not observed with DNP-PE-containing liposomes in the presence of anti-DNP antibody; the rate of selective lipid accumulation was $12\% \cdot h^{-1}$, similar to the second rate observed with PC, PS-containing, or DNP-PE-containing liposomes.

Quantitation of liposome leakage

Cell-induced dilution of liposomal contents was detected by co-encapsulating HPTS and a non-fluorescent quencher, DPX, into liposomes. The quenching of HPTS with DPX was calibrated by coencapsulating 35 mM HPTS with increasing concentrations of DPX (0–50 mM). The amount of fluorescence (413 nm) observed was compared to the fluorescence in the presence of 0.1% Triton X-100 (defined as 100%). As shown in Fig. 5 (inset), 50 mM DPX was required to achieve greater than 99% quenching of 35 mM HPTS. This concentration of HPTS and DPX was used for subsequent studies of liposome leakage. To calibrate the effects of liposome leakage and dye/quencher dilution, a solution of 35 mM HPTS + 50 mM DPX was diluted with buffer and encapsulated in liposomes. Increasing dilution of the HPTS/DPX solution resulted in an increase in fluorescence (Fig. 5), however a significant increase in fluorescence was observed only at high dilutions; a 43% increase in fluorescence corresponded to greater than 90% dilution of the dye/quencher mixture. This curve was used in subsequent studies to correlate the increase in fluorescence of HPTS/DPX-containing liposomes induced by cells to the amount of liposomal contents that have been diluted.

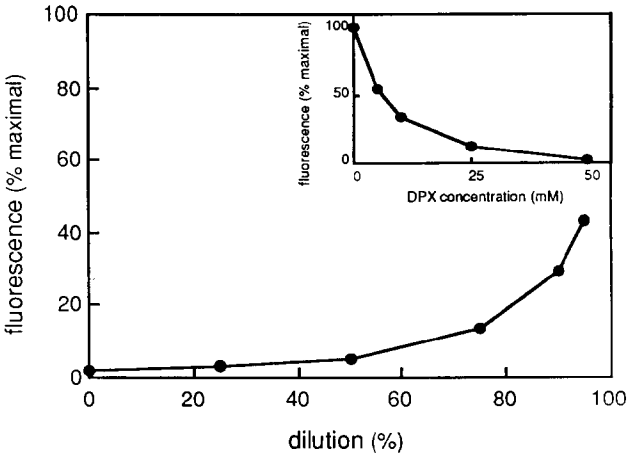

Fig. 5. Quenching of HPTS by DPX. Fluorescence of multilamellar liposomes (PC/cholesterol (3:1)) containing 35 mM HPTS+0–50 mM DPX (inset) or dilutions of a 35 mM HPTS+50 mM DPX solution with buffer was measured in the absence and presence of 0.1% Triton X-100. Data are expressed as maximal fluorescence = $\frac{\text{fluorescence in the absence of detergent}}{\text{fluorescence in the presence of detergent}} \times 100$.

TABLE III

Rate and extent of uptake of [^{3}H]DPPC-containing liposomes by J774 cells

Liposome [a]	Initial rate (liposomes/cell per h)	Extent at 5 h (liposomes/cell)
PC	2360	3090
PC/PS	3080	5870
PC/PS/DNP-PE	1990	4310
PC/PS/DNP-PE +antibody	5900	14700

[a] PC = PC/cholesterol (3:1); PC/PS = PC/PS/cholesterol (2:1:1); PC/PS/DNP-PE = PC/PS/DNP-PE/cholesterol (2:1:0.04:1); antibody = anti-DNP antibody. All liposomes contain approx. 3.8 Ci [^{3}H]DPPC/mol phospholipid.

Cells were treated with PC/PS/cholesterol (2:1:1) liposomes containing 35 mM HPTS + 50 mM DPX at 37°C. Fig. 6 shows phase contrast (a and c) and fluorescence (b and d) micrographs of cells treated for 1 h (a and b) or 4 h (c and d). Punctate fluorescence was observed with illumination at λ_{ex} 350–410 nm at both short (1 h, Fig. 6b) and long (4 h, Fig. 6d) incubation times. Illumination at λ_{ex} 450–490 nm resulted in fluorescence too dim for photography, indicating that almost all of the dequenched dye was at low pH (not shown). Thus, endocytosed liposomes had leaked their contents but the dye remained within low pH compartments and was not present in the cell cytoplasm.

The uptake of HPTS/DPX-containing liposomes by cells and their subsequent leakage was measured by fluorometry. Cells were treated with PC/PS/cholesterol liposomes containing HPTS or HPTS/DPX at 37°C, washed, and fluorescence was measured as above. The samples were treated with 0.1% Triton X-100 and the

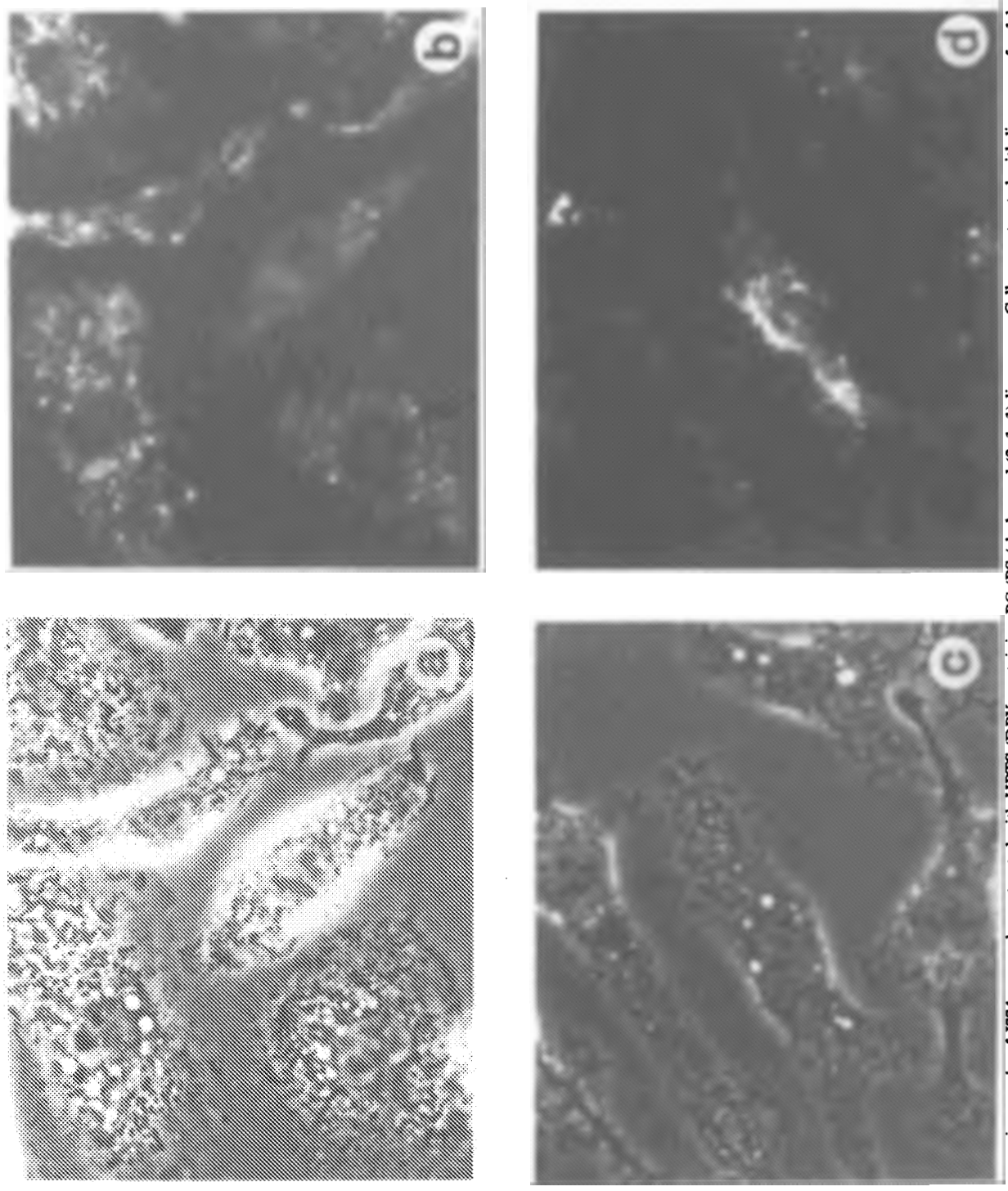

Fig. 6. Fluorescence micrographs of J774 macrophages treated with HPTS/DPX-containing PC/PS/cholesterol (2:1:1) liposomes. Cells were treated with liposomes for 1 h (a, b) or for 4 h (c, d) at 37 °C, washed with PBS-CM and viewed with a water immersion objective by: phase contrast (a, c), or epifluorescence with λ_{ex} 350–410 (b, d) filters.

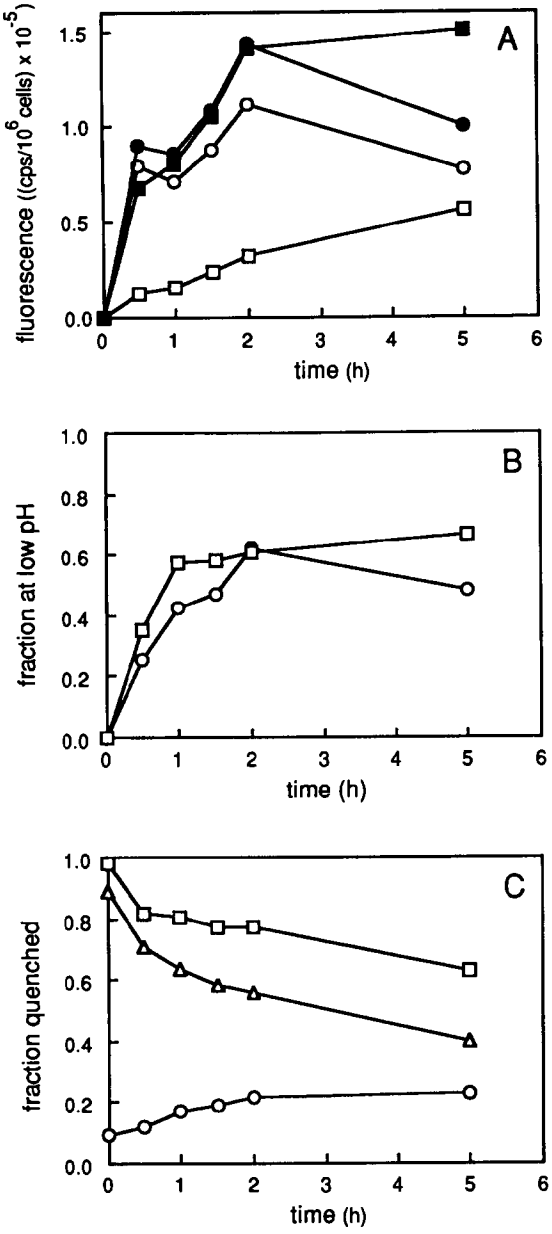

Fig. 7. Time-course of uptake of HPTS and HPTS/DPX-containing liposomes by J774 macrophages. Cells were treated with PC/PS/cholesterol (2:1:1) liposomes containing 35 mM HPTS (circular symbols) or 35 mM HPTS+50 mM DPX (square symbols). Fluorescence at λ_{ex} 413 and 450 nm was measured, the ratio 450/413 nm was calculated, and the amount of HPTS incorporated into the cells was calculated using equation (1). (A) Fluorescence intensity at λ_{ex} 413 nm (photon cps/(10^6 cells)), before (○, □) and after (●, ■) the addition of 0.1% Triton X-100, (B) fraction of HPTS endocytosed (at low pH) and (C) fraction of HPTS remaining quenched (○, □) and corrected fraction remaining quenched (fraction quenched$_{HPTS/DPX}$ − fraction quenched$_{HPTS}$, △).

fluorescence was measured again. As shown in Fig. 7A, less fluorescence was associated with cells treated with HPTS/DPX liposomes (open squares) than with HPTS liposomes (open circles). This difference was a result of quenching of the HPTS by DPX; when these samples were lysed with 0.1% Triton X-100 and remeasured, approximately equal amounts of HPTS fluorescence were observed (closed symbols, Fig. 7A). The uptake of HPTS was coincident with a decrease in the 450/413 nm ratio (not shown) and thus, acidification of HPTS (Fig. 7B). The fraction of dye incorporated into low pH compartments (60%) and the half time of acidification (roughly 30 min) was similar for liposomes containing HPTS or HPTS/DPX.

The increase in HPTS fluorescence in the presence of detergent is a measure of the quenching of the dye. For HPTS/DPX liposomes, fluorescence quenching decreased rapidly and reached a plateau at approximately 60% quenched dye within 5 h (squares, Fig. 7C), corresponding to approximately 95% dilution of the dye/quencher solution (Fig. 5). Liposomes containing HPTS alone became quenched over the same time-course when incubated with cells. The fraction of quenched HPTS rose from an initial value of 10% to approx. 20% after 5 h (circles, Fig. 7C). The net leakage (dequenching) of HPTS/DPX liposomes associated with cells was obtained after correcting for quenching of liposomes containing HPTS alone (triangles, Fig. 7C). Within 5 h, the fraction of dye that is quenched reaches a plateau at approx. 40%, corresponding to about 97% leakage of the liposomes (Fig. 5). There are two possible explanations for this result. The absolute amount of dilution of the dye/quencher mixture of liposomes internalized by J774 cells may be 97%. Alternatively, in the presence of excess liposomes a steady state may develop of liposome binding, internalization, and replacement at the surface with intact exogenous liposomes. The continual binding of intact liposomes would decrease the average value of liposome contents dilution and would increase the average liposome pH.

To eliminate interferences in measurements of liposome leakage and internalization by exogenous liposomes, the previous experiment was modified. Cells were treated with PC/PS/cholesterol liposomes containing HPTS or HPTS/DPX at 37°C for 30 min, washed with PBS-CMG to remove excess liposomes, and reincubated in PBS-CMG at 37°C in the absence of additional liposomes (Fig. 8). At the times indicated, cells were washed again, and fluorescence was measured as above (Fig. 8A, open symbols). Removing exogenous liposomes after 30 min resulted in a rapid loss of dye from the cells upon reincubation; only 25% of the HPTS or HPTS/DPX-containing liposomes remained after a 30 min reincubation. The samples were treated with 0.1% Triton X-100 and the fluorescence was remeasured (Fig. 8A, filled symbols). Detergent treatment resulted in a large increase of fluorescence at 30 min and a smaller increase at later times (Fig. 8A, square symbols). In comparison, when cells are treated continuously with liposomes the fractional increase in fluorescence in the presence of detergent is greater at all

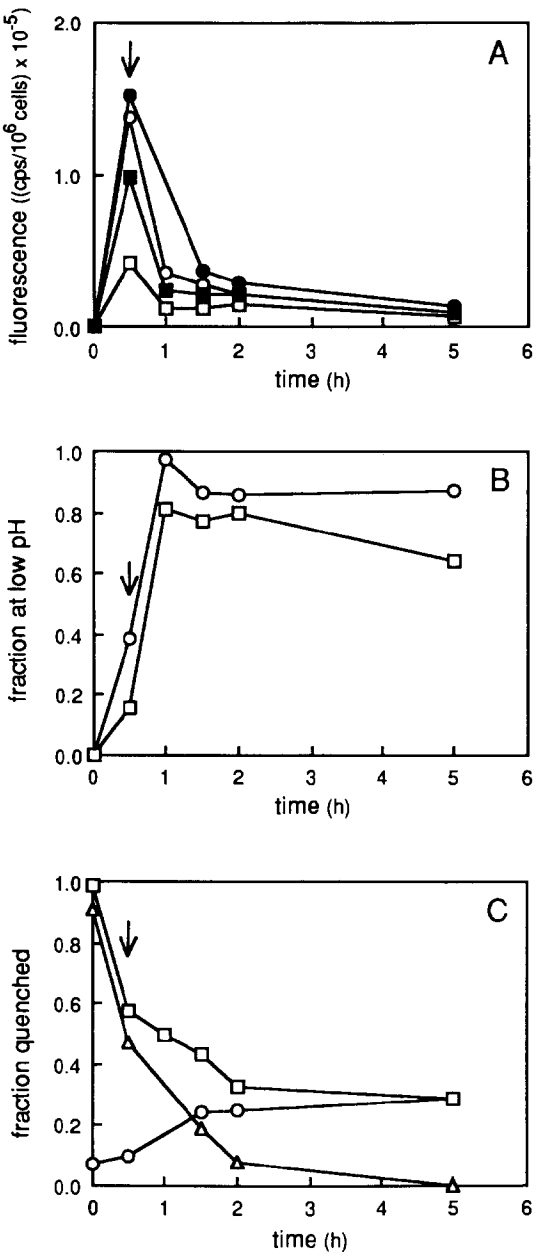

Fig. 8. Time-course of uptake of HPTS and HPTS/DPX-containing liposomes by J774 macrophages. Cells were treated with PC/PS/cholesterol (2:1:1) liposomes containing 35 mM HPTS (circular symbols) or 35 mM HPTS + 50 mM DPX (square symbols) for 30 min at 37°C. Cells were washed (indicated by arrows), resuspended in PBS-CMG and incubation was continued at 37°C. Fluorescence values at λ_{ex} 413 and 450 nm were measured, the ratio 450/413 nm was calculated, and the amount of HPTS incorporated into the cells was calculated using equation (1). (A) Fluorescence intensity at 413 nm (photon cps/(10^6 cells)), before (○, □) and after (●, ■) the addition of 0.1% Triton X-100, (B) fraction of HPTS endocytosed (at low pH), (C) fraction of HPTS remaining quenched (○, □) and corrected fraction remaining quenched (fraction quenched$_{HPTS/DPX}$ − fraction quenched$_{HPTS}$, △).

time points (Fig. 7A, filled square symbols) than that observed in the absence of exogenous liposomes (Fig. 8A, filled square symbols). This indicates that under conditions of continuous exposure, cell associated liposomes have leaked less on the average. After removing exogenous liposomes, the fraction of dye remaining bound to the cell was primarily (> 80%) in a low pH environment (Fig. 8B). In comparison, when incubated continuously with liposomes the fraction of dye in a low pH environment was not greater than 60% (Fig. 7B).

Dye quenching by DPX was quantitated by comparison of fluorescence in the absence and presence of detergent (Figs. 5 and 8A). Fig. 8C shows the fractional quenching as calculated from the increase in fluorescence in the presence of 0.1% Triton X-100. Before exposure to cells, HPTS-containing liposomes were approx. 10% quenched and this fraction increased to approx. 30% during the incubation (Fig. 8C), similar to those values measured in Fig. 7C. The quenching observed in HPTS/DPX-containing liposomes decreased to about 60% during the initial 30 min incubation and continued to decrease to approx. 30% over the time-course of the experiment. The corrected quenching (triangles, Fig. 8C) indicated that after an initial rapid decrease (53% within 30 min, corresponding to 96% leakage (Fig. 5)) liposomes endocytosed by cells eventually leaked all of their contents. During continuous incubation (Fig. 7C) the maximum amount of leakage observed was 97% within 5 h. Thus, removing exogenous liposomes resulted in a greater fraction of dye at low pH and greater degree of average liposome contents dilution, consistent with continual binding of exogenous liposomes to the cell surface if not removed by washing.

Discussion

In the design of liposomes as drug carriers, all modes of liposome-cell interaction must be considered: lipid and protein exchange, adsorption to the cell surface, serum and cell-induced leakage of liposome contents, fusion with cells and endocytosis [56]. Each of these factors affect the efficiency of drug delivery and the choice of liposome components. Although initial studies indicated that liposomes fuse with the cell plasma membrane [57,58], subsequent work established that liposomes are endocytosed in coated vesicles and encounter a low pH compartment inside the cell [37]. Evidence for the low pH compartmentalization of liposomes inside cells has come from the use of cytotoxic agents [21,22] and the pH dependent fluorescent markers carboxyfluorescein and calcein [27,37,58,59]. Both carboxyfluorescein and calcein exhibit a pH dependent quenching of their fluorescence, while only the former becomes membrane-permeant at low pH values [37]. In contrast, the properties of HPTS make it a good marker for liposome endocytosis. It is useful for both microscopic (Figs. 2 and 6) and fluorometric (Figs. 3–5, 7, 8) analysis and accurately reports the pH of its environment [42–45]. It is highly water soluble, membrane imper-

meant, shows a pH dependent shift rather than quench of its fluorescence spectrum, and has an isosbestic point at 413 nm, permitting correction of the measurements to the total amount of dye present in the sample (Fig. 1). Furthermore, the properties of HPTS allow for the use of fluorescence microscopy to detect the location and approximate pH of the dye in cells. By choosing appropriate filters, illumination of HPTS in pH-independent (λ_{ex} 350–410 nm) and pH-dependent (λ_{ex} 450–490 nm) regions of the excitation spectrum can be made (Fig. 2). Thus, the binding and progressive acidification of liposomes can be continuously monitored. In addition, this change in the pattern of fluorescence is energy- and temperature-dependent (not shown), consistent with endocytosis.

The incorporation and acidification of liposomal HPTS can be quantitated by spectrofluorometry. The fraction of dye endocytosed is calculated assuming that the HPTS is present in one of two compartments of different pH: either on the external surface of the cell or in the cell cytoplasm at a high pH (7–7.4), or in intracellular endosomes and lysosomes at a low pH (< 7).

Macrophages are highly phagocytic cells and are ideal for studies of endocytosis and intracellular processing of endocytosed material. Negatively charged liposomes bind to and are endocytosed by cells to a greater extent than neutral liposomes [29,55,60,61]. However, for the macrophages used in the present work this difference is not as great as that seen with other cell lines. Negatively charged PS-containing liposomes are taken up by J774 cells to a slightly greater extent, though at a similar initial rate, than neutral PC liposomes (Fig. 3 and 4, Table III). Similarly, Stevenson et al. [55] found that negatively charged liposomes containing carboxyfluorescein were internalized slightly more efficiently than neutral liposomes by J774 cells. The number of PS-containing liposomes associated with cells at 5 h (approx. 6,000 per cell) is 2-fold greater than values obtained by Stevenson et al. [55] (approx. 3,000 per cell) for J774 cells treated for 3 h with 250 μM PS liposomes (egg PC/cholesterol/PS (7 : 2 : 1). In addition, under their conditions J774 cells bound 3-fold fewer neutral liposomes (egg PC/cholesterol). These discrepancies may be a result of incubation conditions: Stevenson et al. [55] used a 10-fold lower concentration of cells and used liposomes containing 2.5-fold less PS.

Macrophages possess Fc receptors on their surface that bind to the Fc portion of antibodies and are subsequently endocytosed via the coated pit pathway. Liposomes containing DNP-PE are endocytosed in the presence of anti-DNP antibody at a greater rate and to a greater extent than uncoated DNP-PE-containing liposomes (Fig. 3 and 4, Table III). The increased uptake of antibody coated liposomes is probably due to specific Fc receptor-mediated endocytosis [62,63]. Uncoated liposomes may bind to the cell surface and be endocytosed by a separate, perhaps nonspecific, endocytotic mechanism.

The binding of liposomes to cell surfaces induces leakage of liposome contents [27–29] that may be the result of surface protein-liposome interactions [64]. As shown in Figs. 3 and 4, cell associated liposomes rapidly lose HPTS relative to the radiolabelled lipid ([^{3}H]DPPC); the ratio of the HPTS liposome contents marker to the [^{3}H]DPPC lipid marker decreases by 50% within the first 30 min of exposure of neutral or negatively charged liposomes to cells. The initial decrease in in the HPTS/[^{3}H]DPPC ratio is absent in DNP-PE-containing liposomes coated with anti-DNP antibody, indicating that the antibody affords some protection to the disruption of liposome membranes induced by cells. This indicates that leakage of liposome contents induced by cells is a result of direct interaction of the liposome and cell plasma membrane; the presence of antibody prevents close contact of DNP-PE liposomes with the cell membrane. Indeed, the process of cell surface-induced leakage may be related to endocytosis; binding of liposomes to surface proteins or to the lipid bilayer may trigger endocytosis and initiate liposome leakage.

Degradation of liposomes after endocytosis is similar with or without bound antibody; the HPTS/[^{3}H]DPPC ratio decreases steadily and the rate of decrease is similar for neutral, negative or antibody coated liposomes. As surface-bound liposomes are endocytosed, more liposomes take their place on the surface and lose contents. If there is no efflux of liposome contents after endocytosis, the HPTS/[^{3}H]DPPC should approach a constant value indicative of surface induced leakage. However, the HPTS/[^{3}H]DPPC ratio decreases continuously (Fig. 4B), indicating that liposomes are endocytosed and liposome aqueous contents continually efflux from the cell. Liposome leakage (within endosomes) after endocytosis may continue by a mechanism similar to that which occurs on the cell surface. In addition, acidification of liposomes and cell surface proteins after endocytosis may alter protein conformation leading to increased protein–liposome interactions and perhaps penetration of proteins into the liposome bilayer. As liposomes accumulate in lysosomes, other mechanisms such as lipid transfer and lipid degradation contribute to liposome breakdown. Liposome contents released into endosomes and lysosomes become aqueous markers of these compartments, and subsequent efflux of liposomal aqueous contents from cells may result from regurgitation of the contents of early endosomes or from excretion from lysosomes [65,66].

The decrease in HPTS fluorescence associated with cells is not due to degradation of the dye; 80–90% of HPTS originally encapsulated in liposomes can be recovered from the cells and incubation medium (not

shown). In addition, the leakage of HPTS from liposomes after endocytosis is not a result of increased permeability of the dye at low pH; HPTS encapsulated in liposomes similar to those used in this work does not leak readily in the pH range 5–8 [42,67].

In order to measure independently the leakage of liposome contents, an assay based on quenching of HPTS fluorescence by the non-fluorescent molecule, DPX, was developed. DPX has been extensively used as a quencher of aminonapthalene trisulfonate in model studies of membrane fusion and leakage [68], and recently as a liposomal HPTS quencher for microscopy [69]. When coencapsulated with 35 mM HPTS, 50 mM DPX efficiently quenches HPTS fluorescence (Fig. 5). The quenching of HPTS (35 mM) by DPX (50 mM) is efficient even at relatively high dilutions (Fig. 5); greater than 80% dilution is required to achieve appreciable (20% maximal) fluorescence. Liposomes containing HPTS/DPX will fluoresce only if they have leaked more than 50% of their contents. Fluorescence microscopy of HPTS/DPX-liposome uptake demonstrates that leakage subsequent to endocytosis is greater and at a lower pH than leakage at the cells surface; fluorescence is observed only in low pH, punctate compartments within the cells, and not on the cell surface (Fig. 6), although surface bound HPTS-containing liposomes are present (compare Figs. 2b, c and 5b).

Liposome leakage, as monitored by fluorescence dequenching with HPTS/DPX, is concomitant with acidification (Fig. 7). Cells induce an initial rapid dilution of liposome contents; the quenching of cell-associated dye decreases to about 70% within 30 min (Fig. 7C), indicating a 9-fold dilution of liposomes contents (Fig. 5). This dilution represents dye lost to the environment from surface-bound liposomes or by regurgitation from the cells (50% as measured by the [^{3}H]DPPC/HPTS ratio) and leakage of dye from endocytosed liposomes, but retained within cells (remaining 40%), presumably in endosomes. Fluorescence microscopy indicates that the amount of leakage at the cell surface is small compared to leakage that occurs after endocytosis (Fig. 6). A continual slower dilution of liposome contents occurs and quenching eventually plateaus at approximately 40% (Fig. 7C). This signifies an average 5-fold dilution of the dye/quencher mixture remaining with the cells (Fig. 5). During the same time, most of the liposomes (60%) rapidly accumulate in a low pH compartment.

In the preceding experiments, excess unbound liposomes are available to bind to the cells and replace those that have become internalized. Hence, the fraction of dye at low pH and the amount of liposomes that have leaked their contents may be greater for the liposomes that are internalized. To clarify the question of leakage at the cell surface, the experiment described in Fig. 7 was repeated, except unbound exogenous liposomes were removed after a 30 min incubation (Fig. 8). Liposomes initially bound to the cell either desorb from the cell surface or are endocytosed, and are not replaced by exogenous liposomes. As a result, the total amount of dye associated with the cells decreases continuously, possibly due to liposome loss from the cell surface or regurgitation of liposome contents from cells (Fig. 8A). In addition, the fraction of dye in a low pH environment increases to greater than 80% (Fig. 8B), indicating rapid internalization of remaining liposomes. Liposomes remaining associated with, or incorporated into, cells leak all of their contents (Fig. 8C). These results are consistent with nearly complete endocytosis of those liposomes bound to the cell within 30 min followed by leakage and breakdown of liposomes within 2 h, similar to results found with Kupffer cells [70]. The rapid leakage of liposomes occurs on a time scale faster than hydrolysis of liposomal phospholipid in lysosomes [71], indicating that liposome leakage probably occurs in endosomes without lipid breakdown. Finally, if the leakage at the cell surface was much slower than leakage after endocytosis, liposomes containing HPTS/DPX would report a lower pH than liposomes with HPTS alone. As shown in Figs. 7B and 8B, the time-course of acidification of HPTS liposomes and HPTS/DPX liposomes is identical. Thus, the rate of leakage of liposomes at the cell surface is at least as great as leakage after endocytosis. However, microscopy experiments indicate that leakage at the surface is less than 50%, while leakage after endocytosis is greater than 80%. An alternative explanation is that fewer liposomes remain bound to the cell surface compared with the number endocytosed and thus contribute less to the pH measurements.

The small amount of diffuse cytoplasmic fluorescence seen in Figs. 2 and 6 may represent a pathway for the delivery of material to the cytoplasm. Average pH measurements of HPTS pinocytosed by J774 cells differs significantly (0.9 pH units higher) from measurements made with the larger fluorescent probe fluorescein isothiocyanate dextran. Other macrophage cell lines do not show significant differences between these two measurements (Table II). These results imply that J774 macrophages, and not CV-1 fibroblasts [43] or other macrophages (RAW 264.7 and P388D1), have a mechanism for accumulation of HPTS in a higher pH compartment. This compartment may be the cytoplasm and represents 10–20% of the dye remaining associated with the cell after liposome treatment. Furthermore, J774 cells treated with HPTS-containing liposomes do not retain significant amounts of the dye after removal of exogenous liposomes (Fig. 8), however CV-1 fibroblasts treated similarly retain substantial amounts of dye up to 24 h [43]. It is possible that HPTS leaks out of endosomes or lysosomes into the cytoplasm via probenecid-inhibitable organic anion channels [72] or through leaky endosome-lysosome fusion. Once in the cyto-

plasm, HPTS may be transported out of the cell via anion channels in the plasma membrane resulting in rapid loss of the dye from the cell.

The present work has several consequences for liposome-mediated delivery of macromolecules. Cell surface-induced leakage lowers the effective concentration of drug for delivery to cells. The apparent protective effect of antibody binding on cell-surface-induced leakage could indicate that in vivo opsonization of liposomes by plasma proteins may afford some protection to the cell-surface-induced leakage of liposome contents. Leakage of contents during endocytosis results in labelling of the aqueous compartments of endosomes and exposure of the drug to lysosomal enzymes. Efflux of dye from endosomes into the cytoplasm before exposure to lysosomes indicates a (minor) pathway whereby small anionic molecules may avoid degradation in lysosomes. Finally, retention of the liposomal lipid component after endocytosis indicates that lipophilic compounds may be delivered more effectively to cells than small water-soluble compounds.

In conclusion, the use of HPTS as a liposomal contents marker allows a detailed kinetic analysis of liposome binding, endocytosis and leakage by macrophages. It is readily applied to fluorescence microscopy and can be easily quantitated by spectrofluorometry. In conjunction with liposomal lipid markers or fluorescence quenchers, the dye reveals information regarding the selective uptake of liposomal components and the leakage of liposomal contents from liposomes and subsequently from macrophages. Ongoing work is directed towards understanding the mechanisms that trigger liposome endocytosis and requirements for the recognition of liposomes by cells, with emphasis on liposomes of lipid compositions that show decreased in vivo uptake by macrophages [33–35].

Acknowledgements

We thank Dr. Robert Straubinger for many helpful discussions. Supported by NIH grants GM 28117 and CA 35340 and American Cancer Society Postdoctoral Fellowship PF2774.

References

1 Gregoriadis, G. and B.E. Ryman (1972) Eur. J. Biochem. 24, 484–491.
2 Hoekstra, D. and Scherphof, G. (1979) Biochim. Biophys. Acta 551, 109–121.
3 Fidler, I.J., Raz, A., Fugler, W.E., Kirsh, R., Bugalski, P. and Poste, G. (1980) Cancer Res. 40, 4460–4466.
4 Poste, G., Kirsh, R., Fogler, W.E. and Fidler, I.J. (1979) Cancer Res. 39, 881–892
5 Fidler, I.J. (1980) Science 208, 1449–1451.
6 Fidler, I.J., Sone, S., Fogler, W.E. and Barnes, Z.L. (1981) Proc. Natl. Acad. Sci., USA 78, 1680–1684.
7 Kleinerman, E.S., Erickson, K.L., Schroit, A.J., Fogler, W.E. and Fidler, I.J. (1983) Cancer Res. 43, 2010–2014.
8 Koff, W.C., Showalter, S.D., Hampar, B. and Fidler, I.J. (1985) Science 228, 494–497.
9 New, R.R.C. and Chance, M.L. (1980) Acta Trop. (Basel) 37, 253–256.
10 Lopez-Berestein, G., Mehta, R., Hopfer, R.L., Mills, K., Kasi, L., Mehta, K., Fainstein, V., Luna, M., Hersch, E.M. and Juliano, R. (1983) J. Infect. Dis. 147, 939–945.
11 Tremblay, C., Barza, M., Fiore, C. and Szoka, F. (1984) Antimicrob. Agents Chemother. 26, 170–173.
12 Allison, A.C. and Gregoriadis, G. (1974) Nature 252, 252.
13 Alving, C.R. (1987) in Liposomes, (Ostro, M.J., ed.), pp. 195–218, Marcel Dekker, New York.
14 Mayhew, E., Papahadjopoulos, D., Rustum, Y.M. and Dave, C. (1976) Cancer Res. 36, 4406–4411.
15 Kataoka, T. and Kobayashi, T. (1978) Ann. N.Y. Acad. Sci. 308, 387–394.
16 Rahman, A., Kessler, A., More, N., Sikic, B., Rowden, G., Woolley, P. and Schein, P.S. (1980) Cancer Res. 40, 1532–1537.
17 Forssen, E.A. and Tökés, Z.A. (1981) Proc. Natl. Acad. Sci. USA 78, 1873–1877.
18 Olson, F., Mayhew, E., Maslow, D., Rustum, Y. and Szoka, F. (1982) Eur. J. Cancer Clin. Oncol. 18, 167–176.
19 Cohen, C.M., Weissmann, G., Hoffstein, S., Awasthi, T.C. and Srivastava, S.K. (1976) Biochemistry 15, 452–460.
20 Heath, T.D., Fraley, R. and Papahadjopoulos, D. (1980) Science 210, 539–541.
21 Leserman, L.D., Machy, P. and Barbet, J. (1981) Nature (London) 293, 226–228.
22 Heath, T.D., Montgomery, J.A., Piper, J.R. and Papahadjopoulos, D. (1983) Proc. Natl. Acad. Sci. USA 80, 1377–1381.
23 Kimelberg, H.K. and Papahadjopoulos, D. (1971) Biochim. Biophys. Acta 233, 805–809.
24 Black, C.D.V. and Gregoriadis, G. (1976) Biochem. Soc. Trans. 4, 253–256.
25 Zborowski, J., Roerdink, F.H. and Scherphof, G. (1977) Biochim. Biophys. Acta 497, 183–191.
26 Scherphof, G., Roerdink, F., Waite, M. and Parks, T. (1978) Biochim. Biophys. Acta 542, 296–307.
27 Szoka, F., Jacobson, K. and Papahadjopoulos, D. (1979) Biochim. Biophys. Acta 551, 295–303.
28 Fraley, R.T., Subramani, S., Berg, P. and Papahadjopoulos, D. (1980) J. Biol. Chem. 255, 10431–10435.
29 Fraley, R.T., Straubinger, R.M., Rule, G., Springer, E.L and Papahadjopoulos, D. (1981) Biochemistry 20, 6978–6987.
30 Poste, G. (1983) Biol. Cell 47, 19–38.
31 Weinstein, J.N. (1984) Cancer Treat. Rep. 68, 127–135.
32 Alving, C.R., Steck, E.A., Chapman, W.L., Jr., Waits, V.W., Hendricks, L.P., Swartz, G.M. and Hanson, W.L. (1978) Proc. Natl. Acad. Sci., USA 75, 2959–2963.
33 Allen, T. and Chonn, A. (1987) FEBS Lett. 223, 42–46.
34 Gabizon, A. and Papahadjopoulos, D. (1988) Proc. Natl. Acad. Sci. USA 85, 6949–6953.
35 Allen, T., Hansen, C. and Rutledge, J. (1989) Biochim. Biophys. Acta 981, 27–35.
36 Finkelstein, M. and Weissmann, G. (1978) J. Lipid Res. 18, 289–303.
37 Straubinger, R.S., Hong, K., Friend, D.S. and Papahadjopoulos, D. (1983) Cell 32, 1069–1079.
38 DeDuve, C., DeBarsy, T., Poole, B., Trouet, A., Tulkens, P. and Van Hoof, F. (1974) Biochem. Pharm. 23, 2495–2531.
39 Ohkuma, S. and Poole, B. (1978) Proc. Natl. Acad. Sci. USA 75, 3327–3331.
40 Weinstein, J.N., Blumenthal, R., Sharrow, S.O. and Henkart, P.A. (1978) Biochim. Biophys. Acta 509, 272–288.

41 Wolfbeis, O.S., Furlinger, E., Kroneis, H. and Marsoner, H. (1983) Fr. Z. Anal. Chem. 314, 119–124.
42 Hong, K., Straubinger, R.M., and Papahadjopoulos, D. (1986) J. Cell Biol. 103, 56a.
43 Straubinger, R.M., Papahadjopoulos, D. and Hong, K. (1990), in press.
44 Clement, N.R. and Gould, J.M. (1981) Biochemistry 20, 1534–1538.
45 Biegel, C. and Gould, J.M. (1981) Biochemistry 20, 3474–3479.
46 Damiano, E., Bassilana, M., Rigaud, J.-L. and Leblanc, G. (1984) FEBS Lett. 166, 120–124.
47 Comfurius, P. and Zwaal, R.F.A. (1977) Biochim. Biophys. Acta 488, 36–42.
48 Lowry, O.H., Rosebrough, N.J., Farr, A.L. and Randall, R.J. (1951) J. Biol. Chem. 193, 265–275.
49 Szoka, F. and Papahadjopoulos, D. (1978) Proc. Natl. Acad. Sci. USA 75, 145–149.
50 Szoka, F., Olson, F., Heath, T., Vail, W., Mayhew, E. and Papahadjopoulos, D. (1980) Biochim. Biophys. Acta 601, 559–571.
51 Bartlett, G.R. (1959) J. Biol. Chem. 234, 466–468.
52 Savistsky and Golay (1964) Anal. Chem. 36, 1627–1639.
53 Kimelberg, H.K. and Mayhew, E.G. (1978) CRC Crit. Rev. Toxicol. 6, 25–79.
54 Reggio, H., Bainton, D., Harms, E., Coudrier, E. and Louvard, D. (1984) J. Cell Biol. 99, 1511–1526.
55 Stevenson, M., Baillie, A.J. and Richards, R.M.E. (1984) J. Pharm. Pharmacol. 36, 824–830.
56 Pagano, R.E. and Weinstein, J.N. (1978) Annu. Rev. Biophys. Bioeng. 7, 435–468.
57 Poste, G. and Papahadjopoulos, D. (1976) Nature (Lond.) 261, 699–701.
58 Weinstein, J.N., Yoshikami, S., Henkart, P., Blumenthal R. and Hagins, W.A. (1977) Science 195, 489–492.
59 Blumenthal, R., Weinstein, J.N., Sharrow, S.O. and Henkart, P. (1977) Proc. Natl. Acad Sci, USA 75, 5603–5607.
60 Rimle, D., Dereski, W. and Petty, H.R. (1984) Mol. Cell. Bioch. 64, 81–87.
61 Heath, T.D., Lopez N.G. and Papahadjopoulos, D. (1985) Biochim. Biophys. Acta 820, 74–84.
62 Geiger B., Gitler, C., Calef, E. and Arnon, R. (1981) Eur. J. Immunol. 11, 710–716.
63 Derksen, J.T P., Morselt, H.W.M., Kalicharan, D., Hulstaert, C.E. and Scherphof, G.L. (1987) Exp. Cell Res. 168, 105–115.
64 Van Renswoude, J. and Hoekstra, D. (1981) Biochemistry 20, 540–546.
65 Brown, M.S. and Goldstein, J.L. (1983) Annu. Rev. Biochem. 52, 223–261.
66 Pastan. I. and Willingham, M.C. (1985) in Endocytosis, (Pastan I. and Willingham, M.C., eds.), pp. 1–44, Plenum, London.
67 Kano, K. and Fendler, J.H. (1978) Biochim. Biophys. Acta 509, 289–299.
68 Ellens, H., Bentz, J. and Szoka, F.C. (1985) Biochemistry 24, 3099–3106.
69 Chu, D.-J., Dijkstra, J., Lai, M.-Z., Hong, K. and Szoka, F. (1990) Pharmac. Res., in press.
70 Dijkstra, J., van Galen, W.J.M., Hulstaert, C.E., Kalicharan, D., Roerdink, F.H., and Scherphof, G.L. (1984) Exp. Cell Res. 150, 161–176.
71 Dijkstra, J., van Galen, M., Regts, D. and Scherphof, G. (1985) Eur. J. Biochem. 148, 391–397.
72 Steinberg, T.H., Newman, A.S., Swanson, J.A and Silverstein, S.C. (1987) J. Cell Biol. 105, 2695–2702.